NASA Conference Publication 2317

Astronomical Microdensitometry Conference

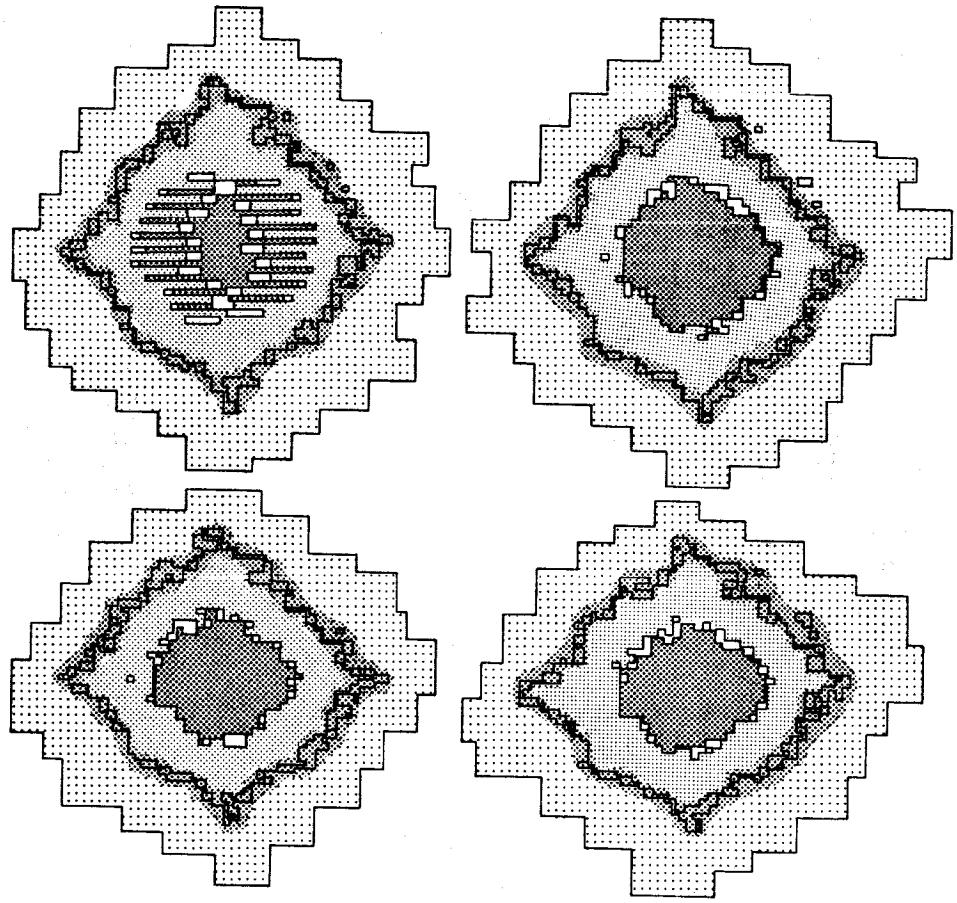

Proceedings of a workshop held at
Goddard Space Flight Center
Greenbelt, Maryland
May 11-13, 1983

NASA

NASA Conference Publication 2317

Astronomical Microdensitometry Conference

Daniel A. Klinglesmith, *Editor*
Goddard Space Flight Center
Greenbelt, Maryland

Proceedings of a workshop held at
Goddard Space Flight Center
Greenbelt, Maryland
May 11–13, 1983

NASA
National Aeronautics
and Space Administration

Scientific and Technical
Information Branch

1984

PREFACE

These proceedings are a result of two and one half days of intense paper presentation and discussion on the subject of Astronomical Microdensitometry. There were over 70 scientists and engineers from around the world in attendance. The conference was sponsored by NASA, Goddard Space Flight Center and the American Astronomical Society.

This conference was unusual in the sense that most of the time that astronomers get together they only talk about their science and not the tools needed to extract the scientific information. At this conference we were concerned mainly with one of the tools -- the microdensitometer. This conference had given us the opportunity to spend a large amount of time on the very important subject of how to extract scientific information. We have pulled together in one volume most of the current understanding of the one commercially available microdensitometer, the PDS. We have discussed how to diagnose a microdensitometer. We have looked at all of the modern high speed machines and we have begun some discussion on the subject of what the next generation machine should be capable of doing. We have also talked about the problems of data storage and retrieval.

The success of the conference was due in a large measure to the participants themselves. They shared their secrets about the PDS and their fears and desires about the future of astronomical microdensitometery. The organizing committee which is listed below was a great help to me because they keep me on track, introduced ideas other than mine and generally were very supportive of the many details needed to accomplish a conference like this one. Mr. Jean DellAmore and the staff at Birch and Davis are to be congratulated on the smooth running of the conference. The attendees are forever in the debt of Mr. James Horton, the designer of the "PDS" for a delightful and very factual account of the history of the 150 or so PDSs that have been built. But we will never know where the dropped machine is! My sincere thanks to all who were involved.

We have attempted to transcribe the question and answer periods after each paper. I have tried to retain the flavor of the comments. The transcripts are very much verbatim. In several instances the questions from the audience could not be heard on our tapes, in those cases I have deleted both the question and answer. The tapes have been heard by several people, myself included, and I take full responsibility for the errors that still remain.

At every conference there is usually one very pertinent remark heard from the back of the audience. Ours was no exception, and I quote:

"You can't take a steel machine for granite"

and

"You can't get a granite machine for a steal"

ORGANIZING COMMITTEE

Dr. Daniel A. Klinglesmith, Chairman
Dr. Peter Boyce
Dr. Robert Cornett
Dr. Harry Heckathorn
Dr. Barry Lasker
Dr. Arthur Poland
Dr. Francois Schweizer
Dr. Donald Wells

CONTENTS

SESSION I

Chairman: Harry M. Heckathorn

I. How to Diagnose a Microdensitometer

The ultimate goal of modern-day astronomical microdensitometry is the fast, faithfuly conversion of analog information, stored as blackened grains of silver in a recording emulsion, into digital format for subsequent computer processing. However, either by design or by malfunction, the various optical, mechanical, and electronic components in even the current generation of microdensitometers impose limitations on the accuracy (both photometric and positional) and speed of digitization. The diagnosis of a microdensitometer is the process of test and evaluation in order to understand these limitations (some of which may be fundamental), to isolate specific problems and to provided the basis against which various "improvements" may be judged. Contributions which describe and illustrate by example useful techniques for testing the hardware and its compatability with the requirements of the astronomer are welcome (as are specific examples of hardware failures or the results of uncouscious misuse).

DIAGNOSING A PDS MICRODENSITOMETER

William van Altena

and

Jin-Fuw Lee

YALE UNIVERSITY OBSERVATORY

and

Alan Wandersee

YALE CENTER FOR ELECTRONIC SERVICES

Abstract

Over the past four years a number of diagnostic tests have been developed for the PDS 2020G microdensitometer to monitor its performance and to isolate various electro-mechanical problems. In this paper we describe a number of tests which have helped us to diagnose problems with the photometer, positional accuracy and data collection. The tests include: scanning a razor blade edge to study the response of the photometer and zero-point losses in the coordinate system; scanning a long straight line to evaluate the drunkenness of the stage motions; scanning photometric step-wedge calibrations to study the response of the photometer; measurement of a series of high signal-to-noise plates of the same region of the sky to evaluate the overall performance of the microdensitometer; and a variety of electronic tests to isolate electromechanical problems.

I. Introduction

In this paper we describe a number of simple diagnostic tests that we have used with the PDS 2020G microdensitometer to identify problems in the hardware. The Yale PDS is the "translator" version, which gives us more accesibility to the various registers. However, all of the tests described here should also be applicable to the "microprocessor" version.

II. Loss of the coordinate zero-point

Our most common problem has been with a loss of the zero-point in a coordinate. To identify such a loss, we have found it to be a good practice to repeatedly measure a test object every ten to fifteen minutes during an extended scan. In this way, we can monitor thermal drifts and possible zero-point losses by comparing the repeat measurements. If image positions or spectrum line positions show unexpectedly large errors in the reductions, or excessively ragged edges, then a zero-point loss may be indicated. To confirm the existence of a zero-point loss, locate a sharp fiducial mark on the platten, such as a speck of dust, and note the coordinates. Run the x-axis back and forth manually at maximum speed several times and then reposition the PDS carriage on the fiducial mark. The coordinate should repeat to within one micron. Repeat this test with the y-axis. If both coordinates repeat accurately, then try the test again, only this time run the carriages into the electronic overtravel limits a number of times. If a failure occurs here, then a possible solution is to add an R-C network across the offending "over travel" lamp. On the other hand, if a loss of the zero-point is indicated in the rapid motion test, then the encoder signal level is probably too low for the detection circuitry.

Two common sources of this problem are fogging of the encoder lamp condenser lens due to outgassing of the epoxy cement, or a misalignment of the encoder assembly. First, check the lens for fogging by removing the cover plate and then the two screws that hold the lamp housing to the encoder box. The lamp housing should then be easy to pull out and unplug. Loosen the screw that holds the clamping spring on the lamp and pivot it out of the way. Gently remove the lamp assembly from the housing using needle-nose pliers, if necessary. If the lens is fogged, a Q-tip soaked in alcohol readily removes the dirty coating on both the lens and the lamp. Put the encoder back together and run the high speed manual test again. If the zero-point test still fails, then it will be necessary to use an oscilloscope to monitor the waveforms coming from the encoder on the "scale amplifier" board. Locate the test points where both the "a" and "b" waveforms can be examined. The encoder waveforms should appear sinusoidal and symmetric and have amplitudes greater than some minimum voltage. Check the manual for the minimum voltage and procedures for aligning the encoder, as poor alignment might result in damage to the encoder.

III. Failure to detect limit crossings

Another common problem associated with low signal levels in the encoder, is the missing of limit crossings. The usual symptom of a missed limit crossing is that the PDS will continue past its destination to the over travel limit switch and wait for some kind of operator intervention. To fix this problem, adjust the phase and dwell times of the squared "a" and "b" encoder signals on the scale amplifier board using an oscilloscope to monitor the results. When properly adjusted, the phases should differ by 90 degrees and the dwell times of the positive and negative going signals should be identical. If this procedure does not correct the limit-miss problem, then it is often necessary to use a logic probe to locate the point where the limit signal is getting lost. The solution to the limit-misses now becomes more difficult and depends on your ingenuity in locating the "dead" component!

IV. Cross talk between the coordinates

The occurrence of cross talk between the coordinates can be easily identified by manually running one of the coordinates at high speed while the other coordinate is at rest. If counts appear in the coordinate at rest, then we can suggest two possible locations for the problem. The x- and y-axis motor drives produce a certain amount of electrical noise, which can be reduced by installing an 0.1 uf capacitor across the motor brushes. This may introduce a dc offset voltage in the drive circuit, which has to be compensated for elsewhere. Another potential source of cross talk may be found in the PDS power supplies. Check that the logic and analogue power supplies are isolated and not tied together in any way.

Finally, mechanical vibrations can cause an interaction between the axes in an undesireable manner. For example, an offcenter or slightly out-of-round drive shaft will shake the PDS and result in detectable counts in the other axis. This problem can be identified by attaching the oscilloscope to the sinusoidal encoder test points and switching to a high gain. If the opposite axis is then manually run at high speed and a detectable signal is noticed, then there is a good chance that the drive shaft is bent. This unfortunate state of affairs can be confirmed by mounting a precision feeler gauge adjacent to the drive shaft and manually rotating the shaft to check for any eccentricity. Unfortunately, the only solution to this problem is to replace the drive shaft.

V. Photometric response

The next series of diagnostic tests are performed with two unused razor blades, mounted perpendicular to each other on a small piece of cover glass. The razor blade fixture can then be taped to the platten at any position for the tests. We have found the single-edge "injector" razor blades to be the most convenient ones to use.

Scans of the razor blade in one axis are made using a pixel width of 5-25 um and a sample spacing of 1 to 2 um. Normally, if we are scanning in the x direction, we will use a scan length of 100 um or more and twenty to several thousand scans at the same y coordinate. The edge of the razor blade is defined as being that point where the transmission reaches 0.5. In practice, the half-transmission point is found by fitting the data by least-squares to the equation:

$$T = A + B*X, \qquad (1)$$

where T is the transmission, X is the coordinate (X or Y), and B is the slope of the transfer curve. It has been our usual practice to derive the transmission from the measured density and to include only transmission values lying in the linear region between 0.1 and 0.9 in the solution. Occassionally, we have found it useful to find the edge at higher densities, in which case it is necessary to use a cubic solution to allow for greater curvature in the transfer curve.

$$D = A + B*X + C*X^2 + D*X^3 \qquad (2)$$

In either case, the solution is inverted and the edge position corresponding to the half-transmission point or to the desired density value is found.

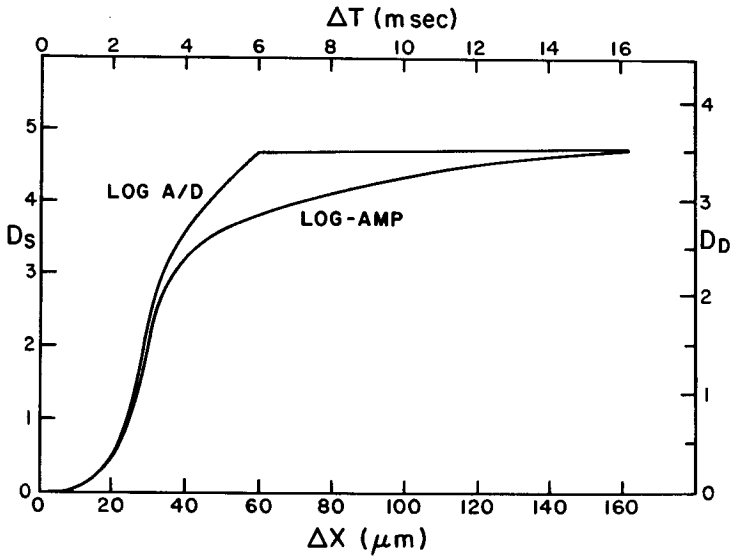

Figure 1: Response of the 0 - 5D logarithmic-amplifier and the 0 - 4.65D logarithmic analogue to digital converter to a 10 mm/sec scan across a razor blade edge from light to dark. The left and right ordinates show the PDS specular and Kodak diffuse densities, respectively, while the upper and lower abscissae show the elapsed time in milliseconds and the distance in microns, respectively, both relative to a point near the edge.

In Fig. 1 we illustrate the response of the logarithmic-amplifier to a razor blade scan at a speed of 10 mm/sec. Also included in Fig. 1 is the response of a high speed logarithmic analogue to digital converter recently installed on the Yale PDS and described by van Altena and Lee(1983). (Kodak diffuse density is approximately equal to 3/4 the PDS density.). Note that significant delays in the response of the log-amp are already present at diffuse densities above 2.0. Due to these delays, it is necessary to deal with the forward and reverse scans (light to dark and dark to light) separately. The effect of these delays is to progressively offset the forward and reverse lines of a raster scan as, for example, we go to higher and higher densities in a raster scan of a stellar image.

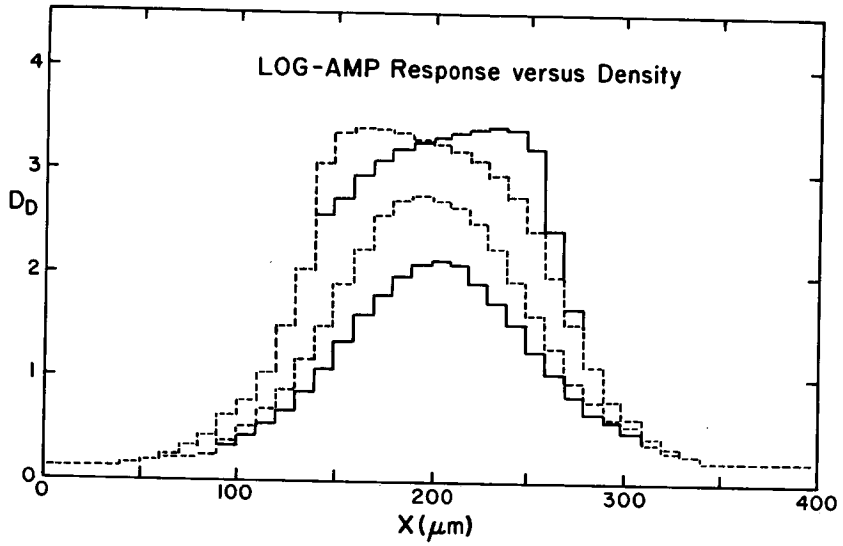

Figure 2: Response of the log-amp to a 10 mm/sec raster scan across a dense stellar image. The diffuse density is plotted against the x coordinate in microns for four scans moving towards the center of the image. The solid curves represent scans in increasing x, while the dashed curves represent scans in decreasing x. A noticeable skewing of the image appears at densities above 2.0 and becomes very large above density 3.0.

Figure 2 illustrates several raster scan lines through a dense stellar image as we move in toward the image center. Solid lines represent the forward scans and dashed lines the reverse scans. At diffuse density three, the offset between lines is more than 50 um, which can lead to serious errors in the derived photometry and position of the image. The solution to this problem is to replace the slow log-amplfier with a faster unit such as described elsewhere in this volume or with the log A/D converter described by van Altena and Lee(1983).

Turning now to the noise characteristics of the photometer, we will evaluate the extent to which the photometer is photon noise limited.

Latham(1978) defines the micronoise as the local rms point-to-point fluctuations in the density. Using this definition, we scan a clear part of the platten with a 20 to 30 um aperture and compute the micronoise from 2000 or so points. If the system is photon noise limited, then we expect the noise to be a function of the square-root of the number of detected photons.

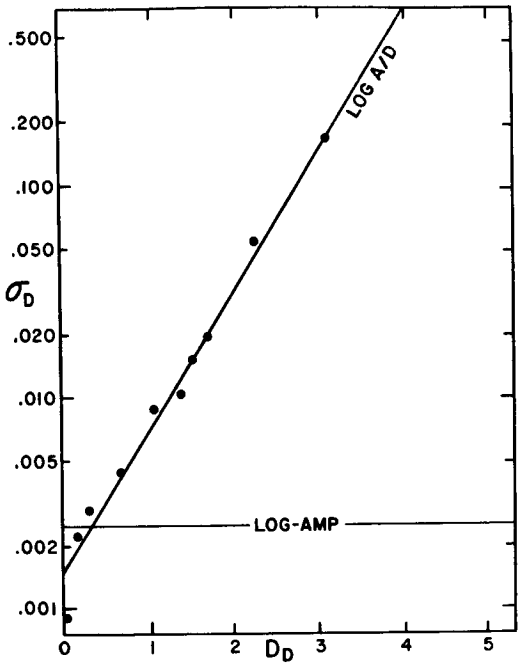

Figure 3: The diffuse density noise versus the diffuse density for a series of clear plate scans using different PDS filter settings. The log A/D converter data points follow the slope one-half line, indicating that it is photon noise limited. The log-amp is very quiet at all densities, indicating that it has a very long time constant which integrates the photon noise to achieve its low noise characteristics.

In Fig. 3 we show the diffuse density micronoise for the Yale PDS log-amp and the log A/D converter as a function of the diffuse density, where the micronoise has been scaled to an aperture of 1000 um. The log-amp is very quiet for all densities, while the log A/D converter micronoise follows the photon noise limit relationship illustrated by the slope one-half line. The log A/D relationship predicts a detection rate of one photon/sample through an aperture of 1000 square microns at a diffuse density of 5.4.

We can reduce the photon noise either by multiple sampling, or by integrating the output from the photomultiplier. While taking multiple samples and averaging the results in software is simple, it results in averaging the data over a much longer distance in the direction of the scan. This can result in serious problems, if there are significant density gradients in the region being scanned. For this reason, we have chosen to integrate rather than to take multiple samples. For reasonable integration

times, the spatial averaging only amounts to a fraction of a micron. We have found that an additional integration time of 24 usec reduces the system micronoise to a value that is below the IIIa-J emulsion micronoise. It is important not to use too much integration, since real density fluctuations in the emulsion will be artificially smoothed.

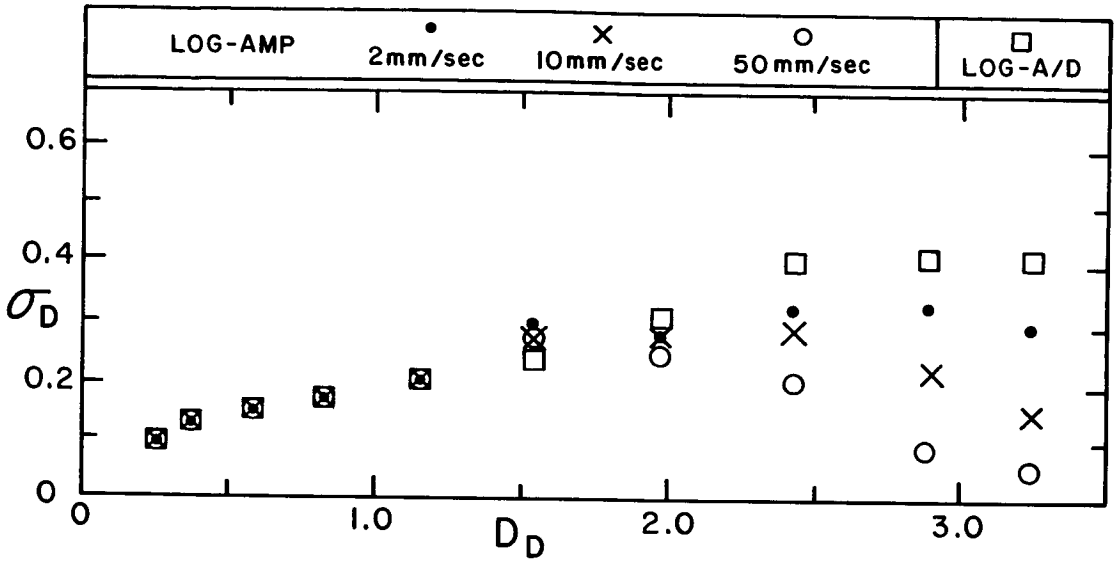

Figure 4: Response of the log-amp and log A/D converter to scans across a Kodak IIIa-J step wedge. The diffuse density micronoise is plotted versus the diffuse density for three different scan speeds. At density 2.0 the data are artificially smoothed by the long time constant of the log-amp. The input to the log A/D converter has been smoothed by the addition of a 24 usec time constant R-C circuit, which minimizes the photon noise, but does not artificially smooth the grain noise.

In Fig. 4 we show the diffuse density micronoise plotted against the diffuse density for scans of a IIIa-J density wedge from our inter-observatory calibration step wedges, Sewell(1975). The square boxes represent the emulsion noise as measured by the log A/D converter with an integration time of 24 usec, while the dots, crosses and circles represent, respectively, the noise determined with the log-amp at speeds of 2, 10 and 50 mm/sec. At diffuse density 2.0 the log-amp data are seen to fall significantly below the log A/D converter data, indicating that the emulsion noise is being artificially smoothed. Theoretically, it has been shown by Dainty and Shaw(1974) that the emulsion micronoise should be proportional to the square-root of the density. Furenlid, Carder and Shoening(1977) have shown that the square-root relationship holds experimentally. Therefore, we have a very convenient diagnostic for the response of the photometer. If your PDS photometer produces a square-root relationship between the density micronoise and the density, then the photometer is probably not photon noise limited or artificially smoothing the data. If, on the other hand, the data turns up for

D > 2.0, then you are probably photon noise limited; if the data turn down, then the photometer has an integration time that is too long.

VI. Positional accuracy

We now turn to diagnostics related to the repeatability of the PDS. First we look at the local repeatability of the PDS with scans of the razor blade. In Fig. 5a we plot the edge position, determined from Eq. 1, versus the scan number for scans in one direction only. In other words, the abscissa is a time sequence and any thermal drift would be represented by an systematic drift in the ordinate. The scans were made with an aperture of 10x10 um at a speed of 10 mm/sec at the same value of the y-axis. The data appear to have a bimodal distribution, however this feature is not always present and we have no explanation for its existence. The dispersion of the edge determinations is +/- 0.25 um (s.e.). The most curious feature of this diagram is that when the experiment is repeated, but with a time delay forced before the next scan, then the dispersion is reduced. In Fig. 5b we show a diagram identical to Fig. 5a, except that the PDS has been forced to wait 1/6 sec before the next scan. As is obvious, the dispersion (+/- 0.09 um) has been greatly reduced.

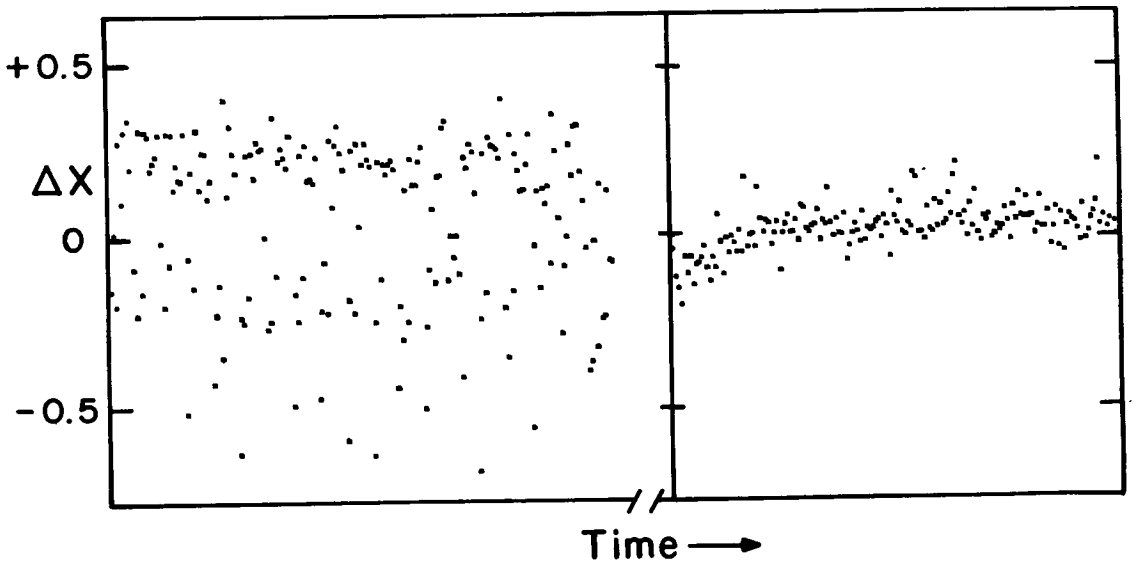

Figure 5: In Fig. 5a the edge position relative to a point near the edge is plotted versus the scan number, or time. The edge position has a dispersion of 0.25 um when the PDS scans back and forth without any delay between successive scan lines. In Fig. 5b, a delay of 1/6th of a second has been forced between successive scan lines, resulting in a decrease in the dispersion to 0.09 um. Note that only alternate lines are included in these plots. The apparent bimodal distribution in Fig. 5a is not present in all scans and its origin is unknown.

In Fig. 6 we show a plot of the dispersion versus various delays before the next scan. The dispersion reaches a minimum of +/- 0.05 um after a delay of 1/3 sec before the next scan, and remains constant thereafter. No completely satisfactory explanation for this behaviour has been found so far. Notice that at the beginning of the scan in Fig. 5b, there is evidence for a small drift in the coordinate. The kink has been correllated with closing the door to the PDS room just before the scan was started. The small temperature difference between the inside and the outside of the room was sufficient to cause this drift.

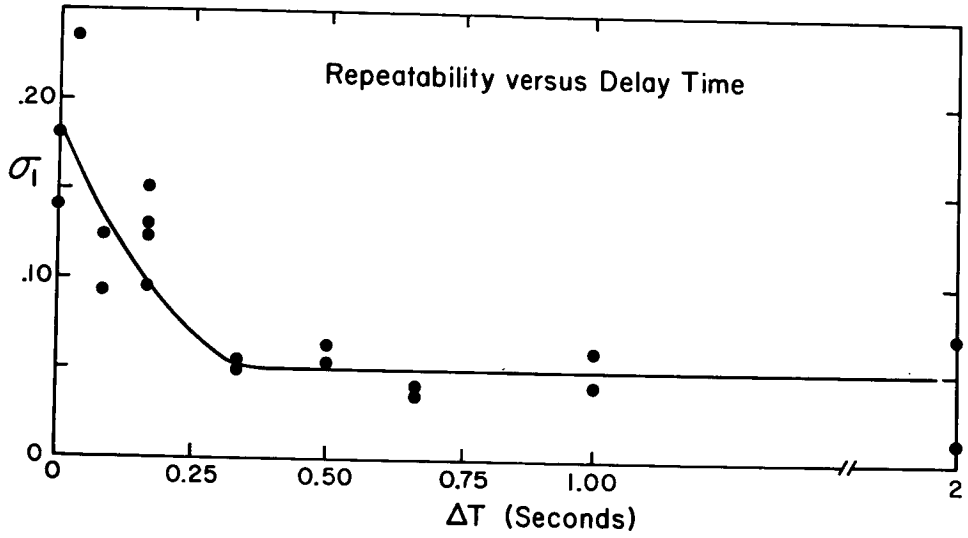

Figure 6: The dispersion of the edge position is plotted versus the delay time before starting a scan line. A minimum dispersion of 0.05 um is reached with a delay of 0.33 sec before starting a scan.

VII. One micron glitches

One problem that has plagued us for most of the time that we have had the PDS, is a more of less random change in the zero-point of exactly one micron. We refer to this phenomenon as the one micron glitch. The problem is usually suspected when the positions of test objects fail to repeat to the expected accuracy, and is confirmed by razor blade scans. Depending on the severity of the glitch problem, the frequency may be anything from one in 40 scans to one in several thousand. We therefore will typically scan the razor blade a few thousand times, remove any long term thermal drift in the edge positions, and plot the results as shown in Fig. 7. As can be seen in the figure, the edge position changes in discrete amounts of 1.0 um, more or less randomly. At times the direction of the glitch may continue in one direction and result in a serious change of the zero point. For a considerable length of time we took advantage of the fact that a two micron glitch was a very rare event, and scanned in the mode where the PDS counted by twos. This procedure filtered out the one micron glitches very effectively, but it did not cure the basic problem.

Since we have not been able to absolutely identify the source of the glitch, we will list the various areas that we have felt, at one time or another, may have been responsible for the problem. The first area that we always look at is the encoder signal level in the x-axis (we have never seen glitches in the y-axis). If the levels are low, then the encoder condenser lens may need to be cleaned. Second, check for excessive electrical noise in the system. For example, are the motor brushes contributing noise? If so, then try placing a capacitor across the motor brushes as suggested in Sec. IV.

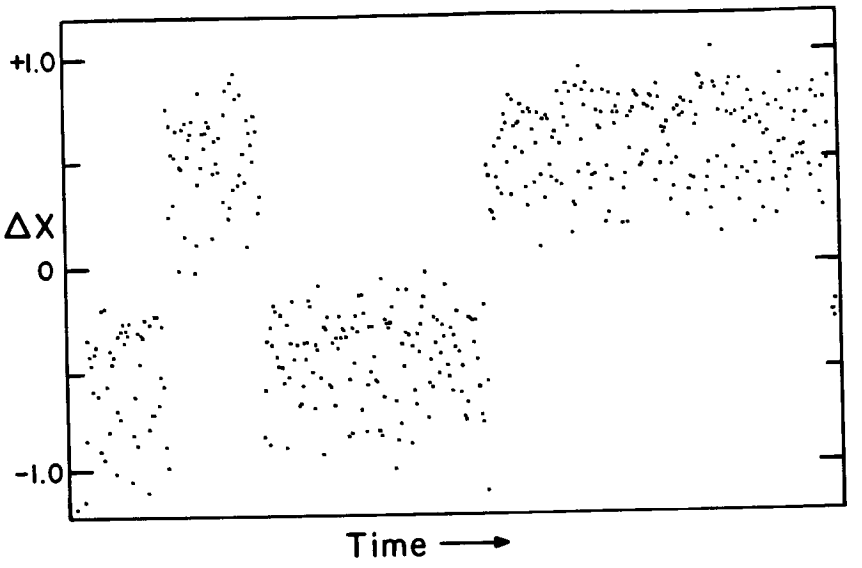

Figure 7: The edge position is plotted versus the scan number or time in arbitrary units. The discontinuities in the edge position are referred to as the one-micron glitch, since they are zero-point shifts of exactly one micron. The frequency of the glitches may be anything from one in 40 to several thousand when the problem exists.

In our search for the solution to the glitch problem, we found that the encoder signals, as monitored at the scale amplifier board, appeared to be very noisy when the stage was reversed. Several attempts were made to clean up the waveforms by smoothing the signals. However, these attempts were largely unsuccessful, since they had the ultimate effect of reducing the maximum speed that the scale amplifier could respond to the incoming signals. The glitch problem disappeared following a major disaster with the electronics, when an over-voltage protection circuit failed and burned out 90% of the electronics in the translator drawer. Through the kind assistance of the NSF, funds were provided to replace the 200-odd integrated circuits and rebuild the system in the Yale Center for Electronic Services. Rebuilding the electronics seems to have largely cured the elusive problem of the one micron glitches. Our best guess is that the source of the glitches was somewhere in the scale amplifier board, so if this problem occurs, then it might be wise to try replacing that board completly.

VIII. Premature completion of a scan

Very early in our tests, we discovered that the PDS would "complete" a scan well before it had reached the end of a line. The source of this problem was identified as being due to jitter in the x-carriage motion during the scan, which produced some reverse counts when the carriage jittered backwards. The "divide-by-n" circuitry provided with the PDS, which counts the encoder pulses between adjacent pixels, expects only up counts and will count a down pulse due to carriage jitter as an up pulse. Our solution to this problem was to build and install an up/down counter for the divide-by-n circuit. We have reasons to believe that the jitter problem may be more severe with the granite machines than with the metal machines.

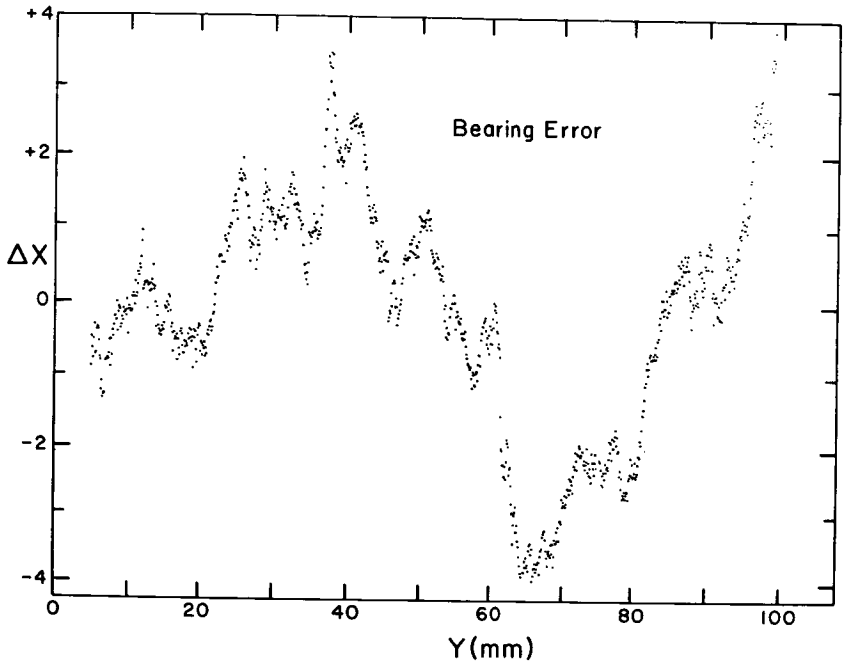

Figure 8: The edge position of one line in a Ronchi ruling oriented with the lines parallel to the y-axis versus the y position in mm. The peak to peak amplitude of the bearing errors in this scan is about +/- 4 um. The fundamental periodicity has a period of about 60 mm, which is the nominal circumference of the bearings, while the shorter period of 4-5 cycles per 60 mm may be due to a squareness of the bearings. The major patterns repeat approximately from scan to scan, but the phase and relative amplitudes can change significantly.

IX. Bearing errors and non-repeatability in the coordinates

Shortly after the PDS was installed at the end of 1978, we discovered that the repeatability of the system was not adequate to do astrometry, in contrast to the excellent repeatability obtained previously with the metal machines.

The basic source of the problem was traced to errors in the side guide bearings in the two axes. The errors in the x-axis were in the +/- 1-2 um range, while those in the y-axis were in the +/- 5 um range. It is common practice in astrometry to correct for errors in the stage motions by having a well calibrated table of corrections to linear motion. However, the positional errors were not repeatable even on a time scale of 20 minutes.

To diagnose the extent of the problem, we oriented a linear Ronchi ruling on the platten with its lines parallel to the y-axis. X raster scans were made along the y-axis at intervals of 50 um, and the edges at the half-transmission point were computed by Eq. 1. The results are shown in Fig. 8, where the relative edge position in x is plotted as a function of the y coordinate. The most obvious periodicities seen are a basic 60 mm cycle, which is the nominal circumference of the bearings, and a shorter ragged periodicity of about 4-5 cycles per revolution of the bearing. The latter periodicity indicates that the bearings are a bit "square" on top of their elliptical shape. The sharp peaks may be due to the circulation of the balls in the bearing races. As mentioned above, these errors are not repeatable; two consecutive scans do not reproduce each other, but tend to show some phase shift of the peaks with respect to the major features, but not precisely.

Since the errors are not repeatable, we have resorted to the construction of an optical micrometer which records the error of the stage relative to a fixed fiducial line each time a measurement is made. Details of the system are given in another paper in this volume by Lee and van Altena(1983b). The optical micrometer enables us to correct for the drunken motion of the stages after the fact, when we compute the positions of the images. The accuracy of the correction is good to about +/- 0.6 um over the 20x20 inch platten. If we repeat the measurements of a plate within a few hours, then we may be able to correct the positions to an accuracy of +/- 0.3 um. However, long term drifts prevent us from reliably achieving a positional accuracy comparable to the emulsion grain noise limit of +/- 0.2 um on the fine-grained class IIIa emulsions, Lee and van Altena(1983a). As a final solution to this problem, we have ordered and will install a Hewlett-Packard dual axis laser interferometer on the PDS. The dual axis laser interferometer system will enable us to fully eliminate the drunkenness of the stages from entering into the output coordinates of the PDS.

It should be noted that in the granite machines the two axes are completely independent. The x and y positions are recorded by their respective linear encoders and it is assumed that the granite guide rails constrain the motions to ones that are strictly linear. This would be very close to true, were it not for the ball bearings which cause the stages to move within the nominally straight granite surfaces in a drunken fashion. If the bearings are too loose, then the stage will slop from one side to another and exhibit considerable hysteresis in its motion, as illustrated in the paper by Kinsey(1983) in this volume. On the other hand, if the bearings are too tight, then the drunkenness of the stage increases, probably due to overloading the bearings.

An additional danger of adjusting the bearings too tightly is that the granite rails are not strictly parallel, and at some points in their motion

the bearings will be over loaded, while at other locations they will be loose. Kinsey(1983) has commented that even the ellipticity of the bearings produces such a variable loading on the granite that the granite surfaces may fracture along the rolling path of the bearings. Fortunately, this has not happened to the Yale PDS. To prevent its occurrence we have recently installed "spring" loaded bearings on one side of the x axis. The "spring" loading was accomplished by replacing the rear single bearings with double bearings on each shaft. A thin O-ring was then placed around the vee-shaped groove between the bearings, which keeps the O-ring from rolling off the bearing as the stage moves. The resiliancy of the O-ring provides nearly constant loading against the front rail independent of the bearing ellipticity and variations in the spacing between the granite rails. It remains to be seen how well this simple and inexpensive solution will hold up with time. A more elegant spring loaded assembly is described by Kinsey(1983) and would be the preferable long range solution. In both cases, care must be taken to prevent excessive sideways motion of the stage due to failure of the spring loading mechanism, since that might damage the encoder.

X. Tests of the overall positional accuracy

The positional accuracy of the final data may be tested by measuring a series of parallax plates and determining the accuracy of the derived parallaxes and proper motions. This test will monitor the accuracy of the whole system, including the algorithm used to compute the image positions. The basic concept behind this approach is that if the positions have been determined without error, then the derived parallaxes and proper motions should have zero errors. The extent to which their errors are not zero, is then a measure of the accuracy of the system. It should be clear however, that this approach will not identify the source of the error, it will only give a measure of the improvement or degradation in the accuracy following a change in your procedures.

For our test, we have used a parallax series of IIIa-J plates taken with the KPNO 4 meter telescope at the prime focus. The high accuracy of the IIIa-J plates makes this series an almost ideal one for testing the ultimate accuracy of the PDS. Measurements of this series made on the Berkeley PDS 1010A yielded an accuracy of +/- 0.4 um (s.e.). On the other hand, similar measurements with the Yale 2020G PDS have yielded errors no smaller than +/- 0.5 um, at the best. The results of Lee and van Altena(1983a) show that the limiting accuracy of the IIIa-J plate should be 0.2-0.3 um, so we are still far from the limit of the emulsion. For this reason, we have ordered a dual-axis laser interferometer that should allow us to fully eliminate the errors of the ways and of the ball bearings.

In this paper we have tried to describe the most significant problems that we have had with the Yale PDS microdensitometer. We hope that the approaches given to diagnosing the problems and where possible, the solutions to the problems, will prove useful to others using similar microdensitometers. While

the tests have been designed specifically for the Perkin-Elmer PDS 2020G microdensitometer, most should be useful with some modifications to other systems.

XI. Acknowledgements

It is a great pleasure to acknowledge the help of many individuals who have made it possible to transform the Yale PDS into a precision microdensitometer. Without the generous financial support of the NSF over several years, this research would not have been possible. Specifically, Drs. Peter Boyce and Kurt Weiler have provided the financial support and understanding, while we searched for the solutions to our various problems. In the initial stages of this research, Dr. Liang-Tai George Chiu was responsible for setting up the computer and the PDS. Co-author Dr. Jin-Fuw Lee has been responsible for much of the testing of the PDS during the past three years.

Co-author Alan Wandersee has sleuthed out most of the electronic problems and designed solutions to them, occassionly in consultation with Walter Lund, Director of the Yale Center for Electronic Services and Lawrence Averil of the Perkin-Elmer Corp.. Several individuals in the Gibbs Instrument Shop at Yale have provided advice, design and construction of various components for the PDS. Adrian Disco and his recent successor as Director of the Gibbs shop, Gilbert Vogel and instrument maker Anthony Massina have provided many hours of friendly consultation, design and construction of test fixtures, calibration devices such as the optical micrometer, and miscellaneous components such as plate holders.

Our colleague Dr. Augustus Oemler has discussed many of the PDS problems with us over the years and more recently we have had helpful converstations with Dr. James Kinsey of the Space Telescope Science Institute. Finally we would like to thank James Brosious and Sandra Olenik for preparing the illustrations and the many individuals at Perkin-Elmer with whom we have discussed all of our PDS problems at length: Lawrence Averil, James Horton, Anthony Hull and James Jenkins. This research has been supported in part by the National Science Foundation and the National Aeronautics and Space Administration.

XII. References

Dainty,J.C., and Shaw,R. 1974. Image Science. London. Academic.

Furenlid,I.,Schoening,W.E., and Carder,B.E. Jr. 1977. Am. Astron. Soc. Photo-Bull. 16: 14.

Kinsey,J.H. 1983, in Astonomical Microdensitometry, edited by D.A. Klinglesmith, III.

Latham,D.W. 1978. Am. Astron. Soc. Photo-Bull. 18: 3.

Lee,J.-F., and van Altena,W.F. 1983a. Astron. J. (submitted).

Lee,J.-F., and van Altena,W.F. 1983b. in Astronomical Microdensitometry, edited by D.A. Klinglesmith, III.

Sewell,M.H. 1975. Am. Astron. Soc. Photo-Bull. 8: 13.

van Altena,W.F., and Lee,J.-F. 1983. Am. Astron. Soc. Photo-Bull. (submitted).

Hemmingway: Were there any conditions under which you could get more glitches more frequently than other conditions? In other words, do you get more glitches just scanning at a constant rate? Or do you get more glitches when it is ramping up or down?

Van Altena: Because we are never really able to identify the cause of the glitches, I can't say that we found anything aside from switching from counting by one's to counting by two's. There was a very definite effect there. We often felt that the problem arose at the turnaround, when the stage was stopping and then turning around for the reverse scan. We felt this way because when you look at the wave forms on the oscilloscope you find that they are extraordinarily choppy, and it makes you wonder how the system is working. We tried a number of things to try and smooth out the wave forms. Occasionally we thought that we had solved the problem, but then we would find that having fixed that we're no longer able to scan at high speeds. By and large, we never really found out why the glitches came and went.

Opal: Why does waiting a 1/6 of a second at the end of each scan help to improve the reproducibility?

Van Altena: Perhaps Jim Kinsey would like to comment on that. He has had some ideas as to what it is in the photomultiplier that might be doing this.

Kinsey: I think I would like to put that on hold. I have to talk to you about that.

Van Altena: Okay. This is still under discussion, so we will wait on that answer.

Kinsey: It could be vibration because we have observed vibration in the scan, but...

Hemmingway: On this specific point, last week we were looking at the pulse which comes out of the black box, I'm not sure exactly what's going on, which actually triggers the A/D converter and that's obviously directly linked to the position system. As each scan would start up this pulse would eventually settle down to an interval which was commensurate with the speed in which the PDS was supposed to be driving at that particular scan. But it would take about two or three seconds for the interval of these pulses to settle down. They really jitter by a factor of two or three more than what the actual pulse interval should have been. I don't know whether stopping the scan and turning it around would cause it to be much more stable so that, in fact, it seems that there is a rate jitter that settles down as the PDS gets into the scan that might have something to do with it.

Van Altena: I think it might depend if thats the case, in part, on the drive system. We have the activators; if you have much back-lash in the bearings in the activators it will cause the stage to vibrate—so you get an oscillation back and forth. You get rid of most of this by pre-loading the bearing and then you get a much smoother drive on your stage, however, if you have a screw drive you don't have this problem. I'm not sure.

Hechathorn: I'd like to ask a question. On the one plot that you had with of the scans of razor blade where scatter was quite large, I had the impression that there was a bi-modal distribution? Is this going light to dark and dark to light?

Van Altena: No generally speaking, there will be more data on one side than the other; so it's not just light/dark. I don't know why you have that bi-modal distribution. Sometimes its very obvious and sometimes its not there at all.

Lasker: In your index line scans you show a spacial frequency that is strong of the order of 1 centimeter. Can you identify that with any specific mechanical component?

Van Altena: The bearings are square. If you take the diameter of the bearing and measure out the length on it you can find a component that varies more sinusoldally as the bearing is rolling over on the order is about 60 mm. There is also a wave length of about 15 mm (1/4 of it) that indicates to me that the bearing is a little on the square side. Sometimes it looks like there are components with about five oscillations per revolution I'm not sure if this represents the balls rolling inside the bearings itself.

The problem is that you can't deal with them the way you would normally deal with errors in ways of the machine by calibrating them and developing calibration which is then applied. Because the waveform changes with time, you cannot make one scan of your index line to develop the calibration. If you come back 20 minutes later and make another scan you can see that these waves have migrated and changed in form. So that it is impossible to make any calibration for it; you have to constantly monitor what's happening with the bearings.

MacNamana: You showed a plot of scatter versus change in temperature over about 1/2 hour with your PDS. What was the temperature change over that period?

Van Altena: I did not measure it. I am not sure. It may have been a degree.

Horton: You do indeed have a ball problem as the ball passes the bottom dead center of the bearing. Each time the ball passes you will have a fluctuation.

Van Altena: Unfortunately its not repeatable so you can't calibrate it.

Horton: There may be some skidding.

PERFORMANCE TESTING OF THE HIGH ALTITUDE OBSERVATORY PDS MICRODENSITOMETER

A. Poland
Laboratory for Astronomy and Solar Physics
NASA-Goddard Space Flight Center
Greenbelt, MD
R. Munro and D. Friend
High Altitude Observatory
Boulder, Colorado

I. Introduction

The High Altitude Observatory (HAO) PDS microdensitometer, purchased in 1972, is one of the earlier machines produced. Particular features of this machine include: PDP-8 control, 12 bit A/D converter, high density log amplifier, updated locking microscope head, auto-loc, teflon drive screws and nuts, and high speed operation (up to 60 mm/sec). The microdensitometer is generally used with 10 or 50 micron apertures on 35mm and 70mm film so performance requirements are not as stringent as for some astronomical machines. The HAO microdensitometer undergoes monthly testing to assure its consistent performance. These tests are designed to check positional and photometric stability at the 10 micron aperture level.

II. Performance Test

The HAO test procedure is designed to run without operator intervention following initial configuration of the microdensitometer for each subprocedure. Specialized test software is resident in the PDP-8. The operator selects the proper subprocedure by entering commands; once computer control is established, it is not relinquished until the test is complete. A sample of the operator's instruction sheet appears in Figure 1. Figure 2 shows the special film used for the evaluation of the microdensitometer's performance. The results from computer processing and reduction of the data are presented in Figures 3 through 8.

There are four sections to the HAO microdensitometer test procedure. The first is designed to examine the positional accuracy of the scanning system. Because the position of an individual measurement is computed from the starting point of a scan, the number of values recorded from the beginning of a scan, and the incremental step size, this computational algorithm must be specifically compared with the Digital Coordinate Readout System (DCRS) position. A scan is initiated that records the DCRS x and y values instead of density values from the A/D converter. Differences between the computed and DCRS values exist primarily due to timing variances in the x direction and vibration in the y direction. As the scan speed is reduced, the positional error should become smaller. Tests are run at speeds of 255, 200, 150, and 10 (the maximum speed of 255 corresponds to 60 mm/sec). Both raster scans, in which information is recorded as the stage moves in alternate directions, and edge scans, in which information is only recorded each time the stage moves in the same direction, are used. Degradation of test

results over time can indicate loosening adjustments or excessive wear in the drive systems.

The second test monitors the performance of the photometric system independent of position. Both the signal to noise and linearity of the gain are examined. The optical system is adjusted so that the clear glass platten is slightly out of focus (to remove the effects of dust and scratches on the surface of the glass). A 10 micron slit is selected and the photomultiplier is adjusted to produce a density of 0.03. Several hundred measurements are made through each of the five neutral density filters. Variations in the mean values from month to month indicate changes in linearity while fluctuations in the standard deviation imply a change in the noise level of the light source, photomultiplier, or associated electronics.

The third test evaluates the consistency of the signal to noise of the entire system as a function of time. Differences in measured density can be caused by either photometric changes or positional error. Thus, this procedure examines the combined error. The wedge from the test plate shown in Figure 2 is scanned lengthwise (i.e. parallel to the film edges) through its center. Two raster scans, at speeds of 200 and 10, and one edge scan at a speed of 200 are taken. The fast raster scan scans the same area 50 times, the others scan it twenty. For each scan, all 50 (or 20) density values from six different positions along the wedge are printed out to monitor systematic changes. Also, the mean and standard deviation are computed from all density values at a given scan location for fifty positions along the wedge to obtain a signal to noise estimate throughout the dynamic range of the microdensitometer.

The final test is designed to examine the repeatability of the system for periods on the order of an hour. This time the central picture from the test plate shown in Figure 2 is used. The picture is scanned twice, all scan parameters and the microdensitometer configuration remaining identical for the two scans. Point by point differences between the two pictures are then computed and the results presented as a histogram. The more skewed the results are toward small differences, the more stable the system.

III. Results

Sample output of the results for a position check is shown in Figure 3. The labels of each column have the following meanings: x mean--the mean difference between the computed and actual x value; x signma--the standard deviation of mean differences; xlo--the lowest difference and its location (at); and xhi--the highest difference and its location. The columns referring to y have similar meanings. Odd numbered records are scanned in the positive x direction; even numbered records are measured in the opposite sense. The results are tabulated for speeds of 255 and 10. Differences greater than 10 are caused by DCRS values changing during examination. Errors at the highest speeds can be several microns while errors at the slowest speeds are less than one micron. Large errors can sometimes be corrected by tightening the belts on the x and y drives.

Figure 4 lists the results for the evaluation of the photometric system alone. Differences in mean values have changed by less than 0.02 over a ten year period and less than 0.01 during the last five years even though the system was physically relocated a number of times. Thus no real change in the linearity has occurred. The standard deviations have also shown no significant variation; the signal to noise of the photometric system has remained high and unchanged over this long period of time.

The results from the scans and rasters of the step wedge display the signal to noise expected from a typical grainy film. While the signal to noise for the photometric system alone is quite good, positional errors (as observed in the position test) can lead to a lower signal to noise on a grainy or high contrast film. The results from 50 rasters through the step wedge obtained at high speed are presented in Figure 5. The first part of the figure shows all of the measured densities for points 1, 540, etc. Note that for approximately the same density level, the signal to noise can vary significantly depending on the graininess at that particular location. Figures 6 and 7 list the data for a slow raster and an edge scan respectively. Measurement accuracy is improved for slow scan mode.

The results for the system repeatability procedure are shown in Figure 8. In the figure a "cell" refers to differences between the limits shown (i.e., cell 2 has the differences between .01 and .02). Variations in the comparisons of two identically rastered objects are most frequently caused by a drift of the microscope head. However, an excessive number of large errors can indicate a need for tightening the drive belts or electronically realigning the drive system.

Figure 1

MICRODENSITOMETER MONTHLY ACCEPTANCE TEST

MAGNETIC TAPE NO. DATE

1. POSITION TEST
   A. LOAD SCANSMORE
   B. DENSITY VALUES ARE NOT MEASURED. HENCE NO WARM-UP IS NECESSARY.
   C. SCAN WITH THE FOLLOWING INPUT PARAMETER SEQUENCE:

      SCAN TYPE? X BACKUP? N EDGE? N
      DELTA = 100 TRAVEL = 30000
      STEP = 100 NUMBER = 20
      SPEED = 255
      X = Y = /D - TP

   D. REDEFINE THE SPEED PARAMETER WITH THE COMMAND RV200, AND SCAN. /D - TP
   E. REDEFINE THE SPEED PARAMETER WITH THE COMMAND RV150, AND SCAN. /D - TP
   F. REDEFINE THE SPEED PARAMETER WITH THE COMMAND RV100, AND SCAN. /D - TP
   E. REDEFINE THE SPEED AND MODE WITH COMMANDS RV200,RE, AND SCAN. /D - TP

2. ADC NOISE TEST
   A. ALLOW WARM-UP PERIOD OF AT LEAST ONE HOUR BEFORE PROCEEDING.
   B. ADJUST DENSITOMETER FOR TEN MICRON SCAN AS FOLLOWS:

      UPPER AND LOWER OPTICAL SYSTEM MAGNIFICATION ON "2"
      UPPER AND LOWER OPTICAL SYSTEM APERTURES ON "B"
      NEUTRAL DENSITY AND COLOR FILTERS ON "C"

   C. SET VOLTAGE TO 1.00 WITH CLEAR GLASS IN FIELD OF VIEW.
   D. RECORD VOLTAGE V = _____
   E. ADJUST LOGARITHMIC AMP SO THAT DENSITY IS 0.03, AND SCAN. /D - TD "C"
   F. REPEAT FOR EACH SMALL FILTER POSITION BELOW; RECORD DENSITY.

      POSITION 2 DENSITY (~0.40) _____ /D - TD
      POSITION 5 DENSITY (~1.92) _____ /D - TD
      POSITION 6 DENSITY (~2.95) _____ /D - TD
      POSITION 7 DENSITY (~3.74) _____ /D - TD

      go back to "C"

   G. SET VOLTAGE TO 3000 AND RESET LOG AMP SO THAT DENSITY IS 0.03. CHECK DENSITY AT FOLLOWING POSITIONS:

      POSITION 2 DENSITY _____
      POSITION 5 DENSITY _____
      POSITION 6 DENSITY _____
      POSITION 7 DENSITY _____

3. WEDGE
   A. PUT CALIBRATION PLATE IN 4" X 5" HOLDER ON PLATTEN WITH EMULSION UP, PICTURE TO THE FRONT, WEDGE TO THE REAR.
   B. FOCUS ON CENTER OF LOWER RIGHT FIDUCIAL AND SET THE X AND Y DISPLAYS OF THE DCRS TO ZERO.
   C. RECORD THE POSITION OF THE LOWER LEFT FIDUCIAL:

      X = _____ Y = 0

   D. REFOCUS ON FILM.
   E. SET DENSITY (0.05) AND VOLTAGE (>300) ON CLEAR GLASS AND NOTE:

      X = 0 Y = -600
      D = _____ V = _____

      X = 0 Y = 600
      D = _____

   F. SCAN WITH THE FOLLOWING INPUT PARAMETER SEQUENCE:

      SCAN TYPE? X BACKUP? N EDGE? N
      DELTA = 10 TRAVEL = 30000
      STEP = 0 NUMBER = 50
      SPEED = 200
      X = 0 Y = 52000
      /D - CD

   G. REDEFINE NUMBER PARAMETER WITH THE COMMAND RN20, REDEFINE SPEED PARAMETER WITH THE COMMAND RV10; SCAN. /D-CD
   H. REDEFINE SPEED AND MODE WITH COMMANDS RV200, RE, AND SCAN. /D-CD
   I. CHECK DRIFT:

      X = 0 Y = -600
      D = _____

      X = 0 Y = 600
      D = _____

4. PICTURE PICT1
   A. VERIFY FOCUS AND ALIGNMENT.
   B. RESET VOLTAGE AND DENSITY IF NEEDED:

      X = 0 Y = -600
      D = _____ V = _____

      X = 0 Y = 600
      D = _____

   C. SCAN WITH THE FOLLOWING INPUT PARAMETER SEQUENCE:

      SCAN TYPE? X BACKUP? N EDGE? N
      DELTA = 10 TRAVEL = 24000
      STEP = 10 NUMBER = 1000
      SPEED = 200
      X = Y =
      /D- CD

   D. CHECK FOR DRIFT AND RESET IF NEEDED:

      X = 0 Y = -600
      D = _____ V = _____

      X = 0 Y = 600
      D = _____

   E. RESCAN THE PICTURE AS ABOVE. /D - CD , PICT2
   F. NOTE DRIFT:

      X = 0 Y = -600
      D = _____

      X = 0 Y = 600
      D = _____

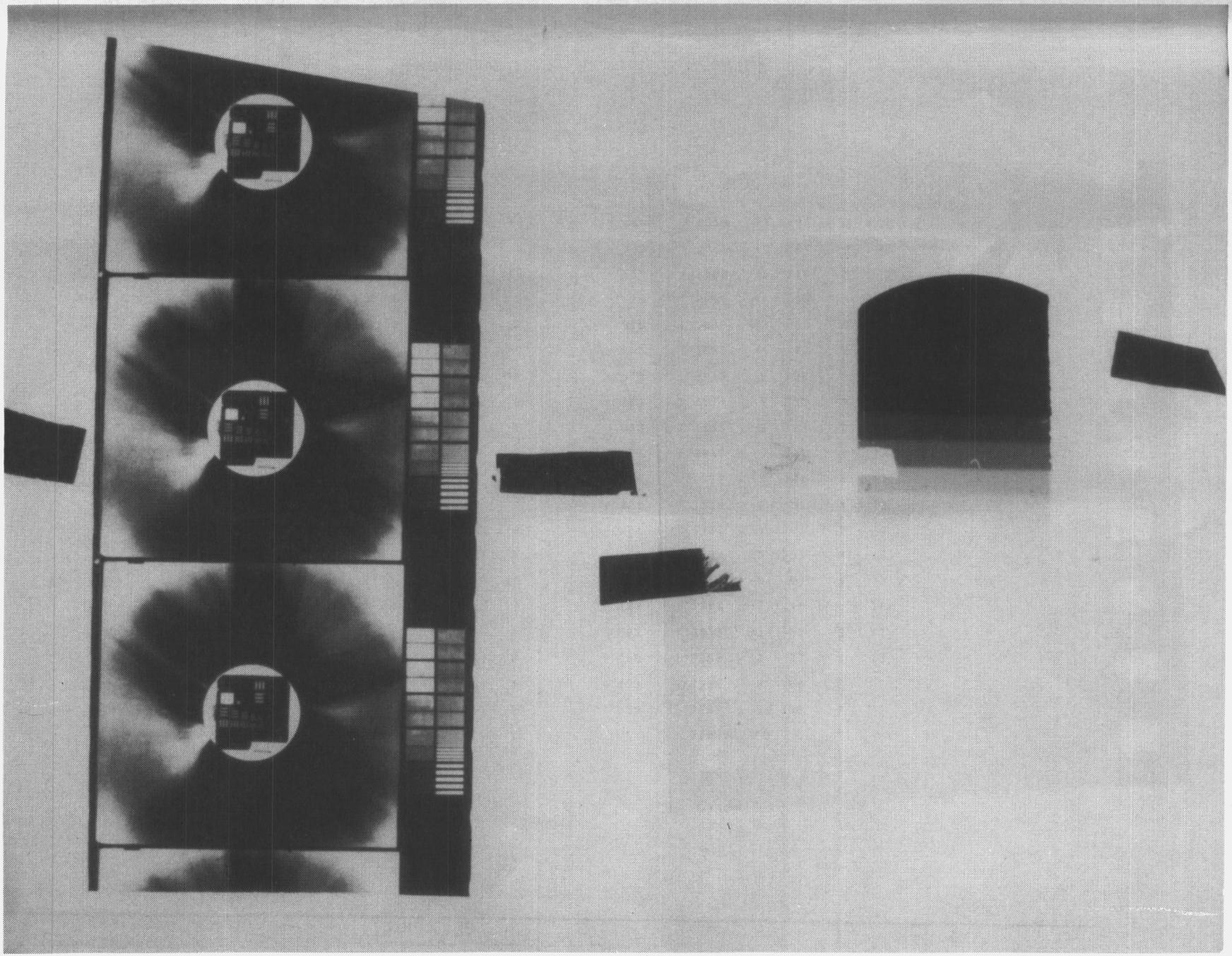

Figure 2. Special film used for the evaluation of the microdensitometer's performance.

Figure 3a

I.D.: 4APR83/ACT/POS255

POSITION TEST; SPEED = 255

FILE	RECORD	XMEAN	X SIGMA	XLO	AT	XHI	AT	YMEAN	Y SIGMA	YLO	AT	YHI	AT
1	1	7.ØØ3	4.7697	Ø	273	11	6	.ØØØ	1.1282	-2	ØØ5	3	1
1	2	-7.627	4.6369	-29	16	-1	1	-.423	1.4274	-3	66	3	1
1	3	7.75Ø	4.4886	Ø	269	12	5	-.ØØØ	1.5985	-5	38	4	17
1	4	-7.623	4.8616	-29	16	-1	1	-.26Ø	1.2Ø79	-3	65	3	1
1	5	-75.757	39.5734	-96	177	12	5	-.15Ø	1.7381	-5	41	4	16
1	6	-8.38Ø	4.9412	-27	1Ø3	-1	44	-.143	1.2421	-3	64	4	3
1	7	7.8Ø3	4.4816	Ø	269	12	5	.197	1.4135	-2	ØØ2	4	16
1	8	-74.947	28.3943	-138	17	-52	115	-.597	1.2439	-4	61	3	1
1	9	7.857	4.4313	Ø	269	12	5	-.353	1.721Ø	-5	37	4	19
1	1Ø	-1Ø9.883	6.4984	-13Ø	1Ø2	-1Ø1	43	-.29Ø	1.3213	-2	191	4	1
1	11	7.83Ø	4.4581	Ø	267	12	3	.163	1.3675	-2	217	4	17
1	12	-7.32Ø	4.3517	-2Ø	17	-1	1	-.Ø33	1.4232	-3	63	9	39
1	13	7.89Ø	4.41Ø4	Ø	269	12	5	-.1Ø7	1.9Ø14	-6	37	4	21
1	14	-7.487	4.6494	-27	18	-1	44	-.81Ø	1.5813	-4	239	4	1
1	15	7.923	4.3891	Ø	269	12	5	-.ØØ3	1.7272	-4	43	5	19
1	16	-87.52Ø	25.3893	-129	17	-58	175	-.Ø1Ø	1.2Ø96	-3	61	4	1
1	17	7.93Ø	4.393Ø	Ø	269	12	5	-.21Ø	1.687Ø	-5	39	4	22
1	18	-1Ø9.463	6.7426	-149	17	-1Ø1	43	-.22Ø	1.1158	-2	11Ø	4	2
1	19	7.917	4.3859	Ø	267	12	3	-.Ø93	1.7Ø82	-4	54	4	15
1	2Ø	-111.537	9.4Ø12	-159	17	-1Ø1	43	-.2ØØ	1.222Ø	-3	63	3	1

FILE 1 RECORD 21 NSTATE= 1

Figure 3b

I.D.: 4APR83/ACT/POS1Ø

POSITION TEST; SPEED = 1Ø

FILE	RECORD	XMEAN	X SIGMA	XLO	AT	XHI	AT	YMEAN	Y SIGMA	YLO	AT	YHI	AT
4	1	.997	.Ø576	Ø	1	1	2	Ø.ØØØ	.1826	-1	62	1	3
4	2	-.997	.Ø576	-1	3ØØ	Ø	1	-.ØØ3	.1527	-1	217	1	1
4	3	.997	.Ø576	Ø	1	1	2	.ØØ7	.1413	-1	6	1	1
4	4	-.997	.Ø576	-1	3ØØ	Ø	1	Ø.ØØØ	.1826	-1	221	2	1
4	5	.997	.Ø576	Ø	1	1	2	.ØØ7	.1825	-1	2Ø3	1	1
4	6	-.997	.Ø576	-1	3ØØ	Ø	1	-.ØØ3	.1915	-1	232	2	1
4	7	.997	.Ø576	Ø	1	1	2	.Ø17	.2375	-1	264	2	1
4	8	-.997	.Ø576	-1	3ØØ	Ø	1	.Ø1Ø	.1524	-1	5Ø	2	1
4	9	.997	.Ø576	Ø	1	1	2	.Ø13	.14Ø8	-1	4	1	1
4	1Ø	-.997	.Ø576	-1	3ØØ	Ø	1	Ø.ØØØ	.1826	-1	21Ø	2	1
4	11	.997	.Ø576	Ø	1	1	2	.Ø1Ø	.2Ø79	-1	2Ø2	2	3
4	12	-.997	.Ø576	-1	3ØØ	Ø	1	.Ø1Ø	.1912	-1	47	2	1
4	13	.997	.Ø576	Ø	1	1	2	.ØØ7	.1999	-1	27Ø	1	1
4	14	-.997	.Ø576	-1	3ØØ	Ø	1	.Ø13	.1996	-1	69	2	1
4	15	.997	.Ø576	Ø	1	1	2	.Ø17	.19Ø8	-1	6Ø	2	2
4	16	-.997	.Ø576	-1	3ØØ	Ø	1	.ØØ3	.1527	-1	47	2	1
4	17	.997	.Ø576	Ø	1	1	2	.Ø1Ø	.1729	-1	276	1	1
4	18	-.997	.Ø576	-1	3ØØ	Ø	1	.ØØ7	.1632	-1	57	2	1
4	19	.997	.Ø576	Ø	1	1	2	.ØØ3	.1527	-1	282	1	1
4	2Ø	-.997	.Ø576	-1	3ØØ	Ø	1	.ØØ7	.1825	-1	69	2	1

FILE 4 RECORD 21 NSTATE= 1

Figure 4

ADC NOISE TEST

FILE	1	MEAN =	2.89612E-02	SIGMA =	1.77327E-03	MEAN/SIGMA =	1.63321E+01
FILE	2	MEAN =	4.28533E-01	SIGMA =	2.42388E-03	MEAN/SIGMA =	1.73553E+02
FILE	3	MEAN =	1.96144E+00	SIGMA =	8.14889E-03	MEAN/SIGMA =	2.40781E+02
FILE	4	MEAN =	3.01276E+00	SIGMA =	1.10433E-02	MEAN/SIGMA =	2.72815E+02
FILE	5	MEAN =	3.91027E+00	SIGMA =	1.19757E-02	MEAN/SIGMA =	3.26518E+02

Figure 5a

I.D.: 4APR83/ACT/WEDGE200

WEDGE TEST; SPEED = 200

NSTATE = 1 RECORDS = 50
NWDS = 3001 RECORDS = 50

1	540	1080	1620	2160	2700
4.60455E-01	3.86250E-01	4.26250E-01	8.45000E-01	2.28750E+00	4.02875E+00
3.49200E-01	4.15000E-01	4.45000E-01	7.52500E-01	2.26125E+00	4.11625E+00
4.60469E-01	3.88750E-01	4.16250E-01	8.45000E-01	2.26625E+00	3.99875E+00
3.54200E-01	4.12500E-01	4.51250E-01	7.55000E-01	2.24625E+00	4.10000E+00
4.60464E-01	3.98750E-01	4.16250E-01	8.46250E-01	2.25875E+00	4.01500E+00
3.56700E-01	4.17500E-01	4.55000E-01	7.61250E-01	2.27125E+00	4.11250E+00
4.60461E-01	3.95000E-01	4.05000E-01	8.45000E-01	2.26500E+00	3.97875E+00
3.57950E-01	4.15000E-01	4.51250E-01	7.57500E-01	2.24500E+00	4.10875E+00
4.60461E-01	3.97500E-01	4.11250E-01	8.40000E-01	2.27625E+00	3.99875E+00
3.56700E-01	4.20000E-01	4.58750E-01	7.58750E-01	2.26875E+00	4.09375E+00
4.60464E-01	3.91250E-01	4.13750E-01	8.38750E-01	2.26625E+00	3.98000E+00
3.64200E-01	4.18750E-01	4.56250E-01	7.48750E-01	2.28000E+00	4.10500E+00
4.60462E-01	3.96250E-01	4.12500E-01	8.40000E-01	2.26875E+00	3.98500E+00
3.64200E-01	4.21250E-01	4.53750E-01	7.62500E-01	2.28625E+00	4.11125E+00
4.60458E-01	3.88750E-01	4.12500E-01	8.43750E-01	2.26875E+00	4.08750E+00
3.60450E-01	4.15000E-01	4.51250E-01	7.58750E-01	2.26500E+00	4.09625E+00
4.60464E-01	3.91250E-01	4.13750E-01	8.40000E-01	2.26625E+00	3.99000E+00
3.60450E-01	4.20000E-01	4.55000E-01	7.71250E-01	2.26125E+00	4.10500E+00
4.60467E-01	3.91250E-01	4.11250E-01	8.43750E-01	2.26125E+00	3.97750E+00
3.59200E-01	4.21250E-01	4.55000E-01	7.58750E-01	2.27125E+00	4.11250E+00
4.60466E-01	3.91250E-01	4.15000E-01	8.40000E-01	2.27875E+00	3.97625E+00
3.66700E-01	4.20000E-01	4.53750E-01	7.58750E-01	2.27750E+00	4.10500E+00
4.60464E-01	3.92500E-01	4.13750E-01	8.55000E-01	2.26625E+00	3.98375E+00
3.62950E-01	4.18750E-01	4.56250E-01	7.61250E-01	2.25750E+00	4.09500E+00
4.60459E-01	3.95000E-01	4.13750E-01	8.43750E-01	2.27375E+00	3.98125E+00
3.62950E-01	4.21250E-01	4.52500E-01	7.66250E-01	2.26500E+00	4.08875E+00
4.60458E-01	3.92500E-01	4.15000E-01	8.42500E-01	2.26125E+00	4.01250E+00
3.67950E-01	4.20000E-01	4.55000E-01	7.66250E-01	2.28000E+00	4.10500E+00
4.60469E-01	3.96250E-01	4.10000E-01	8.40000E-01	2.27125E+00	3.98875E+00
3.64200E-01	4.22500E-01	4.52500E-01	7.60000E-01	2.29250E+00	4.09500E+00
4.80466E-01	3.95000E-01	4.11250E-01	8.45000E-01	2.26375E+00	3.99625E+00
3.66700E-01	4.22500E-01	4.55000E-01	7.63750E-01	2.27000E+00	4.11500E+00
4.60461E-01	3.92500E-01	4.13750E-01	8.45000E-01	2.26875E+00	3.98500E+00
3.59200E-01	4.21250E-01	4.56250E-01	7.68750E-01	2.26625E+00	4.12500E+00
4.60461E-01	3.88750E-01	4.13750E-01	8.40000E-01	2.26750E+00	3.98125E+00
3.65450E-01	4.18750E-01	4.53750E-01	7.58750E-01	2.24875E+00	4.11250E+00
4.60458E-01	3.96250E-01	4.12500E-01	8.40000E-01	2.24875E+00	3.98875E+00
3.65450E-01	4.17500E-01	4.55000E-01	7.63750E-01	2.24500E+00	4.10375E+00
4.60458E-01	3.88750E-01	4.10000E-01	8.40000E-01	2.26500E+00	3.98125E+00
3.61700E-01	4.22500E-01	4.56250E-01	7.60000E-01	2.27875E+00	4.11125E+00
4.60456E-01	3.95000E-01	4.11250E-01	8.40000E-01	2.28000E+00	3.98375E+00
3.66700E-01	4.13750E-01	4.53750E-01	7.62500E-01	2.25250E+00	4.09375E+00
4.60458E-01	3.91250E-01	4.11250E-01	8.46250E-01	2.26250E+00	4.00625E+00
3.66700E-01	4.20000E-01	4.51250E-01	7.60000E-01	2.26000E+00	4.00875E+00
4.60464E-01	3.92500E-01	4.10000E-01	8.41250E-01	2.26875E+00	3.98375E+00
3.66700E-01	4.17500E-01	4.53750E-01	7.60000E-01	2.25625E+00	4.10875E+00
4.60461E-01	3.93750E-01	4.15000E-01	8.41250E-01	2.26625E+00	3.99375E+00
3.62950E-01	4.21250E-01	4.51250E-01	7.60000E-01	2.27500E+00	4.10500E+00
4.60458E-01	3.90000E-01	4.13750E-01	8.37500E-01	2.27500E+00	3.98125E+00
3.64200E-01	4.20000E-01	4.51250E-01	7.56250E-01	2.27250E+00	4.12125E+00

Figure 5b

POINT =	3000	MEAN =	4.37775E-01	ST DEV =	1.39223E-02	OF	50 POINTS	MEAN/DEV =	3.14441E+01
POINT =	2940	MEAN =	3.66400E-01	ST DEV =	1.62397E-02	OF	50 POINTS	MEAN/DEV =	2.25620E+01
POINT =	2880	MEAN =	4.48185E+00	ST DEV =	1.55751E-01	OF	50 POINTS	MEAN/DEV =	2.87758E+01
POINT =	2820	MEAN =	4.20482E+00	ST DEV =	8.48178E-02	OF	50 POINTS	MEAN/DEV =	4.95748E+01
POINT =	2760	MEAN =	4.12015E+00	ST DEV =	3.39987E-02	OF	50 POINTS	MEAN/DEV =	1.21185E+02
POINT =	2700	MEAN =	4.04837E+00	ST DEV =	5.81809E-02	OF	50 POINTS	MEAN/DEV =	6.95826E+01
POINT =	2640	MEAN =	3.58142E+00	ST DEV =	2.71455E-02	OF	50 POINTS	MEAN/DEV =	1.31935E+02
POINT =	2580	MEAN =	3.45302E+00	ST DEV =	2.92415E-02	OF	50 POINTS	MEAN/DEV =	1.18086E+02
POINT =	2520	MEAN =	3.58292E+00	ST DEV =	2.72576E-02	OF	50 POINTS	MEAN/DEV =	1.31447E+02
POINT =	2460	MEAN =	2.78035E+00	ST DEV =	1.86280E-02	OF	50 POINTS	MEAN/DEV =	1.49256E+02
POINT =	2400	MEAN =	2.79757E+00	ST DEV =	1.42136E-02	OF	50 POINTS	MEAN/DEV =	1.96824E+02
POINT =	2340	MEAN =	2.82380E+00	ST DEV =	1.44048E-02	OF	50 POINTS	MEAN/DEV =	1.96032E+02
POINT =	2280	MEAN =	2.37885E+00	ST DEV =	1.21677E-02	OF	50 POINTS	MEAN/DEV =	1.95506E+02
POINT =	2220	MEAN =	2.25615E+00	ST DEV =	2.04004E-02	OF	50 POINTS	MEAN/DEV =	1.10593E+02
POINT =	2160	MEAN =	2.26712E+00	ST DEV =	1.04709E-02	OF	50 POINTS	MEAN/DEV =	2.16516E+02
POINT =	2100	MEAN =	1.77345E+00	ST DEV =	2.57021E-02	OF	50 POINTS	MEAN/DEV =	6.98002E+01
POINT =	2040	MEAN =	1.60640E+00	ST DEV =	4.82530E-02	OF	50 POINTS	MEAN/DEV =	3.32912E+01
POINT =	1980	MEAN =	1.71045E+00	ST DEV =	8.19588E-03	OF	50 POINTS	MEAN/DEV =	2.08696E+02
POINT =	1920	MEAN =	1.24502E+00	ST DEV =	1.82131E-02	OF	50 POINTS	MEAN/DEV =	6.83586E+01
POINT =	1860	MEAN =	3.14200E-01	ST DEV =	1.98554E-02	OF	50 POINTS	MEAN/DEV =	1.58244E+01
POINT =	1800	MEAN =	3.51625E-01	ST DEV =	1.45457E-02	OF	50 POINTS	MEAN/DEV =	2.41738E+01
POINT =	1740	MEAN =	3.64675E-01	ST DEV =	4.42867E-03	OF	50 POINTS	MEAN/DEV =	8.23441E+01
POINT =	1680	MEAN =	7.44350E-01	ST DEV =	4.62164E-02	OF	50 POINTS	MEAN/DEV =	1.61058E+01
POINT =	1620	MEAN =	8.01525E-01	ST DEV =	4.12873E-02	OF	50 POINTS	MEAN/DEV =	1.94133E+01
POINT =	1560	MEAN =	6.48975E-01	ST DEV =	4.03149E-02	OF	50 POINTS	MEAN/DEV =	1.60976E+01
POINT =	1500	MEAN =	6.27850E-01	ST DEV =	4.07937E-02	OF	50 POINTS	MEAN/DEV =	1.53908E+01
POINT =	1440	MEAN =	6.34900E-01	ST DEV =	2.95823E-02	OF	50 POINTS	MEAN/DEV =	2.14621E+01
POINT =	1380	MEAN =	5.03800E-01	ST DEV =	7.96700E-02	OF	50 POINTS	MEAN/DEV =	6.32358E+00
POINT =	1320	MEAN =	5.13475E-01	ST DEV =	4.78411E-02	OF	50 POINTS	MEAN/DEV =	1.07329E+01
POINT =	1260	MEAN =	4.53550E-01	ST DEV =	2.52913E-02	OF	50 POINTS	MEAN/DEV =	1.79331E+01
POINT =	1200	MEAN =	4.64075E-01	ST DEV =	2.55292E-02	OF	50 POINTS	MEAN/DEV =	1.81782E+01
POINT =	1140	MEAN =	4.55675E-01	ST DEV =	9.39817E-03	OF	50 POINTS	MEAN/DEV =	4.84855E+01
POINT =	1080	MEAN =	4.33375E-01	ST DEV =	2.04683E-02	OF	50 POINTS	MEAN/DEV =	2.11729E+01
POINT =	1020	MEAN =	4.42350E-01	ST DEV =	3.97639E-02	OF	50 POINTS	MEAN/DEV =	1.11244E+01
POINT =	960	MEAN =	3.39275E-01	ST DEV =	2.69966E-02	OF	50 POINTS	MEAN/DEV =	1.25673E+01
POINT =	900	MEAN =	3.61875E-01	ST DEV =	1.41868E-02	OF	50 POINTS	MEAN/DEV =	2.55078E+01
POINT =	840	MEAN =	3.42175E-01	ST DEV =	3.57472E-02	OF	50 POINTS	MEAN/DEV =	9.57208E+00
POINT =	780	MEAN =	4.06600E-01	ST DEV =	1.06977E-02	OF	50 POINTS	MEAN/DEV =	3.80083E+01
POINT =	720	MEAN =	3.85225E-01	ST DEV =	1.88906E-02	OF	50 POINTS	MEAN/DEV =	2.03924E+01
POINT =	660	MEAN =	3.43850E-01	ST DEV =	2.37366E-02	OF	50 POINTS	MEAN/DEV =	1.44861E+01
POINT =	600	MEAN =	4.15250E-01	ST DEV =	1.17845E-02	OF	50 POINTS	MEAN/DEV =	3.52369E+01
POINT =	540	MEAN =	4.05800E-01	ST DEV =	1.34763E-02	OF	50 POINTS	MEAN/DEV =	3.01122E+01
POINT =	480	MEAN =	3.87775E-01	ST DEV =	1.51725E-02	OF	50 POINTS	MEAN/DEV =	2.55577E+01
POINT =	420	MEAN =	3.99575E-01	ST DEV =	2.39447E-02	OF	50 POINTS	MEAN/DEV =	1.66874E+01
POINT =	360	MEAN =	3.44325E-01	ST DEV =	2.07981E-03	OF	50 POINTS	MEAN/DEV =	1.65556E+02
POINT =	300	MEAN =	3.34700E-01	ST DEV =	7.47312E-03	OF	50 POINTS	MEAN/DEV =	4.47872E+01
POINT =	240	MEAN =	3.23350E-01	ST DEV =	5.22877E-03	OF	50 POINTS	MEAN/DEV =	6.18406E+01
POINT =	180	MEAN =	3.54025E-01	ST DEV =	2.52846E-03	OF	50 POINTS	MEAN/DEV =	1.40016E+02
POINT =	120	MEAN =	3.53050E-01	ST DEV =	3.23894E-02	OF	50 POINTS	MEAN/DEV =	1.09002E+01
POINT =	60	MEAN =	3.80075E-01	ST DEV =	8.41283E-03	OF	50 POINTS	MEAN/DEV =	4.51780E+01

Figure 6a

I.D.: 4APR83/AT/WEDE1Ø

WEDGE TEST; SPEED = 1Ø

NSTATE = 1 RECORDS = 2Ø
NWDS = 3ØØ1 RECORDS = 2Ø

1	54Ø	1ØØØ	162Ø	216Ø	27ØØ
4.ØØ45ØE-Ø1	3.6875ØE-Ø1	4.Ø875ØE-Ø1	8.1625ØE-Ø1	2.26ØØØE+ØØ	4.13ØØØE+ØØ
4.2545ØE-Ø1	4.2ØØØØE-Ø1	4.5375ØE-Ø1	7.4ØØØØE-Ø1	2.21625E+ØØ	4.37ØØØE+ØØ
4.2Ø445E-Ø1	3.8ØØØØE-Ø1	4.1375ØE-Ø1	8.225ØØE-Ø1	2.26875E+ØØ	4.13625E+ØØ
4.267ØØE-Ø1	4.225ØØE-Ø1	4.5625ØE-Ø1	7.4875ØE-Ø1	2.215ØØE+ØØ	4.37625E+ØØ
4.4Ø461E-Ø1	3.9125ØE-Ø1	4.25ØØØE-Ø1	8.2625ØE-Ø1	2.2925ØE+ØØ	4.13875E+ØØ
4.34225E-Ø1	4.3875ØE-Ø1	4.6875ØE-Ø1	7.6ØØØØE-Ø1	2.22125E+ØØ	4.42375E+ØØ
4.4Ø467E-Ø1	3.8875ØE-Ø1	4.3125ØE-Ø1	8.325ØØE-Ø1	2.28375E+ØØ	4.1575ØE+ØØ
4.292ØØE-Ø1	4.45ØØØE-Ø1	4.75ØØØE-Ø1	7.6625ØE-Ø1	2.225ØØE+ØØ	4.375ØØE+ØØ
4.4Ø473E-Ø1	3.8875ØE-Ø1	4.2875ØE-Ø1	8.3625ØE-Ø1	2.295ØØE+ØØ	4.12375E+ØØ
4.4545ØE-Ø1	4.4125ØE-Ø1	4.7375ØE-Ø1	7.6375ØE-Ø1	2.21875E+ØØ	4.375ØØE+ØØ
4.4Ø47ØE-Ø1	3.9625ØE-Ø1	4.3375ØE-Ø1	8.325ØØE-Ø1	2.29125E+ØØ	4.15ØØØE+ØØ
4.417ØØE-Ø1	4.45ØØØE-Ø1	4.7ØØØØE-Ø1	7.6125ØE-Ø1	2.225ØØE+ØØ	4.3775ØE+ØØ
4.4Ø461E-Ø1	3.85ØØØE-Ø1	4.2625ØE-Ø1	8.275ØØE-Ø1	2.3Ø5ØØE+ØØ	4.145ØØE+ØØ
4.417ØØE-Ø1	4.3625ØE-Ø1	4.725ØØE-Ø1	7.625ØØE-Ø1	2.2325ØE+ØØ	4.4Ø25ØE+ØØ
4.4Ø478E-Ø1	3.9625ØE-Ø1	4.2875ØE-Ø1	8.4125ØE-Ø1	2.3Ø5ØØE+ØØ	4.155ØØE+ØØ
4.46725E-Ø1	4.45ØØØE-Ø1	4.775ØØE-Ø1	7.65ØØØE-Ø1	2.2Ø875E+ØØ	4.38625E+ØØ
4.4Ø47ØE-Ø1	3.8875ØE-Ø1	4.2875ØE-Ø1	8.3125ØE-Ø1	2.3Ø125E+ØØ	4.13625E+ØØ
4.367ØØE-Ø1	4.375ØØE-Ø1	4.6875ØE-Ø1	7.625ØØE-Ø1	2.21125E+ØØ	4.36625E+ØØ
4.4Ø464E-Ø1	3.875ØØE-Ø1	4.25ØØØE-Ø1	8.3125ØE-Ø1	2.2975ØE+ØØ	4.15125E+ØØ
4.417ØØE-Ø1	4.35ØØØE-Ø1	4.6875ØE-Ø1	7.6ØØØØE-Ø1	2.2Ø625E+ØØ	4.37125E+ØØ

Figure 6b

POINT =	300	MEAN =	4.27187E-01	ST DEV =	8.61390E-03	OF	20	POINTS	MEAN/DEV =	4.95928E+01
POINT =	294	MEAN =	3.39125E-01	ST DEV =	1.04515E-02	OF	20	POINTS	MEAN/DEV =	3.24474E+01
POINT =	288	MEAN =	5.09344E+00	ST DEV =	2.83446E-02	OF	20	POINTS	MEAN/DEV =	1.79697E+02
POINT =	282	MEAN =	4.38156E+00	ST DEV =	8.63169E-02	OF	20	POINTS	MEAN/DEV =	5.07614E+01
POINT =	276	MEAN =	4.25662E+00	ST DEV =	1.12053E-01	OF	20	POINTS	MEAN/DEV =	3.79877E+01
POINT =	270	MEAN =	4.26237E+00	ST DEV =	1.20822E-01	OF	20	POINTS	MEAN/DEV =	3.52781E+01
POINT =	264	MEAN =	3.63200E+00	ST DEV =	1.43581E-02	OF	20	POINTS	MEAN/DEV =	2.52958E+02
POINT =	258	MEAN =	3.34162E+00	ST DEV =	3.47066E-02	OF	20	POINTS	MEAN/DEV =	9.62822E+01
POINT =	252	MEAN =	3.69794E+00	ST DEV =	1.64377E-02	OF	20	POINTS	MEAN/DEV =	2.24966E+02
POINT =	246	MEAN =	2.80481E+00	ST DEV =	4.71157E-02	OF	20	POINTS	MEAN/DEV =	5.95303E+01
POINT =	240	MEAN =	2.85900E+00	ST DEV =	6.48587E-02	OF	20	POINTS	MEAN/DEV =	4.40804E+01
POINT =	234	MEAN =	2.77587E+00	ST DEV =	3.22735E-02	OF	20	POINTS	MEAN/DEV =	8.60110E+01
POINT =	228	MEAN =	2.39775E+00	ST DEV =	4.06021E-02	OF	20	POINTS	MEAN/DEV =	5.90548E+01
POINT =	222	MEAN =	2.23162E+00	ST DEV =	2.93260E-02	OF	20	POINTS	MEAN/DEV =	7.60971E+01
POINT =	216	MEAN =	2.25400E+00	ST DEV =	3.78000E-02	OF	20	POINTS	MEAN/DEV =	5.96296E+01
POINT =	210	MEAN =	1.79494E+00	ST DEV =	3.43772E-02	OF	20	POINTS	MEAN/DEV =	5.22130E+01
POINT =	204	MEAN =	1.63294E+00	ST DEV =	3.16556E-02	OF	20	POINTS	MEAN/DEV =	5.15845E+01
POINT =	198	MEAN =	1.71737E+00	ST DEV =	1.97203E-02	OF	20	POINTS	MEAN/DEV =	8.70866E+01
POINT =	192	MEAN =	1.23344E+00	ST DEV =	1.40694E-02	OF	20	POINTS	MEAN/DEV =	8.76678E+01
POINT =	186	MEAN =	3.42937E-01	ST DEV =	1.93378E-02	OF	20	POINTS	MEAN/DEV =	1.77341E+01
POINT =	180	MEAN =	3.59062E-01	ST DEV =	1.84640E-02	OF	20	POINTS	MEAN/DEV =	1.94467E+01
POINT =	174	MEAN =	3.70687E-01	ST DEV =	7.80099E-03	OF	20	POINTS	MEAN/DEV =	4.75180E+01
POINT =	168	MEAN =	7.29250E-01	ST DEV =	3.16238E-02	OF	20	POINTS	MEAN/DEV =	2.30602E+01
POINT =	162	MEAN =	7.94375E-01	ST DEV =	3.61129E-02	OF	20	POINTS	MEAN/DEV =	2.19970E+01
POINT =	156	MEAN =	6.62250E-01	ST DEV =	2.66710E-02	OF	20	POINTS	MEAN/DEV =	2.48303E+01
POINT =	150	MEAN =	6.22562E-01	ST DEV =	3.64788E-02	OF	20	POINTS	MEAN/DEV =	1.70664E+01
POINT =	144	MEAN =	6.52875E-01	ST DEV =	3.18201E-02	OF	20	POINTS	MEAN/DEV =	2.05177E+01
POINT =	138	MEAN =	4.92375E-01	ST DEV =	6.82526E-02	OF	20	POINTS	MEAN/DEV =	7.21401E+00
POINT =	132	MEAN =	5.25625E-01	ST DEV =	5.05910E-02	OF	20	POINTS	MEAN/DEV =	1.03897E+01
POINT =	126	MEAN =	4.66687E-01	ST DEV =	3.64955E-02	OF	20	POINTS	MEAN/DEV =	1.27876E+01
POINT =	120	MEAN =	4.77250E-01	ST DEV =	3.10332E-02	OF	20	POINTS	MEAN/DEV =	1.53787E+01
POINT =	114	MEAN =	4.60812E-01	ST DEV =	1.34529E-02	OF	20	POINTS	MEAN/DEV =	3.42538E+01
POINT =	108	MEAN =	4.46750E-01	ST DEV =	2.29653E-02	OF	20	POINTS	MEAN/DEV =	1.94532E+01
POINT =	102	MEAN =	4.39562E-01	ST DEV =	3.48059E-02	OF	20	POINTS	MEAN/DEV =	1.26290E+01
POINT =	96	MEAN =	3.38062E-01	ST DEV =	2.67467E-02	OF	20	POINTS	MEAN/DEV =	1.26394E+01
POINT =	90	MEAN =	3.68500E-01	ST DEV =	1.77817E-02	OF	20	POINTS	MEAN/DEV =	2.07236E+01
POINT =	84	MEAN =	3.32062E-01	ST DEV =	1.04079E-02	OF	20	POINTS	MEAN/DEV =	3.19049E+01
POINT =	78	MEAN =	4.09437E-01	ST DEV =	1.61945E-02	OF	20	POINTS	MEAN/DEV =	2.52825E+01
POINT =	72	MEAN =	3.89562E-01	ST DEV =	2.34630E-02	OF	20	POINTS	MEAN/DEV =	1.66033E+01
POINT =	66	MEAN =	3.53250E-01	ST DEV =	2.84726E-02	OF	20	POINTS	MEAN/DEV =	1.24067E+01
POINT =	60	MEAN =	4.28125E-01	ST DEV =	1.17120E-02	OF	20	POINTS	MEAN/DEV =	3.58712E+01
POINT =	54	MEAN =	4.11875E-01	ST DEV =	2.60303E-02	OF	20	POINTS	MEAN/DEV =	1.58229E+01
POINT =	48	MEAN =	3.80937E-01	ST DEV =	9.10765E-03	OF	20	POINTS	MEAN/DEV =	4.18261E+01
POINT =	42	MEAN =	4.07437E-01	ST DEV =	2.19640E-02	OF	20	POINTS	MEAN/DEV =	1.85502E+01
POINT =	36	MEAN =	3.49062E-01	ST DEV =	7.20107E-03	OF	20	POINTS	MEAN/DEV =	4.84737E+01
POINT =	30	MEAN =	3.17687E-01	ST DEV =	1.93741E-02	OF	20	POINTS	MEAN/DEV =	1.63975E+01
POINT =	24	MEAN =	3.20937E-01	ST DEV =	1.27652E-02	OF	20	POINTS	MEAN/DEV =	2.51417E+01
POINT =	18	MEAN =	3.68437E-01	ST DEV =	9.85738E-03	OF	20	POINTS	MEAN/DEV =	3.73768E+01
POINT =	12	MEAN =	3.68125E-01	ST DEV =	1.83435E-02	OF	20	POINTS	MEAN/DEV =	2.00684E+01
POINT =	6	MEAN =	3.89062E-01	ST DEV =	1.31985E-02	OF	20	POINTS	MEAN/DEV =	2.94779E+01

Figure 7a

I.D.: 4APR83/ACT/WEDGE200E

WEDGE TEST; SPEED = 200, EDGE SCAN

NSTATE = 1 RECORDS = 20
NWDS = 3001 RECORDS = 20

1	540	1080	1620	2160	2700
4.0047 0E-01	3.9125 0E-01	4.4500 0E-01	8.5125 0E-01	2.32875E+00	4.05000E+00
4.0045 2E-01	3.8625 0E-01	4.3500 0E-01	8.4250 0E-01	2.31125E+00	4.02875E+00
4.0045 2E-01	3.9000 0E-01	4.3125 0E-01	8.4875 0E-01	2.30500E+00	4.05125E+00
4.0045 8E-01	3.9000 0E-01	4.3125 0E-01	8.5375 0E-01	2.33250E+00	4.07000E+00
4.0045 0E-01	3.8875 0E-01	4.3375 0E-01	8.5375 0E-01	2.31500E+00	4.03625E+00
4.0045 2E-01	3.8875 0E-01	4.3125 0E-01	8.4750 0E-01	2.32625E+00	4.04500E+00
4.0045 2E-01	3.8875 0E-01	4.3125 0E-01	8.5250 0E-01	2.32000E+00	4.03500E+00
4.0045 8E-01	3.8875 0E-01	4.3250 0E-01	8.4750 0E-01	2.30625E+00	4.04000E+00
4.0044 8E-01	3.8875 0E-01	4.3125 0E-01	8.4875 0E-01	2.32000E+00	4.06375E+00
4.0045 2E-01	3.9000 0E-01	4.3250 0E-01	8.4625 0E-01	2.33000E+00	4.02875E+00
4.0044 8E-01	3.8625 0E-01	4.3500 0E-01	8.4875 0E-01	2.31500E+00	4.04250E+00
4.0045 2E-01	3.8625 0E-01	4.3250 0E-01	8.4875 0E-01	2.32000E+00	4.04000E+00
4.0045 8E-01	3.8750 0E-01	4.3000 0E-01	8.4125 0E-01	2.31875E+00	4.03500E+00
4.0045 6E-01	3.9125 0E-01	4.2875 0E-01	8.5125 0E-01	2.31875E+00	4.04500E+00
4.0045 6E-01	3.8625 0E-01	4.2875 0E-01	8.4625 0E-01	2.32625E+00	4.04750E+00
4.0045 3E-01	3.8500 0E-01	4.2875 0E-01	8.4875 0E-01	2.32000E+00	4.03875E+00
4.0045 2E-01	3.8125 0E-01	4.2625 0E-01	8.4500 0E-01	2.32500E+00	4.03125E+00
4.0044 8E-01	3.8375 0E-01	4.2875 0E-01	8.4625 0E-01	2.33625E+00	4.02875E+00
4.0045 2E-01	3.8500 0E-01	4.3125 0E-01	8.4625 0E-01	2.30875E+00	4.05625E+00
4.0044 5E-01	3.8250 0E-01	4.2625 0E-01	8.4625 0E-01	2.31625E+00	4.05000E+00

Figure 7b

POINT =	3000	MEAN =	4.31375E-01	ST DEV =	4.99844E-03	OF	20 POINTS	MEAN/DEV =	8.63020E+01
POINT =	2940	MEAN =	3.63250E-01	ST DEV =	4.46164E-03	OF	20 POINTS	MEAN/DEV =	8.14162E+01
POINT =	2880	MEAN =	4.32919E+00	ST DEV =	8.69873E-03	OF	20 POINTS	MEAN/DEV =	4.97680E+02
POINT =	2820	MEAN =	4.38031E+00	ST DEV =	1.29716E-02	OF	20 POINTS	MEAN/DEV =	3.31518E+02
POINT =	2760	MEAN =	4.09794E+00	ST DEV =	1.01879E-02	OF	20 POINTS	MEAN/DEV =	4.02236E+02
POINT =	2700	MEAN =	4.04319E+00	ST DEV =	1.11487E-02	OF	20 POINTS	MEAN/DEV =	3.62661E+02
POINT =	2640	MEAN =	3.58537E+00	ST DEV =	1.14161E-02	OF	20 POINTS	MEAN/DEV =	3.14062E+02
POINT =	2580	MEAN =	3.50200E+00	ST DEV =	1.08426E-02	OF	20 POINTS	MEAN/DEV =	3.22985E+02
POINT =	2520	MEAN =	3.66362E+00	ST DEV =	1.22340E-02	OF	20 POINTS	MEAN/DEV =	2.99461E+02
POINT =	2460	MEAN =	2.82719E+00	ST DEV =	1.15777E-02	OF	20 POINTS	MEAN/DEV =	2.44193E+02
POINT =	2400	MEAN =	2.87587E+00	ST DEV =	1.19707E-02	OF	20 POINTS	MEAN/DEV =	2.40243E+02
POINT =	2340	MEAN =	2.80600E+00	ST DEV =	9.46705E-03	OF	20 POINTS	MEAN/DEV =	2.96397E+02
POINT =	2280	MEAN =	2.38375E+00	ST DEV =	1.12152E-02	OF	20 POINTS	MEAN/DEV =	2.12546E+02
POINT =	2220	MEAN =	2.35000E+00	ST DEV =	1.03153E-02	OF	20 POINTS	MEAN/DEV =	2.27816E+02
POINT =	2160	MEAN =	2.32000E+00	ST DEV =	8.31978E-03	OF	20 POINTS	MEAN/DEV =	2.78854E+02
POINT =	2100	MEAN =	1.72369E+00	ST DEV =	8.96586E-03	OF	20 POINTS	MEAN/DEV =	1.92250E+02
POINT =	2040	MEAN =	1.54194E+00	ST DEV =	8.31485E-03	OF	20 POINTS	MEAN/DEV =	1.85444E+02
POINT =	1980	MEAN =	1.71356E+00	ST DEV =	6.26592E-03	OF	20 POINTS	MEAN/DEV =	2.73474E+02
POINT =	1920	MEAN =	1.27287E+00	ST DEV =	4.85895E-03	OF	20 POINTS	MEAN/DEV =	2.61965E+02
POINT =	1860	MEAN =	3.03375E-01	ST DEV =	2.40767E-03	OF	20 POINTS	MEAN/DEV =	1.26004E+02
POINT =	1800	MEAN =	3.62187E-01	ST DEV =	2.04920E-03	OF	20 POINTS	MEAN/DEV =	1.76746E+02
POINT =	1740	MEAN =	3.78812E-01	ST DEV =	2.14604E-03	OF	20 POINTS	MEAN/DEV =	1.76517E+02
POINT =	1680	MEAN =	7.62437E-01	ST DEV =	3.27097E-03	OF	20 POINTS	MEAN/DEV =	2.33092E+02
POINT =	1620	MEAN =	8.48062E-01	ST DEV =	3.24699E-03	OF	20 POINTS	MEAN/DEV =	2.61184E+02
POINT =	1560	MEAN =	6.49937E-01	ST DEV =	5.89591E-03	OF	20 POINTS	MEAN/DEV =	1.10235E+02
POINT =	1500	MEAN =	6.66750E-01	ST DEV =	3.94097E-03	OF	20 POINTS	MEAN/DEV =	1.69184E+02
POINT =	1440	MEAN =	6.34875E-01	ST DEV =	4.14390E-03	OF	20 POINTS	MEAN/DEV =	1.53207E+02
POINT =	1380	MEAN =	5.77187E-01	ST DEV =	3.64166E-03	OF	20 POINTS	MEAN/DEV =	1.58496E+02
POINT =	1320	MEAN =	4.86687E-01	ST DEV =	3.77647E-03	OF	20 POINTS	MEAN/DEV =	1.28874E+02
POINT =	1260	MEAN =	4.43125E-01	ST DEV =	2.48433E-03	OF	20 POINTS	MEAN/DEV =	1.78368E+02
POINT =	1200	MEAN =	4.44187E-01	ST DEV =	1.90702E-03	OF	20 POINTS	MEAN/DEV =	2.32923E+02
POINT =	1140	MEAN =	4.73437E-01	ST DEV =	4.53932E-03	OF	20 POINTS	MEAN/DEV =	1.04297E+02
POINT =	1080	MEAN =	4.31562E-01	ST DEV =	3.89059E-03	OF	20 POINTS	MEAN/DEV =	1.10925E+02
POINT =	1020	MEAN =	4.09750E-01	ST DEV =	2.22205E-03	OF	20 POINTS	MEAN/DEV =	1.84402E+02
POINT =	960	MEAN =	3.76125E-01	ST DEV =	2.76417E-03	OF	20 POINTS	MEAN/DEV =	1.36072E+02
POINT =	900	MEAN =	3.92562E-01	ST DEV =	3.17399E-03	OF	20 POINTS	MEAN/DEV =	1.23681E+02
POINT =	840	MEAN =	3.51687E-01	ST DEV =	9.18793E-03	OF	20 POINTS	MEAN/DEV =	3.82771E+01
POINT =	780	MEAN =	4.00312E-01	ST DEV =	1.67122E-03	OF	20 POINTS	MEAN/DEV =	2.39533E+02
POINT =	720	MEAN =	3.98500E-01	ST DEV =	4.15707E-03	OF	20 POINTS	MEAN/DEV =	9.58607E+01
POINT =	660	MEAN =	3.33437E-01	ST DEV =	2.67731E-03	OF	20 POINTS	MEAN/DEV =	1.24542E+02
POINT =	600	MEAN =	4.13937E-01	ST DEV =	3.56360E-03	OF	20 POINTS	MEAN/DEV =	1.16157E+02
POINT =	540	MEAN =	3.87312E-01	ST DEV =	2.74645E-03	OF	20 POINTS	MEAN/DEV =	1.41023E+02
POINT =	480	MEAN =	3.76500E-01	ST DEV =	2.75568E-03	OF	20 POINTS	MEAN/DEV =	1.36627E+02
POINT =	420	MEAN =	4.32937E-01	ST DEV =	2.77475E-03	OF	20 POINTS	MEAN/DEV =	1.56028E+02
POINT =	360	MEAN =	3.54375E-01	ST DEV =	2.14695E-03	OF	20 POINTS	MEAN/DEV =	1.65060E+02
POINT =	300	MEAN =	3.35562E-01	ST DEV =	5.14592E-03	OF	20 POINTS	MEAN/DEV =	6.52095E+01
POINT =	240	MEAN =	3.37062E-01	ST DEV =	2.77475E-03	OF	20 POINTS	MEAN/DEV =	1.21475E+02
POINT =	180	MEAN =	3.71625E-01	ST DEV =	3.03881E-03	OF	20 POINTS	MEAN/DEV =	1.22293E+02
POINT =	120	MEAN =	3.27687E-01	ST DEV =	5.64960E-03	OF	20 POINTS	MEAN/DEV =	5.80019E+01
POINT =	60	MEAN =	3.73250E-01	ST DEV =	3.17214E-03	OF	20 POINTS	MEAN/DEV =	1.17665E+02

Figure 8

```
PICTURE COMPARISON


I.D.: 4APR83/ACT/PICT1


CELL 1 CONTAINS ABS(DENSITY) < .Ø1
CELL 2-     .Ø1  <=  ABS(D)   < .Ø2
CELL 3-     .Ø2  <=  ABS(D)   < .Ø3
CELL 4-     .Ø3  <=  ABS(D)   < .Ø4
CELL 5-     .Ø4  <=  ABS(D)   < .Ø5
CELL 6-     .Ø5  <=  ABS(D)   < .Ø6
CELL 7-     .Ø6  <=  ABS(D)   < .Ø8
CELL 8-     .Ø8  <=  ABS(D)   < .1Ø
CELL 9-     .1Ø  <=  ABS(D)   < .15
CELL 1Ø-    .15  <=  ABS(D)   < .2Ø
CELL 11-             ABS(D)   > .2Ø


I.D.: 4APR83/ACT/PICT2

IN CELL  1     MEAN =     .ØØ426     WITH   93Ø7Ø6  POINTS
IN CELL  2     MEAN =     .Ø1394     WITH   7Ø9318  POINTS
IN CELL  3     MEAN =     .Ø2372     WITH   417125  POINTS
IN CELL  4     MEAN =     .Ø3369     WITH   2Ø4137  POINTS
IN CELL  5     MEAN =     .Ø4363     WITH    97613  POINTS
IN CELL  6     MEAN =     .Ø5367     WITH    45262  POINTS
IN CELL  7     MEAN =     .Ø6693     WITH    31772  POINTS
IN CELL  8     MEAN =     .Ø8724     WITH     82Ø3  POINTS
IN CELL  9     MEAN =     .1169Ø     WITH     457Ø  POINTS
IN CELL 1Ø     MEAN =     .17Ø28     WITH      748  POINTS
IN CELL 11     MEAN =     .3122Ø     WITH      546  POINTS

     245ØØØØ.ØØØØ
         951.8Ø43
          18.5453
           -.ØØ23
```

Barry Lasker: I'd like to comment on your histogram. You rather warm my heart. We've been doing similar sorts of things, very sensitive tests to test how well the low order bits are working. But often that can get away from one in a rather insidious way. Something we have done with our experimental software is to occasionally do a histogram of the distributions of the individual "bin" values. Of course, the bottom ones should be 50/50. Anything else would stick out like a sore thumb. The other thing I would like to raise is, I noticed that you, like everyone of us, has a need to document the things that the operator can do with the knobs on the PDS. I would be curious to hear if anyone in this room has done anything about making anything other than the standard functions into anything readable.

Arthur Poland: The only thing that we've made computer readable was the DCRS, X and Y value readings.

Barry Lasker: That's an interesting comment on the flexibility of the translator incarnation also. Doing the same thing on the microprocessor PDS would be quite a challenge I think.

PHOTOMETRIC AND POSITIONAL ACCURACY OF THE PDS BONN IN VIEW OF ASTRONOMICAL REQUIREMENTS

H.J. Becker
Sternwarte der Universität Bonn (FRG)

The PDS 1010A of the Astronomical Institutes of the University of Bonn is the PDS version characterized by the 10x10 inch measuring field, density range 0...5, and 4 cm/s maximum scanning speed. The system is controlled by a PDP 8/m computer, which is now being replaced by a link to the VAX computer of the institute with image processing facilities. Until now, PDS measurements were stored on magnetic tape and reduced off-line at the CYBER 172 of the Max-Planck-Institut für Radioastronomie. - In 1977 we began extensive tests of the PDS performance and accuracy (see Becker 1978, Becker 1979, Becker and Becker 1979a, b). Since then the system has been used in spectroscopic studies, astrometry, and two-dimensional photometry.

The PDS measures either transmission $T=I/I_o$ (where I_o=incident intensity) or density $D=\log(I_o/I)$. In either mode the output is digitized into 1024 linear steps, setting obvious limits: since $D=\log(1/T)$ no density variations above D=3 can be distinguished in transmission mode. The 10 bit digitization on the other hand sets all transmission values T>99% to D=0 in density mode. Most authors seem to measure in density, but instead of stating that measures are best done in density mode for $D \geq 3$ (Wray and Benedict 1974) we should ask at which density one step $\Delta D=0.005$ just equals one digital step $\Delta T=1/1024$ in transmission (for T=0...1). From

$$\Delta D = \Delta T \cdot dD/dT \qquad (1)$$

or

$$T = \log e \cdot \Delta T/\Delta D \qquad (2)$$

we find that the density mode is to be preferred for T<0.08 or D>1.07, while transmission mode is more accurate for densities below 1.07 (Becker 1978). There are indeed numerous cases where faint features on underexposed plates are better recorded in transmission. - To keep track of the mode selection, we store this as part of the scan identification mark on magnetic tape. This information is then used for a fully automatic transformation into standard density units (without restriction to 10 bits) when data values are decoded for further reduction (Becker 1979, Becker and Becker 1979b).

We have confirmed earlier findings that the measured density (or transmission) is a slight function of the slit size or PMT high voltage. This non-linearity is quite pronounced for low PMT voltages so that measurements with large apertures require grey filters placed into the beam. No difficulties should arise if identical slits and PMT voltage settings are used for the plate under study and for the calibration plate. We have to consider that for photographic plates the transformation from density to intensity anyway requires a non-linear calibration given by the characteristic curve of the emulsion.

Measuring the photometric stability, variations of $\Delta D=\pm 0.03$ in density or $\Delta T=\pm 1.5\%$ in transmission during 7 hours of operation were found after 3.5 hours warming up. This is slightly more than the $\Delta D=\pm 0.02$ ($\Delta T=\pm 1\%$) in 10 hours after 1 hour warming up as given by Boller&Chivens (see Becker 1978). It may cause a photometric drift in time-consuming two-dimensional scans.

The photometric accuracy of the PDS on a short time scale can be investigated with the "noise test", e.g. on a calibration plate where areas of different densities are available (Becker 1978, Becker and Becker 1979b). On each of these points we took 500,000 measures (30 sec) without stage movement (and thus measuring only system noise) and studied the density scatter $\sigma(D)$ as a function of D. Results for three different apertures both in transmission and in density mode are presented in figure 1 after converting the density scatter $\sigma(D)$ into transmission values $\sigma(T)$. It is seen that for the transmission measurements $\sigma(T)$ increases with T, and also $\sigma(D)$ becomes larger for higher densities. Of course the noise increases with decreasing aperture size, as indicated by larger values of the PMT high voltage parameter, and transmission mode becomes more accurate than density mode for $T \geq 0.1$ as expected (with a slight dependence on slit size).

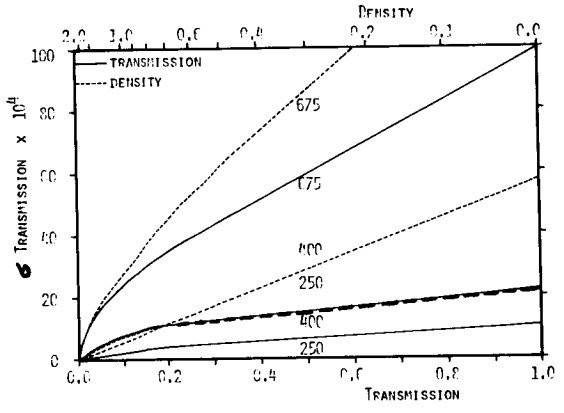

Figure 1: PDS system noise in density and transmission as a function of the PMT voltage parameter.

Is the photometric accuracy of the PDS sufficient to record the complete information contents of photographic plates? A simple test is shown in figure 2, where the same 200µm of a Kodak IIIa-J plate with constant density were scanned 100 times (aperture 10x400 µm, step width $\Delta x=2$ µm). The regular

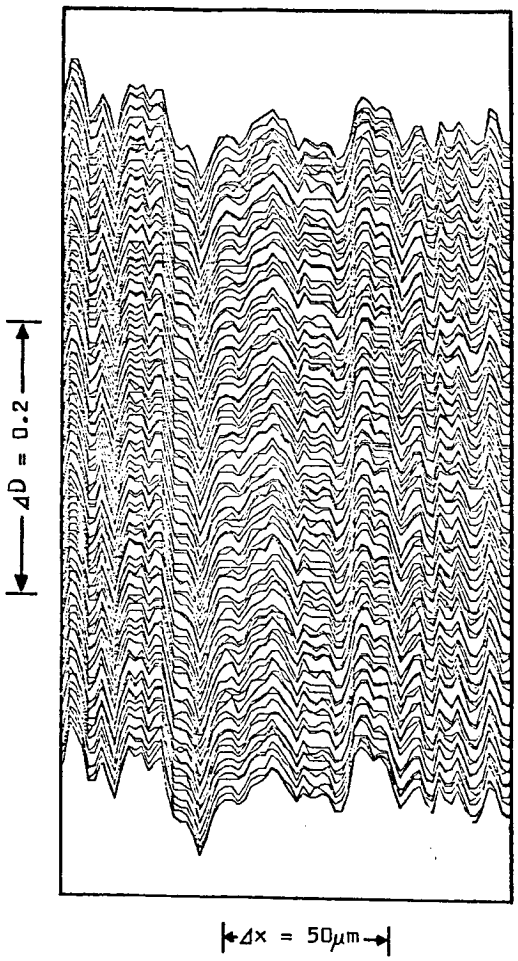

Figure 2: 100 PDS scan lines of the same area on a IIIa-J plate show the repeated pattern of grain noise with only small contributions from system noise.

pattern indicates that grain noise dominates over system noise even for the fine-grained IIIa-J emulsion. - More detailled studies of the graininess of IIa-O were made by measuring the macro-noise (Furenlid 1978)

$$\sigma(D) = \left[\frac{1}{n}\sum_{i=1}^{n}(\bar{D} - D_i)^2\right]^{1/2} \quad (3)$$

(n=number of pixels, $\bar{D}$=mean density) on calibration plates. Plates from different years could be combined to produce figure 3, but there seems to be a wavelength dependence of the $\sigma(D)/D$-relation (Becker 1983). For comparison with other data we must convert to diffuse densities and to the 1000 μm^2 standard aperture (see e.g. Latham 1978). Of course the micro-noise values of Furenlid et al. (1977) and of Latham (1978) are somewhat lower but macro-noise is probably a better measure for practical purposes. - Recalling the PDS tests above we find that for the IIa-O emulsion graininess is about 10 times larger than system noise. Even for IIIa-J this is still a factor of 5 except for high densities. At these high densities, however, the photographic signal-to-noise ratio and the detective quantum efficiency are already reduced as shown in figure 4. This means that for nearly all cases of practical interest the PDS noise is considerably smaller than grain noise of the emulsion.

We will now turn to the positional accuracy of the PDS. A systematic error arises from the non-orthogonality of the axes. For the PDS Bonn this was determined as $\phi = 3.5 \pm 0.3$ arcsec, which amounts to a maximum shift of 2 μm relative to the stage center (Becker 1979, Becker and Becker 1979b).

A quite serious problem in determining PDS positions is the distortion of high-density profiles due to the time constant of the amplifier and PMT. This is obviously speed-dependent. However,

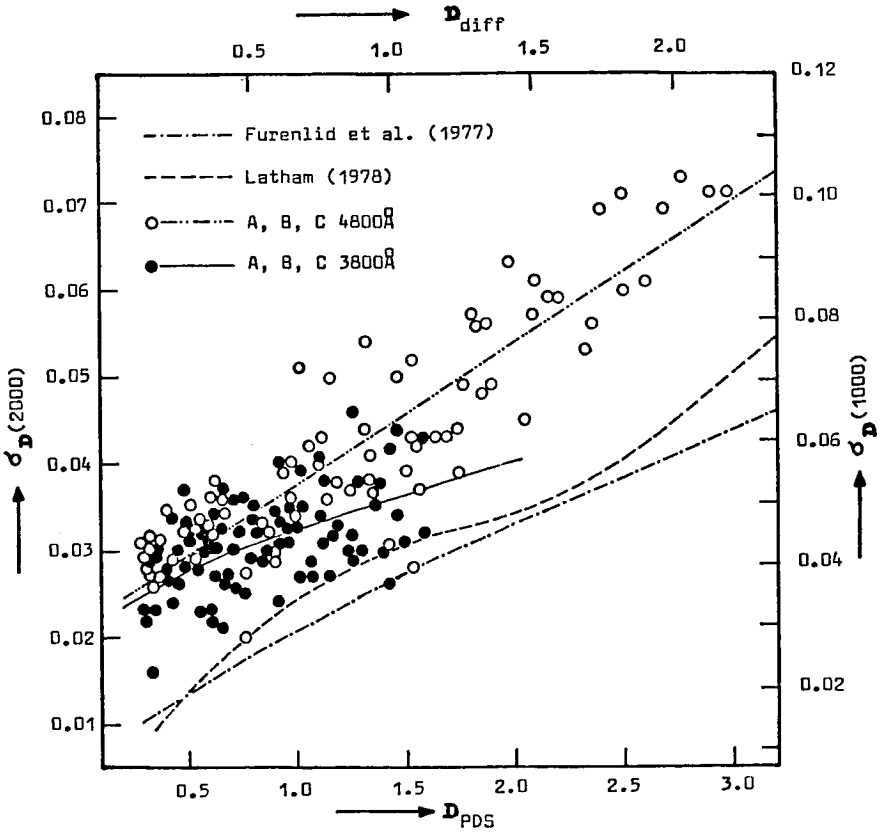

Figure 3: Graininess of IIa-O as a function of PDS densities (lower abscissa) or diffuse densities (upper abscissa). Macro-noise measurements at two wavelengths are compared with micro-noise data (Becker 1983).

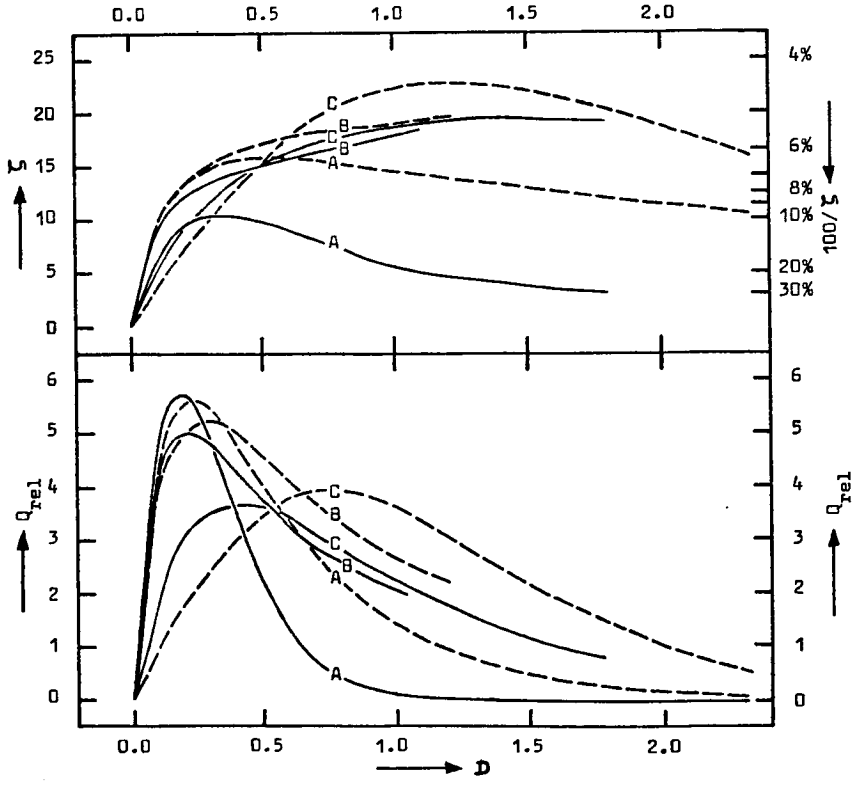

Figure 4: Output signal-to-noise ratio (upper graph) and relative DQE (lower graph) as a function of density for 3 groups of IIa-O plates at λ=3800 A and at λ=4800 A (dashed curves) (Becker 1983).

Figure 5 (right): Speed-dependent distortion of a profile (scanning with increasing x from left to right) after adjusting the ramp distances.

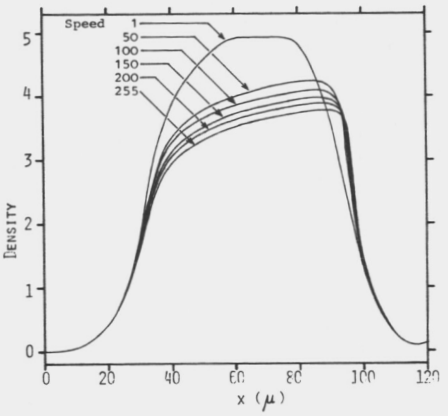

Figure 6 (below): Plotting density gradients as grey levels produces a relief image. Areas of higher density show the raster scan pattern due to a distortion of the profiles.

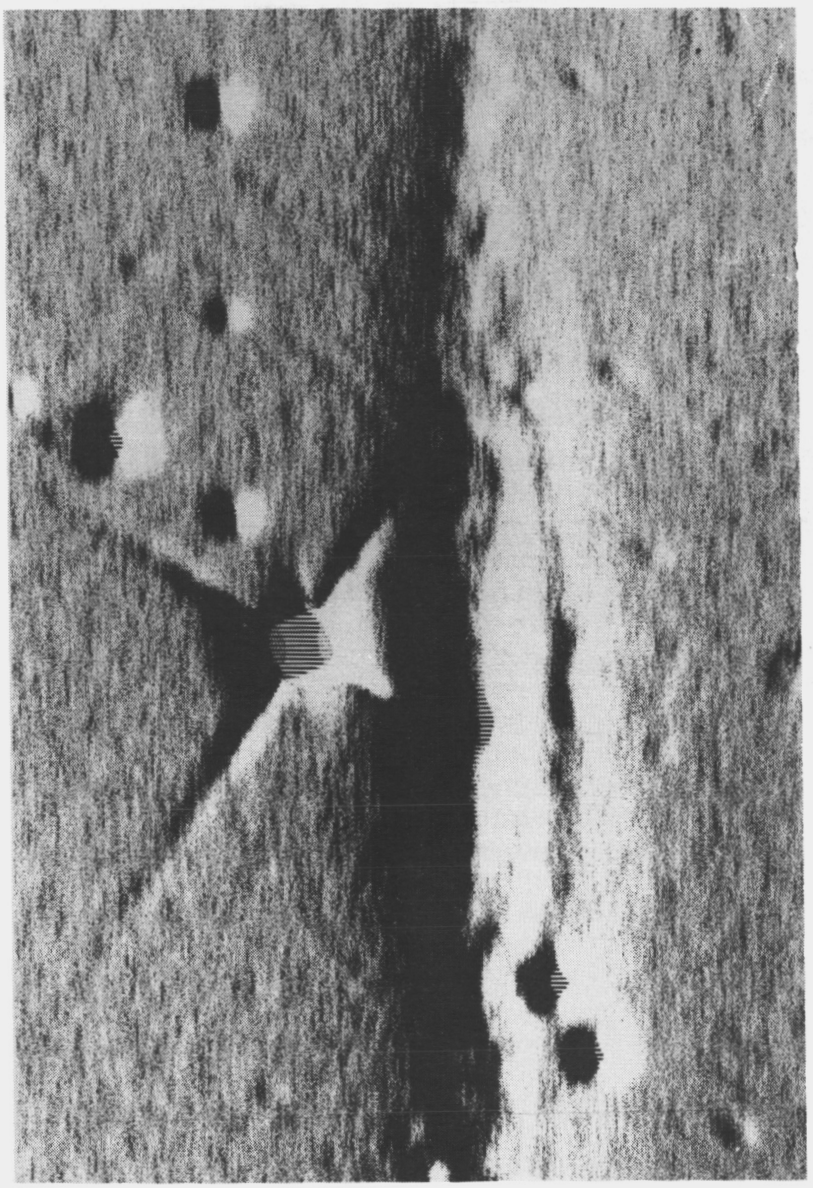

the standard ramp distance of 100 μm is not sufficient for an acceleration to medium or higher scanning speeds so that for short one-dimensional scans these speeds are only nominal and never reached (Becker 1979). Only with fully speed-adapted ramps can we see the true extent of system-induced asymmetries as in figure 5. The distortion starts at $D \geq 2.0$ and is present even for moderate speeds (Becker 1979, Becker and Becker 1979b). This situation is encountered in comparison spectra or other strong emission lines as well as in images of brighter stars (figure 6). Although the true positions can be recovered by averaging forward and reverse scans this will not reproduce the correct peak density.

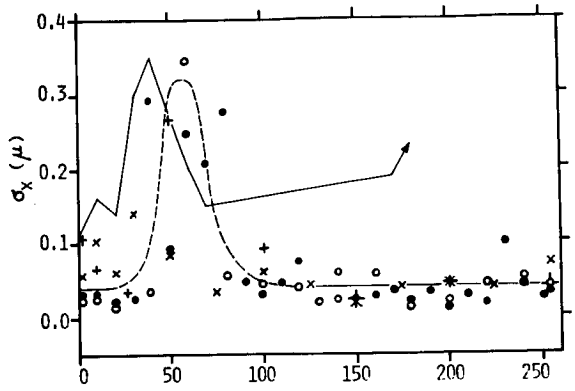

Figure 7: Repeatability of PDS positions as a function of scanning speed. Measurements from Bonn are compared with data for the PDS Vienna (upper curve).

The ability of the PDS to reproduce position measurements was tested in more than 1500 scans of a sharp edge (method as Wray and Benedict 1974). To overcome the finite resolution of photographic plates a metal wire was used for the edge measurements and directly fixed unto the PDS stage. The results of four independent test series in figure 7 demonstrate that the repeatability, measured as standard deviation from the mean position, is $\sigma(x)=0.05$ μm and rises to a maximum of $\sigma(x)\approx 0.3$ μm around SPEED 50 (0.8 cm/s). The same trend on a somewhat higher error level was observed for the PDS in Vienna (Albrecht et al. 1977) and we suspect resonance vibrations of the optical position encoders to cause this effect (Becker 1979, Becker and Becker 1979b). There is however no reason why this speed range, once established, could not be avoided for precise measurements.

One of the astronomical applications where accurate positions are required is the measurement of radial velocities. This is in turn based on a wavelength calibration with a comparison spectrum. Recently 2050 such lines in ESO Coudé spectra at 20 A/mm were measured with the PDS and Gaussian profiles were fitted to derive the positions (Becker 1983). The distribution function in figure 8 shows that the positional error of each line in this sample is $\sigma = 0.6$ μm. This is quite satisfactory in comparison with conventional results, but even so the PDS is not the limiting factor with its positional repeatability a factor of 10 better. This is also true when we consider the actual stellar spectra

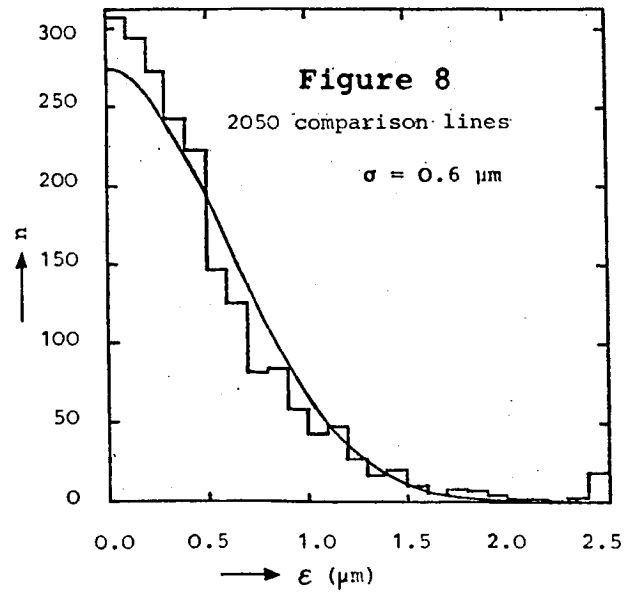

thus calibrated (see table 1), where the achieved internal error of the radial velocities is about 0.4 km/s or 0.3 μm at this dispersion, and the precision in the individual lines 1.8 km/s or 1.3 μm.

Table 1: Radial velocity of κ Ceti from ESO Coudé spectra (20 A/mm) on IIa-O emulsion digitized with the PDS Bonn (Becker 1983).

		Plate		
		F-7370	F-7376	F-7381
number of lines		17	18	18
mean RV helioc.	(km/s)	19.57	17.63	17.86
standard deviation	(km/s)	1.58	1.94	1.88
	(μm)	1.12	1.37	1.33
internal error	(km/s)	0.38	0.46	0.44
	(μm)	0.27	0.33	0.31

We can conclude that, but for certain limitations and provided that some precautions are taken, the PDS is able to digitize the complete information contents of astronomical plates.

References

R. Albrecht, H. Jenkner, W.W. Weiss and H.J. Wood (1977). Astron. Astrophys. 58, 93.

H.J. Becker (1979). Untersuchungen zur Radialgeschwindigkeitsmessung bei Sternen mit Hilfe eines automatischen Mikrodensitometers. Sternwarte der Universität Bonn.

H.J. Becker (1983). Thesis, in preparation.

M. Becker (1978). Untersuchungen zur spektralen Photometrie von Sternen. Sternwarte der Universität Bonn.

H.J. Becker and M. Becker (1979a). Mitt.Astron.Ges. 45, 151.

H.J. Becker and M. Becker (1979b). Veröff.Astron.Inst.Bonn,Nr.90.

I. Furenlid (1978). in: R.M. West and J.L. Heudier (eds.), Modern Techniques in Astronomical Photography, p.153. ESO.

I. Furenlid, W.E. Schoening, and B.E. Carder (1977). AAS Photo-Bull. 16, 14.

D.W. Latham (1978). AAS Photo-Bull. 18, 3.

J.D. Wray and G.F. Benedict (1974). Proc. SPIE 44, 137.

Heckathorn: Bill (Van Altena) are you interested in that variation in positional accuracy with speed?

Van Altena: Yes. I think it's very interesting. I'm not so sure that our granite machine has the same characteristics. A long time ago we made those razorblade scans that showed the correlation between the accuracy and the delay in the scanning. I believe we did that at a number of different speeds, but I don't remember off hand. The comment that I want to make though is that we find the transmission varying as a function of time. That may be just due to the drifting of your upper aperture; your upper slit. We found that it is necessary for us to open our upper aperture one notch so that it is simply collecting all the light that is transmitted, or sent up by the lower aperture. In other words, it is large. So if it does tend to drift around, which ours does, you will end up with an apparent change in the output which, if you then recenter the aperture it would go back to the original balance. So I don't think it's anything in the power supply. It's probably just a thermal drift of the upper aperture.

Becker: I think this would be true for scans that require longer times. When we were discussing the edge scans it was far very short time scales in which we did not find very serious photometric drifts or thermal drifts that could cause the aperture to change in position.

Van Altena: We found that even for the razor-blade scans where we are talking about very short intervals of time, that the accuracy decreases substantially if we use matching upper and lower aperture. In other words, to get the 500ths of a micron accuracy we have to open the upper aperture and then that is repeatable. Two other comments that I wanted to make relate to my discussion of the photometer. It was apparently not clear that the noise graph that I showed was the raw one without the integration. By putting in 24 micro-seconds of integration right after the photomultiplyer, the noise was reduced below the noise in any of the currently used astronomical emulsions. The resolution of the convertor is 14/5. We can measure the outer envelopes of the galaxy without any problems.

Hewitt: I would like to say that our experiences seem exactly the same, but if you use the nominally matching lower and upper apertures the drift is photometrically significant, on the time scale as short as five minutes. Of course, if you're trying to do astrometry all the plate positions are measured with respect to the lower aperture rather than the upper aperture, so it is hopeless trying to do astrometry if the upper aperture is affecting your results.

Hemmingway: On the Texas PDS, which is a metal PDS, I found that we have a slightly more severe thermal problem than other people might because we have a cooled PMT. From the time we turn it on, to a period of half an hour to an hour afterwards, the upper aperture will drift up to five or ten microns and then it will settle down. So you will actually drift the size of the aperture that we're trying to measure it with. The interesting thing is if you turn it off and let it coll down, the aperture will drift back. So it's clearly a thermal problem involved in the cooling system coming to equilibrium.

Hewitt: We find, despite our best attempts to control the environment, they are not very good attempts because the PDS is not our PDS, it's Lowell Observatory's. There are limits to what we can do. The upper aperture continues to drift around in a semi-random path. I think that depends whether the air conditioning system for the computer in the adjacent room is on, all this kind of stuff...you just confirmed that it's at the level of one or two microns, and that does not hurt very much, except that when you are talking about doing photometry at the 1 or 2 percent level, it matters a lot!

Heckathorn: I think there is a paper co-authored by Hemmingway that we'll bring up later on in the session, where they do tests on the airconditioning, and variations—its quite interesting.

MICRODENSITOMETER ERRORS:

THEIR EFFECT ON PHOTOMETRIC DATA REDUCTION

E. P. Bozyan
Department of Astronomy, University of Texas
Austin, TX 78712

C. B. Opal
E. O. Hulburt Center, Naval Research Laboratory
Washington, D.C. 20375

ABSTRACT

We analyze the performance of densitometers used for photometric data reduction of high dynamic range electrographic plate material. We test densitometer repeatability by comparing two scans of one plate. We examine internal densitometer errors by constructing histograms of digitized densities and find inoperative bits and differential non-linearity in the analog-to-digital converter. Such problems appear common to the four densitometers used in this investigation and introduce systematic algorithm dependent errors in the results. We suggest strategies to improve densitometer performance.

I. Introduction

PDS scans of Texas Mark II Electrographic Camera (Griboval Camera)[1] plates result in UBV magnitudes and colors accurate to better than 0.02 magnitudes.[2] The plates were scanned with the University of Texas 1010A PDS (Texas PDS). The noise in this data and data reduction process has been divided into three catagories for analysis: 1. the noise introduced by emulsion granularity and defects, 2. noise added by the PDS scanning and 3. noise added by the algorithm used to estimate stellar magnitude. In this paper we report the results of the tests we have performed to estimate the size of the three sources of noise, discuss in detail the noise introduced by the Texas PDS and then extend this discussion to include the Lowell Observatory PDS (Lowell PDS), the Goddard Space Flight Center PDS (Goddard PDS) and the Grant microdensitometer belonging to the Space Science Division at the Naval Research Laboratory (Grant).

The tests we describe use astronomical plate material obtained with the Griboval Camera. We have demonstrated elsewhere the uniform sensitivity and distortion free properties of the Camera.[2] Plates exposed with the Camera differ from normal astronomical plate material in that the cesium-antimony photocathode (with typical peak quantum efficiencies of 10 to 15 percent) releases photo-electrons which are accelerated to 50 kev and on impact, upon electron sensitive emulsion, render 5 to 20 silver-halide grains developable. This together with the fine grain of the electron sensitive emulsion results in a linear or nearly linear response over a much wider range of density and much higher ultimate densities ($D \geq 6$) than conventional photography.[2] In order not to degrade this data by the scanning process stringent requirements must be placed on the densitometer.

II. PDS Repeatability

To separate plate to plate emulsion noise from the combined PDS-magnitude algorithm noise we took two, out-of-focus, 12 minute, V plates of M67. The plates were taken sequentially and on the same place on the photocathode to eliminate error introduced by any small, spatial variation in photocathode sensitivity. M67, an old open cluster, was chosen because it provides a large number of reasonably bright but well isolated stars which have also been observed photoelectrically. The observations were taken at the f/13.6 Cassegrain focus of McDonald Observatory's .76m telescope using Kodak 4489 electron microscope film.

The two plates (plates A and B) were then scanned sequentially with the Texas PDS. Three weeks later plate B was again scanned (called plate BP). All microdensitometer scanning reported in this paper was done in the same manner: 2048 by 2048 raster scan, with a 16 by 16 micron square aperture, using x and y steps of 16 microns, at a speed of 4 mm per second. The density of the clear emulsion was set to .1. For the three scans (A, B, and BP) density to intensity corrections were applied[2], the arrays collapsed to 512 by 512 and stellar magnitudes estimated using an automatic star finding and centering algorithm. Stellar magnitude was estimated by integrating the intensity within a numerically simulated circular aperture of 320 micron

radius centered on the star from which the median of the local background was subtracted. This median was that within a numerically simulated annulus centered on the star with inner and outer radius of 768 and 896 microns. The out-of-focus star images were typically 200 microns in diameter. This produced a list of 188 stars common to the three data sets spanning a four magnitude range. The zero points for the individual scans were estimated from published photoelectric observations.[3,4]

The noise in this data reduction process (PDS scanning plus magnitude algorithm) and its dependence on magnitude was estimated by comparing the stellar magnitudes for the one plate scanned twice. The magnitude differences (plate B - plate BP) were plotted versus the plate B magnitudes. A 0.4-magnitude-interval running mean was calculated. The results are shown in Figure 1: the crosses are the individual stars and the solid line is the running mean. The noise in the data (emulsion noise) plus data reduction process was estimated by comparing the magnitudes for the scans of the two plates (plates A and B) using the same technique. The magnitudes of plate A - plate B were plotted versus plate B. The results are shown in Figure 2: the crosses are the individual stars and the solid line is the running mean. Figure 3 shows the 0.4-magnitude-interval running standard deviation corresponding to the running means in Figures 1 and 2: the dotted line is the one plate scanned twice, the solid line is the scans of the two plates. There is obviously more scatter for the two plates than the one plate scanned twice. For approximately a two magnitude range the standard deviation of the magnitude difference, for the one plate scanned twice, is less than 0.01 magnitude, giving a PDS-magnitude algorithm error of 0.007 magnitude for one plate. For the same magnitude range, the standard deviation of the magnitude difference for the two plates is 0.02 magnitude giving a 0.014 magnitude error for one plate and, assuming quadrature addition of errors, a 0.012 error due to emulsion noise for a single exposure. However, for both, the scatter starts to increase suddenly at a magnitude of 14.3 This increase is not what is expected from the errors caused by Poisson statistics.

The only ostensible difference, other than microdensitometer noise, between the two scans of the one plate, was the registration of the pixels on the plate. This might cause the sudden increase in the standard deviation if the star centering algorithm became particularly sensitive to the registration of the stellar image in the pixel array as the plate limit is approached. We investigated this possibility by trying different centering algorithms and by artificially displacing the image center and concluded that neither was responsible. We then turned our attention to the PDS itself.

III. Non-linearity and Noise in the Analog-to-Digital Converter

The densitometers investigated use successive-approximation analog-to-digital converters (ADC). These use a binary-sort principle: the input voltage is compared successively with a reference voltage determined by a resistor switching network which progressively halves the voltage increments for comparison. The accuracy of the converter is usually expressed as a percentage of full scale plus a quantization error in terms of the least significant bit (LSB). These specifications imply an average linearity, but do not

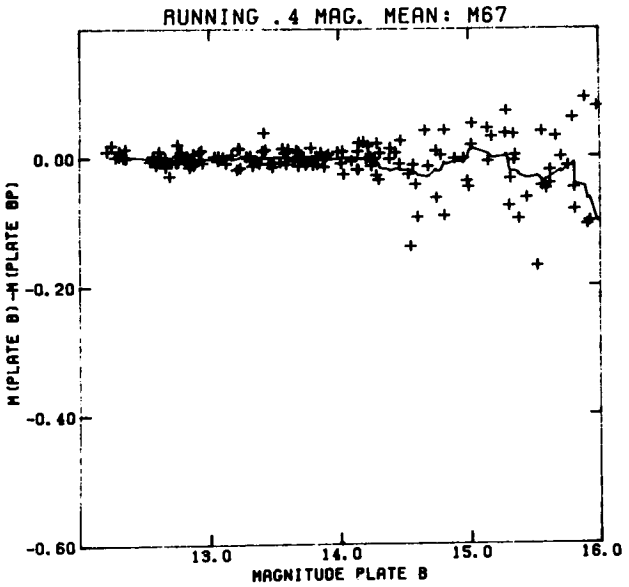

Figure 1. The difference in magnitude for one plate scanned twice versus magnitude for 188 stars in M67. The plate is an out-of-focus, 12 minute V, Griboval Camera plate. The two scans were done 3 weeks apart with the Texas PDS. The crosses are the individual stars. The solid line is the 0.4-magnitude-interval-running mean.

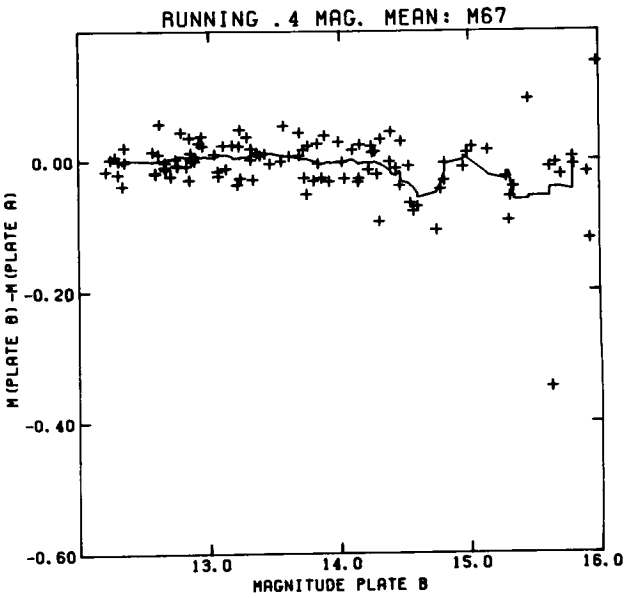

Figure 2. Similar to Figure 1 but for two different plates: plate B of Figure 1 and plate A. The two plates were taken sequentially on the same place on the photocathode to eliminate error introduced by small variations in photocathode sensitivity. The plates were scanned sequentially.

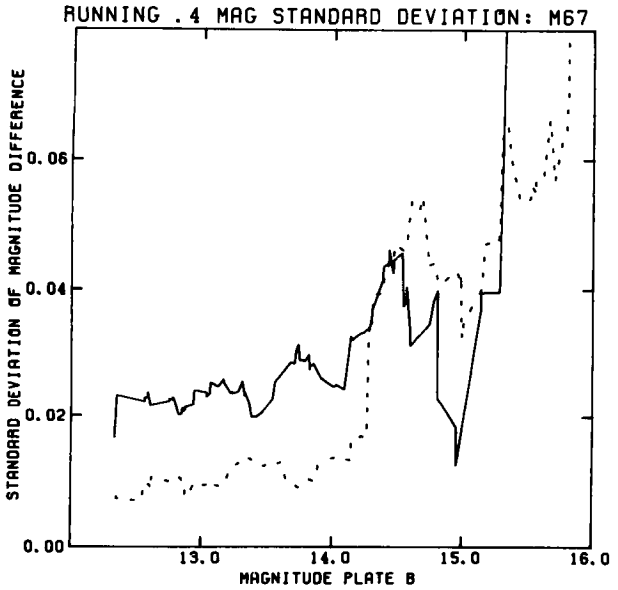

Figure 3. Standard deviations of the 0.4-magnitude-interval running means shown in Figures 1 and 2. The dashed curve is the same plate scanned twice and the solid is the two different plates.

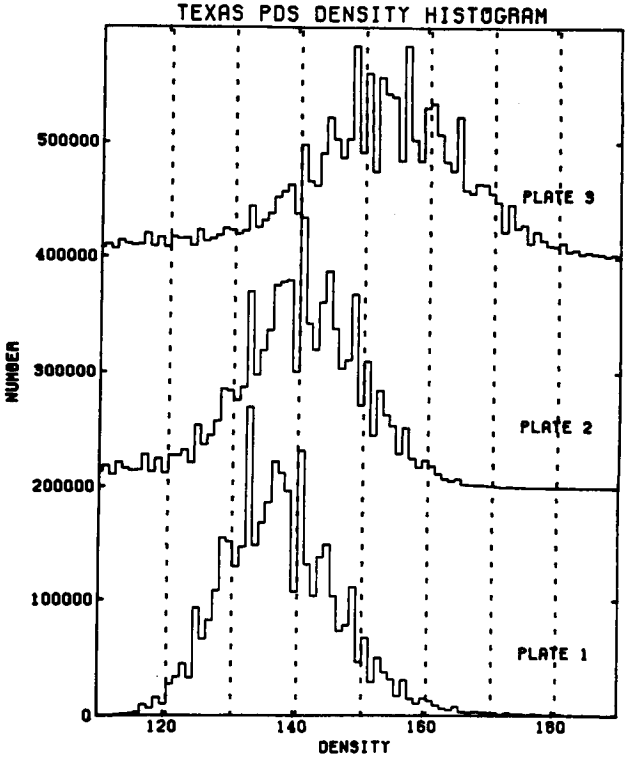

Figure 4. Frequency histograms of the DNs for three different plates scanned with the Texas PDS. Plate 2 and Plate 3 are offset from Plate 1 by 200,000 and 400,000 respectively.

address the possible range of values which can convert into a given data number (DN); thus, the width of a DN is not accurately specified in terms of fractions of a LSB. This effect is known as differential non-linearity.

To demonstrate these effects we have constructed histograms of plates scanned with the Texas PDS, the Lowell PDS, the Goddard PDS and the Grant microdensitometer. These PDS machines all have 10 bit ADCs, the Grant has a twelve bit ADC of which we have used the 10 most significant bits. In all cases, most of the numbers represent sky background, with a tail to high density due to stars and galaxies.

Figure 4 shows frequency histograms of the DNs for three different plates scanned with the Texas PDS. With four million numbers the expected distribution is Gaussian in the vicinity of the mean density. Near the peak, fluctuations in DN frequency should follow Poisson statistics and thus be of order $N^{\frac{1}{2}}$. Thus, fractional fluctuations in the present data, with peak frequencies of 10^5 should be 1/300, yet observed variations are as great as a factor of 2. Although the mean density is different on each plate, examination of the histograms reveals that specific DNs occur with an unusually high or low frequency and repeat this performance plate to plate. Figure 5 shows similar data obtained with the Lowell PDS for our two M67 plates, the same effect is apparent. In Figure 6 we show histograms of scans from all four densitometers, which have been normalized to Gaussian distributions fit to the mean and standard deviation of each scan. Also included is a Monte-Carlo simulation to emphasize the severity of the problem. The effects of differential non-linearity are quite evident: considerable variation in bin widths (the range of values that convert to a given DN) is apparent. The variations in bin width range from about 35% for the Lowell PDS to 18% for the Goddard PDS.

These fluctuations and their repeatability on the Texas PDS are conclusive evidence that differential non-linearity contributes to these strange distributions. While each converted number may be within the specifications of the ADC, the statistical properties of a set of such numbers introduces bias in estimates such as the mean, median and standard deviation. The bias arises from the difference between the actual and the nominal center of that bin. If the bin widths varied but were centered on the nominal value, the mean and standard deviation would not be biased and the median could be corrected. The importance of this problem is due to the failure of expected improvements in signal-to-noise ratio from averaging large numbers of noisy samples.

Another problem with the ADC has been detected with DN frequency histograms. Figure 7 shows the histogram for the Texas PDS scan of the 10 minute B plate used in the picture of M51 shown on the frontispiece of these proceedings. Note that half the DNs are missing, an effect caused by a "sticky bit" problem in the ADC: the 8 bit was stuck on during the entire scan. The problem, while obvious in Figure 7, was not detected by displaying the scan on an image processing system. The effect of an improperly working ADC is to seriously increase the noise in the data; however, it is extremely difficult to detect unless a histogram is examined.

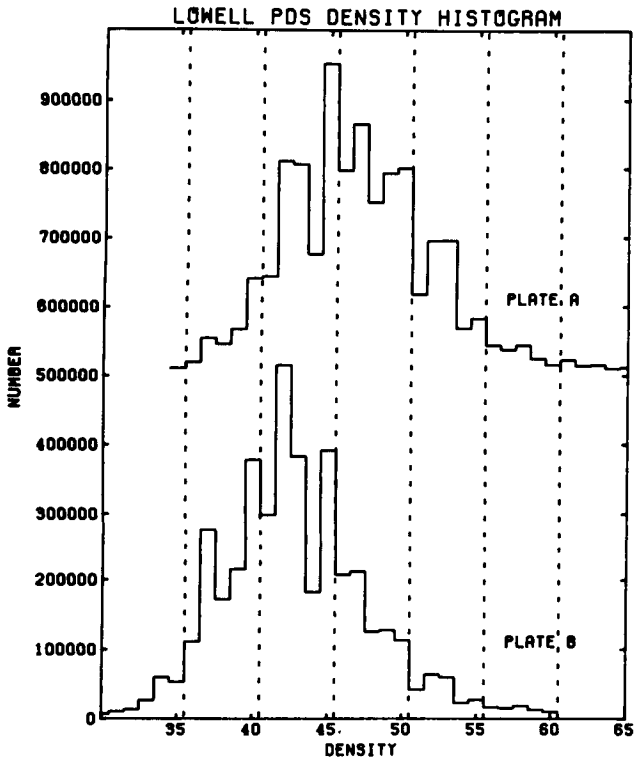

Figure 5. Frequency histograms of the DNs for the two M67 plates scanned with the Lowell PDS. Plate A is offset from Plate B by 500,000.

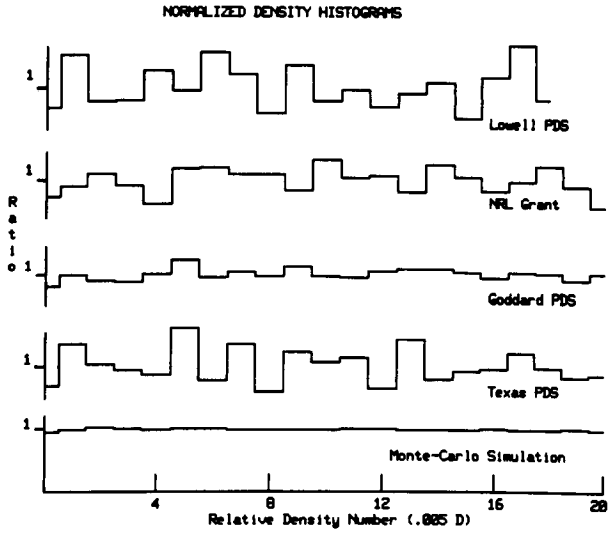

Figure 6. Frequency histograms of DNs for all four microdensitometers. The histograms have been normalized to Gaussian distributions fit to the mean and standard deviation at each scan. A Monte-Carlo simulation is included for comparison.

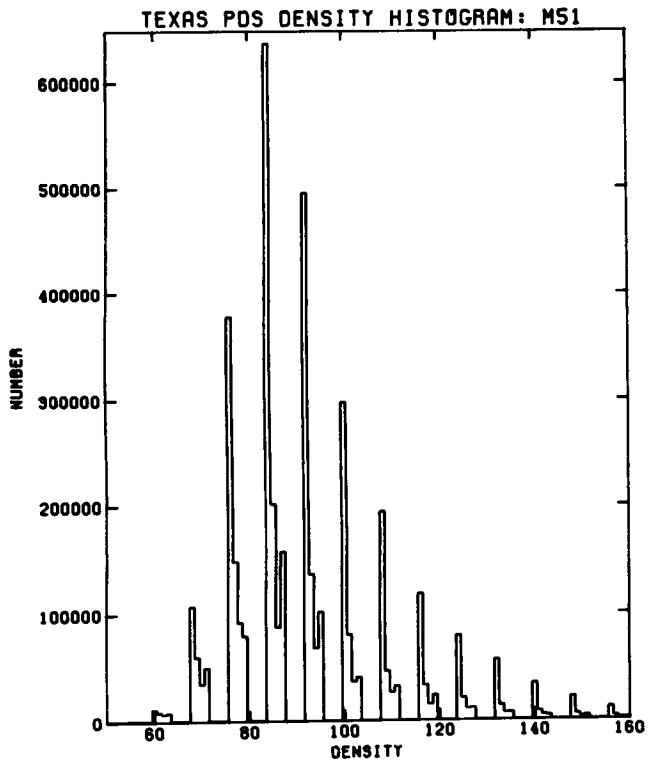

Figure 7. A frequency histogram of the DNs for the Texas PDS scan of the 10 minute B plate of M51. Half the DNs are missing because the 8 bit in the ADC was stuck on during the entire scan.

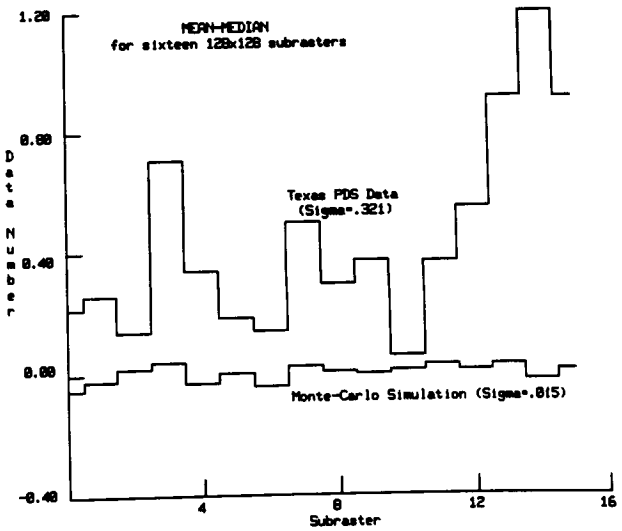

Figure 8. A plot of the difference between the mean and the median for 16 subrasters taken from a Texas PDS scan. The subrasters are 128 by 128 pixels. Also plotted is a Monte-Carlo simulation.

IV. Photometric Data Reduction and Differential Non-linearity

What is the effect of differential non-linearity on photometric data reduction? In section II the median of the distribution is used to estimate sky background for two reasons: 1. when a low probability non-Gaussian distribution is added to a high probability Gaussian distribution (for instance lint, pinholes or cosmic rays plus sky background) the median, not the mean, of the combined distributions is the better estimate of the mean of the Gaussian distribution, and 2. for a very large sample of DNs with a limited range of values (for instance, here the 4 million DNs are limited to 1024) an efficient median algorithm can be used. In the presence of differential non-linearity the interpolated median will be biased by both the variations in bin widths and the difference between the actual and nominal centers of the bins.

To estimate this bias we have chosen 16 subrasters, from a Texas PDS scan and found the mean and median for each. The subrasters are 128 by 128 pixels and are predominantly sky background. The median was interpolated linearly between the DNs immediately below and above the integer median. For reference we have constructed Monte-Carlo simulations of similar data for an ideal ADC. Shown in Figure 8 is a plot of the difference between the mean and the median for the 16 subrasters for both sets of data. For the Texas PDS data the difference is always greater than zero while the Monte-Carlo simulation is centered on zero. For the Texas data the standard deviation of the difference is 0.321 DN; results for the other densitometers are similar. Clearly there is considerably more variation in the actual densitometer data than in the simulations, indicating that differential non-linearity is a non-negligible effect. For example, an error in background determination of a .321 DN produces a .2% error in the intensity of a stellar image 20 DN (0.10 D) above sky. As the plate limit is approached, this source alone limits the accuracy of photometry to a few percent.

There are 3 other sources of noise in the Texas PDS which we did not discuss but also are important: 1. the photomultiplier has only a 50 microsecond time constant and is only sampled once for each step in X, (at a speed of 4mm per second the photomultiplier is being sampled for only 1/50th of the scanning time), 2. the time constant of the log amplifier is a strong function of input current, and 3. the input voltage to the ADC is not held constant during the conversion process and ADCs are known not to operate properly under these conditions.

III. Conclusions and Recommendations

In the above discussions we have demonstrated the value of two tests of densitometer performance: 1. to repeat scans of a field and reduce the data in the normal manner to ascertain that no unexpected sources of error are present and 2. to construct histograms of the PDS output to examine the performance of the ADC.

We recommend that successive-approximation ADCs be used with extreme caution. Ramp-type (Wilkinson) converters of the type used in nuclear

instrumentation are available and do not suffer from differential linearity and "sticky-bit" problems. Economic versions of these devices operate at speeds 10 kilo-samples per sec for 13-bit resolution, sufficiently fast for most densitometer applications. By using an exponential decay reference rather than a linear ramp reference, this type of converter could be modified to yield logarithmic data numbers directly without need for the logarithmic amplifier used in present machines.

Acknowledgements

We are grateful to P. J. Griboval for help with the use of his camera, to A. V. Hewitt for scanning our plates on the Lowell PDS and for useful discussions, to G. W. Torrence for evaluating the Texas PDS hardware, to H. M. Heckathorn and P. D. Hemenway for useful discussions, and to F. A. Bozyan for many stimulating discussions, assistance in evaluating the Texas PDS, and for reading and making helpful suggestions for improving this paper.

References

1. Griboval, P. J., Adv. Electronics Electron Phys., Vol. 40B (Proc. Sixth S.P.I.E.D.), p. 613, 1976.

2. Opal, C. B., Bozyan, E. P., and Griboval, P. J., S.P.I.E., Vol. 331 (Instrumentation in Astronomy IV), p. 453, 1982.

3. Johnson, H. L., and Sandage, A. R., Astrophys. J., Vol. 121, p. 616, 1955.

4. Eggen, O. J. and Sandage, A. R., Astrophys. J., Vol. 140, p. 130, 1964.

Wells: The histograms that you showed and the comments you made about your A to D cause me to remember experiences at Kitt Peak National Observatory about five years ago and maybe Ed Carter can say more about this. At one point we were using an algorithm to get background estimates for star magnitudes, just like you working in an annulis and it's key element is mean minus median. In the course of the working on that algorithum we were looking at histograms of the densities in these annulli and seeing this on a graphics terminal and one could not help but notice that the histograms were weird. There were peculiar peaks and missing values in the histograms. The other thing that occurred was that certain images, when they were enhanced on the image display, if you cranked up the enhancement, you could detect contours in the data. They were very subtle contours in certain images and this was also very peculiar. This led to an elaborate study of the A to D convertor at Kitt Peak. A program was built which analyzed the statistics of the A to D convertor and it was shown that certain values were much more common than others. Now, one of the key things that I believe came out of that was that in front of the A to D convertor there is a sample and hold.

Boyzan: Well, there are three different ways you can go. You can go sample and hold, you can go Wilkinson Convertor...We haven't decided. They're all reasonably priced, technologically well available within the kind of speeds that we want to work in now.

Wells: Agreed. Let me explain just for those who haven't looked into this that the A to D is usually a successive approximation device which is deciding the bits one by one as it progresses through the bits during the conversion. If the input to that A to D is noisy, which it is with no sample and hold, it follows that occasionally the convertor makes the wrong decision on the choice of a high order bit and is unable to correct the decision as it proceeds in the approximation. This leds to the peculiar statistics.

Boyzan: We're picking up noise all the way back here. It's in a higher level bit than where we're getting the other stuff, so we're being dominated because we can bring down our noise by a factor of square root of two. We're up here in the 16th bit picking up noise. It's going right through the whole chain. You were sampling at a low speed, we're not.

Wells: The Kitt Peak PDS was changed after this study.

Boyzan: Yeah, well one of the things I'd like to know is about the transfer function. Has anyone studied the transfer function of the photomultiplier? Do we know what we can get away with? How to do it? These are things that we are just beginning to look into. One of the problems you have to take into account is variable scanning rates and you want to be able to run your PDS. Some people could run it very fast with new electronics and get the same accuracy we get now. I could run it very slow, the way I do now, and increase my accuracy tremendously. I mean, Jeffrey Tarnam said he could build me a little black box so I could take it and stick it in anybody's PDS.

Lasker: May I make an appreciation of what you're saying while you have this diagram up? As you'll recall, earlier I drew an explicit filter on the block diagram. Just to be a bit pedantic it is in everybody's system, it behooves us to know where it is and how much we're respecting Shannon. And as we do this it's not only time conditioning but when you think about the relation between time and scanning speed, were also with what we do about filtering, affecting the shape of the affective aperture we're using...I think we're on a very important point as a group and we're only coming to...

Boyzan: Coming to appreciate it now.

Hewitt: A couple of past things occurred to me and this is all news to me. Particularly about what exciting things are being discovered about the law of the PDS. (Laughter) One might consider going back to rather old-fashioned technology of digitizing which is inherently rather glitch free, what is wrong with the voltage to frequency convertor?

Boyzan: Uh...I'll let my co-author answer that question.

Opal: I think the answer is buy off the shelf for one thousand dollars an 8192 Staff Wilkinson A to D converter which will have at least 13 bits and 50 kilo-hertz with a differential linearity in the area of a quarter of a percent. That's what we're talking about here.

Oliver: First the problem with the voltage to frequency convertor, is of course, generally you can't get enough bits, that is you've got one megahertz full scale frequency conversion and you get one part of a thousand ten bits which will give you one millisecond sample and a one megahertz V to F is pushing the V to F Technology...I wonder why people aren't looking at going to a 15 bit or so A to D?

Boyzan: I'll take ten. For seventy bucks and an afternoon's time, we can put in a nice 12 bit A to D convertor.

Van Altena: Now, that's what we've done. We put in a logarithmic A to D convertor up at the front end. We still have sticky bits but they're down to the 14th bit level. So this means only those lower bits are affected. The higher bits don't seem to affect our densities at all. So this is a logarithmic A to D convertor. We're getting out densities down to the thousandth of a density and those don't seem to be affected by sticky bits. They're down below that level.

Boyzan: Well, one thing I still think that's very important is something we do with Texas interferometer is that we, anytime you do anything, any plug that goes into a A to D convertor, you should run a bit histogram on it. I think it's something that we all ought to do just on a regular basis, it's not difficult to do.

Horton: The so-called sticky bit is inherent in A to D convertor. It is the differential linearity that we are playing with. The industry standard is that the width of each bit is plus a minus 1/2 of the least significant bit. We can get a significant change in the number of samples going into the buckets shall we say so that would instead be improved just by going to a higher resolution A/D converter and just ignoring all the lower bits. Just to get the higher accuracy of the differential linearity.

Opal: I haven't experimented with much of this, but I did divide the numbers by four. You seem to get this histogram, as it depends on the bunch of resistors in this and hold it at all levels so that the bin width of the zero to five volts versus the five to ten volt range varies by this amount, so that you do not gain anything by going to higher precision.

Boyzan: The thing that of course is interesting about it is the fact that it is so systematic and so repeatable. The fact that it's the same numbers all the time that are high and low, that's what you want. If it were a random process that would be better, you wouldn't see it.

Horton: It's not a random process. It's actually fixed in each A/D converter and each bit will have the save characteristics in any given A/D converter.

Boyzan: Okay, but don't you think that modern A to D convertors are less prone to this problem?

Horton: No, because the industry standard is plus or minus one-half of the least significant bit.

Hewitt: It is to say that they are not correlated from one bit to the next. We could have 12 consecutative bits screwed up. You may recall that I said that I had two points to make. Perhaps less directly related to the counter problems and that is that algorithm that we used to do to Stellar photometry does not take the median. We typically don't have enough noise for us to be able to trust the median in any real sense. The noise in the sky is a standard deviation of plus or minus one bit and that doesn't leave a thing. If you take the median in photometry instantly you have a resolution of plus or minus half a magnitude at the kind of level where we might be producing something that is at least half way sensible. I think if you don't take the median you're a little less troubled by this kind of thing.

Boyzan: Yes, we've fooled around with it both ways and haven't noticed any really great differences in our results. We have not been able to establish, to get systematically different results.

Opal: We do interporlate the mean.

Boyzan: We fooled around with data for two years before we finally got down to trying to establish why we have this jumping noise at low levels. But I think it's important to educate people to let them know these machines are marvelous and can be used successfully but you've got to understand the source of your error. And you've got to be well aware of where the error can creep in.

Oliver: I'd like to suggest with the appropriate input circuity to switch amplifiers, you can go in straight transmission mode with 15 bit or 16 bit A to D with small manipulation and get the kind of accuracy that you like. At least down to a density of 4 or 5. Many people still tend to believe that the system with the log amplifier introduces not only the problem with time resolution and it's a very severe one and I'm astonished to find people who are discovering this now. I thought that this was well known 15 years ago. You have not only that problem but there are other inaccuracies involved in a analogue logarthmic amplifiers as you are going down towards density five that people just ignore and say, we'll I've got a 12 bit A-D on the output log on density 5, so I've got 17 bits for density 5-

plus 12 bits for the A to D conversion - you have not got anything of that sort?

Boyzan: No - you have a percentage accuracy for the input that's coming in...

Oliver: So when you look at the alternate approach of straight transmission operation, do the log conversion later on it can be done in software quite rapidly. Don't compare that approach to some mythical performance that is not being achieved. I know that you can take samples at intervals at 40 micro seconds with 15 bit A to D conversion...

Hewitt: Without wishing to belittle my paper—I would like to point out that photomultipliers interact. That is inconsistently non-linear behavior due to the fact that is a Monday, Wednesday or Friday.

Boyzan: On some of these tests where the gain of the photomultiplier was varied by factors of 20 - we get the same response through the system.

Hemmingway: Course that's over a real short period of time.

Boyzan: Yes, a couple of hours but it's all very interesting to find out. Sometimes I feel like I've just opened Pandora's box I would have been just as happy if I had never learned about it, but I think they are all very solvable problems and everyone is beginning to approach to solving them.

Positive-Feedback Photometric Drift in the PDS

R. H. Cornett (SASC), R. C. Bohlin (ST-ScI), J. K. Hill (SASC) and T. P. Stecher (GSFC)

I. Introduction

The intensity calibration of many types of images made by modern detectors such as image tubes and microchannel plates requires determining and removing variations in gain across the image field, or flatfielding. The straightforward and customary way to do this is to uniformly illuminate the detector input and digitize the resulting flatfield image.

We have found that digitizing flatfield images produces conditions in the PDS 1010A at the GSFC Laboratory for Astronomy and Solar Physics which cause the measured density to drift by as much as .1 DN during a 10 minute interval. The drift occurs when the PDS, set up in equilibrium at fog level, subsequently scans a reasonably dense (>1.2) region for periods of longer than a few minutes. The drift is manifested primarily as a positive shift in density that is approximately the same for all densities.

II. The Problem

This behavior is characterized in Figure 1, which is adapted from plots made by a strip chart recorder connected to the analog PDS output. The PDS was focussed and set up in the conventional way and the PMT voltage was adjusted to give density readings of 0.0 on clear glass in equilibrium. In this example a 20 micron square aperture was used with no neutral density filters, giving a PMT voltage control setting of 5.2. The stage was then moved to bring into the aperture a large uniform region with density about 2.5, and left in that position. Figure 1a) shows the resulting plot of measured density as a function of time. The densitometer measurement drifts upward from D = 2.46 asymptotically toward D = 2.56 with a halving time of about 20 minutes.

Figure 1b) shows the response of the PDS to clear glass after having been allowed to reach equilibrium at D = 2.56 at the position described above. The asymptotic drift is toward 0.0 but the initial halving time is much shorter (about 5 minutes).

Our investigations have shown that this behavior also occurs in the PDS "transmission" mode at approximately the same level, and varies in severity by only a factor of two in total drift over the range of aperture sizes and PMT voltages commonly used (10 - 80 microns; voltage settings 3.9 - 6.8). The drift occurs for all densities greater than about D = 1.5 when a significant fraction of the scan line contains that density.

The instrument for which we require flat field data produces flat fields that are 39 mm diameter circles centered in the 41 mm square digitized region. The flat fields have nearly uniform densitites of up to about 3.0. Therefore, flat field scan lines consist of between 0% and 98% dense film in a fog level background. Scanning this image with a 20 micron aperture at the highest available speed requires about two hours and produces easily detectable drift.

The flat field scan pattern was simulated by using the PDS to scan steps of a density wedge. The scans were arranged so that 80% of the scan length was across fog level material. These scans were alternated with scans of fog level material to permit the PDS to return to equilibrium fog level. Successive density wedge steps of D = 0.33, 0.89, 1.20, 1.75, 2.23, and 2.55 were scanned in this manner.

Scanning was done in the x-direction only so that, for each "image" the densitometer repeatedly scanned the same line. Therefore plotting the density of a given sample versus line number is equivalent to plotting measured density at that position versus time.

Figure 2 presents the results of the scan of the wedge segment with D = 1.20. The upper curve of Figure 2(a) describes D(t) in PDS units for the average of 20 adjacent columns at the high density end of the scan while the lower curve plots the average of 20 adjacent columns at fog level. Figure 2(b) displays D(t) at fog

level for the average of 20 adjacent columns during the fog-level scan immediately following that of figure 2(a).

The behavior is qualitatively similar to that shown in Figure 1. Figure 2 also shows, however, that the drift in measured density for a given scan is nearly the same at all times for the high-density region and the fog-level region. This is true for all measured values of the high density. Table 1 summarizes the results of a sequence of scans like those of Figure 2 and demonstrates this. For each pair of scans of the flat-field-like region the change in measured density at the wedge density is equal to the change in measured density at fog level. Scans of complete wedges show that the shift in density is constant for densities between fog-level and wedge values.

III. Correction Procedure

The above characteristics suggest a straightforward correction procedure for removing the effects of this densitometer drift. If the fog level is assumed to be in fact constant and is monitored during scans of flat fields, the PDS drift may be removed by subtracting the difference between the observed fog level and its assumed constant value for each pixel.

This is done for our flat fields by arranging each scan line to include some fog level pixels at each end, and using those pixels to generate the measured fog level as a function of time for the scan. This function is then smoothed and subtracted, as a function of scan line, from the measured density. The fog level is then adjusted to a standard value by adding a constant. The result is a "flattened" scan with PDS drift removed to the accuracy within which the fog level drift matches the drift at other levels (about 2 PDS units).

Figure 3 shows this procedure. The noisy curves are the averages of 10 fog-level pixels at the edge of 2048 x 2048 flatfield frame with central density about D = 2.0, plotted as a function of scan line. The thick line is the smooth background curve fitted to that function shifted upward by 10 PDS units. It was produced by

a) boxfiltering over 15 lines, b) median filtering over a 5 - line interval, c) selecting the smaller density of the smoothed left and right sides, and d) fitting a cubic function to the result. We have tested this procedure by using it to correct scans of a density wedge made daily during densitometry of our flight data. The reproducibility of all densities on the wedge from 200 to 600 PDS units is improved from a mean standard deviation of 5.0 PDS units to a mean standard deviation of 2.1 PDS units by this procedure.

IV. Conclusions

Densitometry of extended regions of moderately high density causes the PDS measured density to drift upward by as much as 0.10 D in ten minutes. This drift is nearly constant for all density values and can be corrected by subtracting the measured fog level from all density values.

Table 1

Scan	Type*	Mean Density PDS units	ΔD at ff	ΔD at Fog
1	FF	67	2	1
2	Fog	20	—	-1
3	FF	177	5	5
4	Fog	20	—	-2.5
5	FF	238	5	5.5
6	Fog	20	—	-3
7	FF	350	7	7
8	Fog	20	—	-5
9	FF	445	7	7
10	Fog	20	—	-5
11	FF	512	7	7
12	Fog	20	—	-5

* "FF" denotes scan of 80% density wedge, 20% fog (to simulate flat field scan).

"Fog" denotes fog level scan. All scans were 30 minute, 1024 x 1024 pixel scans.

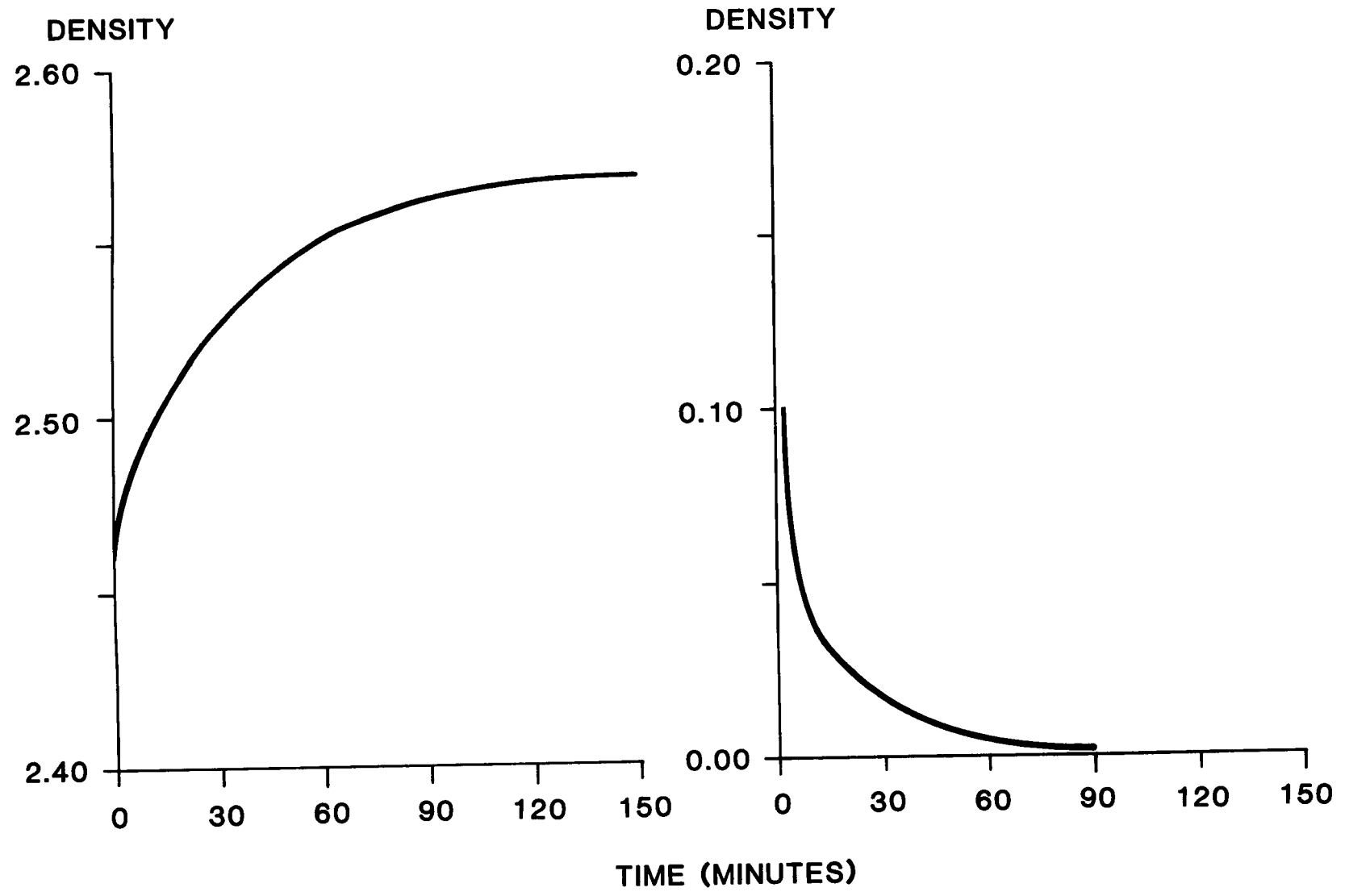

Figure 1

a) Strip chart record of a quasi-static experiment in which the PDS aperture was moved to a region of density 2.5 and left there. Plot is of density at the analog output vs. time.

b) Subsequent behaviour after the experiment of figure 1a). The PDS aperture was quickly moved to clear glass and left there.

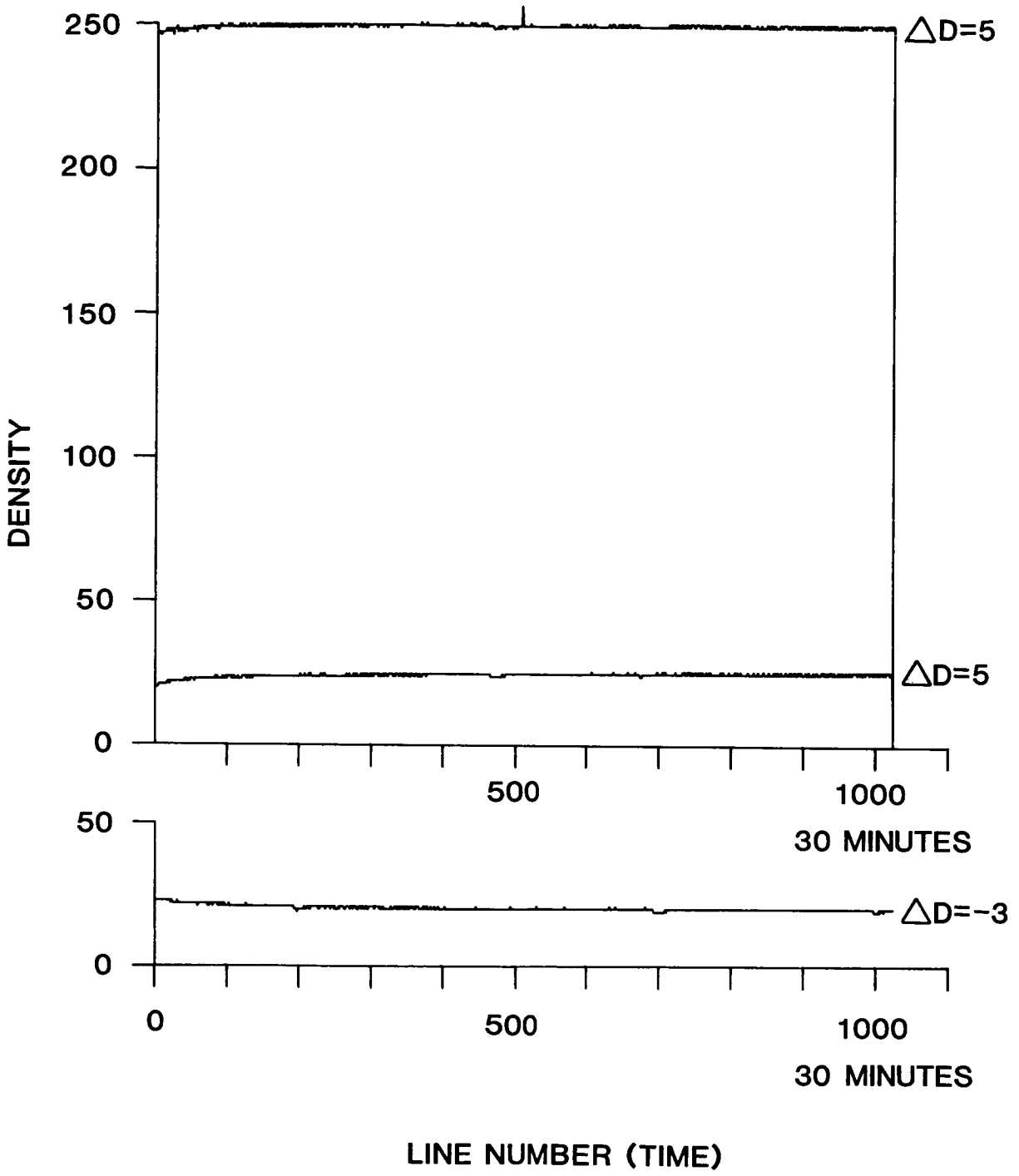

Figure 2 "Image" from repeated 1-dimensional scans off the edge of a constant density patch, as described in the text. The upper plot (Figure 2(a)) displays the average of 20 columns at the high and low density ends, respectively, of the initial scan. The lower plot (Figure 2(b)) displays the average of 20 columns at fog level during the subsequent fog-level scan.

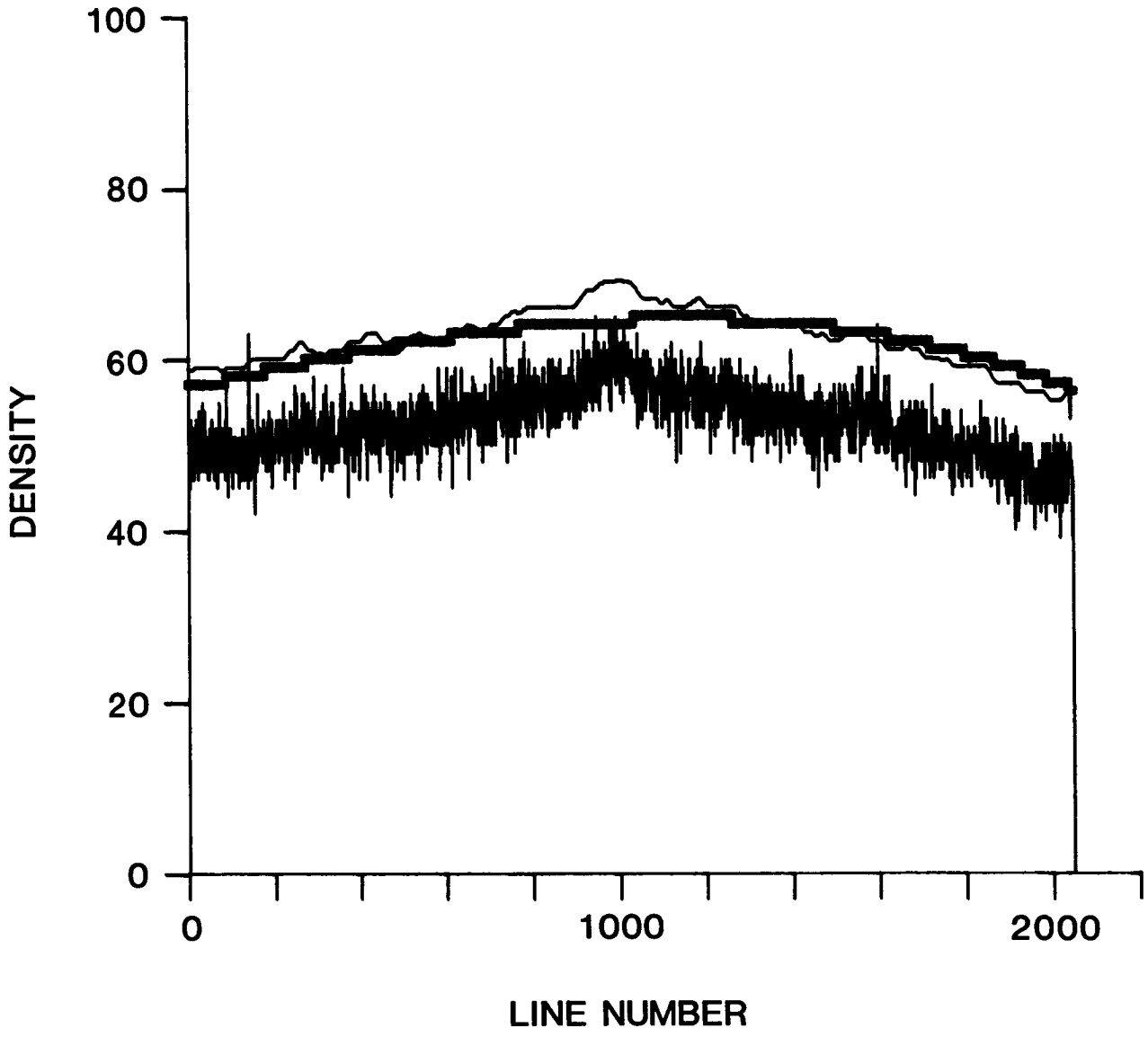

Figure 3 Correction procedure for flatfield scans. The noisy curve is the average of 10 columns at fog-level along the edge of a flatfield image. The thin line is a smoothed version of the noisy curve (raised by 10 units, for visibility). The thick line is result of choosing between lower of the thin line plotted and a similar one for the other side of the image, and fitting a cubic to the result. The thick line is the one subtracted from the fog-level.

Cornett: I'd be interested to know if anyone has any comments specifically on whether it's aperture drift?

Tony Hewitt: The question I had - is why do you think it happened?

Cornett: No, I did until this morning have a leading contender, that was that it was a PMT effect.

Hewett: That was what I was going to suggest.

Cornett: Yeah, it has happened in two PMT's here at Goddard, which as we know is the best PDS in the world. (laughter) I should mention that it happens over a wide range of PMT voltage settings and a wide range of aperture; by that I mean from 10-80 microns, we are not interested in much smaller aperture sizes than that.

Oliver: Yeah, this looks like, initially it looked like fatigue but that would happen only in the lowest densities and not at high densities. Have you looked at the current out of the PMT, since you are in a static monitoring situation, you have a constant current level. Can you look at the actual current to see if that is showing this effect or whether it shows only after you have gone through the logarithmatic amplifier and the A/D converter?

Cornett: It also occurs in tranmission, so I know at least one step back. Has it ever happended to anyone else?

Tony Hewitt: We had a birght idea, which was not at all bright, some years back realizing that the Hamawatsu photomultiplier of the PDS had been mistreated we decided that rather than replacing with an identical one we talked to some other photomultiplier manufacturers to see what we could find - EMI said, oh yes the PDS, we can select you somthing or other to handle exactly what you need out of a PDS. So we said fine, send us one. So they sent one after a few weeks and we collected all kinds of test data - we put it in and it turned out to show this affect on a time scale of a couple of minutes - which was gross. I think the indications are that is very probably in photomultiplier.

Chett Opal: The direction of the effect is generally color centered formation value - it also holds the photomultiplier to what occurs as variations in the electro-static potential to wall charging and that can go in either direction.

Heckathorn: Bob did you do a scan down, in the vertical direction?

Cornett: Yes to make sure that wasn't the way it looked. That's right.

Heckathorn: did you do that?

Cornett: Yes, yes.

Boyzan: It's not static this test which you used?

Cornett: Yes, this test is not static and we have one that is and it shows the same problem. Yes, I mean on our PDS it's quite obvious.

Dittmore: Can some of this be photographic process on your actual data?

Paul: Some of it could be, except we have repeatedly scanned; well we do know that. I better not get into a separate question. It isn't a photographic process. I know what you're talking about. By rotating on the same flat field 90 degrees and getting the same plot down the same scan direction. It will prove that this is the real effect in the PDS.

Don Wells: I wanted to give another piece of information about the Kitt Peak machine. Sometime in the middle 70's Jack Harvey from Kitt Peak got worried that the original photomultiplier was being overloaded that is, it was carrying heavier current than it was designed to carry and as a result of that along with the other modification. PDS came back and put in new photomultiplier which I think is about 2" cathode instead of the original smaller one and I think that was thought to be a better photomultiplier capable of higher current as I recall.

Don Hewitt: This just about completes my paper for this afternoon. (laughter) I point out the only reason for producing such a high anode current in the photomultiplier seems to be the limitation of the logarithmic amplifier which is awfully slow and needs a high input current. So if you fix the input electronics you could then operate the photomultiplier at a lower current.

Eric Crane: Is the peaking of the curve always at the center of your field?

Cornett: It is always nearly at the center within the constraints of the time scale. Yes.

Eric: Have you done some checking to see that it's not in the optical system itself. That looks like nothing more than vigoretting.

Cornett: Yes. But you can turn it 90 degrees and it would and it would be vignetted the other way and it'll be flat along this "column." In other words what I've done is to take a flat field that I scanned with this in the X direction, turn it this way and scan it again. Perform the same tests and compare line scans to column scans and it turns out the same way as far as scan directions are concerned not as far as flat field is concerned.

Craine: Do you still get the same peak and thats what you would expect?

Cornett: I don't believe so. No matter what happens, when I scan this way the vigoretting occurs like this and it's flat in this direction.

Anderson: What if you scan right along there so that you get something that's flat?

Cornett: Yes.

Anderson: But it seems then to have something to do with the distance say from here to here on the amplifier recovery versus from here to here does it? That's what we're talking about.

Horton: What is the length of time it takes to make the scan?

Paul: About two hours for the whole thing.

Horton: No, for the each scan line?

Cornett: Well, it's two hours over 2,000—a few seconds.

Horton: There is a space charge effect that you'll see in photomultiplier curves that usually shows up mostly going from a low density to a high density region. That will cause a drift effect. Usually it doesn't show up at all so if that were it would it be a skewed curve but still maybe something to do with that?

Characteristics of the MSFC, PDS Microdensitometer

by

W. F. Fountain
G. A. Gary
H. Oda
George C. Marshall Space Flight Center

Introduction

This report summarizes the results of several parametric studies carried out on the Marshall Space Flight Center (MSFC) PDS-10 microdensitometer for the purposes of documenting and understanding the operation and limitations of the system for inhouse research and to provide a bench mark for comparison with other microdensitometers.

This study is independent of photographic emulsions and represents the system response. The results are grouped into four general areas. These are (1) system overall stability to drift (2) photometric linearity and noise, (3) reproducibility and (4) scanning performance.

The MSFC system is a 1978 version of the PDS 1010A, manufactured by Perkin Elmer Corporation with a density range of 0 to 4 and includes a DecWriter keyboard; a 9-track PerTec DMT, and digital strip chart output. Data analysis and image processing is carried out on various other independent systems within the laboratory. The instrument is being used in a wide varity of applications including astronomy, contamination studies, atmospheric research, Shuttle engine analysis, and cosmic ray analysis.

Since becoming operational we have experienced only three significant problems with the system. Eratic scanning which was traced to a bad element on a motor control board, several sample table bearing failures, and eratic scanning at scan speeds below 2 mm/sec. (speed setting of 10). This problem has been improved by a factory adjustment in the divide by N function, however scan rates below 0.5 mm/sec. remain unreliable for our system. A change out of the original PM tube (Hamamatsu HTV-268) resulted in an overall improvement in system noise characteristics in 1981.

Parametric Tests

Test data taken in order to evaluate the interdependency of scan speed, noise and position are summarized in the following graphs. Shown also are results of tests for system stability, reproducibility, stray light and PMT settling time.

Figure 1 shows the long term stability of the system measured at a density of four over a 12 hour period. The large deviation during the 8th and 9th hours is unexplained. However, overall stability is normally with $\pm$ 0.05 density units.

The signal to noise ratio as a function of PMT high voltage is shown in figure 2 for a constant density value of 4.16. These measurements were made using a density wedge and the 12.5 x 12.5 micrometer square aperture. 20,000 readings were binned for each data point. The signal value is defined as the number of readings that fall within $\pm$ .02 of D=4.16. The S/N drop below a high voltage setting of 2.5 is attributed to PMT non-linearity at low voltages. Operating near a setting of 3 (500 volts) is recommended. Figure 3 shows the system noise statistics as a function of sample density for three effective measurement areas (100 μm^2, 400 μm^2, and 2500 μm^2), using 50,000 data readings at each density. The deviations from linearity at low densities is attributed to the digital resolution of the A/D converter. The rate of change of the standard deviation as a function of density for a 20 micrometer square aperature is S_2=0.27.

Following the standard calibration procedures thru clear glass for each effective scannning aperature produced the data show in figure 4. The corresponding aperture nomenclatures are listed in Table 1. For apertures with area greater than $\sim(100\mu m)^2$ a neutral density filter should be inserted into the optical path to maintain operation on the linear portion of the PMT response curve. This result is again reflected in figure 5 where the density reading for each system aperture is shown versus the PMT calibration voltage thru clear glass. Two of the standard internal neutral density filters of D=0.2 and D=4.0 were used. The density variations reflect both tube nonlinearities at the voltage extremes as well as system noise and possible alignment variations encountered when changing apertures and eyepiece optics. Also, each data point is an discrete measurement rather than an average value. The curves are eyeballed estimates of the trend.

Figures 6 and 7 were obtained by scanning into an opaque region from various initial density levels, in order to test the system response in moving from regions of high signal to low signal. This was done for a series of increasing scan velocities. Figure 6 shows the signal response lag in terms of aperture position for the 12.5 μm square aperture (B4). At a density reading of 4 and scan velocity of 39.2 mm/sec. the digitized signal lags are 2, 35, 45, 52, and 65 micrometers for initial densities of 4, 3, 2, 1 and 0 respectively. For the initial density case of 0, this converts to a time lag of 1.7 ms. Figure 7 shows the time lag for a wide range of scan velocities for the two cases of initial density equal to 0 and 1 with a

typical lag time 0.5 msec at a density of 4.0.

This signal lag, a PM tube phenomena, is most severe when going from high to low photometric signal and can introduce significant positional error in certain types of data, such as star images or high density spectral lines.

Figure 8 shows the effects of scattered light using the x4 optics and the 12.5 x 12.5 micrometer effective aperture. A sharp edged opaque sample was manually positioned in 1 micron intervals across the aperture plane. Residual signal due to scattered light remains evident to a distance of $\sim$25 µm beyond the theoretical cut-off point.

The remaining figures 9, 10, 11, and 12 graphically indicate the system response as a D=3 neutral density filter is scanned from both high signal to low and low signal to high at speeds of 980 µm/sec., 9800 µm/sec. and 39,200 µm/sec. All scans were done in the x-direction with no movement in the y-direction using the same 12.5 x 12.5 µm effective aperture as the other tests. Figure 11 shows a comparison of the system response at scan speed 5 (980 µm/sec) for the two cases of high to zero and zero to high density traverses. The data showing the high to zero density scan is reverse plotted for the comparison. At this speed it is seen that no distortions are due to scan speed and the curves represent true system response.

Figures 9 and 10 clearly show that the system response time is exceeded at the higher scan velocities for these conditions, with the maximum effect seen at high speeds moving from low to high density. This is a result of the electronics having been saturated with current and coming abruptly into a region of much less light. The optical transfer functions derived from these results were noisy and noise removal is an art, hence for the purpose of this paper these results are not presented.

Figure 12 compares a sharply focussed image with a defocussed (PMT objective) image with the visibly defocussing producing a displacement of 0.128 density units.

Summary

This parametric study of the MSFC microdensitiometer provides the operational characteristics of the system without reference to any optical sample. The test data establishes the operational region of confidence for our system. Calibration drift is minimal, in terms of a few hours, but should be checked periodically on long runs. Scan speeds between 500 and 20,000 micrometers/sec. can be reliably used with apertures with effective areas between 10^2 and 10^4 square micrometers with PMT voltages between 550 to 900 volts, and target elements greater than $\sim$20 micrometers. Outside these limits, effects due to noise, stray light, system time response and coherency effects require special handling of data in order to achieve reliable and consistent results with the system.

Table 1

Effective Scanning Apertures
for the MSFC Micro-10
with the 4x Objective
(micrometers)

A1(1)	50	E1	25 x 1000
A2(1)	25	E2	12.5 x 500
A3(1)	16.7	E3	8.3 x 333.3
A4(1)	12.5	E4	6.3 x 250
B1	50 x 50	F1(2)	75 x 1000
B2	25 x 25	F2(2)	37.5 x 500
B3	16.7 x 16.7	F3(2)	25 x 333.3
B4	12.5 x 12.5	F4(2)	18.8 x 250
C1	125 x 125	G1(1)	10
C2	62.5 x 62.5	G2(1)	5
C3	41.7 x 41.7	G3(1)	3.3
C4	31.3 x 31.3	G4(1,3)	2.5
D1	25 x 500	H1(2)	250 x 250
D2	12.5 x 250	H2(2)	125 x 125
D3	8.3 x 166.7	H3(2)	83.3 x 83.3
D4	6.3 x 125	H4(2)	62.5 x 62.5

(1) Diameter of circular aperture
(2) Neutral density filter needed for calibration
(3) Not able to calibrate

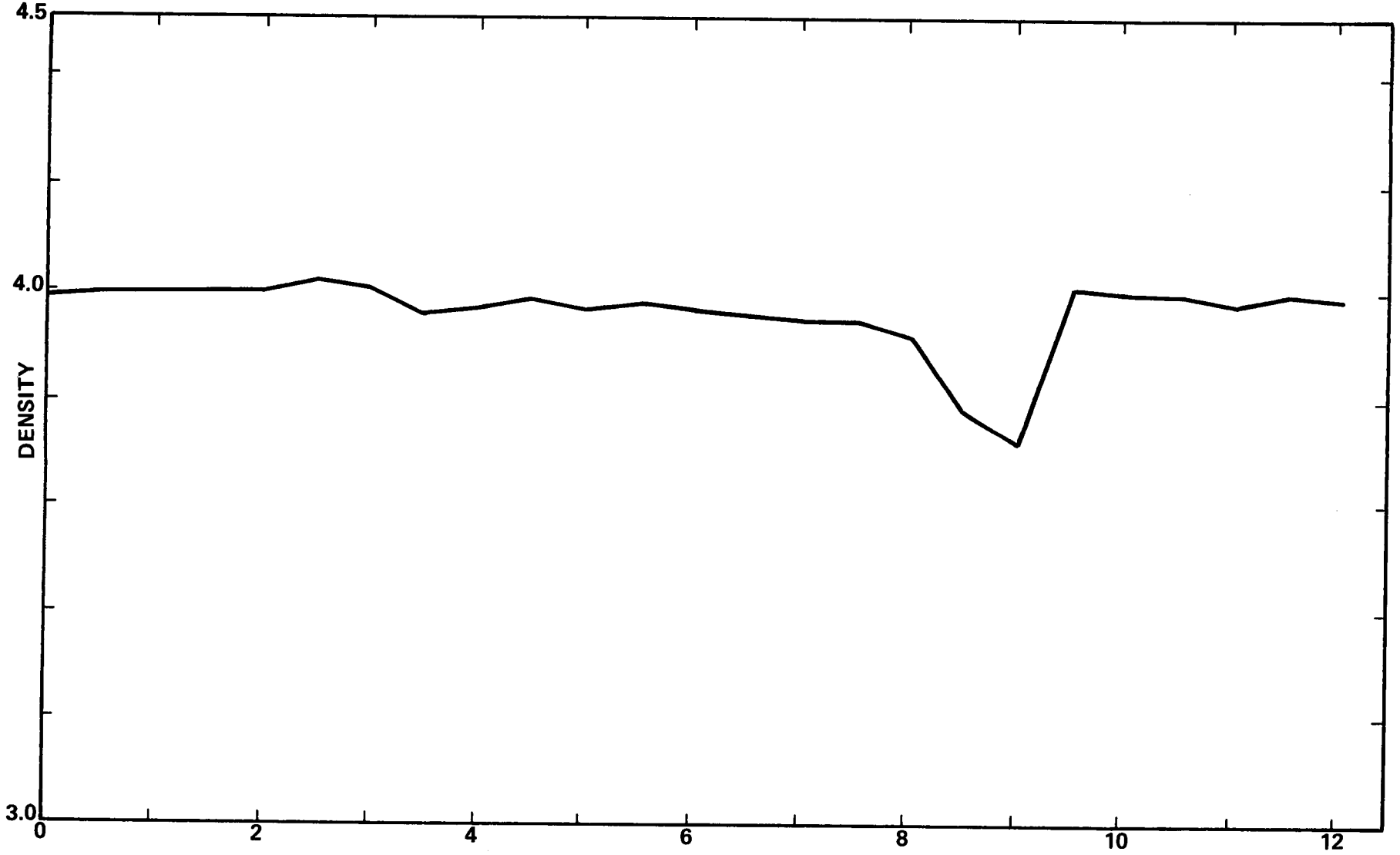

Figure 1. Long term stability of system at a density of 4 with 12.5 x 12.5 micrometer effective aperture over a 12 hour period.

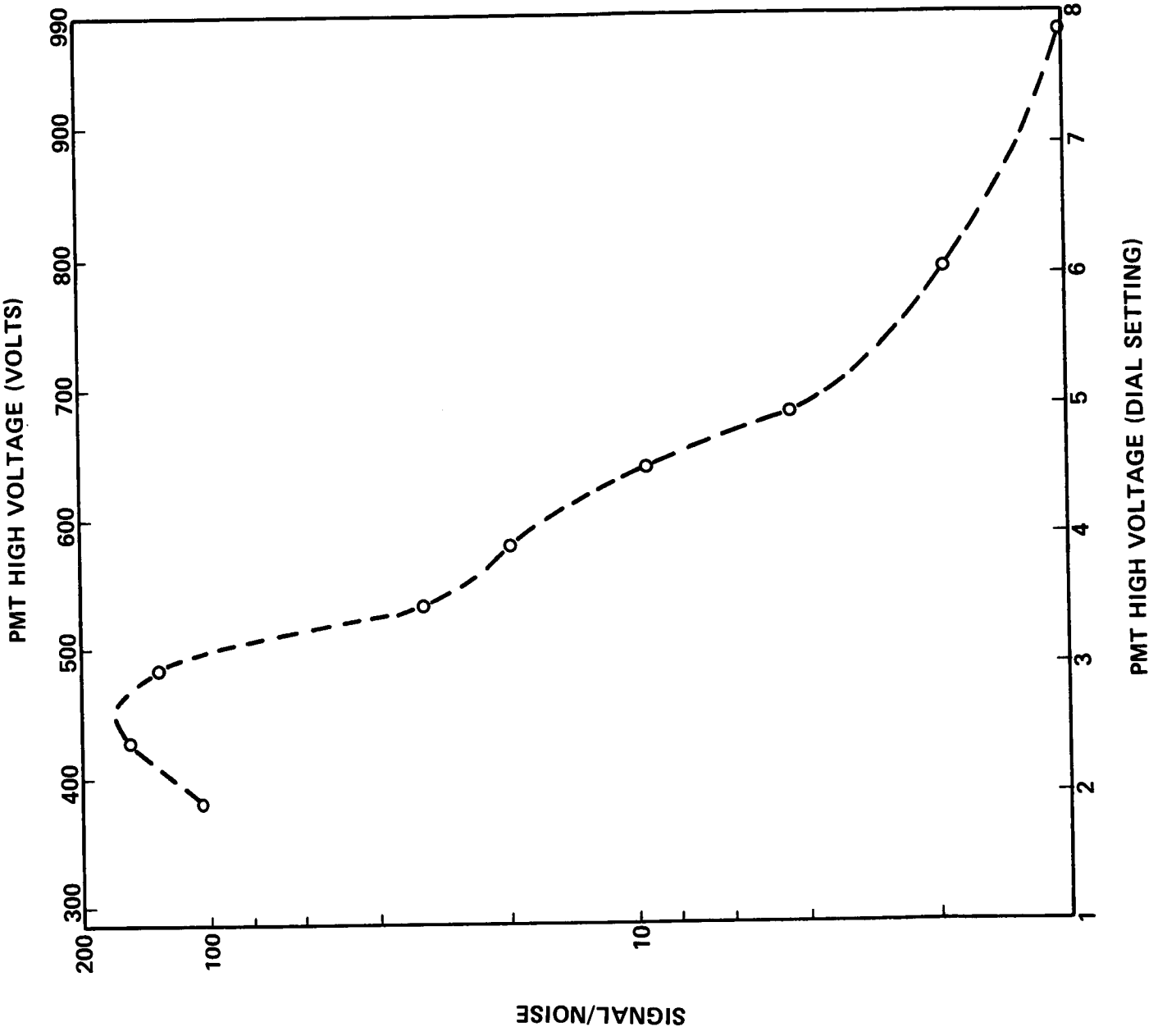

Figure 2. System signal/noise vs. H.V. setting for a density of 4.16, with a 12.5 x 12.5 micrometer aperture. The signal is defined as the number of readings within $\pm$ .02 of 4.16.

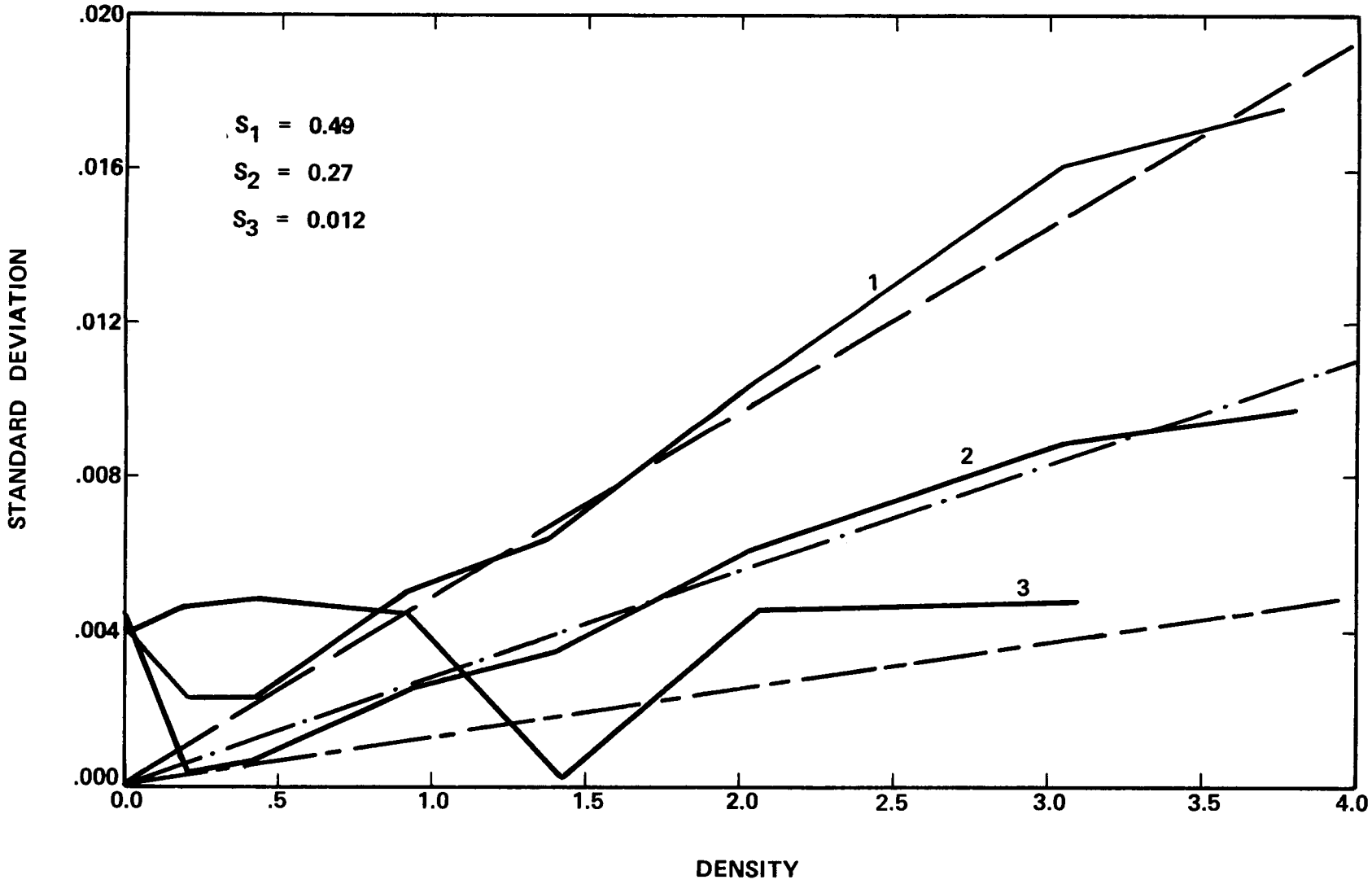
.020
.016
.012
.008
.004
.000
0.0
.5
1.0
1.5
2.0
2.5
3.0
3.5
4.0
S_1 = 0.49
S_2 = 0.27
S_3 = 0.012
1
2
3
STANDARD DEVIATION
DENSITY

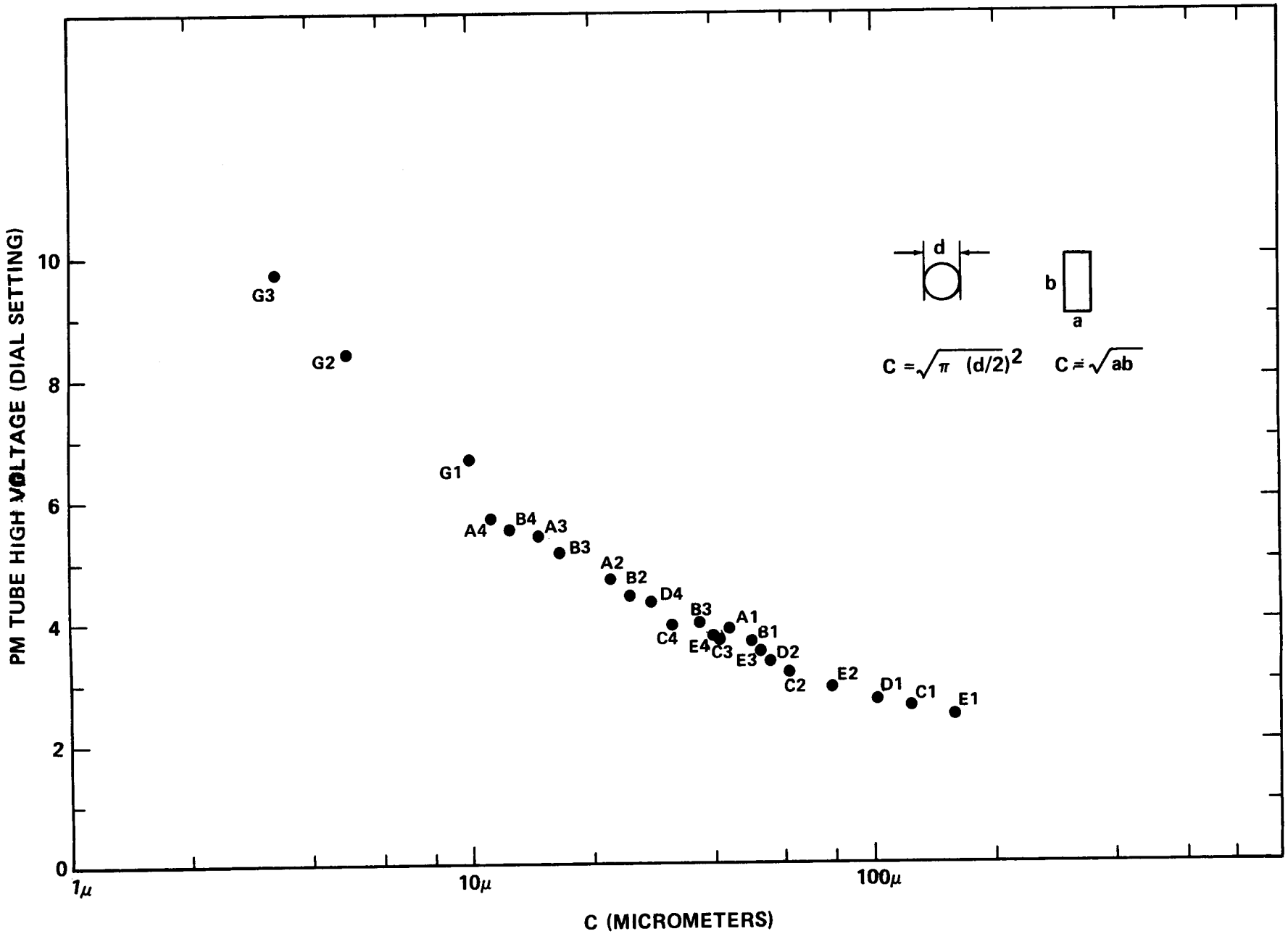

Figure 4. Calibration voltage level vs. scanning aperture area. The aperture nomenclature is given in Table 1.

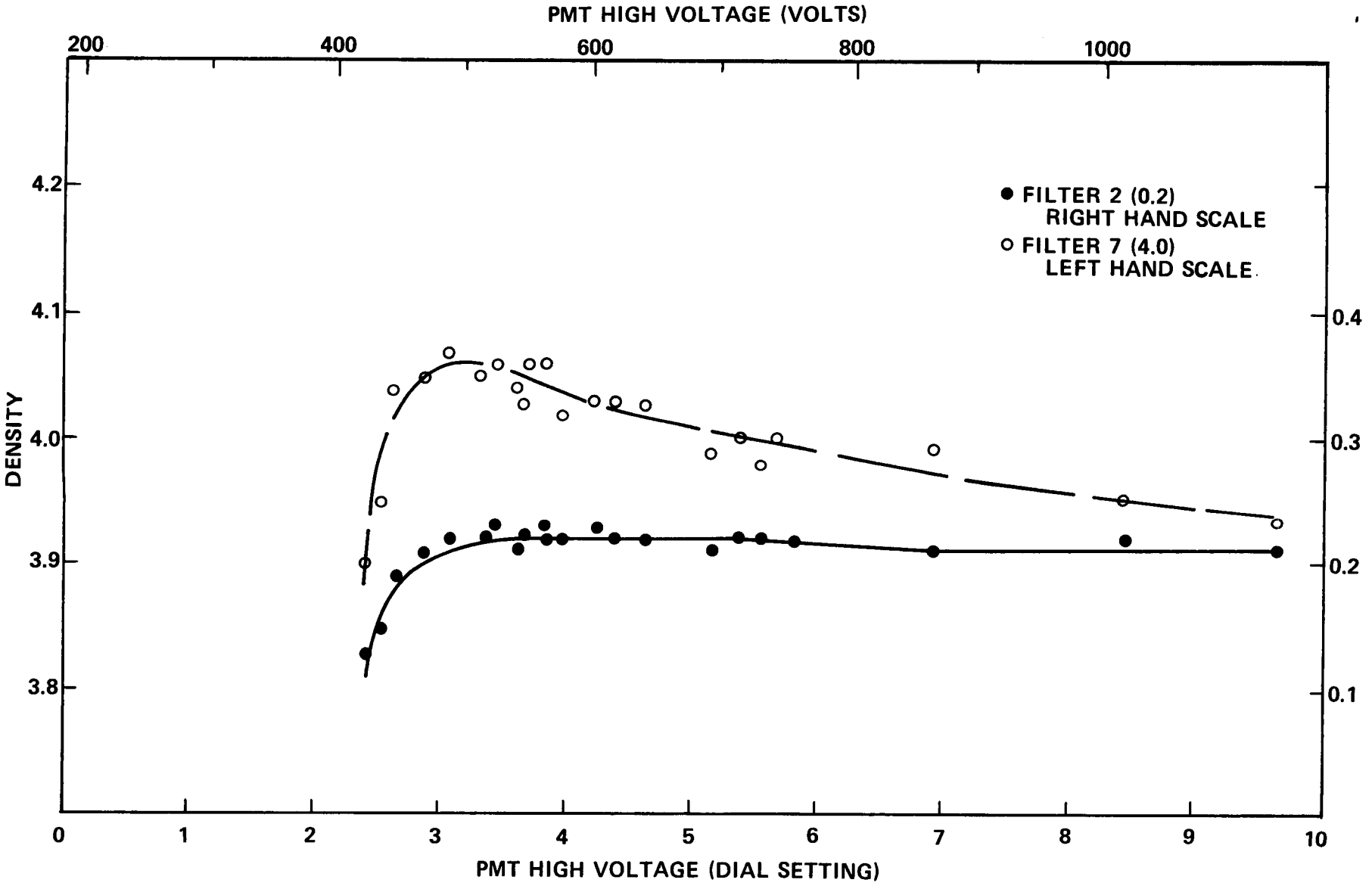

Figure 5. Composite of all system apertures vs. clear glass calibration voltage for 0.2 and 4.0 sample densities.

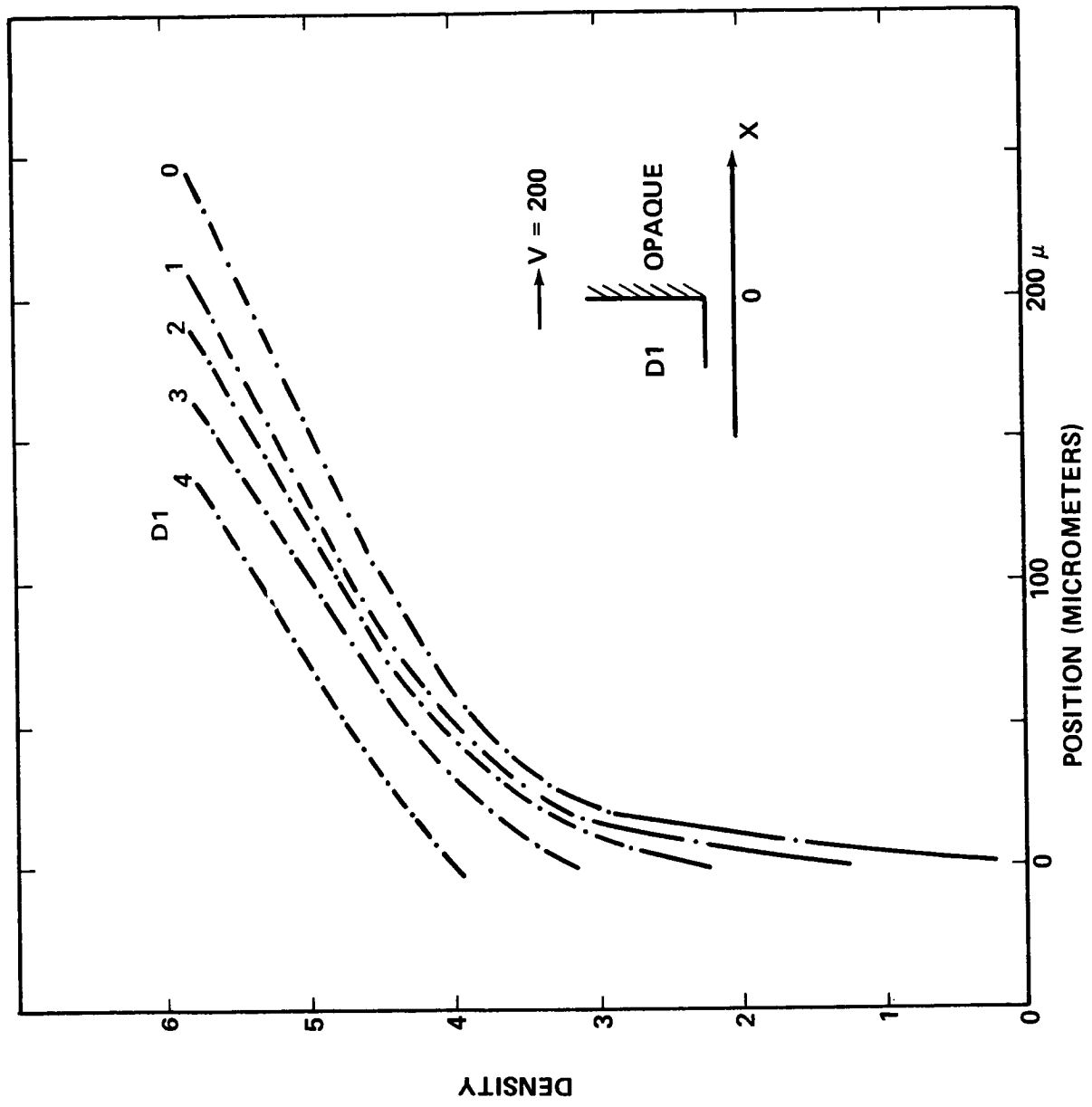

Figure 6. System response using opaque boundary and high scan speed (39.2 mm/s) showing signal lag for low density high density traverse. At a density of 4, lags are 2, 35, 45, 52, and 65 micrometers for initial densities of 4, 3, 2, 1, and 0 respectively. For an initial density of 0, this converts to a lag of 1.7 ms.

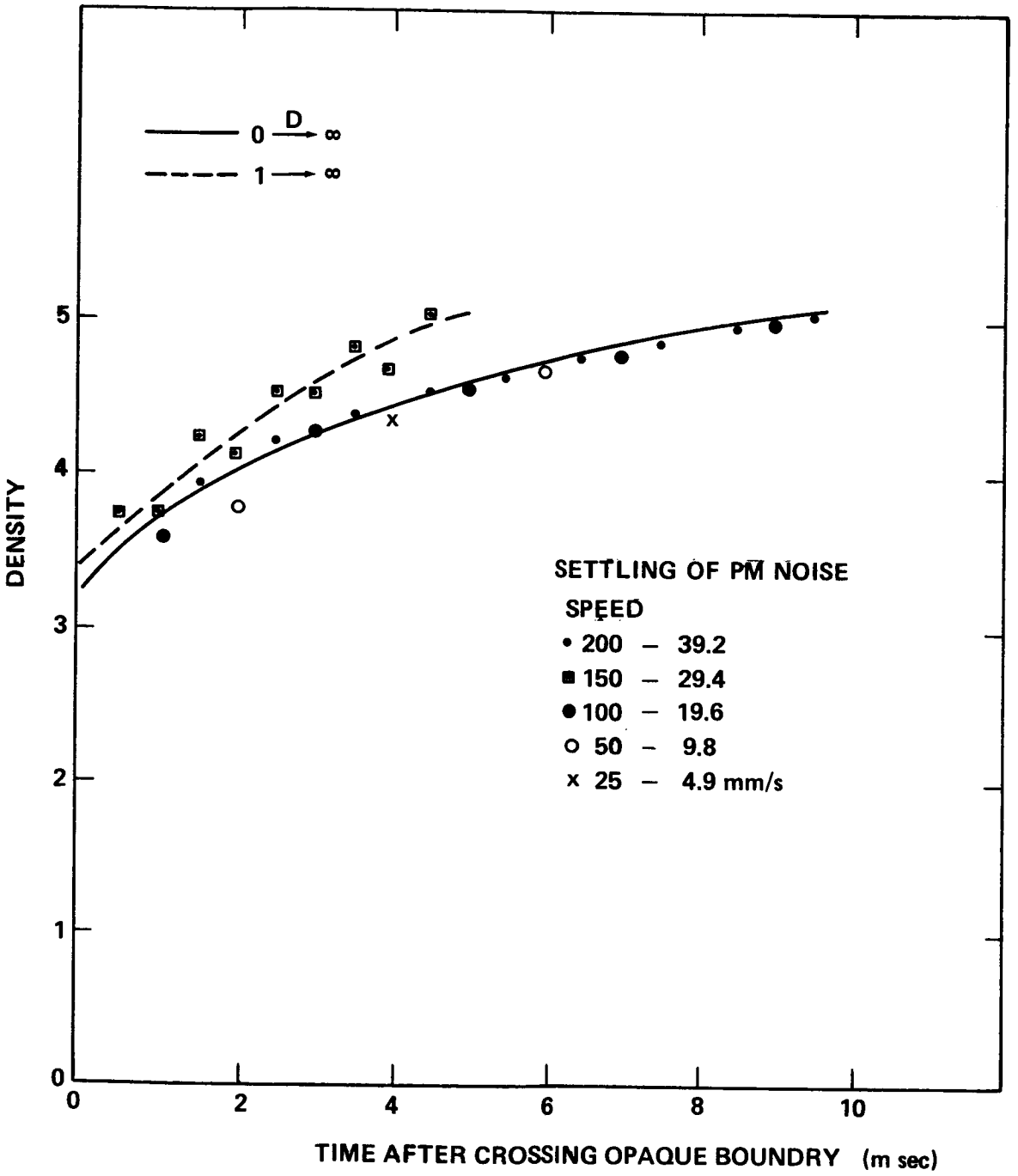

Figure 7. System response using opaque boundary and a scan direction giving low density to opaque traverses, for low side densities of 0 and 1. Aperture is 12.5 x 12.5 micrometers. The data is plotted for scan velocities of 4.9, 9.8, 19.6, and 39.2 mm/sec. A scan velocity of 29.4 was used for the D=1 to opaque scan.

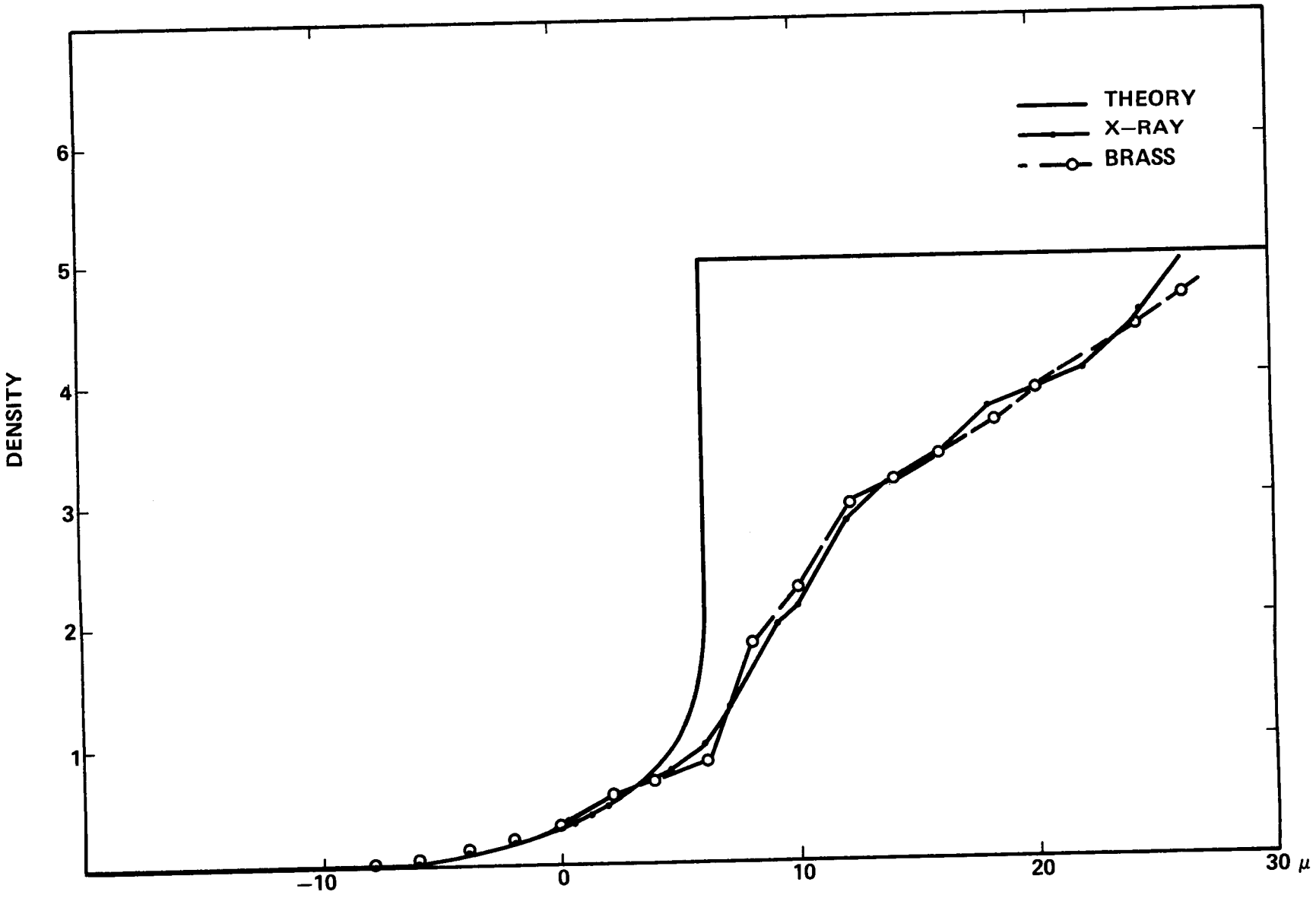

Figure 8. Stray light test for x4 optics and 12.5 x 12.5 micrometer aperture with manual positioning.

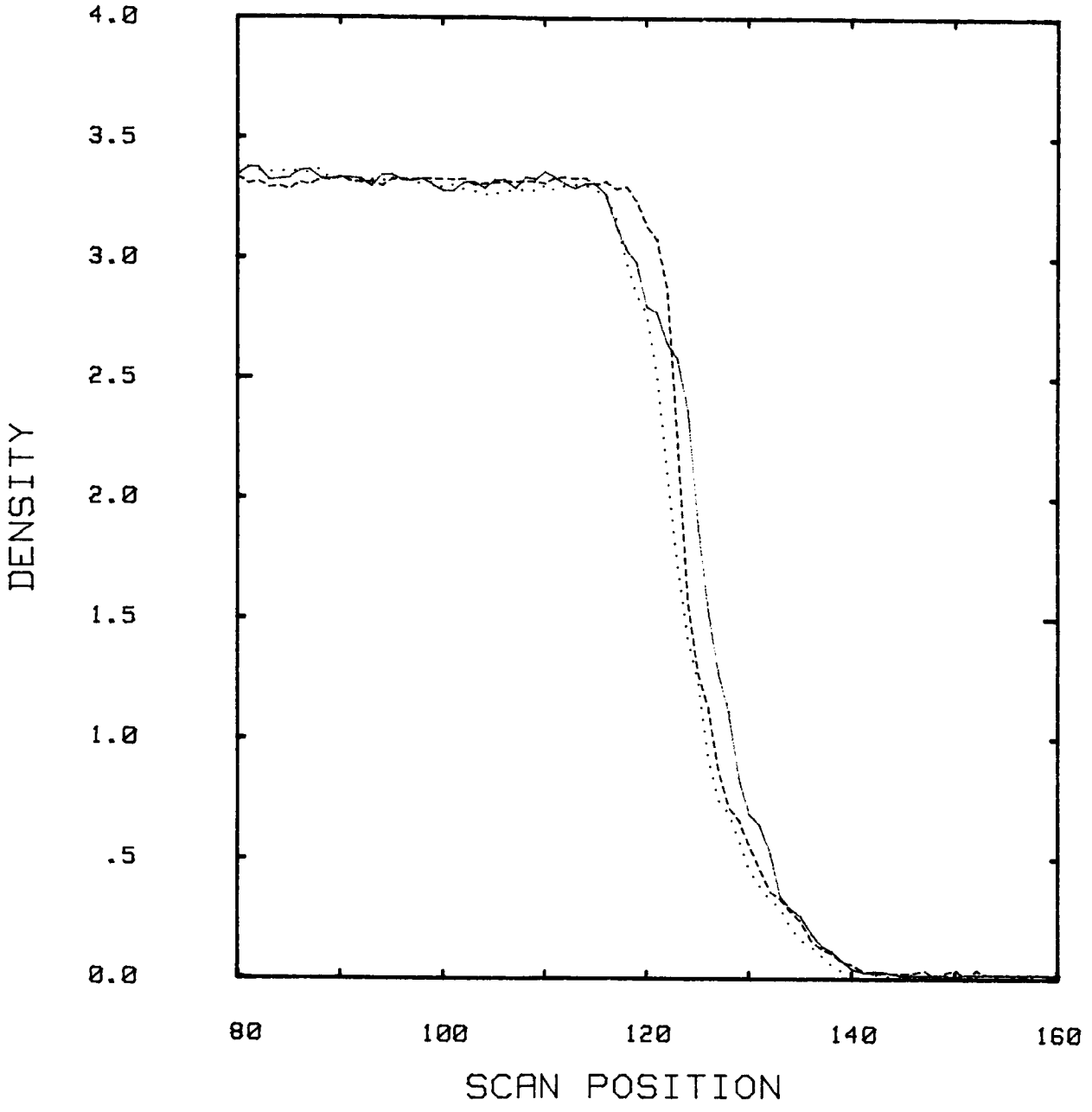

Figure 9. Response of system for high to zero density traverse of edge scans of a D=3.0 Wratten filter with an aperture of 12.5 x 12.5 micrometers at speed settings of ——5, ·····50, ----200 (or 980, 9800, 39,200 micrometers/sec.).

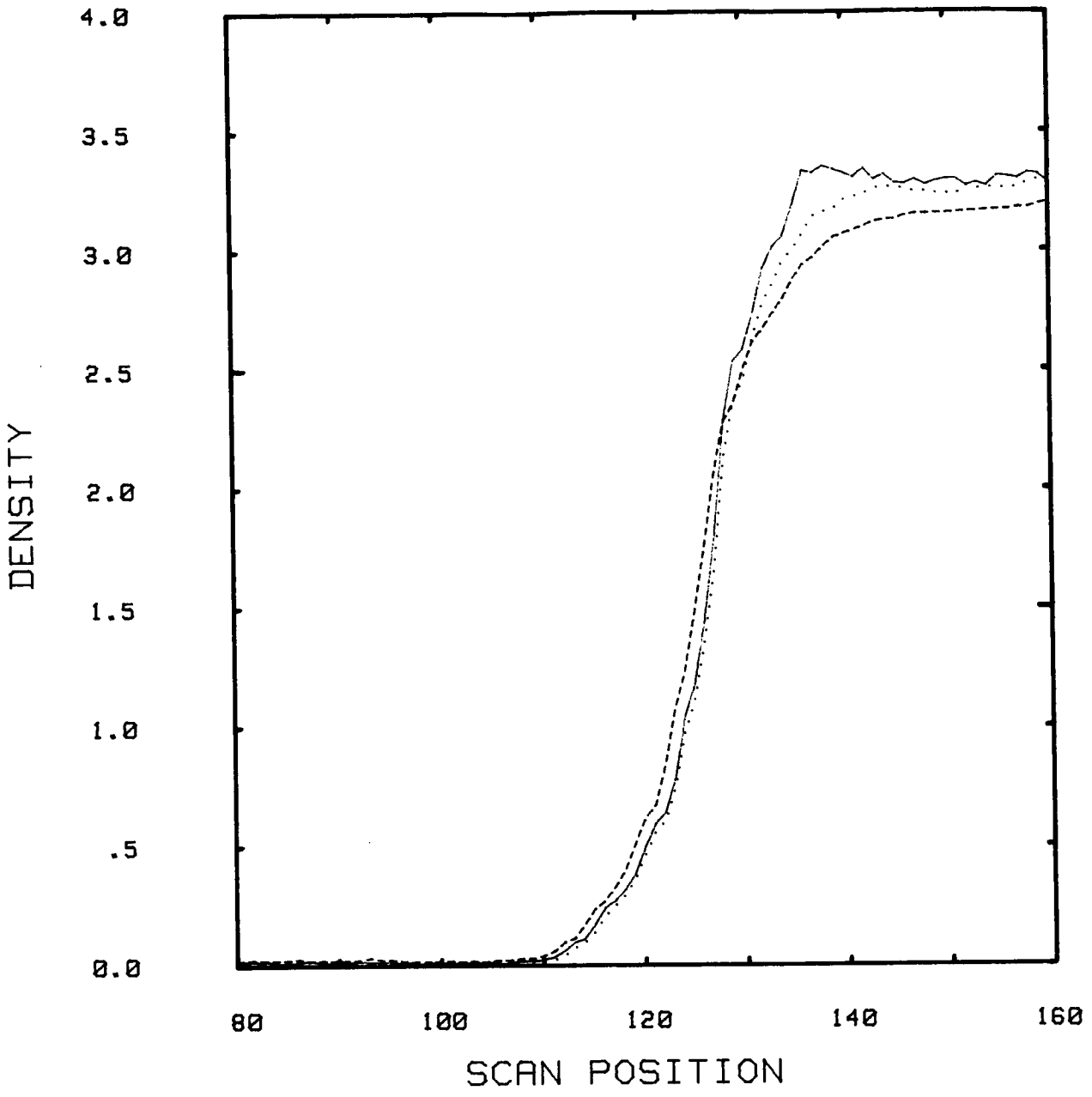

Figure 10. Response of system for zero to high density traverse of edge scans of a D=3.0 Wratten filter with an aperture of 12.5x 12.5 micrometers at speed settings of ———5,.....50, ------200 (or 980, 9800, 39,200 micrometers/sec.).

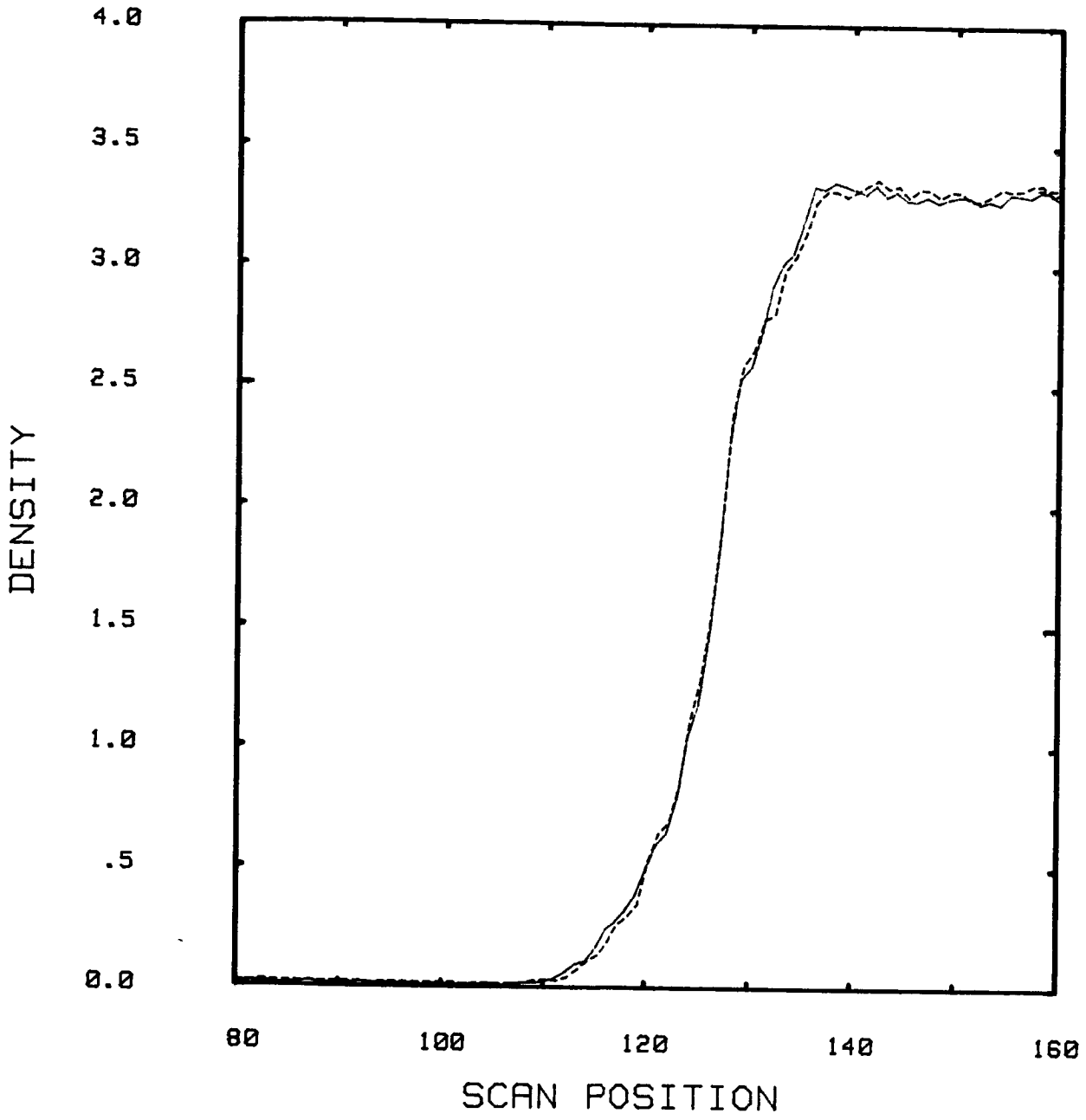

Figure 11. Comparison of system response at speed 5 (980 um/sec) for high to zero, and zero to high density traverses, with direction of high to zero reverse plotted for the comparison.

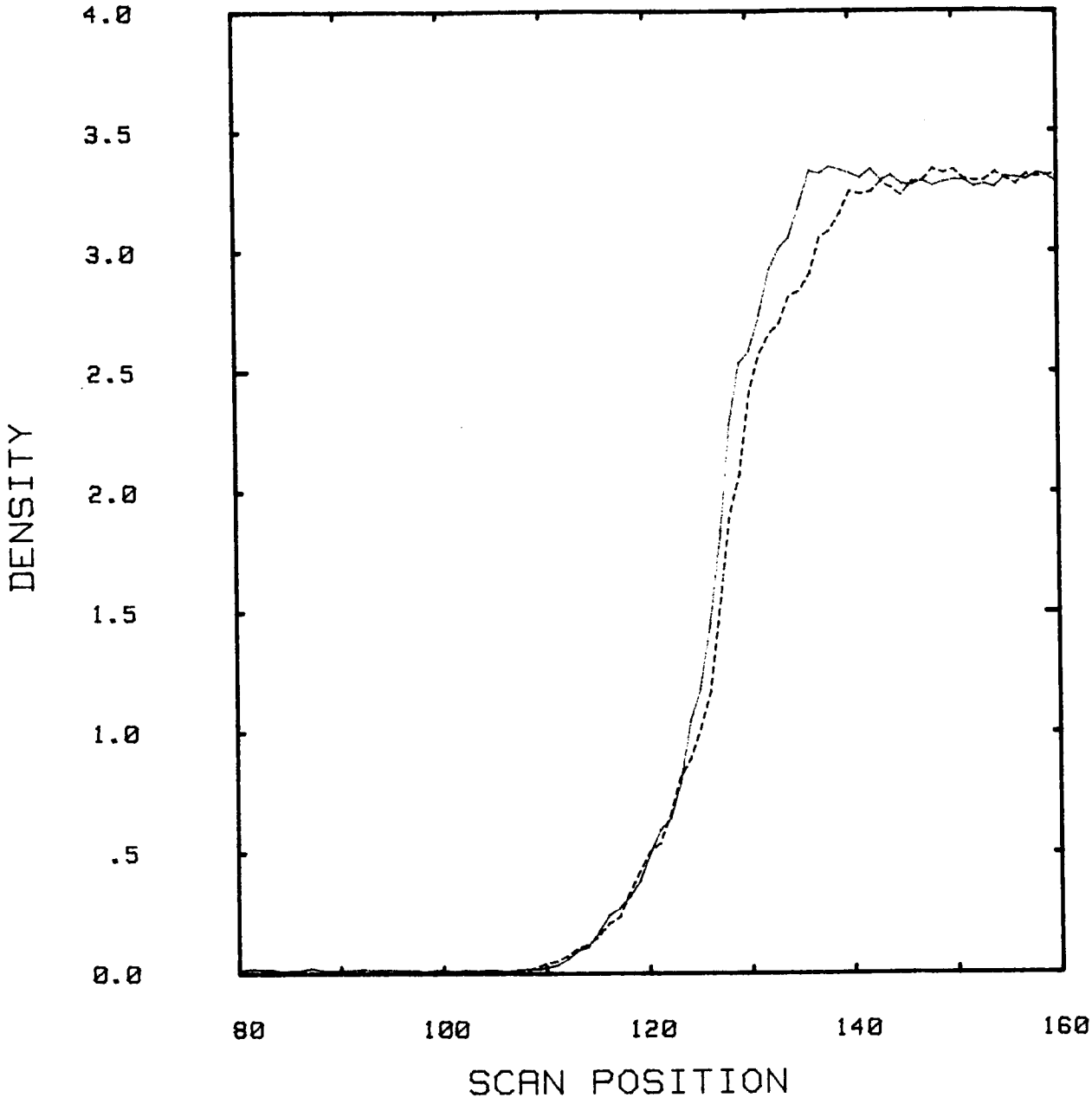

Figure 12. Comparison of sharply focused scan vs. defocused scan (PMT objective) with the visibly defocused scan displaced by 0.128 density units.

B. Lasker: Your first chart showing that glitch of eight hours in the sense of you're getting more light at the aperture. I guess it must have alarmed all of us who make very long scans. Seems to me superficially, it can exclude everything you said this morning about aperture misalignment because we're going through a light condition to more light and then back down. You said that you had an old lamp and regulated power supply. Where does one look to explain things like this?

Fountain: Well, I was hoping that we had some suggestions from this group. That's really a mystery to me. You have a comment about that.

Hewitt: Yes. I do have a comment about that. We did not discover this for ourselves, we were told about it and I'm surprised it hasn't been put in the record. The lamp socket oxidize because of the heat and our routine procedures is to place the lamp and place the socket at the same time. If we don't do that we find zero point shifts of 10 percent, pretty much random.

Dittmore: We got around that by silver sodering the lamps.

Angellio: You don't say what time this data happens but its been reasonably common that at quitting time all kinds of things happen on the line and not only this type of data but other type of data that shows similar kinds of glitches in and around quitting time expecially around 5 o'clock or so in the afternoon and to a lesser extent in the morning presumbly people come at different times in the morning. So it is not quite as prevelant. Even though you have things like regulated power supplies and what have you sometimes the loads on the line are really fantastically different at that time of day.

Fountain: I may not have mentioned it but this data was started at 6 o'clock in the afternoon.

Poland: Is there any chance someone came in the room?

Fountain: That's a possibility because security people do wander around in those buildings at night. The door is not locked, it's closed.

Horton: That is probably a thermal drift problem and you can get more light through, at least more signal out because of thermal drift just by having the light spot that hits the PMT move to a more sensitive area of the PMT. So, just because you get more light does not mean that is was not a thermal drift problem.

Fountain: That's why I mentioned that I was sorry I didn't monitor the temperature. They do at times cut off the air conditioning units and cut off the power to conserve energy. I am not aware if they did anything right at that time of the morning. It's possible.

Landau: Did you look to see if this happened again? Is it one of many glitches?

Walter: No. That is only one such one. I have seen what appears to be possibly that type of thing occurring but of course in the midst of making measurements then you see some change occurring with calibration; what I do is stop and recalibrate. And probably when I that then I don't see any further drift. I've never seen anything of that magnitude before.

PERFORMANCE OF THE ESO PDS

P. J. Grosbøl
European Southern Observatory
Karl-Schwarzschildstr. 2, D-8046 Garching, FRG.

ABSTRACT

The astrometric and photometric performance of the PDS 1010A microdensitometer at ESO is discussed including the tests used for checking it.

1.0 INTRODUCTION

A PDS 1010A microdensitometer with a 10-bit A/D converter and the 5D option was ordered by ESO in 1978 to compliment the Measuring Machine Facility (MMF) which consisted of a one dimensional GRANT 800 series comparator/densitometer and a two dimensional OPTRONICS S-3000 flat bed microdensitometer. Since the OPTRONICS already offered a high positional accuracy and could accommodate 14 inch Schmidt plates the main objective of the purchase was to get a densitometer which could digitize densities up to around 5 and had a fast moving stage. The PDS was delivered during the last half of 1979 to ESO in Geneva where it was incorporated into the existing system and tested. The whole MMF was then moved with ESO to its new headquarters in Garching in the summer of 1980.

2.0 INSTALLATION AND OPERATION

The PDS is standing on a separate concrete floor in an air-conditioned room in the basement. The temperature is kept constant within ±0.5°C, however, sudden changes of the heat disipation in the room may cause a temperature drift of approx. 1°C due to the low air exchange rate of the system. All equipment in the room are kept on continuously to avoid such variations and to improve the stability in general.

The control of the PDS is done by a HP 21MX computer through a Universal Interface 3100UI. This computer performs all real time tasks including storage of data on a 1600 bpi magnetic tape. It is linked to a central HP 1000F computer which takes care of all user interaction and administration. The control software has been written by ESO and looks for the user almost identical for all the measuring machines (see, Melnick,J. 1980 in Proc. of ESO Workshop on Two Dimensional Photometry, Eds. P.Crane and K.Kjaer, Noordwijkerhout, p.53). The usage of the PDS has gradually increased since the installation and is now typically between 300 and 400 hours per month.

3.0 PERFORMANCE

The general level of performance has been found to be very constant with exception of problems caused by componant failures. It is typically checked twice a year, however, the most important test is done by monitoring the data obtained by users.

3.1 POSITIONAL PERFORMANCE

The positional accuracy of the stage was measured by Siemens using a laser interferometer. The differences between the measured and the actual positions are given in Figure 1 where two spatial resolutions are shown for each axis.

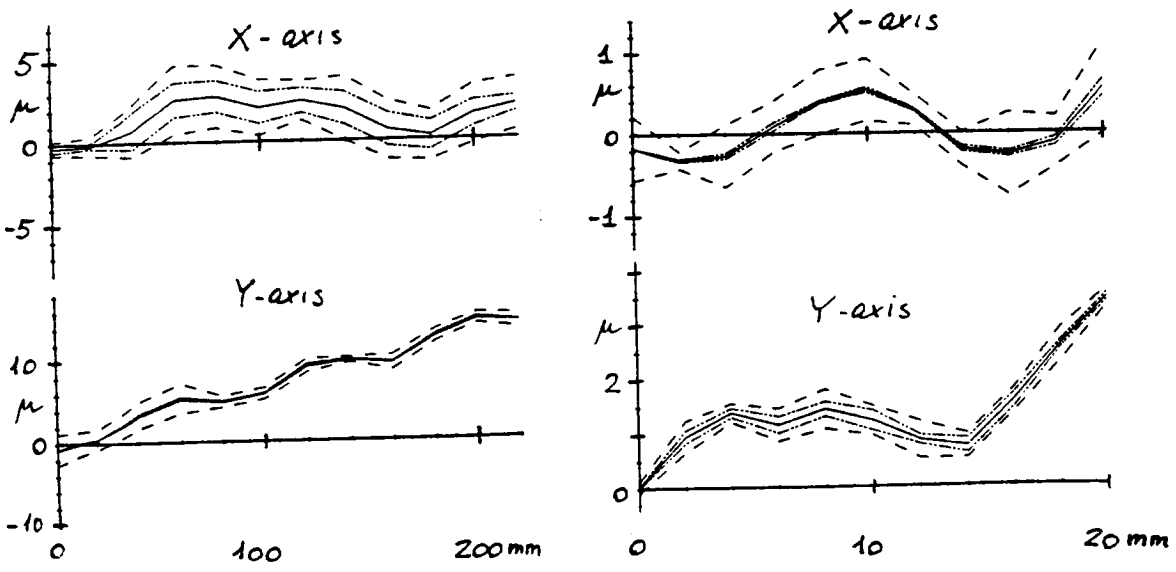

Figure 1: Absolute positions minus PDS readings for X and Y axes.

Besides a general systematic error a cyclic variation with an amplitude of Ø.5 micron is present probably due to the bearings. The positional repeatability is for both axes of the order of 1.5 micron. This is in good agreement with results from measurements of stellar images on plates yielding an internal error of 1 micron. Temperature variations in the room effect the accuracy significantly but were kept much less than Ø.5°C during these measurements.

Moving the stage to a given position one finds that it may start jittering around this location (especially in X) when the AUTOLOCK mode is used. This oscillation can have an amplitude of 5-1Ø micron and will not in all cases be damped out. It is caused by a wrongly ajusted mechanic/electric feedback and can therefore be reduced modifying this feedback loop. We found that the problem could be solved by reducing the AUTOLOCK speeds to 1 and 2 PDS units for X and Y, respectively, in addition to reducing the tension on the linear actuators as much as possible. The ajustment of the tensions is now done by loosening the actuators until the standard error of the deacceleration ramp distance for maximum speed increace to approx. 2Ø micron. After this lower tension setting was used there has not been seen any significant mechanical wear of the bearings.

Scanning with low speeds it was observed that the distance between samples some times was smaller than the specified value. This problem was located to the use of the unsigned positional increment for calculating the distance between samples. Especially at low speeds the stage may still jitter slightly during the first part of lines being scanned causing both positive and negative increments. An electrical circut was installed to remove this problem in the X-axis. Further, a minimum ramp distance of 2Ø micron is used for low speeds in order to give the oscillation time to damp out.

3.2 PHOTOMETRIC PERFORMANCE

An EMI 9789A photomultiplier tube specially selected to have a low dark current is used as detector. The original amplifier board was modified slightly to accommodate an Analog Device 755N amplifier which is 2-3 times faster than the original. The linearity of the photometric system is checked by scanning a continuous metal-film neutral density wedge with the different built-in filters. The departure from linearity can then be obtained by subtracting and normalizing the scans. This are done for both density and transmission mode. A typical curve for density mode is shown in Figure 2 where the difference between the original scan and one with an additional Ø.93 density filter is given. The error varies smoothly over the whole range of 5 densities with a maximum error of less than Ø.Ø5 density units.

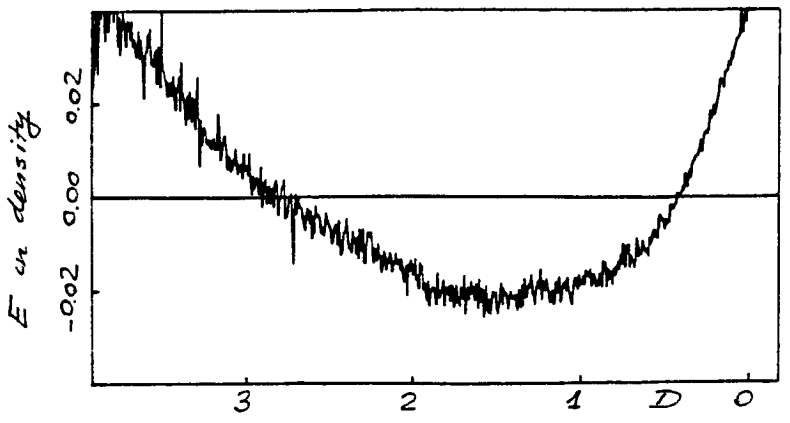

Figure 2: Non-linearity of the PDS density reading R given as the error $E(D) = R(D+\Delta D)-R(D)-\Delta D$ as function of density D for $\Delta D=.93$.

The Interobservatory Densitometer Calibration Plates of set No. 30 and 38 were measured yielding the general transformations to Diffuse Transmission Densities. The mean Callier Q factors for the emulsions are given in the Table 1 using the mean density values listed in AAS Photo-Bulletin No.18, 1978.

Table 1: Mean Q factor for the ESO PDS.

Emulsion	Q (Set 30)	Q (Set 38)
Ia-O	1.24 -+ .02	1.28 -+ .03
IIa-O	1.27 -+ .01	1.28 -+ .01
IIIa-J	1.26 -+ .01	1.19 -+ .01
649-F	1.04 -+ .01	1.03 -+ .01

All measurements were done with a 25 micron square aperture using the central 70 percent of each step to compute its mean density. There was seen no effects from changing the high tension applied to the tube as long as it was kept above 700 V.

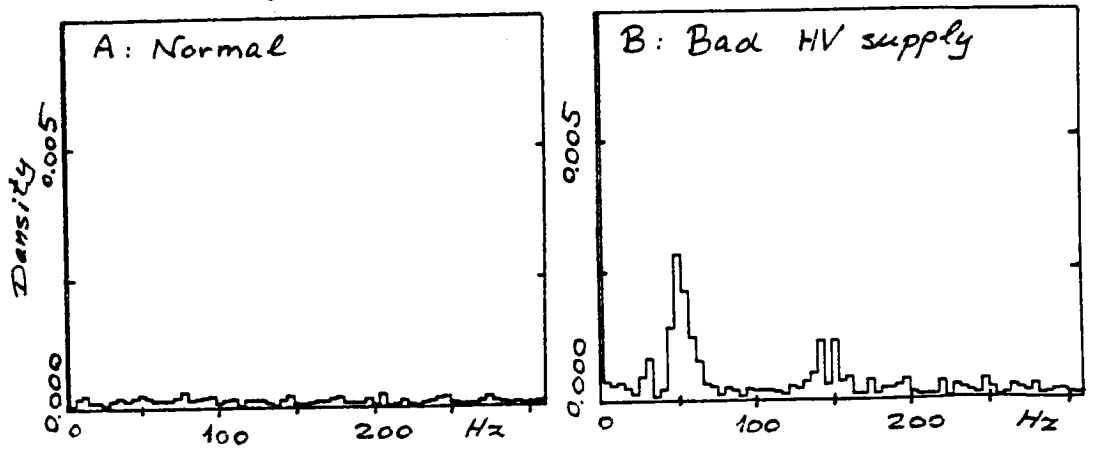

Figure 3: Power spectrum of PDS density readings on clear plate.

Although the AD 755N logarithmic amplifier is faster than the original it is still the limiting factor which determines the maximum usable scan speed for a given application. Scanning with the maximum speed of 50 mm/s the highest reliable density is around 2.5 while only the slowest velocities (i.e. < 1 mm/s) can be used if objects with peak densities above 4 should be measured.

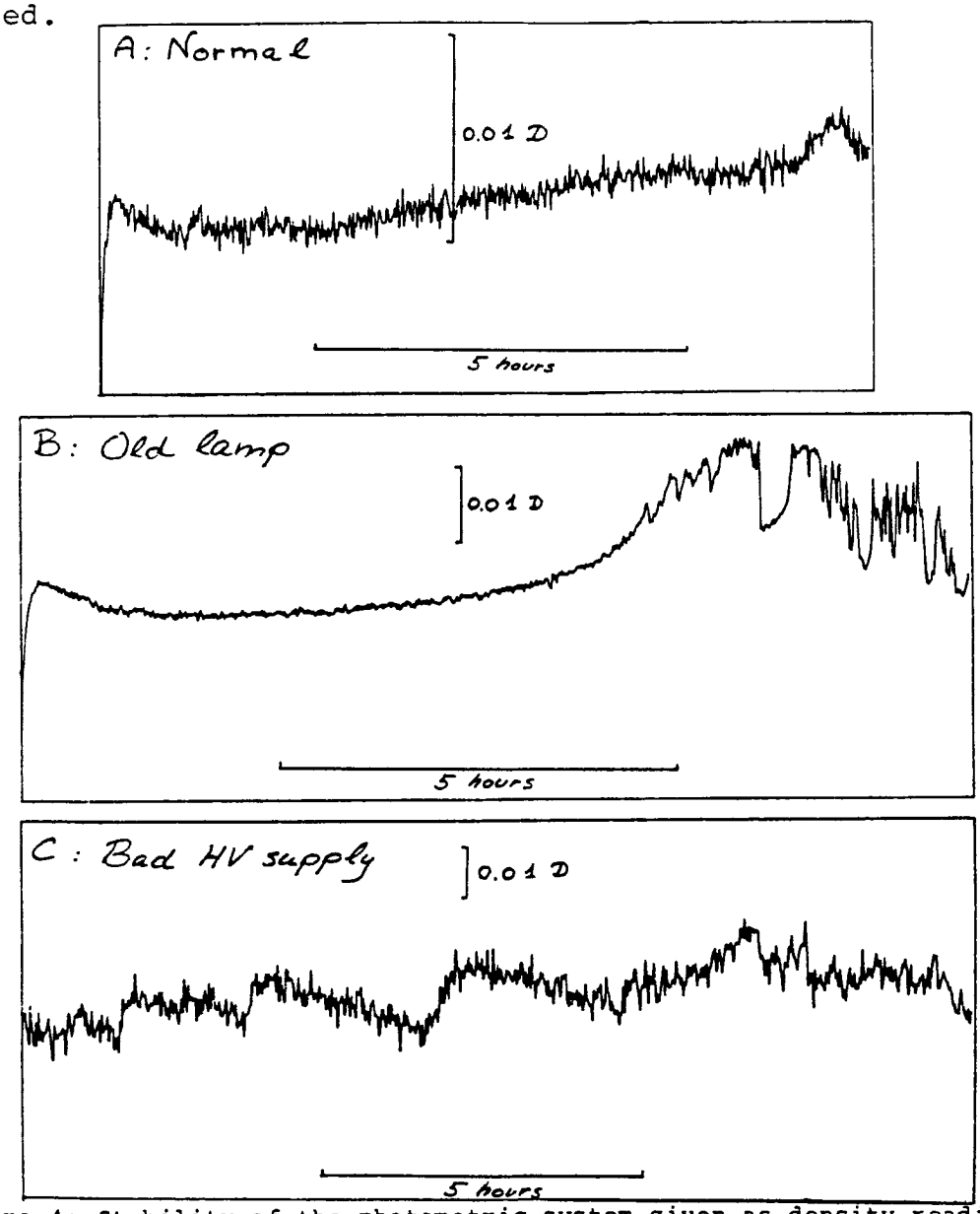

Figure 4: Stability of the photometric system given as density readings as function of time.

The stability of the photometric system is also of high importance for the general performance. Both short and long term variations (i.e. noise and drift) are monitored by digitizing values from the PDS at given time intervals only with a clear glass plate in the beam. One of the built-in density filters is

used to get readings in the typical range. The values are Fourier transformed to analyze the short term variations and to find harmonic fluctuations (e.g. from the power supplies). A normal power spectrum is shown in Figure 3 where also a power spectrum taken with a bad high tension supply is given for comparison. The long term stability of the system is normally monitored over a period of 10-15 hours during the night. Three examples of such long time monitoring are shown in Figure 4 where A) is a normal case, B) is showing lamp variations approx. one day before it failed, and C) gives a worst case when the high tension supply went bad. The actual stability obtained also depends on how well the alignment is done, the fixing of the upper objective, and temperature variations in the room.

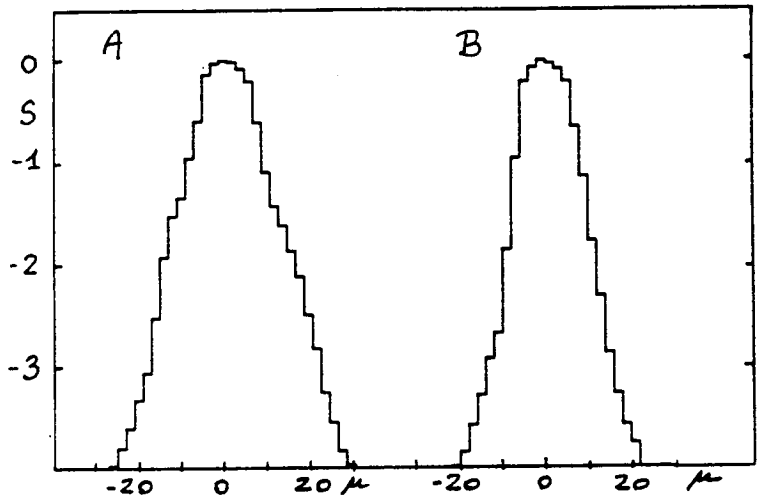

Figure 5: Logarithmic response S as function of distance from center of a 10 micron slit using A) 30 micron and B) 15 micron preslit.

The stray light in the upper optical system was determined by scanning a pinhole with a 2 micron diameter. To estimate the relative importance of the preslit aperture a 10 micron square slit was measured twice using a 15 and 30 micron preslit, respectively. The logarithmic response relative to the central value is given in in Figure 5 for both tests. It can be seen that the larger preslit gives significant more stray light. Thus, it is recommended to use the matched set of apertures.

4.0 CONCLUSION

The PDS 1010A has satisfied our basic needs for photometric measurements of astronomical plates with respect to dynamic range and stability. It is, however, important to know its limitations and use it accordingly. Also its positional repeatability of approximately 1.5 micron is adequate for a number of application.

B. Lasker: Is the scale on that last chart you showed linear or logarthmic?

Grosbol: It's logarithmic. I have numbers for it if you want to see "isoplots" and so on.

Hemenway: What is the scattered light density and what percentage of the scattered light do you get and how much of a problem is it?

Grosbol: Now you may mention that is doesn't come very much light through a 2 micron circular pinhole and that this is a very limiting factor. Basically, I haven't been able to push the PDS so that I can get reliable data varying these different kind of parameters.

Opal: I don't know if you know the answer to this but the cooling of the optics. Do you know anything about this?

Grosbol: We have not, basically even touched the optics. We have used it as supplied. We simply have monitored this so we can present data to the users saying that they should watch out. This will affect the maximum density you can obtain in a very sharp image.

Van Altena: In order to improve the infocus range we have recently changed from the 10 power objective to the 5 power and the coating was not as good and we see considerably more scattered light in the system than we used to.

Grosbol: We had the four power objectives. We don't use them basically because the range, the large aperture are not illuminated smoothly enough.

B. Lasker: Bill (Van Altena) may I ask of you what else haven't you changed and how much easier is the focusing depth?

Van Altena: It solved most of our focus problems. We just use the five power objectives now. We save the 10 power for very special comparisons. We would like to get some better objectives with better coatings on them. We just have not ordered them yet. Our depth of yield is now better by a factor of two.

Anderson: We obtained two power objectives for our PDS. Again no depth of focus problems, but mechanically we are just barely able to get to focus because mechanical setup is such that we can barely do it. We do have a few users who want very large sample areas for them we have to use those.

Dittmore: You get an entirely different density readings when you use different numerical apertures. You can't compare data taken now with the past.

EXPERIENCES WITH A PDS 2020 GM

Dieter Teuber
Astronomisches Institut der Universitaet Muenster
Domagkstrasse 75, 4400 Muenster
Federal Republic of Germany

1 STATUS

1.1 Basic Configuration

In April/May 1982 a PDS 2020 GM connected to a Perkin-Elmer PE 3220 computer was installed at the Astronomical Institute of Muenster University. This microdensitometer is capable of scanning areas up to 20"x 20". The single scan segments are controlled by a microprocessor, while the overall control program resides with the PE 3220. The main part of our PDS is a 52" x 54" x 10" granite block resting in a steel frame. It is the support for the scanning mechanics. Almost all electronics is mounted inside the steel frame.

1.2 Computer and Electronics

At the time we planned to buy our microdensitometer, the Perkin-Elmer Applied Optics Division (PE AOD) normally offered the PDS in combination with a 16-bit DEC computer. Because we are ultimately interested in digitizing large areas and in performing on-line reductions we decided to equip the system with a 32-bit computer.

The overall control program is a rewritten version of SCANSALOT. It comprises the major functions of the basic program. Only the driver for the parallel interface inside the PE 3220 had to be created in the assembly language of the PE-system.

The largest data blocks which can be transferred to the host computer contain 3200 data points. Scans longer than that are automatically segmented. An extension to a block size of 16 000 is in preparation.

The scanning speeds range from 30 to 255 PDS units. The equivalent speeds in conventional units are shown in Fig. 1.

The analog electronics is equipped with the 0-5 D amplifier.

In cooperation with PE AOD we built additional "electronic fine positioning handwheels" to facilitate exact positioning of the targets.

All reduction programs running on the PE 3220 can be administered by the monitoring system ADAM (Astronomical Data Analyzing Monitor) (1).

2 OPERATIONAL EXPERIENCES

2.1 Thermal Effects

During operation of the PDS the main granite block suffers deformations from being locally heated by the power supplies. Removal of all electronics from the steel frame would solve this problem, but create others, see e.g. 2.3. Instead, cooling with 12 fans mounted in the side panels proves to be an effective measure against unequal heating.

The optical and mechanical parts of the instrument are made of four different materials: granite, steel, glass and aluminum. The latter has a much larger thermal expansion coefficient than the others. Though the temperature of the microdensitometer room is stable within $\pm$ 0.2° C, these small variations still cause shifts of the Heidenhain scales and of the optical parts.

To keep the effects as small as possible various protective arrangements were designed in collaboration with PE AOD:

The scanning mechanics must be insulated from the circulating warm air. This is accomplished for the x-axis through two acryl covers which leave enough space for the glass platen to assure easy mounting of the photographic plates. They alse serve as dust covers and give protection against mechanical damage. Cleaning can be performed without hindrance.

Y-axis scanning is performed by the C-frame which carries at its bottom the illumination optics and at its top the photometer system. Here, most problems arise from the lamp. The heated air gives rise to deformations of the granite bars which support the C-frame thus causing positional errors. They may well also be responsible for the frequent defects of ball-bearings reported by van Altena (2). In order to keep the warm air away from the granite an exhaust pipe was installed through which the heated air is blown beyond the granite in all positions of the C-frame.

The photometer arrangement at the top of the C-frame is also very sensitive to temperature gradients such as are introduced through asymmetries in the cool airstream from the airconditioning system

of the PDS room. The result is a tilt of the upper microscope which causes a shift of the pre-slit relative to the measuring aperture. A ventilated cover to avoid this effect is being developed by PE AOD.

2.2 Vibrational Effects

Vibrations are introduced from inside and outside the microdensitometer. The outside vibrations were studied in great detail because we could not avoid installing the PDS on the seventh floor of a large concrete building, where our institute is located. The specific place was carefully chosen. The PDS room is near the exact center of the building, the y-axis is aligned with the long axis of the building, the support structure of the machine is not connected to the floor of the PDS room.

Fig. 2 shows the positional repeatibility of our PDS (3). There seem to be no resonance effects, a good indication of the stability of the driving mechanics. At speeds less than 30 PDS units spurious effects occur which are not yet clearly understood: the x-carriage sometimes drives into overtravel while executing a regular scan. This may be due to transient excessive shocks, but so far we were not able to record one of these events with a storage oscilloscope.

The vibrational noise of the x-axis has a peak-to-peak amplitude not larger than $\pm$ 0.2 µm. The frequency range of these vibrations extends from about 5 Hz to 125 Hz. Even at speed 1 the deformation of the sine wave signal of the Heidenhain encoders should not be affected by more than 5% in the x-direction.

The much larger mass of the C-frame makes it more sensitive to vibrations. Here the positional noise has a peak-to-peak amplitude of 2 µm. This is well within the range of the autolock. We have, however, to take into account that the C-frame is not yet damped as is the x-carriage. PE AOD is prepared to install frictional brakes on the C-frame, too.

2.3 Transient Electrical Noise

While the 1010A microdensitometers come with closed steel housing, the 2020 GM microdensitometer is electrically essentially unshielded. The effect is obvious when watching the panel while switching incandescent lamps. Since the power lines are completely seperated the transient signals observed must be introduced via the unshielded PDS-cabled.

Short cable lengths and complete shielding of the cables are highly recommended.

2.4 Photometric Perturbations

Fig. 3 shows that photometric stability is generally reached after 3 hours of warm-up time. The relative peak-to-peak scatter is here about 1.3%, it is, however, highly dependent on the density or transmission and on the photomultiplier voltage.

No stability is reached for equal pre-slit and scanning apertures as shown in Fig. 4. This is an effect of the relative aperture drift due to thermal instability of the C-frame.

Fig. 5 shows the well-known lag of the logarithmic amplifier.

All photometric tests were carried out by J. Tucholke as part of his master's thesis (4).

3 SCIENTIFIC RESULTS

First astronomical results obtained with our 2020 GM microdensitometer became available 9 months after commencement of operations. They are part of a master's thesis by H. G. Scheuer (5) and concern quantitative morphology of ellipsoidal galaxies using the SRCJ-Atlas.

Fig. 6 shows a sample tracing of a SRCJ-Atlas wedge and Fig. 7 the corresponding density curve. The results are shown in Figs. 8-10, where the most characteristic curves of each kind are presented.

Fig. 8 shows the intensity gradient of the E0-galaxy NGC 1379 obtained from the present study. Error bars are less than twice the size of the symbols. The excellent agreement with the computed $r^{1/4}$-curve shows that NGC 1379 is indeed an elliptical system. The slight deviation of the last point is real, its divergence being supported by studies published in the literature (6).

Fig. 9 is a sample of the measured ratios of major and minor axes as a function of distance from the center of the SA0-galaxy NGC 5102.

Fig. 10 shows the change of position angle of the S0-galaxy IC 5063. This result is of particular interest because it shows an unexpected variation of the position angle in a S0-galaxy.

The results testify both, the excellence of the SRCJ-Atlas and the promise of performance of the 2020 GM microdensitometer.

LITERATURE

1. Teuber, D., to be published
2. van Altena, W., private communication
3. Becker, H.J., Master's Thesis, Bonn, 1979
4. Tucholke, J., Master's Thesis, Muenster, 1983
5. Scheuer, H.G., Master's Thesis, Muenster, 1983
6. Kormendy, J., Ap. J. 218 (1977) 333

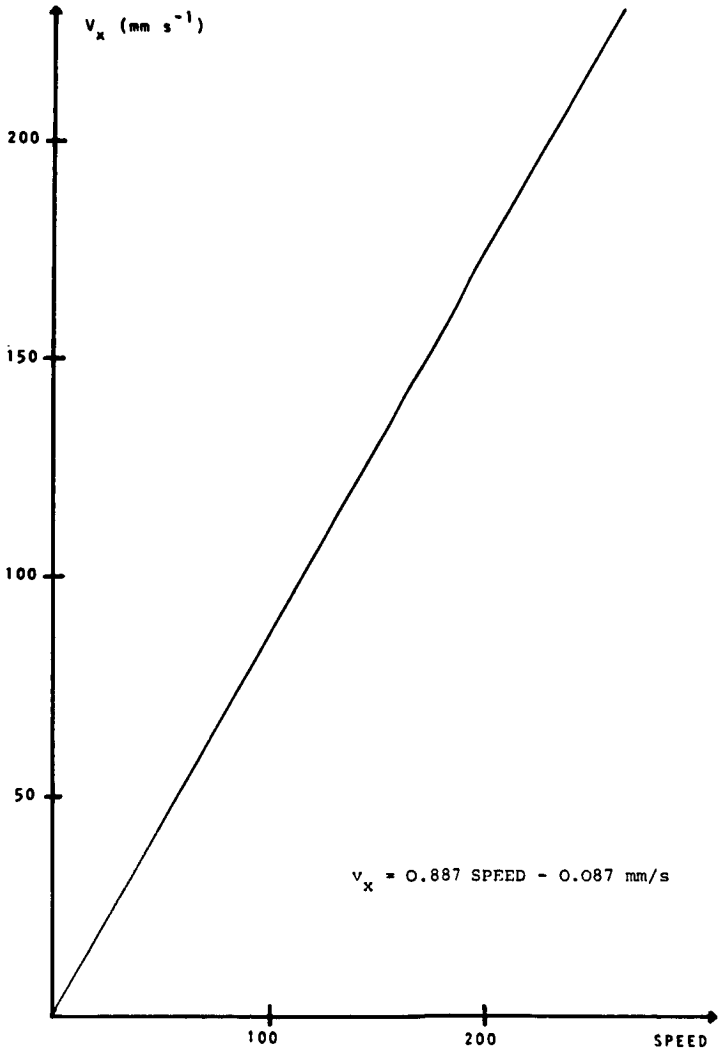

Fig. 1. PDS speed versus speed in conventional units

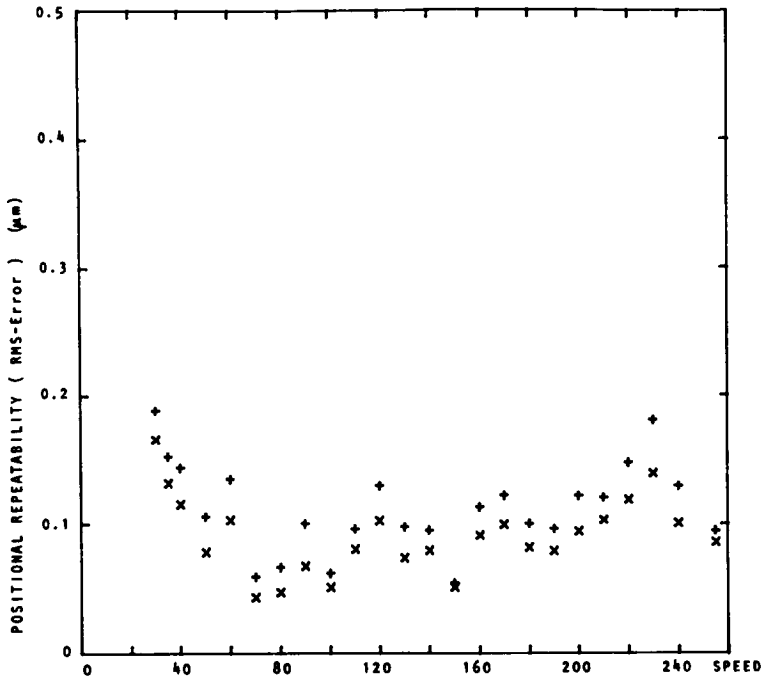

Fig. 2. Repeatability of the PDS 2020 GM

+ method of Becker (3) x statistical method
The statistical method subtracts the influence of lamp variations and thus leads to lower values

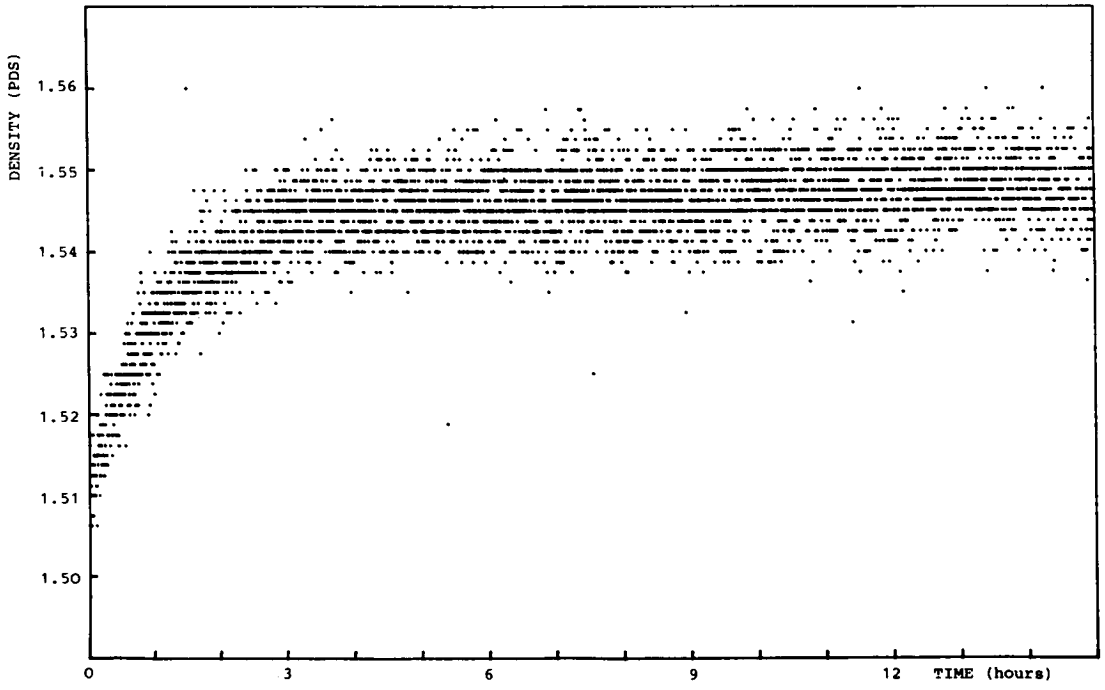

Fig. 3. Photometric drift of the PDS 2020 GM with pre-slit 50 x 400 µm, scanning aperture 20 x 20 µm.
Stability is reached after 3 hours warm-up time

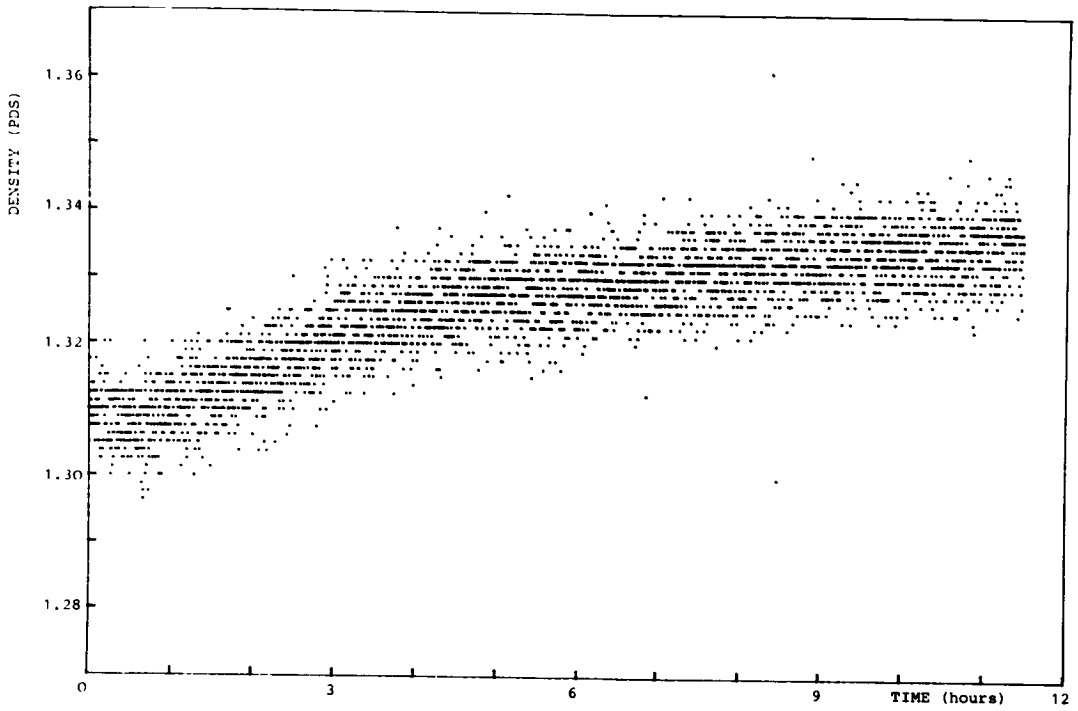

Fig. 4. Photometric drift of the PDS 2020 GM with pre-slit = scanning aperture = 5 x 100 µm. No stability is reached, obviously an effect of relative aperture drift due to thermal instability of the C-frame

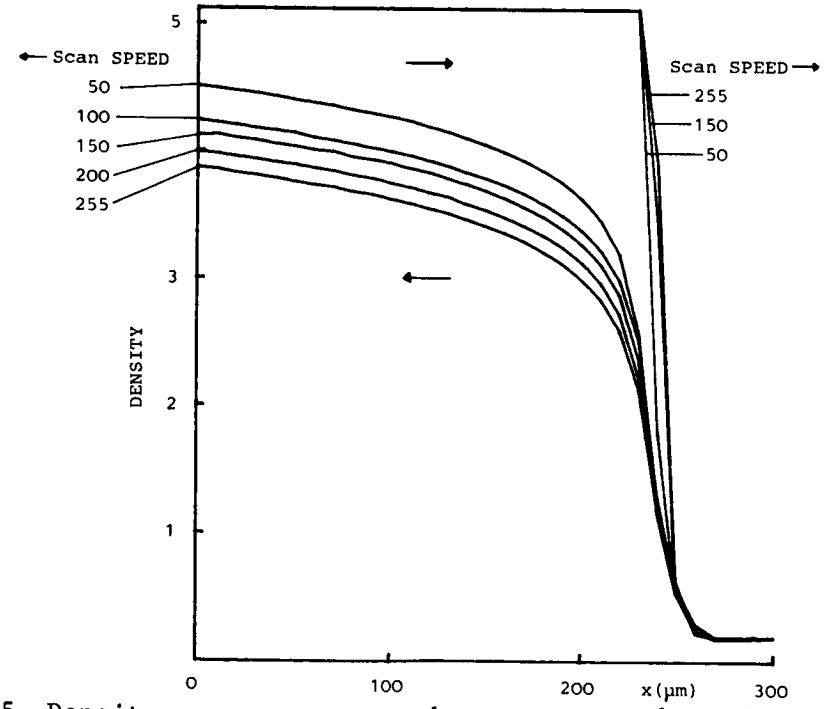

Fig. 5. Density scans across a sharp, opaque edge. The well-known lag of the logarithmic amplifier is clearly seen

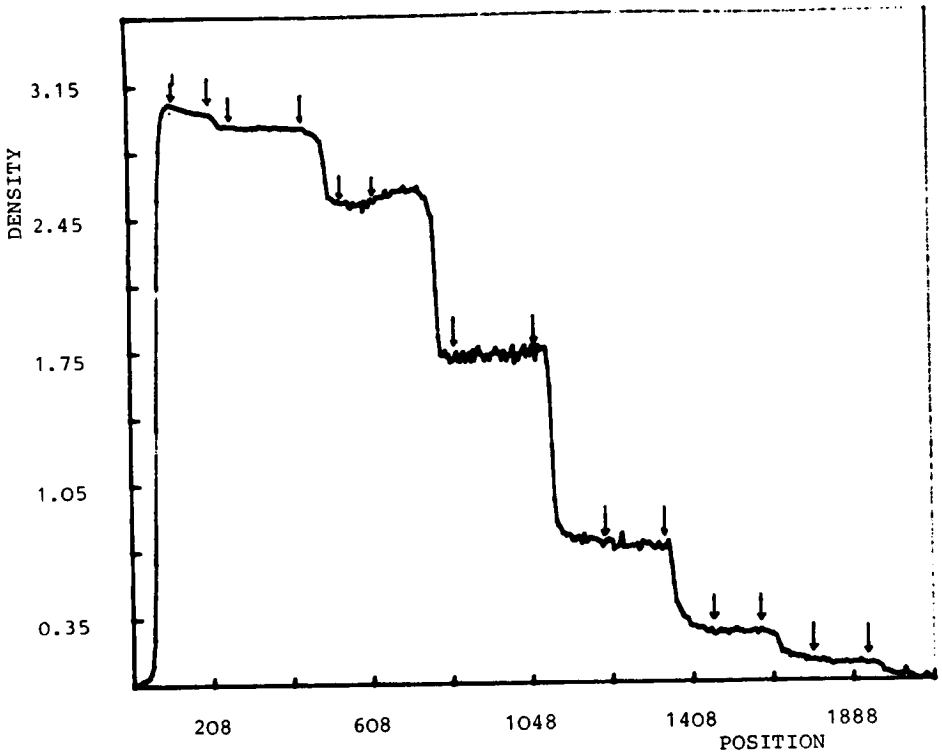

Fig. 6. Wedge tracing from the SRC-J atlas plate No. 085 made with the PDS 2020 GM

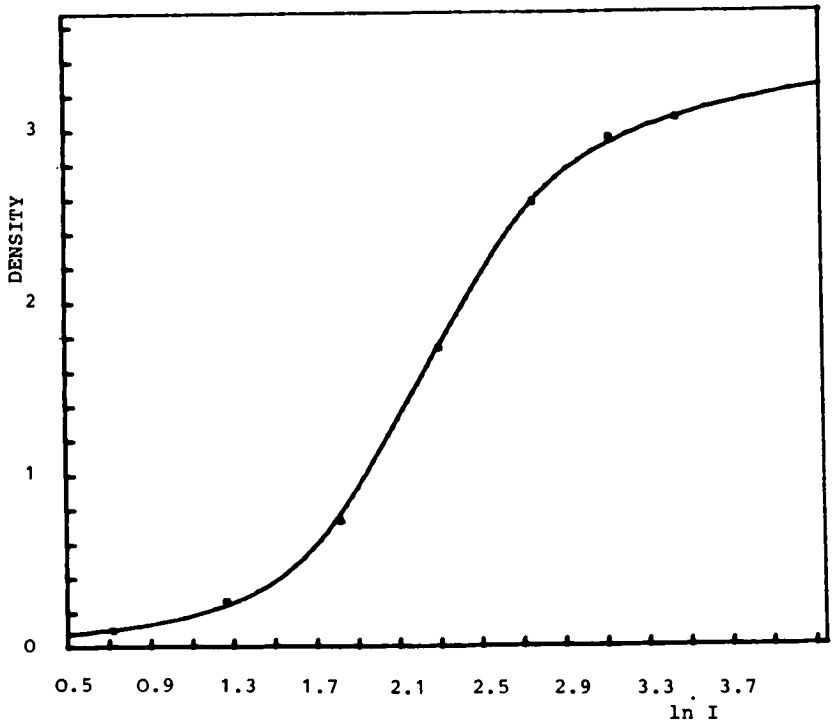

Fig. 7. Density curve for the SRC-J atlas plate No. 085 from the North wedge

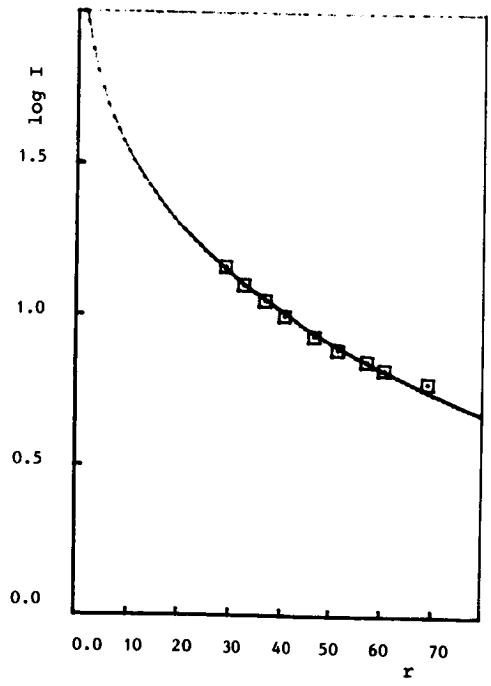

Fig. 8. Log I - distance diagram of the E0 galaxy NGC 1379 obtained from SRC-J atlas scans and reduced with the density curve shown in Fig. 7

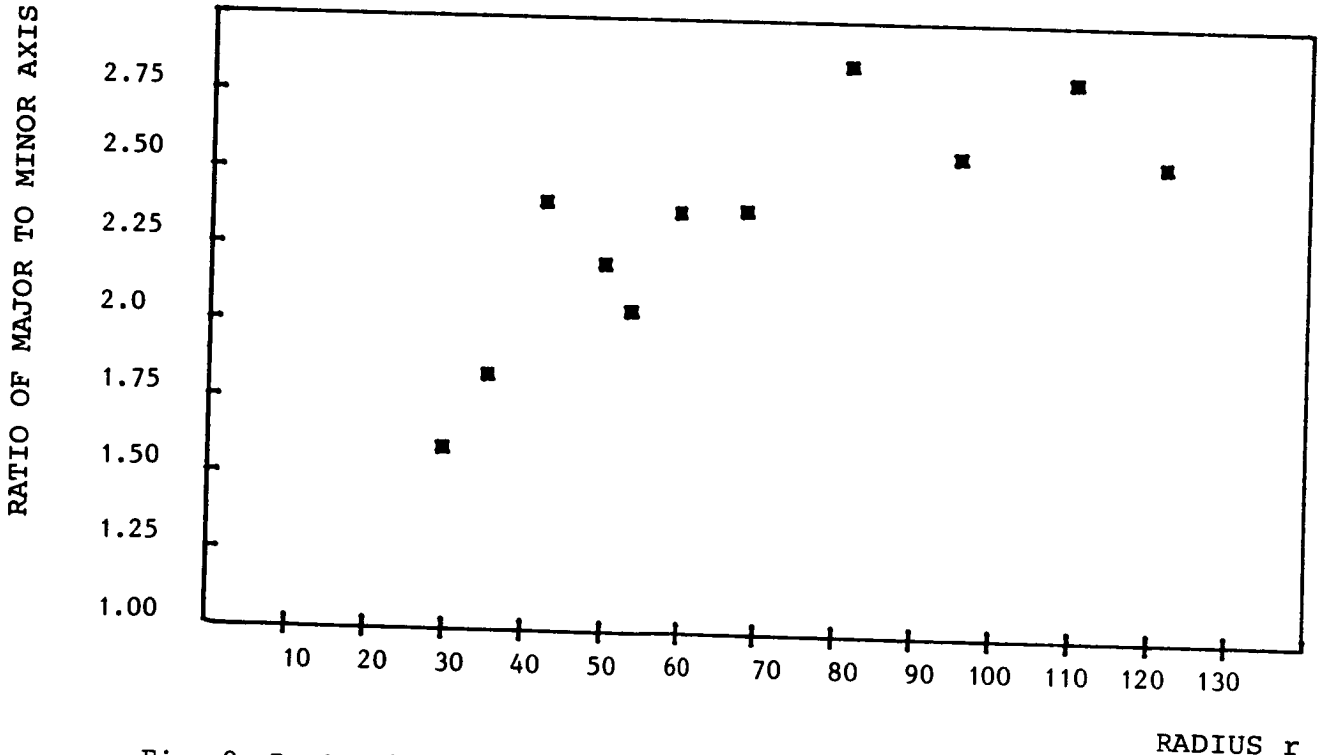

Fig. 9. Ratio of major to minor axis for the SAO galaxy NGC 5102 obtained from SRC-J atlas tracings

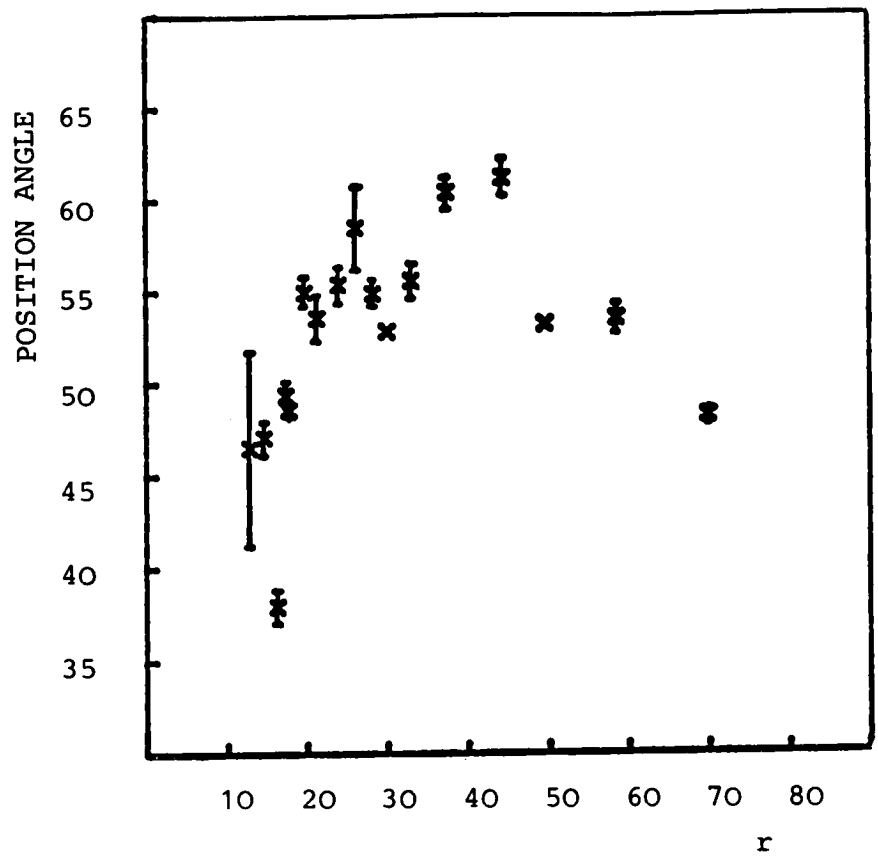

Fig. 10. Change of position angle of the major axis with distance r from the center of the S0 galaxy IC 5063

SESSION II

Chairman: Robert H. Cornett

II. PDS Status and Improvements

PDS scanning microdensitometers are in routine use at many astronomical institutions. All of the machines have been modified to some extent in response to discovering insufficiencies, to increase measuring accuracy, or in order to make them work better for specific applications. It is the purpose of this session to present an overview of known PDS problems, discuss solutions as they have been implemented in different places, and to investigate suggested improvements. The emphasis should be on detailed technical information so as to maximize the usefulness to those interested.

PDS CONCEPTS AND ASTRONOMICAL APPLICATIONS: AN OVERVIEW[+]

Barry M. Lasker
Space Telescope Science Institute*

ABSTRACT

This paper introduces the topic of PDS status and improvements by reviewing the basic concepts of PDS scanning microdensitometers, including their major electronic, optical and mechanical variations. Certain improvements to the basic PDS design have been found necessary for the effective collection of astronomical data and have been widely implemented in the community; an overview of these improvements is also presented.

I. INTRODUCTION

As an introduction to our topic, "Status and Improvements to the PDS Microdensitometer," I wish to review the instrumental concepts underlying the PDS design and to present an overview of the modifications on the basic instrument. While my orientation (and presumably that of most of the participants at this meeting) is astronomical, one should note that a significant community of industrial PDS users does also exist.

The acronym PDS is attributable to the first manufacturer of the instrument, Photometric Data Systems. While the corporate history of the instrument involves various transitions (explained in the Appendix and also by Jim Horton elsewhere in this proceeding) to bring us to its present production by the Applied Optics Division of the Perkin-Elmer Corporation (Garden Grove, California), the phrase PDS has become a generic description of these microdensitometers.

An immediate corollary to this historical development is that the PDSs started (and remain to this day) well-defined commercial products. This means that for a fefinite price and delivery wait, one can acquire a specific capability to perform microdensitometry and that with this capability one is brought

---

[+]At the conference, this paper was presented in two parts: Sections I and II were given at the beginning of Session II; and the remainder at the beginning of Session III. Figure I was added after the conference.

*Operated by the Association of Universities for Research in Astronomy, Inc. under contract NAS5-26555 to the National Aeronautics and Space Administration.

to share the set of experiences and skills that incorporate over a decade of astronomical experience with PDSs. The concomitant disadvantage clearly exists, namely because the PDS is standardized, it can not fit each application perfectly. Of course, this near-fit of the PDS to specific applications is the catalyst for the modifications that are so common in astronomy; for each experimenter knows that the right combination of good engineering, realistic management, and inspired tinkering can bridge this gap between PDS production specifications and the specific requirements of individual PDS installations.

The matter of evaluating features of the standard commercially produced microdensitometers with respect to capabilities required in the astronomical laboratory will arise repeatedly in this conference. Our perspective on this must be governed by economic realities. By industrial standards the astronomical microdensitometry market is very small (a few machines per year), and it therefore tends to be slow to respond to consumer-generated requests for new products. Correspondingly on the academic side, funding tends to come for one development program at a time and therefore results in a dispersed community of instrumentalists working on PDSs. At this meeting we have an obligation to invent ways to nurture cooperation between the small industrial marketplace and this dispersed community of users and developers. I do hope that our discussions can make a significant contribution in delineating the overall needs and in distilling them into two kinds of identifications:

1) the kinds of changes, embellishments, or new products that are commercially sustainable and therefore of interest to industry, and
2) the kinds of improvements are so limited in demand that the astronomical community must internally find effective ways to share the effort of development and distribution, either among ourselves or in collaboration with contractors or consultants.

II. THE PDS CONCEPT

The PDS design is based on a photometric subsystem to measure the astronomical plate (or other specimen), two positional servos to manipulate the measuring spot over the specimen, and a data system for control and recording. Figures 1 through 3 give the concepts underlying the optical layout, the photometer electronics, and the motor controls, respectively, and an overall system diagram appears in Figure 4.

PDSs exist in various mechanical and electronic configurations. Their platen size may be 25 cm square (i.e. the 1010 series) or 50 cm square (the 2020 series). The smaller machines are manufactured with metal construction or, for use where

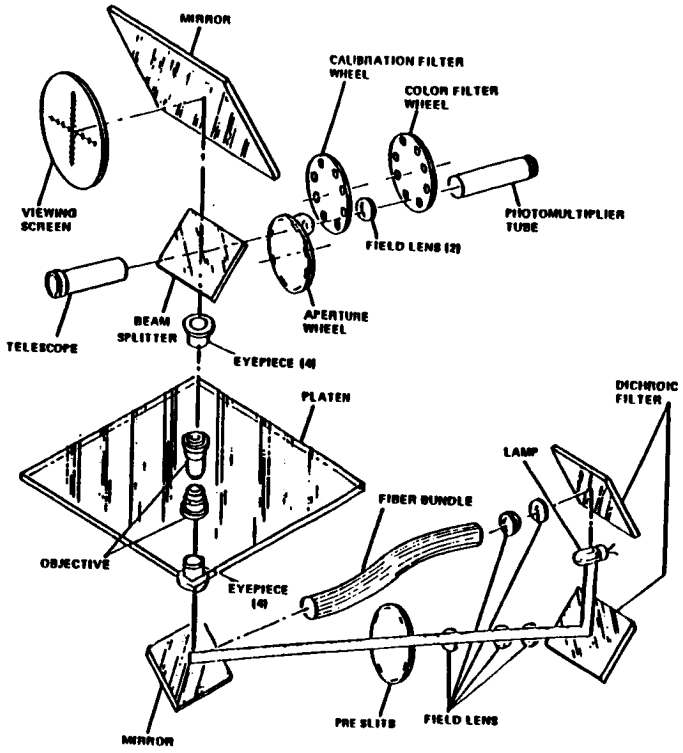

Figure 1. The optical layout of the PDS, reproduced by permission of Perkin-Elmer, from a PDS manual.

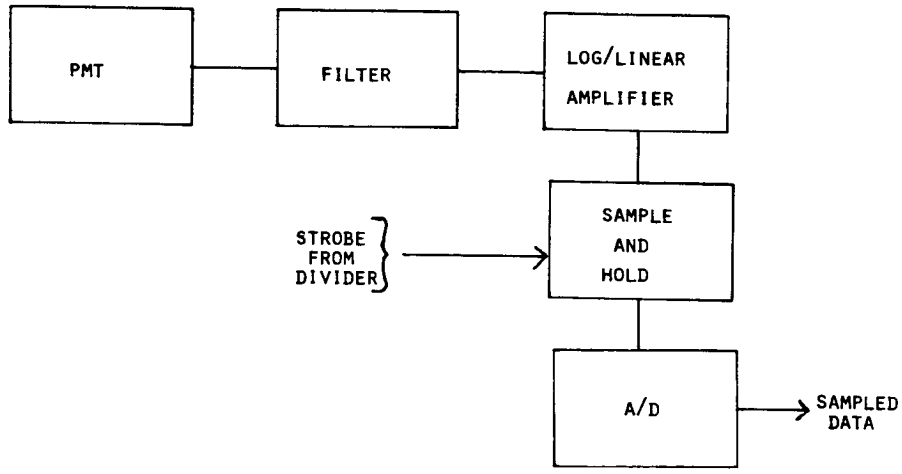

Figure 2. The photometer electronics. The filter, which does not exist as an explicit circuit element in some installations, is shown separately.

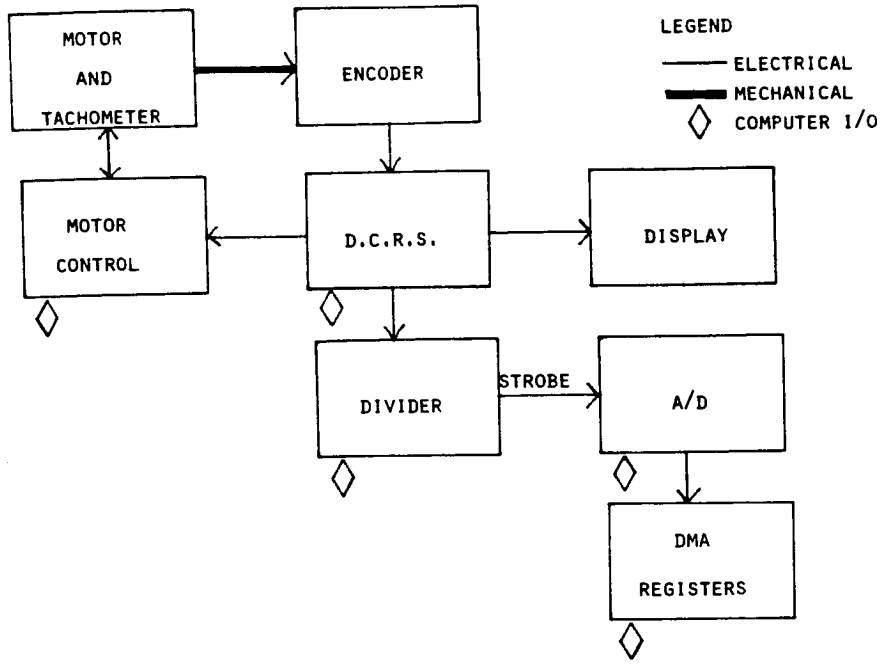

Figure 3. The motor controls and related data processing elements. "D.C.R.S." is an abbreviation for Digital Control Readout System. Depending on register settings, the control elements can be used either as a position servo (AUTOLOCK) or as a velocity servo.

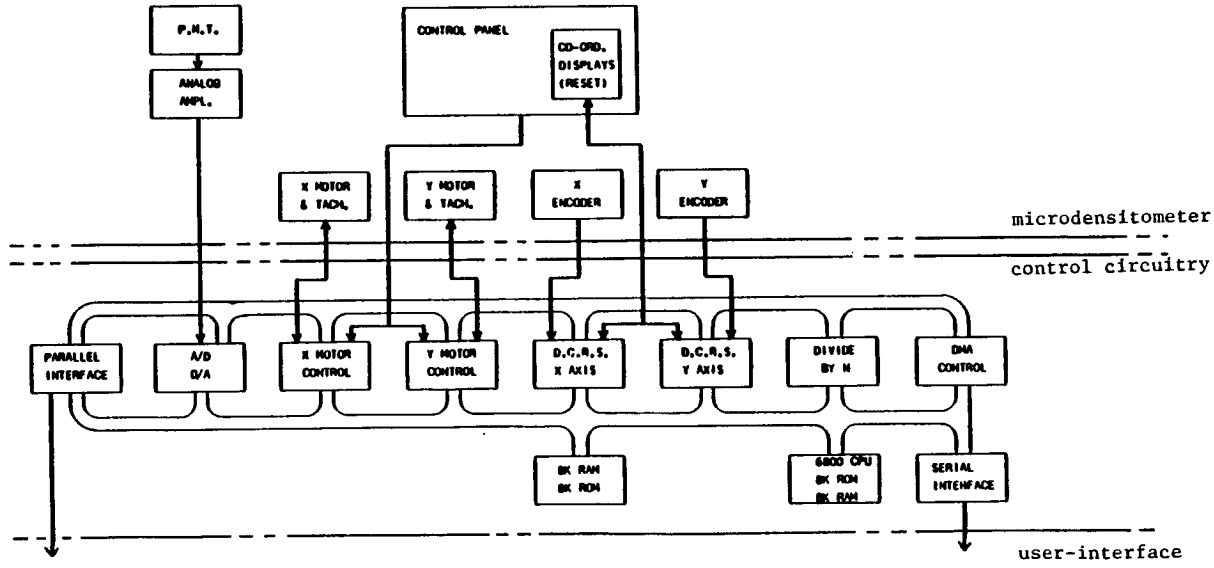

Figure 4. A PDS system diagram, adopted by permission of Perkin-Elmer from a PDS manual. Microprocessor elements shown in the lower line of the diagram (RAM/ROM, CPU, Serial Interface) do not exist in the translator implementation.

greater stability and thermal inertial is required, with granite construction; the larger machines are made only in the granite version, denoted by the letter "G" in the product number (e.g. 1010G).

The photometric subsystem is a rather conventional arrangement of light sources, microscope objectives, apertures, and one photomultiplier. The photomultiplier gain is generally set by manipulating the high voltage; the photomultiplier output, processed by a linear preamplifier, is further amplified by either a linear or a logarithmic main amplifier; and the amplified output is converted by an analog-to-digital (A/D converter) into digital data that is recorded (directly or through a host computer) for further processing.

The servos are based on positions sensed by linear encoders, on motions provided by dc motors, and on velocities sensed by dc tachometers. (One should also note that early versions of the PDS used stepping motors and drive screws in place of the present dc servo motors and Rholix^{R} actuators.) In the metal 1010 PDS implementation, scanning is performed in both axes by moving the plate. For the granite machines (both 1010 and 2020) scanning in one axis (x) is performed by moving the plate; and in the other (y), by moving the optical system; in the latter, the x translation is generally much faster than the y. These mechanical distinctions become especially important when comparing properties of different kinds of PDSs, especially test data related to positional accuracy.

PDSs are made in two electronic configurations. The "translator" version provides relatively straightforward and directly accessible logic paths between the PDS registers and the host computer. This configuration has relatively little local intelligence and is based on 1970 epoch electronic design. The "microprocessor" version uses an internal Motorola M6800 microprocessor to control the PDS. This configuration has substantial local intelligence and great potential for modifying PDS characteristics in firmware; however, the microprocessor architecture does preclude direct access to the PDS's internal registers by the host computer.

The versatility of the PDS is largely attributable to the logic connecting the positional servos and the A/D converter. For each line segment to be scanned, this logic, initialized to contain the starting coordinate of the scan and the sample increment, strobes the A/D every time a required sample point is crossed.

While some PDSs are provided with stand-alone control and recording capability, the complexity of the control registers and the voluminous quantities of data produced lead to the

practice of directly interconnecting PDSs to host computers. The DEC PDP-8, PDP-11, and VAX series are the most common, but other mini- and microcomputers have been installed both by Perkin-Elmer and by the users.

III. IMPLEMENTATION CONSIDERATIONS

While there are doubtlessly users who buy a PDS, plug it into their ac outlet, and begin working, these represent relatively uncritical groups which are unlikely to contribute (or even attend) a meeting such as this. For the most part we, the astronomers, are a group of very demanding users who recognize that a successful PDS installation is a major investment. I suggest a good rule of thumb is that the implementation costs of a viable PDS system are comparable to the purchase costs of the equipment.

As I look around the community, certain characteristics appear common to productive PDS installations:

1. The dedication of several people who collectively provide a broad knowledge of the astronomical problems and of the hardware and software necessary to operate a PDS,
2. A willingness (together with the financial resources) to modify PDS hardware as required to meet specific astronomical goals, and
3. The incorporation of a moderately powerful computer, either a host minicomputer or an off-line mainframe. (The size of host minicomputers varies considerably with the application and often approach rather large VAX configurations.)

Obviously the integration of a PDS system is a delicate matter requiring substantial cooperation among the participants (Perkin-Elmer, the users, consultants, etc.). My own perception is that the greatest potential for smooth PDS development exists when the roles of the customer and the manufacturer in such developments are precisely defined. Attention to these matters at the time of preparing a purchase contract can set a very early stage for smooth PDS installation and improvement and can avoid confusing (and possibly costly) misunderstandings later. In this regard I would draw particular attention to the need for well defined acceptance tests. While some astronomers tend to do acceptance tests in an ad hoc manner that leads to a slow identification of problems and a hazy definition of the responsibility for fixing them, tests that are properly defined from the beginning (and negotiated between the buyer and the vendor) lead to well-determined capabilities at their conclusion; and in the event of problems, it is clear who must take the corrective action.

Another critical area is documentation. Even if one plans no modifications, obvious basic matters (what a PDS is, how it is interfaced, how it works, how to fix it, and especially how to use it) are of substantial importance. Some confusion in documentation may be attributed to the variety of PDS configurations (Section II above); and some, to the extremely varied tastes and requirements of the users. Other holes in the documentation are obviously attributable to the distributed nature of expertise, particularly in the areas of maintenance and operations. I'd like to identify this as a discussion topic at this meeting: What more needs to be done on PDS documentation and who should do it?

Even more than the ordinary documentation is needed to support PDS modifications, as one is then concerned with internal PDS engineering details that may not be in the standard user documentation. Thus the user should be absolutely clear at the time of purchase as to what special kinds of documentation are required to support planned modifications. (For example, a user planning to add another device to the M6800 microprocessor needs the specification of the PDS internal interface-bus and considerable software data.)

There is a considerable variety in the kinds of astronomical work done with PDSs. Our addressing a few specific cases forms a convenient basis for appreciating the motivations that have lead to the existing variety of PDS enhancements:

One-Dimensional Spectrophotometry: In one of its simplest applications, the PDS, configured with a slit aperture, is used to make a single scan that measures a widened spectrum. Even though this is an emulation of the microdensitometers developed in the 1950-1960 epoch, the requirements for positional accuracy and photometric precision may be quite demanding.

Two-Dimensional Spectrophotometry. The need for sky subtracting long-slit spectra and for measuring separate spatial points in them (e.g. for abundance gradients in galaxies) makes this a truly two dimensional problem that also has strong requirements on positional accuracy and on photometric precision.

Surface Photometry, e.g. luminosity distribution in galaxies for example. The large areas to be covered and the need for precision near the plate limit lead to requirements for time stability and for A/D resolution.

Stellar Photometry. The PDS is smarter and faster than an iris densitometer, but concomitant requirements are

placed on control flexibility and on response speed in the photometer electronics.

Astrometry. This application has positional and photometric requirements similar to those for spectroscopy, but additionally the performance must be maintained over relatively large areas, for example over 35 cm square Schmidt plates.

Obviously, these examples involve a tremendous cross section of astronomical research. Any one of the above could be expanded into a treatise, and the obvious generalizations to electrography and to playback functions (in image processing and in radio astronomy) have been neglected. In fact, PDSs have been (or at least could be) put to good use in every area of astronomical research involving photographic observing. However, research directly related to even these few examples has led to sufficiently great expenditure of critical effort that the limitations to the basic PDS became evident and motivated the specific PDS modifications that this session is devoted to, specifically

1. Photometric Precision and Stability. The various successful modifications in this area include the current driver for the lamp (and other electrical and mechanical aspects of the illumination system), the optical system, the high voltage power supply, the A/D converter, the logarithmic amplifier (see Item 2 below, also), and the filtering circuitry preceding the sample-and-hold unit.

2. Speed. The standard logarithmic amplifier has time lags that (at the higher scanning speeds of the PDS and typical astronomical plate scales) gives unacceptable image skew. In response to this, several successful logarithmic amplifier replacement circuits have been developed in the community.

   Other approaches to increasing PDS speed may be in the direction of mechanical adjustment, alternative scan strategies, or optical changes involving multiple detectors. While there has been much discussion and some experimentation in these areas, I am not aware of anything that can be reported as a successful modification.

3. Positional Accuracy. The nominal positional accuracy of the PDS is specified as 5 microns in precision (i.e. relative to a perfect measuring grid) and 1 micron in reproducability. At least for the 2020Gs in use at Yale and at the ST ScI, the reproducability is not sufficiently stable to be meaningful in terms of determining a calibration function, and the machine is to be regarded as a

5 micron device both in precision and in reproducability. Various means of achieving 1 micron or better capability (based on fiducial plates, auxiliary micrometers, or commercial lasers) have been and are being developed.

4. Control and Data Processing. Substantial effort has been expended on developing control systems both for PDSs purchased separately from their host computers (and interfaced by their users) and also for PDSs purchased with a dedicated computer running Perkin-Elmer's Scansalot^{R} program. These activities often involve creating relatively subtle hardware and software interfaces and replacing the Scansalot program or even the host computer with more modular and flexible software and hardware. Most of this activity involves DEC PDP and VAX computers. Although I am not aware of a successful reprogramming of the microprocessor version, there is substantial interest in this.

   To the extent that many of us are now controlling PDSs with hierarchically structured software written in a high level language (generally FORTRAN), hardware-dependent functions tend to be well isolated in a few modules with most of the remainder being dedicated to data collection and processing. This, I believe, gives us an opportunity that should not be missed for software sharing.

5. Miscellaneous. Other efforts that have been made in the astronomical community and that are of some general interest involve environmental control and monitoring (temperature, humidity, atmospheric pressure, ac power), the design for the support of the translating devices (platen and yoke - particularly as related to bearing supports in the 2020Gs), and special plate mounting fixtures.

   The PDS typically has a depth of focus of the order of 10 microns, and maintaining plate flatness to that tolerance is at best a chore. Many of us have recollections of a plate that took an hour to bring into flatness with a creative combination of shims and masking tape. Various fixes have been proposed and built (active schemes based on air puck sensor, laser sensor; passive ones based on vacuum, cover glasses, and clamps), but I am not aware of a generally accepted solution.

I thank R. Albrecht, J. Kinsey, W. van Atlena, and D. Wells for teaching me about PDSs and J. Horton and A. Hull for helping me with some historical details.

APPENDIX

EXCERPTS FROM A LETTER BY A. HULL

One of the purposes of this introductory paper for this Astronomical Microdensitometry Conference is to facilitate the understanding and interpretation of PDS studies and test results by clarifying the differences among them that may be attributed to the history of their design and manufacture. In reply to inquiries on this topic, Anthony B. Hull of Perkin-Elmer Corporation (Applied Optics Division, Garden Grove, California) collected historical material which was contained in a letter dated 26 April 1983 to the author. With his permission, major parts of that letter are quoted this appendix.

"Ten years ago (May 7, 1973) the Boller and Chivens Division of Perkin-Elmer purchased Photometric Data Systems Corporation (PDS) of Webster, New York. We learned of PDS from astronomical users and thought that these microdensitometers would be a logical compliment to our line of astronomical telescopes and instruments. The microdensitometer has been marketed to both astronomical and non-astronomical users.

"The first PDS system was delivered to Corning Glass in June of 1969 and the first astronomical customer was Leopold FIGL of Austria (November 1971). In September of 1972, PDS delivered a model 1010A to KPNO, the first domestic astronomical user. The first granite machine, a 14x20 inch model, was made by PDS and delivered in November of 1972.

"The first machine that B&C Division delivered was the numbered one 1010G shipped in June, 1972. The second 1010G went to JPL in June of 1974. Production of the Micro-D remained in the hands of the Boller & Chivens Division until February of 1977 when Perkin-Elmer made some divisional changes. The Micro-D was moved to the Electro-Optical Division in Connecticut for six months and then returned to the Applied Optics Division in California where most of the B&C work had been transferred. The first 2020G machine was shipped to Yale University Observatory in August 1978. To this date, Perkin-Elmer (and PDS) has delivered 152 microdensitometer systems, a substantial fraction of these to astronomical users.

"Although a mature product, a number of substantial improvements have been made and will continue to be made. The original Micro-D's were driven by stepper motors until May of 1972 (SN 21) when the stepper drive was replaced by the translator direct screw drive. The screw drive was changed in 1976 to a Roh'lix actuator. With SN85, the microprocessor controlled microdensitometer was introduced in April, 1979. Since that date, 37% of

our orders have been for microprocessor machines, but 90% of current orders are for microprocessors.

"Aside from the drive changes and several other improvements, the Micro-D mechanics are largely unchanged through the years. Consequently, even the earliest machines can be serviced by Perkin-Elmer. The computer interface is another matter, and Perkin-Elmer has frequently and extensively modified its electronic hardware to accomodate developments in mini-computer architecture. Today, we offer a machine that is compatible with virtually all mini-computers. Considering the mechanical and software options, there are well over one hundred "standard" possibilities to choose from. We now offer basic translator machines in the 1010A, 1010G and 2020G models, plus basic microprocessor machines as 1010M, 1010GM and 2020GM models."

PDS Microdensitometer Electronics Modifications

A.V.Hewitt

U.S.Naval Observatory
Flagstaff Station
Flagstaff, AZ 86002

ABSTRACT

The design of the detector and front-end electronics in the PDS cause nonlinearity and instability of the system at both low and high densities. Minor and reversible modifications (replacement of the photomultiplier and front-end analog circuitry) have significantly improved the performance. The modified PDS has no transmission mode.

Requirements

At the Flagstaff Station of the U.S. Naval Observatory the Kron electrographic camera is used to make broad-band stellar observations using Ilford L4 nuclear track emulsion. The plates have high information content and are linear (or nearly so) up to a density far beyond the capability of any conventional microphotometer. Lowell Observatory kindly allowed us extensive use of its PDS 1010A. However, photometric errors less than 1% on star images smaller than 50 microns full width half maximum and central density as high as 4D were required. The unmodified instrument did not meet this specification.

Photometric performance limitations

The fundamental limitation of the PDS is the quantum noise due to the low light level at the detector with small apertures and high densities. For stellar photometry, a 5-micron aperture would have been advantageous since it would have reduced transmission averaging. However, tests carried out by Harold Ables of the U.S. Naval Observatory showed

that the light throughput of the PDS was inadequate with such an aperture even after the installation of new optical components supplied by Perkin-Elmer Corporation. Therefore, the smallest aperture used on the Lowell PDS is 10 microns; if there are no neutral-density filters in the beam, the quantum noise is then negligible compared to the plate noise even for a fine-grain emulsion such as L4.

However, the original detector and analog electronics have significant performance problems. Even with small apertures, the photomultiplier is required to operate at very low gain, so that the voltage across the last stage is less than 30V and only about 20V at zero density. In addition, the design of the logarithmic amplifier is such that the anode current at zero density is 0.1 mA, two orders of magnitude above the limit recommended by Hamamatsu, the manufacturer of the photomultiplier. As a result, stability and linearity are poor at the low-density end of the range.

At the high-density end, the photomultiplier dark current (at least for small apertures) and the amplifier voltage offset introduce a bias. This appears as a curvature of the density reading vs. true density curve, which becomes asymptotic to a line of either zero or infinite slope, depending on whether the offset corresponds to positive or negative transmission. It changes on a short timescale and is difficult to null out because the offset adjustment is inaccessible and has poor resolution.

The high input impedance of the amplifier limits the speed of the system at low densities. Worse yet, the speed of the logarithmic amplifier decreases by an order of magnitude for unit increase in density, causing a nonlinear response unless the scan speed is restricted.

Modifications

Since the PDS belongs to Lowell Observatory, we were unable to undertake modifications which were extensive or irreversible. Neither were we in a position to carry out complex changes involving the interface with the computer.

Initially we left the amplifier unchanged and replaced the detector with an EMI 6094B photomultiplier specially selected by EMI for operation in a PDS. It showed intolerable fatigue effects.

We therefore replaced the amplifier and installed a 6-stage RCA 7764 photomultiplier, operated at an anode current

of 1 microampere at zero density. To optimize the performance at high output, the voltage across the last stage was stabilized at 75V with a zener diode.

The new amplifier is faster and requires a lower photomultiplier anode current. It lacks a transmission mode, which we have found to be unnecessary. Its installation releases a front-panel control for setting the zero (high-density) level, the adjustment that was difficult to make with the original design.

The set-up procedure is to adjust the photomultiplier voltage to give a reading of about 0.1D on unexposed emulsion, then insert a high-density neutral filter and adjust the front-panel control so that the density reading agrees with the known value for the filter. Of course, high-density readings are systematically affected by errors in the assumed value for the density of the neutral filter. In practice, this is not a problem provided one uses a filter beyond the useful density limit of the PDS, which is 3.5D for this particular machine with a ten-micron square aperture.

Amplifier design

The amplifier is shown in Fig. 1; it is extremely simple. The logarithmic amplifier, Analog Devices 755N, is still available and there are alternatives which could be substituted if necessary. The front-end amplifier is a FET-input device with 25pA bias at 25C and a fairly stringent requirement of 10 microvolt/C voltage offset, corresponding to 1% at 4D. The speed of the system is set by the time constant R1C1, which is chosen to match the maximum sampling rate of the PDS. For extremely fine-grain emulsions, the photon noise may be unacceptably high with such a short integration time. We prefer to co-add samples in software to circumvent this problem rather than offer the user an adjustable time constant.

The function of amplifier A3, together with Z1 and R2, is to provide a current source of about 130 microamperes to offset the output to zero at zero density. Amplifier A4 provides a smoothed output to the panel meter.

Performance

A comprehensive series of tests of the photometric performance was carried out, mainly by Harold Ables. The test procedures were designed to measure aspects of the

performance of the PDS important to our programs, not to determine absolute parameters such as the transformation of measured density to diffuse density. However, since we require good photometric data from plates with low noise and small scale, the tests were necessarily stringent. We needed to know if the density measures were repeatable over a period of days, independent of photomultiplier gain and anode current and reliable at high table speed.

Bench tests showed the amplifier itself to deviate from linearity by about 0.1% at densities less than 4D. The errors were consistent and so could be corrected if necessary. Measures of astronomical plates showed that, for stellar photometry, the photometric differences between repeated measures of the same plate were much smaller than those between measures of comparable plates of the same field.

To investigate the bandwidth of the system, I repeated at different table speeds measures of a star image with peak density 3.5D and full width at half maximum approximately 70 microns. At the maximum speed, the measured peak density was decreased by about 10% and the total density-area product by about 2%. These changes are negligible compared to the effect of transmission averaging when such an image is measured with a 10 micron aperture.

To look for nonlinearity in the overall system response we mounted a neutral filter of approximate density 0.1D in the filter wheel. We then measured a plate of a density wedge first without the filter in the beam and then immediately afterwards with the filter, all the operating parameters being held constant. The filter is mounted in the filter wheel of the PDS and is presumably illuminated in a consistent fashion. The form of the image on the plate is irrelevant, provided it has a wide range in density without any steep gradients. We found a density wedge to be ideal; it is important to note that we did not need to determine the characteristics of the wedge.

Subtracting the two arrays point-by-point and sorting the data in terms of density gives the measured density of the filter as a function of the plate density. The advantage of this method is that it should introduce no systematic errors.

With the modified PDS we found that there are no significant changes in the value of the function at low density, where photomultiplier nonlinearity might become important.

At high density the value often diverges, presumably because the photomultiplier dark current changed between the two scans. Below the density limit set by this effect, typically between 3D and 4D, the function may be fitted by a line with residuals less than 0.03D. Ideally, the slope of the line should be zero; our measures show that it varies from one determination to the next but does not exceed 3%.

In contrast, the PDS in its original form showed significant deviations from ideal behavior at densities below 1D, presumably because of photomultiplier saturation effects. In addition, the high-density divergence occurred at a lower density than in the modified design; this may have been an intrinsic problem or merely the result of a high dark current in the photomultiplier installed at the time.

The function of measured filter density vs. sample density is noisy, particularly at high density. It is therefore unsuited to the determination of nonlinearities extending over small ranges in density, such as might be caused by a non-ideal A/D converter. These are better investigated by the traditional technique of looking at the number of samples in each density increment.

Conclusions

The modifications described are simple and inexpensive but significantly improve the performance of the PDS 1010A microphotometer. The improvement in density repeatability is marked and the permissible density slew speed is greatly increased.

Acknowledgements

I wish to thank for their assistance and encouragement: Harold Ables of the Naval Observatory; Arthur Hoag, Stuart Jones, Bjarne Thomsen and Lawrence Wasserman of Lowell Observatory; the Perkin-Elmer Corporation.

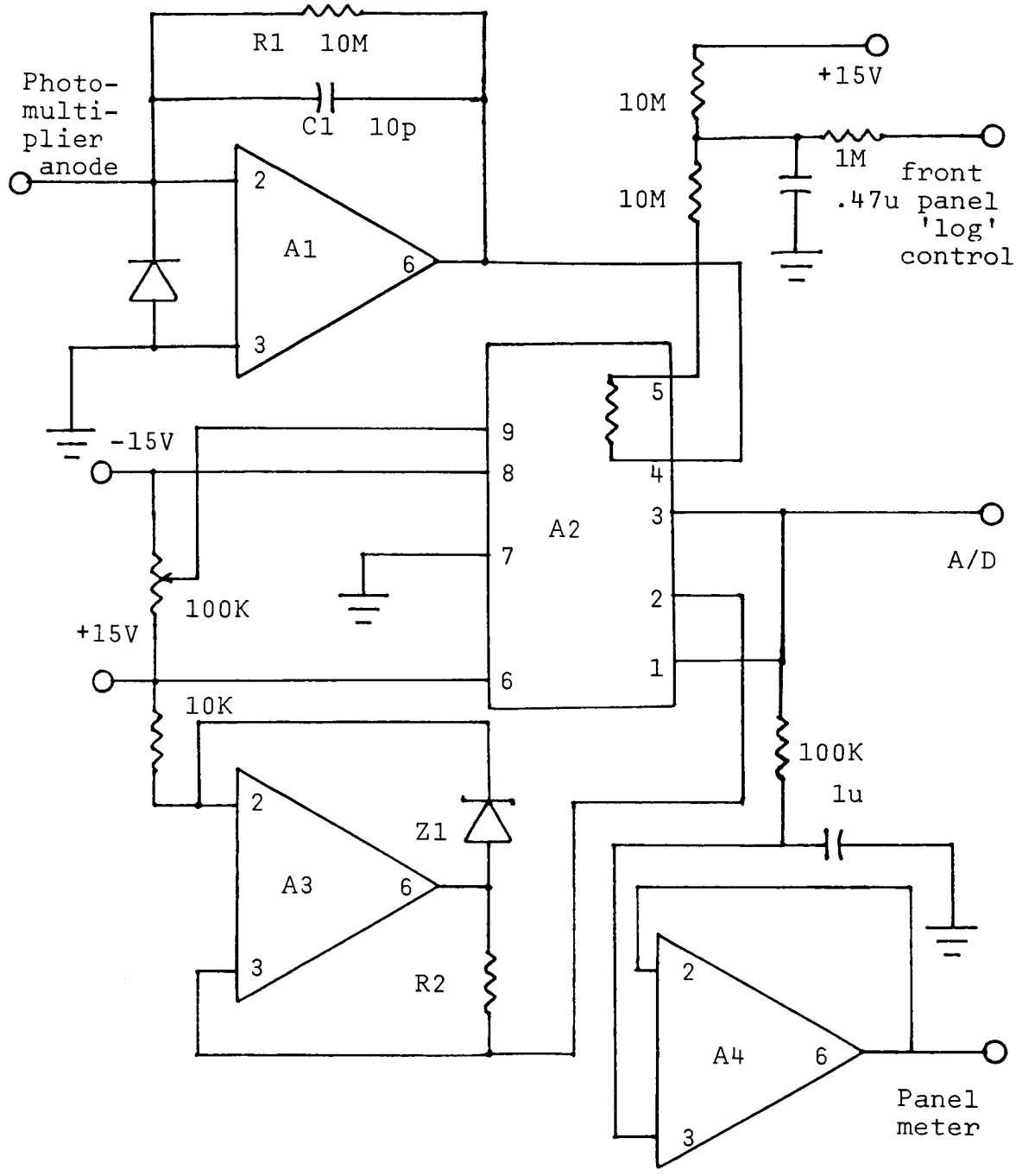

A1 Teledyne-Philbrick 1426-02
A2 Analog Devices 755N
A3/4 Analog Devices 741JN

Figure 1

Boyzan: What do you think that you ought to replace your A/D converter with?

Hewitt: I've only been thinking about it since you gave your paper. Do you have any suggestions?

Bozyan: We an discussing it among ourselves.

Hewitt: I gather that the logarithmic A/D seems to work pretty well. Is that true?

Oliver: It works very well.

Hewitt: I don't know what interfacing problems that you come up against installing the logrithmic A/D.

Van Altena: Not too many. We have just taken in parallal the existing systems so that we can switch with a plug connector from one to another and then the bit stream goes right down into the computer.

Hewett: Sounds like a good solution. I hope that it would be. I crossed my fingers when I suggested this to you.

Van Altena: There is a substantial amount of electronics that surrounds analogic module.

Hewitt: Do you have a model number for that unit?

Van Altena: There is a preprint of a paper that discusses the photometer with the log A/D convertor that we have installed and my colleague Jin-Fuw Lee has one copy here and if anybody wants a copy can have it xeroxed.

Stobie: I would just like to say that we have had an experience very similar to yours with the photomultiplier that we were using in our detector system (COSMOS). We orginally had a 12 stage tube and we were getting far too much gain, so we had to cut the EHT supply down to such a level that it was really low compared to what had been recommended for proper operation. We realized something was wrong because we were not getting the signal to noise out of the system that we should expect from photon counting statistics. Eventually one of our people tracked this down by shorting out six of the stages. We could then improve the signal to noise by a factor of 2 or 3. And this prompted us to buy a six stage tube which could be operated at the correct voltage.

Hewitt: It wouldn't surprise me at all. Certainly it's our experience that even though we worked with 10 by 10 micron apertures most of the time. The six stages tube has more than adequate gain. We would like to go to smaller apertures yet, but the problem is that with our particular PDS the filament of the lamp is found is focused on the first aperture and although Perkin-Elmer supplied us with alternative optics which we hope will help to solve that problem. In fact we still find the machine unusable in aperture smaller than 10 by 10. We just couldn't get enough light through it.

Bozyan: You referred to the fact that the new photomultiplier would solve some heat problems also solves the problem of driving too fast or exhileration.

Hewitt: We have never been exhilerated by using the PDS. We don't measure plates that look like that but it's quiet conceivable that the problem exists with our PDS. It's just that we, what we generally do is set our zero level to the background rather than to clear plate because we often don't have any clear plate.

Kibblewhite: What photocathode were you using?

Hewitt: It is an S-11 photocathode.

Kibblewhite: The saturation properties of the S-20 photocathode are much better than the S-11.

Hewitt: I have not seen any evidence of saturation effects in the photomultiplier cathode. I think we can rule out the cathode character of the problem because we run our photomultiplier with constant voltage on the first stage as well as the last. This means that if there are cathode separation effects they should operate independently of how much gain we have across the photomultiplier. So that if you should put a neutral density filter in and then adjust the gain things should look exactly the same as they do with the cathode problems, but they don't. In any case let me go back a step with a six stage tube with the S11 cathode, we do not see any fatigue effect, it works.

Hemenway: Where is your nutral density filter in the optical path?

Hewitt: We just mounted it in the regular filter wheel of the PDS. In fact we like the next speaker, have removed the color filters and put low density neutral filters and that yields 0.1-0.2 something like that so we could make them differential comparisons. Then we have the regular filters in the other wheel.

The current status and future upgrade of the PDS at the Royal Greenwich Observatory.

I G van Breda, H E Davies, A J Penny and C D Pike.
Royal Greenwich Observatory, UK.

Abstract

The PDS at the Royal Greenwich Observatory is a Model 1010A purchased in 1974 with a PDP 11 interface. Comprehensive scanning facilities are available using Forth software. This paper describes some aspects of the machine's present performance and gives the outline of an upgrade proposal which we feel will be necessary in order that our PDS can continue to offer a convenient and reliable service to the astronomical community.

Current performance

The density calibration method that has been adopted is to choose a particular PMT voltage and LOG amplifier offset setting and calibrate the PDS for that setting. When the PDS is used in measuring a plate, those settings are used and the density readings are brought within a suitable range by choosing a combination of the two N.D. wheels. The calibration table between reading and true density value can then be used. The table is calculated as follows. A Joyce-Loebl density wedge is placed on the platen and the PDS scanned along it for a short distance. The mean density reading, R_M and the mean slope $S = \Delta R/\Delta x$ (x = distance along wedge) are then calculated. (ΔR is small ~ 0.1-0.05D). The N.D. setting combination is then changed, and exactly the same section of wedge scanned again. This produces a new R_M and S. This is done for many N.D. combinations to give R_M covering the whole PDS density range. These are plotted and a smooth line drawn.

We have $S = \frac{\Delta R}{\Delta x} = \frac{\Delta R}{k\Delta D}$ as the scan Δx along the wedge always covers the same density range ΔD

and so $\Delta R = k\Delta D.S$

or $\sum_{D_1}^{D_2} \Delta D = D_2 - D_1 \simeq \frac{1}{k} \sum_{R_1}^{R_2} \frac{\Delta R}{S}$

so by numerical integration of the graph of S vs R, the density change between a reading and some arbitrary zero can be found, scaled by k. The constant k is then found by means of a long scan along the wedge, using the Joyce-Loebl factory calibration to give the absolute density change. Thus a calibration table between R and D can be set up. The advantage of this method is that (apart from the constant, k) it is entirely independent of standards, it is extremely accurate and produces a calibration at a very fine gradation over the density range. It has been found that these calibrations are stable over years.

The machine noise defined as the RMS scatter in density readings taken from scans without any object in the beam but with different ND filters inserted can be a useful check on the performance of the PDS. Typical results for a 7μ aperture show a nearly linear increase in noise from 0.002D at D=0 to approximately 0.01D at D=2.5, considerably less than normal emulsion noise. These data can also highlight problems that are present in the A/D converter. Histograms of the data show markedly that the converter has 'preferred' bits sometimes set in the output.

We have detected three forms of photometric instability in the PDS. The first arises from the relative movement of the upper and lower apertures. Despite the fitting of a locking device on the upper objective this drift still occurs occasionally. The situation is greatly helped by leaving the machine and computer permanently on since much of the drift used to happen during the warm up period. When drift does occur during a scan the effects are normally bad enough to invalidate any photometric properties the scan might have. Secondly there appear to be irregular and erratic variations on the photometric zero point of the order of several percent. We suspect that these arise either in the lamp output or in the supply to the detector electronics. The third instability is coupled with the ambient temperature variation. The air conditioning currently installed gives a temperature variation of ±2oC with a period of 10 minutes. There is a corresponding variation in the PDS zeropoint of amplitude 0.01-0.02D with the same period but with a slight phase lag. We have not yet isolated the cause of this though our tests suggest that

neither small movements of the apertures nor the detector electronics are responsible.

The PDS continues to perform very well astrometrically. Measures of a uniform distribution of 25 stars over a 140 mm square area yield RMS differences between independent runs on the PDS of 0.3μ and 0.7μ in X and Y respectively. When compared to measures of the same plate made with the GALAXY machine the RMS differences were 2.0μ and 1.3μ. The errors from the GALAXY machine are independently estimated at between 1.0μ and 1.5μ in each coordinate. Another test done was to use a small aperture and to scan forwards and backwards over a grainy piece of film. The forwards and backwards scans were compared and a relative shift of less than 0.1μ found after a 1μ displacement inserted by the hardware was corrected in the movement software.

Proposed upgrade

A number of features of the present configuration make a change desirable. In particular we have a heavy requirement for a facility to perform accurate photometry on 14" square Schmidt plates. To this end we have redesigned the carriage assembly. The new carriage will accommodate the 14" square plates and will have motor driven rotation. We intend to base the control of the carriage on a microprocessor which would be responsible for generating the servo ramps and would receive simple commands from the host PDP 11/34. Because of space restrictions imposed by the throat depth the scan length in Y will be limited to 10" but the full 14" will be accessible in the X direction.

The ability to perform accurate photometry is limited both by the detector electronics and by the light source stability. We have commissioned a design study with the aim of redesigning the detector electronics around Analogic's AN 8020L logarithmic ADC. This is a 15 bit device which will allow up to $4\frac{1}{2}$ decades in output signal to be covered with a digitization time of 200μ (this allows 160μ for signal integration and internal zeroing of the device). The maximum sampling rate of 5000 samples/second this would achieve is far inexcess of that presently permissible at moderate to high densities if distortions in the output are to be avoided.

As a single beam instrument the PDS suffers from problems with the stability of the light source. We have inserted a photodiode into the lamp housing to monitor long term changes in the lamp output and this gives a warning of lamp decay, but we feel that a separate monitor channel with feedback to the reference input of the logarithmic ADC should be incorporated as soon as possible.

If we are to scan effectively Schmidt plates without a platen we require an autofocus system to compensate for plate sag. The limitations of space and the accuracy needed (few microns) are rather severe requirements on any device. The most promising system we have investigated so far is a device designed by the National Physical Laboratory in the UK and is a proximity focussing device based on the principle of controlled astigmatism. We have yet however to investigate its effectivness under the conditions we require.

Van Altena: I have a question about the auto focusing. Were you planning on focusing simultaneously both the upper and lower apertures?

Pike: Yes.

Unidentified: If you take your output and highpass it the grain noise when it's in focus will give you a large dispersion between the maximum and minimum. And when its out of focus it will all be smoothed out you can focus on the data

Pike: Yes. That's the principle we thought of but I don't know why we dismissed it.

Horton: Apardine in Massachusetts has a auto focus mechanism that's been designed specifically for a PDS microdensitometer.

Pike: How much does it cost?

Horton: About $30,000. (laughter)

Pike: Even with the exchange rate that's not a very good price.

Hewitt: There is a point that I would like to raise about your possibility of monitoring the lamp. It is tempting to think about simulating a dual beam machine. I think you might get into some problems because it is not like a Joyce-Lobel which has a ribbon filament, what it has is a regular coil filament. It is very hard to make sure that you are on the same place.

Pike: That was entirely motivated by these strange variations we have over and above the ones that I have showed.

Dunn: Actually our earliest 1950 microdensitometer, pre-PDS, also built by Boller and Chivens, did have a lamp monitor of its filament. It works fine. You just have to use a little care and put a filter over it.

Oliver: I would just like to comment. I did a little work on that instrument after Sac Peak got rid of it. I think it is the same instrument which had a photo cell monitoring the lamp. I had a problem there with the fatigue of the photo-diode that was being used to monitor the lamp during the warm up period of about an hour. The photo-diode fatigued and changed! The lamp was absolutely rock stable (laughter). That is the photomultiplier that look at the lamp showed the lamp to be rock stable but the monitor diode drifted slowly downward by about 15 percent. So if you start introducing additional monitoring channel you have another thing to worry about.

Pike: Does anybody have any ideas about the temperature variation levels?

Horton: Yes, the instrument will move if you have a temperature gradient. The best way to control the temperature is to have plenium type of air-conditioning where the cold air gets mixed with the warm air outside the microdensitometer room then the air that gets pumped into the room is at the final temperature. If you just pump cold air into the room, the minute that the cold air hits the machine you are going to get a gradient and the machine is going to move. There is nothing you can do about it.

THE PDS FOR SPACE TELESCOPE GUIDE STAR SELECTION SYSTEM: STATUS AND IMPROVEMENTS

J. H. Kinsey
Space Telescope Science Institute*

I. OVERVIEW OF SPACE TELESCOPE REQUIREMENTS FOR GUIDE STARS

Pointing the ST (Space Telescope) requires that the onboard guidance system be provided with the coordinates and magnitudes of at least two guide stars for each observation region. Initial target acquisition is provided by the Pointing and Control System to an accuracy of the order of 1 arc minute utilizing information from the gyros. It is then possible for the FGS (Fine Guidance System) to search a region about 3 arc minutes across for objects that match each guide star. Once two such guide stars are acquired in each of two FGS apertures, the tracking servo loop maintains guidance to a tolerance of 0.007 arc seconds RMS jitter, (ref. 1).

The positions of a guide star pair relative to a target must be known to ± 0.33 seconds of arc so that an instrument such as the High Resolution Spectrograph (with an aperture of 2 arc seconds) will have a high probability of having the desired target region within its aperture. A Gaussian model for the error budget allocates 0.22 arc seconds of error to proper motions and 0.25 arc seconds to the positions of the two stars at the plate epoch; then an error of about 0.1 arc second is allowable for the actual scanning measurement. A 48 inch Schmidt survey plate has the dimensions of 35 cm x 35 cm covering a region spanning about 6.5 degrees across, so that 1 arc second is equivalent to 14.5 um on the plate. Therefore to achieve the desired 0.1 arc second precision, the scanning process should have an accuracy of 1 um.

The range of brightness for guide stars is between 9.0 and 14.5 in visual magnitude. A precision of 0.4 units in magnitude is required in order that guide stars not be confused with other stars in the FGS field. The magnitude of a guide star is determined from the relative size of the image on the plate. Schmidt plates are saturated at between 3 and 5 in O.D. (Optical Density).

*Operated by the Association of Universities for Research in Astronomy, Inc. under contract NAS5-26555 to the National Aeronautics and Space Administration.

The task of producing a catalog of potential guide star candidates will require complete scanning of approximately 1500 plates covering the entire sky with appropriate overlap. In the time window available to prepare GSSS before launch of ST (approximately 1.5 years), it will be necessary to scan at least four plates per day to complete this task.

Translating the above requirements into specifications for a scanning system requires that the GSSS (Guide Star Selection System) must have the capabilities summarized in Table I. The values in Table I are nominal and only insure that the measurement precision and scanning rates can be realized. Sampling at 50 um is the design requirement for finding guide star candidates. To prepare for ST operations after launch, it will also be necessary to perform fine scans of both the Schmidt plates and special plates with sampling intervals as small as 10 um in small subregions of a plate. Scanning speed requirements are based on two 8 hour shifts per work day and assume a one hour period for plate setup in preparation for a scan.

TABLE I - GUIDE STAR SELECTION SYSTEM SCANNING REQUIREMENTS

Spatial Precision	+/-1 um
Reproducibility	+/-1 um
Spatial Resolution	1 um
Density Range	0-5 O.D.
Scanning Area	50 cm x 50 cm *
Digital Resolution	greater than or equal to 12 bits

Scanning rate required to scan 4 plates (35 cm x 35 cm) per 16 hour day (for 2 scanning engines):

Sampling Interval	50 um
No. of Scan Lines	7000
Scanning Time per Line	3.6 s

* Special plates from several sources, which are of this size, may be expected.

Perkin-Elmer specifies that the Model 2020G PDS is capable of providing 1 um spatial resolution at a linear scanning rate of 200 mm/s with a precision of ± 5 um over its 50 cm x 50 cm scanning aperture. Repeatability is specified as ± 1 um. An optional density range of 0 to 5 in O.D. is available. This device, which is built on a 3.25 ton black granite (black gabbro) base, is of very rugged construction. These specifications would satisfy the guide star requirements of ST provided the spatial precision can be enhanced to 1 um and that two machines are used to provide the required scanning rate. It

should be noted that although a 200 mm/s scanning rate implies a time per scan line for a 35 cm plate of 1.75 s, the overhead required for turning around between lines is between 1 and 1.5 s.

The remainder of this discussion will be directed to an assessment of the limitations of the PDS as it is delivered and the modifications that must be made to improve its performance for the designated task. We are currently in the process of implementing the modifications. This presentation is a report on progress to date; completion of the modifications is expected in third quarter of 1983.

II. EXPERIMENTAL DETERMINATION OF PDS ACCURACY

Actual performance characteristics of the two machines acquired for the project have been measured in order to facilitate design and implement improvements in the GSSS. Positional precision is of primary concern to the success of the project and hence those measurements have been carried out which indicate the magnitude and nature of positional errors.

In order to determine the errors in each axis separately, a 20 um diameter wire was stretched under moderate tension on a frame which could be positioned on the x carriage in place of the platen. The wire could be aligned parallel to either the x- or y-axis by iterative adjustments of the frame, and it could be easily brought into focus along its entire length by means of adjustment screws on the frame.

Scans of this wire were made by performing a raster scan along its length using the smallest aperture (5 um) provided. For instance, with the wire aligned parallel to the y-axis 100 samples at 1 um intervals were taken across the wire alternately in the positive and negative x-direction, with a 500 um step in the y-direction between each scan. The data from each scan line was analyzed by fitting a straight line to the points representing the edgesof the wire. The mean x value for the two half-intensity points for the two edges was determined and taken as the center of the wire for each scan. It should be noted that the wire was ascertained to be straight with no "kinks" or periodicities with a magnitude greater than 1 um. This was accomplished by comparison of a number of scans of the wire both before and after rotating the frame 180 degrees about the wire's long axis and by repeated visual examination of the aligned wire in the PDS viewing screen as it was scanned along its entire length at high magnification.

Figure 1 is a representative plot of one such wire scan. This was performed on PDS 1 (We arbitrarily designate the two they were received.). Identical scans performed on PDS 2 are very similar, but show some differences which are attributable

to variations in the guidance systems between the two machines. Casual examination of the two frames in Figure 1 shows that there appear to be three distinct frequency components. The lowest of these contains at most two cycles over the 350 mm length of the wire. The medium frequency has a period of about 14 mm and the shortest is at the y-sampling interval of 0.5 mm.

At least part of the lowest frequency component is caused by a slight curvature in the guide rails. This is probably unchanging unless the machine is moved, or unless adjustment is made to these rails (the granite will measurably deflect). One of the fundamental mechanical problems with the PDS is seen by comparing Figures 1 (a) and (b). These two plots represent a scan in the positive y-direction of the wire followed immediately by the a scan in the negative direction. Note that at the beginning of each of these scans there is a steep x-offset followed by a relatively modest variation in x-position for the remainder of the scan. The two of these taken together illustrate a mechanical hysteresis such that the mean x-position of the wire is dependent on y-scanning direction. The total magnitude of the deflection of the wire position is consistent with the $\pm$5 um positional accuracy given by Perkin-Elmer.

The medium frequency is not commensurate with either the rotation of the entire bearings or the balls. The period is too large for the ball diameter and too small for the bearing race. It is possible it may be because of an ellipticity of one, or more, bearings. It appears related to bearing rotation since the phase is easily changed by manual rotation of a bearing. It appears then that the Perkin-Elmer specification of 1 um reproducibility does not hold. Our measurements would indicate that the reproduciblity is indeed the same as accuracy, i.e. 5 um.

The high frequency is easily explained as the quantum of uncertainty in the PDS position encoder which has a resolution of 1 um, so that alternate scans have an apparent jitter of 1 um. This particular "error" is easily corrected computationally.

Figure 2 is the result of averaging multiple left-to-right and right-to-left scans across a Ronchi ruling at 4 mm/s. This particular scanning rate is commensurate with a sampling rate of 4 kHz which is the same for 50 um sampling and a scan speed of 200 mm/s. The scans in each direction are averaged separately. The results depicted were obtained using a new log amplifier in place of the one supplied by Perkin-Elmer since the latter device was found to have much too long a rise time for the scanning operations. The new log amplifier is based on the Analog Devices AD757 6-decade logrithmic amplifier module. Above density 3 (Perkin-Elmer units which are essentially semi-diffuse density) there is some distortion of the signal. This

is currently under study.

The result of scanning a step wedge spanning 3 in diffuse O.D. are shown in Figure 3. This plot is an average of 200 scans along the same line across the wedge. All steps are clearly defined and the noise increases as expected with decreasing light. Measurements made directly at the output of the photomultiplier with an oscilloscope give a S/N for the photo-signal of 500 with a 50 um aperture. The noise equivalent dark signal was 2 mV into 100 Kohms, giving a dark current of 20 nA. The Hamamatsu R268 photomultiplier being used has a specified maximum dark current of 20 nA.

III. LIMITATIONS OF THE PDS

The PDS as specified by Perkin-Elmer and as shown by the measurements of the previous section does not meet the requirements of the ST GSSS. In order to modify and enhance this measuring engine it is necessary to examine critically its inherant limitations. No criticism of the PDS is intended since design specifications appear to be met except in the case of reproducibility, which has been determined to be 5 um rather than the 1 um Perkin-Elmer specifies.

Several design problems which either have to be corrected, or circumvented in order for the machines to be used for GSSS, will be discussed. Aside from several relatively minor electronic concerns, there are four major mechanical problems that limit the performance characteristics of the PDS.

The first of these problems is related to the cross-coupling between the motions in x and y which are a form of mechanical hysteresis. This effect manifests itself in an offset in x-position which is dependent on the y-scan direction. An explanation entirely consistent with the observed data and the operation of the device is that the y-axis motion is produced by an off-center drive on the granite yoke which carries the entire optical system. Because of the application of the driving force to one side of the center of gravity of this subsystem, a torque is produced which causes the yoke to rotate either counter-clockwise or clockwise depending on whether the y-motion is positive or negative. This in turn produces the corresponding offset in x. Because of the construction of the Model 2020G PDS, correction of this difficiency by redesign of the drive is not considered feasible.

The second limitation to precision appears to be related to the use of ball bearings for lateral guidance of the both the x and y-axes. This is apparent because of the 14 mm period component of the x and y-scans of the wire parallel to the orthogonal axes, as shown in Figure 1.

The third problem has to do with the indirect manner in which the position measurements are made on each axis with respect to the optical axis. Because of the way the encoder/ruling subsystems are mounted on x- and y-axis, the counts derived from their outputs tell precisely only where the encoders are with respect to the base. For higher precision measurement it is necessary to measure the relative position of the plate with respect to the optical axis of the microdensitometer optics, i.e. with respect to the focal spot on the image being scanned. The encoders measure their relative position along the ruling, but cannot account for any rotational motion of the x carriage or the y yoke. Furthermore, from the evidence in Figure 1 there is coupling between x and y measurements because of this rotational motion, but the the motion control for the two axes are completely independent.

The last difficiency is one which is related to long term use of the PDS scanners. There has been an inordinate amount of wear on the bearing surfaces of the granite x guide-rails which define the lateral position of the carriage. The origin of this is primarily because two opposing parallel surfaces are being used to define the direction of motion. Geometrically this is not correct and functionally it is wrong since it is next to impossible to produce exact parallelism even in structures much smaller than large granite rails. The variations in separation inherent in this design cause a wide variation in bearing pressure. On PDS 1 this loading has been high enough to roughen the granite bearing surface after less than 100 hours of operation. Considering that during the coarse scanning of one 35 cm x 35 cm Schmidt plate the x bearings roll in excess of 2.45 km, it is easily seen that the wear problem is of fundamental concern to the project. There is some reason to believe that the granite used for these machines is not as wear resistant as can be obtained. Black gabbro does not appear to be as ideal a material for the bearing surfaces as pink granite (refs. 2 and 3). It should also be noted that the 14 mm period component shown in Figure 1 and discussed in the last section may indeed be caused by permanent deformation of the guide bearings due to overloading.

IV. MODIFICATIONS

In this final section a brief summary of the actions being implemented to correct for the measurement errors will be given. As a necessary introduction to this material a brief description of the motion control on the PDS will be given. This description is equally valid for the machines which have a translator controller connected directly to the host computer instead of the onboard microcomputer.

In Figure 4 is shown a very much simplified schematic of the motion control for x and y on the PDS. This diagram depicts the servo feedback loops by which motion is controlled. A motor control circuit is provided for each axis. Movement in the x-direction of the carriage is accomplished by the M6800 microprocessor sending an appropriate command to the x-motor control circuit including a digital speed with sign. Voltage of the appropriate magnitude and polarity is applied to the x-motor and motion commences. The x-tachometer returns a voltage to the motor control proportional to its speed of rotation. This voltage is compared to the voltage equivalent of the required speed and the resultant error signal controls the drive voltage of the motor.

As the carriage moves the x-scale/encoder provides the pair of sinusoidal signals to the x-digital coordinate readout system (DCRS) which increments, or decrements, the x-position register according to the sense of motion. The DCRS circuit also sends its pulses to the special AUTOLOK register on the motor circuit board. When the AUTOLOK feature is invoked by the microprocessor an increment, or decrement, count from the DCRS will cause a motion of the motor such as to return the encoder to its previous position. The position of the carriage may be determined by the M6800 at any time simply by reading the x-position register. The motion and location of the y-motion is provided in an identical manner to that of x using a set of circuits that are completely independent.

In typical operation the microprocessor would perform a scan by positioning the yoke to give an appropriate y starting location for the scan and setting the x-position of the carriage at a location preceding where density samples are to commence being taken; this is to permit "ramping" up to the desired speed by the time sampling starts. X-motion is commenced by sending the appropriate command to the x-motor circuit. Y-axis motion is frozen by enabling the y AUTOLOK feature so that any drift of y will be eliminated.

The feedback loops provided by the velocity error detection and the AUTOLOK as well as the precision of the encoder/scale would make it possible to maintain higher accuracy if the measurements were referenced to the optical axis rather than to the base. Reference to the optical axis and therefore the measurement locus could be achieved if the measurement devices were somehow attached between the carriage and the optical head, which indeed they are not, and cannot be made so. An optical interferometer could realize this goal by measuring the distance between each of two orthogonal reflectors attached to and parallel to the sides of the platen and two corresponding reflectors forming the opposite ends of the interferometers attached to the optical measurement head. The positional

signals produced by such devices would take the place of those which are provided by the existing optical encoders.

The virtue of such an arrangement would be that now any variations in y position produced by the x-motion of the carriage would cause a corresponding correction of that error by a motion produced by the AUTOLOK feedback loop on the y-motor board. Similarly the correct starting position in x would be directly read from the interferometric distance between the platen and the optical head. Any variation in x caused by motion of the yoke would be automatically corrected.

It is planned to implement such an enhancement by utilizing a Hewlett-Packard Model 5501A laser interferometer system equipped with two orthogonal plane mirrors attached parallel to the x and y-axes on the x carriage. The pulse output from this system will replace that which is now provided by the linear scales and optical encoders. This system will correct for both the medium and low frequency components shown in Figure 1. It should increase precision to the 1 um range. A simplified schematic of this implementation is presented in Figure 5. The plane mirrors designed for this system are 50 cm long by 3.8 cm x 2.5 cm in cross-section. They will have lamda/2 flatness over the entire working area and lamda/8 over any 2.5 cm region. Because of the use of plane mirrors the measuring speed must be reduced from the 350 mm/s quoted by Hewlett-Packard for use with retroreflectors to one half that value. The latter form of reflector is not compatible with the measurement geometry required by the PDS.

A fix for the granite wear caused by the over-constrained x guide bearings has already been implemented and sucessfully tested on PDS 1, and the second machine is soon to be upgraded. The modification consists of replacing the hard mount of the bearings on one side of the carriage with spring loaded bearings. These bearings are free to follow variations in spacing, but produce a constant force by the remaining hard mounted bearings against a single surface , a geometrically and functionally correct solution.

The remaining minor mechanical, optical and electronic quirks of these machines have essentially been mastered. Engineering software has been developed since installation of the first PDS in September 1982 and production coarse scanning will start in the near future.

ACKNOWLEDGEMENT

I wish to acknowledge the expert assistance in carrying out this project provided by Messrs. R. Denman and A. Evzerov.

REFERENCES

1. O'Dell, C. R. The space telescope. in Telescopes for the 1980s, ed. by G. Burbidge and A. Hewitt, Annual Reviews, Inc., 129-193: 1981.

2. Starrett. Catalog No. 28, The L. S. Starrett Co., pp 400-401, Athol, Massachusetts, 1982.

3. Steele, R. S. and Douglas, R. A. Experimental Determination of Dynamic Stress-Strain Relationships During Wave Propagation in Brittle Materials, Technical Report 74-1, North Carolina State Univerity, Raleigh, 1974.

FIGURE CAPTIONS

Figure 1. Raster scan of 20 um diam. wire parallel to y-axis. Scanning aperture = 5 um, x sampling interval = 1 um, y sampling interval = 500 um, and scanning speed = 5 mm/s. Alternate x-scans are in opposite directions. (a) positive y-direction. (b) negative y-direction.

Figure 2. Repetitive scan of same x-segment across a Ronchi ruling. Scan aperture = 5 um, x sampling interval = 1 um, and speed = 4 mm/s. Solid curve represents the average of 100 scans in the positive x-direction and the dashed curve 100 scans in the negative direction.

Figure 3. Repetitive x-scan of Kodak No. 2 Step Tablet. Plot represents average of 200 scans in alternating directions across tablet. Scanning aperture = 50 um, x sampling interval = 400 um, and scan speed = 100 mm/s. Kodak step wedge is calibrated and has 21 diffuse density steps ranging from .05 to 3.05.

Figure 4. Simplified block diagram of PDS motion control system. Solid lines represent digital signals and dashed lines analog circuits.

Figure 5. Simplified schematic of planned implementation of laser measuring system for improving positional accuracy of PDS. Design is based on components of the Hewlett-Packard 5501A laser positioning system.

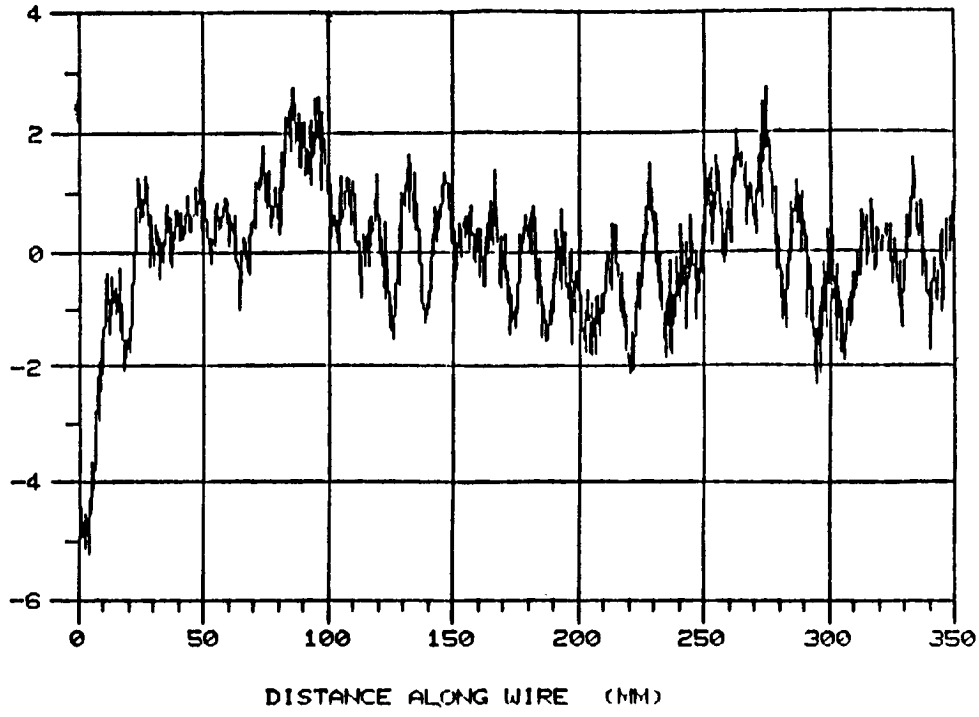

Figure 1 (a)

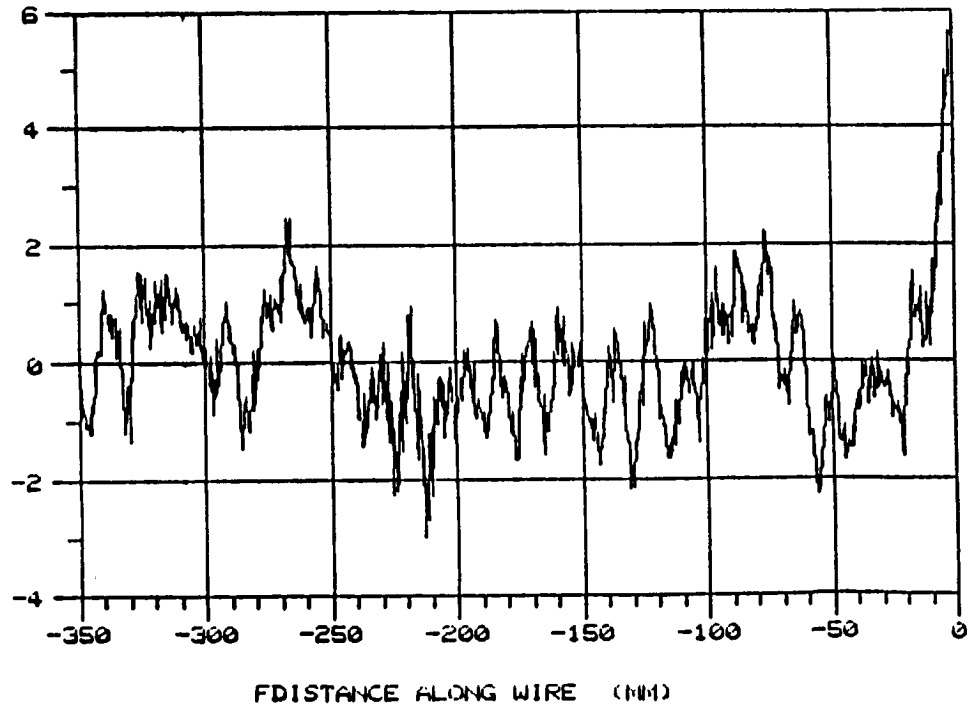

Figure 1 (b)

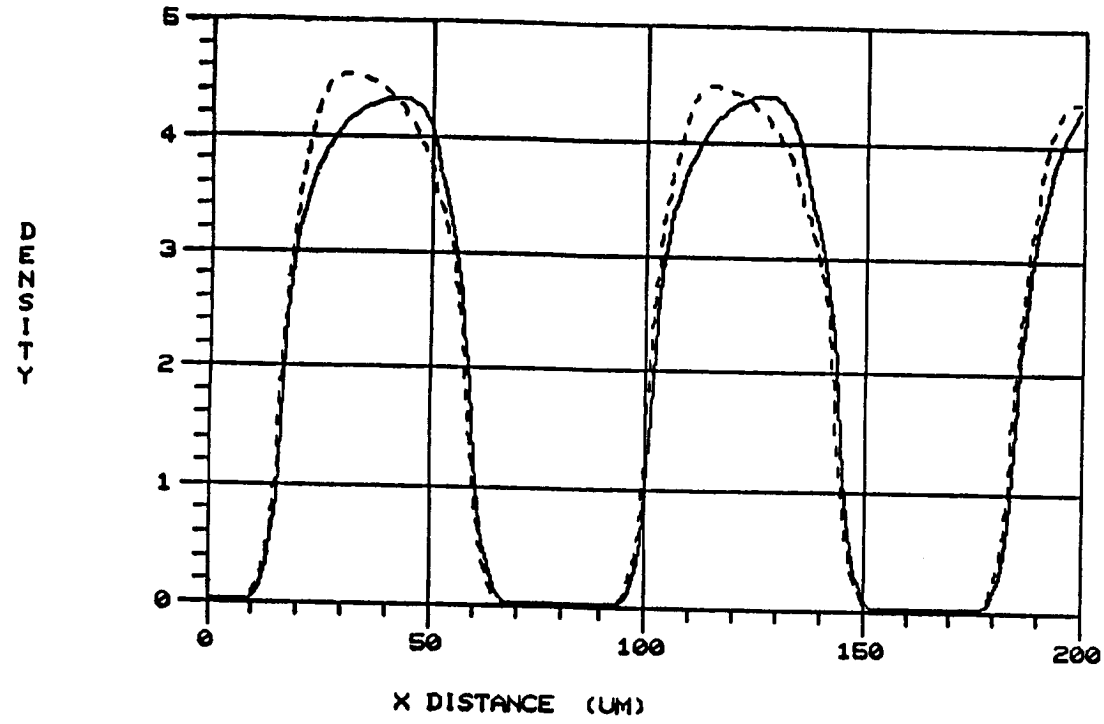

Figure 2

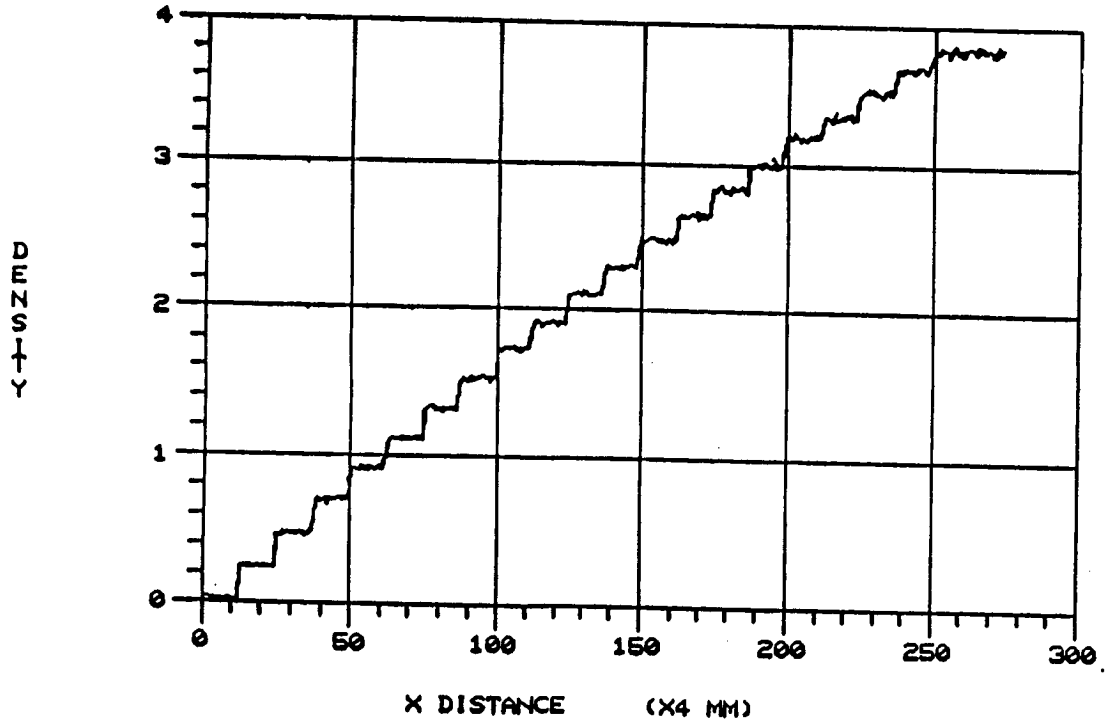

Figure 3

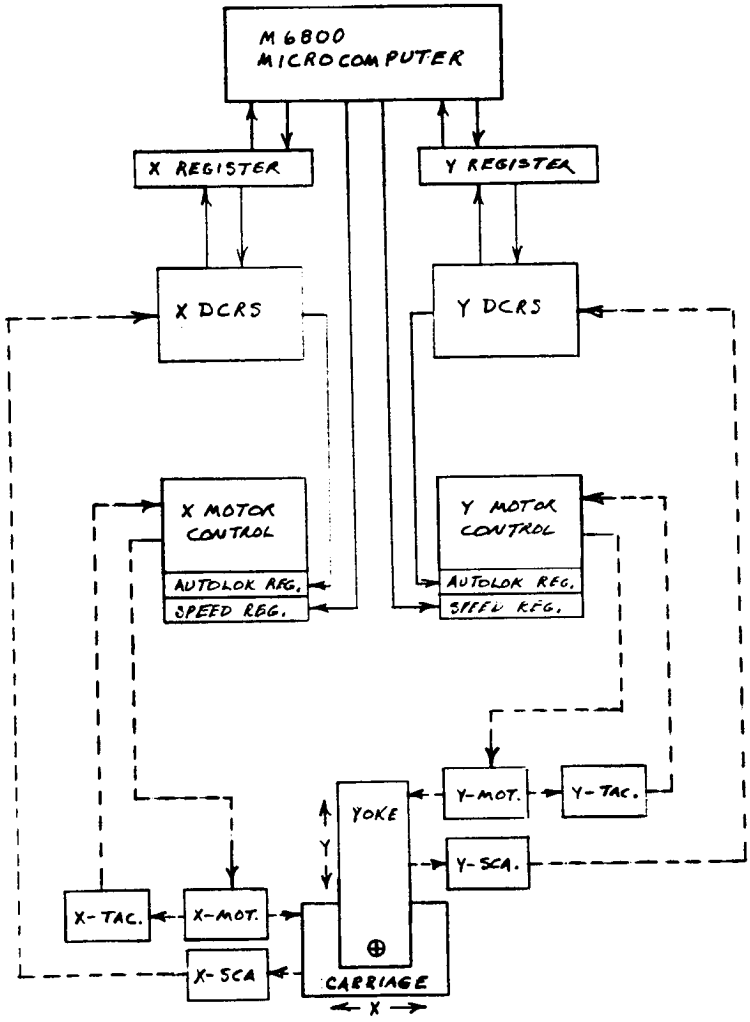
M6800
MICROCOMPUTER
X REGISTER
Y REGISTER
X DCRS
Y DCRS
X MOTOR
CONTROL
AUTOLOK REG.
SPEED REG.
Y MOTOR
CONTROL
AUTOLOK REG.
SPEED REG.
Y-MOT.
Y-TAC.
YOKE
Y
Y-SCA.
X-TAC.
X-MOT.
X-SCA
CARRIAGE
X

Figure 4

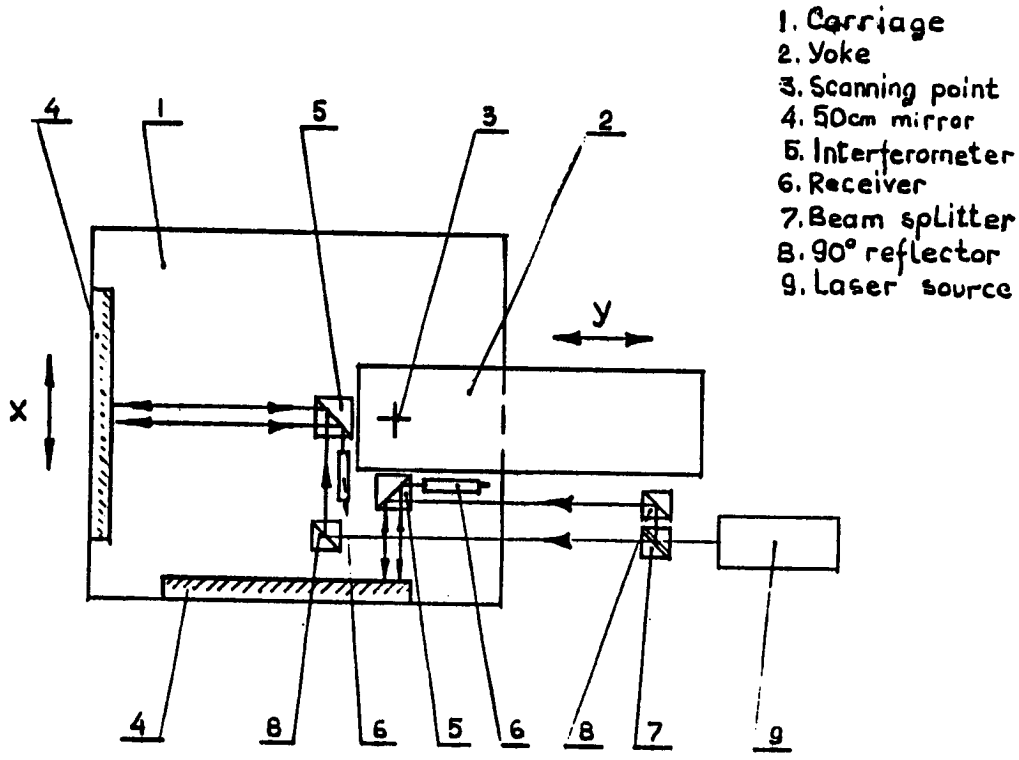
1. Carriage
2. Yoke
3. Scanning point
4. 50cm mirror
5. Interferometer
6. Receiver
7. Beam splitter
8. 90° reflector
9. Laser source
4
1
5
3
2
y
x
4
8
6
5
6
8
7
9

Figure 5

Monet: Are you going to use active feedback?

Kinsey: Yes, that is correct. Our intentions are to actually replace the encoder output normally that goes into the DCRS which is the position sensing electronics in the PDS; we will go into this with the output of a pulse generator hooked to the output of the Hewlett Packard position sensors. So the positive feedback then would be the fact that any motion no matter what its source, that causes a change say in the fixed axis (y-axis) so if there's curvature in the x-rail for instance and it causes a change in the Y distance that feedback will drive the servo-mechanism so that the y-axis will correct itself.

Van Altena: When you talk about this possible uncertainty I would think that probably would not be the effect because permanent head position repeatable to about 5 hundredths of a micron, I think that probably would be visible. I think what you are seeing is just noise in the hearings as the balls are rolling in the races.

Kinsey: Are you talking about on the wire scans?

Van Altena: Yes.

Kinsey: It's different depending on which type of scanning you do. But I guess that's consistent with what you just said. It has a different character and I'll show you the two scans here from the X and Y scans.

Van Altena: Yes. I have another comment about that. There is another factor, the width of the wire varies on a scale of about 100 micron. It varies with an RMS variation of about 0.7 microns. So that you have this width variation of the wire depending on where you determine the position. It ultimately wonders around.

Kinsey: Are you talking about the actual physical width of the wire?

Van Altena: Yes.

Kinsey: I don't know what the tolerances on the wire are. This is one that our optical engineer selected very very carefully. We have looked at it under high magnification. We flipped it around its longitudional axis and are pretty sure it has no kinks larger than a micron, which is 20 percent of the diameter of the wire.

Van Altena: Depending on where you come across the wire it will be thicker or thinner and this can introduce some noise.

Kinsey: And you're estimating what?—on the order of the micron, variation?

Van Altena: We can actually map it out to see the width. The other thing is the different noise in the X and Y axis. I think that our X axis is considerably better than the Y axis. I believe that the difference for this is that the axis bearings have to be cinched up more tightly to keep this 300 lb. of granite moving on the same line and this overstresses the bearings and this amplifies the noise you can see.

Kinsey: I remember you once made a suggestion to me that if we loosen the bearing up we would not see as many of the oscillations. That was true but we began to see more of this torquing effect. So, you can't win either way.

Van Altena: We are not so concerned with the torquing effect because we have the ultimate micrometer that measure the errors from the various positions. I do have to say that we are going to the dual axis laser interferometer as you are.

McNamara: Perhaps if you looked at it with both a 10/10 and a 20/20 you could determine if it is something that is peculiar to the 2020 machine. That is, are you getting the same oscillations when you do the same experiments on both machines?

Kinsey: Do you mean in scanning the wire?

McNamera: Yes. Or if it's not the wire if it's actually the fact that you're using such a heavy machine.

Kinsey: Well, I don't see in this particular case where that would help us. We have two machines and if you want I'll be specific. I think it's sort of an academic problem really. I don't know that much about the 10/10 but I think mechanically it's not quite the same. The carriage moves in two directions. Isn't that right? What we have here is a carriage that moves in one direction only that's constrained with granite rails then we have about 160 Kilogram yoke which holds the optics which moves in orthogonal direction. So I don't see what we would gain here.

McNamara: I guess what I'm trying to flush out here is what machine would give you better astrometrics accuracy—the 10/10 or the 20/20? I guess originally the 20/20 is more stable. Is that necessarily true?

Van Altena: No, in fact the 2020, the granite machine, seems to be a far inferior in terms of its accuracy when compared to the metal machine and whether or not it is a result of the fact that the design of the metal machine was scaled up. I did a lot of work on the 1010a at Berkely and at Austin and what I found there is that the internal calibration of the ways that I developed was constant over a period of 2 years. This allowed me to make a correction with respect to an RMS repeatability on an external basis of 0.4 micron.

McNamara: That is exactly the impression I was getting. Virginia also has an installation in Australia where they had a 1010a. They stripped it down and took it apart and put it back together and it repeatabilities to within a micron. It just seems to me from all the discussions that the astometrist would use the 1010.

Kinsey: We have to handle the 14" plates and large so we will have to go to a large machine.

IMPROVEMENTS TO THE PHOTOMETRIC RESPONSE AND POSITIONAL ACCURACY OF THE YALE PDS 2020G MICRODENSITOMETER

Jin-Fuw Lee and William van Altena

YALE UNIVERSITY OBSERVATORY

In the course of optimizing the Yale PDS 2020G microdensitometer for photometric and astrometric research, it has been necessary for us to incorporate several hardware changes. In this paper, we describe the properties of a new high speed photometer and a positional calibration system. The new photometer incorporates a high speed logarithmic analogue-to-digital converter with more than ten times the resolution of the former system and a cycle time of approximately 50 usec. The positional calibration system monitors the drunkenness of the stages with respect to fixed index lines and enables us to correct the +/- 5 um stage errors to an accuracy of better than 1 um.

I. Introduction

The slow photometric response of the logarithmic amplifier and the drunkenness of the stage motions in the existing PDS microdensitometers are the main obstacles for precision investigations involving photometry and astrometry (See another paper in this volume by van Altena and Lee(1983b), hereafter referred to as Paper I). Two hardware systems, a new fast photometer and a positional calibration system, were therefore implemented on the Yale PDS 2020G microdensitometer as the remedy to these inaccuracies. In this paper we report on the properties and accuracy of these new systems.

II. The new photometer

The characteristics of the new photometer have been described by van Altena and Lee(1983a). In the following, a brief review of its salient features is given. As a replacement for the slow logarithmic amplifier, we installed an Analogic AN8020L 15-bit logarithmic A/D converter, which first transforms the photoelectric current from the photomultiplier tube (pmt) linearly into a voltage in the range 8v to 178 uv and then converts logarithmically to the density through a special digital algorithm. The module features a 13 usec integration time and an 18 usec conversion time. The hardware configuration of the PDS electronics limits us to an output resolution of 12287 levels between 0 and 4.65D, corresponding to 0.00038D per level, which is more than ten times the resolution of the log-amp. The noise of the new system is found to be dominated by the photon counts, so a R-C circuit has been designed to provide for a longer integration time. With an additional 24 usec of integration in the R-C circuit, the photon noise is reduced to below the grain noise level of most astronomical emulsions, including the IIIa-J.

The response to a razor blade scan shows that the log A/D converter is much faster than the log-amp, as described in Paper I. A detailed analysis of the response curve involves the evaluation of the edge positions at different density levels by using Eqs. (1) and (2) in Paper I. In Fig. 1, we plot the edge positions determined at T=0.5 (D=0.3), D=2.5, and D=3.0 for razor blade scans at different speeds for the log-amp and the log A/D converter. (Note that we use the PDS specular density in this paper). At T=0.5 both the log-amp and the log A/D converter yield edge positions that are independent of speed and direction, while at D=2.5 and D=3.0 only the dark to light log A/D scan is independent of speed. The average light to dark response of the log A/D converter scans yields response times of 20, 50, 150 and 600 usec at densities 2.5, 3.0, 3.5 and 4.0 respectively. On the other hand, the log-amp is some seven times slower at densities 2.5 and more than ten times slower above density 3.5.

Since a change of either the voltage or the filter setting will alter the indicated density, a direct comparison will be meaningless unless the photometer is a linear system, or a density-calibration curve is available. To test the linearity of the new photometer, the Interobservatory comparison step wedges, Sewell(1975), with 21 density levels were scanned on the PDS

using a large aperture (100x100 um) and a long integration time (450 usec) in order to cut down both the grain noise and the system noise. Each scan was then repeated with a change of voltage or filter setting and the differences between the two sets of output densities compared. From these comparisons, we found that the photometer is linear to 0.005D for D < 3 and voltage settings between 3.5 and 5.0. A nonlinearity due to the nonzero dark current becomes prominent above D=3 and also nonlinearity is dominant at both low (V < 3.0) and high (V > 5.0) voltage settings.

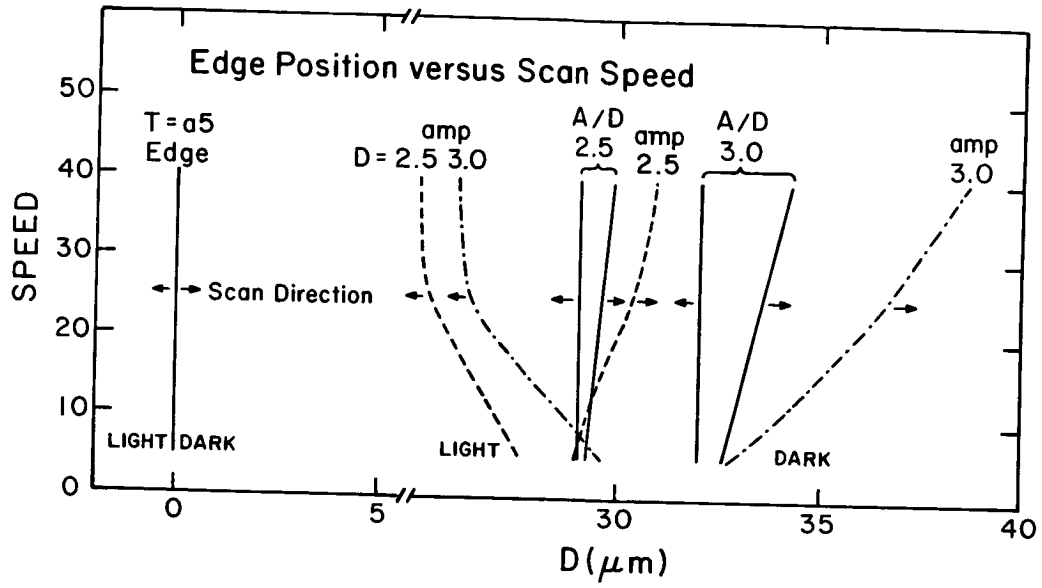

Figure 1: The edge position in microns is shown as a function of the scan speed in mm/sec for a series of razor blade scans. At a transmission level of 0.5, the log-amp and the log A/D both produce the same edge position regardless of the scan direction, which is also indicated in the figure. At a density of 2.5 the edge position is shifted approximately 30 um towards the dark side, due to the point spread function of the microdensitometer. Only the log A/D dark to light scan produces an edge that is independent of scan speed. The light to dark scan indicates that the effective response of the log A/D is about 50 usec at D=3.0. The response of the log-amp is about 7 times slower at D=3.0 and more than 10 times slower than the log A/D above D=3.5.

As described in Paper I, the fast response of the photometer enables us to measure the grain noise at the reasonably high speed of 10 mm/sec. Tests with the Interobservatory comparison step wedges show that the specular density measured by the PDS is linearly related to the Kodak diffuse density with a proportionality constant 0.76. In addition, the grain noise of the Ia-, IIa- and the IIIa- emulsions obeys the square-root of the density law approximately, as described by Furenlid, Schoening and Carder(1977).

The new photometer also allows a rapid digitization of stellar image profiles with a negligible amount of skewing. Normally, a small raster scan

of size 600 um square is made around each image at a scan speed of 10 mm/sec. The density array D(i,j) is then fitted to a Gaussian profile

$$D(i,j) = B_o + D_o \exp\langle -[(x-X_o)^2 + (y-Y_o)^2]/2R^2 \rangle \qquad (1)$$

and optimally weighted by the inverse square of the grain noise to achieve the best fit.

To study the photometric and positional errors, approximately 40 stars on a IIIa-J plate were measured with both the log-amp and the log A/D converter for comparison. The formal errors of the positions are plotted in Fig. 2 versus the peak density D_o.

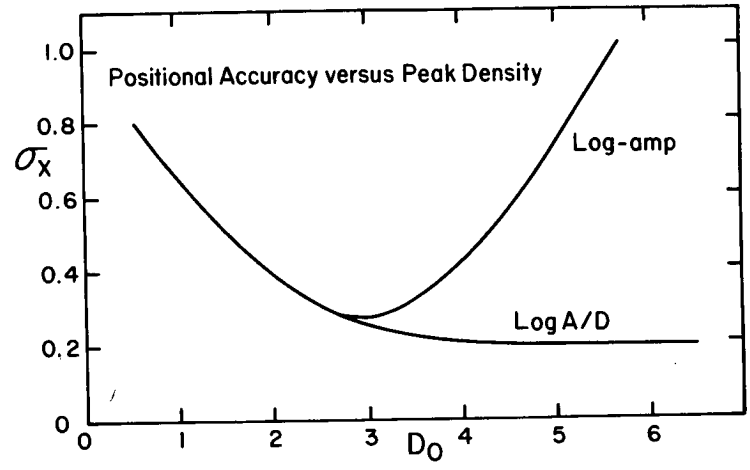

Figure 2: The formal error of the position in um is shown as a function of the peak density for images fit to a bivariate Gaussian. The log-amp curve diverges from the theoretical relationship above peak densities 2.5 due to the slow response of the log-amp, which causes the high density regions of the image to be skewed in the scan direction and therefore not correctly modelled by the fitting function. The log A/D curve follows the theoretical grain noise limit very closely and therefore extracts all of the positional information from the image.

The increasing error at large peak densities for the log-amp implies that the measured profiles of these bright stellar images are dominated by skewness, while the errors obtained from the log A/D converter agree fairly well with the theoretical limit placed by the grain-noise of the IIIa-J emulsion (see Lee and van Altena, 1983). In Fig. 2, we see that the errors are about E = 0.2 - 0.3 um for most images, except for the faint images which have peak densities less than 2.5 and slightly larger centering errors, 0.3 - 0.7 um.

For an estimate of the stellar brightness, we use the pseudomagnitude defined by Stetson(1979) as

$$m = \text{const.} - 2.5 \log_{10} (D_o R^2). \qquad (2)$$

The theoretical standard error in m is roughly E/R, which for a typical size image with R = 50 um, will be about 0.005 - 0.006 for bright images ($D_0 > 2.5$) and 0.006 - 0.014 for faint images ($D_0 < 2.5$). These high signal to noise images are therefore suitable tools for assessing the overall performance of the PDS, and are scanned routinely to check the repeatability in both positioning and photometry.

III. Photometric repeatability

Short term repeatability is tested by making about a dozen scans of the same plate over a period of a few hours. The voltage and the filter settings are kept constant, while the orientation and the position of the plate are changed. The repeatability in the magnitude, m, is generally better than 0.01 for all images. Tests on the long term repeatability were made by comparing measurements of the same plate spread over a period of a few months. In this case, it is not possible to keep the voltage settings the same for all of the tests. The repeatability in m is within 0.02 mag., except for a few bright images. The nonrepeatability in m for these bright images is probably due to the non-linearity in the photometer at densities above 3.0. In the high density region in the center of these bright images the photometer is susceptible to drift in both the dark current and the gain of the system. These systematic effects can be removed with a polynomial transformation of second order between the magnitudes in the various runs. They can therefore be absorbed in the calibration curve, if sensitometric spots are available on the plate. Similary, if photoelectric standards are used, the transformation from pseudomagnitudes to real magnitudes will remove any non linear effects.

IV. Positional repeatability

The positional accuracy of the PDS was tested by raster scanning the same set of stellar images on a IIIa-J plate as mentioned in Sec. II. The plate is then moved by a distance L, scanned a second time and the two sets of coordinates computed with an optimum centering algorithm. The second set of coordinates is then reduced to the first set using linear coefficients allowing only for rotation and translation. The unit weight errors from the least-squares fit are our indicators for the positional accuracy of the machine. For repeat measurements (L=0) on the Yale PDS, the accuracy is about +/- 1 um and +/- 0.4 um, in x and y respectively. For L >> 1 mm, the accuracy degrades to +/- 2 um and +/- 0.4 - 0.6 um in x and y respectively. These tests were performed before the implementation of the positional calibration system.

Paper I describes three possible causes for the nonrepeatability in the positions: (1) one-micron glitches, (A thorough clean-up of the circuitry will probably remove the glitches); (2) thermal drift, (A pre-scan warmup both electronically and mechanically will minimize the drift); and (3) drunken stage motion due to curvature in the granite ways and distortion in the shape

of the guiding bearings. The stage motion problem is very important especially for the y-axis on our 20-inch granite machine. Therefore, positional calibration systems were designed to reference the stage motion to a straight line. The calibration system on each axis consists of a straight "index-line" (used as the new reference edge) and a monitor which continuously measures the relative position between the measurement axis of the PDS and the index line. Assume that the displacement between the x-axis and the respective x index-line is DY(x), and the displacement between the y-axis and the y index-line is DX(y), then the true position (x', y') will be corrected in the reductions after scanning by,

$$x = x + DX(y)$$
$$y = y + DY(x) \qquad (3)$$

V. Positional calibration system

A long straight index-line (at least 20-inches long) is not readily obtained in the commercial market. We have therefore made our own using the following method. First, a clean 25 or 50 um diameter tungsten wire is stretched over a clean glass strip with dimensions of about 520x30x6 mm. Epoxy cement is applied to the ends of the wire while it is under tension to keep it straight. The glass strip is then placed in a vacuum chamber and aluminized. The wire is then removed and a clear line remains on the glass strip in the background of the reflective aluminum coating.

The 50 um index-line is viewed in reflected light by an optical micrometer, in which light from a fiber optics light source passes through a beam splitter and is focussed by a 10X objective on the index-line. The reflected light traverses the same objective, but is then diverted by the beam splitter to the split photodiode, where the index-line is imaged as a dark 0.5 mm line on the two 0.5x4.0 mm photo detectors, A and B, which have a separation of 0.1 mm.

The intensity difference, A - B, between the two channels, is a measure of the relative position, D, of the index-line and the photodiodes. The transfer curve, R, is defined by

$$R = (A - B)/(A + B), \qquad (4)$$

where the ratio is taken to conpensate for fluctuations in the intensity of the reflected light. The transfer curve can be derived as follows: If the width of the index-line is W, then the intensities A and B are proportional to W + D and W - D respectively, if the displacement D is less than half of the index-line width. Within this range, the transfer curve is linear and is given by,

$$R = D/W \quad \text{for } |D| < W/2 \qquad (5)$$

For our 50 um index-line, the linear region of the transfer curve is approximately W = 50 um, which is large enough to cover the range of lateral motion of the axes. The corresponding sensitivity is dR/dD = 1/W = 2% per micron. This is equivalent to a scale of 0.01 um per resolution unit (R.U.).

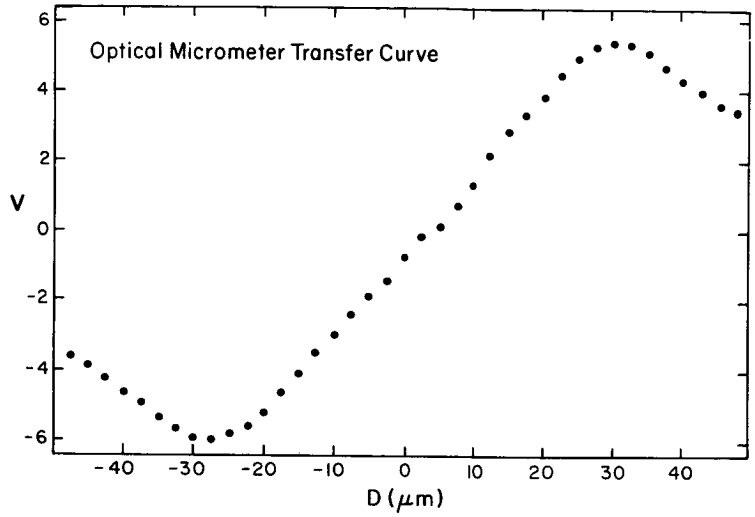

Figure 3: The actual shape of the transfer curve is found by moving the index-line across the field of view of the optical micrometer in steps of 2.5 um and recording the output voltage of the micrometer. The ordinate can be approximately converted to the transfer function in Eqs. 4 and 5 by dividing 'V' by ten.

Tests with the optical micrometer show that it has low noise (2 - 3 R.U.) and a fast response (< 1 msec). A major problem with the system is associated with the precise determination of the scale. Since the nonrepeatability of the lateral motion of the axes can be as large as +/- 5 um, a 5% error in the scale will result in an error of 0.25 um in D. Several factors prevent a better determination of the scale from being made: (1) Defocusing of the optical micrometer may result in a blurring of the image of the index-line, and a correspondng change in the transfer curve. The index-line therefore has to be carefully adjusted to a horizontal plane so that the focus can be maintained over the full length of travel. (2) The variation in the width of the index-line is about 2 - 3 um, as is shown in Fig. 4, which amounts to a 5% variation in the scale from one point to another. (3) The lateral motion of the axis may contain rotational or vibrational components in addition to a simple displacement. which would then vitiate the corrections indicated by the optical micrometer, since the optical micrometer only measures the displacement. In view of these problems, the following method is used to determine an average scale for the optical micrometer: A long straight line is placed on the PDS platten and aligned parallel to one axis, say the y-axis. The line is then raster scanned and the edge positions are determined along the length of the line. A repeat scan is then made and the change in the edge positions due to changes in the bearing errors are then fitted linearly with the change of the micrometer readings. The slope of the relationship then yields an average scale.

A second major problem is the existence of a few hundred pinholes on or near the index-line, which introduce errors into the derived corrections. Our strategy for correcting for the pinholes is to cover 3/4 of the length of the photodiode so that it collects reflected light only from a 100 um length of the projected index-line instead of 400 um. For a typical raster scan of 30x30 pixels with a 20x20 um step size around stellar images, the frame size is 600 um, and only 1/6th of the micrometer data (namely 5 pixels out of 30) will be contaminated, if one of the pinholes falls within the frame. These bad data can then be detected and smoothed later on in the software.

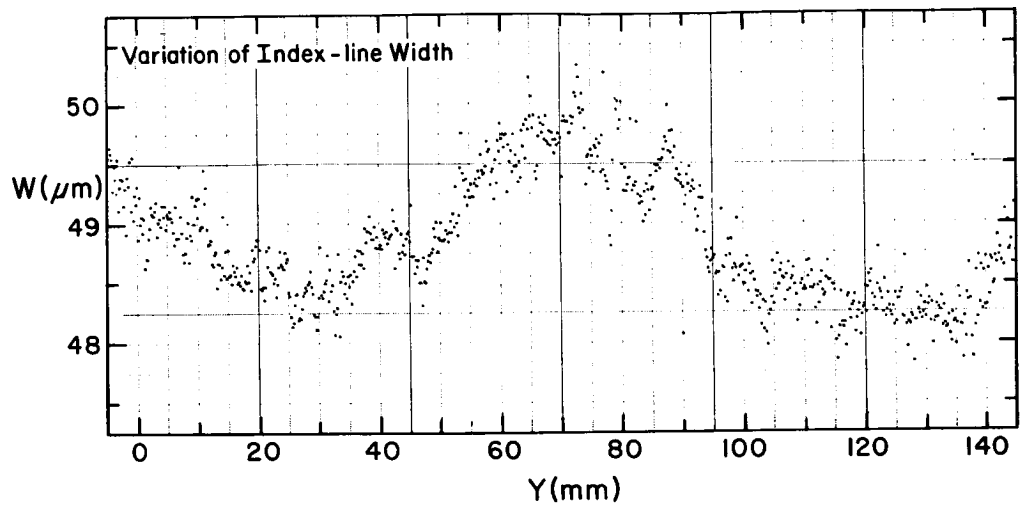

Figure 4: The width of the index-line as a function of position along its length, shows that the line is rather rough even on small length scales. Due to this roughness, it is not practical to calibrate the line to a precision that does not limit the IIIa-J image position accuracy.

The use of these index-lines as the new reference system significantly improves the repeatability for stellar images on IIIa-J plates to +/- 0.3 um. For measurements with a displacement on the plate of the order L < 1 mm, the error is about +/- 0.7 um. However, for L >> 1 mm, there is no improvement at all when using the correction system. This implies that the index-line is neither straight nor smooth on a scale longer than 1 mm, and that we need a method to calibrate the shape of the index-line on a very fine scale.

VI. Calibration of the index-line

The shape FY(x) of the index-line can be calibrated, if an absolute straight line can be found and scanned on the PDS. The following method is used to produce our ideal straight line. First, a calibration line is made by the same method as the index-line. This time, a second glass strip of the same thickness (3 mm this time) was glued on the top of the calibration-line strip. This allows the line to be scanned from both the top and bottom sides

using approximately the same focus of the PDS. The average edge of these two scans is defined to be the new reference straight line. A tick mark is made close to the end of the calibration line so that it can be placed in approximately the same position (within 50 um) during the flip side measurements. The reason for this careful alignment, is that the calibration line is also not smooth. The roughness, G, of a line over a scale, s, can be defined as

$$G^2(s) = N^{-1} \sum_{y=y}^{y_n} [F(y + s) - F(y)]^2 \qquad (6)$$

where F(y) is the shape of the line. For the index-line, we find that G(100 um) = +/- 0.25 um, G(200 um) = +/- 0.3 um and G(1 mm) = +/- 0.7 um. This means that we have to calibrate the index-line with a step size as small as 100 um in order to achieve an accuracy of 0.25 um. There are about 5000 calibration points for the index-line on each axis. To go to an even smaller step size is impractical, since the scan then takes more than two hours and thermal drifts may contribute significant errors. The PDS position relative to the new reference line is then given by

$$\begin{aligned} x' &= x + DX(y) + FX(y) \\ y' &= y + DY(x) + FY(x) \end{aligned} \qquad (7)$$

where FY(x) and FX(y) are the interpolated values for the shape of the index-lines for the x- and y-axes respectively. In practice, since the index-lines may not be smooth even over the 600 um field of a stellar image, we first apply the corrections FX(y) and FY(x) to the micrometer data DX(y) and DY(x). We then smooth over the 600 um field, and finally go through the digital image centering algorithm with the pixel positions corrected accordingly. In this way, the positional accuracy of the machine is improved to +/- 0.4 to 0.8 um.

VII. Measurements of a parallax series

Since our primary interests are in astrometry, a parallax series taken on IIIa-J emulsions with the Kitt Peak National Observatory 4-meter telescope was measured on the Yale PDS. This series has been measured on the Berkeley PDS1010A metal machine with the resulting astrometric accuracy of +/- 0.4 um, see van Altena and Mora(1977). To repeat these measurements on the Yale PDS, a plateholder was built in the Yale shops and used in the scan as a replacement for the glass platen. The new plateholder keeps the plates close to the same part of the ways, to minimize problems with curved ways, and flattens the plates with adjusting screws to achieve good focus over the whole plate. The two-dimensional Gausssian digital image centering program, with optimum weighting according to the grain noise, was used to provide stellar positions and the pseudo-magnitude, m. The plate-to-plate variation in m is well fitted with a second order polynomial transformation with the standard

errors of the fit around +/- 0.02 to 0.04 mag, which is comparable to the values found by Stetson(1979) and Chiu, et al(1979). We note that they are larger than the errors from the repeatability of the photometer and the errors from the grain micronoise. This implies that the errors are probably dominated by large scale macronoise and nonlinearities in the photometer.

The astrometric central-overlap program in use at Yale with optimum weighting was used to compare the stellar positions and the mean residuals obtained were +/- 0.5 to 0.7 um. This indicates that the positional accuracy is limited by that of the machine, and we will soon install a dual-axis laser interferometer to replace the linear encoder and the optical micrometer.

VIII. Acknowledgements

We would like to thank the National Science Foundation for its support of this research during the past five years. A number of individuals in the Yale instrument shops have helped with the design and construction of the instrumentation described in this paper. In particular, Alan Wandersee was responsible for the electronic design and construction and Adrian Disco and Anthony Massina designed and built the mechanical parts. We would also like to thank James Brosious and William Sacco for preparing and photographing the illustrations.

IX. References

Chiu,L.-T.G.,van Altena,W.F., and Stetson,P.B. 1979. in Image Processing Techniques in Astronomy, edited by G.Sedmak,M.Capaccioli and R.J.Allen, Trieste Obs.,p.240.

Furenlid,I.,Schoening,W.E., and Carder,B.E. Jr. 1977. Am. Astron. Soc. Photo-Bull. 16: 14.

Lee,J.-F., and van Altena,W.F. 1983a. Astron. J. (submitted).

Stetson,P.B. 1979. Astron. J. 84: 1056.

van Altena,W.F., and Lee,J.-F. 1983a. Am. Astron. Soc. Photo-Bull. (submitted).

van Altena,W.F., and Lee,J.-F. 1983b. in Astrononomical Microdensitometry, edited by D.A. Klinglesmith, III.

van Altena,W.F., and Mora, C.L. 1977. Bull. Am. Astron. Soc. 9: 599.

Sedmark: How do you take into account the dark current of the photomultiplier?

Lee: I did not do anything to correct for the dark current. So I have problem with repeatability for bright star. The non-repeatability is below the level of the plate to plate variations.

Sedmark: Which is your effective scanning speed for 24 micro second duration time?

Lee: For all these tests the scan is very small scan across a star. The length of the scan is about 600 micron so we use 10 mm per second because that's the best speed to achieve minimum scan time.

Sedmark: And with 10 mm/sec you maintain your accuracy?

Lee: Yes

Horton: As far as the darker current is concerned it just has to calibrated out and then is nothing you can do about off setting it because the magnitude is of the order of a fraction of a nano-amp and there is no controls on the machine to zero it out and you just have to accept it and come up with the calibration code.

Hewitt: Not caring this variable I think the best way you can get a handle on this is to adjust the machine so that the dark current gives as limit to the limit to the maximum density and then set up your plate so that there is an opaque area that gets with each standard raster and subtract it out and hope that it does it.

Horton: It will vary as you change the high voltage, but it should be fairly stable for the same operating parameters.

AN IMPROVED LOGARITHMIC AMPLIFIER CIRCUIT FOR PDS MICRODENSITOMETERS

Christopher M. Anderson and Mark H. Slovak
Department of Astronomy, University of Wisconsin-Madison

Donald E. Michalski
Space Astronomy Laboratory, University of Wisconsin-Madison

ABSTRACT

A high speed logarithmic-amplifier circuit for the Perkin-Elmer PDS microdensitometer is discussed. The circuit is designed around an Analog Devices 757P log-amp module which replaces the Function Modules, Inc. FMI 531 "Negative Log/Anti-log" device of the original. The new amplifier is capable of producing undistorted profiles of rapidly changing, dense (>4) images over the available range of scanning speeds. The circuit board has been designed to replace directly the manufacturer supplied unit; neither electrical nor mechanical modifications of the basic PDS are required. The performance of the circuit is illustrated through its effects on the overall Modulation Transfer Function of the instrument and by scans of a well-exposed stellar image. Circuit diagrams and parts lists are presented and a mechanism for obtaining either circuit board lay-out art work or finished circuit boards will exist.

1.0 INTRODUCTION

The determination of accurate spatial and radiometric information from diverse photographic media is a common astronomical data reduction task. The use of flat bed, scanning microdensitometers in now the standard first step in the reduction of large format photographic records such as wide field Schmidt plates or multi-order echellograms. The solution of astronomical problems of current interest requires not only extreme positional accuracy over large fields, but also photometric precision over an extreme range in density. The Perkin-Elmer "PDS" microdensitometer is by far the most widely used device of this type.

The great utility of the PDS is the increase in speed of data reduction over comparable manual methods and has been discussed by Albrecht (1980). Weis, Upgren and Dawson (1981) described a program of determining radial velocities from microdensitometer scans of objective-prism spectra obtained with the CTIO Schmidt telescope. They concluded that a PDS quickly provides

radial velocities of accuracy comparable to slower hand measurements. Auer and Van Altena (1978) have discussed the use of the PDS for astrometric work previously done by manual cross wire micrometers. Stetson (1979) extended those methods to include the stellar photometry heretofore accomplished with iris photometers.

However, as discussed by Massey and Welch (1979), rapid, accurate determinations of line profiles and centroids using a PDS are limited by the inherent slow response of the electronic logarithmic amplifier circuitry, especially for photographic densities >3. This problem is particularly exacerbated when the PDS platten is driven at fast scanning rates. The problem is characterized by two effects: (1) at progressively faster scanning rates, symmetric profiles become "ramped" or skewed in the scan direction and (2) the recorded peak density is a function of the scanning speed, decreasing from the slowest to the fastest scanning speeds by nearly 15%. While Massey and Welch (1979) discuss an *ex post facto* software algorithm to determine line centroids from profiles distorted by this effect, an *a priori* hardware modification stands as a clear desiderata.

In this paper we present a logarithmic amplifier (log-amp) circuit design for the Perkin-Elmer PDS Micro-10 microdensitometer. This circuit has been tested on the PDS that is part of the Midwestern Astronomical Data Reduction and Analysis Facility (MADRAF). The PDS is interfaced to the facility's VAX 11/780 computer. This VAX/VMS system also supports a variety of peripheral devices including a Grinnell image processing system. Using the improved circuit containing a fast log-amplifier, we have found that the problem is virtually removed, permitting the PDS to be operated at the fastest scanning rates without significant degradation of even dense images.

2.0 THE LOGARITHMIC AMPLIFIER

The 5-decade logarithmic amplifier supplied by Perkin-Elmer with the MADRAF Micro-10 (microprocessor controlled) PDS was designed around a Function Modules, Inc. FMI 531 "Negative Log/Anti-log" device. In order to overcome the problems which will be illustrated in section 3, one of us (DEM) was commissioned by Professor A.D. Code to design a newer and faster unit.

We chose to require that:

1. There be no internal or external, electrical or mechanical modifications to the rest of the PDS;
2. The "transmission" mode of the original amplifier be retained;
3. The calibration of the amplifier be at least as stable and no more complicated than that of the original, and if at all possible, more stable and simpler.

The first of these in essence required that the new device be designed onto a circuit board of the same size and connector layout as the original and that no power or other services not already available in the PDS be required. Furthermore, any calibration or setup adjustments to be made by the operator would have to be accomplished by the use of the existing switches and potentiometers of the control console. Although the transmission mode of the original has rarely been used for research purposes (nor has it been used in the

new model) its availability seemed desirable.

The device which met the additional criteria above and, according to manufacturer's specifications, appeared to offer better performance was the Analog Devices 757P. In the existing configuration a range in density from 0 to density 5 corresponds to a change in input current to the log-amp from 100 microamps to 10 nanoamps. According to manufacturer's specifications the AD 757P handles this in 95 microseconds while the FMI 531 requires about 260 microseconds for the same slew. Laboratory measurements of the entire circuit containing the FMI 531 indicated that its actual performance was substantially worse than would be suggested by these specifications. On the other hand the PDS at speed parameter 128 (corresponding to 25 mm/s or 2.5 microns/100 microseconds) travels about one half the width of the smallest available pixel in the advertised rise time of the AD 757P.

The circuit which resulted from this design effort is shown in Figure 1 and a parts list is given in Table 1. The layouts of the two sides of the circuit board are shown in Figures 2a and 2b. It was found that the circuit diagrams provided by the manufacturer did not correspond to the amplifier board provided. Thus it is judicious to assume that machines of other vintages may well have still different circuits. Before the amplifier herein presented is adopted, potential users should verify that the pin assignments of amplifier board are the same as in the MADRAF machine. To this end, we provide in Table 2 a list of the assignments which apply in our case.

3.0 SCANNING PERFORMANCE

The standard figure of merit for comparison is the Modulation Transfer Function (MTF). The MTF of the entire microphotometer system is determined by scans of a standard resolution test pattern consisting of alternating dense and transparent bars of various spatial frequencies. The product of the spatial frequency (cycles/mm) and the scan speed (mm/s) then yields the frequency (Hz) at which the instrument is attempting to respond. The "modulation" is the ratio (in percent) of the output amplitude to the amplitude of the test pattern. The test pattern available to us had a density amplitude of 3. In order to derive the MTF in the important high density regime, a neutral density 2 filter was introduced into the beam. The pattern was scanned at 50 mm/s with a 5x50 micron slit (5 microns in the direction of the scan) and samples taken at either 5 or 2 micron spacings (low and high spatial frequencies respectively). The scans were then plotted, normalized to the density 2 to 5 range and the observed amplitudes measured. The results are plotted in Figure 3. The manufacturer supplied amplifier suffers measureable degradation even at frequencies as low as 15 Hz and simply cannot reach density 4.0 (from a starting D = 2.0!) above 250 Hz. The new amplifier shows no detectable degradation out to 150 Hz and declines in response only gradually out to 1 kHz. Density 4.0 is still easily reached at 1.5 kHz. Beyond a kilohertz the roll-off in response is due to a combination of the amplifier, the microphotometer optics and the test pattern itself.

Although the MTF is the usual means of measuring performance in this context, a more graphic comparison of the old and new circuits was made by scanning a dense stellar image at selected scanning speeds across the available range provided by the PDS. For illustration three speeds were chosen at speed parameters of 4, 130 and 255, which corresponds to platten speeds of approximately 0.78, 25.4 and 50 mm/s respectively.

A 5 x 7 inch plate taken by one of us (CMA) using the Palomar 48-inch Schmidt telescope on 1966 August 20 was chosen for these illustrations. The plate is centered on the Omega Nebula (NGC 6618) and covers a region of approximately 2.5 x 2.5 square degrees. The images on the plate resulted from a 35 minute exposure obtained under good seeing conditions (~1") using a GG-11 filter and a 103a0 plate. A bright well-exposed star, HD 168415 = BD-15 4927 (V = 5.39, K4III), northwest of the nebula was selected for test purposes. The dense image is symmetric, showing a sharply focused diffraction pattern from the secondary support structure.

The image was scanned using the PDS in a raster mode, creating a square 'map' of 128 x 128 pixels, using a 20 micron spot and 10 micron steps in both the x and y scan directions (roughly aligned with right ascension and declination). Each pixel corresponds to about 0.67" on the plate. The resulting map spans approximately 1.43 x 1.43 square arcmin centered on the star. This process was repeated for each of the three speeds first using the manufacturer supplied circuit and then the new circuit.

Density centroids were calculated for each of the 128 x 128 pixel maps and the results are given in Table 3. The results from the two amplifiers differ at worse by 0.3% (o.18 pixels = 1.8 microns) and confirm the results of Massey and Welch (1979) that density centroids can be accurately determined from even distorted profiles.

Density profiles near the center of the image are shown in Figure 4. Two consecutive rows are superposed and the scans at the three speeds are tacked end to end. The scans from the new amplifier have been displaced upward by two units in density. The density profiles obtained at slow speeds agree quite well for both log-amps. The FWHM of the profiles are 34 pixels (~23") and reach the same peak density (4.8). At moderate speeds, however, the comparison is less favorable and the profiles depart radically in appearance. The profiles produced by the original log-amp not only become asymmetric, skewing in the scan direction, but are reduced in peak density by nearly 15%. The profiles obtained with the new log-amp remain virtually constant in appearance and peak density, even at the fastest scanning rate, varying by less than two precent.

4.0 STABILITY, CALIBRATION AND OPERATION

In order to check the stability of the two amplifiers, the blank platten was scanned with a large aperture, small step size and dead slow scan speed. Raster scans 64 pixels square, requiring 5 minutes each, were collected repeatedly over the course of about an hour with each of the two amplifiers.

The PDS neutral density 3 filter was used to sample lower current levels. After a warm up time of about 15 minutes, neither amplifier showed either short (c. 10 sec) or long (c. 1 hour) time scale drifts greater than one half of one percent.

In order to verify that the density to intensity conversions derived with the new and old amplifiers were consistent, several KPNO spot sensitometer plates were measured with each circuit. Each of the 16 spots on the plate were rastered in a 40 x 40 grid, the median filtered mean density of each spot was determined and a spline fit to the characteristic curve. The resulting curves were indistinguishable.

The procedure for the initial calibration of the manufacturer supplied amplifier is a multi-step process involving the adjustment of three potentiometers in two different positions of a "Calib" switch. Due largely to the slow response of the log-amp, the adjustment of the high voltage to the photomultiplier is found to be extremely sensitive and subject to substantial drift. The new amplifier simplifies this substantially. The "Calib" switch is left in the "N" position at all times and the only adjustment is the high voltage. The instrument is set on the location which is to be identified as zero density and the voltage potentiometer adjusted until the built in meter registers zero. The speed of the log-amp is such that this can be done quickly with only the "coarse" high voltage potentiometer.

5.0 CONCLUSION

We have presented a circuit for a log-amplifier which can significantly improve the performance of commercial PDS microdensitometers. On the P-E Micro-10 PDS microdensitometer, the existing circuit board is easily replaced by a simple swap-out procedure with no other modifications. The improved response of the new circuit obviates the need for software algorithms to recover centroid information from density profiles and provides undistorted profiles at even the fastest scanning speeds. We will provide detailed circuit diagrams to interested parties who wish to implement this circuit.

We would like to thank M. Dearing and D. Bucholtz for their competent assistance in circuit design and implementation and T. Lynch for providing the superb PDS applications software. MADRAF was established through NSF grants AST-7900894, 8011445, and 8121099. DEM was supported by NASA contract NAS-52677 for the Wisconsin Ultraviolet Photopolarimeter Experiment for Spacelab.

REFERENCES

Albrecht, R. 1980, AAS Photo-Bulletin, 25, 9.

Auer, L.H. and van Altena, W.F. 1978, A.J., 83, 531.

Massey, P. and Welch, S.M. 1979, AAS Photo-Bulletin, 22, 11.

Stetson, P.B. 1979, A.J., 84, 1058.

Weis, E.W., Upgren, A.R., and Dawson, D.W. 1981, A.J., 86, 246.

TABLE 1

PARTS LIST FOR THE WISCONSIN PDS LOG AMP

Resistors All are 1/4 W size

No. Req.	Res. in Ohms	Type	Tol.
3	10 k	Metal film	1%
1	11 k	Metal film	1%
1	100 k	Metal film	1%
1	100	Carbon	5%
2	200	Carbon	5%
1	1.2 k	Carbon	5%
1	2 k	Carbon	5%
1	10 k	Carbon	5%
1	20 k	Carbon	5%

Capicitors

No. Req.	Val. in micro f	Type	WVDC
1	.01	Disk Cer.	25
4	.1	Disk Cer.	25
2	10	Electrolytic	25

Diodes

No. Req.	Type
4	1N4148

Integrated Circuits

No. Req.	Type	Description	Mfg.
3	LF356P	FET input op amp	Nat, Mot
2	DG200BA	Analog Switch Dual SPST	Intersil
1	AD581J	10 v IC Ref.	Analog Devices
1	AD757P	6 Decade log ratio module	Analog Devices

TABLE 2

CIRCUIT BOARD[1] PIN ASSIGNMENTS

PIN[2,3]	FUNCTION
C	Transmission Inverted Output
D	-15V
F	+15V
J	Ground
K	Density Output
L	Transmission Mode Control
M	Density Mode Control
S	Signal Input
T	Transmission Off Set
X	????
Y	Transmission Output

Notes

1. The connector is a CINCH type 50-44A-30 Printed Circuit Board Edge Connector.
2. Circuit components are down when board is installed; the finger board connector tabs which are used are then up and labeled alphabetically from left to right.
3. Letters G, I, O, Q, are not used by CINCH; other missing letters in this table are unused in this design.

TABLE 3

COMPARISON OF DENSITY CENTROIDS AND CENTRAL DENSITIES FOR DIFFERENT LOG-AMPLIFIERS

Speed	Old Log-amp		New Log-amp	
	CENTROID(X,Y)	PEAK D	CENTROID(X,Y)	PEAK D
4	(65.90, 65.73)	4.89 + .21	(65.90, 65.91)	4.82 + .30
130	(66.16, 64.58)	4.12 + .13	(66.14, 64.56)	4.74 + .20
255	(66.12, 64.67)	4.11 + .12	(66.12, 64.64)	4.74 + .19

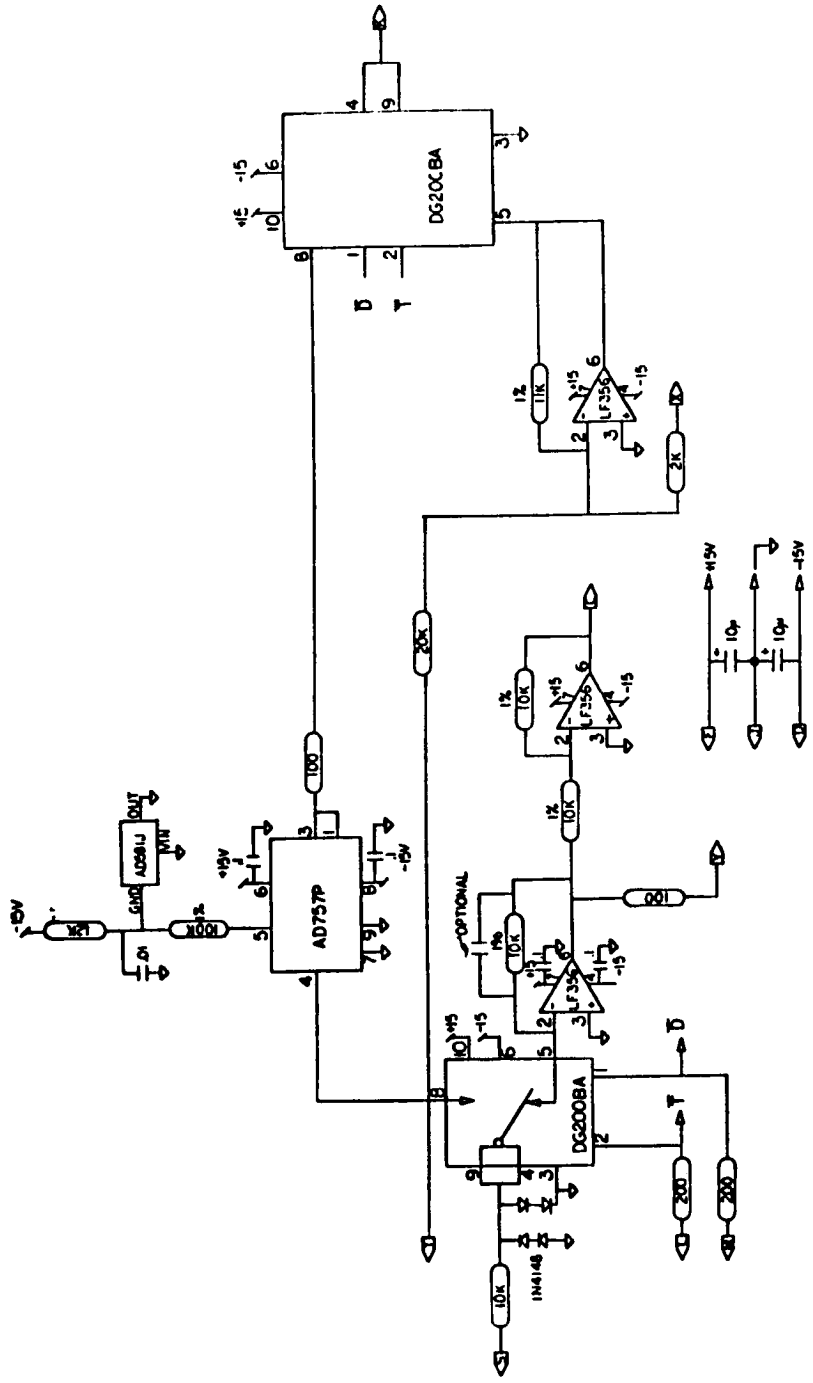

Figure 1. The revised logarithmic-amplifier circuit for the Perkin-Elmer Micro-10 PDS microdensitometer.

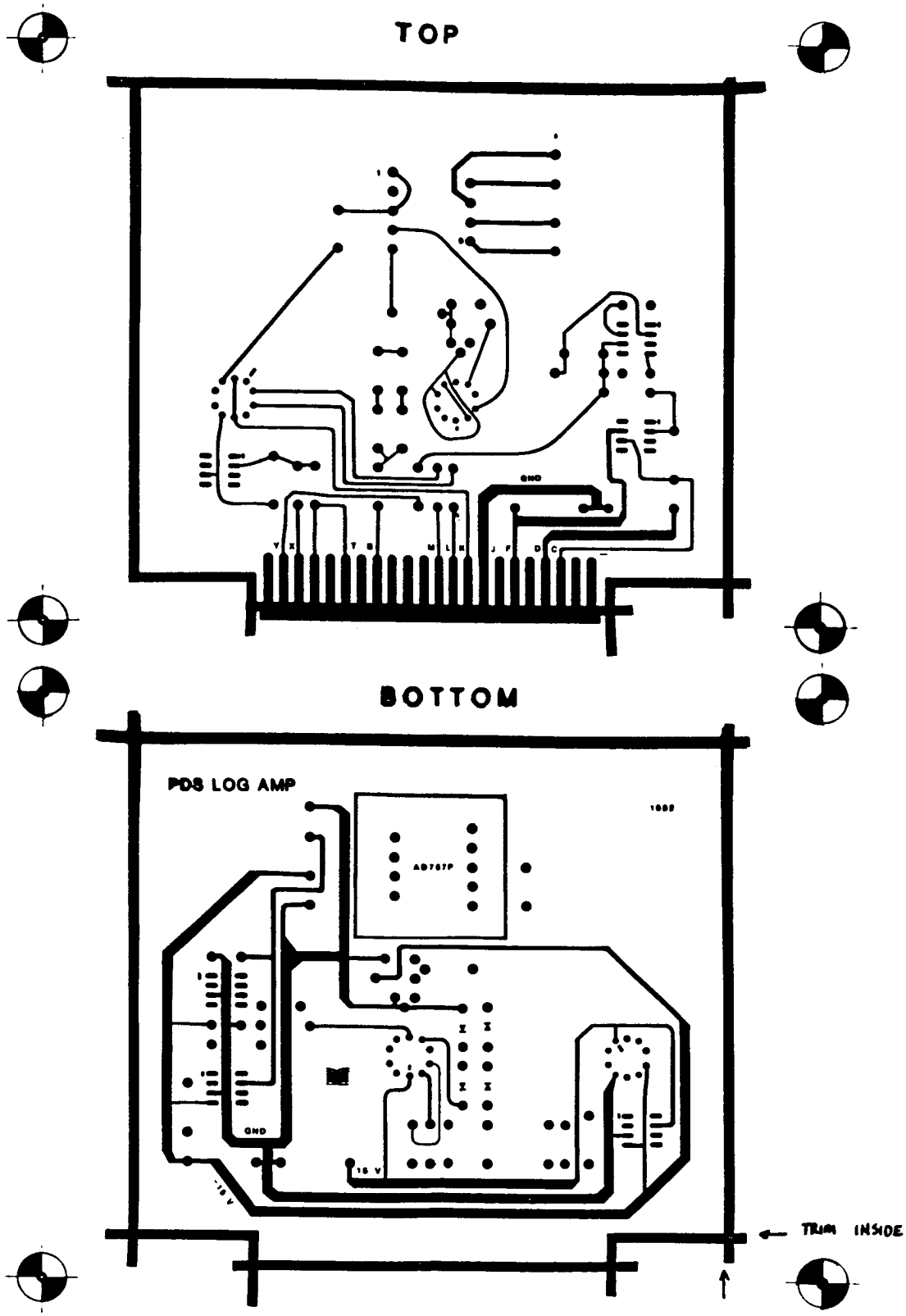

Figure 2. The circuit board layout of MADRAF PDS Log amplifier.

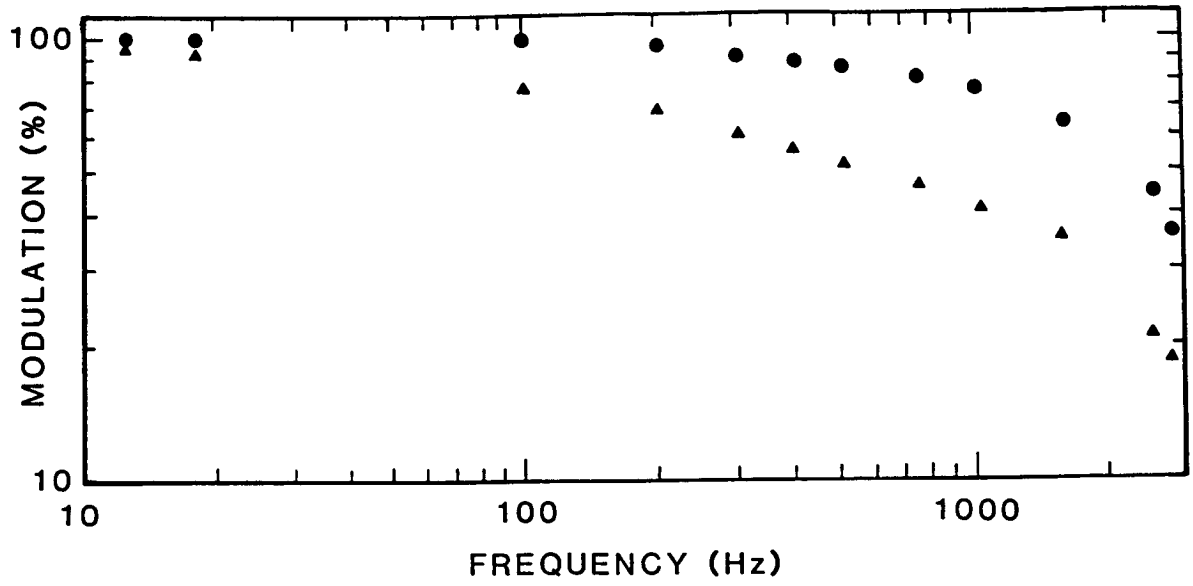

Figure 3. The Modulation Transfer Function (MTF) of the entire PDS system with the new (dots) and the old (triangles) amplifier circuits.

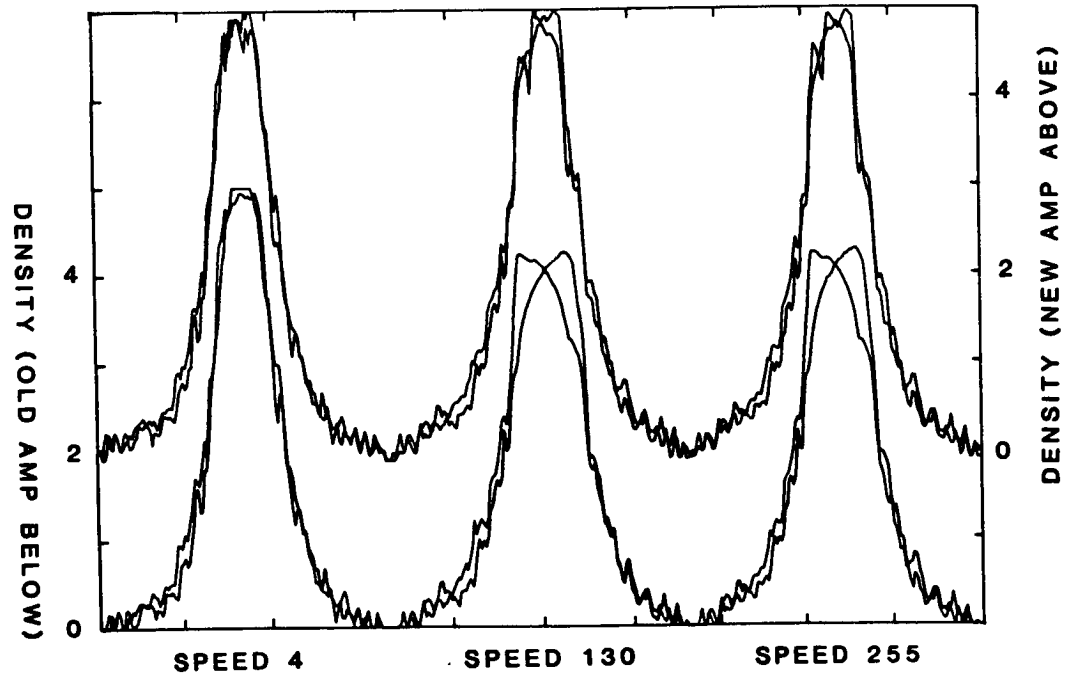

Figure 4. Density profiles at the center of the images described in the text. Shown superimposed are two successive scans which are taken in opposite directions. The slow, medium and fast speed scans for each of the amplifiers are displayed end-to-end and the scans for the new amplifier are displaced upward by two units of density.

Lasker: I'd like to make two comments. One is my compliments that you leave tracks that others can follow relatively effortlessly. My other comment is in trying to compare what you're showing with what we have seen elsewhere. I think it's very easy to get a qualitative feel that this is very good. In fact, I can confirm from some experiments we've had done that whatever positional concerns that we have using the Yale bi-dimensional centrorder are well below micron. It might be useful when we get to our discussion time tomorrow to open the question of "How do you test our Log amplifier, such that we can all talk to each other without trying to do calculations between the various tests?

Hewitt: What in fact does limit the band width of your system now? Is there a time filter in there?

Anderson: Partly, let me put it this way; in order to get to 3 kilohertz. I was driving full speed using 5 micron aperture. Ten power objectives and magnification four, four below and probably a little bigger. Incidently, I very much endorsed the idea of using larger upper apertures that I was doing. Then I had to drive at full tilt across the bar pattern that I had available to me. And I found that even at zero frequency I couldn't get up to the highest density just from the scattered light in the optics.

THE PDS-VAX INTELLIGENT PLATE SCANNING SYSTEM OF TRIESTE ASTRONOMICAL OBSERVATORY

Mauro Pucillo and Giorgio Sedmak
Osservatorio Astronomico di Trieste
Via G.B.Tiepolo 11
34131 Trieste, Italia

ABSTRACT:

An intelligent subsystem for interfacing a PDS1010A digital microdensitometer to a DEC DR11W DMA 16 bit UNIBUS port in DEC VAX VMS environment was designed and is presently under test at Trieste Observatory. The subsystem employs two MOTOROLA M68000 microprocessors with 128 KB data memory. The PDS primitives and the user-defined high level scanning functions and preprocessing modules are loaded from the host computer into two 8 KB RAM memories in the microprocessors using a dedicated PDS control language. The subsystem is planned to employ a non-standard photomultiplier electronics. Two design schemes are being tested, one based on three amplifiers of gain 10 cascaded and multiplexed to a 12 bit AD converter, and a second based on a single amplifier of gain 100 and two 14 bit AD converters. Either solutions should yield a 1 percent accuracy at density 4 above the photon noise and the photomultiplier non-linearities, working at the maximum scanning speed of the PDS1010A machine.

1. INTRODUCTION.

The Perkin-Elmer PDS1010A digital microdensitometer is a field-proven, astronomy standard facility for the digitization of photographic material. Recent astronomical research programs involving the digitization of echelle spectra and the guided extraction of clusters of subimages from large plates for automated statistics pointed out the operational limits of the tape-oriented stand-alone PDS configurations. The availability at Trieste Observatory of a second new PDS1010A machine close to the DEC VAX11/750 system of the Trieste ASTRONET pole recommended for the implementation of a PDS-VAX intelligent plate scanning subsystem to be operated in DEC VMS software environment.

The PDS-VAX intelligent subsystems should carry out the user-defined plate digitization programme and transfer the data to the

host environment without any substantial degradation of the host performance. The PDS control software should allow the user to define easily the PDS programme while being able to address a host-resident library of special purpose procedures and preprocessing modules for the implementation of complex, multistage digitization procedures.

One key problem of PDS digitization is concerned to the standard logarithmic amplifier, which is known to be too slow to match the PDS maximum scanning speed at densities above 3. Improved logarithmic amplifiers or logarithmic AD converters improve dramatically the performance of the standard component, but do not solve the problem in a clearly controllable manner. We must emphasize that the real problem is to have an electronics that is able to be modelled so as to allow the user to compensate the effects of the sampling filter equivalent to scanning a non-stationary density signal. The straightforward solution of measuring the transmittance linearly up to density 4 would require an AD converter of length non commercially available. However, it is easy to design and built an autoscale equivalent of a long-word AD converter by means of commercial components. We will follow this last approach.

It must be pointed out explicitly that any design will be limited by the photon noise and by the non-linearities of the detector used. The photon noise can be averaged to the wanted accuracy by increasing the integration time, that is decreasing the scanning speed, or by increasing the source level. The non-linearities of the detector are much more difficult to be managed. In principle, a model of the non-linearities should be built and a post-digitization compensation applied to the data.
The limiting problem, however, remains the sampling filter effect of digitizing a non-stationary density signal. We believe that this problem prompts for a much deeper physical insight than normally made by astronomers. It is probable that this problem, as well as the detector non-linearity problem, could be faced by means of a suitable reciprocal filter built from the model of the direct one.

This paper contains the description of the hardware and software of the PDS-VAX microprocessor subsystem and new photomultiplier electronics which was designed and is presently under test at Trieste Observatory.

2. ARCHITECTURE OF PDS MICROPROCESSOR CONTROLLER AND VAX INTERFACE.

The configuration of the DEC VAX11/750 system of Trieste ASTRONET pole employed for the assistance of the PDS1010A machine includes 4 MB central memory, 1 GB disc mass memory, VERSAPLOT-compatible raster printer-plotters, and ANSI standard VT100/125 alfanumeric and graphic terminals. The pictorial terminals available in the system are one AYDIN 5214, one SIGMA ARGS, and one DEC VS11

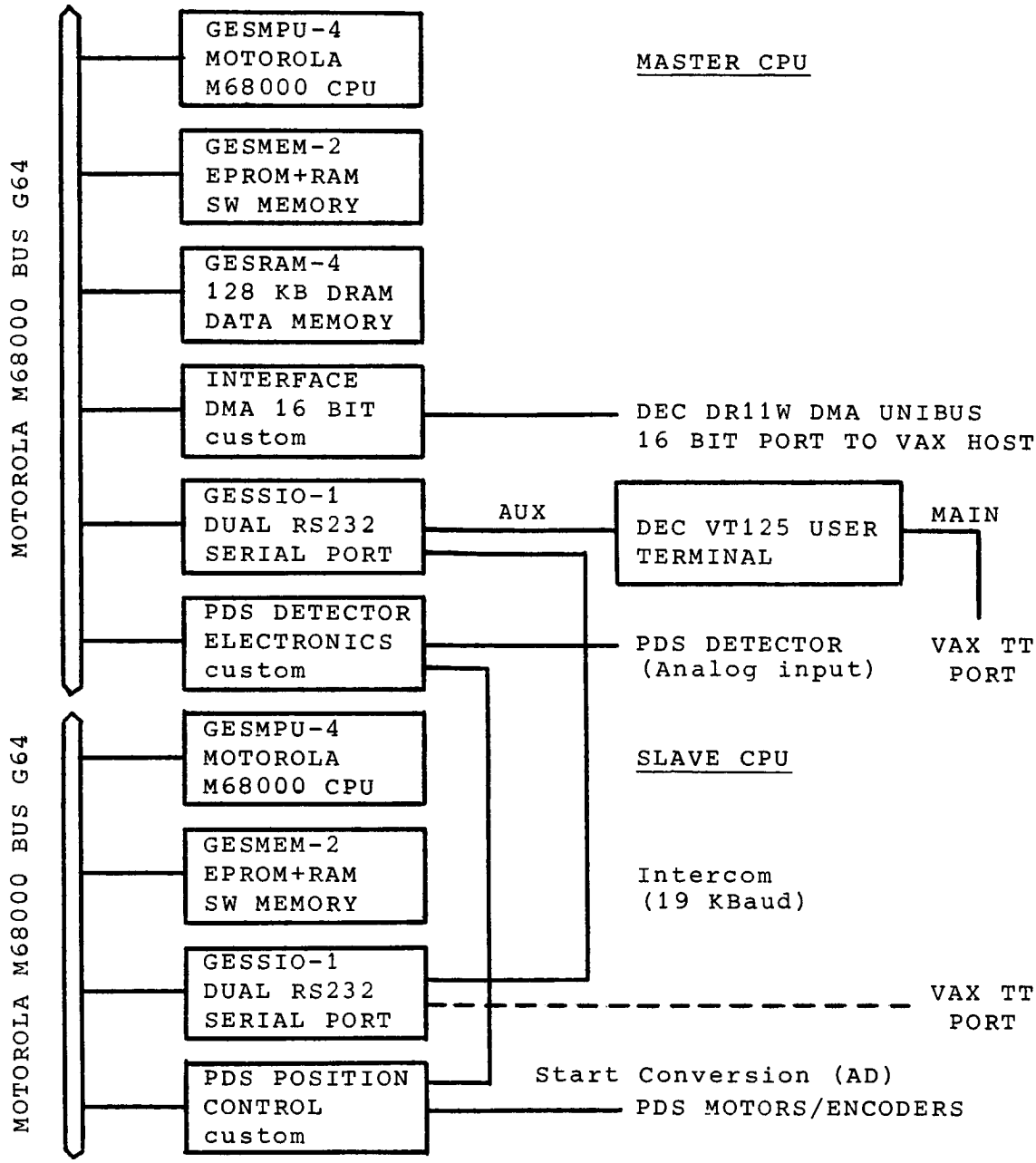

Figure 1

Architecture of the PDS-VAX intelligent microprocessor controller.

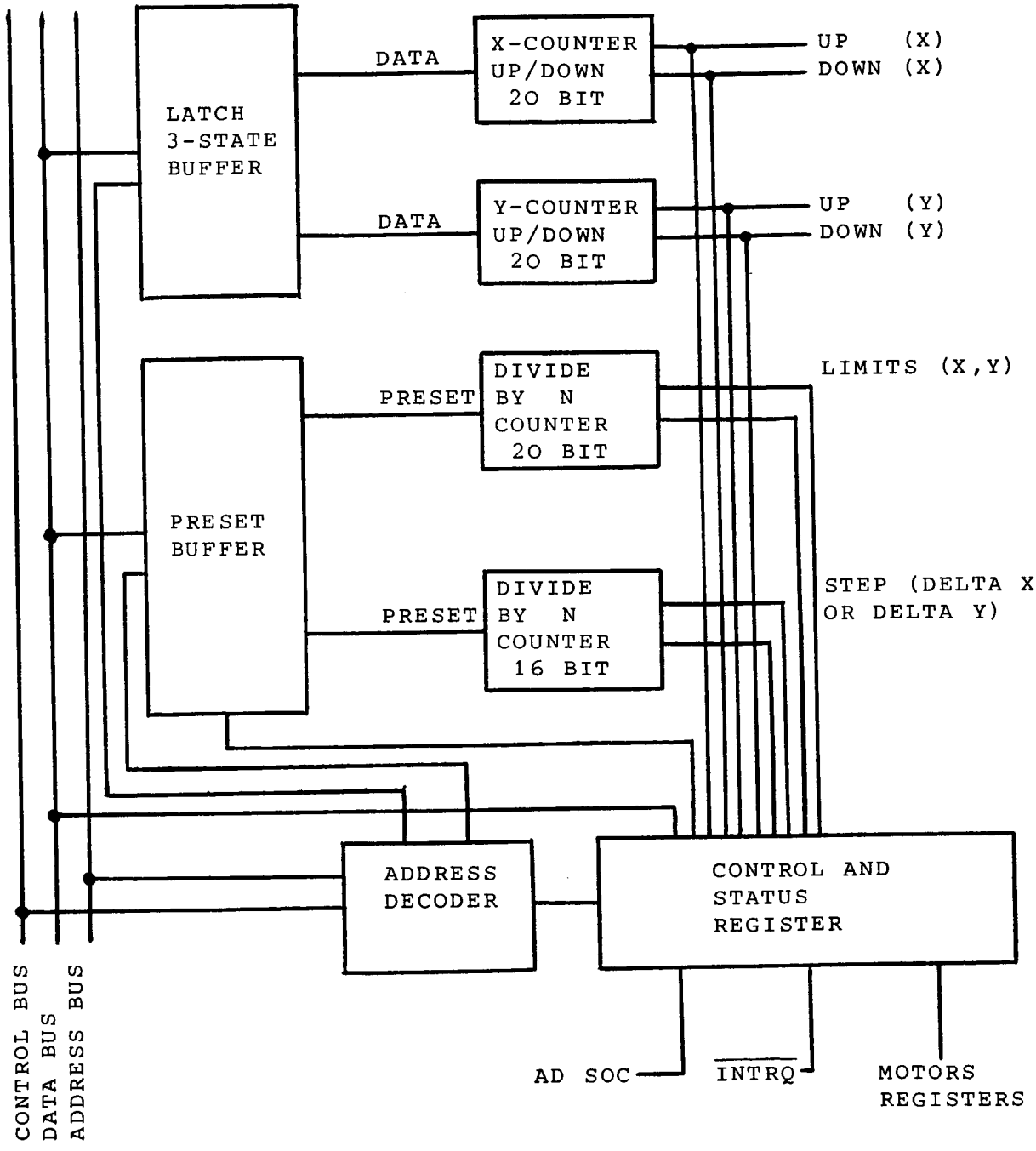

Figure 2

Architecture of the PDS positioning and data acquisition control.

machine. This configuration is the fall 1983 one. Some devices are presently on delivery by DEC.

The architecture of the PDS1010A machine is the standard one. The PDS-VAX intelligent controller inputs the positional counts from the Heidenhain encoders, here to be used with the absolute zero marker option, inputs/outputs the data/controls of the photomultiplier electronics, monitors the operational status of the PDS machine, and transfers data and commands to/from the host environment. The user commands the PDS through the controller directly from the host computer. The user terminal, presently one DEC VT125, is also used to monitor alfanumeric and graphic information from the microprocessor controller in feedthrough mode.

The architecture of the intelligent microprocessor controller is shown in Fig. 1. The controller is based on two MOTOROLA M68000 microprocessors with 4 MHz clock rate interconnected through 19 KB serial ports for the interchanging of commands/parameters. Each microprocessor uses one 8 KB RAM memory for storing the firmware loaded from the host environment. The controller was designed taking into account the availability of the standard DMA access to the large volumes of central and mass memories in the host environment. This facility allows the controller to be dedicated to carry out the PDS scanning primitives and user-defined plate digitization programme and preprocessing applications with the only requirement of a sufficiently large data memory. The data memory size of 128 KB was set so as to accommodate one full scan of 250 mm length at 5 microns sampling step.

The controller is built by means of commercially available modules of the MOTOROLA M68000 line, with the only exceptions of the PDS interface, the VAX interface, and the detector electronics/ interface. One of the two microprocessors is the master dedicated to carry out the AD conversion and data acquisition, the eventual preprocessing, and the dialogue to/from the host environment. The second slave microprocessor is dedicated to carry out the control of the positioning of the PDS platen on the scanning axis and the autolock on the non-scanning axis.

The configuration of the PDS interface is shown in Fig. 2. The configuration of the VAX interface is typical of any DMA 16 bit port, and is not reported here. The configurations of the photomultiplier electronics are detailed in next section.

3. AUTOSCALE PHOTOMULTIPLIER ELECTRONICS.

The high accuracy measurement of the full PDS density range would require a long-word AD converter not commercially available if the standard logarithmic amplifier/logarithmic AD converter approach is not accepted. One possible alternative approach is the autoscale electronics, equivalent to a long-word AD converter at the expense of the conversion time or of the cost.

Two autoscale electronics designed for the PDS-VAX subsystem are

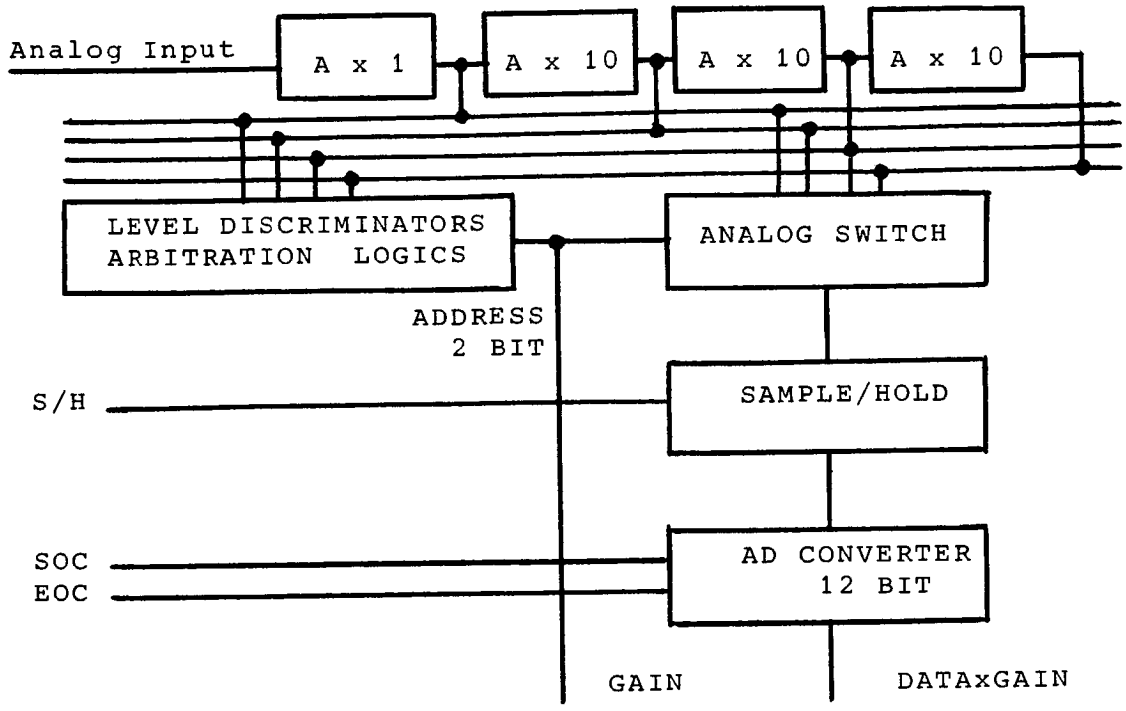

Figure 3

Autoscale photomultiplier electronics with hardware arbitration.

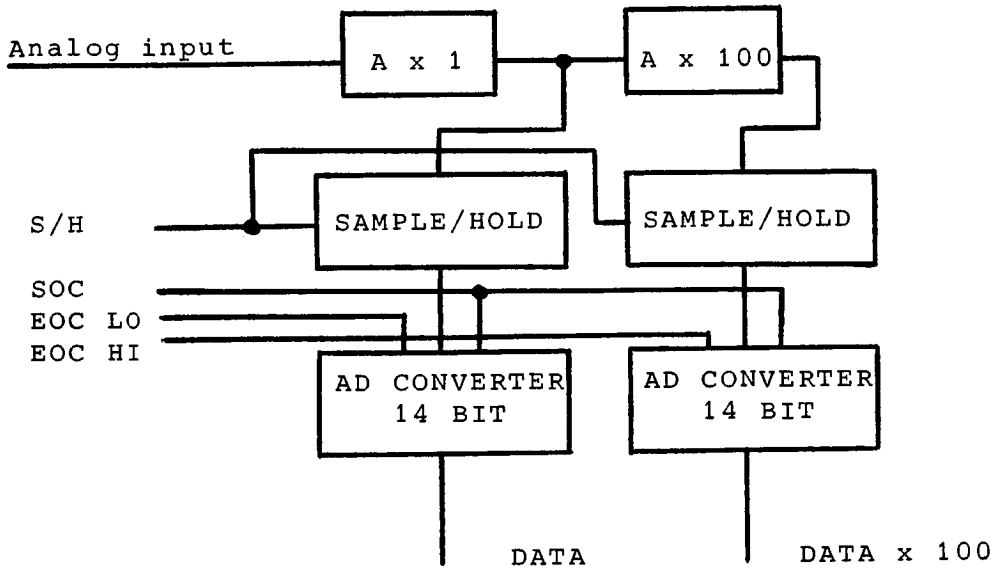

Figure 4

Autoscale photomultiplier electronics with firmware arbitration.

shown in Fig. 3 and 4. The design of Fig. 3 converts the photomultiplier anode current into voltage by means of a first low-noise high-impedance amplifier. This signal is fed into three amplifiers of gain 10, cascaded and multiplexed to one single 12 bit AD converter through a sample-hold module. All circuitry is managed by an arbitration logics driven by three level discriminators that monitor the voltage range. The system performs like a conventional AD converter with the only excpetion of 2 additional gain address bits. The typical settling time with standard components results about 20 microseconds.
The design of Fig. 4 is similar to that in Fig. 3 but uses only one extra amplifier of gain 100. The normal and the amplified-by-100 signals are fed through two sample-hold modules to two 14 bit AD converters directly coupled to the microprocessors controller. This scheme has the disadvantage with respect to the first one of a higher cost and a slightly more complicated firmware, but it offers the advantage of a superior stability and a potentially lower settling time. The arbitration for the design of Fig. 4 is directly made by the master microprocessor.

The test made up to now on the scheme of Fig. 4 shown that the autoscale electronics may result competitive to the standard solutions. The only defect revealed up to now is a thermal drift due to the saturation of the bottom amplifiers in case of saturations of long duration. A modified scheme with non-saturable configuration is being now developed to face this problem. No data are presently available on the second approach of Fig. 4 which is presently under developement.

4. PDS CONTROL LANGUAGE FOR VAX-VMS ENVIRONMENT.

The standard stand-alone control software is perfectly acceptable for using the PDS as an off-line digitizer. However, many astronomical applications require rather complex and sometimes interactive digitization programmes, on-line preprocessing and/or data presentation, and/or multistage digitization procedures.

A special PDS interactive control language (PDSICL) was developed to take into account all these requirements. The language allows to emulate very simply any given standard stand-alone environment to accommodate users trained in such environment, but of course exploits its capabilities in applications requiring a high degree of interaction between the user/host environment and the PDS/sample assembly.

The PDSICL software is logically structured into three main components, the user interface to guide the user in building and executing the scanning procedures, the data and commands encoder /decoder to control the flow of commands and data to/from the PDS, and the commands interpreter/executor to interpret and execute the commands.

This logical structure is physically distributed among the three

PDSICL COMMANDS LIST

Command	Description
B - BATCH	Equivalent to MACROSCAN command. The name associated with the command can have up to 9 characters.It is used to open a file of that name and extension .PDB where the MACROSCAN is stored.
D - DIAGNOSE	Executes one of the diagnostic programs built for the PDS control system.
F - FORMAT	Defines the physical specifications of a scanning operation. The specifications include the scan area, scanning speed, sampling step, etc.
L - LOAD	Loads the platen acceleration ramps data stored in the host or determined by a direct measurement. Loads an executable code segment from the host.
M - MACROSCAN	Defines and executes or erases a PDS procedure built by many individual PDSICL commands. It must have a two characters name.
P - POSITION	Moves the PDS platen to the assigned position. The positioning may be absolute or relative according to using signed or unsigned values.
R - REPORT	Reports to the host the position of the PDS platen or the content of a MACROSCAN.
S - SCAN	Performs a scan to an assigned position. It may use the data defined by the last FORMAT command.
W - WORKSET	Defines the working parameters of the PDS. In the context of another command supersedes for the duration of that command any other definition.
Z - ZERO	Resets the coordinates origin. Checks the platen positioning with respect to the absolute zero markers of the platen encoders.

The general PDSICL command string is written as follows:

<COMMAND NAME>| [POSITION]||(<QUALIFIER>|<ARGUMENT>||(<QUALIFIER>|<ARGUMENT>|)|

TABLE 1
List of PDSICL commands.

processes that cooperate to control the PDS. The VAX processor runs the user interfaces and the VAX section of the encoder/decoder. The master microprocessor runs the PDS section of the encoder/decoder and the data acquisition section of the interpreter/executor. The slave microprocessor runs the positioning section of the interpreter/executor.

Three interfaces are provided to allow the user to work at different levels on the PDS. The first is a high level interface built to aid the unexperienced user to work with the PDS without being involved in the PDS structure. The second interface is dedicated to emulate the SCANSALOT and the ESO PDS environments for astronomers used to employ such systems. The third level of interfacing is the low level that uses the basic PDSICL commands.

The preliminary version of PDSICL includes 10 basic commands, all identified by one single alfa-character and specified by means of qualifiers/parameters. Defaults are used whenever is possible for any optional name, qualifier, or parameter. The basic commands are listed and described concisely in Table 1. The commands may be combined in procedures of any complexity, that can be stored and then run in batch mode. The emulated ESO and SCANSALOT environments are examples of this facility.

5. CONCLUSION.

The intelligent PDS-VAX microprocessor subsystem described in this paper is presently under test. No particular problems were seen and are foreseen with respect to the positioning the PDS platen and controlling the data acquisition up to the limits set by the mechanical design of the PDS machine.

Some problems were already found in the photomultiplier electronics. However, all known types of electronics suffer of some defects. It seems unovoidable to have to compromise between speed, stability, and accuracy. The most important problems are of course the photon noise at high densities and the effects of the sampling filter equivalent to digitizing a time-varying density signal. No solution can be found for the photon noise that exceed the limits of the statistics of the photons carrier. On the contrary, the sampling filter effects can be taken into account and we believe that these effects have been up to now completely underestimated by astronomers. We plan to work deeper into this problem, and to use the facility of the on-line preprocessing allowed by the master microprocessor of our system to eventually implement the reciprocal sampling filter.

Finally, we stress that the effective speed requirement of a plate scanning machine should be evaluated in terms of the ratio between the time spent on the digitization phase of any scientific work and the total time needed to publish that work, with a weight given by the cost and availability of such a machine. If one accepts this point of view, low speed macines like

the PDS may result to yield a quite large rate of scientific data, particularly if the data are to be accurate contemporarily from the positional and the photometrical point of view.

In this last case, we believe that a strategy of digitization based on a maximum speed pre-scanning dedicated to the detection of the relevant objects followed by a guided digitization of the target objects selected may result in an overall winning strategy in regard of the price-to-performance ratio.

ACKNOWLEDGEMENTS.

This research program was carried out under contracts of the Consiglio Nazionale delle Ricerche of Italy, Gruppo Nazionale di Astronomia (GNA-CNR).
The prototype hardware was built in the laboratories of Trieste Astronomical Observatory with the cooperation of M.Comari, S.Furlani, L.Lampi and with the technical cooperation of G.Dainese. F.Marchesini contributed to the design of the host intercommunication software as part of thesis work. F.Pasian and P.Santin of Trieste Observatory contributed to the definition of the PDSICL language and to the tests of the subsystem.

Lasker: There are so many fasinating things here it is hard to know where to ask the first question. But one thing I would appreciate hearing a little bit more about your low pass filters.

Sedmark: In the PMT electronics? For the standard PMT electronics. We use all the standard Perkin-Elmer electronics or we plan to use different electronics of the type for example shown here (shows slide). I didn't have information of the types of new logarithmic amplifiers presented here at this meeting. We were testing our own logarithmic amplifier. And for that kind of electronics, yesterday all the details regarding the importance of using or not using a certain time constant.

For the other circuit, that is the auto scale circuit the matter is slighlty different. In practice you have a certain busy time an equivalent to a deadtime is given to the system for performing the gain arbitration. This time is of the order of the recovery time of its amplifier and the recovery time of its trigger. Because of course some amplifiers work in saturated mode so we must allow for a recovery of the saturation. For variable amplifiers I have detailed a critical diagram. The recovery time is of the order of a few microseconds. That means we lose some 10 or 12 microseconds. Then we have to switch to the switch and perform the sample and hold and A/D conversion. All this implies some 20 microseconds. So this is not an integration time this is a busy time which is dead regarding integration. In the event that we have to integrate and for integration we have two possibilities: (1) integration against the photon noise and one against the electronic noise. For the photon noise the only right choice is to put integration here on the character of the voltage convertor. Photon noise is to use, and this is a test we will perform in the next few weeks to replace the sampling module by means of an integrating module—it should allow the minimize electronic noise of this part. But this is a fast problem and for this reason we are trying to pass this solution. It is to have the minimum possible amount of electronic noise in the electronics by selecting properly amplifiers, very low gain units, and working at a relatively good right light level. Evidently you have to integrate for the time constant to set the photon noise below your density accuracy required. But this is a characteristic not due to the electronics this is due to physics. So my idea is that, and this is an argument that we can discuss here, I hope to have bit of discussion. We have the problem of how much to integrate versus how much higher may be the scanning speed. Evidently, all is ok if your gradient density is zero. But if we think of a practical case, like an astronomical range from 0.2D to 4.0D, that is we have four decades in a few pixels. Evidently, in that case the importance of the time constraint has to be weighed according to your scanning speed. Probably another scanning machine is a better solution for this kind of thing. It is very difficult to obtain from the PDS, which is a mechanical machine. We tried also to perform a start stop operation for such cases. But we abandon this after a few catastrofic tests. Now with we perform a different format for data acquisition; for example, in the galaxy we first perform one acquisition it a certain speed on the all the galaxy then we repeat the data acquisition near the center with a different speed.

This is a practical comprise working well. In that case it is possible to move from one time constant to another time constant. I don't know if this is an answer to your question. It is a comment to the problem.

Lasker: It is certainly pertinent to the problem. I would add to all of that of course we must not permit a signal to change at a rate that is so rapid that there is more information in the signal than the information we are sampling and that was fact why I asked you about this problem.

Sedmark: If I understand correctly, I'm not so sure that there is a thing I have not said before that is this system is operated by supposing that the density gradient is relatively small between two pixels. And so the gain arbitration, the timing of the gain arbitration with respect to the time of the sample and hold and A/D conversion is shifted. The programming of this system by means of the information on one pixel and then making the system operate, that is converting the data, on the next pixel. So this is part of an answer to your question. But this is not a method regarding the time constant. So we have two points: (1) how to have measurement made in stationary condition with respect the electronics. This is one point. I call it busy time or dead time as you prefer. The other point is the time constant that is the band pass of your system. This is connected to your density gradient not to the electronics. So I separate. I say for the second which is electronics or busy time or dead time, as you prefer, we can solve the problem, on the first we cannot solve, call this my personal opinion. For this we have to comprise because the first problem can be solved. And that's the reason for yesterday I proposed the comment for further discussion to the paper presented on the PDS machine used in astronomy. If we perform integration on say 450 micro seconds, how slow must be that the effective scanning speed of the machine to accommodate with this. This is a method strictly concern to the gradient in density. We cannot give an answer for the general condition. And so in case of PDS, evidently PDS is not a stop/start machine. In case of PDS that according to our opinion is the core of the problem. Our practical solution is to assign different formats, this is the reason that you have such complex software. To sign not a start/stop operation but a different parameter and different parts of the region for perfect scanning image and to modify this.

Opal: A lot of these problems can be overcome by running your A&D converter at full bore and setting your time constant so that is all optimized for the highest density that you expect and then doing in 68000 the digital average and feeding that digital average to the mainframe when ever it wants a new word.

Sedmark: I agree. This deals with the noise in the electronics of course. If you think with the PDS moving in a region of strong density gradient then you are averaging incorrectly because your average of course, noise but you average also granularity noise, and this is not correct and you average also systematical errors in the seeing and this is completely not correct. So I agree with this kind of approach for the electronic noise but the problem of the density gradient is maintained. You of course can not average in software if you suppose that you signal is varying at the input of the system.

Opal: This does average the density gradient directly. Instead of taking the logarithm of the sum you are taking the sum of the logarithms which is the right thing to do.

Sedmark: I want to make another comment on this kind of problem according to my opinion is very strictly application dependent. For example it is possible to think of applications like radial velocity in coude spectra in that case what is your main purpose is to maintain very accurate centering of the lines so as not to introduce false biases which is the same problem in galaxy photometry not to create PDS originated twisting of the isophotes and so on. So for that application probably that averaging is not particularly recomendable for other applications for example surface photometry in the wings of a galaxy maybe that kind of solution that you propose is very very effective and very fine to use but I do not have data on this kind of solution on my system of course.

Moderator: Sounds like we're getting into detail things maybe we should talk about some of them later. This is the last question.

Hewitt: In the presence of a gradient in transmission what you want is to average is the exposure.

Sedmark: Exactly, but remember that we have a non-linear characteristic curve so it's very difficult to perform such operation. It is possible to do it. We intend to put a shutter in the main beam so as to monitor the dark current in case dark current is important in strong density part.

THE VAX/VMS DEVICE DRIVER AND USER OPERATION PROGRAM FOR THE MIDWESTERN ASTRONOMICAL DATA REDUCTION AND ANALYSIS FACILITY PDS MICRODENSITOMETER

Christopher M. Anderson and Thomas W. Lynch
Department of Astronomy, University of Wisconsin-Madison

and

Michael P. Dearing
Instrumentation Systems Center-College of Engineering
University of Wisconsin-Madison

ABSTRACT

The Midwestern Astronomical Data Reduction and Analysis Facility (MADRAF) PDS microdensitometer was the first astronomical PDS which was provided with a Motorola 6800 microprocessor control/interface and the first which was to be interfaced to a 32-bit instruction computer operating in a multiuser environment. Command and response hand shaking are handled on an RS 232 serial line while data transfer occurs on a dedicated Direct Memory Access line. This set of conditions necessitated the creation of a specialized device driver for the system. The general outline of this software will be discussed. The availability of an extraordinarily powerful computer opened the possibility of a user operating program of great versatility with diverse data destinations and formats, automatic documentation, and an extensive set of utilities which facilitate operations especially by the occasional visiting astronomer.

I. INTRODUCTION

Once upon a time, astronomers from a bunch of Midwestern university departments of astronomy got together and decided that they needed modern data reduction facilities in their own back yard. The result was the Midwestern Astronomical Data Reduction and Analysis Facility (MADRAF) funded by NSF Grants AST-7900894, 8011445 and 8121099 to the Committee on Institutional Cooperation# through its financial agent, Northwestern University, and subcontracted by Northwestern to the University of Wisconsin. Atop the wish list was a fast photograph digitizer of high photometric and positional accuracy like the Perkin-Elmer PDS microdensitometer. Of the roughly 120 PDS's in

A committee composed of the Vice Presidents for Academic Affairs (or the equivalent thereof) of the "Big Ten" Universities plus the University of Chicago and dedicated to expediting cooperative ventures in education and research in the Midwest.

existence, about one third are used by astronomers and are controlled with dedicated small computers (e.g. PDP-8's or PDP-11's) and specialized hardware interfaces. But it was the dawning of the age of the VAX.

Although the data rates generated by the PDS are modest by most modern standards (800 kbps absolute maximum and 40 kbps typical*), in order to achieve efficient operation without loss of data in a multi-user environment, it was necessary to develop a new scheme for interfacing of the PDS to the VAX/VMS system of MADRAF. Perkin-Elmer agreed to provide their new 6800 microprocessor version of the PDS with parallel data output line which could interface directly with a Direct Memory Access device in the UNIBUS (a DR11B in the MADRAF case, in more recent cases a DR11W). For command purposes, a standard RS232 port would be used. In order to make use of this architecture, one of us (MPD) was commissioned to develop the device driver while TWL under the scientific direction of CMA developed the user interface software. The use of a host computer of the power of the VAX made it possible for the operations program to be provided with many more capabilities that are present in smaller systems (e.g. SCANSALOT on a PDP-8). In the following sections we briefly discuss the characteristics of the device driver (section II), the operation program design (section III), and the utilities available to the astronomer (section IV).

II. THE VMS DEVICE DRIVER

A device driver sits on the edge between the soft and hard aspects of the interface of a device to a computer (in this case, the VAX). This device driver (PDDRIVER) uses standard VMS tables and routines to control the data I/O operations on the PDS parallel interface. PDDRIVER is compatible with VMS Versions 2 and 3 (to release 2), either DR11-B or DR11-W, and either the X-10 PDS parallel interface or the new Micro 10/20 Real Time Data Interface (RTDI).

PDDRIVER supports three DR to RTDI functions, (1) DR Reset, (2) PDS-Direct or PDS Buffered Data Transfer, and (3) PDS M6800 microprocessor hard reset. The PDS-Buffered data transfer mode uses the PDS memory (RAM) as a buffer for collection of the scan data before single block DMA transfer of the data to VAX memory. The PDS-Direct data transfer mode is useful when scan lines will result in data counts exceeding PDS RAM size (typically 6400 bytes) and when multiple buffer transfers per scan are not desirable. PDS-Direct data transfer uses VAX memory as the buffer with the data coming directly from the Analog-to-Digital Converter.

PDDRIVER supports Direct Memory Access (DMA) method block transfers for reasons of throughput and PDS X-10 characteristics. PDDRIVER uses the Direct I/O type of transfer rather than the Buffered to eliminate one more rewrite of the scan data, via a system buffer, on its way to the user and, consequently, to lock the user's (in MADRAF's case, the "PDS Operations Programs"'s) buffer in memory to preclude paging. The PDS is THE key input device at MADRAF and the single greatest consumer of researcher's lab time. Although the Buffered

* Based on 50 mm/s, samples every 1 micron and 25 mm/s, samples every 10 microns respectively.

Data Path (BDP) is generally more efficient, the PDDRIVER uses the Direct Data Path (DDP) for two chief reasons beyond that the DDP is easier to program. (1) The MADRAF VAX started life as a relatively unique UNIBUS VAX (no MASSBUS) with consequent contention for UNIBUS Adapter (UBA) resources with most of the activity involving allocated BDP's. Use of the DDP lessened the potential of such contention. Use of a VAX-11/750, configured with full UBA's, with only 3 BDP's would also reinforce the DDP choice. (2) In RTDI direct transfer mode, a BDP would be kept allocated for a potentially unacceptably long period of time (in computer magnitudes) due to the pace of the electromechanical scan. The DDP, however, can be shared.

III. PDS OPERATIONS PROGRAM DESIGN

The PDS program used at MADRAF was the result of a "Bottom Up", "Top Down" design. It is a modular, structured program written in VAX 11 FORTRAN 77. Data is received from the PDS across a high speed parallel line and can be stored on disk in a number of formats or be sent directly to tape. The program includes extensive help facilities, limit and error checking and other "user friendly" options. The general outline of command, response and data flow are shown in Figure 1.

Bottom Up

A set of subroutines was created to communicate with the PDS microprocessor. First, at the "lowest level", the basic routines for writing (instructions or responses) to, and reading (responses) from the PDS were developed. The implementation of each of the PDS microprocessor instructions came next, including the required responses where applicable. A standard communication with the PDS consists of constructing an instruction, writing the instruction to the PDS, reading the response from the PDS, interpreting the response, and issuing an acknowledgement of message received from the PDS.

Top Down

Next came the "TOP DOWN" phase which was used for the user interface design. First a terminal/user dialogue was developed that would enable the user to successfully set up, specify, and execute a scan. Options for type of scan, number of scan in the session, data format etc. were included. After the basic user ID was decided upon, the routines needed to accomplish any user specified scan were designed using the set of "low level" command subroutines as "building blocks".

The program proceeds as follows. First a global coordinate system is automatically set by driving the PDS platten to (-x,-y) overtravel, stepping out of overtravel, and resetting the coordinates to (0,0). Next the user is asked to manually set up a local coordinate system for the user's convenience. Header information and scan parameters are then set either by the user at the terminal or from a "SAVE" file (a file created by the program during a previous session of by the user using a text editor). This setup must be done at least once during a session. The available menu of options is displayed and

the user can choose among SETUP (described above), SCAN, HELP, CHANGE ("setup" parameters), GO (to a specified coordinate point), or EXIT.

The final phase, which could be termed "INSIDE OUT" or "OUTSIDE IN", is an ongoing process in which enhancements, extensions, and design modifications and improvements are made.

IV. USER INTERACTION AND UTILITIES

Some of the most important features of the MADRAF PDS operations program are its 1) auto-documentation feature, 2) diverse data destinations, 3) multi-rastering, 4) reregistration utility and 5) scan parameter editing.

When the operations program is executed, the aforementioned global and local coordinate systems are established first. The user is then expected to set up the scan parameters. In this operation, the scan to be performed is automatically documented with variables and keywords in standard FITS format. The user must consciously ignore good scientific practice in order to create unannotated, undocumented data files and even then much of the critical data is saved.

The user can select from several data destinations. The default is to the so-called .SAD (for Standard Astronomical Data) file structure used in the data reduction package obtained from Mt. Stromlo (called PANDORA at MSSSO and ROO for Reduce Observations Optionally at MADRAF) through the kind efforts of Dr. S. M. Simkin. The beauty of this destination is that the INSTANT the scan is complete it can be displayed on the Grinnell image display unit without the more common intermediate mucking about with tapes. Another possibility is to write the files to ordinary VAX/VMS .DAT with FITS header information going into a similarly named text file. Should the user wish to go directly to tape, a FITS tape is the automatic result! Should the MADRAF user require FITS tapes at a later date, utilities are available for creating them from .SAD and other disk formats. It is also possible to send the data buffer to a VAX/VMS "Mailbox" from which the user can rewrite the data in any format desired by a user written program executed from within the PDS program. The most frequent use for this option is to write the data to the type of files used by the Yale astronomy, photometry program of Peter Stetson.

One of the most frequently requested options is to execute many similar (relatively small) rasters on a single plate or set-up of plates. To this end, there are utilities for the creation of the ".PAT" ot pattern files which direct the instrument to various locations on the platten relative to the local coordinate zero. The user can either mark the points by moving the PDS platten about manually, or use previously stored patterns or edit and rescale previously created pattern files. Off-line it is possible to create the .PAT files with any text editor from previously measured or computed positions or directly from a print of the plate by marking points on a graphics input tablet (Bit Pad). The data from the various separate rasters can be placed in separate files or in various "maps" within a single .SAD or FITS file. The user can exercise the option of pausing between the separate rasters in order to

refocus as is often required with older, unflat plates.

Another popular option is the "registration" utility which enables the user to reproduce the position angle and location of the local coordinate zero on the platten of a previously set-up plate or for different plates of the same object. To this end a .REG file, similar in structure to the .PAT file is used. The user is instructed to set the platten to the desired location of local zero, the coordinates are zeroed and the platten moved to another position. The user then rotates the platten to bring a second object to the viewing screen cross wire. The platten is then moved back to local zero and the procedure interated until alignment is achieved. If the user is careful to choose the local zero near platten center, three iterrations are usually sufficient.

Finally the actual raster parameters can easily be specified or modified. The user can select any two of the three parameters: 1) number of points; 2) distance between points; or 3) total distance scanned for each axis. The user specifies whether the reference points in the .PAT file are the center or lower right corner of the raster and whether the X or Y axis is to be the fast scan axis. The speed of the scan is also selectable. All parameters are provided with the most frequently selected defaults and a .SVE save file can be used to reestablish a previously accomplished set-up. Finally the user can move the platten to any local coordinates and reset to local zero at this point.

One option which has yet to be implemented is the ability to scan simultaneously in both axes in order, for example, to follow the "S" distortion produced by magnetically focused image tubes. There has been little call for such functions since ROO contains options to perform geometric corrections.

The operators manual, which is essentially a compilation of HELP files, is available on request. Copies of the program itself can also be made available.

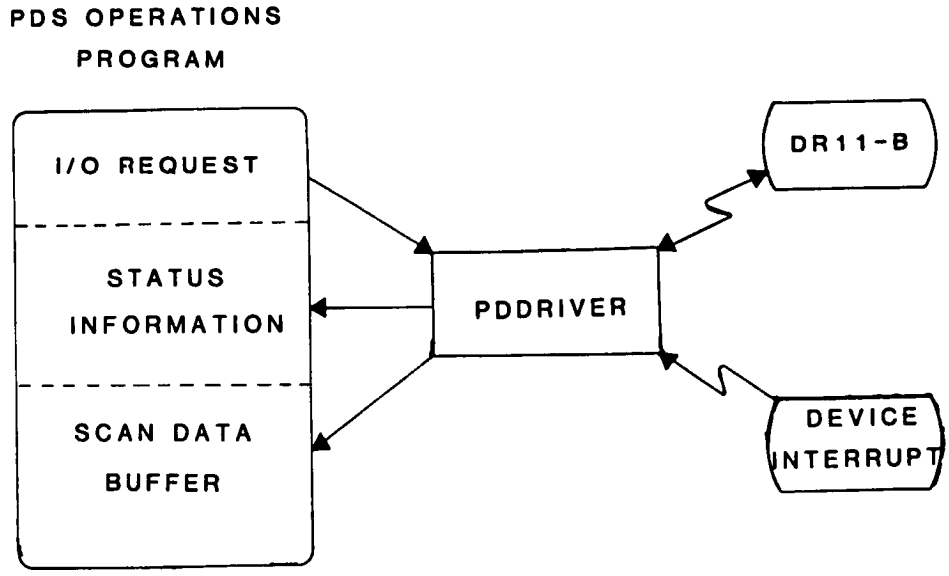

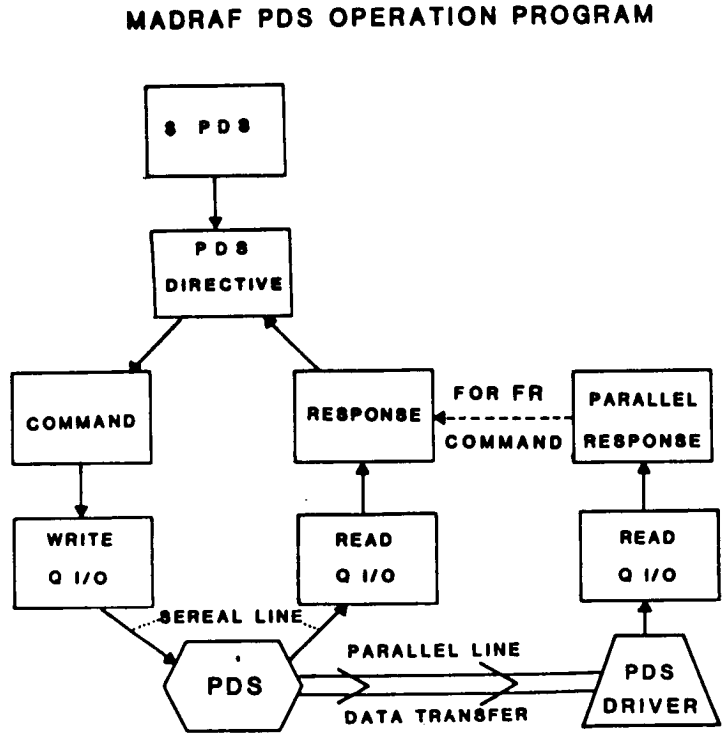

Figure 1 MADRAF PDS Device Driver and Operation Program Flow Charts

Lasker: I would like to add the observation that it is gratifying that sometimes astronomers really can do what we say, namely share each others experiences efficiently. The driver that Chris has been talking about is one we are using, we obtained it from them and it came up quite painlessly. It came up almost as quickly as the ink dried on the consulting arrangement

Anderson: The hardest part was getting the contract from Mike Deering just to go to Baltimore and Tom Lynch too.

Monet: How does your physical driver say the standard DR11W that appears say in 2.x or 3.x. Did you rederive the wheel just because they did not give one?

Anderson: Yes. That's correct. It was not available. We had to send Mike Deering to Maynard Mass to take the device driver course and he had to do.

Monet: It is the same thing now for new systems possibly, probably you're taking, considering starting with a 10W11 driver?

Anderson: I suggest that you talk with Mike on that. I really can't address that.

Lasker: Chris, I have engaged Mike in this discussion and indeed what he does is start with the DEC factory issue & make PDS specific modifications to it.

Anderson: I think he started more or less from scratch well as scratch as any programmer does these days back in 1979.

Opal: It should be trivial to get this to work on RS11M?

Anderson: Yes. I don't know anything about drivers I'm just an astronomer trying to use this darn thing so....

A MICROPROCESSOR-BASED CONTROL SYSTEM FOR THE VIENNA PDS MICRODENSITOMETER

Helmut Jenkner 1)

Space Telescope Science Institute, Baltimore, Maryland 2)
and
Institute for Astronomy, University of Vienna, Austria

Manfred Stoll, Josef Hron

Institute for Astronomy, University of Vienna, Austria

ABSTRACT

The aging DEC PDP-12 computer, serving as the control processor for the Vienna PDS 1010 Microdensitometer, was replaced by a Motorola Exorset 30 system, based on a Motorola 6809 microprocessor. User communication and instrument control are fully implemented in this system; data transmission to a host computer is provided via standard interfaces. The Vienna PDS System (VIPS) software was developed in BASIC and M6809 assembler. It provides efficient user interaction via function keys and argument input in a menu-oriented environment. All parameters can be stored on, and retrieved from, mini-floppy disks, making it possible to set up large scanning tasks. Extensive user information includes continuously updated status and coordinate displays, as well as a real-time graphic display during scanning.

---

(1) On assignment from the European Space Agency - Astronomy Division.

(2) Operated by the Association of Universities for Research in Astronomy, Inc., under contract NAS5-26555 to the National Aeronautics and Space Administration.

1. HISTORY

In 1971 the Institute for Astronomy of the University of Vienna purchased a PDS 1010 Microdensitometer from (then) Photometric Data Systems. A DEC PDP-12 Computer was used for all instrument control, as well as data acquisition, storage and reduction tasks.

With the installation of a DEC PDP-11/34 in 1977, all data acquisition and reduction was transferred to the new computer; the PDP-12 was solely used for PDS control and user interface purposes, communicating to the PDP-11/34 via a unidirectional RS-232 serial interprocessor link.

The decreasing reliability and the extremely high maintenance costs of the PDP-12 made it imperative to replace it by a more cost-effective (and more powerful) microprocessor system. With preliminary planning starting in late 1981, the first version of the system became operational in spring of 1982; several gradually improved versions have been implemented since then.

2. ORGANIZATIONAL AND HARDWARE ALTERNATIVES

From the overall systems point of view, a number of approaches are possible for a PDS control and data acquisition system:

- Stand-alone System:

  All necessary hard- and software for control, user interface, data acquisition and data storage, is concentrated in a self-contained unit. In particular, industry compatible magnetic tape is used as permanent storage medium, in order to allow the user to reduce the data an a large variety of processors. With the possible exception of the magtape format, this solution does not pose any compatibility problems. However, it is comparatively expensive and requires longer development times and more manpower, things which are not too abundant in the typical university environment.

- Pure Control System:

  A system of that type performs instrument control functions only. User communication and data related operations are removed to a host processor. Communication typically consists of command down-loading to and data up-loading from the host processor. While this is a comparatively easy to build and maintain hardware solution, it requires more complicated communication software on two systems in

order to support the elaborate problem-oriented software protocol. In addition, this version poses a considerable processing load on the host computer.

- Communication and Control System:

  In this approach instrument control and user interface are handled by the system. Data only are transmitted to a host processor via a standardized interface. Advantages include the fact that all instrument-related functions are concentrated in one unit, the lack of compatibility problems, the simple software protocol (e.g. RS-232), the comparatively low price for hardware, and the moderate software development needs.

The advantages of the last approach made it the most attractive system for our purposes.

From the viewpoint of the PDS Microdensitometer, a decision had to be reached as to where to start with the new (digital) hardware. Again, three different approaches are possible:

- Replace all electronics:

  New compact hardware would have to be designed and built, starting immediately at the PDS motors. This would allow one to arrive at a system of increased functionality (e.g. fully independent axes), but it would require extensive design work and thus absorb manpower for too long a time. In addition, this would not help to overcome the fundamental hardware problems of the PDS 1010 (motor - encoder arrangement, photometric system, depth of field, etc.), in spite of the fact that it would lead to a major redesign of large PDS subsystems.

- Replace control hardware (DCRS) and control computer:

  This solution would leave the low level electronics (eg. motor drivers) unchanged, but replace the DCRS (Digital Coordinate Readout System) and, of course, the control computer. By virtue of the vendor's policy, however, it was impossible to receive sufficient engineering information on signals and general layout of the DCRS.

- Replace control computer only:

  In this approach the old PDS electronics, including the DCRS, is left unchanged; only the control processor is replaced. The obvious drawback of this solution is the fact that it is not capable of adding new features to the limited drive and control functions. On the other hand, it

provides an easily implemented known protocol requiring little hardware design, and can be done relatively quickly.

Because of the above mentioned advantages the third solution was the most attractive for our institute at that time. A more general solution, in particular the first one above, can still be implemented at a later time. It should be combined with major mechanical changes to the instrument; however, no definite plans for such a change exist at this time.

It should be noted in this context, that the major use of the Vienna PDS is in the field of spectroscopy. That usually implies a moderate number of single sweeps; two-dimensional work measuring large plate areas and thus leading to large data volumes is the exception rather than the rule in our application. Additionally, tests have shown that it is necessary to scan at low speeds in order to obtain satisfactory positional accuracy. All this leads to relatively relaxed requirements with regard to data communication capabilities with the host computer; a serial asynchronous link (RS-232) was found to be sufficient for the current PDS applications.

3. CONTROL HARDWARE

Rather than using existing board designs and components from earlier microprocessor-based control systems (e.g. telescope control) and developing the entire control software in the microprocessor's assembly language, a small microprocessor system was purchased which included all features required for the PDS application. In addition, existing operating system software and high level languages facilitated program design and implementation.

The following sections list the hardware components used in the control processor for the PDS microdensitometer:

- Motorola Exorset 30

  Based on M6809 microprocessor, including:

  -- full ASCII keyboard and 16 user-definable function keys;
  -- CRT display with 22 x 80 or 16 x 40 characters, and 320 x 256 dot graphics;
  -- printer interface;
  -- asynchronous serial interface (RS-232);
  -- 48 kByte RAM storage;
  -- 24 kByte PROM storage;
  -- 2 mini-floppy disk drives.

- Universal Parallel Interface Adapter
  Four 8 Bit parallel input/output ports.

- Quad Serial I/O Module
  Four asynchronous serial interface ports (RS-232).

- A/D Converter
  -- 12 Bit resolution;
  -- 8/16 input channels;
  -- 40 microseconds conversion time
- EPROM/PROM Programmer

- Card Cage

- Power Supply

The parallel interfaces are used for communication to the DCRS. Using on-board firmware, the standard Exorset 30 asynchronous serial interface allows the system to emulate a terminal, communicating with a host. A second serial interface is used for PDS data transmission to the host.

4. SOFTWARE ENVIRONMENT

Several software layers are available in the Exorset 30. The EXORbug Monitor, implemented in firmware, handles basic keyboard and display operation as well as disk I/O, and provides a set of debugging tools.

The disk-based XDOS Operating System provides the interactive environment and access to a number of utilities, as usually available on microprocessor or low-end mini-computer systems.

The BASIC-M Interactive Compiler is available as a (moderately) high-level language. It features both an interactive and a compiler mode, and is enhanced for real-time applications and process-control.

Parts of the system had to be implemented in the Exorset's relocatable M6809 assembler. Time critical parts, DCRS protocol emulation, table driven command parser and value check procedures, respectively, are examples of assembler routines.

Program development and maintenance were performed on the Institute's DEC PDP-11/34 (currently being replaced by a DEC VAX-11/750), for reasons of data storage, better editing capabilities, and multi-user access to the programs. Source modules were downloaded to the microprocessor system and compiled or assembled, and linked.

5. CONTROL SOFTWARE

The following design criteria were used for the control software of the Vienna PDS System (VIPS):

- High level of interactivity.
- Extensive user information.
- Ease of use.
- High fault tolerance.
- Flexibility.

Communication with the PDS is implemented via parallel interfaces to the DCRS and simulation of the DCRS command protocol, and via the connection between the A/D converter and the photo-signal amplifiers.

User communication features command input via function keys, with menu information on the terminal screen, giving the relationship between command and function key number at any given time. If commands require arguments, prompts appear (in reverse video) to guide the user through the input sequence. All arguments are checked for validity upon input, both in general (e.g. simple range checking) and in the current environment (eg. selected scanning speed and sampling interval combination causes exceedingly high transmission speed).

User information is provided by four different displays which always contain menu information on the commands available through the function keys (see also Figures 1 through 4):

- Main Status Display:

  Contains continuously updated PDS coordinates and all primary scan parameters, as well as information on the status of the host link. This display can have two distinct modes of operation:

  -- Command Mode (Figure 1)
  -- Input Mode (Figure 2)

  In the former mode, all keys are used to initiate certain instrument dependant functions (see below), whereas in the input mode individual parameters in the display can be changed.

- Coordinate Storage Block Display (Figure 3):

  Allows inspection, input, and editing of up to 16 coordinate pairs, which are used as starting location of the currently defined scan pattern. As will be discussed later, coordinates (and scan parameters) can be stored on

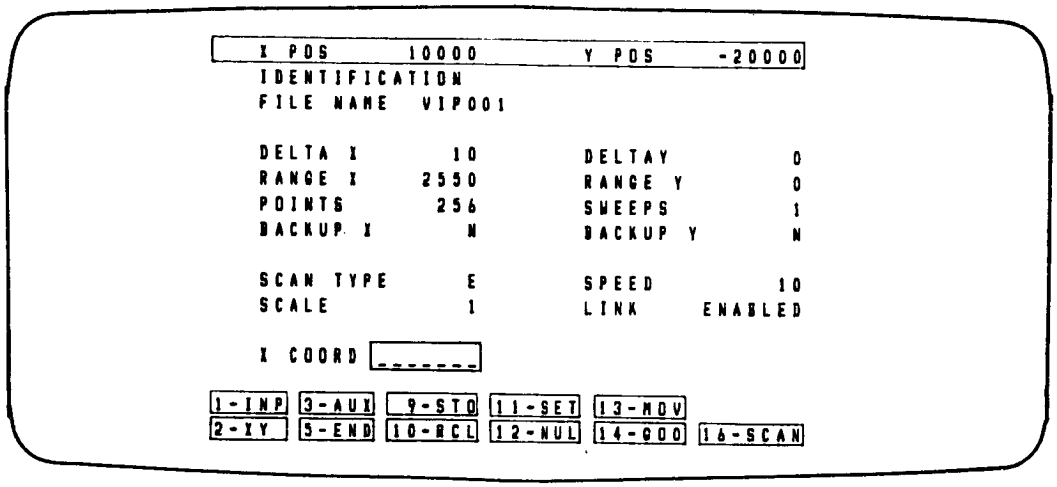

Figure 1. VIPS Main Status Display in Command Mode. Boxed areas denote reverse video display. The first line gives continuously updated PDS coordinates; the last two lines correspond to commands initiated by function keys; the line above this menu area is the input and message line. In the current display, input of an X-coordinate is expected after a MOVE or SET command was initiated via the respective function keys.

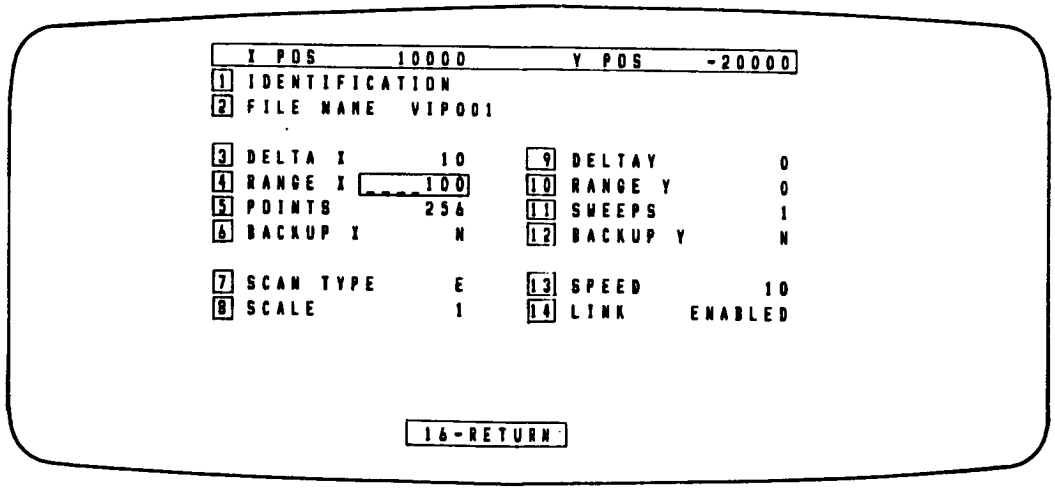

Figure 2. VIPS Main Status Display in Input Mode. Boxed areas denote reverse video display. Numbers to the left of each item correspond to function keys, initiating input of the respective value. In the current display, input of the scan range in X was requested via function key 4.

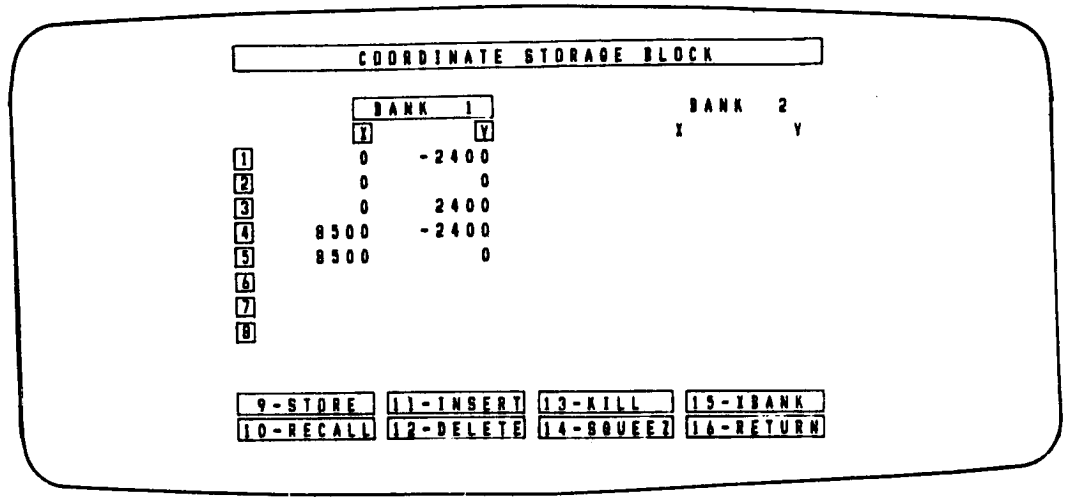

Figure 3. VIPS Coordinate Storage Block Display. Boxed areas denote reverse video display. Function keys 1 through 8 allow the user to input coordinate pairs, the remaining function keys (bottom lines) execute editing functions.

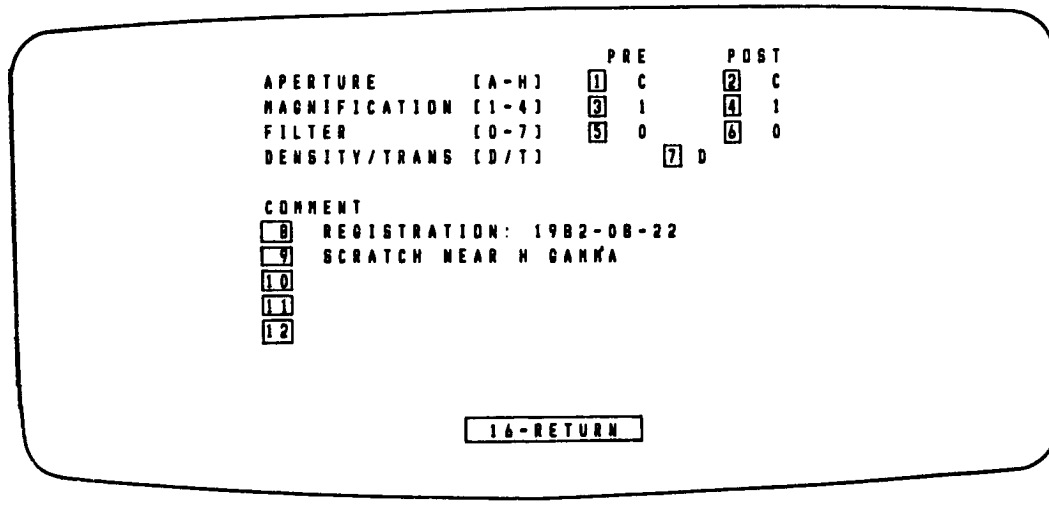

Figure 4. VIPS Auxiliary Status Display. Boxed areas denote reverse video display. Numbers to the left of each item correspond to function keys, initiating input of the respective value.

disk, giving virtually unlimited scanning sequences.

- Auxiliary Status Display (Figure 4):

  Allows inspection and input of manually set PDS instrumental parameters, as well as several comment lines. This information is transmitted as part of the header information and can be stored with the data.

- Real-time Graphic Display:

  During Scanning, the scanned data are scaled by a preset number (in the Main Status Display), displayed on the screen and continuously refreshed. This allows the user to monitor the incoming data and react immediately in case of equipment failure or erroneous instrument setting.

In addition to the commands for input of individual arguments displayed in the respective display pages, the following groups of commands are available:

- Display mode selection commands:

  The respective display pages may be selected from the Main Status Display in Command Mode. All other displays return to this page.

- Parameter storage and retrieval commands:

  All parameters of the current system status can be saved on one of the mini-floppy disk drives. It is therefore possible to set up large scanning tasks in advance, and recall complete sets of parameters at scan time by a single command. One disk can hold up to 160 sets of parameters; exchange of disks is possible.

- Scanning, moving and setting commands:

  The PDS coordinates can be set from the control system to any number within the range of the PDS counters without moving the plate stage. A move command allows the user to direct the stage to given coordinates. Special commands are provided to zero the coordinate system, and to move the stage to the origin. After scanning is requested via the scan command, the user is prompted for affirmative acknowledgement in order to prevent unintentional scanning and synchronization problems with the host computer.

- Coordinate editing commands:

  Commands are provided for inserting of coordinate pairs at certain locations, deletion of single coordinate pairs, deletion of all coordinate pairs of the coordinate storage block, and for rearranging of coordinates in adjacent storage locations (squeezing).

Scanning is done continuously; that is, no fixed maximum buffer size is used within the system. The control system uses a ring buffer to implement the asynchronous read (from the PDS) and write events (to the host computer), whereas the host computer uses double buffering to prevent data loss during output operations to storage devices.

Data transmission to the host can be disabled for test purposes or during the setup phase. In addition, checks on the availability of the host link are performed at various times during scanning.

The BASIC-M mainline consists of event-driven modules, which are invoked by software interrupts from the function keys. This mainline consists of 1300 BASIC statements, requiring 11 kBytes for program storage, 10 kBytes for the associated run-time library, and 3 kBytes of data storage.

Assembler subroutines are used for table-driven terminal I/O, disk I/O, motor driving and scanning, graphic display, and for data formatting, checking, and transmission. These subroutines contain a total of 4000 statements, requiring 6.5 kBytes of program storage and 4 kBytes of data storage.

6. HOST SOFTWARE

A simple receiver task buffers the incoming data and periodically writes them into a temporary disk file, using double buffering to prevent data loss and allow the PDS to scan continuously.

Different formatter tasks can then access the temporary disk file and generate a permanent disk or tape file in several different formats (e.g. standard PDS format, FITS format, etc.), which can then be reduced with the help of general purpose image processing systems, either on the host processor itself, or on other computers.

SESSION III

Chairman: Francois Schweizer

III. Status and Advantages of "Other" Microdensitometers

Although a variety of designs for "classical" microdensitometers have been tried by astronomers over the years, it is obvious that PDS, which has sold at least thirty machines for astronomical research, is dominant in the field, to the extent that the PDS machines are the standard against which alternative instruments are compared. Designers of most "other" machines have aimed to obtain higher data rates than are possible with PDS machines by utilizing non-mechanical scanning mechanisms, currently laser beams or diode arrays. It appears that generally speed has been obtained at the cost of giving up dynamic range and/or the ability to produce large-size continuous digital images. But most of these machines include special computing hardware in order to implement automatic real-time object measurement and/or classification. In what range of astronomical applications can these new machines totally replace the PDS machines? What are the strengths and weaknesses of the various machines currently? Are any of them going to become commercially available? Contributions which discuss the technical and astronomical motivations which have caused several astronomical institutions to undertake these major development projects, rather than just ordering yet another PDS machine, are especially welcome.

Why use a microdensitometer other than a PDS?

R.S. Stobie
Royal Observatory, Blackford Hill,
Edinburgh EH9 3HJ, Scotland, U.K.

ABSTRACT

The motivations for constructing a special purpose built microdensitometer are explored. A brief description of the salient points of some of these microdensitometers is given stressing in particular the advantages and disadvantages of the system in comparison to a PDS machine. The principal gain is in speed though at the expense of loss in dynamic range. Exactly how much this affects the astronomical results is demonstrated. Some of the astronomical results already obtained with these machines and from on-going projects are described. It is shown that there is a large class of important astronomical problems which can be tackled by these machines but which are not feasible on the PDS because of the speed of the machine.

1. Custom-built measuring machines

Over the past 15 years a number of high-speed automatic measuring machines have been built for the astronomical community. A list of such machines is given in Table I. Most of these machines are presently either working or under development. Further information on the machine details can be found in the references. I have restricted the list to include only machines with a full 2-D capability and have excluded custom-built machines designed purely for 1-D spectroscopic work. The machines naturally fall into two categories according to the type of astronomy they were designed for (i) the general purpose measuring machines (ii) the special purpose measuring machines.

The general purpose measuring machines digitise the photographic plate and provide an image analysis system (on-line or off-line). This image analysis system usually has the capability of determining an accurate sky background, following a variable sky background, detecting the presence of an image by connecting pixels above a threshold, rejecting noise pixels above a threshold, connecting the pixels to form a coherent image and simultaneously calculating various image parameters (frequently based on the moments of the image pixel distribution). The parameters contain information on the astrometric and photometric properties of each image and enable simple image classification (eg star/galaxy discrimination) to be carried out. In the end the user is presented with a magnetic tape containing a catalogue of such images, summarising in as meaningful a way as possible the astronomical information on the photograph. A suite of software also exists to aid the user in the further analysis of his data, eg graphical display of images detected together with a listing of image parameters, software to merge data sets from measures of different plates taken on the same area of sky, software to classify stars/galaxies, software to detect variable objects. Because the general purpose measuring machines work with digitised pixel data they can be extremely flexible in the type of application. More specialised applications include for example software for the extraction of spectral information from objective prism plates and the detection of supernovae in external galaxies via the digital differencing of maps.

The special purpose machines have been designed mostly to obtain accurate stellar positions and magnitudes using analogue scanning and servo techniques for automatic centring on circularly symmetric images. In the case of the GALAXY machine, not only does the machine automatically centre on the image, it simultaneously matches the radial profile of the image to a library of profiles to obtain the best fit, thus providing a stellar magnitude parameter.

The reason why such machines have been built seems clear. In the case of the general purpose machines the design has been driven by the

requirements for scanning large Schmidt plates. A PDS microdensitometer (with a fast logarithmic amplifier) measuring a 4m telescope prime focus plate can scan a 200 x 200 mm^2 area at 50 micron resolution in 20 hours (Herzog and Illingworth, 1977). The corresponding figures for a 300 x 300 mm^2 area of a Schmidt plate digitised at 10 micron resolution would be 1000 hours. Thus to realise the scanning of Schmidt plates within a day requires a measuring machine 100 times faster than the PDS. Most of the general purpose measuring machines satisfy this requirement. What is most remarkable is that the Luyten/CDC machine (originally built as a special purpose machine for a large proper motion study using Palomar Schmidt plates, and now being modified to provide a general purpose scanning facility, Humphreys and Landau 1980) not only satisfies the speed requirement by the greatest margin but that it was doing this over 10 years ago.

The machines are all roughly comparable in their positional accuracy. The xy stages are linear to a few microns and orthogonal to a few arcsecs. The positional readout is obtained from Moire fringe gratings or a laser interferometer giving digitisation in the range 0.1 to 2 microns. The repeatability and stability of most machines is of the order of 1 micron. Most impressive is the results obtained by the GALAXY machine on UK Schmidt plates where plate to plate comparision of the same area of sky has shown positional residuals per plate of 1 micron over an area of 250 x 250 mm^2 (Murray and Corben 1979).

Regarding the speed of the machines it should be noted that the peak data rates quoted in Table I correspond to the highest acquisition speeds from successive pixel integrations. The actual time to scan a whole plate gives a considerably lower average data rate than this because the machine is not continuously measuring pixels and is performing other functions (eg scan run-in and flyback time, moving to measure the next strip, determining the sky background).

The major differences between the machines stem from the types of scanning system and detection system employed, how much on-line processing is done relative to off-line processing, whether the plate is used as the storage peripheral or whether the data is dumped to a storage medium (tape or disc) and then analysed asynchronously.

2. Comparison with PDS

The clear advantage of such machines is that the gain in speed has enabled a whole new range of astronomical projects to be tackled which would not be possible with an "off-the-shelf" microdensitometer. Clearly most of these projects involve the use of Schmidt plates and in section 4 I will give examples of projects which could not have been undertaken with a PDS machine.

This gain in speed has been achieved in 2 ways: (i) by using a flying spot scanning technique with detection by a photomultiplier or (ii) with a fixed linear light source and a linear diode array (Reticon) as a detector to gain the multiplex advantage in simultaneously measuring a row of pixels. Both these techniques suffer from the same problem, namely that there is a loss in dynamic range in comparison to a PDS machine. In the case of the flying spot scanners the fundamental problem is caused by the halo or flare surrounding the spot. Although this halo is of very low surface brightness, it is so extensive that the integrated halo amounts to a few percent of the total light. It is surprising that the laser beam has such a significant halo but this is probably due to the large number of optical surfaces (32 in the case of APM) it encounters before the beam reaches the emulsion. Thus in measuring the dense core of a stellar image the photons which are detected come from the halo transmitting photons through the sky background surrounding the image. This effectively limits the measurable density range to $\Delta D \sim 1.5$ above the density of the sky background. In the case of the linear diode array detectors the simultaneous illumination of the pixels causes a loss in dynamic range since light scattering in the emulsion causes photons to be scattered into neighbouring diodes. If the diode array could be held in contact with the emulsion this would minimise the problem but in practice a transfer lens is used to image the emulsion onto the diode array.

The dynamic range can be improved in two ways. For both the flying spot scanners and the linear diode arrays a slit parallel to the direction of the scan or array will reduce the light scattering problem from two dimensions to effectively a one-dimensional problem. With the flying spot scanners since no mechanical aperture can follow the speed of the flying spot the residual 1-D halo will remain. In the case of both the flying spot scanners and the linear diode arrays there is the opportunity for further rectification of the signal by deconvolution (Swaans 1979). In practice this is generally not aplied because of time constraints.

It is significant that no system has attempted to use a two-dimensional CCD detector. Although this has the advantage of a fixed geometry the system does not lend itself to continuous motion of the plate in one direction and more importantly the light scattering problem will be multiplexed reducing even further the density contrast measurable. What needs to be designed is a high-speed microdensitometer (peak data rate in excess of 100 KHz) which has no significant halo or light scattering problem. This would be a major advance on the limitations of the present systems.

I will not dwell here on the limitations of the PDS microdensitometer as these are reasonably well known (cf Wray and Benedict 1974, Elvius et al 1978) and will be discussed elsewhere at this conference.

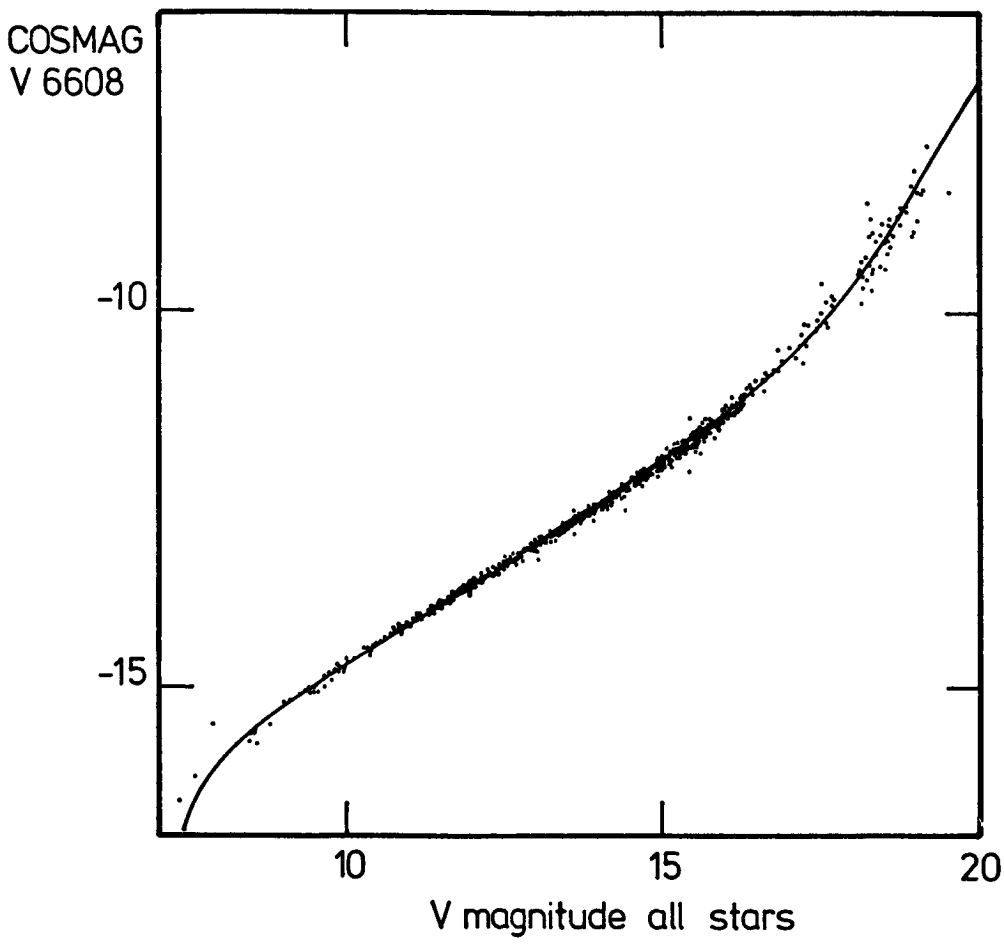

Fig. 1 Stellar magnitude calibration curve for over 2000 photoelectric and photographic standards covering an area of 20 square degrees surrounding the South Galactic Pole. The UK Schmidt Telescope plate V6608 was digitised in COSMOS with an 8 micron increment. The parameter COSMAG corresponds to the volume integral of the intensity in an image bounded by an isophotal threshold. The scatter about the mean relation has an rms of 0.08 magnitude.

3. Astronomical impact of reduced dynamic range

The consequences of the presence of a halo or light scattering problem are predictable. In the case of the spot halo it essentially corresponds to a convolution in transmission space of the spot profile and the structure of the emulsion. For the faint images the density contrast is so low that any halo or light scattering problem has a minimal effect. However as the images become brighter the density contrast of pixels relative to the sky background increases and the densities are systematically measured as less than the true density. The effect is dependent on the structure of the image and will be different for stars and galaxies.

In determining the characteristic curve of an emulsion from a step wedge or sensitometer spots it is essential to mask the step wedge or sensitometer spots so that no halo contribution can be detected from the neighbouring "clear" regions. This is especially important for high density sensitometer spots. The characteristic curve so obtained is then valid for obtaining the intensity of a pixel in a region of uniform density. Thus sky background pixels will be accurately calibrated but pixels in an image will have their density and hence intensity systematically underestimated in comparison to values obtained with a PDS microdensitometer. One of the consequences of this is that the method of determining the magnitudes of stars and galaxies from a knowledge of the brightness of the sky background and the characteristic curve is fraught with danger. An external magnitude calibration is essential to avoid systematic errors.

The one parameter which is not affected (at least to first order) by the presence or absence of a halo is the positional information, eg the intensity-weighted centroid or the profile-fitted centre. Isolated symmetric images should show no systematic error. However any non-symmetric image, for example an image with a nearby companion, will have a second order effect in the error of its xy position.

The accuracy of stellar photometry is not impaired by the presence of a light scattering problem, provided that sufficient reliable standards are available. The reason is that the systematic density errors affect programme and standard stars identically. Fig. 1 shows the stellar magnitude calibration of a UK Schmidt plate measured in COSMOS. The COSMOS magnitudes correspond to a volume integral of the intensity within an isophotal boundary, where the intensity was determined from a step wedge. For a deep Schmidt plate the stars at magnitude 19 are already saturating in the core as a consequence of the spot halo in the measuring machine. The nature of the stellar magnitude calibration curve is complex also as a result of other telescope optical effects such as the stellar halo which for sufficiently bright stars rises above the isophotal threshold and changes the slope of the magnitude calibration. From experience with

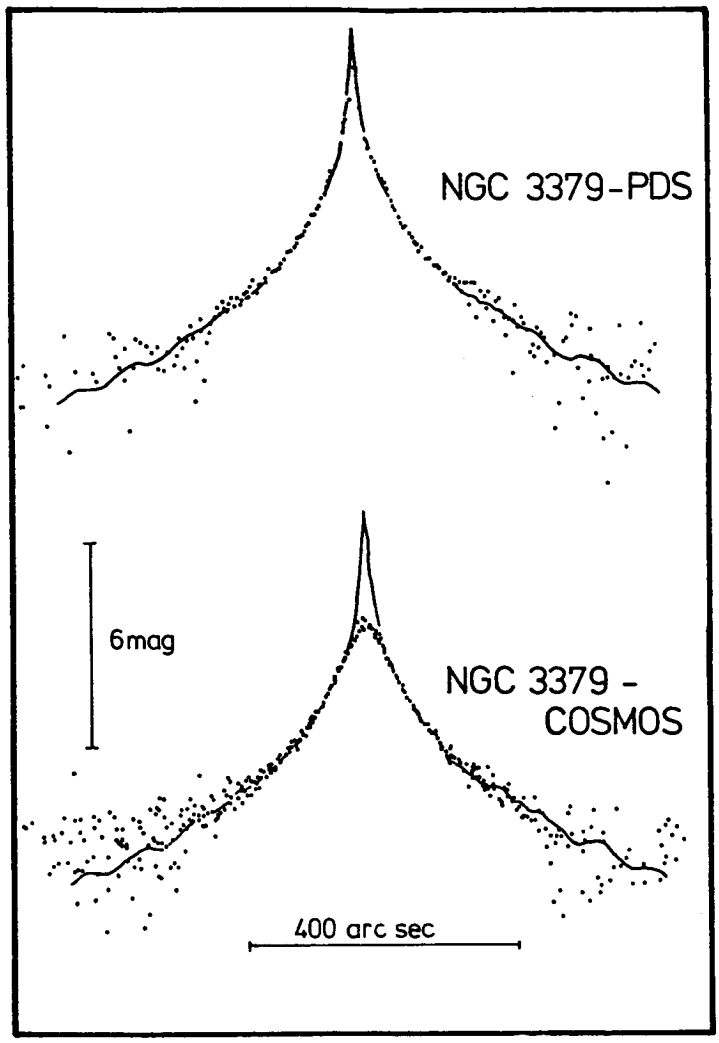

Fig. 2 Photoelectric scans (solid line) of the standard elliptical galaxy NGC 3379 have been used as a check on surface photometry of this galaxy using different measuring machines. The same plate UKST B6669 was digitised both with the PDS and with COSMOS measuring machines. The photographic characteristic curve was derived from a sensitometer spot calibration. The results show that the PDS measures accurately follow the surface brightness profile over the whole range in density. The COSMOS measures, which follow the outer isophotes accurately, systematically underestimate the surface brightness in the nuclear regions of the galaxy. This is a consequence of the spot halo reducing the effective dynamic range.

merging plates of the same area of sky we know that using this technique the stellar magnitude error per plate obtained for isolated stars is $0^m.05$ for UK Schmidt telescope plates and $0^m.03$ for 4m telescope prime focus plates (Stobie 1982). This accuracy is achieved for stars more than $2^m.5$ above the plate limit and compares favourably with stellar photometry using PDS data (Stetson 1979).

The photometry of stellar images in a crowded field is a much more difficult problem. With PDS data it is possible to use profile-fitting techniques which assume that the radial intensity profile of a stellar image is magnitude invariant. However, if a measuring machine has a significant spot halo or light scattering problem, this technique is invalid because the halo causes the meaured intensity profile to become magnitude dependent. Possible methods of coping with this problem are either to work with an algorithm that isn't sensitive to the scaling of the intensity profile or to modify the characteristic curve so that the stellar profiles as measured become magnitude invariant.

Surface photometry of extended objects clearly is affected by the presence of a light scattering problem. Fig. 2 shows a comparison of photoelectric scans, PDS scans and COSMOS scans of the standard elliptical galaxy NGC 3379. The PDS scans follow the galaxy profile as determined by the photoelectric scans over the whole range in density. The COSMOS scans reproduce the low surface brightness region satisfactorily but cannot measure the dense nuclear region because of the scanning spot halo. However it can be seen from Fig. 2 that the integrated magnitude will be very little in error as the volume integral of the missing central intensity is a small fraction of the total intensity of the galaxy. It is for this reason that integrated galaxy magnitudes are accurately measured by measuring machines with a light scattering problem.

Integrated galaxy magnitudes are shown in Fig. 3 as measured on the same plate in the PDS machine and in COSMOS. The results show a 45^o slope with an rms scatter of $0^m.10$ down to B = 21. The fact that the mean relationship is a 45^o slope shows that the scattering problem is much less severe for extended objects than it is for point source objects. The difference between Fig. 3a and 3b is not connected with the spot halo but demonstrates the importance of taking a sufficiently low isophotal threshold to avoid large systematic effects in the integrated magnitude of a galaxy. Results on other galaxies have shown that the linearity of the magnitude relationship and the 45^o slope extends to galaxies as bright as magnitude 13.

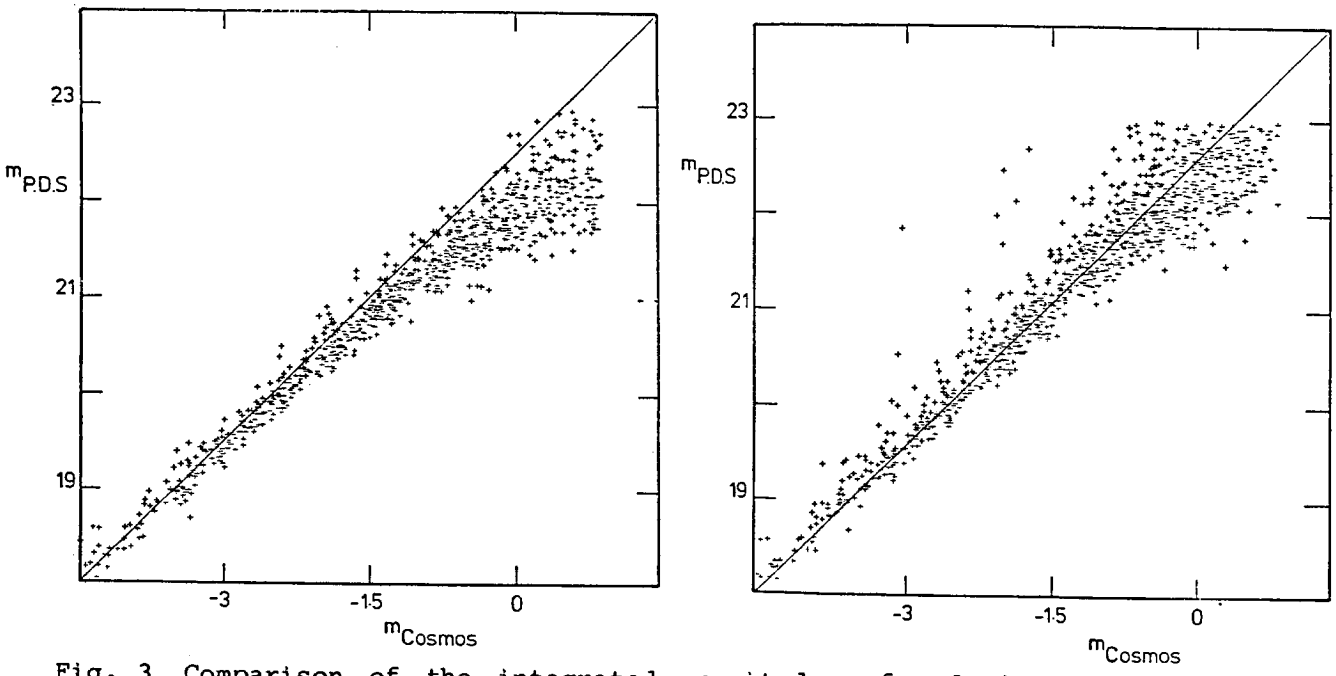

Fig. 3 Comparison of the integrated magnitudes of galaxies on AAT plate J1555 measured in both the PDS and COSMOS microdensitometers. The PDS magnitudes were based on isophotal magnitudes (at a 2.5% intensity level above sky) which were subsequently corrected to give total magnitudes. The COSMOS magnitudes were isophotal magnitudes measured at two thresholds, (a) 7%, (b) 2%, in intensity units above the sky background. For $m_J < 21$ the scatter about the 45° slope drawn is $0^m.1$. Although not shown on the diagram this 45° slope extends and fits the data to much brighter magnitudes ($m_J = 13$). For $m_J > 20$ there is a systematic and increasing deviation in (a) of the points from the 45° slope whereas in (b) the points follow the 45° as faint as $m_J = 23$. This demonstrates the importance of adopting a sufficiently low isophotal threshold to avoid strong systematic errors in the total magnitudes caused by light from the galaxy falling outside the isophotal boundary.

4. Astronomical projects requiring high-speed automatic measuring machines.

A number of major astrometric projects have been carried out using some of the machines in Table 1. The proper motion survey by Luyten (1974) from Palomar Schmidt plates provided 300,000 new proper motions in 2.5 years of operation, exceeding by a factor of 20 the number produced by all other workers in the field in the previous 70 years. The US Naval Observatory machines have been used primarily for the determination of parallaxes and over 50,000 plates have been measured providing much of the fundamental data on the parallaxes of nearby stars (Strand 1975). The third major astrometric survey using an automatic measuring machine involves measuring about 6000 plates with the GALAXY machine to provide accurate positions for southern hemisphere stars (de Vegt et al. 1983). I believe that in future important advances will be made by determining the proper motions of stars relative to the galaxy reference frame. This has already been achieved manually at the Lick Observatory though one inherent difficulty was the relatively small number of galaxies per plate. Using the deep UK Schmidt plates and the APM machine, Kibblewhite et al. (1983) have demonstrated that the plate-to-plate error in a stellar position of 1 micron can be obtained over the whole plate by using 50,000 galaxies as the reference frame.

The combination of automatic measuring machines and deep Schmidt plates is ideally suited to furthering our understanding of the structure of the Galaxy. The first results of such a survey have been published by Reid and Gilmore (1982) and Gilmore and Reid (1983). UK Schmidt plates of the same field in the B, V, R and I bands were measured with COSMOS and the data merged to provide a catalogue of accurate magnitudes of stellar objects. In a field of 18.24 square degrees towards the South Galactic Pole a catalogue of 12,500 stars brighter than I = 18 was obtained. By careful calibration of the absolute magnitudes from the M_V - (V - I) relation this provided the first purely photometric determination of the faint end of the stellar luminosity function to M_V = + 19. The results are consistent with the stellar luminosity functions derived by Luyten and Wielen. In addition the space density of red dwarfs in the solar neighbourhood showed no evidence of any significant excess of M dwarfs and thus no requirement for a significant undetected low proper motion component amongst stars in the solar neighbourhood. An important new result which emerged from this survey was the detection of a Galactic thick disc component. Similar surveys are being extended to 9 selected fields in the Galaxy to improve the statistics and determine any dependence on latitude and longitude.

The discovery of variable objects which was previously carried out by blinking pairs of plates can now be carried out with automatic measuring machines (Hawkins 1981, Stobie and Henley 1983). The technique corresponds to a "multi-blink" procedure wherein all plates

are simultaneously compared with each other. Each plate is scanned in the measuring machine to produce a catalogue of image parameters. These cataloques are then merged to produce a list of magnitudes for each image. Clearly for identification of the candidate variables external magnitude calibration is not necessary and all magnitudes may be converted to a master plate in the natural magnitude system of the telescope/plate/measuring machine combination. The candidate variables are then selected from the objects with the largest rms scatter in the magnitudes. Results have been obtained using UK Schmidt IIIaJ and IIIaF plates measured with COSMOS to derive a complete sample of variables from 100,000 objects to B = 21 in a field of 16 square degrees. The types of variable object discovered included a sample of 88 extragalactic objects (mostly quasars and active galactic nuclei), 3 cataclysmic variables and 26 RR Lyrae variables (Hawkins 1983a, b). The space density of the halo was derived from the RR Lyrae stars as a Galactocentric power law with exponent -3.1. The most distant RR Lyrae discovered was of magnitude B = 20 at a distance of 60 kpc from the Sun with a radial velocity of - 483 km s^{-1}.

Observations of supernovae in external galaxies provide a direct test of the expansion of the universe. This will be an important project for the Space Telescope. The supernova has to be discovered in "real-time" near maximum and for this a high-speed measuring machine is vital. The method proposed by Cawson (1982) using the APM machine is to scan 2000 to 3000 of the brighter galaxies on each Schmidt plate of the same area of sky and to compare the surface brightness distribution of each galaxy with the measurement on a previous plate. This is a more powerful technique than searching for differences in the integrated magnitude of a galaxy and already a number of supernovae have been discovered.

The 2-D distribution of galaxies has been studied on UK Schmidt plates and AAT prime focus plates from COSMOS measurements. Using the parameterised data a star/galaxy classification algorithm is required. Depending upon the seeing a classification accuracy of about 95% is obtained for images brighter than 2 magnitudes above the plate limit. For the faintest images the stars merge with the galaxies in the parameter space and discrimination is lost. Results on the number counts of galaxies have been obtained by Stevenson et al (1983), on the 2-point correlation function of galaxies by Shanks et al (1980) and on studies of rich clusters of galaxies by MacGillivray and Dodd (1979).

The previous projects have all involved the measurement of direct plates. There are two projects I would like to mention in connection with objective prism plates. The method of data reduction is different from the analysis of the direct plate. The location of the objects on the prism plate is determined either by measuring the prism plate itself with thresholding software or by measuring the

corresponding direct plate and applying a non-linear coordinate transformation. A rectangular pixel array is extracted surrounding each object and this is used to determine the local sky level and obtain a 1-D spectrum of the object. The final output is a catalogue of the intensity-calibrated spectra of the objects. Two major projects are in progress using UK Schmit unwidened prism plates (dispersion 2400Å mm^{-1} at a wavelength of 4300Å) digitised by the COSMOS measuring machine.

In comparison to the 2-D distribution of galaxies, the 3-D distribution is a far more sensitive test of the theories of galaxy formation. Redshifts of galaxies out to $z = 0.25$ can be obtained with an accuracy of $\Delta z = 0.01$ from low dispersion objective prism plates (Cooke et al 1983). A survey on one prism plate can contain about 2000 galaxies with measurable redshift and provide 3-D information out to 600 h^{-1} Mpc. Initially redshifts had to be determined by interactive techniques displaying each spectrum in turn because of the complexity of the problem but recently techniques have been developed which are capable of deriving automatic redshifts. The first results have been presented by Beard (1983).

The automatic detection of quasars from objective prism plates has been proved feasible by Clowes et al. (1983). Comparison of the machine-based sample with an eyeball search of the same plate has shown that the software is capable of detecting all eyeball candidates and furthermore detects candidate quasars missed by the eyeball search. The importance of such techniques is not just that they are capable of providing lists of candidate quasars but that the selection effects can be more carefully controlled and quantified and thus the sample will be more statistically uniform.

Apart from the major projects already mentioned a vital role played by the measuring machines is the selection of interesting objects from these large scale surveys for detailed study by 4m telescopes. For example it is a direct result of the measurement of UK Schmidt plates with COSMOS that discovery highlights have included one of the intrinsically faintest stars known (Reid & Gilmore 1981), the existence of a Galactic thick disc (Gilmore & Reid 1983), the faintest RR Lyrae star (Hawkins 1983c) and the second most distant quasar (Shanks 1983).

A word of caution: The previous paragraphs may well have given the impression that obtaining results from Schmidt plates using automatic measuring machines is trivial. I have not gone into any of the many checks necessary to be certain that everything is working correctly, nor all the software/hardware development that is required to extract the information. Indeed it is essential that the astronomer understands the telescope, the photographic emulsion and the measuring machine for a proper analysis of the data. To give but one example on variable stars - one might think that the extraction of candidate

variables is based simply on the rms scatter of the magnitudes using chi-square statistics. This would be true if the magnitude errors always followed Gaussian statistics. It is however the effects that give rise to non-Gaussian statistics that cause the spurious variables to appear. Non-Gaussian statistics can be caused by effects such as emulsion flaws, emulsion sensitivity variations, stellar image profile variations (e.g. as a result of differential atmospheric refraction), two images appearing as a merged double on one plate and two separate images on another, an image falling inside the halo of a bright star will appear as spuriously variable, and different atmospheric seeing causing a constant brightness galaxy to appear variable as a result of differing amounts of light falling outside the isophotal threshold. Most of these effects can be handled (or alternatively the image rejected) to produce a list of candidate variables from which the majority of the spurious variables has been eliminated.

I have only mentioned some of the larger projects being carried out on such machines. There are many smaller projects as well. It should be recognised that the time to measure the plate and process the data is small in comparison to the time that the astronomer will spend analysing the data. With the speed of these automatic measuring machines there is a need for more astronomers to be involved in analysing the data.

5. Conclusions

Apart from the major astrometric surveys it is only within the last 2 to 3 years that the general purpose high-speed measuring machines have been developed to a stage where large scale surveys of the Galaxy and the Universe are possible. The hardware and software development has enabled the extraction of the astronomical information on a few hundred thousand images on deep Schmidt plates (or 4m telescope prime focus plates) in a timescale less than a day. It is now feasible to consider projects involving the measurement of up to 100 plates in a field and to merge all the parameterised data sets. Alternatively very wide angle surveys can be carried out by the measurement of plates in neighbouring fields.

Despite the limitation of a measuring machine with a reduced dynamic range it was demonstrated that a wide variety of important astronomical projects are possible. For the majority of these projects the wide angle capability of a Schmidt telescope is essential (and hence access to a high-speed automatic measuring machine essential), for others the ability to measure very faint objects on deep 4m telescope plates is equally important.

Most of the measuring machines mentioned here are either currently being used for such projects or under development. It was considered that the most important improvement that could be made to such a high-speed measuring machine is to design one with no significant light scattering problem and a peak data rate in excess of 100,000 samples per second.

References

Beard S M, 1983. Workshop on Astronomical Measuring Machines, Occ. R. Obs. Edin., 10, 219.

Cawson M, 1982. Measuring Machines Workshop (Cambridge),unpublished.

Clowes R G, Cooke J A, Beard S M, 1983. Workshop on Astronomical Measuring Machines, Occ. Rep. R. Obs. Edin., 10, 253.

Cooke J A, Emerson D, Beard S M, Kelly B D, 1983. Workshop on Astronomical Measuring Machines, Occ. Rep. R. Obs. Edin., 10, 209.

Danguy T, 1981. Conference on Astronomical Photography, p291, Institut National Astronomie Geophysique (eds. J-L Heudier, M E Sim).

de Veqt Chr, Nicholson W, King D C, Penston M J, Murray C A, 1983. Workshop on Astronomical Measuring Machines, Occ. Rep. R. Obs. Edin., 10, 75.

Elvius T, Lindgren H, Lyngå G, Wihlborg N, 1978. Lund Obs. Report No. 14.

Gilmore G and Reid N, 1983. Mon. Not. R. astr. Soc., 202, 1025.

Hawkins M R S, 1981. Nature, 293, 116.

Hawkins M R S, 1983a. Mon. Not. R. astr. Soc., 202, 571.

Hawkins M R S, 1983b. Mon. Not. R. astr. Soc., submitted.

Hawkins M R S, 1983c. Preprint.

Herzog A D and Illingworth G, 1977. Ap. J. Suppl. Ser., 33, 55.

Humphreys R M and Landau R, 1980. Sky and Telescope, 59, 16.

Kibblewhite E J, Bridgeland M T, Hooley T and Horne D, 1975. Image Processing Techniques in Astronomy (D Reidel), p245.

Kibblewhite E J, 1981. APM Handbook.

Kibblewhite E J, Irwin M J, Bridgeland M T, Bunclark P S, 1983. Workshop on Astronomical Measuring Machines, Occ. Rep. R. Obs. Edin., 10, 79.

La Bonte A E, 1970. Proc. IAU Coll. No. 7, 26.

Luyten W J, 1970. Proc. IAU Coll. No. 7, 48.

Luyten W J, 1974. Science, 185, 351.

MacGillivray H T and Dodd R J, 1979. Mon. Not. R. astr. Soc., 186, 743.

Maehara H, 1981. AAS Photo-Bulletin No. 26, p14.

Maehara H, 1982. Tokyo Astronomical Observatory, Kiso Information Bulletin, Vol. 1, No. 6, p137.

Maehara H and Watanabe M, 1980. Optical and Infrared Telescopes for the 1990's, p677.

Murray C A and Nicholson W, 1975. Image Processing Techniques in Astronomy (D Reidel), p171.

Murray C A and Corben P M, 1979. Mon. Not. R. astr. Soc., 187, 723.

Newcomb J C, 1970. Proc. IAU Coll. No.7, 5.

Newcomb J C, 1975. Image Processing Techniques in Astronomy (D Reidel), p159.

Pratt N M, 1971. Publ. R. Obs. Edin., 8, 109.

Pratt N M, 1977. Vistas in Astronomy, 21, 1.

Reid N and Gilmore G, 1981. Mon. Not. R. astr. Soc., 196, 15p.

Reid N and Gilmore G, 1982. Mon. Not. R. astr. Soc., 201, 73.

Sebok W L, 1980. Applications of Digital Image Processing in Astronomy, SPIE, 264, 213.

Shanks T, Fong R, Ellis R S, Macgillivray H T, 1980. Mon. Not. R. astr. Soc., 192, 209.

Shanks T, 1982. Workshop on Astronomical Measuring Machines, Occ. Rep. R. Obs. Edin., 10, 247.

Stetson P B, 1979. Astron. J. 84, 1056.

Stevenson P R F, Shanks T, Fong R, MacGillivray H T, 1983. Workshop on Astronomical Measuring Machines, Occ. Rep. R. Obs. Edin., 10, 185.

Stobie R S, Smith G M, Lutz R and Martin R, 1979. International Workshop on Image Processing in Astronomy, Trieste, p48.

Stobie R S, 1982. COSMOS User Manual.

Stobie R S and Henley R C, 1983. Workshop on Astronomical Measuring Machines, Occ. Rep. R. Obs. Edin., 10, 49.

Strand K Aa, 1971. Publ. U.S. Naval Obs., 2nd Ser., XX Part I, 19.

Strand K Aa, 1975. Proc. Soc. of Photo-optical Instr. Eng. (SPIE), 54, 17.

Swaans L, 1979. International Workshop on Image Processing in Astronomy, Trieste, p77.

Walker G S, 1971. Automation in Optical Astrophysics, Publ. R. Obs. Edin., 8, 103.

Wray J D and Benedict G F, 1974. Proc. Soc. of Photo-optical Instr. Eng. (SPIE), 44, 137.

Table I. Custom-built automatic measuring machines

1. General purpose (astronomy - stellar/galaxian, direct or prism plates)

Machine	Place	Light source/ scanning system	Detection system	Pixel increment (μm)	Peak data rate (K Hz)	Time to scan one Schmidt plate (300 x300 mm^2)	References
APM	Cambridge UK	laser/acousto-optic	photomultiplier	8	250	10 hours	1, 2
APS (Luyten/CDC)	Minnesota	laser/rotating prism	photomultiplier	5	1000	2.5 hours (2 plates)	3, 4, 5, 6, 7
COSMOS	Edinburgh	CRT	photomultiplier	8, 16, 32	63	6 hours (at 16 μm) 18 hours (at 8 μm)	8, 9, 10
KIDS	Kiso	lamp	linear diode array Reticon (1728)	13		24 hours	11, 12, 13
MAMA	Paris	quartz iodine lamp	linear diode array (1024)	10, 25	300	4 hours (at 10 μm)	14
Modified 2-D Grant	Caltech	quartz iodine lamp	linear diode array (512)	10	3	80 hours	15

2. Special purpose (astronomy - stellar, photometric/astrometric)

Machine	Place	Light source/ scanning system	Detection system	Speed	
GALAXY	Royal Greenwich Observatory	CRT	photomultiplier	900 stars/hour	16, 17, 18
SAMM	US Naval Observatory	Xenon arc lamp/ rotating disc	photomultiplier	4 x manual	19
STARSCAN	US Naval Observatory	Xenon arc lamp/ vibrating mirrors	photomultiplier	5 x manual	20

References: (1) Kibblewhite et al. 1975 (2) Kibblewhite 1981 (3) Newcomb 1970 (4) La Bonte 1970 (5) Luyten 1970 (6) Newcomb 1975 (7) Humphreys and Landau 1980 (8) Pratt 1977 (9) Stobie et al. 1979 (10) Stobie 1982 (11) Maehara 1981 (12) Maehara 1982 (13) Maehare & Watanabe 1980 (14) Danquy 1981 (15) Sebok 1980 (16) Walker 1971 (17) Pratt 1971 (18) Murray and Nicholson 1975 (19) Strand 1971 (20) Strand 1975.

COMMENT:

Eric Crane: I just want to comment that in case of the one-dimensional linear detectors, for example in CCD's they use a slit to limit the scattered light. Another scheme that goes along with that you can use a polarizer in systems that tend to constrain along the slit to allow the slit to block the scattering. Secondly is that you can use a very low frequency light source and minimize the scattering results involved.

Stobie: What light source are you talking about? How low a frequency?

Eric Crane: We talking about using about red lazor.

Dittmore: I have a comment on photographic emulsion. I found it is extremely difficult to develop images of high density to any repeatability and what we've done is developed to a lower gamma using a soft brush with continuous agitating and it actually increases the dynamics range of the straight portion of the D log E curve. And it actually increasing the dynamics range while the density comes down so that you can scan faster.

Stobie: Very interesting.

Boyce: I want to bring up one aspect that you didn't dwell on in terms as to why use these other machines. And in at least one case up there, our over whelming driver was caught involving malfunction and redoing of the 2-D Grant machine. It was the machine they had and they didn't want to make it faster and rather go for another machine, go for a PDS they opted to make a much lower cost diode array for their machine.

Stobie: They choose the most cost effective way. Maybe even if one wanted to build a machine like that, you may be better off to buy a PDS just to get the carriage to start up and build the rest of the machine on top of that. Because we've looked at prices of the carriages and some special purpose carriages were more than the cost of the machine. It's much greater than just a PDS itself.

Van Altena: I'll like to point out one problem in doing astrometry with the spots and the halo around them. You are addressing the union of high signal to noise region while you are measuring the image profile and therefore preventing you from getting the highest possible astrometric accuracy while getting all of the positional information that is in the image.

Stobie: I think if someone can design a high speed machine that doesn't have a halo that would solve a lot of the problems.

Hewitt: You mentioned going down to 24 in magnitude with the 2.5 meter telescope. That would be photographic range? (ANS-yes). Even measuring with a PDS microdensidometer and using electrographic camera, with a quantum efficiency response of better than 10 percent we recognized a 24th magnitude object. I'm talking here about two-hour exposure with a 1.6 meter aperture. What is your image finding algorithm?

Stobie: We haven't measured a single one of these yet. They have been taken. As regards the image finding algorithm, we would be able to take very low threshold cuts in the region of 1 to 2 percent and this would essentially image pixels which came above that threshold level.

Hewitt: If you look at a display for an image like that; there are more pixels above the background than below in that region but they are not very far above the background. There no contigous pixels. These are changes of high density pixels at any one spot relative to anywhere else. Even if you use cross correlation, it takes forever.

A. **Stobie:** Yes, one of the things you mentioned is the way we actually get rid of the noise pixels is to raise the threshold. The problem of the noise pixel comes about in increasing numbers. Generally they should be uncorrelated and we have a error routine that gets rid of images that don't form coherent set of pixels under a certain limit. If it is less than that number we just throw it away as a noise image.

Unidentified: I'll just add one comment on that remark about what you do with these very faint images? The answer is to get two plates. Better yet, three or four. Set your threshold very low and pickup all the noise and cross correlate from this. It is extremely effective. Surely you do some work at this.

Stobie: Yes, in fact we get problems with bright stars where essentially the halo starts to sort of sputter and break up and you get lots of sperious noise as the images around the bright star caused by the halo. What you actually do is measure successive plates and pair things up and of course that sputtering doesn't really pair up and you get rid of ninety-nine (99) percent of it.

Hewitt: You can do even moderately well if your effective aperture is the optimum size; to give you the best possible signal to noise ratio for the faint images but even doing that you can miss a lot of images that could produce some information. If you look at the plates with a microscope and you can't see an image if it's there. I doubt that the computer is going to help much.

Schweitzer: I should perhaps say it does depend on various things, Las Campanas often has half arc second seeing. It is a superb seeing site and it does have 10 arc seconds per milimeter scale and that helps you. I still think 24 is a bit over optimistic you might get close to.

Automated Microdensitometer for Digitizing Astronomical Plates

J. Angilello, Wei-Hwan Chiang,†

Debra Meloy Elmegreen and Armin Segmüller,

IBM Thomas J. Watson Research Center,

Yorktown Heights, N. Y. 10598

Abstract

A precision microdensitometer has been built under control of an IBM S/1 time-sharing computer system. The instrument's spatial resolution is better than 20μm. A raster scan of an area of $10\times10mm^2$ (500×500 raster points) takes 255 minutes. The reproducibility is excellent and the stability is good over a period of 30 hours, which is significantly longer than the time required for most scans. The intrinsic accuracy of the instrument was tested using Kodak standard filters, and it was found to be better than 3%. A 'comparative' accuracy was tested measuring astronomical plates of galaxies for which absolute photoelectric photometry data were available. The results showed an accuracy excellent for astronomical applications.

---

†Also affiliated with Astronomy Dept., Columbia University.

Automated Microdensitometer for Digitizing Astronomical Plates

A precision microdensitometer has been built under control of an IBM S/1 time-sharing computer system. The instrument's spatial resolution is better than 20μm. A raster scan of an area of $10\times10mm^2$ (500×500 raster points) takes 255 minutes. The reproducibility is excellent and the stability is good over a period of 30 hours, which is significantly longer than the time required for most scans. The intrinsic accuracy of the instrument was tested using Kodak standard filters, and it was found to be better than 3%. A 'comparative' accuracy was tested measuring astronomical plates of galaxies for which absolute photoelectric photometry data were available. The results showed an accuracy excellent for astronomical applications.

---

†Also affiliated with Astronomy Dept., Columbia University.

I. Introduction

Since its invention over 60 years ago, the microphotometer or microdensitometer has been considered as one of the most useful instruments to extract information contained in photographic images (Swing, 1973). In recent years, other methods of image detection have been developed, such as the use of television-type devices (Boksenberg, 1975) and of direct photoelectric or electronographic photometry (Ring and Worswick, 1975). Nonetheless, photographic photometry is still extremely valuable. Some of the main reasons are: (1) the significant improvement of the quality of the photographic materials, i. e. developments in emulsion technology etc., (2) availability of fast speed and high precision measuring machines, (3) the extensive employment of computers for the data processing, (4) the convenience of storing photographic materials for future usage, (5) the high angular resolution of photographic emulsions, and (6) the wide wavelength and band pass coverage of photographic emulsions (Smith and Hoag, 1979). To this end, a microdensitometer has been contrived for the purpose of measuring photographic plates or films of wide varieties. These include astronomical plates of extragalactic objects with wide ranges of densities, and x-ray diffraction films for the determination of crystal structures. The system is fully automated and operates at high speed. Within the linear response region, the system has excellent reproducibility. Therefore, large amounts of otherwise unobtainable information contained in plates or films can be extracted for analysis.

II. Basic Principle of Microdensitometer

For an exposed photographic plate, one can define a function of position $E(x,y)$ which represents the amount of energy received within a certain frequency interval and within a differential area centered around the point (x,y) on the plate. The goal of photographic photometry is to determine this function (Latham, 1974).

Let $T(x,y)$ be the fraction of the illuminating light transmitted through the differential area centered around the point (x,y) on the plate, and define the density scale $D(x,y)$ to be

$$D(x,y)=-\log T(x,y). \tag{1}$$

Then the density $D(x,y)$ and the exposure $E(x,y)$ are functionally related as:

$$D(x,y)=f(E(x,y)). \tag{2}$$

This function can usually be determined from a calibration curve. If the inverse function of f exists uniquely, the preceeding equation can be written as:

$$E(x,y)=g(D(x,y)), \tag{3}$$

where g is the inverse of f. If g is known, it is clear that one simply needs to measure the density D to determine the exposure, or equivalently, the amount of energy received on the plate. This can be done by passing a narrow beam of light through all the points of interest on the plate. In general, the optical system is operated under the condition that an intensity reading is dependent on $D(x,y)$.

III. Design of Microdensitometer

An existing microdensitometer (Segmüller and Cole, 1971) was mechanically and optically improved to perform raster scans of large astronomical plates. The basic design of the microdensitometer and its associated facility is schematically represented in figure 1. The light source is provided by a tungsten lamp attached to a regulated lamp power supply. The light from the lamp passes through one of the apertures and is then deflected by a fixed mirror before passing through lens 1, which reduces by a factor of ten the cross section of the light beam on the image stage. Arranged on a slide are five circular apertures with diameters ranging from 200 to 800μm, resulting in an image size from 20 to 80μm. Available is also a slit for the execution of linear scans of x-ray diffraction films. The image on the stage is at the focal plane of lens 2. The stage can be moved in two directions, x and y, by two stepping motors controlled by an IBM S/1 computer. The ranges for the x and y translations are 25 and 15cm, respectively, and the minimum increment in both direction is 5μm. The operational scanning speed is 20mm/min in x and 7 mm/min in y, respectively. For a raster scan of an area $10\times10\text{mm}^2$ large, with 500×500 raster points, the running time is 255 minutes. The scanning speed could be increased by at least a factor of three, using high-torque stepping motors. After passing through lens 2, the beam is reflected by a deflectable mirror through lens 3 into the photomultiplier tube (PMT). The function of lens 3 is to bring the cross section of the beam to a proper size such that the maximum useful detecting area of PMT can be utilized. The

deflectable mirror can be adjusted so that the light after passing through lens 2 goes through the eyepiece to enable the user to focus the image of the light source and the viewing microscope on a grain in the emulsion. The PMT is connected to a regulated high voltage supply and its output signal is read by the analog input feature of the S/1 computer with 14-bit resolution. The S/1 computer is operated under the EDX multiprogramming and multitasking system, controlling also several x-ray diffractometers in time-sharing mode, and it is linked to the host, a VM/370 based computer, on which the scanned data can be analyzed efficiently.

In order to avoid the possible sagging problem of some thin and large plates, the image stage is designed to have movable supports beneath the plates. The contact surface is always the glass side of the plates in order to protect the emulsion. The microdensitometer is contained in a well-shielded frame. There is essentially no detectable stray light from outside or air convection when the frame is closed, assuring that the system is in equilibrium during operation.

VI. Operation and Performance of the Instrument

During a scan, each intensity reading may be an average of up to twenty readings with a delay from zero to ten milliseconds between successive readings. Thus, fluctuations in the reading can be reduced. If several samples are taken per reading, the scanning time is of course increased from the value quoted before. The sensitivity of the analog input amplifier reading the PMT output can be set by program control to several ranges from 10mV to 5V maximum. The lamp power supply is operated at an output voltage between 2 and 6V, corresponding to a range of power roughly between 3 and 14 Watts. The voltage to be applied to the PMT electrode is between 500 and 1500V.

In principle, one can operate the microphotometer using any one of the possible combinations of the parameters within the range specified above, as long as the intensity readings do not reach the saturated region of the PMT. To achieve the highest signal to noise ratio, one should, however, always try to use a combination of parameters such that the intensity readings are as high as possible within the linear range of the characteristic curve.

To calibrate the microdensitometer and to obtain its characteristic curve, the transmission of standard Kodak filters has been measured in several runs. A typical one is shown in figure 2, the parameters being: the lamp voltage $\approx$4.5V, the PMT anode potential $\approx$1300V, the analog input range 5V and the aperture image size 20μm. The dynamic range is close to three decades. By least-squares methods a straight line has been fitted to the data points in the double-log plot. The slope of the straight line, i. e. the exponent of the density function, has a value of 1.06, very close to 1. The rms deviation of this plot, the intrinsic accuracy, has a value of σ=0.027. In order to obtain the higher densities, several filters were stacked, introducing an error due to partial reflection at each filter. The reproducibility of the microphotometer was checked by comparing two successive raster scans of the same white noise plate. The parameters used were: 4V for the lamp voltage, 1000V for the PMT voltage, 20μm for the aperture image size and 20 μm for the step increment in both, the x and y

direction. For the 10545 data points $D(x,y)$ in each scan (1 and 2), we computed the quantity:

$$\sigma = \frac{D(x_1,y_1)-D(x_2,y_2)}{D(x_1,y_1)+D(x_2,y_2)} \qquad (4)$$

and expressed these 10545 numbers in percentage form. The histogram of the result is shown in figure 3. Apparently more than half of the points in the sample have a deviation less than 2%. The uncertainty will be larger if the average intensity readings are lower, since the noise is roughly independent of the intensity readings.

The spatial resolution of ~20μm was determined by conducting a linear scan across a sharp edge. The stability of the instrument was tested by recording the density readings over an extended period for a given voltage and aperture. The result indicates that there is a shift of about 8 percent over a 30 hour period which is significantly longer than the time required for most scans. The shift is, however, not exactly monotonically increasing or decreasing.

V. Comparison with Astronomical Standards

To test the comparative accuracy of the microdensitometer in applications, we performed raster scans of seven photographic plates of galaxy images in blue and near-infrared passbands, for which absolute photoelectric photometry data were published by Schweizer (1976). The measured densities were converted to relative intensities by using the calibration wedges which were recorded on the unexposed ends of the galaxy plates (Elmegreen and Elmegreen, 1983). The pixel resolution corresponded to 1.3 arc sec for the Palomar 1.2 m Schmidt plates scanned with a 20μm aperture image size. The photoelectric photometry data consist of a series of measurements along the eastwest galaxy axis, using apertures some 15 to 18 arc sec in diameter. These data had been calibrated on an absolute scale by comparison with standard reference stars. In order to compare the photographic measurements with the photoelectric measurements, the intensities of the pixels from the photographic scans which corresponded to each region measured with the photoelectric apertures were added together. A linear least-squares fit was applied to the data in order to determine the zero-point magnitude, and the photoelectric minus the photographic residuals were obtained. These fits are shown in figure 4. The residuals represent an accuracy of about 0.1 magnitude, or about 10%, which is adequate and typical for astronomical applications.

VI. Applications

Figure 5 shows the grey scale representation of the near-infrared plate of the spiral galaxy NGC5194, scanned with the following parameters: lamp voltage 4V, PMT voltage 1800V, analog input sensitivity 5V, aperture image size 30μm and x and y step increment 30μm. The digitized figure was produced by the APS-5† photocomposer. Though no means were employed to enhance the contrast, it shows already very detailed features of the galaxy.

We are extremely grateful to Janusz S. Wilczynski for the design of the high-resolution optics and to Philip E. Seiden for his encouragement and involvement in the modification of the microdensitometer. Thanks are also due to Bruce G. Elmegreen for discussions and permission to use unpublished results, to Humberto Gerola for his encouragement and suggestions, to Herbert Gertling for the excellent execution of the mechanical modifications and to Richard F. Voss for valuable discussions and for his programs to prepare the data for the APS-5 photocomposer.

†Manufactured by Autologic, Inc.

VII. References

Bokensenberg, A. (1975). *In* "Image Processing Techniques in Astrophysics", (C. de Jager and H. Nieuwenhuijzen, eds). pp. 59-78. D. Reidel, Dordrecht.

Elmegreen, D. M. and Elmegreen B. G. (1983). *Astrophys. J. Suppl.*, submitted.

Latham, D. W. (1974). *In* "Astrophysics" (N. Carleton, editor),pp. 221-236. Academic Press, New York.

Ring, J. and Worswick, S. P. (1975). *In* "Image Processing Techniques in Astrophysics", (C. de Jager and H. Nieuwenhuijzen, eds.),pp 117-124. D. Reidel, Dordrecht.

Schweizer, F. (1976). *Astropys. J. Suppl.* 31, 313-332.

Segmüller, A. and Cole, H. (1971). *Adv. X-Ray Anal.* 14,338-351.

Smith, A. G., and Hoag, A. A. (1979). *Ann. Rev. Astron. Astrophys.* 17, 43-71.

Swing, R. E. (1973). *Optical Engineering* 12, 185-198.

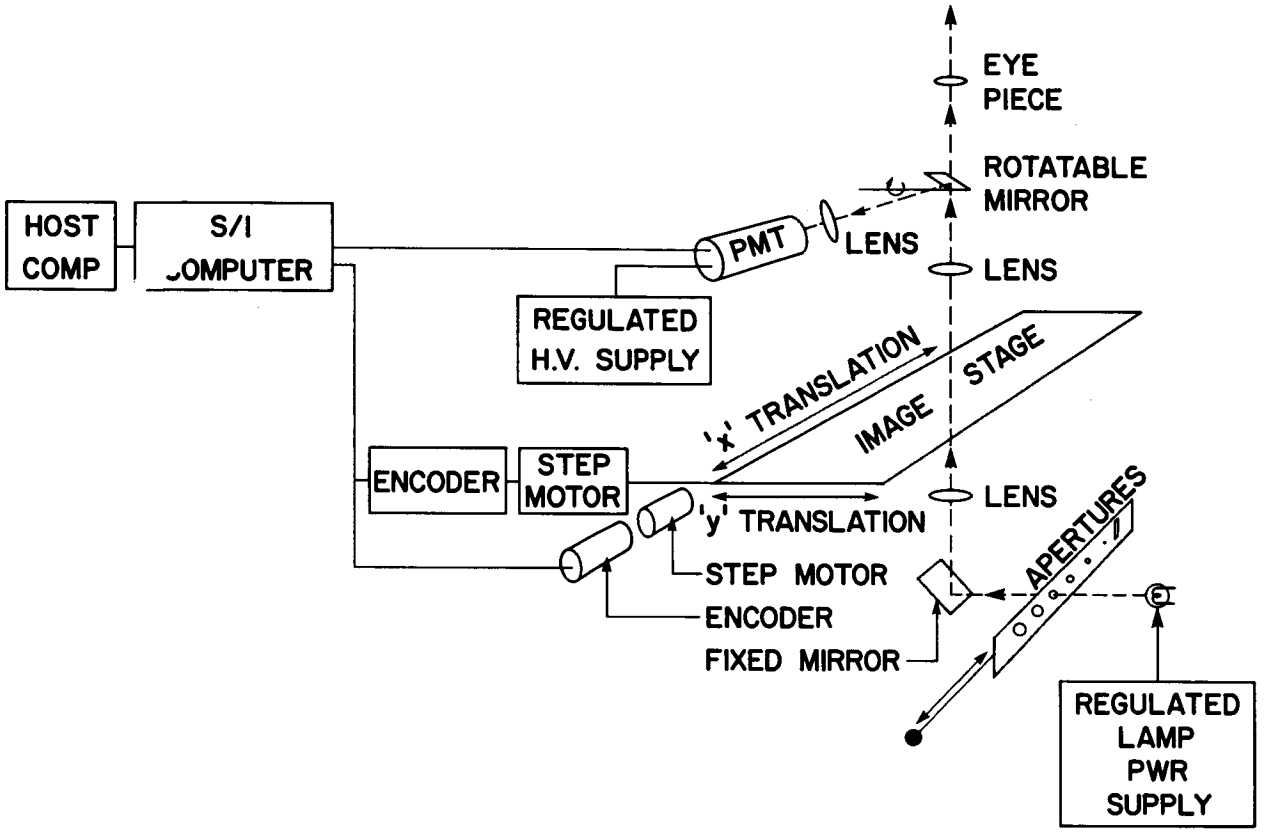

Figure 1: Block diagram of microdensitometer.

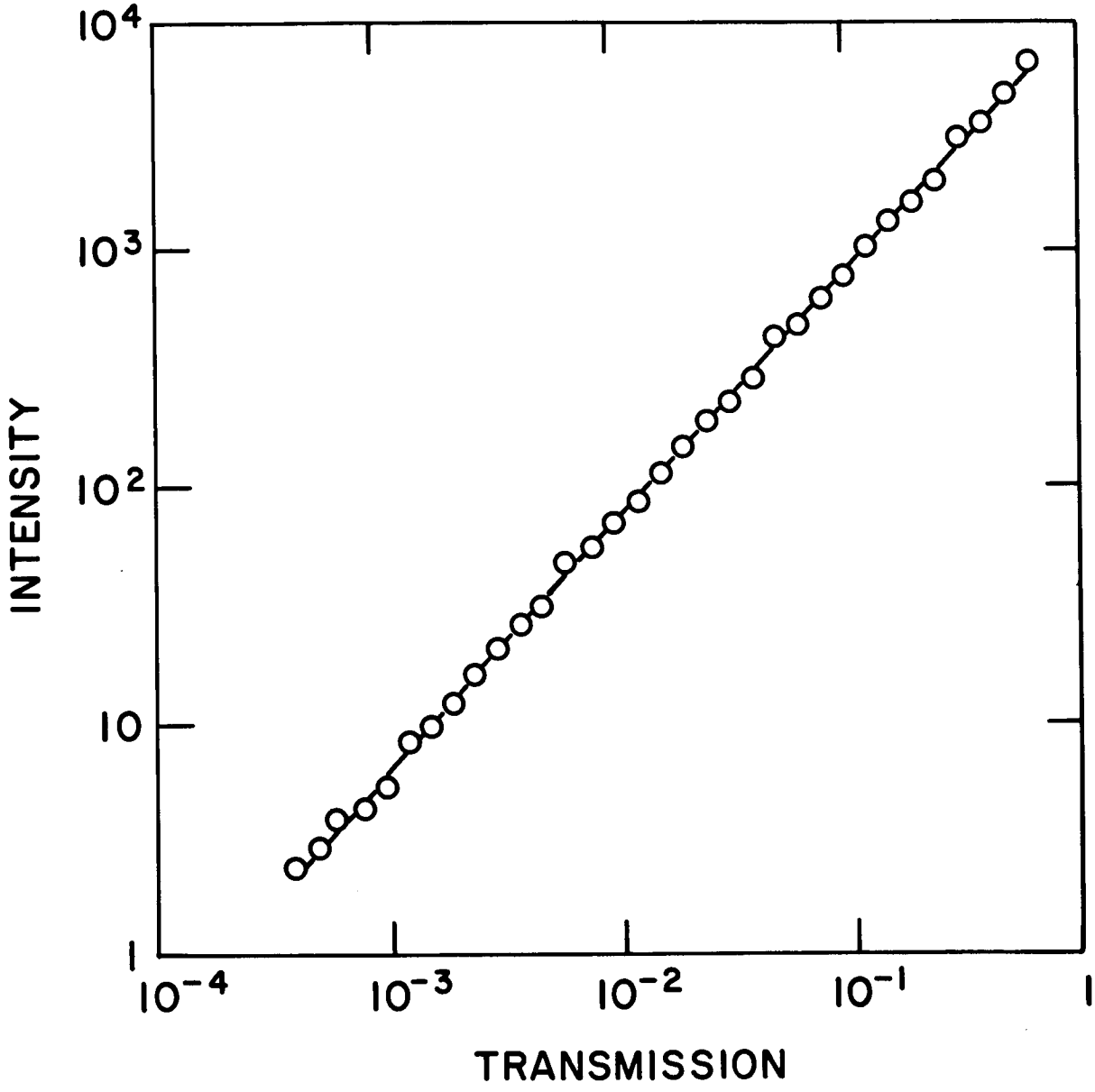

Figure 2: Measured transmitted intensity versus attenuation of standard Kodak filters.

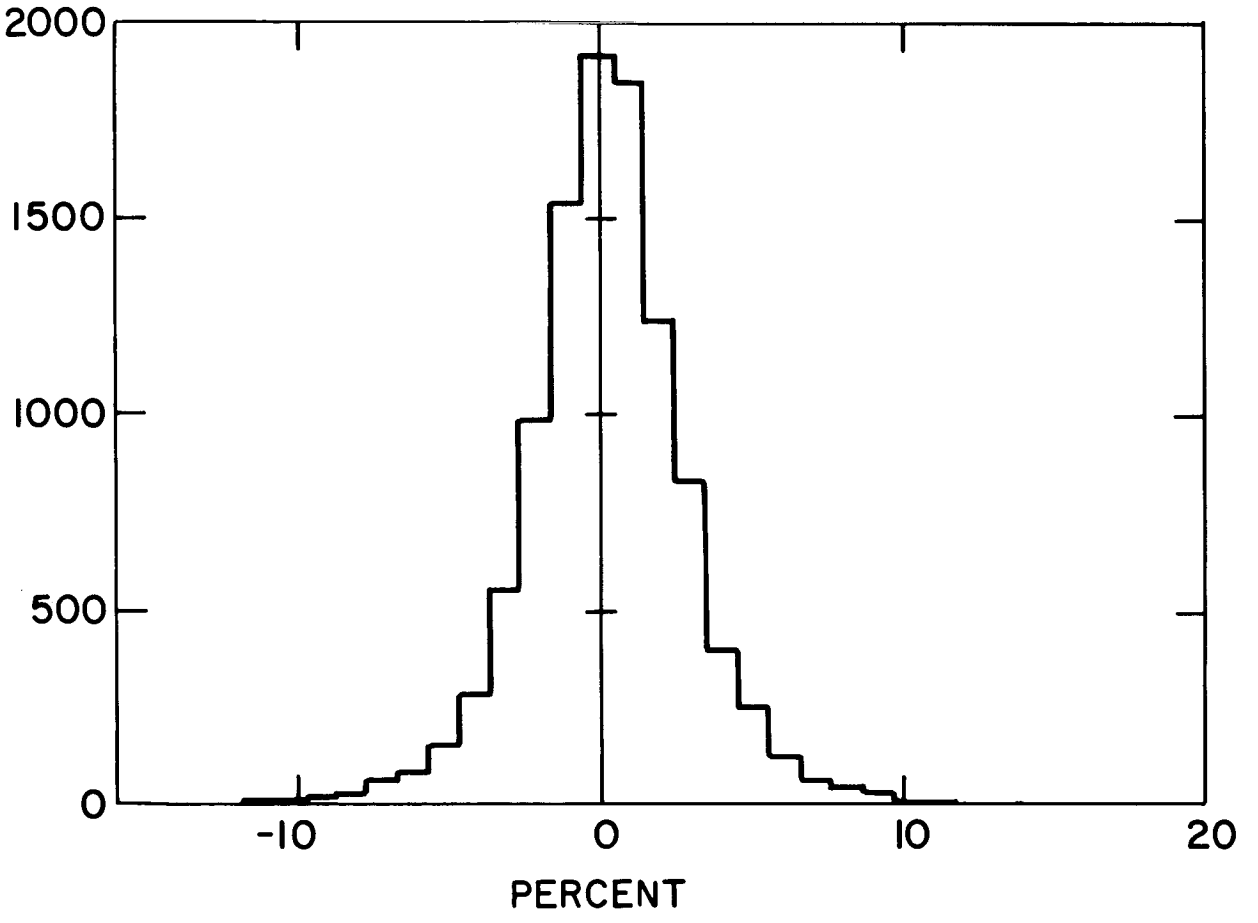

Figure 3: Histogram of 10545 readings of a white-noise plate.

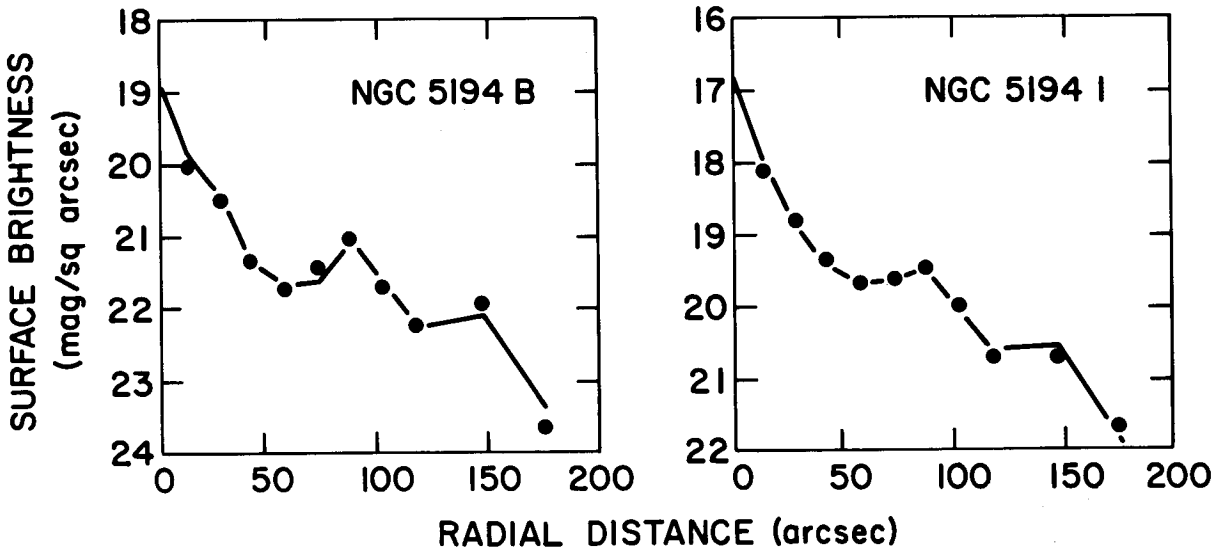

Figure 4: Comparison of photoelectric (———) and photographic (·) surface brightnesses shown as function of the galactic radius for the blue and infrared plate of the spiral galaxy NGC5194. The solid lines connect the photoelectric measurements by Schweizer (1976).

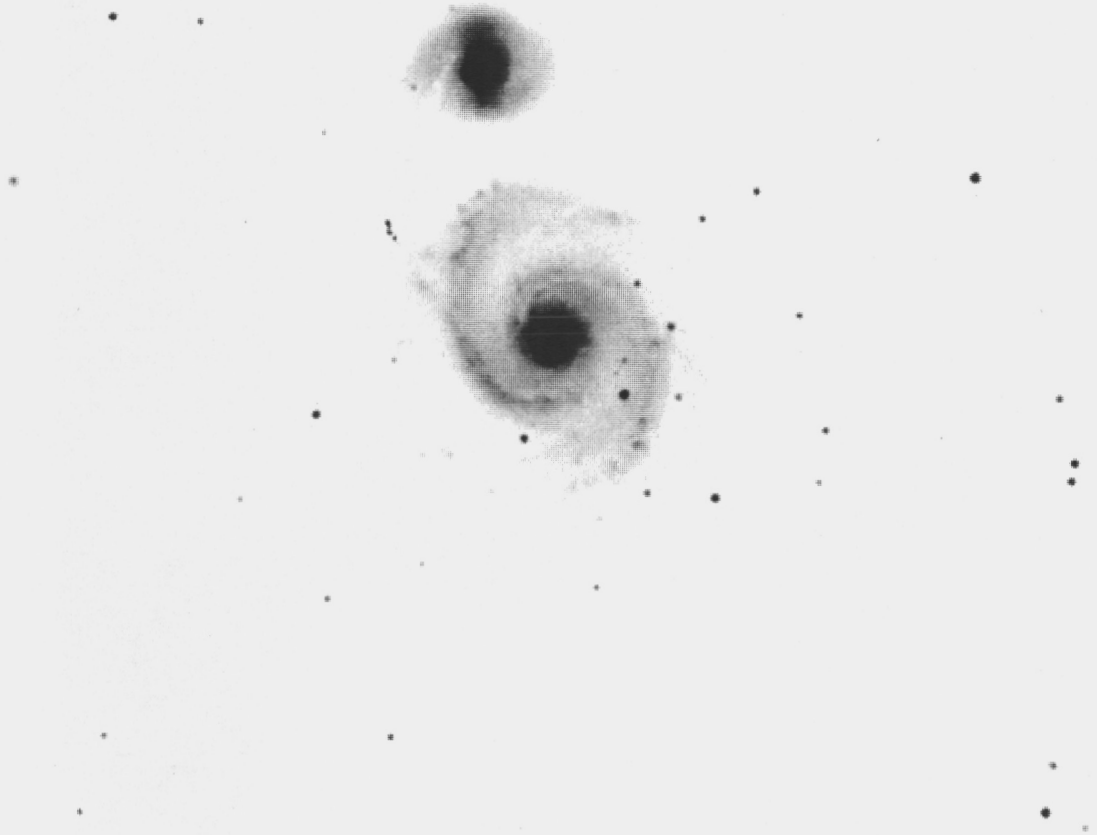

Figure 5: Raster scan of the infrared plate of the spiral galaxy NGC5194 printed by the APS-5 photocomposer.

THE SACRAMENTO PEAK FAST MICROPHOTOMETER

M. R. Arrambide, R. B. Dunn, A. W. Healy,
R. Porter and A. L. Widener
Sacramento Peak Observatory
Sunspot, NM 88349

and

L. J. November† and G. E. Spence
Solar Research Branch
Air Force Geophysics Laboratory
Sunspot, NM 88349

ABSTRACT

The Sacramento Peak Observatory Fast Microphotometer translates an optical system that includes a laser and photodiode detector across the film to scan the Y direction. A stepping motor moves the film gate in the X direction. This arrangement affords high positional accuracy, low noise (0.002 RMS density units), modest speed (5000 points/second), large dynamic range (4.5 density units), high stability (0.005 density units), and low scattered light. The Fast Microphotometer is interfaced to the host computer by a 6502 microprocessor.

1.0 INTRODUCTION

Our previous experience with microphotometers indicated that high photometric precision and low-scattered light can be most easily achieved with a single spot and detector. For a given electronic noise and density the speed of scanning is proportional to the number of photons passing through the light spot on the film and to the quantum efficiency of the detector. The speed may be increased by using a laser, rather than the more conventional tungsten light source. The laser also has a Gaussian distribution of light intensity in the spot. This is a distinct advantage in our system because it lowers the number of points that must be sampled, and reduces the effects of the nonlinear speed of scanning. Furthermore, in our earlier microphotometers we have always obtained good spatial precision and linearity by scanning the film using an X-Y mechanical stage driven by stepping motors. The effect of these considerations on our design is shown in the photograph of the instrument in Figure 1.

The mounting for the entire optical system, including the laser and

*Operated by the Association of Universities for Research in Astronomy, Inc. under contract AST 78-17292 with the National Science Foundation.

†NAS/NRC Resident Research Associate

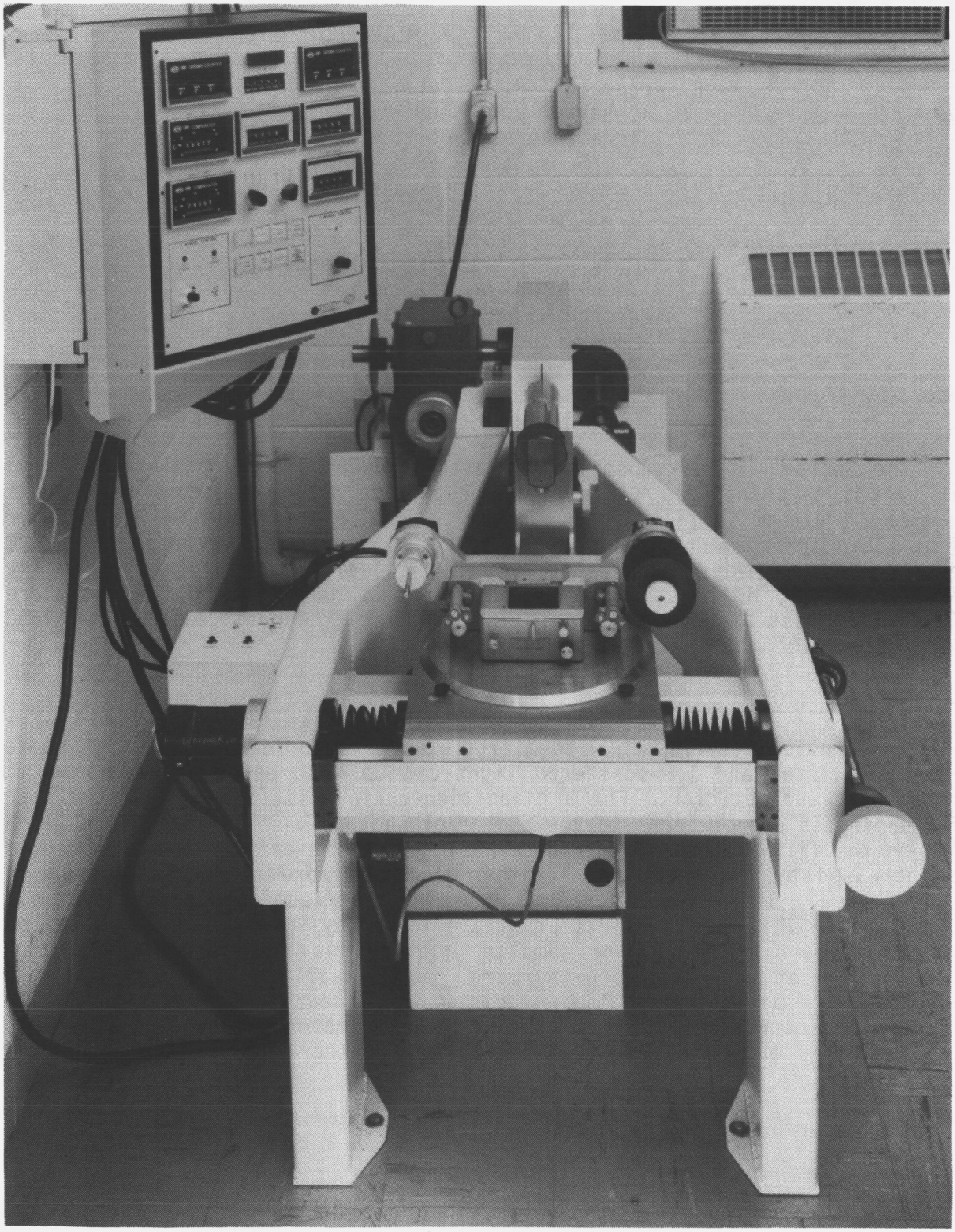

Figure 1: Sacramento Peak Observatory Fast Microphotometer. The large control panel mounted on the wall is no longer used.

detector, is supported on linear ball bearing and ball bearings so that it can be moved by a motor-driven crank to scan the film or plate in the Y direction. A variable-speed DC motor coupled to a gearbox drives the crank through an adjustable eccentric up to plus or minus 3 inches at speeds of up to 2 cycles per second. A stepping motor coupled to a ball screw moves the film gate in the X direction to complete the scan of the film.

The optical system is shown in Figure 2. The laser is mounted in the lower part of the scanning mount. Light passes upwards through the film to the upper path where the intensity is measured with a diode. A large pinhole above the film reduces scattered light. A second pinhole in front of the measuring diode cuts off the Gaussian spot beyond 3 sigma. A tilted glass plate just in front of the laser sends a 4% intensity beam to a second diode that monitors the intensity of the laser. A narrow-band filter at 632.8 nanometers eliminates the unwanted blue light that originates in the laser.

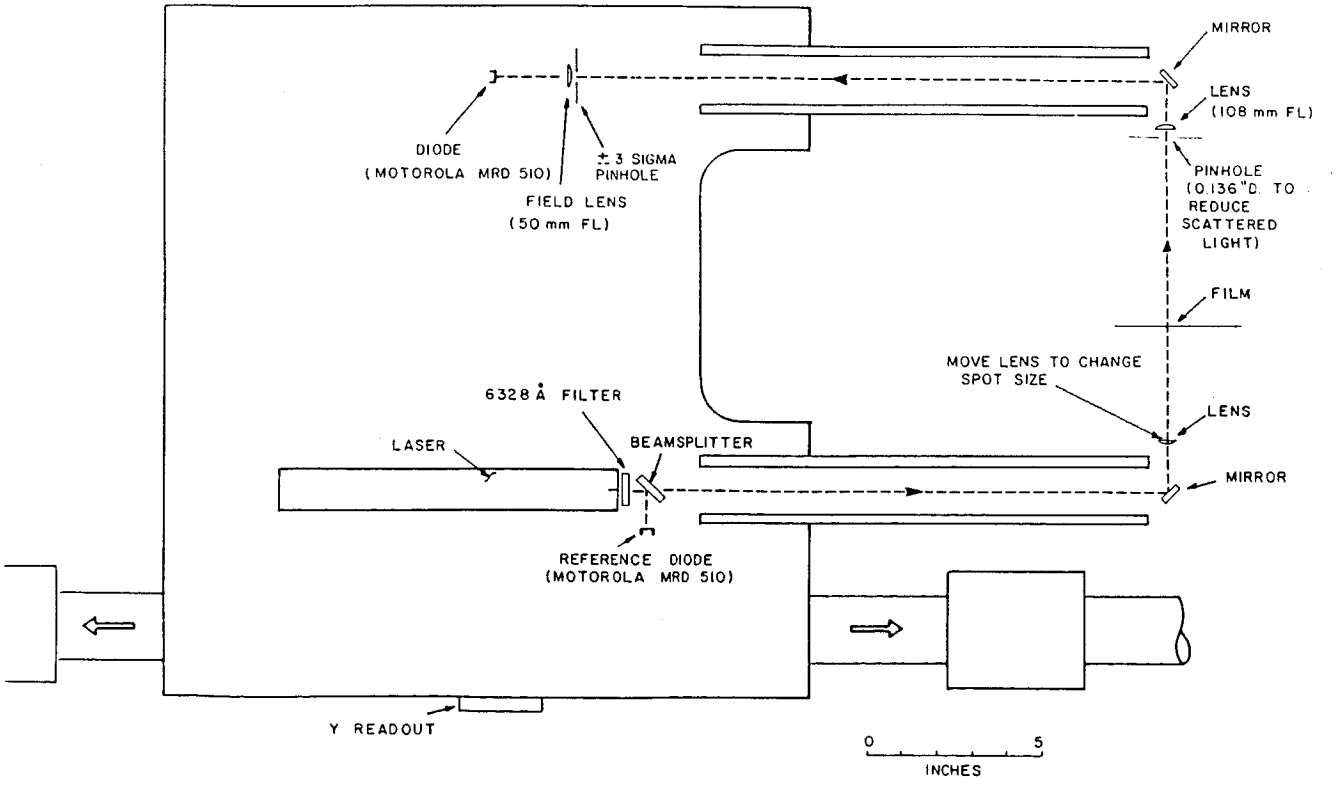

FIGURE 2: OPTICAL SYSTEM

2.0 SPECIFICATIONS:

The performance specification of the SPO Microphotometer is as follows:

Y Motion:	Variable speed DC motor driving a crank through a worm gear reduction. Maximum peak-to-peak amplitude is 6 inches. A linear optical position encoder (Teledyne Gurley model 8712) with a resolution of 0.0001 inches per count defines the position.
X Motion:	A 2000 step-per-revolution Responsyn stepping motor directly coupled to a 0.2-inch lead ball screw. One step equals 0.0001 inches.
Laser:	632.8 nanometers He - Ne Polarized Laser. 1 milliwatt Hughes (P/N 3178H).
Spot Size:	33 to 200 microns Full Width Half Maximum (FWHM) at film plane. Spot Profile is Gaussian and has an equivalent frequency cut-off equivalent to a 9-pole Bessel-type filter.
Analog Signal:	Logarithmic Reponse - Greater than 4.5 decades Sensitivity - 2 volts per density unit
Log Conformity:	±0.5% (2 density units from clear plate) ±1.0% (4 density units from clear plate)
Electrical Filtering:	Low pass 2500 HZ Bessel 6 pole. Digitizing rates and speeds are adjusted so that this filter does not cut off the equivalent Gaussian filter of the laser spot.
Digitizing Rate:	10000 samples per sec max. More typically 3000 to 5000 samples per sec, when set up according to Figure 3.

3.0 GAUSSIAN SPOT PROFILE AND SPEED

Because we are using a laser as the light source, the illumination within the scanning spot has a Gaussian distribution. The frequency response of a Gaussian is equivalent to a 9-pole Bessel filter with a cutoff frequency $\sim 0.31/\text{FWHM}$. The power bandwidth of the spot is such that at a frequency of $1.38/\text{FWHM}$ the amplitude of the intensity fluctuations is attenuated by approximately 870. This is fairly typical of the upper limit for film signal-to-noise ratio with our 50 μm spot size, i.e., Kodak 2415. Interestingly, because of the sharp cutoff of the Bessel filter, appreciably higher sampling frequencies are required to obtain much higher signal-to-noise ratios. If the digitizing rate is set to twice this amount, the data will not be aliased and will be recoverable to at least 0.001 density units.

The electrical filter is a 2.5 KHZ, 6-pole Bessel chosen for its constant time delay so that we can digitize in both directions.

Since the filtering is optical and not electrical, the fact that the scan is sinusoidal in speed is of no concern; however, for the electrical filter to have only a small effect on the signal from the Gaussian spot, the frequency cutoff, fc, of the spot should be approximately 1/5 the fc of the electrical filter. Therefore, $\frac{0.31}{FWHM} < 1/5 \times 2500$ HZ and the FWHM > 0.62 milliseconds. To convert FWHM in seconds to inches so that it can be related to the physical size of the spot, consider that:

$$FWHM_{(inches)} = FWHM_{(seconds)} \times \text{inches/second}$$

and the maximum velocity during a sinusoidal stroke is $2\pi f A$, where A is the amplitude of one half the total stroke and, f is the frequency of rotation of the driver wheel that drives the crank (double strokes/sec). Thus the maximum inches/second = π(Driver RPS)(Total Stroke).

$$\text{Maximum Driver Speed}_{(RPS)} = \frac{\text{in/sec}_{(max)}}{\pi(\text{Total Stroke})}$$

$$= \frac{FWHM_{(inches)}}{FWHM_{(sec)}} \times \frac{1}{\pi(\text{Total Stroke})}$$

$$= \frac{FWHM_{(inches)}}{.62ms} \times \frac{1}{\pi(\text{Total Stroke})}$$

$$\approx 500\ FWHM_{(inches)} \times \frac{1}{\text{Total Stroke}}$$

The relationship between scan speed, spot size, and the Y sample interval is shown in Figure 3. As an example, consider a spot size with a FWHM of 0.003" (75μ). The optimal spacing between the points to be digitized is 0.003/2.8 = .001 inches. Since the position encoder smallest interval is 0.0001 inches, the Y sample interval should be 10. The maximum speed of the driver then depends on the desired stroke, which for this example can vary from 2 cycles/sec for a 0.75-inch stroke to 0.25 cycles/sec for a 6-inch stroke. For all strokes the digitizing rate would average 3000 points per second (4712 max).

A typical 500 x 500 pixel raster would take about 90 seconds within the limitations of the driver speed shown on Figure 3. This is about 15x faster than the older microphotometer at Sac Peak.

The Y encoder count rate is limited to 100 KC. This limit is shown on Figure 3.

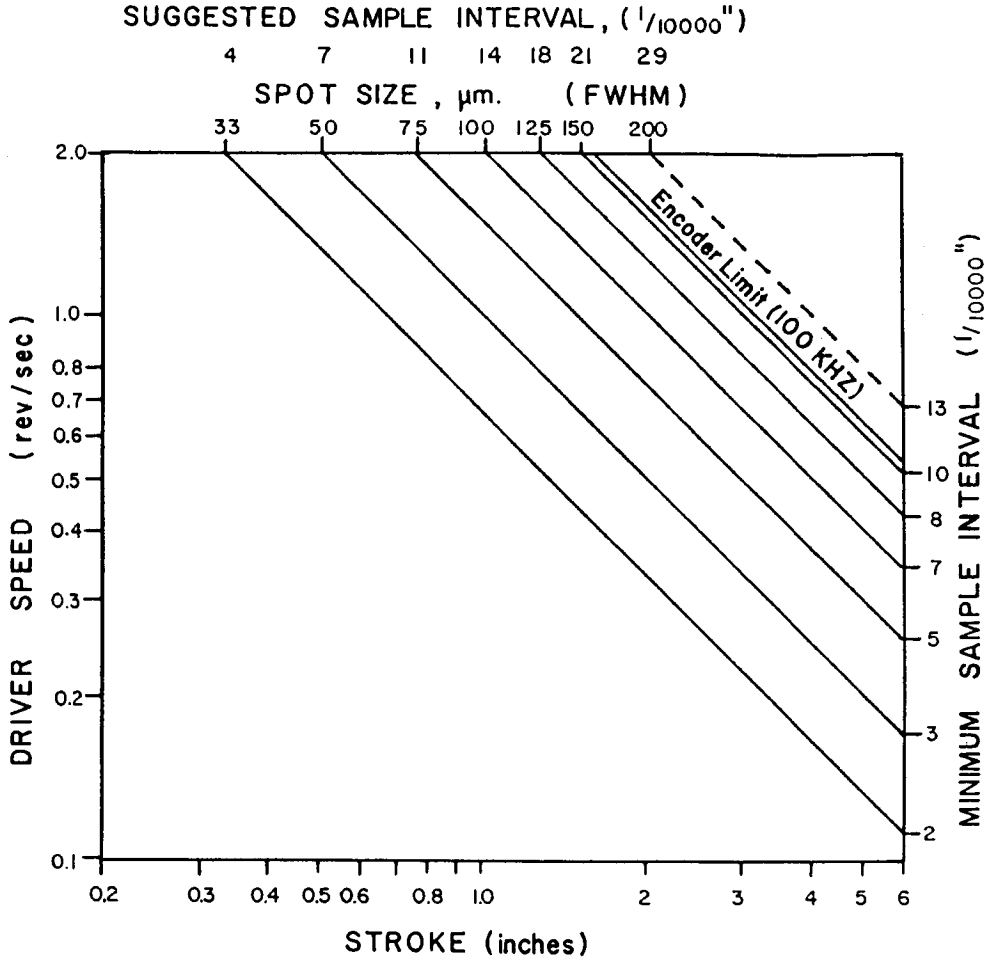

FIGURE 3: Y SPEED AND SAMPLE INTERVAL VS STROKE AND SPOT SIZE.

The depth of focus on the system is very large and we have found that the scan spot can be defocused on the film to change its size without destroying the Gaussian profile.

4.0 ELECTRONICS:

The small-signal bandwidth of the log amplifier (Analog Devices 756N) is shown in Figure 4 and is approximately 4.5KHZ at 4.5 density units which is higher than the cutoff frequency of the 6-pole Bessel filter. The noise at 4.5 density units with a 0.0013-inch spot is < .002 density units RMS.

The overall block diagram of the control electronics is shown in Figure 5. A 6502 microprocessor controls all local functions in response to communications from the host DMA computer through the RS232 serial port. Data is transmitted to the host I/O bus through the parallel I/O port.

5.0 SOFTWARE

Control of the microphotometer by the 6502 microprocessor is initiated by commands from the control panel or via an RS232 interface from a host computer. As data is collected, it is sent via a direct I/O port into the host using its DMA capability. The host is never required to perform time-critical activity.

The host computer is a PE3220 operating in a multi-user, multi-terminal environment. The general user software that controls the microphotometer consists of a number of procedures or tasks which may be envoked interactively by typing a single line specifying parameters, or chained in a program mode using control files containing sequences of these commands. Our definition of a procedure corresponds to that given by Bourne (1978, page 1976).

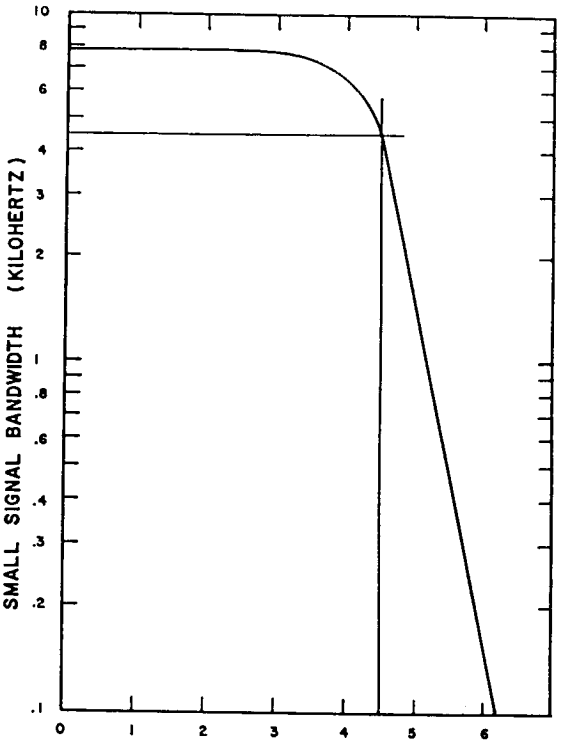

FIGURE 4: LOG AMPLIFIER RESPONSE

The basic procedure library provides setup utilities which allow the user to read and save in a standard output file the present position of the spot or photodiode reading, or move the spot to a designated offset or absolute position, or advance or backspace the bulk film transport. Scanning is done by procedure MSCN with parameters: step size in X and Y, number of points in X and Y, center scan location, and name of file for saving the scan. The scanned image is saved on the disk in the FITS data format, a flexible standard now being developed in the astronomical community (Wells, 1981; November 1981). Other procedures are available for: applying H&D correction to microphotometer images, manipulating images in scalar or matrix algebra, writing images to magnetic tape, or displaying images on our Grinnell image-processing system. Alternatively, MSCN may take the center scan location from a standard input file. This might have been written during the user setup or may have been written by either a frame edge locating procedure (under development) or a correlation tracking procedure (under development).

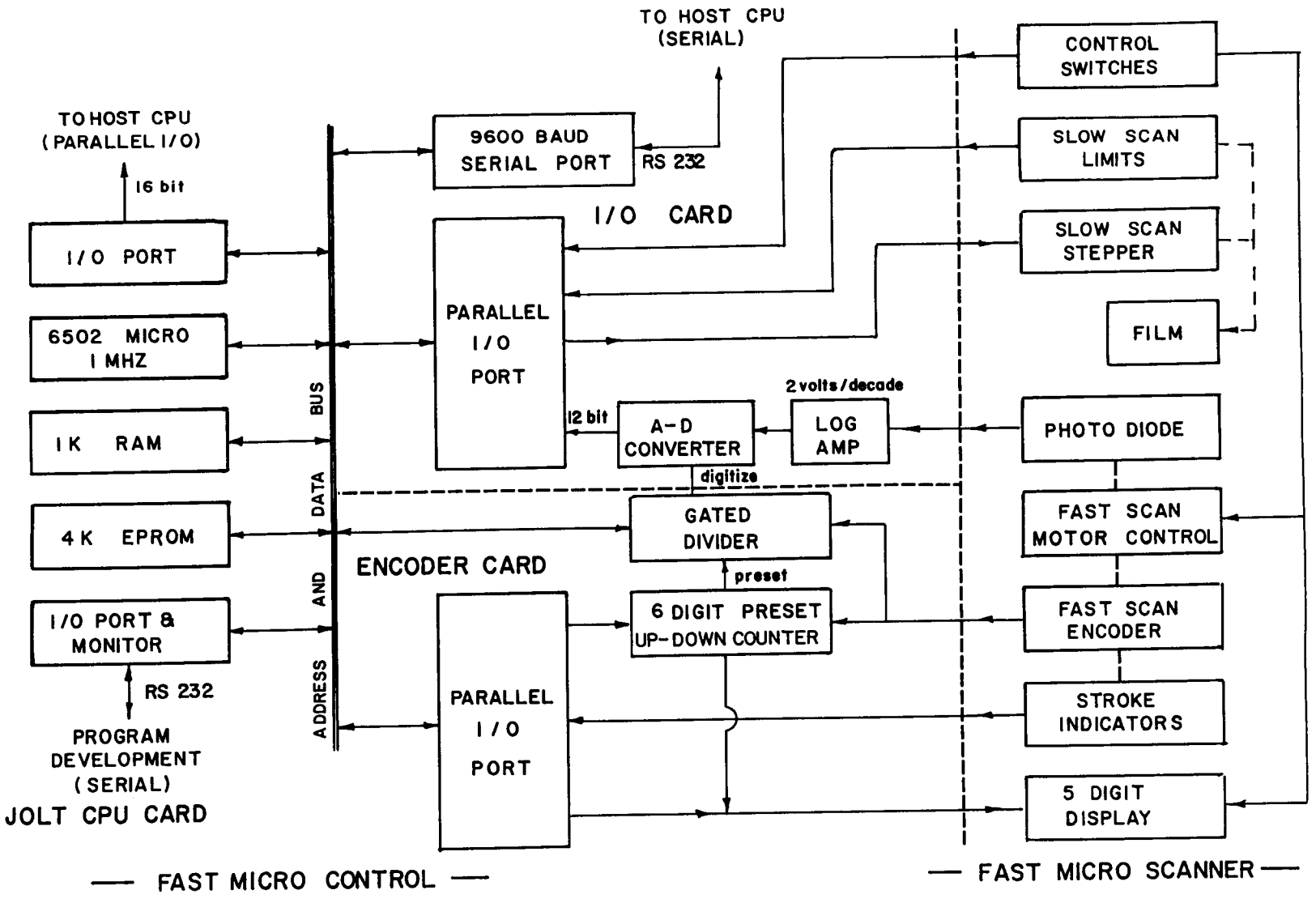

FIGURE 5-ELECTRONICS BLOCK DIAGRAM

6.0 IMPROVEMENTS

The use of coherent light causes interference fringes to occur between the surfaces of every parallel optical element. Since the depth of focus is very large with the laser the film does not have to be pressed between glass plates, and we only have to contend with the interference in the 3- or 4-mil-thick film itself. The coherency of the beam is partially destroyed if the emulsion is towards the laser. We measure an rms fringe amplitude of 0.015 density units if the emulsion is less than 0.6 density. For densities greater than 1.2 the amplitude is insignificant. Below that density the interference fringes often destroy the usefulness of the data. We have made some experiments with tilting the film. Here, if the film is clear, the two interfering beams miss each other and interference does not occur. However, if the film has some density, the emulsion scatters the laser light and forms a larger reference beam that then causes the interference to occur, but with less contrast than if the film were square-on to the beam. Further experiments with tilting the film will be tried to see if the visibility of the fringes can be reduced if the film is below 1.2 density.

We have fabricated a wet film or plate holder that works very well, even with the film square-on. Here the glass plate or film is immersed in a fluid. The external glass surfaces are coated for the laser line with a "V" coating that has a reflectivity of less than 0.1%. This technique is used extensively for holograms. Unfortunately, our cinema movie film gate is not wet and has the problems alluded to previously.

Another possible solution is to decrease the f ratio of the beam where it goes through the film. This technique is similar to that used on the new digital audio disks to destroy the coherency and to discriminate against the fingerprints on the protective plastic. The scheme requires accurate control of focus and may interfere with the mechanical parts of our present gate unless the imaging lenses can be made very long. Nevertheless, it is worth exploring.

The spot size and optical system has been optimized for the larger images found in solar physics.

Some users have found the 33 micron limit to be too large and would like to have smaller spots available. This could easily be accomplished by redesigning the optical system. The principal problem is making the lower objective lens clear the mechanism of the film gate.

7.0 ACKNOWLEDGEMENTS

This microphotometer was started in 1976 by R. Dunn, who layed out the mechanical and optical design, and G. Spence who designed the analog and digital electronics. The mechanical parts were all constructed in the SPO instrument shops by A. Green. When the Sigma 5 computer was replaced by the Perkin Elmer 3240, A. Healy reworked the electronics and M. Arrambide devel-

oped a new software package. More recently the digital electronics were completely changed to a microprocessor by L. Widener, who also programmed this device. L. November reprogramed all the user software. Currently, R. Porter is rewriting the setup manuals and is making the software more "user friendly."

REFERENCES

Bourne, 1978, Bell System Technical Journal, 57-6, part 2.
November, 1981, "The General Data Format for Image Manipulation in Astronomy," SPO Internal Document.
Wells, D.C., Greisen, E.W. and Harten, R.H. 1981, "FITS: A Flexible Image Transport System," Astron. Astrophys., **44**, 363.

Hemenway: I've always been concerned and never sat down think about it what the coherence of the laser light as your light source does as a function of the properties of the photographic emulsion in the grain size and everything else.

Dunn: Well, Spence spent a lot of time working over the years and we're not aware of any problems that way. We put the same different films and all these things. There may be some problems that we haven't found yet. We haven't studied this one I suppose as far as we have studied our pre-PDS one. That was a number of years ago and it's still sitting out there.

Wells: I always wished that I could sample my plates from the gaussian beam instead of a box car. I'm curious to know if you could show your optical diagram again and explain how it is that you get the gaussian beam and secondly whether whatever it is you're doing is applicable to the PDS or is it restricted to laser system.

Dunn: Well, I don't know. I wouldn't see why you couldn't generate a gaussian beam on that PDS without a laser if you wanted to try it. I mean it seems to me that instead of putting in a sharp hole you put in apodized filter somehow. You might be able to do something just with an out focused image. Spence actually changes since we had such a big depth for focus. We change the size of the spot by changing the focus on this thing and he is able to show that was good enough to be the gaussian spot. Of course the laser is inherently a gaussian so now if you come in and you put a pin hole in the front of it so that you taking out the center of the gaussian, that will get you in trouble. I mean if this is the gaussian coming out of the laser and you just put in regular old field lense and enlarge it up and put a pinhole on it you no longer have a gaussian. So you have to let all the light through or if you come down on the lens and you decide I'm going to over fill the lens like we all like to do to get the defraction of the lens. So we put the Gaussian on that thing like this from the center of the laser it's no longer a Gaussian. So the lenses all have to be oversized. The laser just eliminates the center part of the lense and it stays a Gaussian.

Hemenway: That was the thing I didn't realize, the laser makes the Gaussian.

Dunn: Yeah, the laser makes the Gaussiar and Spence realized that back then that they had this cut off and he said "that's great, that should cut everything out." So I see two ways you could try it. I think you could apodize the aperture just to fool around with it—you know your defining aperture—the other one is to put the laser in and try it out.

Hemenway: Just thinking about that, I don't see why one couldn't work it out so that you simply take a pin hole and run the laser as the light bulb and then arrange the optical system so that essentially you're looking at the fourier component so that then what you have is not a Gaussian but a Bessel function when you transfer up the clear aperture.

Dunn: Well I think you might get some other things. You have to look at the filter functions in either and decide whether its really a gaussian.

DATA COMPRESSION TECHNIQUES FOR ASTRONOMY

Robert Landau and Frank D. Ghigo
University of Minnesota

The photometric and astrometric accuracy of the Minnesota automated dual-plate scanner is summarized. The relation between magnitude and isophotometric image diameter is linear on Schmidt plates over a large useful range. We will present results of a study of centroid measurement accuracy and image classification ability of parameters derived from both densitometric and isophotometric scanning techniques. The data analyzed for this purpose are synthesized ideal star and galaxy brightness distributions with appropriate random noise added to simulate plate grain and sky background effects. A preliminary study of image classification using real plates and signle isophote data finds that a parameter describing the raggedness of the isophote may be useful in distinguising stars from galaxies.

Data Compression Techniques for Astronomy

Motivation

The vast amount of raw information from ground-based photography and CCD imagery, the VLA, and, soon, the Space Telescope exceeds what our current data processing facilities can comfortably handle. Two approaches to this problem are possible: we can expand our processing facilities in size and number and we can try at the earliest possible stage of processing to restrict our reduction to only the data that will affect the astronomically desired result. We'd like to describe two procedures for extracting information from photographic plates that directly reduce the amount of information by about a factor of 50 without loss in the accuracy of the astrometric or photometric results. Greatly reduced storage requirements and more rapid plate processing are the benefits, in turn making possible more extensive surveys and searches for rare objects.

Maps

Micro-Adaptive Picture Sequencing is the name given by A.E. LaBonte (1977, 1980) to a method best suited for the analysis of extended images including images already in digital form, such as CCD pictures. It is based on the assumption that it is only for small regions of the image that the maximum spatial resolution is required. For example, to cover a ten inch square plate at 25μ resolution requires 10^8 pixels. However, there exist many regions of the plate of size 50μ or 100μ or 400μ square over which the density will vary only slightly. In these regions fewer pixels of larger size are used to describe the image together with a two or three bit code describing the size of the pixel; or equivalently, the local spatial resolution. To determine whether a reduction in resolution is warranted the intensities of four pixels in a 2 x 2 subarray are examined. If any of several intensity differences exceed preset limits the full resolution is retained; otherwise the average density is assigned to a single pixel four times as large, and four of these are examined to see if the process can be repeated at the next higher level. The result is that regions of high contrast always have full resolution while regions of low contrast are smoothed. Furthermore, by setting the intensity difference limits differently over the field one can

force certain regions to retain full resolution regardless of the image content and force other regions (background) to be averaged.

Although the size of pixels may vary, their position in the field remains implicitly given by their position in the data stream.

Processing a raster to produce a MAPS sequence requires about 20 computer operations per original pixel, all of them integer, with no multiplies or divides, only adds, shifts, memory references and a sign-bit jump. A 68000-based processor could encode the 10^8 pixel raster from a 10-in square plate in about 5 minutes. Alternatively a simple hard-wired circuit could produce a MAPS data stream directly from the output of a plate scanner.

Decompression for display or analysis is even faster than compression and can be done at video rates. Figure 1* shows the results of compressing a scene from 8 bits per pixel to 1/2 bit per pixel by MAPS and by simple 4 x 4 pixel replication. Notice the severe "stair casing" in the replication which is not present in the MAPS restoration. The mean standard error of the intensity of the MAPS restoration compared to the original is 0.15%

APS

The Automated Plate Scanner is a system nearing completion at Minnesota whose primary characteristic is the ability to scan plates fast. (See Figure 2.) Two plates up to 14 inches square are scanned simultaneously. For proper motion work, these would be the first and second epoch plates; for photometry, they might be a red/blue pair. The advantage of scanning two plates, (whether simultaneously or not), is twofold. First, one can work closer to the plate limit by separating randomly developed clumps of grains from true images. (The latter appear on both plates in the same position.) Secondly the difference in the positions of the centroid of images on the two plates is a useful parameter for separating stars from galaxies.

*not included because reproduction obliterates the effects to be demonstrated.

Figure 3

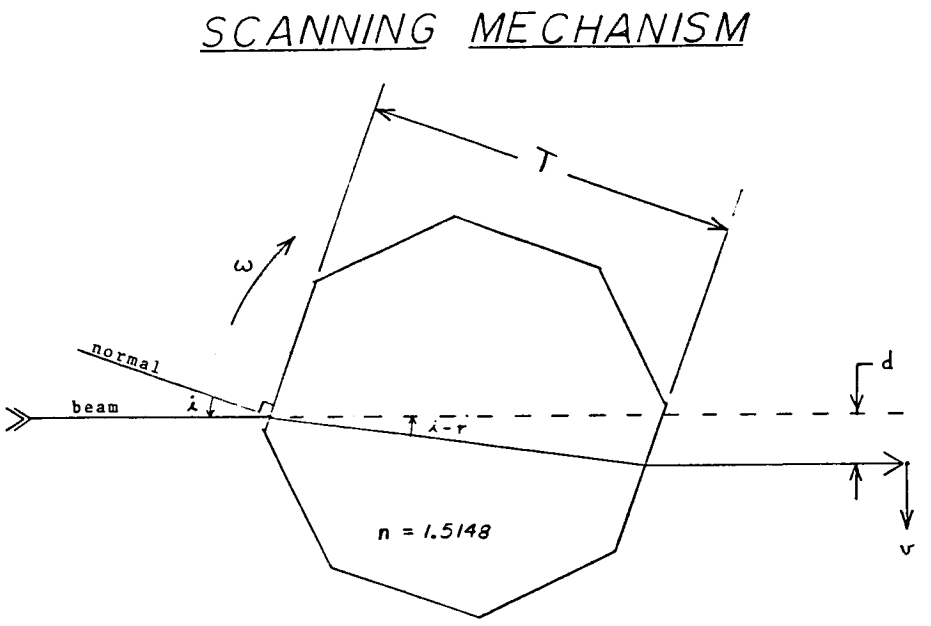

$$\sin r = \frac{1}{n} \sin i$$

$$\text{Beam displacement} \quad d = T \frac{\sin (i-r)}{\cos r}$$

$$\text{Spot velocity} \quad v = \frac{\omega T}{\cos r}\left[\cos(i-r) - \frac{1}{n}\frac{\cos^2 i}{\cos^2 r}\right]$$

The scanning mechanism is a rotating eight-sided prism shown in Figure 3 through which an f/15 laser beam is sent. While the spot is rapidly moving across the plates in the y direction, the plate carriage is moved slowly in the perpendicular direction. Each motion has three independently selectable speeds, producing the scan parameters shown in Table I.

Table I

APS SCANNING SPEEDS

Scanning Prism

	Fast	Med	Slow	
motor speed:	3600	1800	900	rpm
prism speed:	4500	2250	1125	rpm
scanning rate:	600	300	150	scans/sec
spot velocity:	12	6	3	μ/μsec

x-carriage motion

speed	rpm	mm/sec	separation between scans			time for 10x10" plates
Fast:	3600	6	10μ	20	40	30 min
Med:	1800	3	5	10	20	45
Slow:	900	1.5	2.5	5	10	65

In its standard scanning mode the APS makes use of the fact that most of the field of most astronomical photographs is blank sky. Except to subtract its local value (which the APS does during scanning), blank sky is ignored. Most of the data compression achieved comes from this freedom. High scanning speeds are then achieved by trading density information for very accurate positional information. The images themselves often have such sharp boundaries that they can be characterized either by locating the position of the boundary at which the profile crosses a preset density level (an isophote) or by measuring the densities at the centers of a raster of pre-determined positions (pixels).

The APS has, in fact, three scanning modes which are illustrated in Figure 4. The circuitry for achieving these is shown in Figure 5. The laser beam from the scanning prism is split in three and focused to 12μ spots on the two plates and on a precision reticle consisting of 512 alternate light and dark bars 23μ apart that provides the fundamental indicator of the position of the laser spot on the upper and lower plates. As the spots move across the plates and the reticle, the reticle light detector generates a reference frequency, which varies slightly along the scan because the velocity of the spot is non-uniform. A high-frequency oscillator is phase-locked to the reference frequency and is counted in a 16-bit counter. Each count corresponds to a motion of the laser spots on the plates of 3/8μ, thereby defining

the spatial resolution of the scanner. The two shaft encoders on the x and y axis also read to 3/8μ.

After passing through the upper and lower plates the beams are detected by silicon photoconductors to produce the plate channel video outputs. Two ways of processing these signals lead to the three modes of scanner operation. In densitometry mode the video is directly digitized. The A/D is a 12-bit converter running at 1 MHz. Only small regions of the plate can be digitized without indigestion. In the standard (isophotometric mode) from 1 to 7 reference levels are generated by the computer and continuously compared with the video level. When the laser spot encounters an image the video output drops. If the video drops below a reference level (illustrated by the arrow in the video graph of Figure 5), an image gate is generated which triggers the output of the 16-bit counter (the spot position) into the computer. The spot position is reported twice for each image encountered, once on ingress and once on egress as the video recrosses the threshold level. An ingress/egress pair is called a transit and represents two points on the circumference of the image at some reference intensity level. Thus densitometric mode produces densities as a function of position, and the standard mode produces positions as a function of density. The latter can be done at very high speeds and results in fewer bytes of data.

If an image gate is used to gate the A/D then densities inside the image boundary are obtained as well as the transit information - the third, hybrid mode of operation.

The reference threshold levels are continuously maintained with respect to the local background by a two-stage process. Because a scan line is 12 mm long the scanner must first scan a stripe 12 mm wide down the length of the plate then offset y by 12 mm, fly-back, and begin another stripe. A ten inch square plate requires 21 such stripes. During fly-back the plate is coarsly digitized at a resolution of 3/4 mm^2. During scanning these background values are used to adjust the reference levels.

Data compression factors can be calculated from typical scan parameters. A 10-inch square Schmidt plate of a region near M31 contained 70000 stars and 2,000,000 transits, a factor 50 fewer pieces of raw data than digitizing the plate at 20μ resolution would have produced.

During the scanning of one stripe, the raw data from the previous stripe are reduced. Each image is parametrized by x and y centroid, diameter, ellipticity and orientation, and position and diameter uncertainties, a set of 8 words. To maintain a high throughput, it is useful to minimize disk head motion. Consequently we use two disk drives, into one the raw transits are written while the other contains the previous stripe's raw data, which are being converted to image parameters. Data are transfered from the first drive to the second during flyback. To accomodate the non-uniform star density on the sky and hence the sometimes large difference between maximum peak data rates and maximum sustained data rates, each plate has a circular 64-Kbyte buffer in computer memory. The peak data rate is set by the cycle time of computer memory at about 300,000 transits/sec per plate (all threshold levels). The sustained data rate is limited by the disk transfer speed to 100,000 transits/sec per plate.

Consider the photometric accuracy of an isophotometric measuring technique. To the extent that the profiles of all star images are just scaled versions of each other, any parameter which measures the scale can (when calibrated) determine a magnitude. In the absence of grain noise the gradient of a stellar image profile is such that the measurement of the diameter to 3/4μ with a 12μ spot is of equivalent accuracy to measuring the density of the profile to 0.01 with a 15μ pixel. In the presence of grain noise in the image, measurement accuracy then becomes dependent on the number of independent estimates of the scaling parameter: the number of pixels covering the image in the case of densitometry, the number of transit endpoints in the case of isophotometry. For 15μ pixels and 5μ scan separations these are equal for a star of 110μ diameter, about four magnitudes above the plate limit. Brighter stars are measured more accurately densitometrically; the fainter are measured more accurately isophotometrically.

Where a single scaling parameter does not suffice to estimate the brightness of an image, the addition of transit data at a second threshold level provides an important piece of information: the gradient of the image. This, together with the estimated uncertainty in the diameter, and the difference in image position on two plates can form the basis for a star/galaxy classifier. The softness of galaxy images results in a smaller gradient, a

larger uncertainty in the diameter and a larger mean separation on a pair of plates.

The APS is being developed under grant AST79-20382 from the National Science Foundation.

References

LaBonte, A.E. (1977). SPIE Proceedings 119, 99.

——————— (1982). SPIE Proceedings 249, 61.

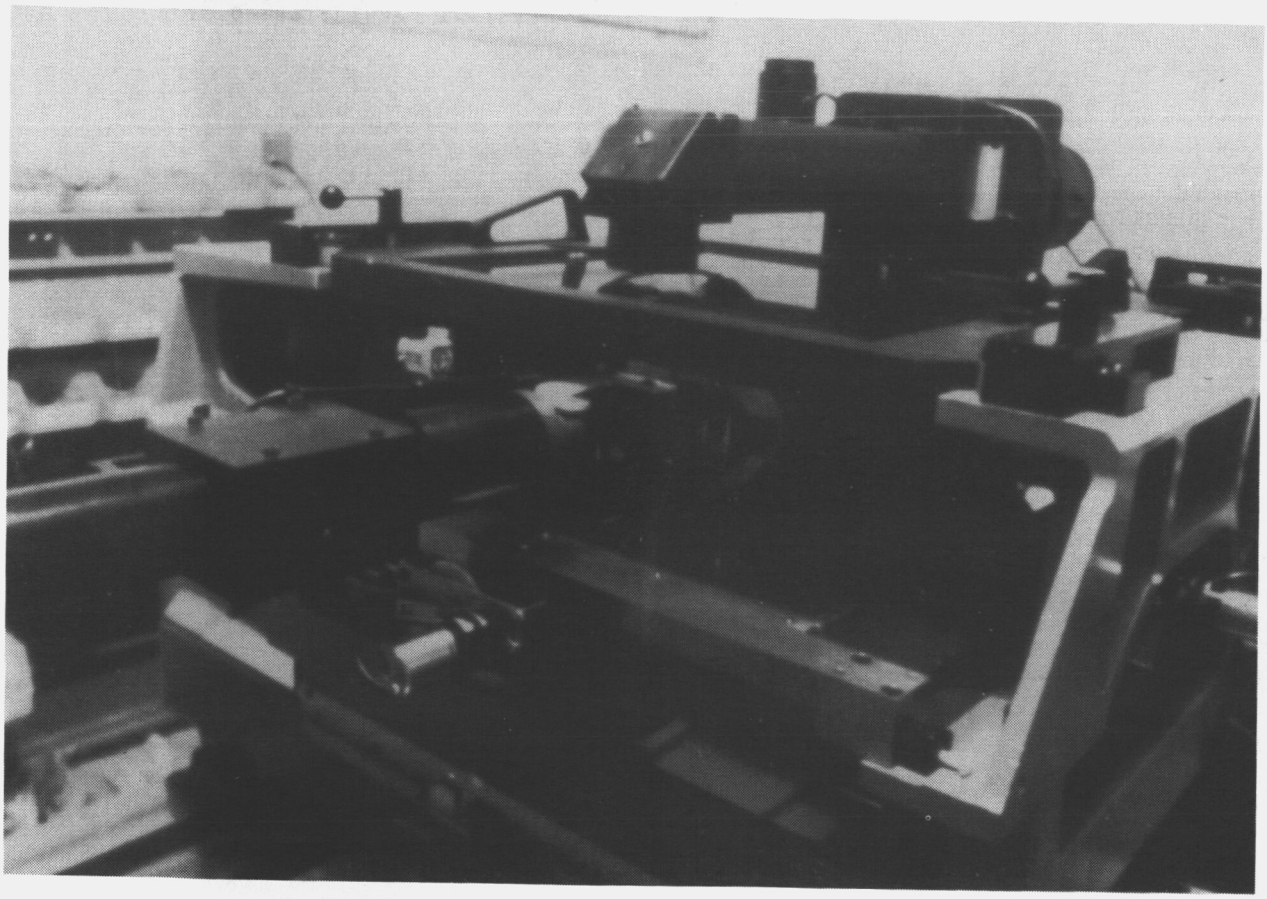

Figure 2. The Automated Plate Scanner

APS SCANNING MODES

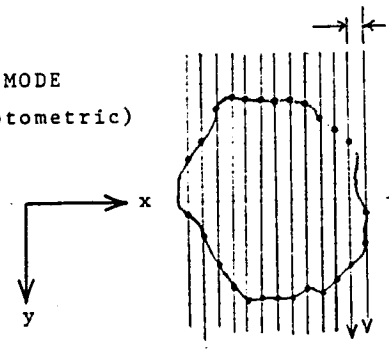

Information per level (8 words)

1. x, y centroid (3 words)
2. diameter (1 word)
3. ellipticity, orientation (2 words)
4. error in y-centroid (1 word)
5. error in diameter (1 word)

Spatial resolution: 0.37 μ

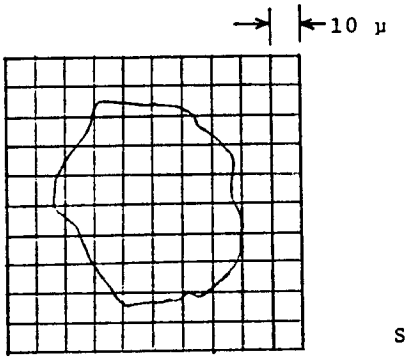

100 words of density or transmission data

Spatial resolution: 1 pixel

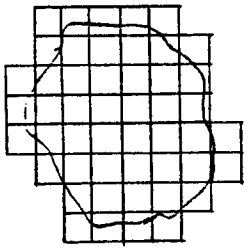

49 words of transmission data (plus one level of transit data)

Figure 4: APS SCANNING MODES

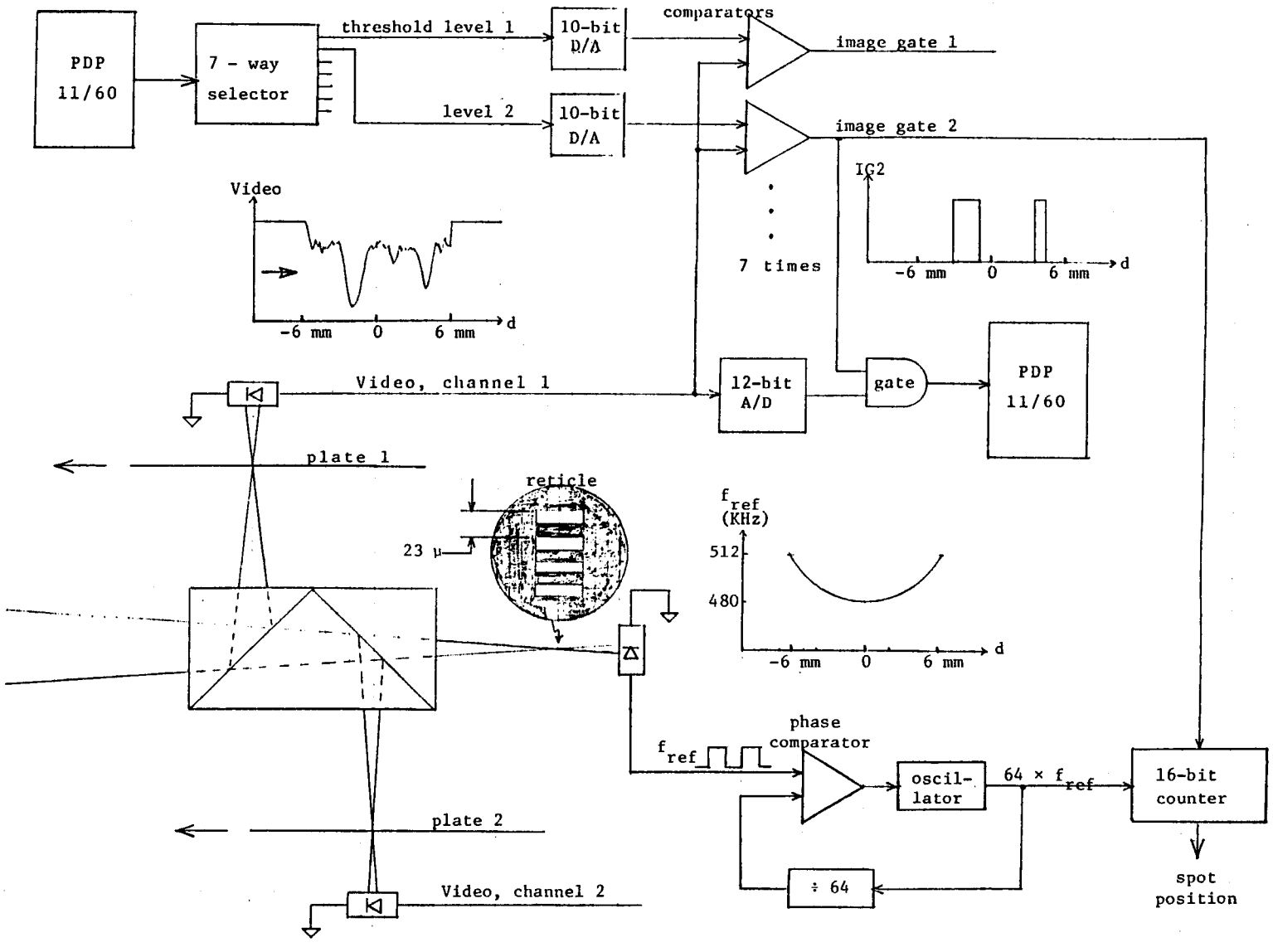

Figure 5: APS SCANNING MODE CIRCUITRY

TECHNIQUES OF ISOPHOTOMETRY

Frank D. Ghigo and Robert Landau

University of Minnesota
Astronomy Department
Minneapolis, MN 55455

I. INTRODUCTION

We will discuss the expected performance of the Minnesota Automated Dual-Plate Scanner (APS) with regard to photometry, position measurement accuracy, and ability to classify images. Since the current rebirth of the machine is not complete, we have not yet done extensive tests with real plate material, and so some of the following discussion is more theoretical than one might wish.

II. PHOTOMETRY

Star image diameters at a selected isophote appear to correlate well with magnitude. The relation, is, in fact, quite linear over a 6 magnitude range, down to the plate limit. (Our method of deriving diameters from the image transits will be discussed later.) Figures 1a and 1b show diameter, in microns, versus magnitude for stars in the Baum photoelectric sequence SA57. We scanned this region on the Palomar sky survey plates, and used PSS plate E and O magnitudes derived from BVR photometry of the sequence done at Kitt Peak by one of us (RL). The relation is linear for magnitudes fainter than 13th on the red plate (fainter than 14th on the blue) with an rms scatter of about 0.1 mag. The turn-up at the bright end is probably due to saturation effects on the plate and incipient diffraction spikes.

The slope of the calibration curve for this and other plates is about 25 microns per magnitude. The typical diameter errors we find on the PSS plates are 2-3 microns, which converts to a magnitude error of about 0.08 to 0.12 mag. This suggests that a significant amount of our scatter in Figure 1 is due to diameter measurement error. Scans of IIIa-J plates indicate that both positions

and diameters can be measured about twice as well as on the 103 emulsions, leading to the hope of doing photographic photometry to 0.05 mag

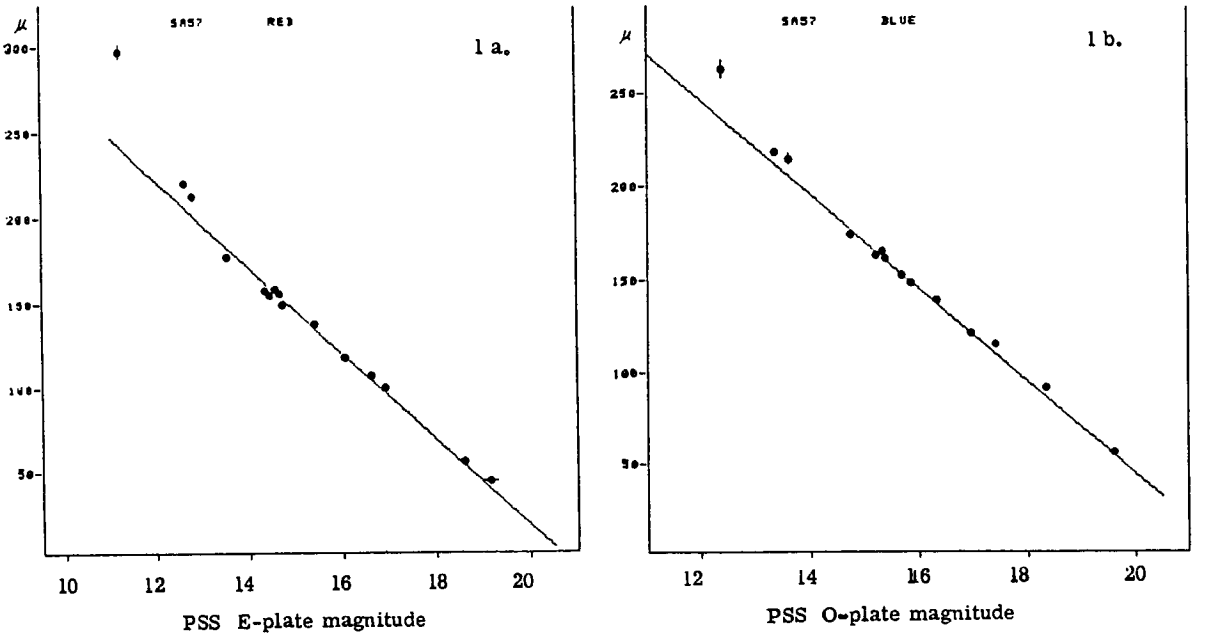

Figure 1. Image diameter-magnitude relation in SA57.

III. ASTROMETRIC ACCURACY

We have done a Monte-Carlo test of the accuracy of measuring star positions by isodensitometric and raster-scan methods. We used idealized star images, represented by circular gaussian density distributions, and simulated a raster scan by sampling points on a square grid and adding gaussian random noise to simulate sky background and plate grain effects. To simulate the APS, we picked a threshhold and created star transit data such as our scanner would produce. Again, random noise was added.

As a guide to choosing a density distribution to represent our idealized star, we used scans of stars made for us by David Koo on the Berkeley PDS using a IIIa-J plate taken at the Kitt peak 4-meter. Table 1 lists the magnitudes of the stars. The data consists of 64x64

rasters of 20-micron pixels. We determined that profiles through these stars were quite well fit by Gaussians. The baseline level, amplitude, and sigma for the gaussians are also listed in Table 1. These Gaussians, after rotation about their centers, are our idealized star density distributions.

Table 1

Idealized Star Profiles on a 4-m IIIa-J Plate

$$D = K + Ae^{-x^2/2\sigma^2}$$

B	K*	A*	σ
18.3	1.32	2.75	54μ
19.3	1.28	2.59	44μ
20.2	1.27	2.23	34μ
21.3	1.26	1.24	30μ
22.5	1.32	0.70	28μ

*density is PDS units ÷ 200

To estimate the background noise, we calculated the standard deviations of background densities in the Berkeley PDS rasters, omitting the stars themselves, and obtained a sigma of 12 PDS units (.06 in density) as an average of the five regions. (Our results, when converted to diffuse density (Latham, 1978), are a little higher than the values found for these plates by Furenlid (1981)). We now have all the ingredients needed for the Monte-Carlo tests.

To determine positions on the pseudo-raster-scan data, we fit a Gaussian with a flat baseline by least squares to the marginal distributions in x and y. This method was found to be the most accurate of several centering methods by Auer and vanAltena (1978) and by Chiu (1977). We also calculated the centroid by taking the first moment of the marginal distributions.

We sampled the simulated stars on the simulated IIIa-J plate at pixel sizes of 10 and 20 microns. For each of these cases, we made 100 trials and obtained the mean and standard deviation of the x and y position differences from the true position, with the results shown in Table 2. The numbers shown are the quadrature

sums of the x and y standard deviations. We may note that the accuracy, as expected, is better for a finer pixel spacing, and that the moment calculation gets worse rather rapidly with increasing magnitude.

Table 2

RMS Position Errors for Raster-Scan Simulations (microns)

	marginal moment pixel size		gaussian fits pixel size	
Star	10μ	20μ	10μ	20μ
$18^{m}.3$	0.7	2.4	0.5	0.6
$19^{m}.3$	1.7	3.4	0.6	0.7
$20^{m}.2$	2.9	6.2	0.8	1.0
$21^{m}.3$	4.9	12.0	1.4	1.9
$22^{m}.5$	8.3	23.4	2.7	3.7

In the APS simulations, we used scan spacings of 5 and 10 microns. The image center and diameter were determined by two methods. The first was to fit a circle by least squares to the positions of the transits of the star image. The second method also finds ellipse parameters for the star data, but uses a computationally very fast method which we will describe later. The threshhold was set to 5 sigma above the mean background. Again, 100 trials were run for each case. The results are shown in Table 3, and are the quadrature sums of the standard deviations in x and y.

Table 3

RMS Position Errors for APS Simultations (microns)

	least-squares circle scan spacing		fast ellipse scan spacing	
Star	5μ	10μ	5μ	10μ
18.3	0.4	0.8	0.9	1.0
19.3	0.4	0.7	0.8	0.8
20.2	0.4	0.6	0.9	0.9
21.3	0.5	0.7	1.0	1.3
22.5	0.8	1.1	1.4	2.1

If we compare the least-squares circle fit results for a 10 micron scan spacing with the 10 micron pixel results of Table 2, we find the Auer and vanAltena method somewhat superior for the brightest stars, but for stars near the plate limit, the isophotometric method gives a definite advantage. An explanation of this effect may be that the number of independent samples in the raster scan technique increases as the square of the image size, whereas the number of samples of an image with the APS is the number of transit endpoints, which increases proportionally to the circumference, that is, linearly with image diameter. The preceding paper (Landau and Ghigo, 1983) discussed this effect in more detail.

IV. FAST CALCULATION OF IMAGE PARAMETERS

A fast algorithm for finding ellipse parameters was written for us by Charles Moore of Forth, Inc. Table 3 shows that the position accuracy degrades by less than a factor of two using this algorithm, compared with the more rigorous circle fit. The main advantage of this method is its speed. It processes, on the average, 50 to 100 stars per second on our PDP 11/60 computer. The circle fit method takes about 2 sec per star, the marginal distribution fitting applied to 64x64 rasters takes 8 to 10 seconds per star, and the moments of the marginal distribution require about 2 sec per star (most of this to simply generate the marginal distributions).

The fast algorithm makes use of a representation of the ellipse in which the ellipse is sliced perpendicular to the X-axis, which is, of course, just the way our machine samples it. A common way to represent an ellipse is with a semi-major axis (a), semi-minor axis (b), and a rotation angle (θ). An alternate way is to use A, half the length of the projection of the ellipse onto the X-axis, B, the y-intercept, and ΔY, the Y position of the tangent line (see Figure 2). In these terms, the equation for an ellipse is:

$$y = (B/A)\left(A^2 - X^2\right)^{1/2} + \Delta Y \cdot X/A$$

Given a, b, and θ, one can convert to A, B, and ΔY, and vice-versa. For example, the area of the ellipse is given by: AREA = π ab = π AB

The parameters we record for each star are the diameter, D, the axial ratio (e = A/B), ΔY, the position (x0, y0), a position error and a goodness of fit parameter.

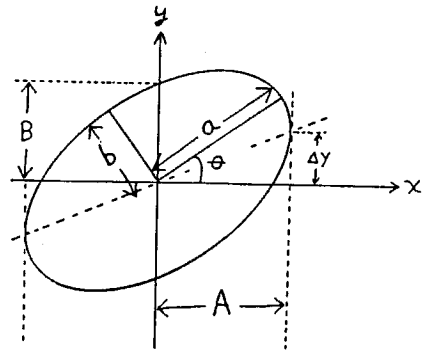

Figure 2. Ellipse parameters. (see text).

The method does no fitting, but simply estimates each parameter in a straightforward manner. The sum of the length of all the transits, multiplied by the scan spacing, is the area. The diameter follows from $D = 2\,(AREA/\pi)^{1/2}$. The A parameter is half the total number of scans of the image times the scan spacing. From A and D, the axial ratio is $e = A/B = 4A^2/D^2$ The Y centroid is the average of the y coordinates of the transit endpoints. An estimate of the position error is the mean absolute deviation of the center of the transits from the Y centroid. The X centroid is found by starting at one side of the image and summing transit lengths until half the area is exceeded. This identifies the central transit, and the x centroid is found by interpolation between the central and adjacent scans. Finally, the ΔY parameter is found by calculating the Y centroid (Yc) of the left half of the image, from which $\Delta Y = 2Yc$. An estimate of how well the ellipse fits is found from the mean absolute deviation of the transit endpoints from the ellipse.

The whole procedure requires 14 multiplies, 10 divides, and one square root, in addition to numerous additions and subtractions. The use of absolute deviations rather than standard deviations as error estimates avoids extra multiplies and square roots. Furthermore, they can be easily converted to standard deviations, since $\sigma = \sqrt{\pi/2} \cdot$(mean absolute deviation). This relation is true for a normal distribution, and we have verified experimentally that it holds for our star transit data.

V. IMAGE CLASSIFICATION

It may seem ridiculous to attempt to distinguish galaxies from stars using single isophote data, but we did make the attempt, just to see how well we can do. In a 1.5 cm^2 region near SA57 on the PSS plates, all matching images were classified as stellar or non-stellar using deeper 4-m plates lent by King. We plotted several combinations of image parameters versus each other and found that the best separation occurred for η and ρ as shown in Figure 3, where η is the sum of parameters describing the non-circularity and edge raggedness of an image on both plates, and ρ is the position difference between the two images on the two plates after transforming upper plate coordinates to lower plate coordinates with a local linear transform.

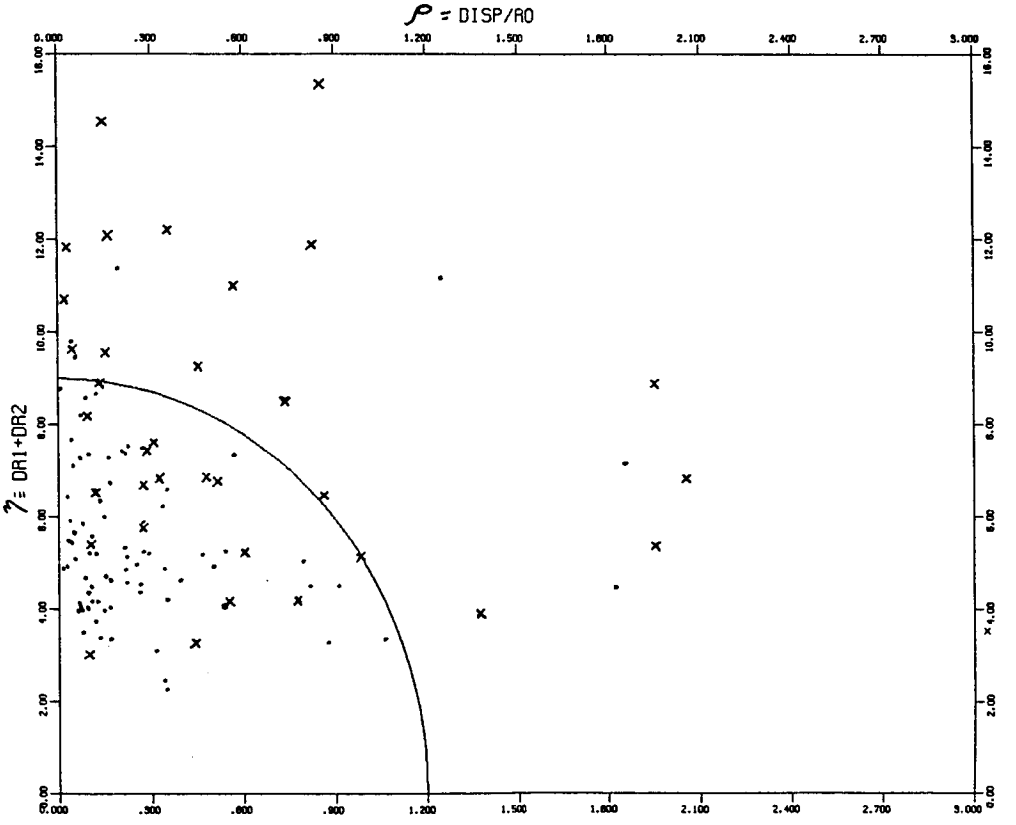

Figure 3. η vs ρ (see text) for 123 objects classified as stellar (dots) or non-stellar (crosses).

With the discrimination curve shown in Figure 3, about half the non-stellar objects are rejected while

losing less than 10 percent of the stars. One can choose a purer but less complete sample of stars, or vice versa, by choosing the discrimination curve differently. This is a promising start, especially for single isophote data. We expect that the addition of a second isophote will improve the situation considerably. The difference in diameters at two isophotes depends on the image edge gradient, which should be a good measure of the softness of the image, and we hope to test this possibility in the near future.

The philosophy we are expounding is to get the most information from as little initial data as possible, in order to increase the data acquisition speed as much as possible. The APS is ideally suited to large search programs involving many plates. For example, if the goal is to find a few objects of interest from among a large number of images, one should carefully choose the threshhold levels and scan spacing to allow one to recognize candidate objects with the fewest initial data. Once the objects are found, they can be studied more thoroughly by re-scanning the candidates in, e.g., densitometric mode, or using a finer scan spacing.

The redevelopment of the Minnesota Automated Plate Scanner is being supported by the National Science Foundation.

REFERENCES

Auer, L.H., and van Altena, W.F., 1978, A.J. 83, 531.

Chiu, G.L-T., 1977, A.J. 82, 842.

Furenlid, I., "Image Analysis Techniques and Applications", Slater and Wagner, eds., Proc. of Conference of the Society of Photographic Scientists and Engineers, January 1981, p. 17.

Latham, D.W., 1978, AAS Photo-Bulletin No. 18, 3.

Jenkner: How do you define processing time?

Ghigo: This was on a PDP 11/60. I meant to mention that, in fact I left out sort of a general statement about processing time. On a pair of 9x9 plates the scanning process of the machine takes about 40 minutes referring to thing that Rob previously showed. Reducing, we found about 70,000 images on each plate; these particular plates happen to be Tottenberg Schmidt plates of the M31 region. We get our parameters, this process again takes about 40 minutes. This is simply running the program. Then of course once we have our star catalog on each plate we have to match two plates to each other and find the transformation from the upper to the lower plate. This we find takes about 30 minutes and we came out in this particular case, I'm talking about with around 35,000 matched stars. This is of course the way that we find what are real stars. We suspect a lot of these maybe spurious streaks, dust specks and so on, and we really don't have any information on how many of those are simple so red that they didn't show up on the blue plate; such things as that.

Hemingway: I had a couple of comments. The first one is just a statement that was obvious, you are simply clipping the data into two levels but then what you're doing in effect is making a two level detector, which is very similar in fact to photographic grain and now you're making your grain size the same as your sample size. Its either on or its off. Now, I am a little worried about the astrometry at very high accuracy, because admittedly what you're trying to do is something that's quick and dirty. But, I am asking you to be careful because its pretty clear that you can get magnitude affects right away if you have something like guiding errors; because what that will do is change the distribution of bright stars and not effect the faint stars if the telescope has one very wicked screw.

Ghigo: I suppose that could happen. We don't really know how well it might be for astrometry, I guess it has to be tested.

Crane: I have two questions. One is what's the current operating status of the machine, and the second question is what is the availability to the astronomical community over the next few years.

Ghigo: The answer to the first question is that its not working at all right now. Sometime in maybe the next year it will start becoming available to the astronomical community in general. The idea is to have it be a national facility.

Boyce: You said that you are going to have more than one level of digitization, how much better will the photometry of stars be if you have two or more levels.

Ghigo: Well it's hard to say, its amazingly good with just one level.

THE AUTOMATED PHOTOGRAPHIC MEASURING FACILITY AT CAMBRIDGE

E.J. Kibblewhite, M.T. Bridgeland, P. Bunclark and M. Irwin
Institute of Astronomy
Madingley Road
Cambridge CB3 OHA
England

ABSTRACT

The design and performance automated photographic measuring facility at Cambridge is described. It consists of a precision laser scanning microdensitometer connected to a series of computers that process the data on-line. Plates up to 350 mm square can be measured. The microdensitometer samples the plate to 12 bit accuracy at a speed of 230,000 samples/second. The positional accuracy is better than a micron. Other features include platen rotation and automatic focus.

1.0 INTRODUCTION

Since this is a conference on microdensitometers I will concentrate on the design of our machine rather than the astronomy it produces. Our machine is probably state of the art at the moment. However, it was designed for specific tasks which I will outline before describing it in detail since microdensitometers and photographic plates are now in competition with TV type detectors.

Almost all astronomical problems still need photographic material to provide observational data and, although CCD and other TV detectors will replace photography for measurement of either single objects or deep small area surveys, photographic techniques will be fundamental for large area observations into the foreseeable future. Although the quantum efficiency of the photographic emulsion is low (a few per cent) the number of pixels is very high (10^9/plate) so that the product of qA exceeds that of CCD arrays by a large factor.

Survey work involves looking for objects in a given volume of space which means either looking in a small area to great depth or a larger area in less depth. The limiting factor is the sky brightness, for as soon as the objects surface brightness falls below that of the sky, exposure times increase rapidly and follow-up work using spectroscopes on big telescopes become correspondingly slow. So while certain problems (such as evolution of galaxies) may need deep exposures with CCD, projects which survey large volumes of space searching for rare objects or improving our statistical knowledge will continue to use photography. On a good night the photographic plate, exposed on a 48" Schmidt, will easily reach 21st magnitude objects and will record 40 x 10^9 bytes of data at an average speed of over 10^6 bytes/sec!

In general, Schmidt telescopes have been used for whole sky surveys. In the future however we can see that comprehensive studies of smaller (say 10° x 10°) areas of sky in many colors (using interference filters or objective prism spectra) and different observing times will be necessary to differentiate between the many different types of object and obtain detailed qualitative data for statistical studies.

For these smaller area surveys high precision is needed, both in photometry in order to measure colors and objective prism spectra, and in position to distinguish faint nearby and distant objects. The ability to collate data efficiently from a large number of plates is also important. Finally the system must be flexible so that different projects can be undertaken without the astronomer having to write a large amount of software.

This last point is extremely important because carrying out survey work is only one example of the use of photographic data. Astronomers have access to enormous archives of plate material collected over a century, only a fraction of which has ever been analysed in detail. Often only a few objects on the plate need be measured (e.g. for parallax work or studies of long period variations of quasars) so that a measuring system must be able to cope with anything from measurements of a small number of objects on many plates to many millions of objects for large survey projects.

The automated photographic measuring (APM) system at Cambridge was designed specifically to carry out these tasks and has been developed over the last decade to meet the present and future needs of astronomers. It consists of a very accurate and fast laser beam scanning microdensitometer to digitise the plate and a series of on-line computers to analyse the data as it is being scanned.

The APM system is interactive. Astronomers come to the unit, learn how to use it, and can leave Cambridge knowing they have good data. The microdensitometer is controlled by a comprehensive software package which enables the astronomer great flexibility without knowledge of the detailed working of the machine. All plates can be aligned using standard reference star catalogs stored on disk, so that all measured image positions are given in R.A. and Dec and data from a number of plates of the same area of sky can be efficiently collated on the STARLINK VAX. A color interactive display allows the user to have a "quick look" at the data either to experiment with different scanning parameters to suit his requirement or be certain he has good data before leaving the facility.

The machine now works in one of four modes, each of which is fully operational: (1) An image analysis mode in which the positions, shapes and sizes of the images are measured. A plate can be measured overnight in this mode and software is available on the VAX STARLINK for star/galaxy separation, collation of data from a set of plates and automated detection of variable or color excess objects and a wide range of plotting and data handling routines. (2) An objective prism mode which produces an uncalibrated intensity versus wavelength data set from each spectra using a direct plate of the field to define each image. These spectra are calibrated on the VAX and automated

classification algorithms can pick up emission line objects. (3) A raster scanning mode which digitises given areas of plate at a speed set by the magnetic tape drive (50,000 samples/second). Software for a wide range of tests such as contouring background removal, Weiner filtering or maximum entropy processing etc. is available. (4) An automated raster scan which digitises round a set of positions stored on magnetic tape. This has been used extensively to obtain contour maps or false color displays of candidate objects selected from one of the first two modes.

The APM machine is extremely accurate. The photometric drift is less than 0.001 D over the period of scan and the transmission measured to 12 bits. The background is first measured and a hardwired interpolator derives a background for every pixel measured on the machine. Photometric accuracies of 0.05 mag for images 2 magnitudes above plate limit and 0.016 mag. 4 magnitudes above the plate limit are routine when measuring stellar images on a set of IIaD or IIIaJ emulsions. Field errors are very small and, indeed, difficult to detect on the APM machine. The positional repeatability of the machine on single images of Allegheny plates in 0.44 microns for 1000 measurements of the same image on the same plate and 1.0 micron between plates.

Most important of all the APM facility is a fully integrated system. Enormous amount of effort has gone into making the system easy to use by astronomers and to provide the software to analyse the data. Software costs now dominate the budget of measuring machine facilities.

2.0 MICRODENSITOMETER

A schematic diagram of the microdensitometer is shown in Figure 1 and the design of the various system elements is discussed below.

2.1 X-Y TABLE

The APM microdensitometer uses a massive X-Y table positioned by direct drive motors coupled to precision ball screws. The position is measured to 0.1 micron using ÷ 100 interpolation of a Moiré fringe grating with a phase lock division technique. Another feature of the encoding system is the provision of a reference point finder so that the counters can be zeroed at a fixed position in the centre of the table's travel.

The machine is built of stabilised Mechanite and weighs 7500 kg of which 4000 kg is the base casting. The mass of the machine gives low temperature drifts of typically 0.04 micron/hr in the X axis and 0.1 micron/hr on the Y axis. Linear Schneeberger bearings are used to define the axis. The loading on the balls is sufficiently high that all balls are elastically deformed so as to be in contact with the ways. Variations in the sizes of the balls (the main source of error) are thus averaged out and the whole table has proved to be exceptionally accurate, stable and reliable.

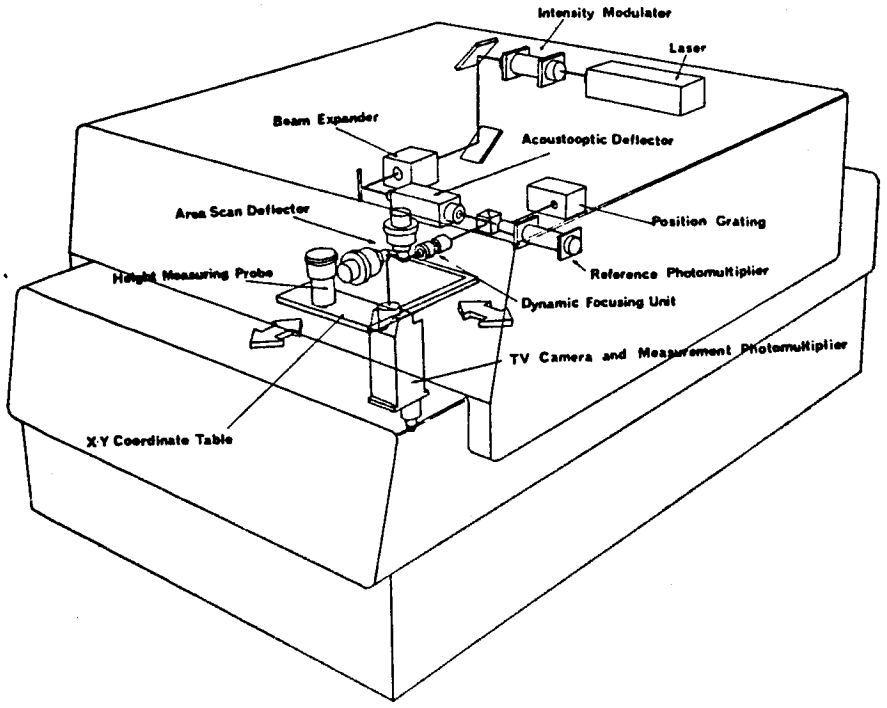

Figure 1. Cutaway of APM Microdensitometer

2.2 PLATEN ROTATION

The current philosophy of the APM machine has been to have computer controlled rotation of the plate over a range of ± 4 degrees with an angular resolution of 2½ arcseconds. This enables us to aline Schmidt plates exactly in a North-South direction and means we can position pixels on the same parts of the sky for a set of plates. We do have problems with 4m plates which often have random orientations but also larger plate scale. For these plates transformation is carried out in the computer. The concept works well though the mechanical implementation has backlash which is taken out by software. Position sensors are currently being added to the APM machine which will speed up the alignment of plates.

2.3 SCANNER

The scanner is the most important single element in the microdensitometer since the pixel positions must be known to sub-micron accuracy, scattered light and photometric drift must be minimised and the plate transmission measured with high accuracy.

To get the smallest possible halo a two-slit microdensitometer (such as the PDS) is usually used. This greatly reduces the effect of scattered light within the optics and emulsion but makes scanning slow due to the inertia of the table which has to be moved under the slit. Raster scanning round a number of small images over the plate (which is especially useful in many projects) is slow and effective scanning speeds of 1000 samples/sec or less are obtained using PDS machines on small (256 x 256 pixel) scans. Orders of magnitude faster scanning speeds can be achieved using CCD detectors or laser beam scanners. CCD detectors are cheaper and have a very stable geometry. They have been used in Holland (Astroscan), Japan and Caltech. They do suffer from a scattered light problem both by diffusion of light and/or electrons in the photoarray and, more importantly, in the photographic emulsion itself.

No system achieves the photometric stability or accuracy which can be achieved with a laser beam scanner. Although more expensive than a CCD system its cost is less than 9% of the total cost of the machine, the beam can be readily stabilised and high speed deflectors now exist. The spot can be intensity stabilised to 0.1% and its gaussian profile reduces the effects of sidelobes and high frequency noise. We use an acousto-optic deflector to scan the beam over a line 256 sample points long. This uses a high frequency (100 MHz) sound wave to diffract the light into a first order and the beam is deflected by changing the frequency of the sound beam. The system has no moving parts and low scattered light (see Figure 2). It can scan at a speed of up to 10^7 sample points/sec although the optics must be adjusted for a given scanning speed. We normally scan at 1 sample/4 microseconds, a speed which matches our computers.

2.3 AUTOMATIC FOCUSING UNIT

The APM machine uses a lens mounted in an air bearing and positioned by a loudspeaker movement to control the focus. The lens is oscillated through ± 20 microns and a phase locked loop used to move the lens so as to maximise the plate grain noise. The effect of this is to cause periodic changes in size of ± 0.3 micron on the 8 micron $1/e^2$ diameter of the scanning spot. Both theory and experiment show that this introduces less than 1% error into photometric measurements. This is a simple, direct and reliable means of keeping focus all over the plate.

2.4 PHOTOMETRY

We use a 6 stage photomultiplier which feeds a sample/hold and 12 bit ADC at its base. A television camera is also available to look at a 5 mm square region round the area being scanned. The camera is switched into the beam when required.

2.5 USE OF FILM

The existing APM machine measures film without any problems. For astrometry and finding charts film copies of the UKSTU/ESO survey still in their transparent envelopes can be scanned. For higher precision, film

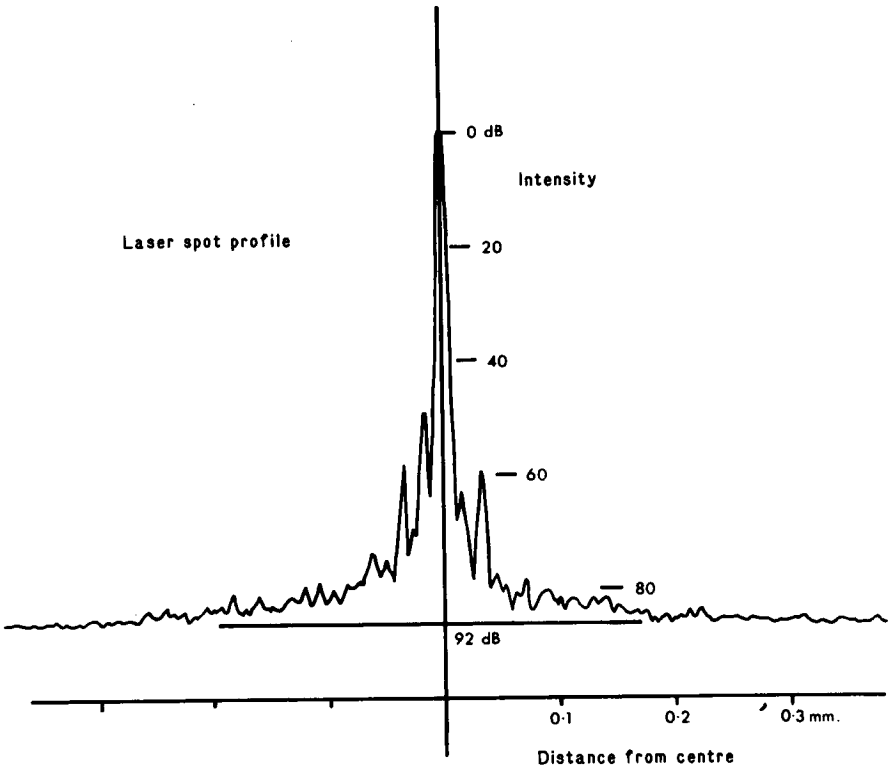

Figure 2.Laser spot profile.Intensity along x axis.

must be held flat on a glass platen. Extensive tests have shown the parafin Nonane is a safe and reliable optical "bond" between the glass and the film, surface tension holding the film flat and the liquid eliminating Newtons rings which can affect accurate photometry. The procedure takes less than a minute to carry out and totally removes the problem.

3.0 IMAGE COMPUTING HARDWARE

The APM system uses a very powerful on-line image analysis computer which was developed specially for the project at Cambridge. The computer was designed to convert a raster scan of the plate into image parameters without loss of information and was built only after image processing algorithms had been extensively tested in software simulations. Because of the raster scan process, each image is perceived as a series of slices from several or many scan lines. The data processing algorithms are therefore structured to work on a line-by-line basis with sufficient details about image position, shape and connectivity being saved to allow complete image reconstruction. The algorithms were implemented in a hardwired processor capable of processing the data as fast as we could scan it. The algorithms break down into three types:

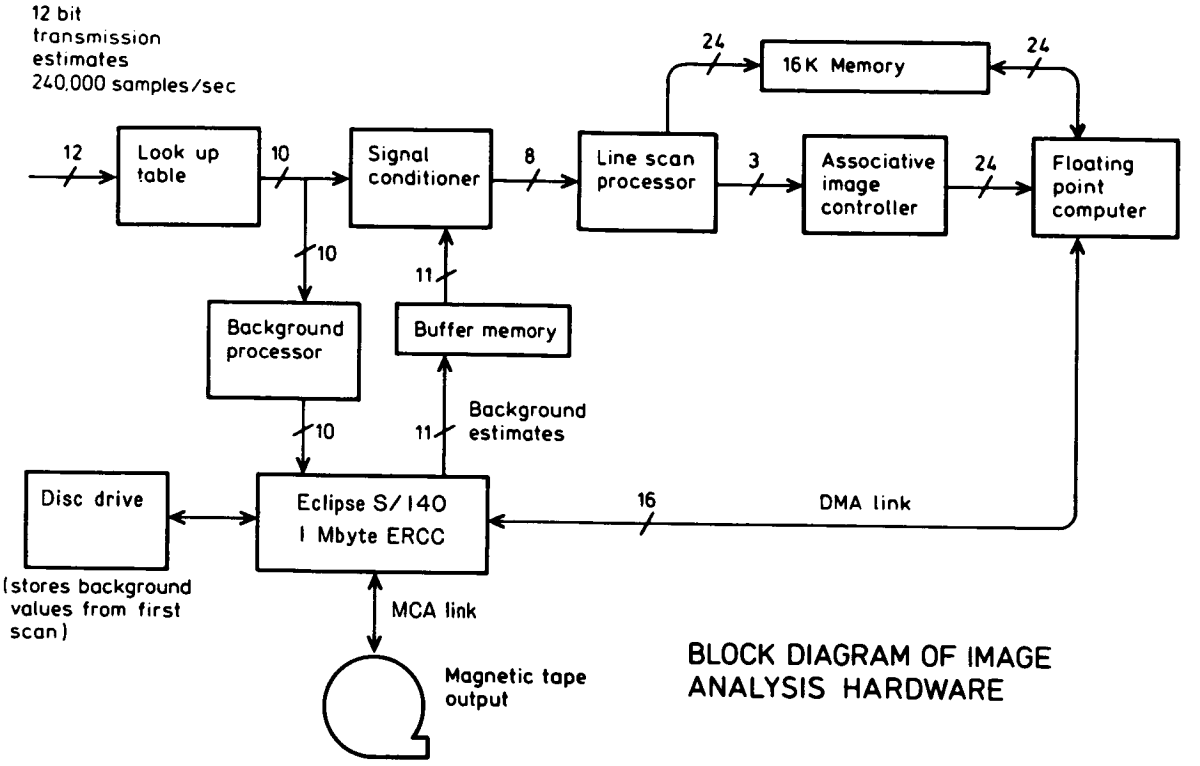

Figure 3.

i) Signal conditioning algorithms which reduce the amount of numerical processing the systems carries out, without degrading the image data.

ii) Connectivity algorithms that determine which data belongs to which images.

iii) Image parameter algorithms that work out the centre of gravity, integrated intensity and shape of the images.

SIGNAL CONDITIONING ALGORITHMS

All astronomical images are recorded superimposed on a background (or more strictly, a foreground) caused by the night sky and photographic noise. This background must be subtracted from the data set produced by the scanner,

and in general only intensities greater than a certain threshold level above the background are considered to belong to images. Even if no astronomical images were present, noise fluctuations appear above the threshold, and the nearer to the background the threshold is set, the more often the noise exceeds it. Unfortunately faint stars can only be distinguished from galaxies if the intensity profiles of these objects are measured to the faintest possible levels. Faint galaxies have a stellar (point-like) core with a faint diffuse halo. This requirement to measure image data as near to the background as possible means that we must not only measure the background extremely accurately, but also cope with the very large number of spurious 'noise images' which can be greater than 10^8/plate. In our system the background is measured using a special processor and noise images are removed by a non-linear shape filter.

BACKGROUND PROCESSOR

There is no unique definition of background in the presence of images. We derive maximum likelihood estimators of the background by forming histograms of the number of times a given intensity occurs within areas of 64 x 64 pixels. These histograms are obtained by a pre-scan all over the plate. The maximum likelihood estimator gives the most likely value of the mode of the histogram. Special purpose hardware derives these modal values and two dimensional smoothing is applied to these data points (10^6 mode estimates all over the plate). We also determine the width of the histogram background bell and this gives us a measure of how good an estimate each histogram can provide. We set a threshold at a fixed intensity above the local background, for every point scanned on the plate.

NOISE REMOVER

Because atmospheric and telescopic distortions smear the images of point sources of light, all earth based astronomical images are at least 1 arcsec in diameter, or about 40 contiguous pixels in area on a Schmidt plate. A geometric window filter is used which rejects 'images' of less than n-points in maximum linear extent ($0 \leq n \leq 6$). Images smaller than this are completely unaltered (Figure 3).

This noise filter is highly non-linear and its parallel nature makes implementations on commercial computers very slow. In our system 8 sequential lines (256 pixels each) of data (the current and previous 7 scan lines) are stored, together with a 1 bit binary image of the threshold data (1, if a point is above threshold, 0 otherwise), in a set of serial shift registers. The final 8 locations of each of the 8 shift registers, are fed into logic which detects a contiguous set of zeroes around small images within this 8 x 8 window. By clocking the data sequentially through the chain of registers, the window effectively sweeps over successive sample points on the plate. The logic removes small images as they are detected so that the data stream out of the last register is considerably simpler than the input stream. Note that the logic is so programmed that portions of images greater than the maximum size to be removed, are left totally unchanged by the process. This filter

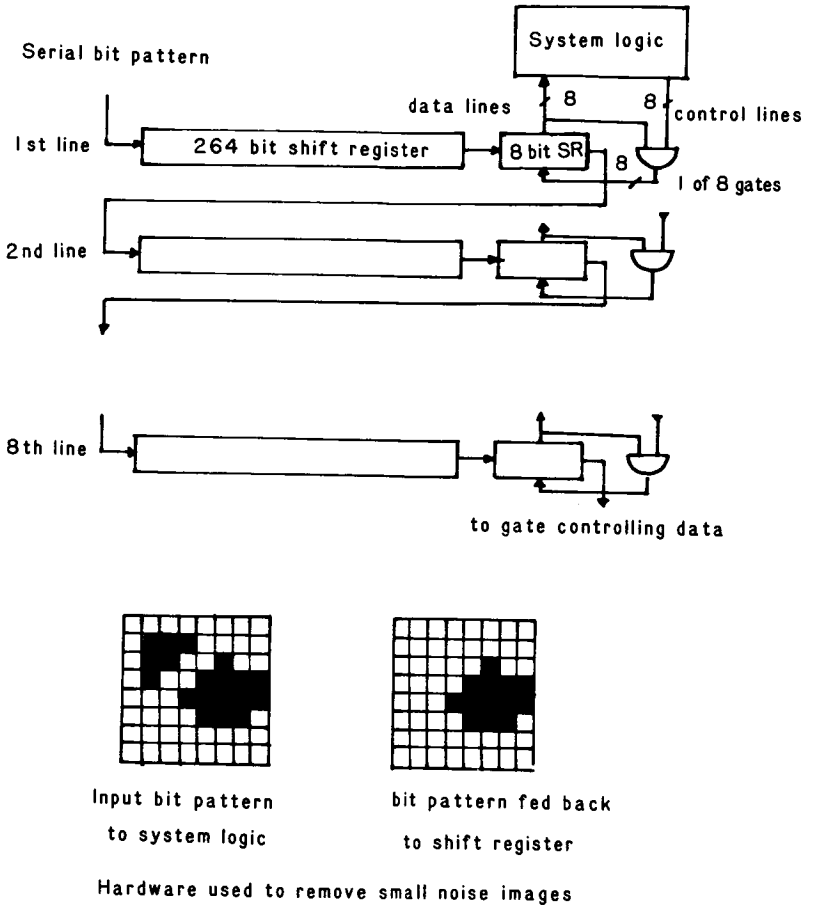

Figure 4. Schematic diagram of noise removal logic.

is crucial to the operation of the system since it reduces the number of spurious images that have to be processed, by a factor of 10 to 100.

SPOT SMOOTHER

The scanner uses a fixed spot size of 8 micron. By using a similar set of shift registers to the noise remover but attached to a set of adders boxcar smoothing is performed on-line to give an effective spot size of 8, 15 or 30 microns. This method of smoothing is more accurate than using a bigger spot size.

IMAGE RECONSTRUCTION

To obtain adequate slope information, the spacing between raster scan lines is much smaller than the size of even the smallest astronomical images.

Every image is therefore scanned in a number of 'slices', ordered in the data stream in a complex manner. Images are assigned numbers (or 'names') in the order in which they are first scanned and in general this is different from the order of termination. Collation of all the slices of a given image is a non-trivial process since noise can (and does) produce complex connectivity relations between segments on different scan lines. The collation algorithm must recognise 5 basic connectivity patterns. These are 1) Start of new image (or image segment); 2) Simple continuation of images; 3) Branching of image into 2 segments; 4) Merging of 2 image segments to form 1 image; 5) Termination of image segment. Some or all of these can conspire to form 'rings', 'halos', 'hairs', etc.

The processor which carries out this task works in parallel with a second processor that determines the parameters (centre of gravity, moment of inertia, etc.) of every image slice on the current raster scan line. These parameters are temporarily stored in a 16K x 24 bit work random access memory (RAM). This memory can hold 1024 blocks of parameters of data and serves to buffer the raster scan data (which is continuous) from the asynchronous operation of the rest of the data processing system. In function the memory acts as a whole set of First-In, First-Out (FIFO) memories, one for each image in the scan area.

The function of the Associative Processor is to store these blocks of data in the RAM and to keep track of the locations of all the blocks belonging to each image. The RAM contents are thus a highly dynamic data base reflecting the recent past history of the plate scan. We should note that after a merge has occurred, the name of the merging image section is in general changed so that we must be able to rapidly undate its connectivity list. Early designs used associative processing techniques to carry out this latter function. A linked list structure implemented in hardware is now used.

The Associative Processor has three linked lists: 1) The Block List: This is strictly a set of sublists, one for each separate image currently being scanned. Each sublist points to the set of memory block addresses containing parameter information from slices belonging to that image. The nodes of each sublist also carry pointers back to the image name which owns the sublist. 2) The Garbage List: A list of unused memory block addresses. 3) The Parent List: A list of unused image names. At the start of the scan the first list is empty and the other two are full. The Garbage and Parent lists each have a hardware register that stores the head of each list.

When a new image is detected, it is assigned a block address from the Garbage list and an image 'parent' name from the Parent list. Both lists are updated by changing the head register contents to the pointer to the previous head's successor. Every image has a number of blocks of data stored in the 16K memory, and a name and a linked list of all the associated blocks stored in the Associative Processor. Each parent (image) name has associated with it, two pointers; one that points to the block list head (LH) and the other to the block list tail (LT). All new images are given different parent names. If a merge occurs, the two parents must be combined.

This is done by joining the two linked lists (easy, because we know both the head and tail pointers of each), and sequencing through the block list of the merging parent, changing the parent name at each node. Special hardware is used to ensure this is carried out efficiently. When a termination is detected, the system checks to see if this is a final termination (it does this by keeping a count of the numbers of new segments, merges, branches and partial terminations in a register associated with each image name). If so, all the block addresses associated with that image are passed to the fourth and final processor called the Floating Point Computer (FPC), (functionally equivalent to many of the commercially available "Array Processors"). The FPC which is optimised for very fast bulk I/O overlapped with simultaneous floating and fixed point computations, takes all the appropriate data from the 16K RAM and combines it, to form for the one image; 1) Image centre of gravity; 2) 2nd moments about C. of G.; 3) Integrated intensity; 4) Areal profile; 5) Number of pixels. As each block is removed from the RAM into the AU, its block address is returned to the Collation Processor Garbage List for re-use. Finally, the image name is returned to the Parent List.

This hardware is fast and reliable (measured MTBF 2700 hours). It is built out of MSI TTL and contains 2500 chips.

ON-LINE COMPUTER

The APM machine uses an Eclipse s/140 to control the microdensitometer and to write the data onto tape or disk. The computer is sufficiently powerful that it can carry out most of the data validation so that the astronomer can check his data before storing it on magnetic tape. A wide range of image processing tasks can be carried out on the machine including comparison of galaxy pictures for supernovae detection, measurement of overlapping images, and detailed analysis of faint objective prism spectra.

OFF-LINE COMPUTERS

Off-line processing using a virtual memory computer is almost essential for efficient collation of plates and image processing of arrays of more than 256 x 256 pixels. Extensive software is available from the APM machine which can be run on a VAX computer. Collation of two plates takes 20 minutes CPU time and the APM unit as a whole uses about 1/4 of the time and resources of a fairly large VAX 11/780.

Peter Boyce: I'd like to take the Chairman's perogative to make a few comments, a few obvious thoughts from the standpoint of the person who was the funding Officer of the National Science Foundation about a number of these projects we've heard about today started some years ago. The focus of the meeting now is turning to where we should go from here and I think we should all keep in mind the differing scientific goals that various groups have which result in different functions that need to be performed by a microdensitemeter; the search function and the measurment function. Now, also different groups will have varying degrees of accuracy that they require out of their machines. So, I think in any consideration of new machines we have to consider the cost of development and construction in making the decision to go to a new machine. There is cost in money which is certainly not unlimited although NSF is looking at a very nice increase in 1984. I'm sure Wayne will tell you that the number of people in the astronomical community have already spend it 10 times over. Secondly, it always seems to be more appealing to fund a tomoscopic instrument than an instrument to analyze a photographic plate. And I think this is a problem on the part of a reviewer who tends often to neglect that once you have the photographic plate or the raw data you've only got part of the job done and the remaining part of analysis is often times harder. But there is another cost as well as money. Its the cost in people and time to complete these projects. Ed Kibblewhite mentions that he is been going at it for 10 years which would certainly be too long. But I think it is about normal for the various projects that are as complex as very highly accurate measuring devices that we are talking about. And, for example the, PDS is a very well defined machine, its fairly well understood. And, we must remember that has it taken 10 to 15 years or so of working with this machine to come to this level of understanding, to understand what the errors are when you are pushing it to or beyond its limit. And new machines will also require large amount of time to come to the stage where we currently are and I think this is one of the reasons that Barry decided to choose PDS in the space telescope project, because it's a machine that, he hoped at the time, was going to be very well understood and that he would have help from a community as large as this carrying the experiences to come out with the best possible measurements. And I think that we mustn't in the excitement to look at what's new overlook the real benefits that we have by sharing the experiences, and indeed perhaps even hardware and upgrading modifications that can be attained for the machines that we have, and together we may be able to do a lot of work better than if we start out to go separately in our own ways.

SESSION IV

Chairman: Peter Boyce

The Next Generation Microdensitometer

Astronomical photography from the ground and from space vehicles will be around for a long time to come. The spatial resolution and the photometric accuracy requirements will increase. What type of digitizing machines will be needed to process the astronomical plate of the future? What are the limits on speed and accuracy that are going to drive the design of the next generation high speed microdensitometer? Contributions which discuss these questions and related ideas or question the need for complete digitization of astronomical imagery are welcome.

A Next Generation Microdensitometer?

David G. Monet
Mount Wilson and Las Campanas Observatories
813 Santa Barbara Street, Pasadena CA 91101

ABSTRACT

Motivations for construction of a Next Generation Microdensitometer are presented and their effect on the NGM design is discussed. A prototype of such an engine has been constructed at KPNO. Its design and performance is reviewed.

I. Introduction

The topic of this session is "The Next Generation Microdensitometer". This paper does not pretend to review or preview this field. It is an attempt to explore the design considerations of the NGM and gaze into the crystal ball in an effort to see how currently available (or announced) products may influence its design. These comments are based on my perception of the scientific programs to be done with such an engine and are therefore reflect my own research interests. I can summarize the direction of my thinking in a statement and a question.

The NGM must be more than a digitizer.

Must a high speed NGM be a high precision NGM?

Before getting into details, I would like to offer the following comments as an amplification.

First, the name "microdensitometer" only partially describes the function of the NGM. Its real purpose is to do astronomy. Digitization of a photographic plate is only the first step. Image processing and analysis is the second step. The final step is to compare current results with previous work and reach conclusions of astronomical interest. The NGM must do as many of these steps as possible.

Second, the NGM must be of an "upward compatible" design. One's desire to produce the perfect microdensitometer must be tempered by the need to produce significant astronomical results as quickly as possible. Astronomy is a fast-moving and fast-changing science. Long lead times must be avoided. Although it may be slow, clumsy, and imprecise, a working prototype of the NGM should be constructed quickly. The final

version, complete with a wide assortment of bells and whistles, can be paced by fiscal resources and community response.

Third, the NGM will not last forever. Because of the rapid changes in technology, particularly in computing and data storage hardware, the half-life of the NGM's greatest productivity is probably only five years. This should not be interpreted as an invitation to mediocrity, but as a challenge to develop general strategies for plate digitization and algorithms for image analysis. The NGM is a particular configuration of hardware and software, and is profoundly influenced by current limitations. The experience gained through building the NGM must be transferable to future microdensitometers and to the general astronomical community.

Fourth, every effort must be made to minimize the cost of the NGM. Because it must include a fast computer for data analysis, the initial cost excluding microdensitometer is already approaching $500,000. The NGM will compete with other major pieces of astronomical instrumentation for funding. It must produce a large quantity of high quality scientific results to justify its cost. Because of its price and performance, the NGM must be a national facility and must serve a large user community.

Finally, a warning must be issued. The photographic plate is, depending on who one talks to, either dead or dying. Examination of the observing requests for the KPNO 4-m and Palomar 5-m telescopes shows little interest in continued astronomical photography by their user communities. For a large and ever increasing number of applications, modern panoramic detectors, particularly CCDs, appear to be demonstrably superior to any conceivable plate/microdensitometer combination. The determination of those areas of modern astronomical research in which the photographic plate is still the detector of choice is a critical prerequisite to the design of the NGM. It should not be designed (and probably would not be funded) to do those projects that should not or cannot be done properly by the photographic process. The NGM is not an all-purpose instrument that will appeal to the entire astronomical community.

Sections II and III present a review of the future. They attempt to identify the scientific goals of the NGM and, to my limited ability to predict the unpredictable, discuss possible design constraints on the NGM. Section IV discusses my own efforts at solving some of the problems posed in Section III. Section V discusses some current technological advances that may affect the NGM design.

II. Possible Uses For a Next Generation Microdensitometer

Scientific justification is the first and most important part of the NGM project. In evaluating what scientific projects should be done photographically, one must understand the alternatives. Currently, Charge Coupled Devices (CCDs) are the principal panoramic detectors in use on large telescopes. Most observatories have (or are trying to start) CCD development or evaluation programs. While not perfect, currently available CCDs have already demonstrated excellent astrometric and photometric performance. By popular consensus, their chief advantage is that their output is digital and that a microdensitometer is not needed!

The best of the currently available CCDs show 6 electron noise with 100,000 electron full-well, no detectable deviations from photometric linearity, and peak quantum efficiencies approaching 80%. While such performance is currently considered exceptional, average device performance is improving and will continue to do so. Currently available CCDs have between 200,000 and 600,000 pixels. Unfortunately, the number of pixels is not increasing at the same rate as their quality. Commercial television markets are satisfied with 512x480 formats. High resolution television, still in its formative stages, will probably require formats with 1024x1024 pixels. GEC (England) is discussing a 1500x1500 device, but these have yet to be evaluated by the astronomical community.

With those properties, CCDs seem to be the detector of choice for faint object imaging (because of the low dark current, low read-out noise, and high quantum efficiency), bright object imaging (because of the large dynamic range), astrometry (because geometric properties are inherent and repeatable), and photometry (because of the linear response). Indeed, the only real disadvantage of CCDs is their small format. With coarse sampling, an 800x800 CCD covers only 0.05 square degree of sky. In attempts to overcome this problem, many groups are using CCDs on telescopes that are either fixed or clocked at a rate different from the normal sidereal rate. The CCD is clocked at the telescope rate so that the charge image of the sky is stationary. This long picture (stripe) is read at a rate of a few rows per second. Preliminary results show that many of the flat field processing problems associated with device "fringing" seem to disappear, although published astrometric and photometric results are few.

The preceding remarks are meant to be realistic and not pessimistic. Photographic plates appear to still be the detector of choice for programs that require large numbers of pixels. Such programs can (must?) tolerate less than perfect detector response, although certain minimum standards must be maintained. Because photography was the standard of the industry for so many years, projects requiring a large included epoch difference can be done photographically. The lack of adequate attention to the archiving current CCD observations is a major problem.

With these preliminaries concluded, the following projects suggest themselves. They appear to be both of great astronomical importance and to belong to the realm of photographic astronomy. Not only is the NGM impersonal and untiring, its detection algorithms may be statistically modeled and corrected for certain selection biases.

1) The Color-Magnitude-Proper Motion diagram of the Galaxy. Many all-sky surveys have been done and the Palomar/National Geographic Sky Survey will be repeated. There is the potential of increasing the Galactic stellar data base by 2 orders of magnitude or more. The various kinematic and photometric populations can be studied with an unprecedented statistical accuracy.

2) The Long Term Study of the Sun. An extensive photographic archive of the sun exists. Accurate, impersonal measurement of spots and other solar phenomena offers an unparalleled opportunity for studying solar behavior.

3) The Extra-Galactic Distance Scale. Variable stars are excellent extra-galactic distance indicators. Because this fact has been known for a long time, extensive photographic studies have been undertaken. Accurate, impersonal detection and monitoring of these stars in nearby galaxies awaits only the machine to reduce the data. Such a project could also assist in the detection of stars of particular photometric properties, such as the brightest red and blue supergiants.

4) Objective Prism Surveys. The search for stars with particular spectral properties is effectively done with a Schmidt-type telescope and an objective prism. Automated pattern recognition can supply approximate spectral types for a large number of stars.

5) A Faint Coordinate System. With HIPPARCOS, an inertial coordinate system will be established to 12th (and occasionally fainter) magnitude. To intercompare observations of cosmological

significance, an accurate coordinate system must extend to 20th magnitude or fainter. This will assure that adequate reference fields can be found in small-field large-aperture telescopes. Precision measurement of photographic plates seems to be the only practical way to process the plethora of stars in the catalog.

6) Counts and Classifications of Galaxies. This is a challenging problem because of the diversity in the morphology of galaxies. Coverage of a large portion of the sky is needed and the counts must be done impersonally.

Clearly, there are other areas for research that have been omitted or slighted. What is important is that there are several classes of extremely important astronomical problems that are, and will apparently remain, the sole property of photographic astronomy. These areas of research are the justification for the NGM. On the other hand, the photometric or astrometric study of small numbers of stars, galaxies, or spectra is no longer in the domain of photographic astronomy. Indeed, many of the projects that justify the NGM provide only finding lists of objects for further study.

III. Possible Design Criteria For The NGM

In light of the preceding remarks, the following design criteria seem important. Where performance specifications are given, they are intended to be guidelines and not absolute requirements.

1) Speed. The entire thrust of the Sections I and II points towards a requirement that the NGM be exceptionally fast. It appears that its great contribution to modern astronomy will come from low precision surveys and not from high precision microdensitometry. Given the great pressures (fiscal, peer, etc.) to produce results, the NGM must be designed with the man/machine interface in mind. I consider a time of about 3x10**13 microseconds (1 year) to be a practical upper limit for the actual measuring portion of a particular program. Significantly longer times will restrict users to those with established careers. As there are 5x10**11 square arcseconds on the sky, one must consider schemes that measure and reduce 1 pixel every 60 microseconds (on average). Even with today's computers, this is a non-trivial data rate.

2) Accuracy. As mentioned previously, the photographic plate is no longer the detector of choice for projects needing extremely accurate measures of a few objects. It must also be

remembered that the digitization of the image is only an intermediate result. What is desired is object detection and parameterization (position, magnitude, shape, etc.) within the framework defined by the scientific objectives of a particular program. Once the minimum accuracy has been attained, additional efforts should be made only so long as the requirements of time and budget are not compromised.

It is difficult to quantify the minimum acceptable accuracy because it varies with each program. For example, photometric segregation of "interesting" objects from the field requires only enough astrometric accuracy for identification. On the other hand, searches for nearby stars can tolerate crude photometry but require high astrometric accuracy. Separation of the various kinematic and photometric populations of the Galaxy requires excellent photometry and astrometry. For the sake of completeness, I think that a target accuracies of Ø.1 arcseconds for astrometry and Ø.1 magnitudes for photometry are reasonable. This level of performance should be maintained over a range of at least 5 stellar magnitudes. For the Palomar Schmidt, Ø.1 arcseconds corresponds to 1.5 microns. I know of no simple translation between single pixel densitometry and the accuracy of the derived magnitude for a stellar image. These specifications refer to the internal units of the NGM. The transformations to external units, such as RA, Dec., and UBVRI colors, is a separate non-trivial problem. I consider such transformations separately because they are not unique to a particular realization of the NGM hardware and software.

3) Automation. The engine should require a minimum of human intervention. The processing speed requirement leads naturally to a stage that can accommodate many plates at once. Stage sizes of 28x28 inches are commercially available today. Assuming Palomar Sky Survey plates, this stage size allows about 12 hours of unattended operation. Substantially larger stage sizes may not be cost-effective. Similarly, the processing software must require minimal operator intervention. Quick and easy changes in the detection and measuring algorithms will be needed.

In summary, the NGM must
1) demonstrate proof-of-principle now,
2) be constructed in less than 6 months,
3) measure the entire sky in less than 12 months,
4) meet the previously stated accuracy requirements, and
5) cost less than 1 million dollars including computer.

The similarity between this list and the requirements for the Advanced Guide Star Selection System for Space Telescope is not a coincidence.

IV. ACME: The KPNO Prototype NGM Experiment.

A machine that satisfies the design criteria presented in Section IV appears to be possible. I began numerical and laboratory experiments along these lines in March 1982. These were culminated by a four month visit to KPNO where a working prototype of the NGM was built around the KPNO 2-axis Grant measuring engine. The code name for this project is ACME (the Astrometrically Compromised Measuring Engine).

The requirement for extreme digitization and processing speed forced ACME to have two unconventional properties. First, there is no intermediate archive of the digitized picture. It is placed in computer memory, processed, and then erased. This strategy is necessary because I do not have access to any computer that can sustain the I/O transfer rate needed to write the images to tape. ACME is, by design, so fast that the time needed to reference, mount, and read a tape is comparable to the time needed to remeasure the plate. A redundant tape archive is simply too expensive, both in time and dollars.

Second, ACME ignores scattered light. Almost by definition, microdensitometers should take great pains to measure the light transmitted through a well-defined area of the plate and reject light scattered by adjacent areas. This forces microdensitometer designs into elaborate mechanical and optical configurations. These become extremely complex when high speed is needed. Instead, ACME uses a CCD television camera as a detector. The RS-170 video output is connected to FrameGrabber attached to the host computer. FrameGrabbers (real-time television frame digitizers) have recently become available from a wide variety of vendors. These devices digitize the incoming television signal to 8 or 10 bits and place the result in the refresh memory of a video display peripheral. This occurs in real-time: thirty 512x512 pixel images per second. This provides efficient and cheap digitization of images at a rate consistent with the ACME specifications.

The choice of a 2-dimensional CCD television detector instead of a 1-dimensional line scanner such as those produced by Reticon was made for the following reasons. First, the CCD is free from many geometric errors present in line scanner data. The geometry of the 2-dimensional detector is fixed over the 512x480 format. Only a single measurement of the relative position of the camera is needed to convert chip to plate coordinates. The 1-dimensional detector needs this information at the start of each scan line. Should mechanical jitter become too large, the resulting image must be repixelized before

analysis. Repixelization is time consuming. Second, I know of no commercially available peripheral equivalent to the FrameGrabber for digitization and storage of 1-dimensional scanner data. While such a device is not complicated, it represented more hardware development than could be done in the time available for these experiments. Finally, the picture produced by a line scanner is inconveniently large unless the scan is started and stopped many times. At the data rates envisioned for the ACME, all images must be in computer memory. There is no time for disk access. The 512x512 format is convenient; the current code requires about 2 Megabytes. Images of size 17000x1024 pixels (typical for a line-scan of a Palomar Sky Survey plate) require prohibitive amounts of memory.

Because of the blatant disregard for scattered light, a prototype of the ACME was needed to evaluate its astrometric and photometric performance. The prototype detector was an old commercial RCA CCD TV camera. Through the kindness of the WF/PC, the host computer was the WF/PC VAX 11/780 in Tucson. It has 3.5 Mb of memory and a Grinnell GMR270 image display. An 8-bit video digitizer board was acquired for the GMR270. The KPNO site was chosen because of the WF/PC VAX and because of the (undersubscribed) 2-Axis Grant measuring engine. The Grant was used for the plate motion stage, and a Z8571 microprocessor was installed so that the VAX could read Grant as if it were a terminal. A human operator was needed to operate the Grant engine because upgrading the stage motion to computer control was outside the scope of this project. KPNO kindly ran 3 RS-170 and 2 RS-232 cables from the VAX to the Grant. Jim Westphal made the DownLooker: a simple bracket that holds the TV camera, an enlarger lens, and a 90 degree flat mirror. The DownLooker fits in the hole normally used by the Grant's lens. The conversion from normal to ACME mode takes less than 5 minutes.

Much of the necessary image processing software has been written. While one should not be preoccupied with execution speed during software development, the ACME timing requirement precludes such traditional approaches as the method of least squares. Consider the time budget. At 20 microseconds per pixel to expose, FrameGrab, transfer, flat field, and detect, our original 1 year time allocation is 1/3 spent. If one allows a similar amount of time for post-measurement processing such as removal of double detections, plate flaws, etc., sorting, and assembling the catalog, the remaining 1*10**13 microseconds is available for detailed processing of each of the entries in the detection list. If we expect 1*10**9 detections, then there are 10 milliseconds to process each entry. This number must be interpreted statistically. Since the apparent stellar luminosity

function is steep (there are many more faint stars than bright stars), one must design the software to handle the typical catalog entry, the faint star, reasonably quickly. One may use leisurely algorithms for the analysis of bright stars because there are so few of them. Given the VAX 11/780 class computer, it appears that algorithms requiring matrix inversion, such as the traditional least square fit of a Gaussian to the marginal distributions, require too much time.

The code is divided into three segments. The first finds candidate objects. Because this code must examine every pixel, it does only minimal processing. It produces a list of approximate positions (typically +/- 4 pixels) and crude magnitudes (the number of ON pixels). The second phase of analysis improves the estimators for position and size (+/1 1 pixel) and provides an estimator of the local sky background. The final phase of analysis computes accurate centers, magnitudes, and simple classification parameters such as image roundness and brightness gradient. Establishment of the analysis hierarchy is critical. One must eliminate as many "unintersting" pixels as possible so that the remaining time can be spent processing "interesting" detections. The current version of the code requires about 5 milliseconds to process the typical faint stellar image.

The success of the prototype ACME is encouraging. A field near NGC2419 was examined. This should be a typical "poor" field because of the onset of image crowding because of its proximity to cluster center, and because it lies about 3 centimeters from the edge of the Palomar Sky Survey plate. Photometry was done by comparing the internal ACME magnitudes from the POSS-O plate with the B magnitudes published by Harris and Racine (1975 Ap.J. 196, 413). The ACME is reliably detecting stars of B=21 and a quadratic fit between instrumental and known magnitudes shows a scatter of Ø.16 magnitudes over the range B=2Ø to B=14. Photometric quality is degrading quickly for the faint stars: the scatter is Ø.7 magnitudes at B=21. Astrometry between POSS-O and POSS-E plates yields an rms scatter of Ø.15 arcseconds (2.2 microns) for the 2Ø stars in common. About 5 seconds elapse between to command to begin the TV integration and the end of the processing. The result is a list of X, Y, magnitude, roundness, and image brightness gradient, sorted in X and corrected for the relative scale and rotation of the TV camera.

V. General Comments and Conclusions

The ACME prototype suggests many areas for further study. The major question, the effect of scattered light on photometric and astrometric precision, has yet to be answered. Measures based on PDS scans of other fields showed that the astrometric precision of the plates was better than ACME produced. Unfortunately, this is probably more a function of transmission vs. density weighting than of scattered light. Figure 1 shows typical row plots through a 103a-0 image and a IV-N image taken by ACME. The grain noise of the 103a-0 is readily seen. This noise appears to be less severe when viewed in density units. Perhaps a transmission to pseudo-density transformation would help the ACME algorithm. One can also see that there are only about 100 data numbers between the black and white pedestals of the TV image. The bright star in both scans is truncated by camera electronics and not by scattered light. Were the camera not on loan from the WF/PC, this would have been fixed.

The true accuracy of the ACME processing algorithms is not known. As Figure 1 shows, the POSS plates provide an extremely noisy environment for precision work. There is, of course, no need to confine the analysis portion of the ACME to photographic data. By the time the code is executed, the photograph is just a 512x512 array of 16-bit numbers stored in computer memory. Also, there is no need to limit the ACME to POSS plates. By changing the lens in the DownLooker, most any plate can be matched to the pixel size of the TV camera.

Most of the ACME is software not hardware. Because of this, it can be quickly and cheaply reconfigured for different tasks. For example, the ACME prototype stressed speed instead of accuracy. Should one be interested in projects with a scope of less than the entire sky, more elaborate processing schemes can be incorporated. The current ACME code has provision for 1-dimensional marginal distribution fitting. This increases the astrometric precision to about 1.8 microns for the NGC2419 field but slows the processing speed by almost an order of magnitude.

The ACME is fundamentally limited by available computing power. Fortunately, this is an area of intense commercial interest and fast-changing technology. Array processors are now available that can do host-independent I/O (so that the CCD can be read directly without using the RS-170 video encoding) and can do vector processing (to do the flat field correction). In addition, currently available microprocessors such as the Motorola 68000 and the National 16000 have speed approaching that of VAX-class processors. The next generation devices, such as

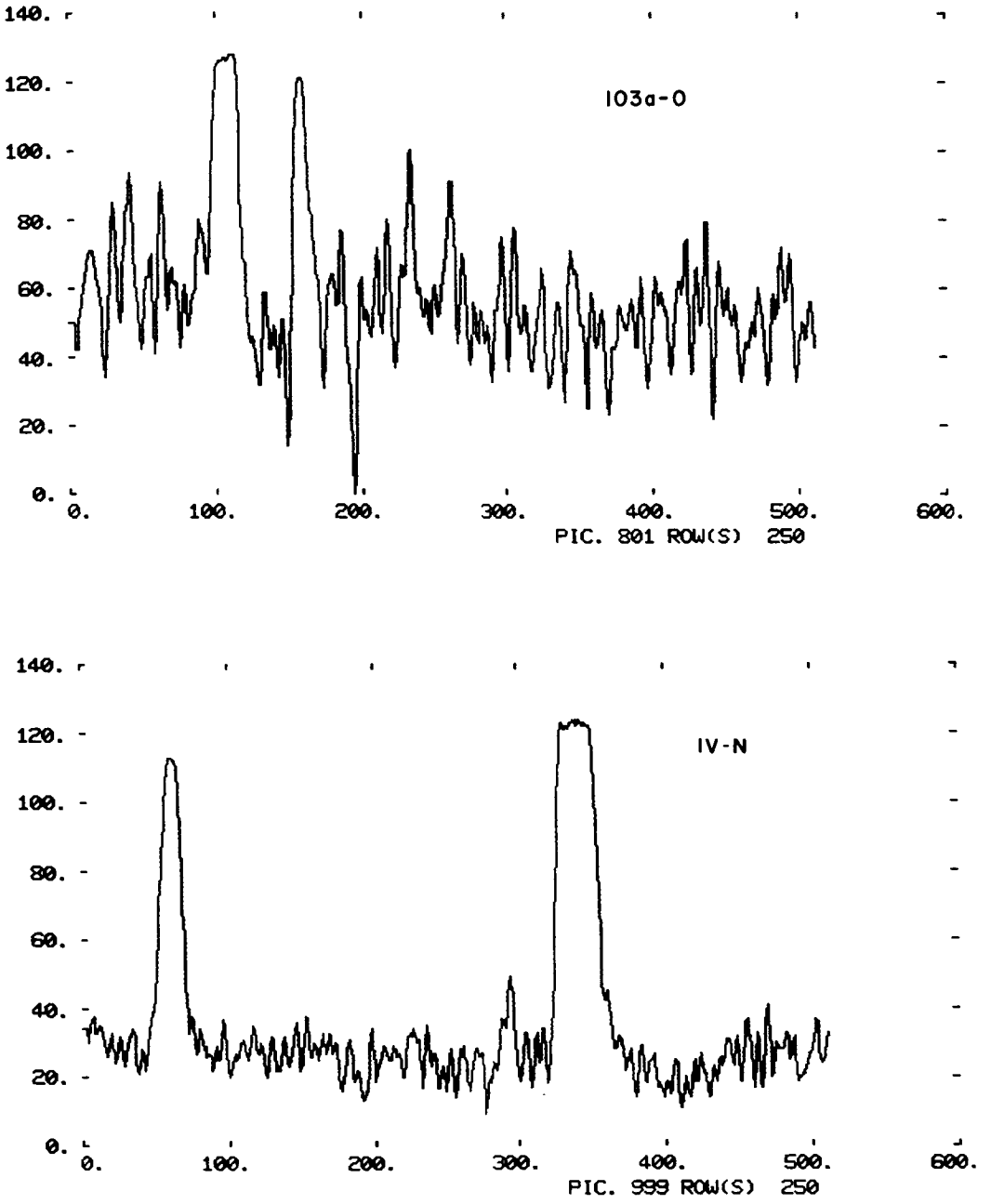

Figure 1. Sample ACME row plots for IIa-O and IV-N emulsions.

the 32132, may provide the necessary computing power for a fraction of the cost. Clearly, if more computing power is available, more detailed processing can be done in the same amount of clock time. Because of the need for stage or camera motion, about one second will always be available for numerical analysis.

The ACME is inexpensive. In a typical university astronomy environment that includes a minicomputer and a (probably decaying) 2-axis positioning stage, $15000 buys a stand-alone FrameGrabber and a precision CCD TV camera. Processing may be slow, but science can be done. For about $100,000, enough front-end computing hardware can be bought to allow processing a 512x512 picture in about 2 seconds. For $250,000, a 1-meter square granite air-bearing XY positioning stage with Michelson interferometers and auto-focus can be purchased. Because of its design, the ACME approach can be built from commercially available "off the shelf" pieces. This means that a minimum of time can be spent building the machine and most of the time can be spent doing science.

I would like to thank Jim Westphal and Roger Lynds for their continuing support. I would like to thank KPNO for allowing my extended visit. Useful conversations with Earl O'Neil, Dave Koo, and Andy Jankevics are also acknowledged.

Boyce: What is the ratio of time between the motion and the actual data taking.

Monet: It turns out that if we did not have electrical problems we could grab in about a 1/30 of a second. There is enough signal to noise ratio because the light bulb is bright enough and all the pixels are integrating in 1/30 of a second. The NNTT boys were testing their Hartmann screens with really bright lights and we're holding four hundredth's of a pixel for these very high signal to noise applications with a single frame grab. So there is plenty of signal to noise in a CCD television camera to hold 8 bits.

What's the translation time between frame grabs?

Monet: I was assuming one second to move and 1/30 of a second to expose, which is roughly one second

Crane: Granted that we want to ignore the scattering problem.

David: I don't want to, its the only thing I can do. You know, we're not done yet. There probably are ways of making microcollimators. I think that we can do some work there. I can do magnitudes at this level. I mean, at some point its the astronomy that drives the whole thing and I don't give a darn about the pixel, the pixel digitization: as long I can hold reasonable stellar magnitude and stellar positions. For surface photometry I suspect all bets are off except for finding the fuzzy objects and giving yourself a finding list of the 30,000 objects per Schmidt plate that you'd like to go back and do reasonably. Like I said the CCD television camera on a PDS is not really a dumb idea if you have a spare of 10 G's in your cash drawer. Its not bad. Very efficient. The first scan of the plate will take something like 20 minutes. Then you can go back and piece by piece digitize those pieces you were interested in. Far faster than digitizing the whole plate: miles faster.

Boyzan: How do you determine your errors and what is the difference in your accuracy when you are working in a crowded field versus an uncrowded field?

David: How is the accuracy determined? I plotted my internal magnitudes versus Harrison-Racine photometry which is presumably good to some factor of three or five, something much better than that. So I am essentially saying this is the external world. I didn't even put in color terms, okay. Its "O" plate versus "E" plate.

Boyzan: Can you run one plate twice and see what differences result .....

Monet: Oh, that is a factor of five better than the numbers I quoted. The astrometry came from taking the "E" plate and the "O" plate and mapping them on to each other. All of that noise is grain noise. You can barely see the system noise in that particular slide. But the internal errors are far better. The repeatability is far better. What's killing me is the external errors from the plate. Now, where this cross over point is I don't know because I haven't done enought testing on it with high quality emulsions. Certainly on the sky survey I am limited by grain noise, and locally determining the sky and all sort of "ick" like that. As far as the photometry in crowded fields I have an auto aperture photometer. I do not believe yet in fixed aperture photometers. We do a half width at full max each of the four directions. Chose an Aperture it then does a look up table go to on the basis of this guess for how the image is, and after transforming the full width at half max to the full width at zero max which took several weeks to understand how that goes, you then go and do the density sum inside that digitally circular aperture. It's not, it sort of ragged, but it's a well defined aperture based on size of the image just computed from the full width at half max. And you have the shape parameter left over. If it truly is a double which you've got. These things will come out as being highly non-round which is presumably a flag which says don't believe this color or this magnitude.

Boyzan: You have to do a lot of flat-fielding.

Monet: Only the CCD.

Boyzan: How effective you can it?

Monet: It costs me two seconds.

Q. **Boyzan:** What about backgrounds?

A. **David:** The detection threshold pulls off with giving QIO's and unibuses and all sorts of "ick" you don't want to hear about. We have to do 17 separate calls to read a frame buffer via DMA, which means with dual ported memory you save huge amounts of time. We take something like from each 1/17 of the picture, they are not equal pieces okay, we take two rows, do a median filter on that for a zeroth guess of the sky, base our detection threshold on epsilon above that. We put temporal filtering on our guess that if all of a sudden it gets something really off the wall for that sky, it blows a whistle and says do something else. I mean that we can impose constraints with software detection limits essentially set empirically from graininess of what we are dealing with. If we run across Sirius or something like that, he will ring a bell and say hey, the sky is 40 data numbers from the last time you gave me sky which is unphysical. Okay, that sort of stuff can be built in with just a few lines of coding. The minimal array that's once per picture, not once per star, and not once per pixel.

Boyzan: That leads to my next question. How stable is your flat field and your gain response?

Monet: On the CCD camera I don't really know. In general an astronomical CCD is one we use for the parallax program is stable over six month time scale. If the flat field holds.

Boyzan: (inaudible)

Monet: You bet, its a nice hunk of silicon. The Westphall chips are somewhat better than that. I assume that you will flat field once every couple of hours. I mean, once you have a reasonable way of doing that. Certainly, every two hour time scale of reasonably isothermal conditions which the engine has to have because of other contraints we've heard about before. But, CCD's are pretty good.

A PRELIMINARY ANALYSIS OF A DIODE ARRAY FOR DENSITOMETRY

Kenneth A. Janes
Boston University

ABSTRACT

A diode-array based image digitizer manufactured by the Eikonix Corp. has been tested to see if it can be adapted to the exacting requirements of astronomical densitometry. As the device is presently configured, a dynamic range of 400:1 can be achieved routinely, with a positional accuracy of 2 microns or better. An area of 2048 X 2048 pixels can be scanned in about 5 minutes. Preliminary tests indicate that several relatively simple enhancements can improve both the photometric and the positional accuracy of the device.

I. Introduction

Most microdensitometers measure the transmission of a photograph one point at a time using a single small spot of light; to measure a larger area of the plate or a succession of star images, the plate (or the spot) must be scanned or moved in some fashion. Consequently, its speed of operation is limited by the mechanical response of its moving stage and by the amount of light reaching its photomultiplier. One of the possible alternative approaches is to use an array detector to sample many picture elements simultaneously. A solid-state diode array would seem to have some considerable attractiveness for extracting the information from a photograph since an array is extremely predictible dimensionally (at least in one dimension in the case of a linear array), and is capable of excellent photometric precision. There are, however, some disadvantages to using a diode array as a densitometer:

1) They have a somewhat limited dynamic range.

2) There is inevitably some scattering of light from brighter regions to fainter ones.

3) There may be diode-to-diode crosstalk and saturation effects.

4) The order of magnitude potential increase in scanning speed will necessitate even more efficient reduction procedures.

Although some of these problems have been examined from an astronomical perspective (see, for example, Swaans, 1979) there still remains some question whether the deficiencies may negate the potential benefits of diode

arrays or how much diode-array based systems may be improved. If they do become practical, they could be of considerable importance for large scale photometric and astrometric surveys such as the Guide Star Selection Program of the Space Telescope project.

II. The Eikonix 78/99 Digitizer

The Eikonix Corporation of Bedford, Mass. manufactures a variety of devices for image processing applications, including diode-array based scanning digitizers. The heart of these digitizers is a linear Reticon diode array (typically 2048 pixels long) which is mounted on a small precision stage to provide scanning perpendicularly to the array. Imaging onto the array is accomplished using a high-quality enlarger lens designed to be used at conjugate ratios near 1:1. The array, its stage and the basic driving circuitry for the array are mounted in a compact camera head. For the model 78/99, light sources, condenser assembly and viewing stand are to be provided by the user.

The signal from the diode array is digitized in either 8 bits or 12 bits through a fast A/D converter. The array is uncooled; integration times range from 12 to 48 millisec. The raw digital signal is sent to a control console where several on line processing tasks can be done. The standard operations include corrections for the diode-to-diode variations in gain and dark noise. After the bias and gain corrections, the signal can be sent to a host computer or to an MC-68000 microprocessor mounted in the control box. The instantaneous output of the array (as modified by the above functions) can be displayed on an oscilloscope. Figure 1 shows a schematic layout of the Eikonix system in use at Boston University.

Virtually all operations of the Eikonix can be controlled by the host computer. Device drivers and fortran-callable routines are supplied. Simple programs can therefore be written and modified at will to handle whatever scanning applications are desired. As implemented at Boston University, the output of the Eikonix is directed through a UNIBUS interface into a VAX 11/730 and programs have been written to operate the digitizer and analyze both spectroscopic and photometric data. In a typical situation with the optics arranged to give a 1:1 conjugate ratio, a 30 mm square area of a plate can be digitized into a 2048 X 2048 array in about 5 minutes. In contrast, a similar scan would take several hours on a PDS machine.

The Astronomy Department of Boston University has acquired an Eikonix 78/99 digitizer for a project to monitor the ionospheric airglow. For the airglow project which involves large numbers of relatively low-contrast 35-mm images, this device is ideal, and has already lead to useful results (Mendillo and Baumgardner, 1982). The purpose of this paper is to discuss the potential of the diode-array image digitizer for astronomical applications and to describe some experiments to relieve some of its known limitations. The ultimate aim will be to apply the device to large scale stellar photometric surveys.

Figure 1 - Schematic of Eikonix System

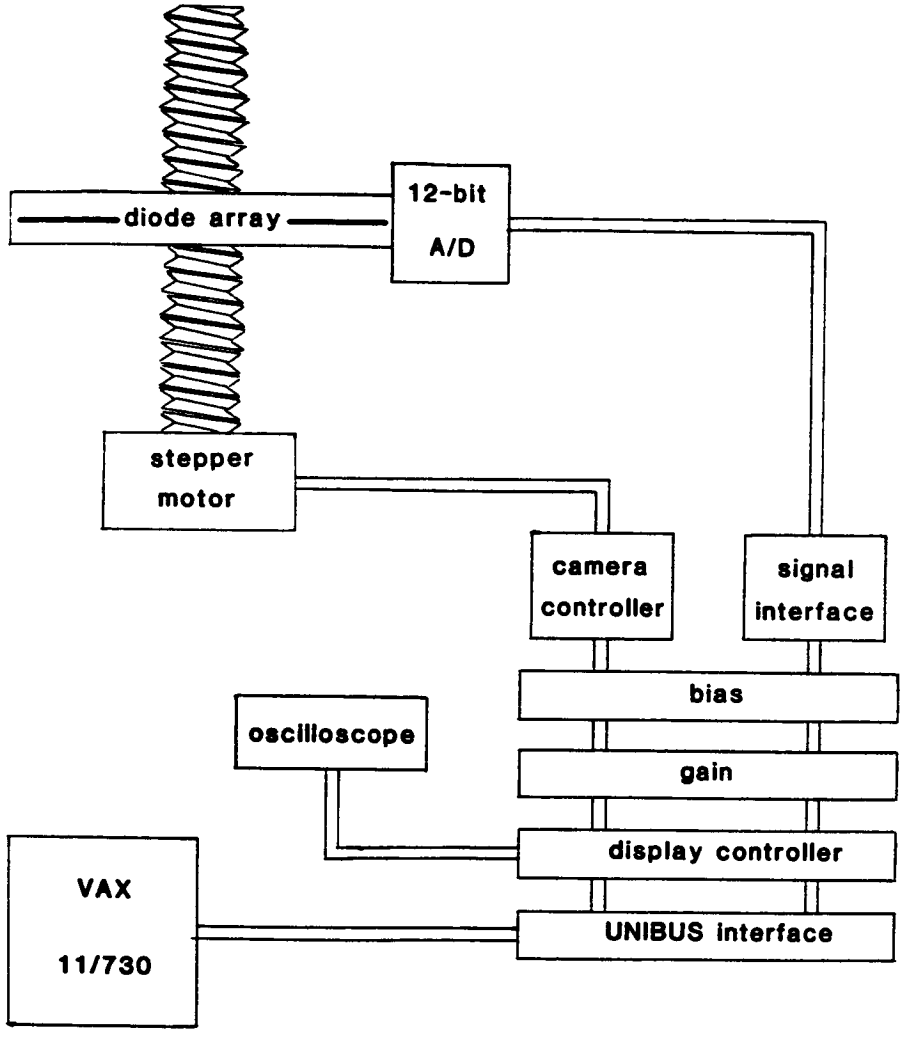

III. A Preliminary Analysis

Since the Eikonix digitizer is a working, commercially manufactured device, it is possible to bypass the lengthy process of building and debugging computer interfaces, writing device drivers and doing other such important, but time-consuming tasks, and get right to the question of evaluating its suitability for astronomical applications. The principal factors which must be considered are the dynamic range, positional accuracy, resolution, scanning speed, possible saturation effects and the problem of scattered light. A few simple experiments not only show what the present capabilities of the Eikonix are, but also indicate possible ways to improve the present device. The results of the tests are summarized in Table 1, along with the

corresponding characteristics of the PDS machine (as determined from Perkin-Elmer ads and private conversations) and estimates as to the ultimate capability of the existing Eikonix digitizer.

Table 1 - Capabilities of the Eikonix

	.....Eikonix.....		PDS
	Actual	Potential	Typical
Dynamic Range.....	400:1	>1000:1	>10000:1
Positional accuracy.....	<2 microns	<1 micron	1 micron
scattered light.....	considerable	moderate	negligible
Resolution.....	1.5 pixels	1 pixel	1 pixel
Scanning speed (at 2048 pixels per line).....	7 lines/sec	10 lines/sec	3 sec/line

a. Dynamic range and photometric stability - The specification sheet for the Reticon "H" series arrays claims a dynamic range of about 375:1 when measured as the ratio of the saturated output to the peak-to-peak fixed pattern noise or 3000:1 when the saturated signal is compared with the rms noise on each pixel. When the dark noise of our array was tested, the rms variations of the noise on a single diode was typically 10.5 on a scale of 0 to 4095 (i.e. 12 bit digitizing), corresponding to a dynamic range of about 400:1. When the light source was set to give an average reading of near the maximum value of 4095, the average of the rms fluctuations in the signal on each pixel was only slightly larger. The fact that the rms variations per pixel do not scale with the size of the signal suggests that the fluctuations in the signal are due primarily to such things as noise in the amplifier or the A/D converter or to variations in the light intensity, rather than to simple dark noise. The observed fluctuations are at least random; when a large number of integrations are averaged together, the noise reduces in approximately a square root of n fashion.

It is well known that the response of a Reticon array varies substantially from diode to diode. One of the nice features of the Eikonix system is the reliable procedure for correcting for bias (dark noise) and gain variations. In one test, the diode-to-diode variations in a small section of the array were on the order of 2 percent (see figure 2); after correction for bias and gain, the variations were reduced to about 0.1 percent (when multiple integrations were averaged).

Figure 2 - Bias and Gain corrections

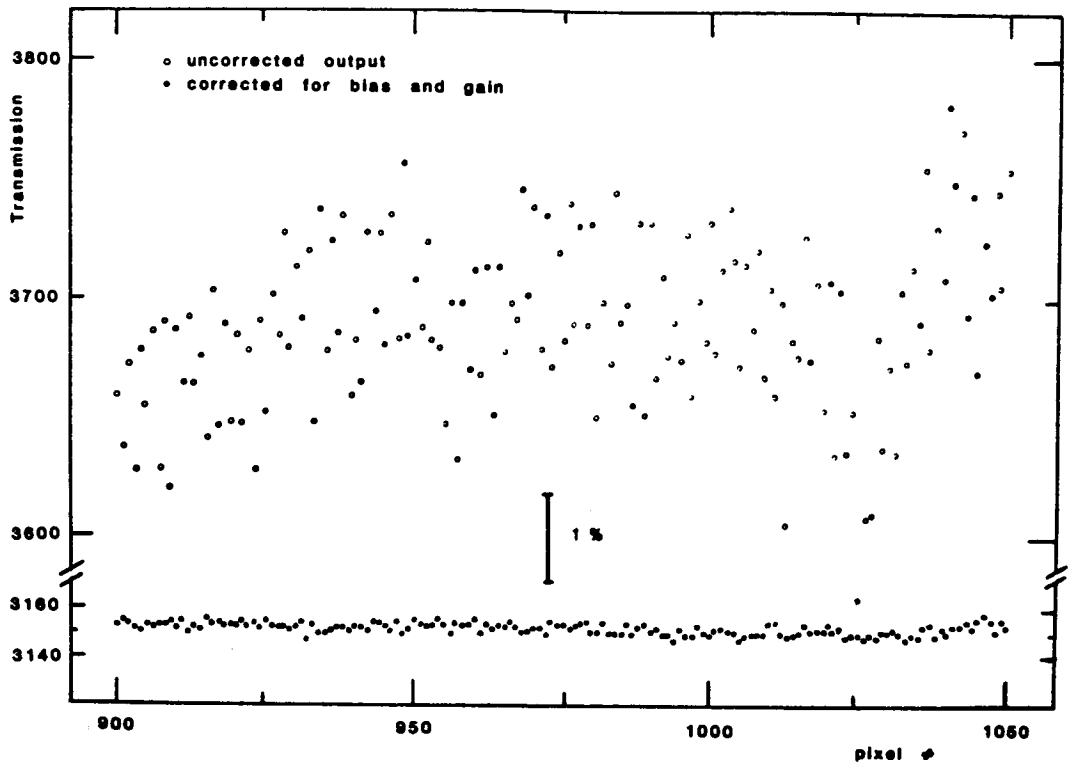

b. Positional Accuracy - Although along the array the dimensional stability and repeatibility should be essentially perfect, in the other dimension, a number of factors could seriously degrade the positional accuracy: the precision of the diode stage, aberrations in the optics and the overall mechanical rigidity of the entire system are obvious factors. Unfortunately,at the present time, the device is mounted on a Polaroid copy stand, so any nearby source of vibrations (such as fan motors in instrument racks) will have a substantial effect on any positional tests. Nevertheless, the device, even on its rather crude stand, is capable of surprisingly good positional measurements. Using a razor blade as a straightedge, a scan was made with the blade set at an angle of about 45 degrees. The deviations from a linear regression of the pixel number (column) of the edge of the blade versus the stage position (row) give an indication of the stepping precision and the mechanical stability of the stage. In several runs, the rms deviations were typically about 1.8 pixels or about 2.5 microns. When the same experiment is repeated except that ten integrations are averaged together at each position of the stage, the deviations were reduced somewhat, indicating that at least some of the deviations are caused by vibrations of the stand. Furthermore, at a 1:1 conjugate ratio, the irregularities of the straightedge are likely to be significant. At present, the best that can be said is that the overall dimensional precision is on the order of 2 microns or better; a one micron precision should be easy to obtain with proper mounting of the apparatus.

c. Resolution (Point spread function) - A rule of thumb in optics holds that the resolution of a lens in line pairs per mm (at the focal plane) is 1000 divided by the focal ratio; the lens we are using (mostly at an effective f/8) should resolve 125 lp/mm or 8 microns. Since the diode spacing is 15 microns the resolution should be set as much by the array, as by the optics. Since the system is set up to operate at close to 1:1 conjugate ratios, it is difficult to set up a small enough pinhole. As an approximation, a narrow slit was placed perpendicular to the array at the maximum working distance, giving a 2:1 one reduction in scale. The slit was roughly 10 microns wide. A scan across this narrow slit gave an approximation to the point spread function which had a full width at half maximum of 1.8 pixels and a nearly gaussian profile.

IV. Limitations

a. Scattered light - The most troublesome problem of diode arrays used as densitometers is the so-called scattered light problem or image flare. The flare is, in effect, the long-range part of the point spread function; it becomes most noticeable in high contrast situations. Unfortunately, this is the situation that is often encountered in astronomy, such as in star images, where there is a density contrast of 3 or 4 in a few hundred microns or less. In a test of this effect, two scans were made across a knife edge. One of the scans was made with a narrow slit placed directly in front of the diode array to mask it from stray light, and the other was made without the slit in place. The difference is substantial, as shown in figure 3.

In another test, a "typical" star image was scanned with and without the slit masking the array. When the slit was in place, the readings at each point were lower by about 150 (on a scale where the clear plate averaged about 3000). In this particular case, where the star images were well isolated from one another, the primary effect of the scattered light is simply to add a positive bias to the signal, on the order of 5 percent of saturation. The dynamic range is reduced somewhat, due to the increased random noise, but the stellar profile is affected little, if at all.

Nevertheless, the amount of scattered light is considerable and in situations where the star images are crowded together, the effects are likely to be much more complex. This experiment demonstrates another important point as well: a major share of the scattering arises from within the array itself. The reason for this can be seen in the construction of the array. The active part of the chip consists of a narrow line of diodes some 15 microns wide, surrounded by a light-colored rather reflecting coating that shields the rest of the circuitry from light. The chip is covered with a thin quartz plate, spaced about 0.025 in. above the array. Thus multiple scattering and reflections between the array surface and the window are inevitable.

Figure 3 - Response to a knife edge

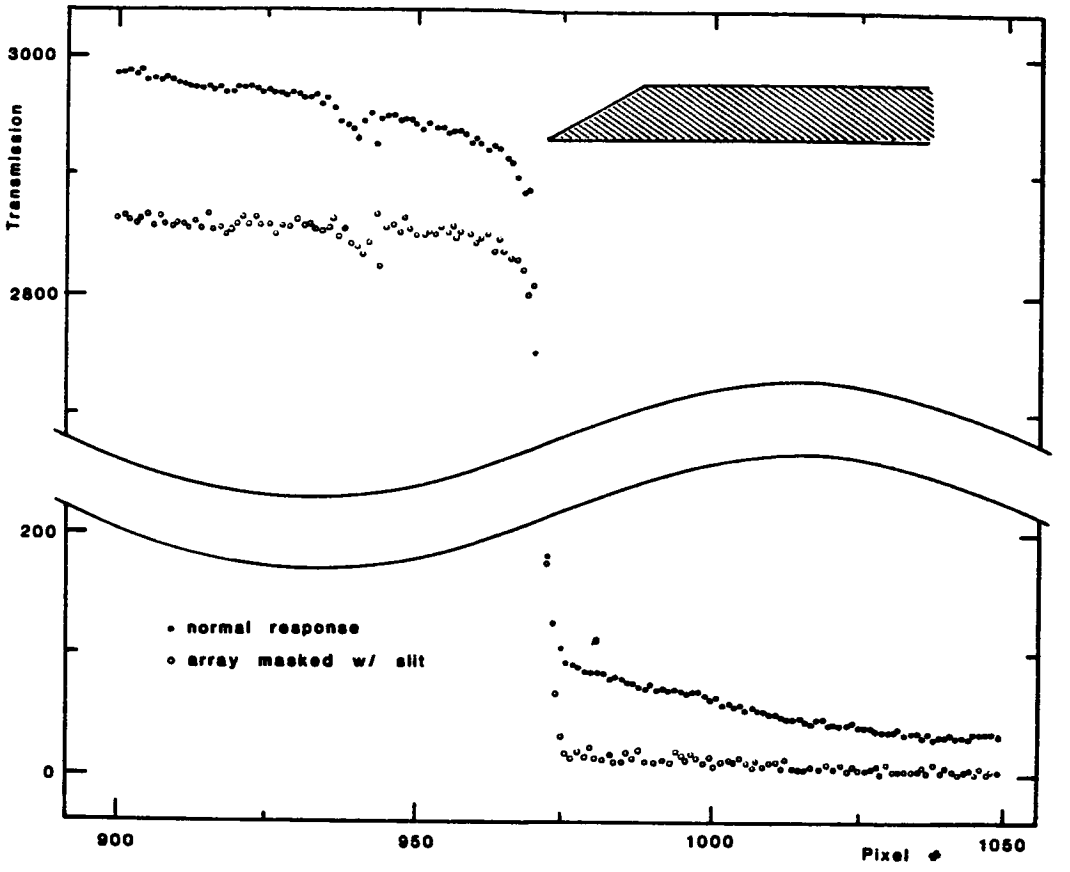

b. Saturation effects - Swaans (1979) has reported that when some diodes are saturated, there is a leakage of charge onto unsaturated diodes. We have not made a careful study of this effect as yet, but the effects, if they exist, do not appear dramatic. This is an important consideration; if some way can be found to prevent saturated diodes from contaminating nearby, unsaturated ones, then it will be possible to extend the dynamic range by combining scans made with alternating high and low intensity light. Further tests of this effect are essential.

V. Discussion

The preliminary experiments discussed in the previous section are consistent with the general characteristics of diode arrays as reported in the specifications given by Reticon and by Eikonix and the results of the analysis by Swaans (1979). The evidence is suggestive, but not yet conclusive that diode arrays can be used effectively for the exacting requirements of astronomical applications. At Boston University we are now in a position to pursue a definitive study of the viability of a diode array system for densitometry. We have a working system, designed and tested for

reliable use in a variety of situations; after several months of learning the system and developing the basic software for scanning and for some analysis of the data, we have become thoroughly familiar with its operation. We can now begin an exhaustive analysis of the potential of the technology and make some of the already obvious improvements necessary to the system, such as:

1) Optical modifications such as masking the array, replacing the full field illumination with a traveling preslit illumination system and adding a system for obtaining alternating high and low light intensity. The goal of these modifications is to cut down on the scattered light and improve the effective dynamic range.

2) Mechanical improvements to replace the present, somewhat crude stand with a more appropriate structure.

3) Software development, including more efficient scanning operations and multiple integrations, improvements to the photometric and astrometric reduction programs and experiments with image enhancement techniques to correct for residual optical degradation of the scanned image.

The goal of this program will be to develop a relatively inexpensive, high-speed scanning device that has a dynamic range in excess of 1000:1 and astrometric positioning capabilities.

VI. REFERENCES

Mendillo, M. and Baumgardner, J. 1982, J. Geophys. Res., 87, 7641.

Swaans, L. 1979, in Image Processing in Astronomy, Eds. G. Sedmak, M. Capaccioli, and R. J. Allen, Osservatorio Astronomico di Trieste, p. 77.

MacNamara: How do you determine your 2 micron acuracy?

Janes: I was scanning a razor blade actually, what I did was to worry about the accuracy in the lead screw direction. And so what I did was to put a razor blade on a 45 degree diagonal and see how jagged an edge it made. Some of that is due to the jaggedness of the razor blade itself. But basically a straight line through and across a few millimeteres of travel, I haven't done it on a large scale yet gave accuracies of that order.

MacNamara: But that doesn't mean that if you scan across a fairly large plate and come back you would read the same values.

Kenneth: Well, if you come back to the same, it does come back to the same place. Of course that small area that you're scanning say within the 30 millimeter square area, Yeah. I haven't done a detail test although in working with it when you put it to a given row, its on that row, and that seems to be looking at the same spot within about the same kind of error which is mainly due to the vibrations of this poorly mounted system, as anything else. I don't think I've tested the stage itself.

Dittmore: You can make your mask out of Kodak high resolution film using a step and repeat machine.

Kenneth: Right, then I'd have to glue it or something under the front...

Opal: Do you put on an intermediate mask and a relay lens?

Kenneth: Ah, I thought about schemes of that sort and the problem is there isn't room in the present thing to put it on the same stage as the diodes. Its a very small little stage and there is very little moving stuff right now. Once you start mounting optics and things on to this little stage you'll have to throw away that whole stage as well. since the whole stage operation is really just that big. It's a little circuit board with the array mounted on it moves back and forth with the scanning for Y dimension. If you gonna put any pre-slit stuff on it you would have to add to that same stage.

PLANS FOR A FAST IMAGE RECORDING SYSTEM AT ESO

P. J. Grosbøl
European Southern Observatory
Karl-Schwarzschildstr. 2, D-8046 Garching, FRG.

ABSTRACT

A 256 diode-array will be installed as detector on the ESO OPTRONICS S-3000 measuring machine in order to increase the acquisition rate. A high intensity LED will be used as light source in a pulse mode. The data will be stored on a random access mass storage device as density values for later reduction. The scanning time for a 30 cm * 30 cm plate with a step size of 10 micron will be less than 10 hours while the dynamic range of the data is expected to be 2.5 density units with an offset of at least 1 unit.

1.0 INTRODUCTION

The ESO Measuring Machine Facility (MMF) consists of three microdensitometers, namely: a GRANT 800, a PDS 1010A, and an OPTRONICS S-3000. The GRANT is used for measurements of spectral plates while the two others can perform two dimensional scans of plates. Most users prefer the PDS for photometric measurements of plates smaller than 25 cm * 25 cm. This is mainly due to its higher dymanic range (i.e. 5 D) and an easy calibration procedure. The OPTRONICS is, on the other hand , mostly used for astrometric programs and for scanning of Schmidt plates. Its photometric system has, however, a limited dynamic range (i.e. 2.5 D) and does not allow dense plates to be measured.

Most of the MMF time is spent on two dimensional scanning of plates. These scans can be divided into two main categories depending on the size of the digitized area : small areas which normally are used for investigations of single objects, and large areas for the study of or search for groups of objects. Only the first category of scans can be performed efficiently at the MMF,

whereas large areas take too much time to be feasible (e.g. a scan of a whole Schmidt plate with 1Ø microm steps would take of the order of three days on the PDS with maximum speed while it on the OPTRONICS would take a week).

A number of arguments suggest that an efficient way of scanning large areas (e.g. Schmidt plates or prime focus plates from the 3.6 m telescope) should be made available to the ESO community. Whereas photometry of small regions may be taken over by electronic detectors such as the CCD the large field photographic photometry will keep its importance in the next decades. The ability to analyze large fields will open a range of new areas of research. It would make it possible to study the distribution of objects over a large area of the sky (e.g. galaxy clustering). On grism and objective prism plates a fast automatic and objective search could be made for objects with special spectral features (e.g. emission line). A fast scanning facility would also enable an accurate digital comparison of large plates taken either in different colors or at different epochs. This ability is necessary for finding objects located in a given region of a color diagram (e.g. object with blue excess), with high proper motions (e.g. nearby red dwarfs or halo stars) or with time variations (e.g. BL Lac objects, QSO's or Super Novae). Digital addition of plates to reach very low surface brightness levels would also be made more efficient by an increased scanning speed. It should further be noted that ESO at present is unable to provide any efficient reduction facility for the plates taken with its Schmidt telescope. Nor are such facilities available in any other of the ESO member states. Finally, the importance of locating special types of objects for later investigations will increase when the Space Telescope becomes operational. As the host institute for the ST/ECF, it would be natural for ESO to offer such search facilities to European astronomers and thereby to help them optimizing their use of the Space Telescope.

The best way to implement a Fast Image Recording SysTem (FIRST) in the MMF would be to modify the OPTRONICS which is a flat bed microdensitometer with a granit base and a stage moving on air bearings. To accomplish this, only the photometric system would have to be exchanged. The stage control system should be maintained because of its high stability and positional accuracy. Further, it can accommodate 14-inch Schmidt plates. The bridge construction of the OPTRONICS would make it possible to do the develpoment on a seperate bridge, and thus minimize the time in which it had to be taken out of use. The general structure of a FIRST is discussed in Section 2 while the performance requirements are given in Section 3. Finally, the feasibility of constructing a FIRST is considered in Section 4.

2.0 GENERAL STRUCTURE OF FIRST

The rapid development in mass storage and computer hardware has changed some of the important parameters in the design of a FIRST. The existing machines for extracting astronomical informations from large areas of plates (e.g. COSMOS in Edinburgh and APM in Cambridge) have included hardware analyzers to reduce the amount of output and increase speed. This concept seems not to be valid today. The information content of a Schmidt plate (i.e. approx. 1 Gpixel) is no longer too big to be stored on fast random access mass storage devices. Further, the fast CPU's now available make it possible to extract the information with sufficient speed using general purpose hardware.

These considerations lead to the proposed general structure of a FIRST as shown in Figure 1. It consists of an optical system which images the plate on a one dimensional diode-array mounted perpendicular to the scanning direction. The detector is operated by a microprocessor which also corrects the readings for the sensitivety and dark current of the individual diodes and converts the measurements to density values. Both the stage and the microprocessor are controlled by a minicomputer. As a first implementation the data will be directed to the minicomputer and then stored on magnetic tape. Later the data could be sent to a mass storage device and to other computers for analyzing through a Local Area Network (LAN).

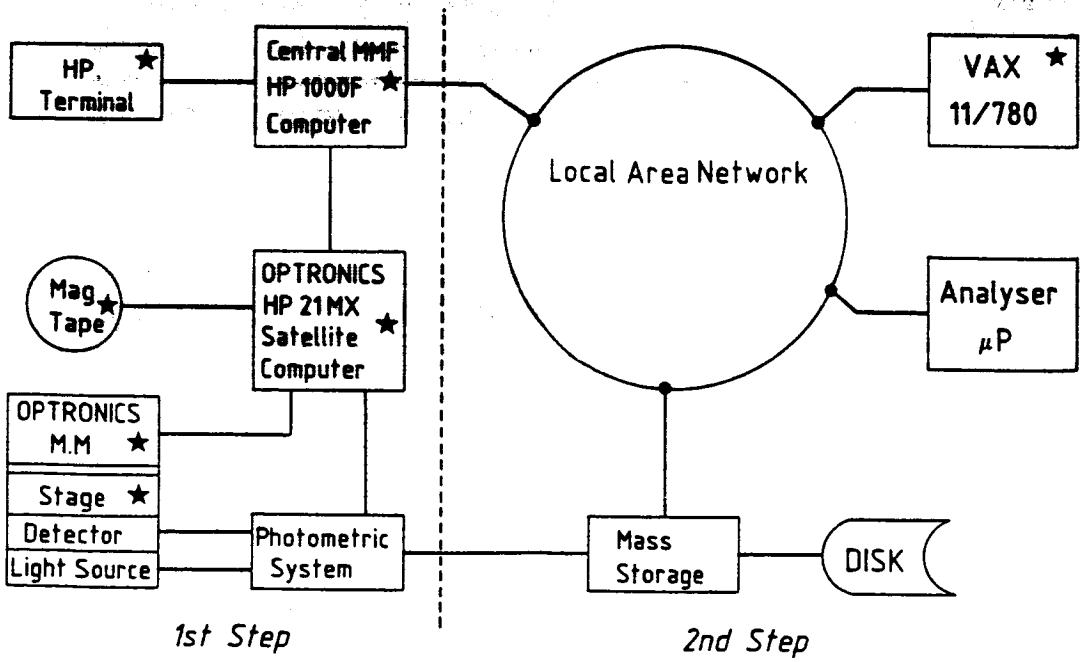

Figure 1: **Block diagram of general structure** (★ available)

The choice of a diode-array (e.g. a RETICON array) as detector was made because of its high performance and stability (see e.g. ESO Technical Report No.5 and Swaans,L. 1981 Ph.D. Thesis, Leiden). Further, this detector can operate with a much simpler optical design compared to that required for a scanning beam system like COSMOS or APM. The calibration of the individual diodes can be done online giving an output in density units.

It will take longer time to analyze the data than to acquire them. In the time from the scan is finished to the data are reduced the mass storage cannot be used for data from a new plate. During this time the FIRST would be used for scanning smaller areas which either could be stored on magnetic tape or analyzed directly in the local computer system. The latter option would be very usefull when astrometric or photometric parameters for a limited number of objects with known positions should be obtained. A LAN will increase the flexibility of the system significantly. This enables data from the FIRST to be analyzed by other computers independently of it being sent to the mass storage.

The proposed structure of a FIRST compared to a hardware analyzer solution gives several advantages, namely :

A) The lack of special analyzing hardware gives a shorter design time. This will fully compensate for the higher cost of the mass storage.
B) A software reduction of the data gives the full benifit of the rapid development in computer hardware. It is expected that processor speed will increase significantly in the coming years.
C) A higher efficiency can be achieved because the FIRST can be used for other purposes while a large plate is analyzed. Further, plates need not be rescanned if small areas around interesting objects have to be extracted.
D) A better and more flexible reduction is possible. Different ways of analyzing the data can be used for different types of applications. Since the processing is offline (i.e. not real-time) there are no restrictions concerning complexity and size of objects which can be handled.
F) No level cut of the data is needed. Therefore, the problem of truncation in the density distribution of faint objects is avoided (e.g. total rather than isophotal magnitudes can be computed).

A more detailed design of the photometric system is given in Section 4 since this will be the limiting factor for the scanning speed of the FIRST. The software reduction of the data is not considered a part of the FIRST and will only be discussed

briefly.

3.0 PERFORMANCE REQUIREMENTS

Since the FIRST will be used for astrometric purposes the positional accuracy must be of the order of 1 micron. It should also be able to resolve the typical point spread function of a photographic plate so that stellar and diffuse objects can be separated. For normal emulsion the pixel size should not exceed 10 micron squared. Measurements which require a smaller pixel size or a large range of densities can be performed on the PDS. Hence, it seems not to be essential to have a higher dynamic range than 2.5 D (see e.g. COSMOS and APM). It must, however, be possible to offset this range by between 1 and 2 density units to allow for plates with high background density.

The computer time needed for processing a plate will decrease in the coming years. Therefore, the FIRST should be designed to scan a plate significantly faster than it at present takes to analyze it. Since it takes approximately 2 hours to expose a deep Schmidt plate a scanning time shorter than this seems not reasonable. On the other hand, a scan of a ESO Schmidt plate should not take much longer than 12 hours in order to process at least one plate per night.

The requirements for a FIRST can be summarized as follows :

1.	Positional accuracy	:	1.0 micron	
2.	Pixel size	:	10 micron	
3.	Dynamic range	:	2.5 D	with 1-2 D offset
4.	Scanning speed	:	2 < t < 12 hours	per Schmidt plate

Laser interferometric tests of the positional repeatability of the OPTRONICS have shown that this accuracy can be achieved. Systematic errors will be determined by the quality of the encoders and the ways. Also the speed of its stage is sufficient to scan a 30 cm * 30 cm plate with 10 micron pixels in 2 hours if an array of more than 200 diodes is used.

4.0 DESIGN AND FEASIBILITY

No parts of the design and construction of the proposed FIRST require developments of new techniques. A number of details in the design are taken from previous studies e.g. ESO Techincal Report No.5, ASTROSCAN (Leiden), and MAMA (Paris).

4.1 Optical System

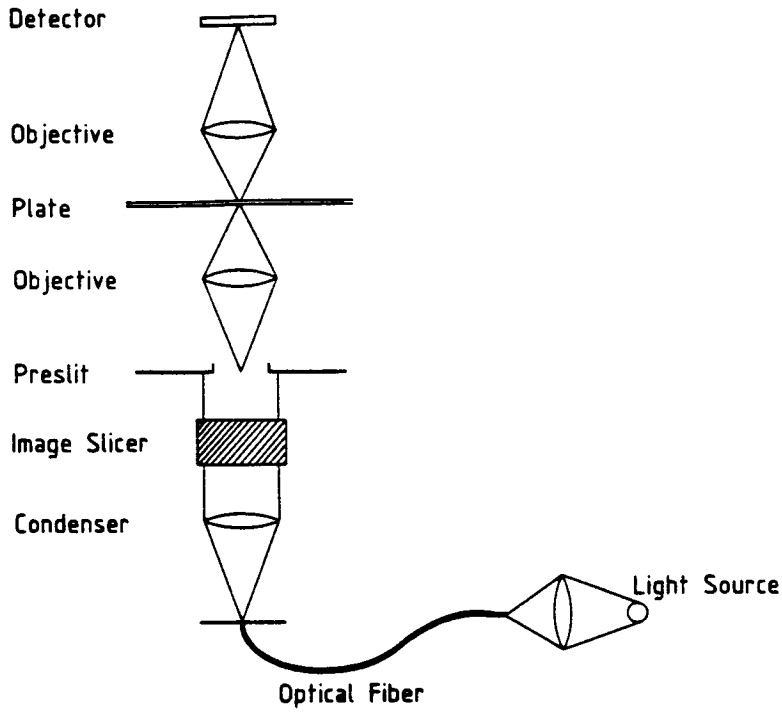

Figure 2: **Optical System** (schematic, not in scale)

The basic optical system is simple as shown in Figure 2. The light from the light source will be transfered to the optical system by an optical fiber. This removes the problem of heat dissipation and makes lignment simpler. A condenser system illuminates the preslit aperture. A cylindrical lens system (e.g. an image slicer) may be included to increase the efficiency. The preslit is then imaged on the plate mounted with the emulsion upwards. A long focal length of this system would be preferred to avoid a significant change of the focal plane due to variations in the glass thickness of the plate. To make intensity calibrations of the diode-array it will be possible to insert a set of neutral density filters in the light part of the lower optical system. Finally, the upper optical system images the emulsion on the detector with a magnification of approximately 3 depending on the actual diode size. The light used will be of a limited spectral bandwidth in order to simplify the optical design and optimize coating. The focus of both the upper and lower optical system should be controlled by the minicomputer. Whereas the best focus should be found automatically it is not foreseen to be changed during a scan. The slit size will be limited to 2.6 mm to reduce problems with optical imaging on the array and effects of stray light (i.e. the array will have 256 diodes). The effective wave length of the light will be between 600 nm and 900 nm depending on the

actual source used and have a total spectral bandwidth of the order of 100 nm.

A normal 200 W halogen lamp can be used as light source when an interference filter is introduced to reduce its spectral range. In this case the detector would be constantly illuminated, while the stage is moving, giving two problems, namely : a strong correlation between successive readings of the array, and a mean position (in the plate coordinate system) of the different diodes in one reading of the array which is depending on the scanning speed (see ESO Technical Report No. 5). The new development of LED's has, however, made it possible to avoid these problems. Their luminosity intensity is now great enough (i.e. greater than 500 mcd) to saturate an diode array in less than 50 microsec assuming a total efficiency of the system of 10 %. One would then only illuminate the plate in this short time before each reading while the time between readings is longer than 1.2 msec. The offset in dynamic range can be achieved by changing the luminosity of the LED keeping the exposure time fixed. It is, however, necessary to monitor the total energy of each light pulse because the efficiency of LED's is strongly depending on temperature.

A full field view will either be implemented as an off-axis TV system or by using flip-in mirors in the main optical system.

4.2 Mechanical Structure

Since the stage of the OPTRONICS will be used the main mechanical task is to fit the optics on it. Although the present bridge could be modified to accommodate the new optics and electronics it is suggested to have a new one made. This would strongly reduce the time in which the OPTRONICS has to be taken out of operation during the installation (i.e. to around two months). Further, an enclosure of the OPTRONICS should be provided to minimize dust and temperature problems.

4.3 Photometric System

The detector will be a RETICON diode array. It has approximately the same performance, at high light levels, as a CCD and does not suffer of problems with crosstalk and blooming. The number of diodes is proposed to be 256 giving a linear size on the plate of 2.56 mm.

A data processing board for reading out the array with a maximum scan rate of 1 MHz is commercially available. The analog video signal will be converted to a 12 bit value and then further processed. The array will be sampled with 1 msec intervals giving a dark current of Ø.Ø3 % of the saturation output signal at room temperature. Thus, cooling of the detector will not be needed.

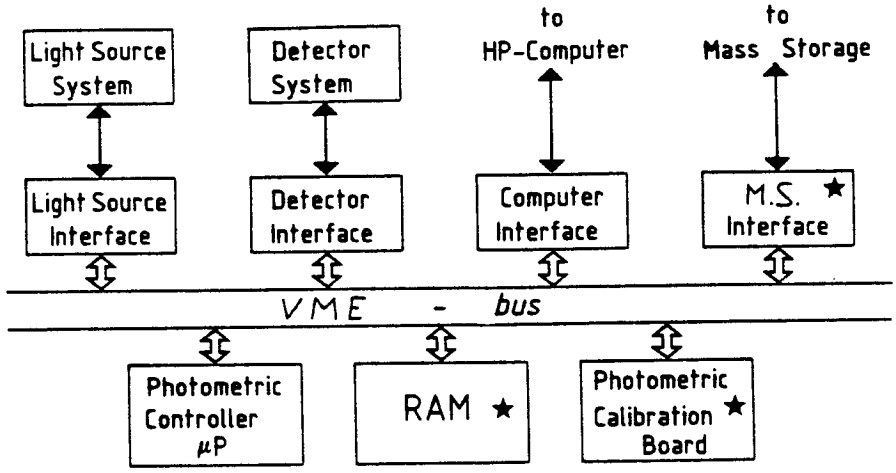

Figure 3: **Photometric System** (★ Optional)

The system should correct all detector dependent feature in the data including a convertion from transmission to density units. The following expression has to be computed for each pixel value :

$$e + s[i] - f(m[i] - d[i])$$

where e is the logarithm of the total exposure of the array since last read-out. The quantities s[i], m[i] and d[i] are the logarithmic sensitivety, the measured value and the dark current, respectively, for the i'th diode. The function f transforms intensity values into density units (i.e. approx. a logarithmic transformation) correcting for non-linear effects in the diodes. The logarithmic exposure e is computed after each light pulse using the measurement from a photodiode located close to the light source. The values of s and d are stored as tables in the microprocessor and can be assumed as constant during a longer period. The dark current is updated after each strip of the plate has been scanned (typically every 2 min) while the sensitivety is measured with intervals of weeks. The calculation of the function f is done by a table lookup. The computation of the expression will limit the maximum sample speed. The fastest way to evaluate the expression would be to use hardware. It is

however suggested to make the computations in the microprocessor during the first implementation in order to simplify it.

The photometric system is controlled by a microprocessor. It will both initiate the sampling sequence and compute the tables for sensitivety and dark current depending on instructions from the minicomputer. The photometric system is shown in Figure 3.

It is foreseen that the array is read out a second time after each measurement in order to remove residual charge in the diodes. Doing this and using a software calculation of the expression a scan time of 8-1Ø hours for a Schmidt plate can be achieved whereas a hardware computation would decrease the time to 2-3 hours.

4.4 Software

The final performance of the FIRST will strongly depend on the quality of the software which is available to control it and to analyze the data from it. The programing tasks can be devided into the four categories discussed below.

4.4.1 Photometric System Microprocessor -

The microprocessor can be operated in a strictly sequential mode (i.e. without interrupts). It has to execute the following 6 functions depending on the instruction received from the minicomputer :

1. Load intensity of light source
2. Load density offset
3. Load density transformation lookup table
4. Compute dark current table
5. Compute logaritmic sensitivety table
6. Perform a diode array reading

The three first commands are updating the memory with values which are sent to the microprocessor directly after the instruction. The computation of sensitivety and dark current tables involves a sequence of 32 readings of the array followed by a calculation of the average for each diode. The last command initiates the measurement of the array. This will first switch on the light source during a given time, then read the photodiode and compute the logarithmic exposure e, start a read-out of the array, and finally compute the expression. After the data is read out a dummy reading of the array will be done to remove

residual charges. The measured data will be sent either to the minicomputer or to the mass storage device. The maximum data transfer rate is approximately 250 Kbyte/s.

A processor like the Motorola MC68000 can perform these operations within the time specifications. A fast 16 Kbyte random access memory is sufficient for both program and tables. A commercial microprocessor board based on the VME-bus will be used for the photometric system. Controllers for the LAN and the communication to the minicomputer are also commercially available.

4.4.2 Scanning Control Program -

This program controls all functions of the FIRST. The principle which now is used for the measuring machine control programs will be maintained, namely, that all administration of data and communication with the user are done by a program running on the central MMF computer while the real time operation is handled by a smaller satellite computer located close to the machine. The existing control program for the OPTRONICS can be used with only minor modifications to accommodate a focusing control and the new photometric system. The transfer of data from the detector is either done directly to the mass storage or through a 16 bit parallel interface to the minicomputer.

4.4.3 Mass Storage Controller -

The controller will both be connected to the photometric system and the LAN. It can accept requests for retrieval of data from all devices connected to the network. This can be done using the concept of the 'intelligent back end' e.g. by Masstor's Shared Virtual Storage System. Such systems may be commercially available in a few years, otherwise, a microprocessor must be introduced to decode the requests coming through the LAN.

The storage of data is a real time process and will have the highest priority. To avoid loss of time to track search on a disk drive retrieval of data from it will first be allowed when no more data are to be written on it. Therefore, the mass storage should consist of at least two disk drives making it possible to start the reductions as soon as the first drive is full.

Modern disk drives (e.g. CDC 9775 SMD with 675 Mbyte, DIGITAL RPØ7 with 512 Mbyte or HP 7935H with 4Ø4 Mbyte) have a rotational latency of 2Ø msec and a track length of the order of 2Ø Kbyte. Since the tracks will be written sequencial the average transfer rate is approximately 5ØØ Kbyte/s being the double of the maximum foreseen acquisition rate.

4.4.4 Analyzing Software -

In the following it is assumed that the VAX computer will be used for analyzing the data from the FIRST , although it later may be more efficient to connect a fast microprocessor to the LAN and let that do the reductions. The transfer of data into the VAX memory is handled by the LAN driver with data rates of the order of 3ØØ Kbyte/s. If an Array Processor is available on the VAX the reduction time will be I/O limited, otherwise, CPU limited.

Two types of standard operations on the data must be available namely, search for objects and extraction of objects found. The fastest methods of searching are level and/or edge detection. Using such algoritms a search time for a 3Ø cm * 3Ø cm plate is approximately 6 hours on a VAX computer without an Array Processor. More sophisticated search algorithms can first be applied to a whole plate when an Array Processor is available reducing the processor time by a factor of 1Ø. It will, however, still be possible to analyze one plate per night with the present VAX system. The list of objects on a plate can then be evaluated by the MIDAS system. Also interesting areas on the plate can be extracted and converted in the standard MIDAS format.

4.5 Implementation

It is anticipated that the FIRST should be implemented in two steps. The first step would include the new photometric system in addition to the mechanical and optical modifications of the OPTRONICS. The operation and performance of the integrated system would be tested and optimized at this level of implementation. Further, it would make in possible to increase the data acquisition rate by a factor of 1Ø (only limited by the magnetic tape drive on which the data would be stored). When it has worked satisfactory for some time the last step could be made in order to increase the performance by a another factor of 1Ø. The last step includes the mass storage system and the connection of the different computers with the LAN.

5.Ø CONCLUSION

The described modification of the OPTRONICS measuring machine will provide the ESO community with an efficient facility to measure and analyze large field photographical plates. Thereby, it will open a wide range of possible investigations for European astronomers. The proposed design gives both a very high acquisition rate and a high degree of flexibility in the evaluation of the measured data. Its performance will be between 1Ø and 1ØØ times better than that of the present OPTRONICS reaching the level of the best existing machines.

6.Ø ACKNOWLEDGEMENTS

I would like to thank the members of the ESO Scientific Division for many interesting discussions. I am especially grateful for the help I have received from the ESO TP Division without which this proposal could not have been made. In particular I wish to express my gratitude to G. Coignet, D. Enard, F. Franza and B. Ljung for their comments and suggestions during the work on this proposal. Finally, I express my sincere thanks to Dr. R. le Poole for many detailed discussions concerning the ASTROSCAN.

A NEW MEASURING MACHINE IN PARIS

Jean Guibert, P. Charvin,
Institut National d'Astronomie et de Géophysique,
77 avenue Denfert Rochereau, 75014 PARIS

ABSTRACT. A new photographic measuring machine is under construction at PARIS Observatory. The amount of transmitted light is measured by a linear array of 1024 photodiodes. Carriage control, data acquisition and on line processing are performed by microprocessors, a S.E.L. 32/27 computer, and an AP 120-B Array Processor. It is expected that a Schmidt telescope plate of size 360 mm square will be scanned in one hour with pixel size of ten microns.

I. THE MICRODENSITOMETER

The microdensitometer combines a X-Y movable carriage, a quasi-monochromatic illumination source, and a multichannel photometer. High scanning speed and flexibility in machine control and data processing are expected from the design of hardware logic and choice of the computer system which includes a parallel processor and a real time oriented mini computer.

Mechanical design

The base is a granit block (1.8 × 1.1 × 0.3 m), plane to within 3 microns. The X-Y carriage consists of two superposed frames with independent perpendicular movements. Each frame is supported and guided by SCHNEEBERGER roller bearings travelling on rectangular ways, and is driven by a feedback loop controlled motor through a ball screw. The positional information is derived from incremental linear moiré fringe transducers (MINILID 300) from HEIDENHAIN. An overall repeatability of 1 micron is expected. The glass table accepts plates of size 550 × 550 mm with maximum thickness 6.35 mm. It can be rotated with respect to the upper carriage in view of some specific applications requiring proper orientation of the plate. The working area being 50 cm

in diameter, a whole 360 × 360 mm Schmidt photograph can be measured with only one positioning.

Optical configuration.

A regulated quartz-iodine lamp illuminates the slit image plane through a hot half-condenser, a broad-band interference filter, a set of neutral densities, and a cold half-condenser. The light is quasi-monochromatic, with wavelength : 633 ± 25 nm. A beam splitter allows a small fraction of the light to be measured by a photodiode for the purpose of flux stability control. The illumination lens forms an image of the slit onto the photographic plate. Finally, the projections lens projects the plate area to be measured onto the 1024 element linear photodiode array (Reticon CCPD 1024). This array can be replaced by a T.V. camera in view of visual examination.

Two magnifications of 1.6 and 1/1.6 (obtained by rotating the projection lens) associate, to each photodiode, a plate element of 10 × 10 or 25 × 25 microns respectively. The field depth is 16 microns for a numerical aperture of 0.2. The system can be operated by remote control. Automatic or programmable focussing is also being considered to compensate for the variation in plate thickness.

II. MACHINE CONTROL AND DATA ACQUISITION AND PROCESSING

The configuration comprises two subsets:

- the host-computer, array processor, and standard peripherals(for data acquisition and processing)
- the microcomputer system (for management of the microdensitometer automatisms).

The host-computer is a S.E.L. 32/27, with 1 Mbyte memory, hardware floating point, input/output processor (IOP), two 80 Mbytes disk units, one 45 ips 800-1600 BPI tape unit, line printer, and consoles.

The AP- 120 B Array Processor (167 ns cycle), with 64 K 38 bits words memory is linked to the acquisition module by a GPIOP (General Purpose Input Output Processor) interface. Due to the parallel organization of the AP- 120 B, floating point adds, floating point multiplies, control arithmetic operations, memory access, host/array processor and peripheral input/output data exchanges can all be overlapped in time.

The microcomputer system is essentially composed of :

. the acquisition module;

. the 6809 master microprocessor which coordinates the different elements of the process (focussing, data acquisition...);

. two slave microprocessor in charge of the X and Y movements.

Data circulation

The output of the reticon array is fed into the analog to digital converter; the data are then corrected for dark current and sensitivity differences from one photodiode to the other, for the inhomogeneities of illumination due to the optical system and for the fluctuations of the source of light.

After a transit through the GPIOP, the output of the acquisition module is compressed by the Array Processor which transmits it to the host computer.

III. OPERATING MODES

X as well as Y motions can be performed at velocities as high as 8 mm / sec in measurement mode, and 40 mm / sec in pointing mode. The acceleration will be limited to 0.5 m /sec^2 , and the standard velocity taken equal to 3.6 mm / sec. With a 10 micron step, this corresponds for the whole set of 1024 photodiodes to a rate of 360,000 measurements per second. At this speed, a 35 × 35 cm plate is scanned in lanes of 10 mm in about one hour.

Each sample being coded with 10 bits, the raw data for the whole plate amount to about 10^{10} bits. Until storage devices of this class have become available and easy to operate, it is clear that one of the two following kinds of operating modes will have to be used:

- scanning of selected areas within the plate, either around successive positions, or along a curve.

- complete scanning of the plate (or of a significant part of the plate), with on-line data compression performed by the array processor.

We are currently investigating the algorithms best suited to these two kinds of data collection, as well as the processing techniques to be used downstream.

REFERENCE

T. Danguy, I.A.U. Working Group on Photographic Problems, meeting on " Astronomical Photography 1981 ", Nice, 1981.

Wells: I'll just remark that the AP120B has a new competitor. If you haven't bought the 120B, look at the competitor before you place a purchase order. Look at the Analysis AP500. It costs half as much. It is a better machine too.

NEXT GENERATION MICRODENSITOMETER

Edward J. Kibblewhite
Institute of Astronomy
Madingley Road
Cambridge CB3 OHA

ABSTRACT

The fundamental limitations of microdensitometers are reviewed and the design of a high speed microdensitometer described. The system will digitise to 16 bits in transmission at a speed of 100 kHz using a laser beam moving over the emulsion. Other features are automatic platen rotation and autofocus. The cost will be of order $200,000.

1.0 INTRODUCTION

In this paper I shall review some of the constraints that affect the design of microdensitometers. At the start we must realize that the microdensitometer is only part of the overall measurement of the photograph. At every stage of extracting data, information is destroyed and it is important to balance the loss of information across the various system elements. The loss is of two types, that caused by the digitisation of the photograph and the other by the algorithms used to analyse the data. Some astronomical programs do not need high measuring accuracy and can use simple algorithms and data of low accuracy (for instance in picking up very blue stars by an automated blink technique). We should design our microdensitometers to be as accurate as possible for there is a natural urge to push instruments to their limits so that more and difficult projects will be attempted. There is also an enormous amount of effort tied up in the software and computing required to extract data. Since the accuracy of the final output is only as good to digitisation of the photograph, we should try to design our machines to meet the theoretical constraints on the digitisation process. In the first half of this paper we will discuss these constraints and how they affect the design of microdensitometers.

2.0 EFFECT OF FINITE SPOT SIZE AND SAMPLE INTERVAL

The most obvious loss of information occurs when we scan the plate with a spot of finite size. This produces an irreversible loss of information. It is a simple application of Cramer-Rao bounds to derive this loss of information for a linear detector (1). More complex calculations using photographic grain models give similar results (2). They show that measurement of intensity is only weakly effected by the spot size provided it is smaller than the smallest images of interest. The estimation of position is more sensitive, the position error being at least $\sqrt{2}$ of the theoretical minimum when the spot size equals the image size. For a linear system the position error is proportional to the image gradient. The loss of information is shown in figure 1.

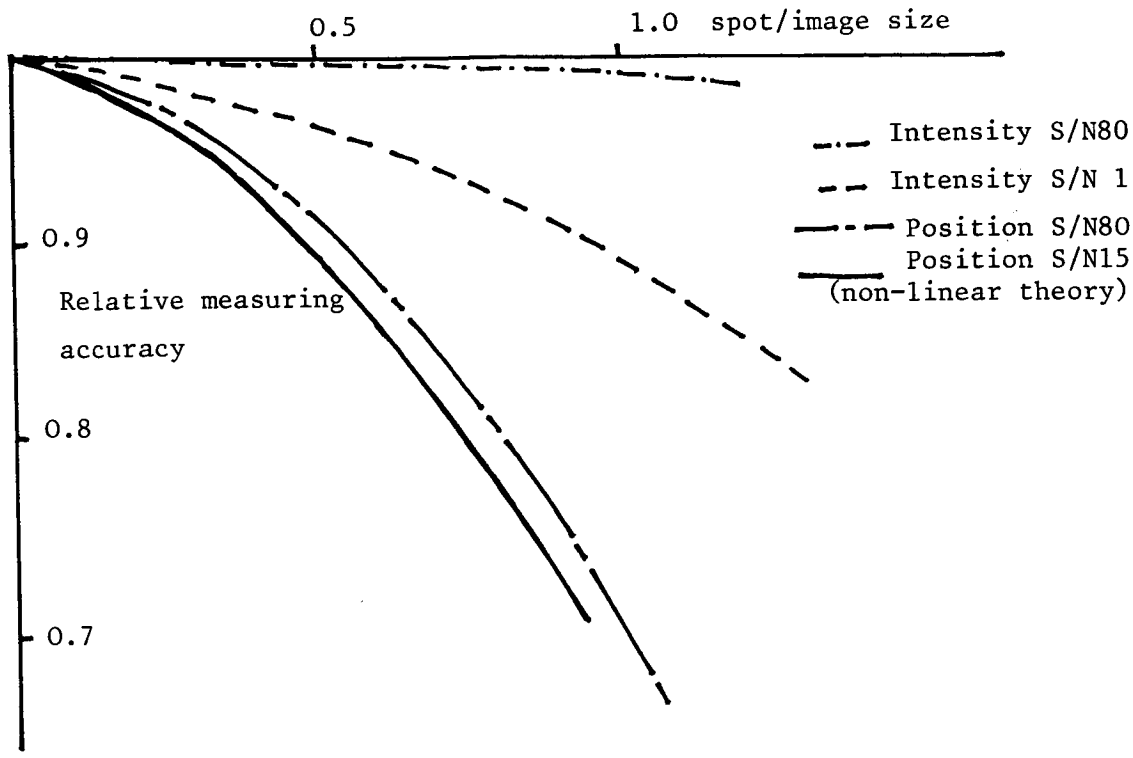

Figure 1. Effect of spot size on measuring accuracy.

There is a much stronger photometric effect if you measure images with appreciable transmission gradients across the spot. This occurs because the area of highest transmission is given most weight within the scanning spot and more weight than is appropriate since there is a non-linear relationship between the transmission and the original light that fell on the plate (3). For an image with a gaussian profile of half width W and spot size L the error in estimating the integrated magnitude is (4)

$$\Delta m = 0.26D \left(\frac{L}{W}\right)^2$$

where D is the peak density of the image.

While corrections for such an effect can be made in principle it is better to design the microdensitometer system to minimise this effect. This can be done by scanning the plate with a small spot and adding the pixels in the computer. Not only is this the best solution theoretically but the use of a single spot size can greatly simplify the design of the microdensitometer.

The sample spacing is also related to the spot size. The exact relationship depends on the use to be made of the data. If Fourier transforms are to

be used in the data analysis it is important that the photograph is sampled at twice the highest frequency present in the data. Failure to meet this requirement can mean the high frequencies are aliased into low frequencies and corrupt the data. The noise spectrum of the photographic grains extends out to at least 1000 cycles/mm and in this case the noise spectrum is defined by the autocorrelation function of the spot size. The spot acts as a low pass filter although we must remember that the edges in a normal microdensitometer are sharp and the power spectrum of the scanning spot extends out some considerable distance. Using a sample spacing of half the spot size therefore only approximates to the Shannon sampling theorem. However this constraint does not apply for measurement of integrated parameters such as intensity or mean position and there is little point in oversampling for this work. On the other hand much tighter constraints exist if we wish to measure accurate shape information from the data. To obtain this information it is usually necessary to interpolate between pixels. Numerical experiments show that as soon as there is an appreciable curvature across the pixel grid the interpolation formula which need to be used depend critically on the shape of the image and need a large number of sample points round each pixel to correct for the curvature. This effect makes the eccentricity of contours round elliptical galaxies always too small. The effect is appreciable at radii of less than 10 pixels from the centre if bi-linear interpolation formula are used. Higher order interpolation formula do not greatly help so that considerable oversampling is needed if we are to get good data. One of the great advantages of photographs is that it is possible to choose the correct sample spacing. Interpolation problems will limit the usefulness of CCD detectors for analysing the shapes of many galaxies and plans to digitise plates for machine readable data bases.

3.0 PHOTOMETRY

A good microdensitometer must be stable, linear and measure each pixel independently of its neighbours. The photographic plate is a detector of remarkable uniformity and measurements of low-light levels above background of less than 1% are readily obtainable. However, small errors in background measurement can cause large errors in the estimation of this light; a 1% error in the background causing 0.2 magnitude errors in estimating the isophotal magnitude of a faint galaxy. With high contrast emulsions such as IIIaJ most of the dynamic range of the detector lies in the region below sky background (i.e. 27 to 22 magnitude/arcsec^2) so it is essential that the microdensitometer does not introduce drifts or step changes into the density measurements. We may include quantisation errors in this error which can be especially bad in contour maps of slowly changing backgrounds. There are therefore advantages in recording the transmission rather than the density or intensity of the data since the quantisation error in transmission space is low near the background. A good analog to digital convertor with 16 bit dynamic range has a worst case quantisation error of 1% at a density of 2.7 and is better for most quantitative work that a log amplifier followed by a 10 bit converter which has an error of 0.5% at the background. Conversion at high speed is a problem since commercial successive approximation converters usually only guarantee monoticity across the range. This can cause jagged histograms and introduce considerable errors. This error is usually not perceived in contour maps but is still present.

Microdensitometers such as the PDS do not have active stabilisation of the light beam and can have major photometric drift either caused by lamp variations or misalignment of the optics. Active control of photometric stability seems essential for any new microdensitometer. The linearity requirement is not important provided the nonlinearity does not change with time since we usually have to calibrate the data in any case. The most serious technical problem is the third requirement which sets tight limits on the scattered light within the optical system.

Scattered light is caused both from dirt or imperfections in the optics and from the diffusion of light within the emulsion. We should note that microdensitometers measure the transmission of the emulsion - the holes between the grains rather than the mass of silver itself, and at high densities these two parameters may be poorly correlated. The two beam system used in the PDS in which the image of a slit is imaged onto the emulsion and then reimaged onto a slit in front of the detector gives most freedom from scattered light since the incident light is restricted within the pixel and the second slit for all but the low angle scattered light. Nevertheless it needs fast optics if it is to give a good throughput of light for high speed measurement, its depth of field is not negligible compared to the depth of the emulsion and when image and detector slits are the same size (which is necessary to minimise the scattered light) coherence effects make the measured transmission depend on phase variations across the spot as well as the mass of silver. Scattering within the emulsion is sufficiently serious to render microdensitometers which illuminate the emulsion uniformly and project an image of the pixel onto a single diode or CCD array unsuitable for precision work. In fact there are many reasons for using a focused laser beam as the light source for the next generation microdensitometer:

1) The energy in the spot is independent of its size and is sufficiently high that photodiodes can be used as the detector.

2) The beam shape has a gaussian profile which minimises the amount of light scattered outside the pixel and acts as a low pass filter with negligible side lobes.

3) The beam has maximum depth of focus and is used with diffraction limited optics. An 8 microm spot is produced by an f/10 lens . These high f ratios minimise flare in the optics and allow a beam of uniform diameter to pass through the emulsion. Fast optics used in conventional microdensitometer defocus the spot as the beam passes through the emulsion (13 to 24 microns thick).

4) The microdensitometer can be made completely linear.

5) Scattered light can be reduced to acceptable proportions by use of baffles or pinholes.

6) The beam can be stabilised to better than 0.1% over long periods of time.

The use of a laser beam also saves money. Much of the cost and complexity of a PDS is due to the large number of slits and optical elements in the light path. We have already seen that scanning a photograph with a small spot size is theoretically desirable. Digital hardware allows us to smooth the data in intensity space at a lower cost than that of a wide range of interchangeable apertures.

Figure 2 shows the design of the autofocus unit used in the Cambridge APM system. The focusing lens is dithered through a small displacement causing the spot to change its size periodically. A phase-lock loop provides error signals which maximise the grain noise. The time constant of the servo can be long and the change in spot size is typically less than 10%. The technique ensures that the beam is always kept in best focus all over the plate.

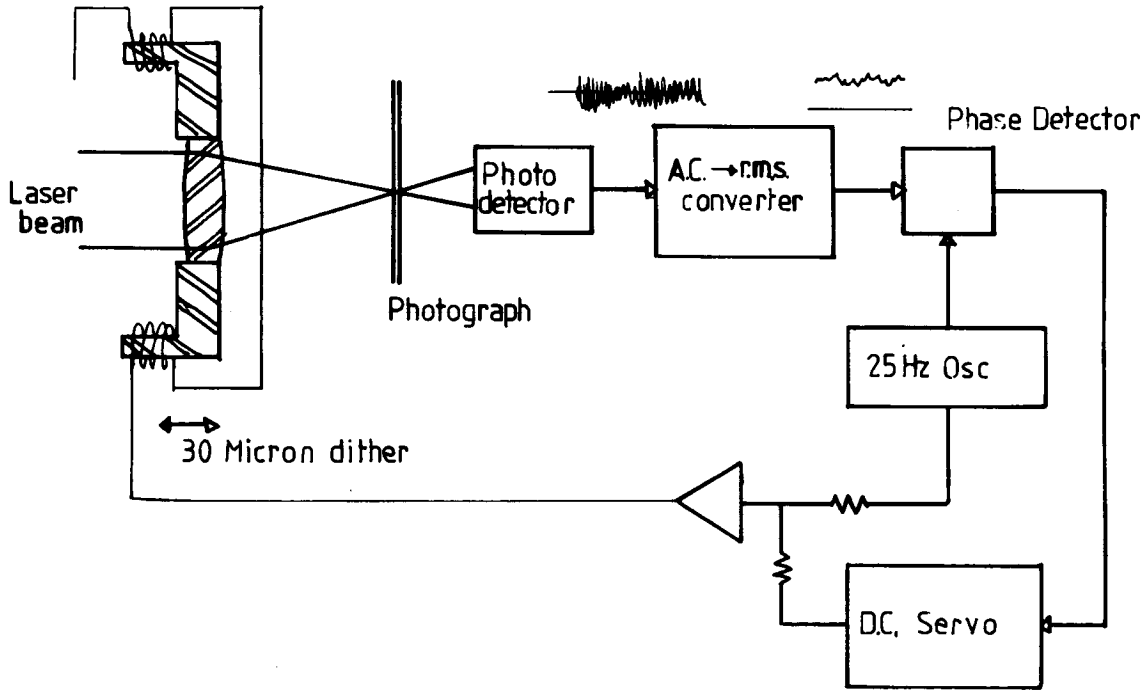

Dynamic Focusing of A.P.M. Microdensitometer

Figure 2.

4.0 SCANNING SPEED

Our microdensitometer at Cambridge will scan at a speed of more than 10^6 pixels/sec and could digitise one Schmidt plate every half hour or more than 10,000 plates/year! Clearly such a speed is excessive for anything but a large national observatory. A small to medium size department is unlikely to scan more than 200 whole Schmidt plates/year since it takes an enormous amount of effort to analyse the data and to provide calibration and follow up observations on large telescopes. Many more projects will use a fraction of the plate in the analysis of individual images. A measuring speed of 10^9 pixels/night is probably adequate. What is more important is that the data is of the highest possible accuracy, that there is adequate software to reduce the data and that the cost of the system is kept as low as possible.

These considerations favour a single spot instrument for which the main limitation in speed is the x-y table slewing under computer control. This is related to the acceleration of the carriage which determines the minimum scanning time T:

$$T = \frac{2.8}{p}\sqrt{\frac{d^3}{a}}$$

where d is the size of plate
p is the pixel size
a is the acceleration of the table. Comparatively modest accelerations of 100 cm/sec^2 will enable a 350 mm square plate to be scanned overnight at a pixel spacing of 10 micron. However high accelerations do need stiff drives. The PDS has an actuator that is extremely thin with a compliance of about 5 micron/kg. This reduces the inertia seen by the drive motor but affects the servo performance. The effects of the compliance cannot really be taken out by any means and certainly not by the small dampers used in the PDS 2020.

5.0 THE NEXT GENERATION MICRODENSITOMETER

In this section we describe a microdensitometer based on the preceding design principles which we have designed for commercial production. This microdensitometer is shown schematically in figure 3. The plate is held in a platen which can be rotated through 360 degrees by hand and through 5 degrees under computer control. The platen is moved along the y axis using a ball screw and direct drive motor. The straightness of the axis is defined by air bearings. Air bearings are now economically viable, the main problem being the provision of a suitable air supply. Preloaded Schebeegreer bearings are also sufficiently accurate and are preferred if lower positional accuracy is acceptable (order of one micron). In both cases small scale imperfections in the mechanical parts are averaged out to give small and smooth variation in the way position from a straight line. The other axis carries a light laser photometer which is moved at high speed. For this we use a recently developed direct drive linear motor. These motors have a long multipole stator which goes across the machine. The moving element consists of powerful permanent magnets which are mounted on a linear air bearing. The x axis

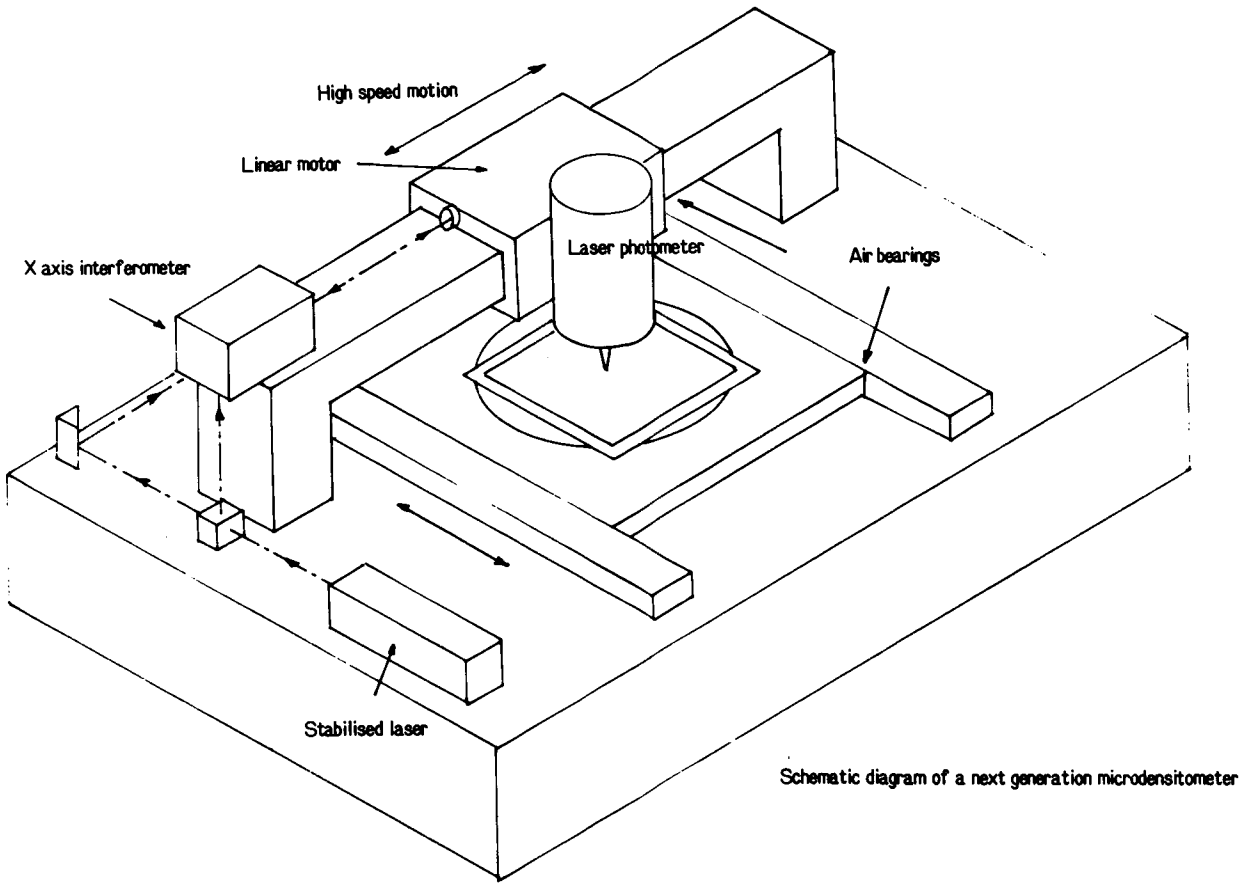

Figure 3.

is thus rather like a shuttle on a loom and accretions of 1-3 g are possible. The laser photometer (described below) is rigidly mounted on the shuttle which also moves the lightweight photodetector under the photograph. The position on both axes are measured by interferometers. These are now available at the same cost as good Moire fringe gratings. Their main disadvantage is that corrections need to be made in the positions to correct for atmospheric temperature and pressure changes. Their big advantage lies in their very fine digitisation spacing (typically 0.08 micron) which enables us to derive velocity information from the encoder. In the past the most effective means of controlling the motion of an x-y table has been to build the tightest possible velocity servo loop and fit the position servo round this. Velocity information is almost always derived from tachos to avoid resonance problems of the drive. However the use of linear drive motors fine encoding and computer control allows us to overcome these problems.

The laser photometer is shown in figure 4. The microdensitometer is designed to be modular and a variety of photometer heads will be available for different types of measuring speed and accuracy. This head uses a semiconductor laser as the light source which is dithered to provide the autofocus signals. An anamorphic prism converts the elliptical beam cross-section in a circle and a pinhole removes the scattered light from

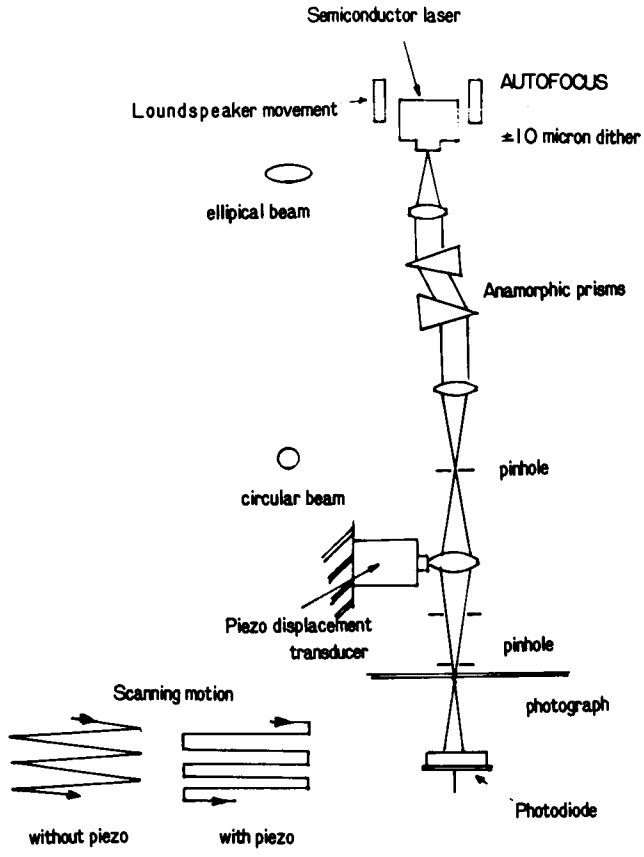

Schematic diagram of laser photometer

Figure 4.

the laser beam. The spot is then refocused onto the emulsion with a relay lens and passes through another aperture a few hundred microns above the emulsion which controls the scattered light. The relay lenses can be moved through small distances using a piezoelectric transducer so that the plate can be measured in both directions. If such a system is not used the plate is scanned in a zigzag, which is unacceptable for most work. The lens is moved so as to give equally spaced pixels.

The output from the photodiode is digitised and fed into a hardware spot smoothing circuit which enables the user to change the spot size in intensity or density space under computer control. Other optional hardware will compute the plate background, remove small noise images and/or compute image parameters.

The machine will digitise to 16 bits at a speed of 50 - 100 kHz at 10 micron spacing which is well matched to a midi computer speed such as a VAX 750. The microdensitometer will be software compatible with the big Cambridge APM microdensitometer system which has already had 20 man-years of software effort devoted to writing the software and has been exhaustively tested by astronomers!

By using new technology we have been able to simplify the design of the microdensitometer and carry out many of the functions in digital hardware. The basic microdensitometer will sell for about $200,000 and a complete system with a VAX 750 and extensive software for about $500,000. No doubt such systems can be reduced further in price in volume production.

(1) H. Cramer (1946). "Mathematical methods of statistics", p. 473.
(2) E.J. Kibblewhite (1970). Thesis University of Cambridge
(3) W.A. Wooster (1964). Acta. Cryst., 17, 878.
(4) J.D.H. Pilkington (1970). I.A.U. Coll. No. 40, 10.

SESSION V

Chairman: Arthur I. Poland

Data Storage and Retrieval

The data storage densities achieved with photographic emulsions (expressed as equivalent bits of information per unit volume) are quite remarkable. If the emulsions are properly processed and stored they can retain information reliably over many decades. The information is visible to the eye, and this is a great asset for the purpose of data retrieval. Also, photographic emulsions are relatively cheap. For these reasons astronomers have always asserted that the original photographic emulsions are the optimum permanent storage medium for the imagery contained within them. Some people have even advocated recording digital television imagery on film in analog form rather than on magnetic media for archival storage purposes. But technology is evolving rapidly and these conclusions are now being called into question. Both magnetic and laser-beam recording techniques are beginning to be competitive with photography in performace and probably in permanence, and digital image displays facilitate retrieval of data from digital archives. Maybe astronomers should now consider completely digitizing all original photographic emulsions soon after developing them. It would then be possible for more than one astronomer to analyze the bits at more than one site using more than one algorithm (bits can be duplicated more reliably than can grains). Maybe future sky surveys should be "published" in digital form. In such a concept the original emulsion is viewed as merely a detector with certain specifications, and the microdensitometer is viewed as merely a tranducer which is required to convert information from silver halide grains into digital bits as faithfully as possible. Contributions which attempt to assess the data storage capabilities of photography relative to those of other technologies will be welcomed for this session.

CRYSTAL GAZING [*], II.
IMPLICATIONS OF ADVANCES IN DIGITAL DATA STORAGE TECHNOLOGY

Donald C. Wells
National Radio Astronomy Observatory [@]
Edgemont Road
Charlottesville, VA 22901 USA

ABSTRACT

During the next 5-10 years it is likely that the bit density available in digital mass storage systems (magnetic tapes, optical and magnetic disks) will be increased to such an extent that it will greatly exceed that of the conventional photographic emulsions like IIIaJ which are used in astronomy. These developments imply that it will soon be advantageous for astronomers to use microdensitometers to completely digitize all photographic plates soon after they are developed. Distribution of digital copies of sky surveys and the contents of plate vaults will probably become feasible within ten years. Copies of other astronomical archives (e.g., Space Telescope) could also be distributed with the same techniques. The implications for designers of future microdensitometers are: 1) there will be a continuing need for precision digitization of large-format photographic imagery, and 2) that the need for real-time analysis of the output of microdensitometers will decrease.

---

* **crystal gazing**, the practice of staring into a crystal ball in order to arouse visual perceptions, as of distant happenings, future events, etc. [from the Random House Dictionary of the English Language, 1971, The Unabridged Edition]

@ The National Radio Astronomy Observatory is operated by Associated Universities, Inc. under contract to the National Science Foundation.

INTRODUCTION

In a previous paper [1] the author speculated upon the probable course of technological development in several areas relevant to astronomical digital image processing. In this paper we concentrate on the subject of mass storage systems with capacities of the order of 1 Terabit (1E12 bits), and especially upon those using removable, distributable media which could permit astronomers to obtain copies of massive digital archives. The most likely form of this technology will be optical video disks (they appear to be less than a year away from commercial realization), but we will also discuss recent exciting advances in magnetic storage techniques.

PHOTOGRAPHY AS A STORAGE MEDIUM

It is instructive to estimate the equivalent bit density of a IIIaJ plate as used for astronomical photography in current large teelscopes. Assume an effective pixel size of 10 microns (100 pixels/mm) and assume 10 bits/pixel of information. We then have 1E6 pixels/sq.cm and 1E7 bits/sq.cm. As we will see in succeeding sections of this paper, optical disks already exceed this area bit density by one order of magnitude, and perpendicular magnetic recording exceeds it by two orders of magnitude, with prospects of gaining yet another order. These facts imply that digitized versions of astronomical plate archives will not greatly exceed either the volume or floor area of the present plate archives, and that they may even be significantly smaller.

ASTRONOMICAL DATA ARCHIVES

Sky surveys made with Schmidt cameras are examples of massive databases which would be interesting candidates for digital distribution. The author believes that during the decade of the 80's it will become technically feasible to distribute such surveys in digital form. In order to see the scope of the problem consider the coarse survey of the STScI Guide Star Selection System. As originally proposed, this would involve scanning the Schmidt sky survey plates with two PDS 2020G microdensitometers. During less than three years of part-time use of the machines the whole sphere (40000 sq. deg.) would be digitized with a pixel size of 3 arcseconds. In the discussion which follows we assume one color and no overlaps. At 1200 pixels/deg we would have 1.4E6 pixels/sq.deg, or 5.6E10 pixels/sphere. If we allow 10 bits/pixel we have 5.6E11 bits total. This is 7E10 bytes (8 bit bytes), or 70000 Mb (70 Gb), which could be transmitted with about 420 reels of conventional 6250 bpi 9-track magnetic tape (using about 165 Mb/reel). The author would like to have a copy of this digital survey and

thinks that other astronomers would also, but none of us will want to purchase or store an archive of more than 400 reels of high density tape, nor will we be patient enough to want to retrieve data from such an archive. We need a storage device technology which will give us rapid random access to a data archive of 1E11 bits or more. Within the next few years it will become possible to record this survey on 3-10 video disks (see the discussion in the next section of this paper). The cost per copy of the survey will probably be below $70 per disk, maybe eventually as low as $20 (current US dollars are used for all cost guesses in this paper). The disks will be about 30 cm in diameter, and thicknesses will be a few millimeters. The video disk playback unit will be a mass-marketed device, and even with a special interface unit it will probably cost less than $3000 total. The random access time will be less than 1 second once a disk is in the unit, and the transfer rate will be 3-5 Mb/sec. This technology will probably make the digital distribution of such surveys an attractive option. Indeed, the costs and physical sizes of the video disk copies and the reader may make it economically attractive for many individual astronomers to have their own digital copies of such surveys.

For our second example we consider the idea of distributing the first decade of the prime focus plate collection of the Mayall 4-meter telescope at Kitt Peak. These plates have an exposed area about 150 mm in diameter, and the scale is 18.6 arcsec/mm. We choose to use a 20 micron pixel size (0.37 arcseconds), or 50 pixels/mm, which implies a raster 7500-square (for this analysis we ignore the unused corners). This is 4.5E7 pixels/plate, and if we assume 10 bits/pixel we get 4.5E8 bits/plate. Let us assume that we want to digitize the best 1000 plates (i.e., about 30% of the collection). We will create a total database of 4.5E11 bits. This project is very similar in scale to the coarse GSSS survey we considered in the previous paragraph, and so we conclude, once again, that complete digitization of large photographic archives is going to become feasible during this decade.

Our final example, taken again from the STScI, is the idea of distributing the <u>entire</u> database of the ST using the distributable database technology. The canonical data rate of ST is 3E9 bits/day. This is about 1E12 bits/year, a problem only slightly larger than the GSSS coarse survey and Mayall collection problems, but done once per year. We infer that by using optical disks, at about 10 disks per year, the ST database will consume less than 1 meter of shelf space per decade of the mission, and may cost as little as $2000 per copy per decade. Many astronomers spend this much on journals, and need more shelf space to store them!

OPTICAL DISK TECHNOLOGY

Optical disks have been studied for most of the decade of the 70's and have long been thought to have a bright future for computer mass storage systems. Many large manufacturers have research programs in this technological area. Any reader of the technical literature of the field in recent years has seen frequent references to this work. The discussion which follows is based on several recent reviews of the state-of-the-art [2,3,4].

Several kinds of optical disks are likely to be marketed specifically for computer systems within the next 3-5 years. Just as with other kinds of computer peripherals we can expect that the performance and capacity of the devices will grow steadily with time. The first technology which will appear uses a laser beam focussed to a spot to record the digital bits as small holes in a thin film of the soft metal tellurium. Many companies have been working on this concept for many years and it is well understood. This technology is "write-once" (i.e., non-erasable). Erasable media are also thought to be possible, especially using magneto-optical techniques, but they are not as well developed and understood at this time. The first and most important fact about optical disks is that diffraction effects imply that a focussed laser beam has a spot size of about 1 micron. This means that we can get 1E4 pixels/cm, or 1E8 pixels/sq.cm. This is a fundamental limit. With current techniques one bit is recorded in each pixel and so current technology yields about 1E8 bits/sq.cm. For example, Phillips reports [4] 0.7 micron holes with track spacing of 2 microns, Burroughs reports 0.6 micron holes with 1.7 micron track spacing, and Kodak reports 0.8 micron holes with 1.67 micron track spacing.

Storage Technology Corporation is reported [4] to be developing a large-scale storage system using 14-inch disks with a capacity of 4 Gb/disk (32E9 bits/disk), access time of about 100 msec, and transfer rate of about 3 Mb/sec. Other firms which are known to be working on analogous systems include Control Data Corporation, Fujitsu, Hitachi, Matsushita, Phillips, RCA, Toshiba, and Xerox. STC expects its 4 Gb disks to cost $100-150 by 1985. The developers expect that the cost per disk will drop to $15 by the end of the decade. It is desirable to construct "jukeboxes" which would hold hundreds of disks. STC is considering a capacity of 500 disks, which, with 4 Gb/disk, will give a total capacity of 2 Tb (2 million megabytes, or 16E12 bits). Suppose that this system is available three years from now. By analogy to previous jukebox mass storage systems (e.g. IBM3850, CDC38500, Calcomp ATL, etc.) we speculate that the hardware cost might be about

$500,000, and if the cost per disk is $100 at that time the total media cost would be $50,000, which implies that it would be reasonable to have several thousand more disks available in an offline library (access time less than a minute) to give a total capacity of about 1E14 bits for a total cost of, perhaps, about $750,000. Obviously the suggested costs are subject to a large uncertainty (factor of 2?). Los Alamos, Livermore, and NCAR have all had mass storage systems with capacities of over 1E12 bits for a number of years (they use older types of mass storage technology), and so we have an indication that there will be at least a modest market for the new mass storage system technology. But the market will need to be large if the costs are to decrease with time, and the history of the last decade of computer systems is littered with mass storage systems which never sold enough of their model to achieve the economies of mass production.

The technology discussed in the previous paragraph is probably not appropriate for the problem of distributing databases to astronomers everywhere. We need something smaller and cheaper. The answer is already visible in the stores: video disks. There are two main types of video disks, Phillips and RCA. The Phillips optical disk technology is easily adaptible to storing digital data (by using a laser beam to read out bits [5]), and it allows easy random access. The RCA scheme resembles phonograph records (a capacitive sensor is used to detect analog signals on a spiral track), and so far there has been no discussion of using it for distributable digital databases, although probably it would work. Apparently both types of disks are reproduced in plastic media by molding from masters somewhat like phonograph records. This permits low reproduction cost, a necessary criterion for mass marketing of recordings for entertainment. We will concentrate on the Phillips digital storage technique because it is almost ready for commercial marketing and its properties are most easily predictable.

All media which are designed for commercial video recording at the present time will have the specification that they must record one hour of broadcast color video. For North American video (NTSC standard) this requires a capacity of about 2E11 bits (PAL and SECAM yield similar numbers). Of course, we can compromise on signal-to-noise ratio (fewer bits) or insist on two or more hours capacity in video media (more bits), but storage capacity in the range 1 to 4E11 bits per disk or cassette is fundamental in current video technology.

There have been a variety of reports of document retrieval systems based on the Phillips-technology video disks and players. Such systems are capable of randomly accessing

individual frames by address, displaying successive frames in slow-motion, and even displaying a single frame continuously. The standard NTSC-format disk will store 54,000 analog video frames per side (30 per second for 30 minutes). Systems based on this technology are likely to be useful for applications such as distributing parts catalogs. They might even be useful for some astronomical applications. For example, during the astronomical image processing conference at JPL in August 1980 a system was shown which used a single video disk to store thousands of planetary mission images. But what we really need are devices which store digital data.

Recently the author received a brochure [6] which describes a system which uses video disk technology to record digital data, and which is intended specifically for distributed database applications. The brochure refers to "characters" (the author assumes this means bytes), and states that the capacity per side is 4800 Mb, or 3.8E10 bits, which is consistent with its statement that the capacity per side is equivalent to about 30 reels of 6250 tape. So, for both sides we would expect a capacity of 7.7E10. The company records master disks for its customers ($16,000 for master and 10 copies), makes duplicates of the disks ($80 per copy), and offers devices to read the disks ($3,000 for simple computer interface, $13,000 for a complete microcomputer system). We can assume that these prices will decrease as the technology matures and competition develops. The brochure implies that analog video imagery can be interspersed with digital data. This type of technology appears to the author to be exactly what we need to make distributable digital databases a practical reality.

Is 1E8 bits/sq.cm an ultimate barrier for optical disks? Probably not, if more than one bit can be recorded in each pixel. A scheme called "cryogenic frequency domain storage" shows some promise [4,7]. The idea is that the recording medium could be such that it has many different energy levels which can be separately activated with a tunable laser. It is expected that up to 1000 data bits might be stored in each pixel in such a system, and this implies a storage capacity of about 1E11 bits/sq.cm., or about 1E14 bits/disk (!).

MAGNETIC DISKS

Several recent reports [8,9,10] have discussed the potential performance of a technique called "perpendicular recording." In this scheme the tiny dipoles representing the bits are oriented vertically in the magnetic medium rather than horizontally. The reason why this idea is exciting is that it will permit recording many more bits per unit area than conventional magnetic recording, and the bit density even

exceeds that of optical disks! The current technology has already demonstrated linear bit densities about four times higher than optical recording, and so the potential area densities are about 16 times higher, about 1.5E9 bits/sq.cm. Some experiments have suggested that linear bit densities another four times higher will become feasible. It is clear that if even a fraction of these possibilities are realized the economics of large magnetic disk systems will be radically changed. If the full potential is realized disk hardware which now holds 1 Gb will be able to hold 100 Gb (8E11 bits), similar to large optical disk system capacities, and the magnetic systems would be erasable.

The first devices using perpendicular recording which will be marketed will be small disks, especially floppy disks. According to the first report mentioned [8], Toshiba has announced that they will market a 3.5 inch microfloppy disk drive with 3 Mb storage capacity which will use the new technology. Small Winchester drives are expected in 1984.

At present it does not appear that perpendicular recording will be useful for distributable databases. This is because of a fundamental problem: the disks probably cannot be replicated by plastic molding or contact printing. The ability to replicate the media cheaply is a fundamental advantage of video disk technology for our purposes.

MAGNETIC TAPE

Conventional digital magnetic tapes do not have large enough capacity for our applications. There is good reason to expect that new tape formats will be developed during this decade but there is not yet enough information available to speculate on their specifications. An alternative is to use video magnetic tape hardware and media to record digital data. The capacity of video tapes is about 1E11 bits, just as for video disks. Radio astronomers have used video tape for many years to record very long baseline interferometry (VLBI) data. A typical current system records 4 Mb/sec for 4 hours (5.8E10 bits total) on a standard video cassette using a slightly modified video cassette recorder [11]. For the proposed Very Long Baseline Array (VLBA) project an improved modulation scheme has been developed which increases this capacity to 2E11 bits [11]. At the VLA there is a problem: the room where the archive tapes are kept is nearly full! NRAO is planning [12] to construct a variation of the VLBI recorders to be used for re-recording the conventional archive tapes at higher density on video cassettes. The unit will use a Golay error correcting code ("23,12", about 50% efficiency) and will scatter adjacent bits down the tape to avoid dropout problems. The effective

capacity will be 3.5 Gb/cassette (2.8E10 bits/cassette). The total parts cost is estimated to be about $5,300, which includes about 200 chips, wirewrap boards and other hardware, a Panasonic VCR, and a DR11-W DMA interface to the PDP-11 Unibus. In principle this technology could be duplicated by other astronomical institutions or by commercial entities.

From the discussion in the previous paragraph we can see that video cassettes give us yet another way to implement distributable digital databases with interesting capacities at interesting prices. But, like magnetic disks, magnetic tapes cannot be duplicated easily. We must spend several hours to copy a cassette. Also, video cassettes have random access times of several minutes, and are generally not able to stop on a given frame.

COMPRESSION AND RETRIEVAL

During the decade of the 70's image processing research workers demonstrated that by use of sophisticated image compression algorithms they could encode most conventional imagery using only 5-10% of the original number of bits. These compression processes generally involve an irreversible loss of some fraction (usually small) of the original information. Because of this corruption of the signal the author is usually reluctant to recommend such algorithms for encoding scientific data. But the scale of the data recording projects we are considering is so large that compression techniques must be seriously considered in any design study.

A database is useless if the end user cannot find the bits he wants in the database sufficiently easily. Therefore the design of indexes, cross-references, search software, calibration tables and software, etc., will be critical in the design of distributable databases. The author thinks that such databases should include the software and special tables along with the data, and these items are not just nice services: <u>they are an integral part of the database</u>.

CONCLUSIONS

1. Distributed databases are going to become technically feasible during the next five years.

2. Planners of astronomical data acquisition systems should be aware of the possibilities for digital distribution of their data.

3. Video disks are the technology to watch for distributable database applications.

4. Microdensitometer system designers should consider carefully what is the role of their machines. If the goal is to deliver a digital facsimile of the entire analog image detected by the silver halide grains, then a microdensitometer is just a precision transducer, and need not have any image analysis hardware and software directly attached to it. It only needs a capability to record the massive digital database which is created when large-format imagery is digitized, and this capability is becoming available. The author contends that this is the best concept for future microdensitometer systems, because it allows multiple data analysts with multiple algorithms to analyze the data, and it allows future workers to apply data analysis techniques which present workers have not yet imagined.

5. If the system concept of the preceding paragraph is accepted it will imply that the microdensitometer is a part of the photographic detector system, and should be purchased with the telescope instrumentation, and probably should be located at or near the telescope so that plates may be fully digitized soon after development.

REFERENCES

1. Wells, D. C. (1979) "Gazing into the Crystal Ball," Image Processing in Astronomy, ed. G. Sedmak, M. Capaccioli, R. J. Allen, (Osservatorio di Trieste), pp. 490-494.
2. Street, J. (1980) "Video Disc Systems Come of Age," Electro-Optical Systems Design, December 1980, pp. 31-37.
3. Bell, A. E. (1983) "Optical Data Storage Technology Status and Prospects," Computer Design, January 1983, pp. 133-146.
4. Rothchild, E. (1983) "Optical-Memory Media," Byte, March 1983, pp. 86-106.
5. Bulthis K., Carasso, M. G., Heemskerk, J. P. J., Kivits, P. J., Kleuters, W. J., and Zalm, P. (1979) "Ten Billion Bits on a Disk," I.E.E.E. Spectrum, August 1979.
6. "Electronic Publishing," sales brochure distributed by Laserdata, Inc., 369 Washington St., Woburn, MA 01801, phone (617)938-8844. Price list dated January 1983.
7. "Spectral Memory", Scientific American, April 1983, pp.73-75.
8. "Perpendicular Recording - A Promising Technique," Computer Design, January 1983, pp. 96-98.
9. Johnson, C. E. (1983) "The Promise of Perpendicular Magnetic Recording," Byte, March 1983, pp. 56-64.
10. Iverson, W. R. (1983) "Perpendicular Bits Up Densities of Prototype Disk Drives," Electronics, April 21, 1983, pp. 47-48.
11. Walker, R. C. (1983), private communication.
12. Escoffier, R. (1983) "VCR Archive Storage," NRAO internal memorandum dated 6 December 1982.

Kinsey: Don, I noticed a couple of years ago in pursuing this optical disk system for some projects I was interested in, both Phillips and RCA indicated at that time the lifetime of the disk was bad then because of oxidation the thyrium layer, what does this laser data actually say about the lifetime of these disk?

Wells: Let me see if they actually say something on that point. Yes, that has been one of the bothersome technical points of optical disk technology. In fact, it's one of the bothersome points of all the tera bit archival type storage units. You always have to demonstrate ten year lifetime and if you haven't operated the machine for ten years, that's surely a hypothetical claim, and that has actually been the downfall of several of the systems. Ten years ago, I investigated a design that used mylar fiches coated with Rodium. There was a company that actually made these and they also ablated them with a laser beam and you probably got really similar numbers on them for the capacities. The technology looked quite fascinating and interesting and yet obviously the company went under because I never heard of them again. Likewise the Ampex teri-art memory. Of course that's permanent and all. So I don't actually know the literal answer. Let me see if they actually say anything. They must have coped with it. They must be claiming a decade lifetime. I'm not sure they actually addressed the question in this brochure.

Kinsey: Yeah, well I just wondered if this had been swept under the rug because Phillips and RCA impiled nothing beyond five to seven years at the minimum.

Wells: Yeah, it turns out that thyrium isn't the only way to go and I actually don't know the technical details. It's discussed in the papers that I reference in my paper—like in the Byte magazine and I reference several of them that are all concerned and obsessed with the properties of the medium-its smoothness, its homogeneity, its lifetime-issues like that. Those are the vital issues of the technical people. I'm principally interested in feasibility question-what can you do with a tera-bit...and so I've actually mostly ignored these technical questions. But if you're going to buy one you want to know how long will it last or how often will I have to re-recode it.

Monet: Two questions—what's the time for reading and writing particularly with respect to-say one megahertz units of accuracy these days on machines? The second one is how many milliseconds per star and per scene given your former interest in optical image processing or current if it's still active?—getting science out of the database.....

Wells: Yeah you can see almost immediately that an optical disk is a fairly fast device because it's going to have speeds comparable to your frame grabber. I mean after all it's video technology.

Monet: Oh I realize that but what's the time to write.....

Wells: Oh, to write the disk?!

Monet: Yeah.

Wells: I think they write at the regular speed that they're reading at. I mean they run fast. The typical rate is going to be several megabytes per second.

Monet: Almost three months per....how long does it take to record the disk I guess?

Wells: You could infer that it takes a couple of hours to record one, because again it's video technology.

Warren: Going back to that question of lifetime, I've talked to Mr. Hinsel a couple of times who is a sales representative of laserdata.

Wells: Oh, you know this company too!

Warren: Oh yes. And he told me that they were guaranteed ten years.

Opal: I have a seven track, 200 BPI copy of Smithsonian Astrophysical Observatory star catalogue. Does anybody here have a machine that can read it? (laughter)

Wells: Fascinating question! A couple of years ago I wanted to get an original copy of the SAO. I was still at Kitt Peak at the time and I scrunged around to find one. And there was still a tape back in the back room of the tape library at Kitt Peak. Nobody had read it in nine years! It read without a single parity error. Most amazing!

Lasker: I'd like to say that I find Don's last sentence extremely exciting. The way my mind goes when I hear him say that is a natural part of major optical telescope is the thing that produces the output. The output of the telescope is an optical disk that goes into the mailbox and if you think about it and think in terms of some number times 10 to six hours for an optical telescope it always seems to fit very well in the area of something you hang on a telescope.

Wells: It's big numbers but they're manageable at this point and probably will get easier with every year.

Anderson: You talked and gave us numbers about the cost of the storage medium and reading medium. What about the writing? It seems that the weak link here is that you've got to go to this company and they write it. We want this thing at the output of the telescope.

Wells: The company says in the brochure that they will negotiate the sale of their disk mastering machine. Now from previous hints that I've gotten of this technology in the last couple of years, I have inferred that the approximate cost is likely to be two or three hundred thousand dollars. But that's something I've not got a number on. The other thing you can say is that optical disk mastering is going to be become a mass activity in the next few years and one presumes it will be a competitive market. But that's the only thing I can say and that's a real guess. I have inferred that number from little hints that appear in the literature.

Craine: I apologize that I missed the first part of your talk so I hope that this isn't covering old ground but I just this past week saw an advertisement from Sony for an optical disk writer that looks like a video cassette recorder and they don't have a price tag on it yet. I've written for the literature. But it's now commercially on the market and since it's geared at the general public.

Oliver: I'm just sort of wondering why you're going with this microdensitometer downstairs at the observatory and the optical disk writer. Why bother to take the plate at all? That is, aren't we looking at the point, where, again, you're arguing in favor of digitizing in the focal plane of the telescope? Why take your plate and go downstairs, slosh it around for awhile, put it in the microdensitometer, wait 5 1/2 hours for it to idigitize the data, and presumably you briefly put it in the trash can.

Wells: Obviously you raise a completely relevant question. My own attitude is I don't care where the bits come from. I have no deep love of photography that would cause me to stick with it if CCD's were better. So I think you have to argue it on a case by case basis. You have to say, "Can I cover sky to a certain signal to noise ratio to a certain area coverage per unit time faster with silver hylaide grains or with silicon chips. And it's a directly calculable thing and you can decide. And the answer keeps coming back still, that if your aim is to cover a large amount of sky in minimum time, photography still wins, and probably will in the future. Now if you get less interested in making Schmidt surveys or surveys with Schmidt telescopes the whole issue reverses because, as we were told yesterday, it appears that certain telescopes that used to do photography no longer support it. I'm not surprised. I had guessed that maybe the Mayhall plate collection will never grow larger than 4,000 plates. That's just a guess on my part.

Janes: I want to point out that with regards to this lifetime business....some of us are talking about archiving. You mentioned ten years for all these databases. The older observatorys around the world have archives that now go back to almost a hundred years.....The information is still useful and its also still readable by modern technology (laughter) seven track tape drives and things are no obstacle.

Wells: Yeah, of course you're right. Incidentally, the fact that you can't guarantee an optical disk for a hundred years should not be taken as any problem of the technology. The answer of all tera-bit memories is that you just simply re-record the data. And there's no problem at all to just set up a program in the system that runs in the graveyard shift every night and re-records one disk. That's obvious and so that in fact is a policy in magnetic tape archives. They choose a certain number of years and re-record tapes....if you intend to keep them for years and years

Boyce: I think this raises a question though that shouldn't be brushed under the rug and that's the thing of indexing. How and all in the 10 to 12 bits can you find the ten to the six bits that are currently of interest to you. I think it's needs a little bit of a dialogue system I think it's not a trivial question.

Parise: I just have two comments. One is for a quick look type of data storage. At the present time JPL is distributing the entire Voyage Jupiter and Saturn encounter on on one video disk. And which you can buy a copy of for $350. And the other thing in reference to low cost video disk mastering equipment, we looked into the problem of putting the IUE quick look facility on video disk. I don't know if you've ever seen it but we have two huge rotary files with 8 by 10 inch films on 26,000 images. In fact, you can fit this all on one video disk. The problem is the inexpensive mastering facilities plus were not set up to take 9 track tape and what you're talking about is now coming available. What they do is they can take master video tapes and movies and things and put it on a video disk for you for just a few thousand dollars. But no one except apparently one or two places put 9 track tape on a video disk.

Wells: You say it's a few thousand dollars to master an analogue video disk? Three thousand? Five thousand?

Parise: I think it was $5,000.

Monet: Just two comments. Frame grabbing off of the JPL disk works like a bandit. It's really a great way to get all sorts of neat Saturn/Jupiter pictures into a VAX, for again an arbitrarily small amount of money, if somebody's got one of those things. Every 1/30 of second you get another picture in 8-bit digital form, very interesting stuff. The other thing I'd like to point out is the great need for some kind of archiving now of on the line ___. In ten years I'm sure we'll all be chuckling at the rather poor data capabilities and how slow it is to use these video disks. I think we need an intermediate storage in the tera-bytes now. Most places I know that have CCDs are not archiving things and, as a astromist, I severely worry that these bits are gone when you hit the digauss button because tapes are $20 a throw. Observatories, for example at Kitt Peak, require visiting astronomers to return tapes for re-recording as differing from returning photographic plates for archiving. It affects me rather personally because the parallax program has 300 rolls of tape already and the choice was "pay for it out of your pocket or we will digauss them "as differing from " return it and we will put it on a shelf for you to come back to in ten years from now." I think it's very important for some kind of a device for intermediate level archiving appear as quickly as possible and we'll worry about the 20 year lifetime in ten years when technology will presumably be far different.

Hemenway: I like to think of myself as one of the few people left who takes photographic plates for non-survey purposes. As soon as somebody comes up with a method for getting hundredth of an arc-second positions over a 20 arc minute field then I'll be happy to fore go getting my hands dirty at the telescope every night.

Poland: I have a couple of comments on the ampex tera-bit memory at NCAR. They have apparently not lost any data, but they've lost a lot of their dictionary. They can't get at it... They can't find it. As far as optical disks go NCAR is apparently in agreement with Storage Technology right now, and they're going to hook one of these optical disks with write and read capabilities onto the NCAR computer so that people will be able to write their data. And I guess we're trying now to get all SMN data-Solar Maximum Mission Satellite that has five or seven telescopes operating for over a year-all of that data fit on one optical disk and we're trying to set up a scheme right now to distribute that to anyone who wants it.

THE PREPARATION OF THE MEASURAMENTS AT THE PDS AT THE PADOVA OBSERVATORY : REPORTS ON AN EXPERIENCE WITH THE DEVELOPEMENT OF AN ASTRONOMICAL DATA BASE ENVIRONNEMENT.

Leopoldo Benacchio
Osservatorio Astronomico
5,Vicolo dell' Osservatorio - 35122 Padova - I

ABSTRACT:
This paper describes some software facilities used mainly for information retrieval and analysis at the Padova-Asiago Observatory. These facilities help guest and resident astronomers to make easier the preparation of plate measurements.
The problems connected with the creation, use and management of a data base in a scientific (astronomical) environnement are reviewed on the basis of the experience gathered during the last three years. The development plan of the 'user session' environnement and its possible applications in a computer network are briefly sketched.

1. BACKGROUND.

The PDS 1010 is a well known and widely used machine in the Padova-Asiago observatory. In almost all the fields presently filled by the astronomical research in the observatory, this machine gave, and gives, an important contribution in the measurament phase. In astrometry, for the measurament of position, mainly on Schmidt type telescope, in the stellar and panoramic photometry, especially of elliptical galaxies, in mono and two-dimensional spectroscopy, especially for echelle images. During these and other reasearches in the last, say, eight years , this machine proved to be, with sometimes great limitations ,a very efficacious and, at the moment, irreplaceable instrument. The installation of a PDS 1010a machine is foreseen, in the Padova observatory, in the end of the 1983.

2.0 THE ASSISTANCE AT THE MEASURAMENT.

In the study and setting up of an astronomical measurament two main different aspects are involved : the study of the criteria of sampling and the retrieval of the exhisting information. We shall deal here only with some aspects of the second problem and its integration with the post-measurament phase, that is data reduction. The experience gathered in these years with the PDS and other computer controlled measuring machine showed, in an encreasing way, the necessity of integrating the retrieval system of scientific information concerning the objects to be

studied with that managing the data coming from the measurament of the object themselves. The big jump of informatic technology from, say, 1975 till now has given the astronomical community computing systems of high power and disc storage capability. Also the software, from operating system to data reduction, takes great advantages from this development especially from the point of view of transportability ,compatibility and documentation.
Let us take, for example, the standard configuration of a 'medium' size pole of the italian astronomical computer network (ASTRONET) :
CPU :Digital Vax 11/750 ; Phys. Memory : 2 Mbytes ; Mass memory from .5 to 1.0 Mbytes ; 'low' and 'high' level colour graphics station ; virtual memory operating systems .
In a computing environnement of this type, by this time enough usual in the international community, we can think that the integration of the information retrieval system with that of data reduction will be an actual possibility.

2.1 THE PRE-MEASURAMENT PHASE

When an astronomer prepares himself to a measurament almost always needs a serie of archives, such as,for example, catalogues, bibliography, observation log-book etc.. The aim of this consultation is that of getting indispensable information and knowledge about the target and field object both, from the astronomical as well as from the numerical point of view. That is, he needs astronomical knowledge to put into his mind and digits in order to put astronomy into the computer. Positions, Magnitude, spectral type, and colour index are the parameters more frequently requested in the pre-measurament phase. For some measuraments, the retrieval of the wanted data is fairly easy. This is the case of spectroscopic images ; these type of observations, in fact, excepting those of objective prisma, takes into account one object only at time. Instead, in many other cases this work is heavy and compells the researcher to take one's attention away from the astronomy to the retrieval of data into paper. This research can be sometimes a long, tedious and tricky task when, for example, a discordance between the retrieved data appears.
In order to aid and make easier this part of the research, some software procedures have been implemented at the Padova-Asiago observatory with the intention to start the integration of the information retrieval system with those of data reduction in a single computing center (Benacchio 1982a,b) . These procedures allow to consult the lists of the Padova-Asiago plate archives (about 65.000 plates as at january 1983), to consult catalogues available from the Centre des donnees stellaires de Strasbourg, and to manage a simple user log-file.

The consultation of the observation register (8 log-books of 4 different telescopes from 1942 till today) is realized through the search, on all or part of the files,of the plates that satisfy the required conditions. The conditions on the search can be based, in a serial way, on nine keys which compose the record of the original observation : object name, year, date, alfa, delta, plate type, filter, exposure time, comment field. The inquiry is builded up by means of single iterations linked by logical operators (AND,OR,NOT). For example : first iteration : object name ; second iteration : AND year ; third iteration : NOT filter. The construction of the final request is, in this way obviously more time consuming than in the case of a complex but synchronous construction.
Nevertheless with this method the user can follow the construction of the wanted final subset step by step. Anyway the execution time of the whole remain in the order of 4-5 minutes for a 4 level inquiry on the whole data set. The experience showed that this method is appreciated by the astronomers who consult the register for the first time, or to those, who are not familiar with computers. Once made the choice, it is possible to schedule directly some utility programs later described. A limitation on the search is due to the concomitance of two factors : at IAU level, a final standard for the codification of the astronomical observation is lacking as for the direct photography as well as for spectroscopy . Moreover in the Asiago records, mainly for historical reasons, some important information are relegated, side by side, in the comment field. Due to this situation we did not think to tranlate, also if possible, th records into a standard form which is not a definitive one. But this implies that many information contained in the comment field, must be searched by means of a variable length string strategy, and can make the search complicate not only from the point of view of the software, but also from that of the practical use of the procedure.
As shown above, it exists a second package that can be reached from the first one to consult the astronomical catalogues. Obviously this package can be invoked directly and, in the practice this is the more frequent case. The catalogues that can be used with this procedure are the most available on magnetic tape from the CDS (see CDS bulletin no. 21, 1982) . The catalogues are consulted with a very similar technique to the one sketched above. Generally each catalogue chosen for the consultation in the CDS list, is inserted in the software system at his arrival from the Centre. The user builds, with the assistance of an utility program of the procedure, a correspondance table between the record on tape and the record on disc. Once the correctness of the translation has been checked, the table is permanently memorized into the system,

while the catalogue is scratched when the interested user do not attend the retrieval work with a daily frequence. This fact depends mainly from the small disc storage capability of the system (60 Mbytes), which inhibits also the adoption of techniques of search more fast than a serial partially indexed one is. Once the list of the wanted objects is obtained, the user can schedule some utility programs. These facilities allow the user to examine the sample by means of histograms, diagrams, lists on paper and overlay. If an user needs applications different from these, he has to link a self developed program to the procedure by means of an interface protocol. In order to use many catalogues at time, it is necessary to run the package on single files with the same requests and then link them togheter by means of the utility programs. This means, for example, to be able to produce mixed lists or diagrams, taking from each catalogue the more useful parameters.
The package has been designed in this way, severely limitated from a philosophical point of view, because, taking into account the limitations of the computers available at the observatory at that time and the poor experience with the problems of the scientific data bases, this seemed to be the best choice.
Finally a third software facility exhists, for the creation, update, and management of an user log-file. Two main parts compose this log file : one created and updated only from the user, the other only from some packages of data reduction. An user can perform a search both in numeric and alphanumeric fields, but the experience has shown that the main use of this facility is that of producing activity documentation.

2.2 POST MEASURAMENT FACILITIES.

When an astronomer come back from a PDS machine to the observatory computing systems (HP 1000.e and .f), can use some resident packages of common access and use. We cannot deal here with a description of these facilities , and only a summary is given below. Besides the retrieval procedures, the following common facilities exhist :
a) a procedure for the management of the PDS files : translation, quick look, computation and image histogram modification, gaussian filtering, image compression (Benacchio, 1983)
b) a procedure for the photographic photometry of extended objects : Interactive Numerical Mapping Technique (Benacchio et al. 1979).
c) a procedure for the reduction of data coming from the Reticon and Digicon detector based spectrographs (Bonoli et al., 1983)
d) a procedure for data reduction of IUE satellite.
e) the IHAP package of the European Southern Observatory (Middlelberg, Crane, 1979)

3.0 AN ASTRONOMICAL DATA BASE.

The experience of these last years, obtained building up, mantaining, and, after all, using these simple retrieval procedures, aided to focus some difficulties, we must consider in designing the layout of a data base system in a scientific environnement, in our case an astronomical one. The first problem we meet is to determine what an astronomical data base is, or could be defined or assumed. In the scientific research, in fact, the concept of data base is more complicated than in the commercial one, for example. That is due to the small, or better limitate usefulness of a data base organized in view of frequent and almost monochromatic requests. Let us take,for example, the case of the consultation of astronomical catalogues. A serie of codified and often repeated requests is typical only of some works of routine, as, for example, the production of charts or overlay for observation and measurament are. The use of catalogues as input in synthesis or model computations or comparison is completely different from the preciding and can require only a very simple interface software between the disc resident structure and the user. But still in this case if the catalogue is large enough and if the structure is not at less indexed, it becomes difficult to be used. These considerations take us immediately into the depths of the problem : on one side we need agile and swift structures of retrieval of the single value of the choosen parameter, on the other hand the construction of any type structure, indexed or hierarchical or inverted, need, more or less strictly, to know the more frequent requests to the inquiry program, before putting up the data base itself. Now, it is difficult to satisfy this condition, because, for definition, the research goes on also through the invention of new structures of correlation, on still known 'data bases'. These structures are revealed also thanks to other requests never put before. Who used software for commercial data base, had, without any doubt, sooner or later, the same experience. On the second hand the complete lack of standardization complicates this situation because each catalogue becomes a self standing case.
Beyond catalogues, an astronomer has to consult other types of 'archives', and should have the possibility to easily get into one's digitized images , as that coming from the PDS and solid state detectors, and 'manipulate' them. Thus in astronomy, the concept of environnement and data base overlap themselves in a way which can create elements of equivocation with respect to the usual definitions. With a merely operative definition, we could assume here as astronomical data base an environnement where 3 fundamental types of files : catalogues, images and 'other' and the procedures to manage them are present and linked

at level of mutual communication. In the type 'other' are included the archives of observations, the tables, the bibliography and the documentation.

3.1 PROBLEMS CONNECTED WITH THE TYPE OF FILE.

If one agrees to accept the previous statement of definition, immediately meets a conceptual as well as operative difference between the types of considered files. This difference is conceptual because, for example, the astronomical catalogues are a collection of data on some objects joined by a common genus, while, instead, the images contain information generally only on one object of any kind. The difference is also operative because these three types of files differ substantially for the use made and for the very different requests put to the software system, that has to manage them. In fact essentially the catalogues are consulted, in the more common, till now, way, that is, as a book. Obviously, their transposition from paper into magnetic support, accessible to a computing system, widen the concept of consultation, as seen above. At the contrary, the image itself is a data base or, better, a file, whose single information elements are used as input to the application of numerical algorithm (filtering, enhancement, integration etc.) in order to obtain the values of parameters which are generally of the same type of them contained in the catalogues (magnitudes, spectral type, colour index etc.). The third type, we called 'other', contains, excepting the tables, various objects : bibliography, log-book and documentation which are consulted and updated, really only at the level of list. With the word bibliography, we mean here only a list of labels, as stellar names, to which are linked bybliographic references.
Data tables, for example of correction or calibration of an observation , are separed because treated in the single procedures with the usual techniques of the matrix algebra.
Beside the difficulties we meet in the use of astronomical catalogues, sketched above and described in the quoted references, it is important to underline that the problems come more from astronomy than from informatics. In fact, if the catalogues were standardized, in their structure and homogeneized in the values, we could choose the query procedure, which makes the best service to the needs of most of the users for most of the catalogues.
That is not possible because the problems of astronomical type in the catalogues can be solved only giving to the astronomers the possibility to work in an agile and easy way on catalogues themselves, in order to do this homogeneization. If we think that the computer can have a key role in the compilation and standardization of the catalogues and in the homogeneization of the data , we must consider that the only way to eliminate the

problems of identification, redundance etc., is that of obtaining wheights by means of procedures that allow an intercomparison between different values from different sources. These wheights can be assigned only from astronomer in their practice. How important and wheighty is the work of the homogeneization of data is shown by the Catalogue of Stellar identifications of the CDS of Strasbourg (Ochsenbein, 1981).
The problems connected with the management of the files like images are really smaller than those of the previous type. In fact the images are managed in a self consistent way in the data reduction software procedures, or better environnement, and exact standard of transportability exhist (Wells, Greisen, 1979). Some of more recent system of data reduction (Albrecht,1982), foresee also log-file, which contain the 'history' of the image during the data reduction. Therefore this situation for the images is good till is considered at the level of data reduction. On the contrary, if the problem of recording is involved, the images present a serie of problems similar to those considered for the catalogues. We talk here, obviously, about the recording only of the main characteristics of an image. The lack of a standard makes also in this case all the matter more complicate, as already mentioned with regard to the observation plate registers. Nowdays this problem is not a crucial one, but it is foreseeable that, with the increasing of the power of the computing systems and after all with the massif use of solid state detectors, it will raise the rate of production of images as well as the necessity to look into lists of preexhisting images.
A last mention deserves the bibliography and documentation. Without dwelling on the problems connected with these two themes, it is worthy to underline, treating about an environnement available to each astronomer in his own Institute, the absolute necessity of local area centers of coordination . Obviously this fact does not preclude that the user can manage a limitate access , in his data base, also to this type of information.

4.0 STATEMENTS FOR A FUTURE IMPROVEMENT.

As it was shown in the above paragraphs, without entering into details, the main difficulties come from the lack of standardization of the information records in astronomy. That is evident for the astronomical catalogues and the log-books of observations. Moreover the dishomogeneity of the data contained in the catalogues themselves can be reduced, and in prospect, eliminated, only with the work of astronomers. To do that, it is necessary to supply astronomers an informatics environnement set up through an integration of three types of files composing what we called astronomical data base and the software which

manages this type of files.
In Italy this task was assumed by one of the working groups of the astronomical network ASTRONET. The projects of this group, which are still at a state of gross layout, include the building up of a very simple software for the aggregation of data coming from several catalogues. It is foreseen the construction in a pole of the network acting as main center, of a system able to accept requests to aggregate data from several files and to satisfy them in a reasonable time, that is in one day. Then in his pole, the single astronomer who made the request, examine the sorted data base with a software as more transparent as possible. This scheme of action, conventionally called 'user session', seems to be particularly interesting because the user is allowed to concentrate himself on the astronomical use of data, and possibly on their homogeneization. Moreover the volatility of the joint file and the relative ease with which it can be get in a network scheme, makes less dramatic the consequences of wrong choises. As a first link step, the access to information contained in log-book, documentation and procedure files is foreseen. The network connection is very important in this scheme because this seems to be the typical problem, where the cooperation is necessary to allow the single researcher to work in the most productive manner. It is desirable that, in a very near future, one could think about a connection, via networks, with still exhisting centers, in order to avoid all the duplication not absolutely necessary. Because of the complexity of the problem to solve, we let begin with a development program with many steps first with reduced aims, which allow, nevertheless, the single user to begin to work in these schemes, as well as to value the efficacy of the scheme itself.

REFERENCES :

Albrecht,R.,1982, in proceedings of IAU coll. no 64
Benacchio,L.,Capaccioli,M.,De Biase,G.,Santin,P.,Sedmak,G. in : International Workshop on Image Processing in Astronomy, 1979, Trieste ,Ed.s Sedmak, Capaccioli, Allen.
Benacchio,L., 1982a, in proceedings of IAU coll. no 64
Benacchio,L., 1982b, Mem. S.A.It, 53,1,209
Benacchio,L., 1983 preprint.
Bonoli,C.,Bortoletto,F.,Falomo,R. 1983, preprint.
Middelberg,F., Crane,Ph., 1979 in : International Workshop on Image Processing in Astronomy, 1979, Trieste Ed.s Sedmak, Capaccioli, Allen.
Ochsenbein,F.,Bischoff,M.,Egret,D. 1981, Astron. and Astroph. Suppl. serie 43,259
Wells,D.C.,Greisen,E.V. 1979, in International Workshop on

Image processing In Astronomy, Trieste, Ed.s Sedmak, Capaccioli, Allen.

STORAGE, RETRIEVAL, AND ANALYSIS OF ST DATA

R. Albrecht*
Space Telescope Science Institute
Baltimore, Maryland

Abstract

Space Telescope will generate multidimensional image data, very similar in nature to data produced with microdensitometers.

This paper presents an overview of the ST Science Ground System between carrying out the observations and the interactive analysis of preprocessed data. The ground system elements used in data archival and retrieval are described and operational procedures are discussed. Emphasis is given to aspects of the ground system that are relevant to the science user (General Observer, Data Archive user), and to general principles of system software development in a production environment.

The system currently under development uses relatively conservative concepts for the launch baseline. Given the 17-year operational life time of the telescope, concepts have been developed to enhance the ground system. This includes networking, remote access, and the utilization of alternate data storage technologies.

Introduction

The data generated by the Space Telescope will be very similar in nature to data generated by scanning microdensitometers. Some of the peculiarities introduced by the measuring engines will be replaced by peculiarities characteristic for the detectors to be used in the science instruments. However, the result will be the same kind of one- or more-dimensional data arrays, and the considerations that go into the planning for the storage, retrieval, and analysis of the data are nearly identical. The major difference is that in the case of the ST there are more severe requirements for throughput, and that outside users have to be able to use the data handling system after only a short period of familiarization.

* On assignment from ESA-Astronomy Division

The Space Telescope

A detailed description of the Space Telescope and the set of scientific instruments can be found in (1). To summarize, ST will be launched by Space Shuttle into an orbit about 500 km above the surface of the earth, an inclination of about 28 degrees with respect to the equator, and an orbital period of about 100 minutes. The diameter of the main mirror is 2.4 meters, the pointing accuracy is in the range of 0.007 arc sec. There are five scientific instruments: two spectrographs, the Faint Object Spectrograph (FOS) and the High Resolution Spectrograph (HRS); two cameras, the Wide Field/Planetary Camera (WF/PC) and the Faint Object Camera (FOC); and the High Speed Photometer (HSP). The Fine Guidance System (FGS) of the telescope, used to lock onto guide stars in order to track objects to be observed, can be considered a sixth scientific instrument since it can be utilized to obtain high-precision astrometry data.

The operational and scientific center for ST will be the Space Telescope Science Institute, located in Baltimore. Communication between the Institute and the Telescope will be through the Tracking and Data Relay Satellite System (TDRSS).

Observing With ST

The orbital geometry of ST makes real-time interaction very complex. Real-time interactions will be possible, but only in a very restricted and pre-planned way. Not more than 20% of the data will be sent to the ground for near-real time viewing and assessment. In addition, the quality of the data received through the Observation Support System (OSS) is not as good as the quality of the final data, which will be available to the observer within 24 hours of taking the observations.

Data Type and Volume

The major source of data points among the science instruments is the Wide Field/Planetary Camera with four CCD detectors of 800 by 800 pixels each. These four subframes can be mosaiced into a single 1600 x 1600 frame. For operational reasons, the detectors have to be read out at least once per orbit.

The Faint Object Camera has a maximum data format of 512 by 512 pixels and works in photon counting mode. Thus, the FOC data volume ordinarily is only a fraction of the data volume of the WF/PC.

The spectrographs operate with linear detectors of 512 pixels, generating a very modest amount of data. The HSP in time series

mode will produce data vectors of several thousand pixels at a time.

The total amount of data received from the ST per day will depend strongly on the instruments used, the observing modes, and the objects observed (i.e. the exposure times). The current basis for planning is several 6250 bpi mag tapes per day.

Hardware

The Science Operations Ground System will be based on DEC VAX-11/780s. Peripherals include 600 Mbyte disks, 6250 bpi magtapes, and facilities to generate output products for the ST observers. The image processing hardware consists of Gould-deAnza image displays and Ramtek graphics devices.

It should be emphasized that the software development considerations given in this paper are not tailored to our particular hardware configuration. In fact, we have to expect substantial changes in the hardware during the lifetime of the ST mission, and, to some extent, even before launch. Thus, hardware independence was one of our major design goals for the development of the analysis software.

Pipeline Processing and Archiving

After the data are received at the ST ScI a calibration will be performed in a "pipeline" fashion. This is really only a preprocessing of the data, and it is not intended to be the final analysis. The operation will be performed in a fully automatic manner to avoid the accumulation of a data backlog. During this calibration step, a number of output products (hardcopies and magnetic tapes) will be generated. The raw data and the calibrated data will then be placed into the data archive. These data sets include the science data, appropriate header information, and a selected subset of engineering data.

Storage and Retrieval

The current plan for the ST data archive is fairly conservative: data will be stored on 6250 bpi magnetic tapes. The main archive will be kept in the ST ScI, with a backup copy in a different building to avoid loss of data in case of a disaster.

The archive will be maintained through a commercial data base management system. Using the DBMS interactive query language the archive can be searched for data that meet a specifiable criterion, or a combination of criteria. The output of such a search operation is one or more frame names, plus the associated magtape reel numbers.

There is a number of constraints both for loading the archive and for retrieving from the archive. Since the data volume is quite formidable, one certainly does not want multiple copies of data sets on the archive. Sometimes, on the other hand, this might be desirable, if, for instance, there are problems with SI calibration.

Retrieval from the archive needs to be even more restricted. The general policy is to keep the data proprietary for one year after the observation was taken to allow the observer to adequately study the material and publish the findings. There are, however, numerous exceptions to this rule. In case of long baseline observations (e.g. astrometry) the one year proprietary period will have to start with the taking of the last data set. Also, if significant changes occur in the calibration procedure the proprietary period will have to be extended.

The data base management system provides for all these capabilities and also has appropriate password and security features to inhibit illegal access to the data. Access to the magtapes themselves is controlled through operational procedures.

The archive data format is FITS (Flexible Image Transport System), with a few modifications to make it more efficient. Even at optimally filled records, FITS is only about 60% efficient on 6250 bpi magtapes. To circumvent this, and to also speed up reading, the records will be blocked (the blocking factor will probably be eight). Also, the high-order, low-order byte sequence will be kept in DEC standard, to avoid having to swap bytes during write and read. These deviations from the standard FITS format can be tolerated since this is only an internal format. Magtapes to be taken from the ST ScI for home institution analysis will be written in standard FITS format, unless otherwise specified.

At this point a remark about FITS is probably in order. FITS was originally developed at NRAO and Kitt Peak and it is well documented (2). In any acquisition software development there is a temptation to go with unique data formats on magtape, simply because this seems to be easier and more efficient. However, it has always turned out that more manpower was spent that way, when changes and additions had to be made and the tapes could not be read anymore. FITS circumvents these problems and should be used whenever possible.

Interactive Analysis

The ST Science Data Analysis System (SDAS), even though it is being developed especially for the instruments on ST, follows very much the design concepts of a number of already existing data analysis systems.

Some of the requirements for SDAS are obvious: it has to provide capabilities to allow adequate analysis of the data produced by the instruments on board of the ST. Other requirements are user-friendliness, expandability, and maintainability. Also, the long lifetime of the mission imposes requirements on SDAS: we have to expect considerable changes in the hardware and software configuration of the analysis system. For this reason, and also because we anticipate the export of software from the Institute, emphasis has been given to transportability and system-independence of the software. In addition, the data analysis host system (command language and utilities) will be government furnished to the ST ScI, and although the development is controlled by an Interface Control Document, we have to expect to have to accommodate considerable changes during the development phase.

To solve these problems, SDAS application software will communicate with the host environment through a series of software interfaces. These routines will solicit (GET) input from and deposit (PUT) output into the host environment. Thus, if the host environment changes, only the PUTs and GETs will have to be changed, and not the application programs.

Hierarchically, these routines will only be used out of the first (uppermost) level of the application software. All lower levels, in particular the science algorithms get their information passed through subroutine calling sequences. All pixel data are kept in VAX virtual arrays. In this manner we achieve a maximum of maintainability: when software is being transported to a different operating system, it is always evident what has to be changed and where in the program the changes have to be made.

As a matter of fact, we are already using these SDAS design features to our advantage in the development of the software. Since the data analysis host system, which is being developed as part of the science operations ground system by a government contractor, will not be available in time for application software development, we are developing SDAS within a different host system. This system, which serves as a testbed system for SDAS, is the NRAO-developed AIPS system.

These design features also contribute to the transportability of the software. Our goal is to achieve "limited transportability", a concept which tries for an optimum trade off between software transportability and development cost. Clearly, the efforts required to develop software that will transport to any computer are prohibitive. On the other hand, a few comparatively simple design guidelines will make sure that the software will port between machines of a certain class. In our particular case we are aiming at 32 bit virtual memory machines,

since these machines can be expected to be used in the majority of astronomical institutions within the next 5 years.

Note that the question of programming language never really enters into these considerations. For practical reasons we are using FORTRAN 77: although other languages are, in some cases, superior to FORTRAN, it is still the most widely used and understood programming language in astronomy. However, the above considerations apply regardless of the language chosen for the implementation of the software.

For SDAS there are severe requirements for documentation and configuration control: not only do all programs and changes made to them have to be documented, we also have to make sure that such changes are not made in an uncontrolled manner. This is particularly important in an environment where a number of people work on the software, and where the authors of the software are not necessarily identical with the users of the software. The approach that we are taking is to utilize software development tools. All documentation is based on the software design document (written in PDL), out of which the different subsets of the documentation (for the user, the applications programmer, etc.) is being extracted by software tools.

The PDL design, the pertinent documentation, the code, test data and other associated files are being maintained as groups and controlled by a utility, the software management system.

While not everybody in astronomy has the same documentation and configuration control requirements that we have, I strongly recommend the implementation of such procedures for any software development project that has more than one component program. Experience shows very clearly that the initial investment of implementing such procedures is more than compensated by the advantages in terms of software maintenance and by the fact that the software will be useful for a longer period of time and for a larger number of people.

The User Environment

To the user these software development considerations are quite invisible. Operational considerations will be more relevant, so let me give a description of SDAS from a more practical point of view.

SDAS is image-data oriented, so typically the user will sit down in front of a work station consisting of an image display device, a graphics CRT, and an alphanumeric terminal. There will also be access to hard copy devices, plotters, and magtapes.

The login procedure will be similar to login procedures on all multi-user computer systems. Through the high level command language the user will then have access to the data and to the SDAS application software.

If the analysis is being carried out immediately following an observation, the data will still be in the working area of the "pipeline" part of the system. Data taken further in the past will have to be requested from the archive. In order to work on them, data will be stored in the user's work space. There also is a software work space, into which the user can pull SDAS modules, modify them, or create special default values for input parameters. After the analysis, requests to generate output products can be queued to the output product generation system.

Like in all other state-of-the-art analysis systems, the user will have access to an on-line HELP function. Not only can HELP be requested on commands and their arguments and qualifiers, HELP can also be asked for when input is being requested from an application program. A menu mode is available for the inexperienced user. The system also logs all input for later reference.

Concepts

As already indicated, the baseline system which is currently being planned is rather conservative in design and technology. We are, however, investigating the possibility of other system concepts and the utilization of alternative data storage techniques.

One of the most dramatic developments in computer systems technology during recent months is the emergence of 32-bit microprocessor based systems. Several companies are now offering packages that are configured around an off-the-shelf microprocessor chip, which is connected to a number of peripherals through an industry-standard bus. The peripherals typically again incorporate a microprocessor, off-loading the central processor, and increasing the overall power of such systems to something in the order of a VAX 11-750.

Even though the vendors of such packages also do a considerable amount of application software development, they usually do not bother with operating system development, but instead use UNIX. Since the price of these systems is only a fraction of the price of superminis of comparable power we have to expect a large number to be in use throughout the community in the near future.

Having powerful analysis systems available at their home institutions, which are capable of running ST analysis software

(exported from the Institute or written locally), will significantly reduce the motivation of users to come to the Institute for data analysis. On the other hand, it will increase the demand for communication, both in the area of software exchange, and for data transmission. The obvious answer is a network solution, and we are currently assessing the viability of different implementations.

Another area with the potential for immediate improvement is the archival data storage. Unfortunately, it was not until recently that alternative storage technologies became available at reasonable prices and a high degree of reliability. For this reason the baseline archive system is designed rather conservatively. Even though the storage on 6250 bpi magtapes is relatively efficient, and the administration of the archive through a Data Base Management System is actually a substantial improvement over other astronomical data archives, there is one considerable disadvantage: random access to the data takes too long. It involves human intervention (an operator has to retrieve the tape from the vault) and can take as long as 30 minutes. We are currently looking into optical disk technology to develop a real-time browse capability.

Acknowledgements

Building the data analysis system for ST can only be a team effort. The team in this case consists of my colleagues at the Space Telescope Science Institute, in particular in the Operations Department, and of individuals at the NASA-GSFC ST Project Office and at TRW, Inc.

References

(1) Hall, D. N. B. (ed.), The Space Telescope Observatory, NASA CP-2244, 1982.
(2) Wells, D. C., Greisen, G. W., and Harten, R. H., Astron. and Astroph. Supplement, 44, pg. 363, 1981.

PHOTOGRAPHIC SURVEYS OF THE SOUTHERN SKY

M. Elizabeth Sim
UK Schmidt Telescope Unit
Royal Observatory
Edinburgh EH9 3HJ
Scotland

The Royal Observatory, Edinburgh (ROE) is an establishment of the UK Science and Engineering Research Council, with the primary task of providing high quality research facilities for the UK astronomical community. The UK Schmidt Telescope Unit is responsible for the operation of a 1.2 metre telescope at Siding Spring Observatory, Australia, and for the Plate Library facility and a suite of associated Photographic Laboratories in Edinburgh.

1. THE TELESCOPE

The 1.2 metre Schmidt telescope has been in operation since 1973. It is a classical Schmidt telescope, very similar in size and design to the Palomar 48" Schmidt. The original BK7 singlet corrector plate was corrected at 420nm for optimal performance in blue light. This was replaced in 1977 by a full-aperture cemented achromat, made by Grubb Parsons. It is corrected at 370nm and 800nm, and is thus capable of giving images of 1 arcsec or less at all wavelengths longward of the corrector plate cut-off at 330 nm. The telescope is also equipped with two full-aperture objective prisms, which may be used separately or in combination, to give dispersions of 2440, 1260, 830 or 620 Angstroms per mm at Hγ.

The telescope is equipped with two step-wedge calibrators, one of which is currently based on the Kitt Peak design. Every plate taken with the telescope automatically receives two calibration exposures on otherwise unexposed areas of the plate. Every plate taken is also subjected to strict quality control. A plate which satisfies the standards required for inclusion in a survey is graded A. Plates which are not quite up to survey standards are graded B, and are very useful for many research programs.

Plates taken with the Schmidt are in two categories, those taken for systematic sky surveys, and those taken at the requests of research users.

2. SURVEYS

2.1 The ESO/SERC SOUTHERN SKY SURVEY

The first task of the UK Schmidt was a collaborative project with the European Southern Observatory (ESO) to undertake a two-colour photographic

TABLE 1

UK 1.2metre SCHMIDT TELESCOPE PARAMETERS

Latitude	$-31^\circ\ 16.'4$	Longitude $-149^\circ\ 04.'2$ $-9^h\ 56^m\ 17^s$
Aperture	1.24 metres	f/2.5
Field of view	6.5 x 6.5 degrees	
Unvignetted field	5?4 diameter	
Plate size	356 x 356 mm	
Plate scale	67.12 arcsec/mm 14.9 microns/mm	
Corrector plate	Cemented Achromat	
Corrected wavelengths	370nm, 800nm	
Image size (excluding emulsion scattering)	< 1 arcsec	

survey of the sky south of -20° declination, to complement the original Palomar Survey. The ESO/SERC survey will eventually consist of blue and red photographs of each of 606 overlapping fields with field centres separated by 5 degrees. The UK Schmidt is taking the blue (J) plates, using hypersensitised Eastman Kodak IIIa-J emulsion exposed through a Schott GG 395 filter. The limiting magnitude of the J survey is approximately B = 23. ESO, having completed a "quick blue" survey using unhypered IIa-O plates, will take the red plates on IIIa-F emulsion. The J survey is now virtually complete. Film copies of the atlas are being produced at the ESO Sky Atlas Laboratory in Munich, and to date copies of 519 fields have been distributed to 150 customers worldwide. For many applications film copies are perfectly adequate, but there is a limited requirement for glass copies, especially for high precision machine measurement. ESO are therefore making 10 sets of glass copies for which 180 fields have been issued to date.

2.2 Near-infrared Survey of the Galactic Plane and Magellanic Clouds

This survey covers the area of sky south of the equator, within 10 degrees of the galactic plane, and also the Large and Small Magellanic Clouds. Eastman Kodak IV-N emulsion, hypersensitised in silver nitrate solution, is exposed through a Schott RG 715 filter, to reach an approximate limiting magnitude I = 19. For comparison purposes a short exposure red (SR) plate (IIIa-F + RG 630) is also taken of each field to reach a similar limiting magnitude. The survey consists of 163 fields, and field centres are the same as those used for the ESO/SERC survey, at 5° centres. Film copies of this survey are being made in the ROE Photolabs, which have been specially designed include the capacity to make limited editions of sky atlases. To date 100 pairs of I/SR film copies have been sent to 68 customers worldwide.

Following considerable user demand, this survey will be extended to high latitude fields, and eventually will cover the whole southern sky. Since moonlight is relatively weak in the near-infrared, plates for this survey can be taken in "grey" time, and they do not compete for telescope time with other projects and atlases.

2.3 The Equatorial Surveys

The ESO/SERC survey covers the area south of -20°, and the second epoch Palomar survey will stop at the equator. The zone between 0° and -15° declination is being surveyed by the UK Schmidt, as the Equatorial J (blue) and R (red) surveys. These were originally planned as relatively low-priority tasks, but now have higher priority since the Southern survey is essentially complete, and the Equatorial J Survey is needed for the Space Telescope Guide Star program. These surveys will contain 288 fields, on 5 degree centres. A very limited number of glass copies of the Equatorial J atlas are being made by ROE Photolabs, and in due course film copies of this atlas will also be made. Most plates for the Equatorial Red (ER) Survey have still to be taken, and in due course they will also be copied and issued as an atlas on film.

Table 2

Characteristics and Progress of UKST Sky Surveys

Survey (& symbol)	Area of Sky (field centres)	Plate & Filter	Approx Limiting Magnitude	Total Fields	Accepted Plates	Total fields distributed
ESO/SERC Southern Sky (J) Survey	$-90° \leqq \delta \leqq -20°$	IIIa-J +GG395	B=23	606	599	519 film 180 glass
Near Infrared Survey of Southern Milky Way and Magellanic Clouds, and Companion Short Red Survey (I and SR)	$\delta \leqq 0°$ $b < 10°$ +LMC +SMC	IV-N +RG715; IIIa-F +RG630	I=19	163	151 (X2)	100 film (X2)
Equatorial Sky Surveys	$-15° \leqq \delta \leqq 0°$					
blue (EJ)		IIIa-J +GG395;	B=23	288	103(EJ)	-
red (ER)		IIIa-F +RG630	R=22		53 (ER)	

2.4 Prism Surveys

There is some customer demand for an objective prism survey. However, different programs require different dispersions and degrees of spectral widening, and as yet no firm decision has been taken regarding the parameters of a prism survey, and nearly all the prism plates taken so far have been in response to specific requests from research groups. Pending a decision on survey parameters, all the available 'A' quality prism plates are being retained to form a basis for a systematic survey.

3. NON-SURVEY WORK

In addition to undertaking the sky surveys for which a large Schmidt telescope is so well suited, the UK Schmidt is also operated on a service basis, primarily for the UK astronomical community. More than half of the plates taken are to fulfill non-survey requests. Plates taken for surveys but which are not accepted as A grades can also be made available for research purposes. Normally plate material is loaned in the form of film copies made by ROE Photolabs. Whilst many plates are used only for visual inspection, the advent and availability of fast measuring machines such as COSMOS at ROE, the APM at Cambridge, and PDS machines, has resulted in a substantial increase in the number and size of requests for plates to be taken specifically for machine measurement. To date we have received requests for material to support some 580 research programs, of which about 200 are still current. Programs range from measurement of parallaxes to automatic searches for quasars. All requests for plate material are dealt with by UKSTU staff in Edinburgh. The UKSTU facilities at ROE are centred around a specially designed Plate Library, which accommodates the bulk of the plate collection and also glass, paper, and film copies of sky atlases. Visitors are encouraged to come and use these facilities, which include light tables and microscopes, and some measuring machines. The Plate Library is conveniently placed very near to the COSMOS measuring machine, and the two facilities complement each other in several major research projects.

REFERENCES

R.D. Cannon, J.A. Dawe, D.H. Morgan, A. Savage and M.G. Smith - Proc. Astronomical Society of Australia 4 (4), 468, 1982.

M. Hartley and J.A. Dawe - Proc. Astronomical Society of Australia, 4 (2), 251, 1981.

Monet: Three quick comments: I have successfully obtained glass copies of the Palomar infared Milky Way atlas and they're available through the Cal-Tech bookstore on special request. The originals are treated as though they are sky survey plates. That is, no one gets to touch them except the photo reproduction department but they are available on special request for those who are willing to pay the cost. I got three-that's all I needed. Second, Sargent did mentioned last week a delay of almost a year for the achromatic corrector involved in the new sky survey so that gives us as software types a little bit more time to figure out what to do with all this data that is coming. The third and most interesting is a comment that Sargent made last week that there is an active debate as to whether there is to be six degree or five degree centers for the northern survey. So for people who have strong feelings in either direction. I think now is the time to start lobbying for your favorite direction. But I think as far as Sargent is concerned, it doesn't really make a whole lot of difference.

Sim: Thank you for raising that. One thing I didn't say, but I should have said, was that both the ESO and the Palamar Schmidts are in the process of getting (achromatic) corrective plates. So these are red surveys. Although it's been delayed, it's probably an advantage because it will come out from the smaller images on the IIIaF emulsion instead of as it was originally planned. I think the (ESO) corrector-I'm not quite sure it's delivered yet-is ahead of the Palomar one in Greg Carsons que.

Monet: Apparently the glass just got delivered and they knew of the slip a year ago or something-I don't know if they have started cutting glass.

Sim: Well, the last time I saw it was about four or five months ago at Greg Carsons workshop. They were polishing one part and fairly well thru polishing one part as I understand it. The second component was coming into the polishing line. That might cheer you up just a little bit.

Lasker: I detect from that comment I was feeling a very similar thing that for those of us who may have to do things in arbitrary place on the sky and do something that requires not just a point on the sky but an area around a position to work with. There are tremendous conveniences in the five degree centers that your plates have adopted. This isn't the place to debate but I do feel that it is useful to say that we do find the five degree centers, presently existing in the South to be very conveniently placed.

Sim: If I can put in another advantage of the five degree centers--bear in mind that on the 1.2 meter Schmidt that we have at Palomar--the unvignetted area of plate is 5.4 degrees diameter. So if you go on six degree centers there is substantial chunks that the sky would always appear on vignetted areas of the plate.

Boyzan: This is a very practical question. What do you recommend for digitizing the film copies? Do you recommend taping it on a glass or sandwiching it between glass plates?

Sim: This is quite a problem. You find if you receive any films from us they are sealed into transparent envelopes. This is largely to keep user fingerprints and ink marks off the emulsion. There's no reason why that bag couldn't be slit and the film taken out. You can always put it back together with tape afterwards for long-term storage. I don't know if I've really solved the problem of how to make that film on a measuring engine. If it's a flat plater machine, on some requirements, for instance we have an X-Y table, just off the plate library, and it seems that it would be quite practical to lay the film down and put a sheet of glass on top of it and that's quite alright. We don't run into any problems due to the transmission through the glass. However, there are some machines where this just isn't practical. If anybody comes up with any ideas—particularly with the more difficult machines--then we'd be glad to hear them. You do what you can when you run into problems.....

Hewitt: The PDS at least does not tolerate a thick piece of glass on it. It was just not designed for it.

Sim: I'm not quite sure what the ideal answer is. Depends really on what the tolerances are on holding it down. If it will go down that's fine but unfortunately it won't. I might put in a little plug for our photographic labs. When they seal the films in clear envelopes, they lie flat. One of the difficulties with the ESO film—they seemed to have picked the curved envelopes that they really do need to be held down.

PHOTOGRAPHIC MEMORY
THE STORAGE AND RETRIEVAL OF DATA

James Horton
Consultant
2242 Highland Vista Drive
Arcadia, California 91006

INTRODUCTION

Photographic emulsion has long been and will continue to be the primary medium for recording the optical phenomena of the world about us. It is fast, easy to use, permanent, low cost, and can have a spectral and spatial resolution and sensitivity far exceeding that of human vision. This spatial resolution capability and sensitivity to intensity modulations enables a higher density of information storage than by any other comparable means.[1,2,3]

The informational content of a photograph consists of not only the optical density of each picture element, but also the location of such elements relative to one another. To utilize this information, especially when it must be input to a digital computer, it has become common practice to digitize the photograph in such a fashion that a "numerical image" is formed of the optical density modulations of the scene depicted.[4,5,6] (Fig. 1) In other words, the photographic record is divided into a two-dimensional array of picture elements, or pixels, which are of a size chosen to be suitable for the intended purpose of such digitization. Each pixel is assigned a numerical value proportional to the optical density modulations integrated over the entire pixel area. This numerical image is then used instead of the photograph as a representation of the phenomena originally recorded. (Fig. 2) An important point to remember is that no sub-pixel modulation exists in the numerical image and none is recoverable without a priori knowledge of the original scene depicted.

STORAGE PROBLEMS

Frequently, the numerical image of a scene must be stored, either for archival purposes, or for subsequent manipulation or modification.[7,8] And since the storage of digital data usually requires many times the volume of the original photograph, it would seem logical and reasonable to use the original photograph for such a purpose, time permitting. One would merely rescan the photo whenever the digital information is required. Unfortunately there are several reasons why this has always been difficult to accomplish. Most of these reasons have to do with errors caused by changes in pixel locations.

The photometric value or "density" of a pixel is determined by evaluating the amount of light transmitted (or reflected) by the geometrical area comprising that pixel. (Fig. 3) Change the location of a pixel and you change its value. This is true even when a pixel is shifted within a "uniform density" area of a photograph due to the granular nature of the photographic emulsion.[9,10,11] (Fig. 4) And if the scene is strongly modulated the effect is even more noticeable. (Fig. 5)

Every film scanner, whether mechanical or electronic, has its own positional error pattern which is due to the inaccuracies of its tracking and position-measuring systems. (Fig. 6) Even though these errors may have a magnitude on the order of only a few microns they can still represent a sizeable percentage of the sampling aperture (pixel) size. Repositioning the photographic record relative to this error pattern has the effect of changing the location of each pixel relative to the photograph. Added to the systematic positional errors are those of non-repeatability due to random positioning of mechanical elements such as bearings, and to electronic noise in the positioning and measuring systems. An additional source of positional error is film distortion such as shrinkage, etc. The net result of these positional errors is that it is extremely difficult to sample analog photographic information at exactly the same locations each time the photo is loaded in the scanner. Therefore, corresponding pixels on successive scans of the same photograph may have different digital values depending upon precisely where each pixel was located when sampled.

Photometric noise also affects digital values of "identical" pixels. The statistical approximation of the quantum nature of electro-optical phenomena leads to the familiar formula which states that the noise content of a signal is equal to the square root of that signal.[12,13,14] (Fig. 7) This implies, among other things, that the relative amplitude of the noise is a function of the optical density of the pixel being sampled.

It can be seen, therefore, that several factors militate against the use of analog photographs as a storage medium for digital data when that data must be readily and repeatedly accessible. Storage of such data must be done so that errors in pixel registration and photometric noise do not affect the recorded values. To be useful as a recording medium each discrete location on the record must be unequivocally identifiable as a unique value.

PROPOSED SOLUTIONS

The photographic storage of digital data can be readily accomplished by using the playback capability of such scanners as the Perkin-Elmer PDS Microdensitometer. (Fig. 8) Basically, digital data is decoded and formatted as a two-dimensional array of discrete pixels, each with an appropriate optical density. The digital data can result from a prior scanning and digitizing operation, or can be generated from non-photographic data. An example of the latter is digital terrain elevation data. Each elevation is associated with a particular location, so the X, Y, and Z coordinates of a terrain feature can be represented on film by X and Y coordinates and optical density level, respectively.

The requirement that the stored data be insensitive to errors of sampling aperture positioning can be met by sampling each pixel with a smaller aperture size than that used to expose that pixel. (Fig. 9) For instance, if each pixel of a photographic record were to be exposed using a 50-micron-square aperture and then sampled using a 25-micron-square aperture, then plus or minus 12.5 microns of pixel misregistration could occur before data errors would be manifested. Also, film distortions are minimized by restricting the size of the film used to record the digital data. Additional

benefits of using a small format (e.g. 70 mm roll film) will be discussed later.

Insensitivity to noise - the final requirement for the storage and retrieval of data - can be attained by the application of the concept of Distinguishable Density Levels to the encoding of the digital data.[15,16] (Fig. 10) The total of all photographic and photometric noise - functions of film granularity, aperture size, and optical density on the one hand and shot noise, Johnson noise, and gain and linearity errors on the other - must be used to determine the increments between successive recording levels. By this method, a nominal density level and all other values which fall within the tolerance zone associated with that density level are identified as having a single, unique digital value. (Fig. 11)

The proposed scheme of data storage and retrieval is, then, that digital data be encoded as Distinguishable Density Levels, stored on photographic film in a two-dimensional array using a relatively large exposure aperture size and then read from the film using a relatively small scanning aperture. To remove exposure and development effects from the error budget and to calibrate the scanner/reader, a step wedge covering the range of DDL's can be laid down at the time of data storage. In addition, fiducial marks can be generated at the same time so the film record can be properly oriented with respect to the coordinate system of the scanner/reader. Some practical aspects concerning the implementation of this storage/retrieval scheme will now be discussed.

IMPLEMENTATION

As to pixel size, a typical requirement might be to store elevation data covering an area of 1° each of longitude and latitude with a data density of one elevation for every 10 meter square.[17] (Fig. 12) If the area in question were centered on South Pasadena, California, the record would contain 9,215 pixels in longitude, and 11,100 pixels in latitude. In order for this to fit within a 9-inch square format (228.6mm) each pixel can be no larger than 20 microns. Considering film shrinkage allowance, available

stage accuracy, film repositioning tolerance, etc., this is clearly too small.

Another approach is to limit each patch of elevation data to a 7-1/2' quad. In such a case, the longest dimension likely to be encountered would contain 1,393 pixels (corresponding to a latitude at 70° N or S). This could fit on a piece of 70 mm film if a 48-micron pixel were used. (Fig. 13) Film shrinkage will be negligible in 70 mm and this is a convenient size for handling. Returning to the example of the South Pasadena-centered area, each patch would contain 1,152 x 1,387 pixels.

The next consideration is that of the number of Distinguishable Density Levels which can be used. In other words, how many different values can be assigned to each pixel location? While the specific number remains to be determined, it will be safe to assume that it will not exceed 100, with a likelihood that it will be considerably less. In any event, it will be a number which is small in comparison with what can be considered as being a useful range of values. The answer to this problem is to multiplex each pixel, forming a two- or three-digit density symbol which is associated with a particular spatial location. (Fig. 14) For example, if 64 DDL's are used and a three-digit multiplexing scheme is employed, then 64 x 64 x 64, or 262,144 different numerical values can be ascribed to one location.

The multiplexing of density-encoded digits can be accomplished by a dual or triple read/write head and by storing or retrieving the data in parallel. (Fig. 15) There would be no geometrical distortion of the data and if 70 mm film were used as a storage medium, handling problems would be minimized. In such a case, with an inter-head pitch of 75 mm, four- and five-head systems are feasible. The extra channels (digits) may be used for encoding choroplethic or cultural information concerning the area covered by the pixel.[17] Such a five-digit recording of 10-meter square elements would require only 80 feet of 70 mm film to cover a 1° quad. If this record were composed of 4096 (64^2) elevations and three 64-level thematic codes for each pixel, an equivalent magtape storage would require 64 10-1/2" dia. reels of 800 cpi tape.

CONCLUSION

The concept of density encoding digital data in a mass-storage computer peripheral is proposed. This concept requires that digital data be encoded as Distinguishable Density Levels of the film to be used as the storage medium. These DDL's are then recorded on the film in relatively large pixels. Retrieval of the data would be accomplished by scanning the photographic record using a relatively small aperture. Multiplexing of the pixels is used to store data of a range greater than the number of DDL's supportable by the film in question.

Although a cartographic application has been used as an example for the photographic storage of data, it will be obvious that any digital data can be stored in a like manner. (Fig. 16) And when that data is inherently spatially-distributed, the aptness of the proposed scheme will be even more evident. In such a case, human-readability is an advantage which can be added to those mentioned earlier: speed of acquisition, ease of implementation, and cost effectiveness.

REFERENCES

1. R. A. Bartolini, H. A. Weakliem, and B. F. Williams, "Review and Analysis of Optical Recording Media," Opt. Eng. 15, 99 (1976).

2. The Theory of the Photographic Process, 4th ed., T. H. James, ed., Macmillan, New York, 1977, p. 630.

3. J. C. Dainty and R. Shaw, Image Science, Academic Press, London, New York, 1974, p. 135.

4. B. R. Hunt, "Computers and Images," Proceedings of the Society of Photo-Optical Instrumentation Engineers, Vol. 74, (1976) p. 3.

5. E. B. Brown, "Parameters of the Sampled Image System," A Symposium of Sampled Images, The Perkin-Elmer Corp. (1971) p. 2-1.

6. A. Rosenfeld and A. C. Kak, Digital Picture Processing, Academic Press, New York, 1976, ch. 8.

7. J. D. Petruzelli, "Archival Mass Storage System," presented at ACSM Fall Technical Meeting, Oct. 17, 1978, Albuquerque, New Mexico.

8. W. T. Riordan, "Digital Data Bases - The Wave of the Future," ACSM Bulletin, Nov. 1977, p. 11.

9. The Theory of the Photographic Process, op. cit., ch. 21.

10. Dainty and Shaw, op. cit.

11. SPSE Handbook of Photographic Science and Engineering, W. Thomas, Jr., ed., John Wiley, New York, 1973, sect. 17.

12. C. J. T. Young, "Trade-offs in Specifying Scanning Instruments," E.O.S.D., Nov. 1975, p. 86.

13. Electro-Optics Handbook, EOH-11, RCA, 1974, pp. 113 and 164.

14. Photomultiplier Manual, PT-61, RCA 1970, p. 56.

15. S. S. Beiser, "Distinguishable Density Levels in Image Recording of Earth Resources Satellite Data," thesis, Rochester Institute of Technology, (1975).

16. R. S. Hoffman, "Photographic Grain Noise Suppression by Density Quantization: Its influence on Image Quality," thesis, University of Arizona (1975).

17. D. H. Alspaugh, Physical Scientist, Defense Mapping Agency Aerospace Center, St. Louis, Missouri, personal communication.

PDS Chronology

Dec. 21, 1967	First Discussions
Mar. 6, 1968	Photometric Data Systems Corp. incorporated
Jun. 14, 1968	Decision made to design new Micro-D
Aug. 19, 1968	PDS opens for business
Oct. 25, 1968	First showing of Micro-D
Nov. 18, 1968	Public offering of stock
Jun. 2, 1969	First Micro-D shipped
Dec. 15, 1969	First overseas shipment
Apr. 30, 1970	First linear encoder, first playback
Jul. 21, 1970	First film transport
Aug. 18, 1970	First Micro-D to GSFC (Resalab)
Jun. 30, 1971	Oldest Astronomical Micro-D built
Nov. 5, 1971	First Astronomical shipment
Dec. 20, 1971	Last 16-mag. Micro-D
May 30, 1972	First 3-color Read/Write Micro-D
Sep. 15, 1972	First domestic Astronomical shipment
Oct. 31, 1972	First PDP-11 Micro-D
Nov. 15, 1972	First Granite Micro-D
Mar. 19, 1973	Last shipment from PDS
May 9, 1973	PDS sold to Perkin-Elmer, Boller & Chivens Div.
Jun. 1, 1973	PDS shut down and moved to South Pasadena, CA
Jun. 14, 1973	First shipment from Perkin-Elmer
Feb. 16, 1974	First Micro-D built at Perkin-Elmer

Feb. 7, 1977	PDS transferred to Electro-Optical Div.
Aug. 1, 1977	PDS transferred to Applied Optics Div.
Oct. 28, 1977	First Microprocessor Micro-D
Aug. 28, 1978	First 2020G Micro-D
Sep. 21, 1979	100th Micro-D shipped
Mar. 1, 1981	PDS moved to Garden Grove, CA

Total Micro-D's shipped - 152

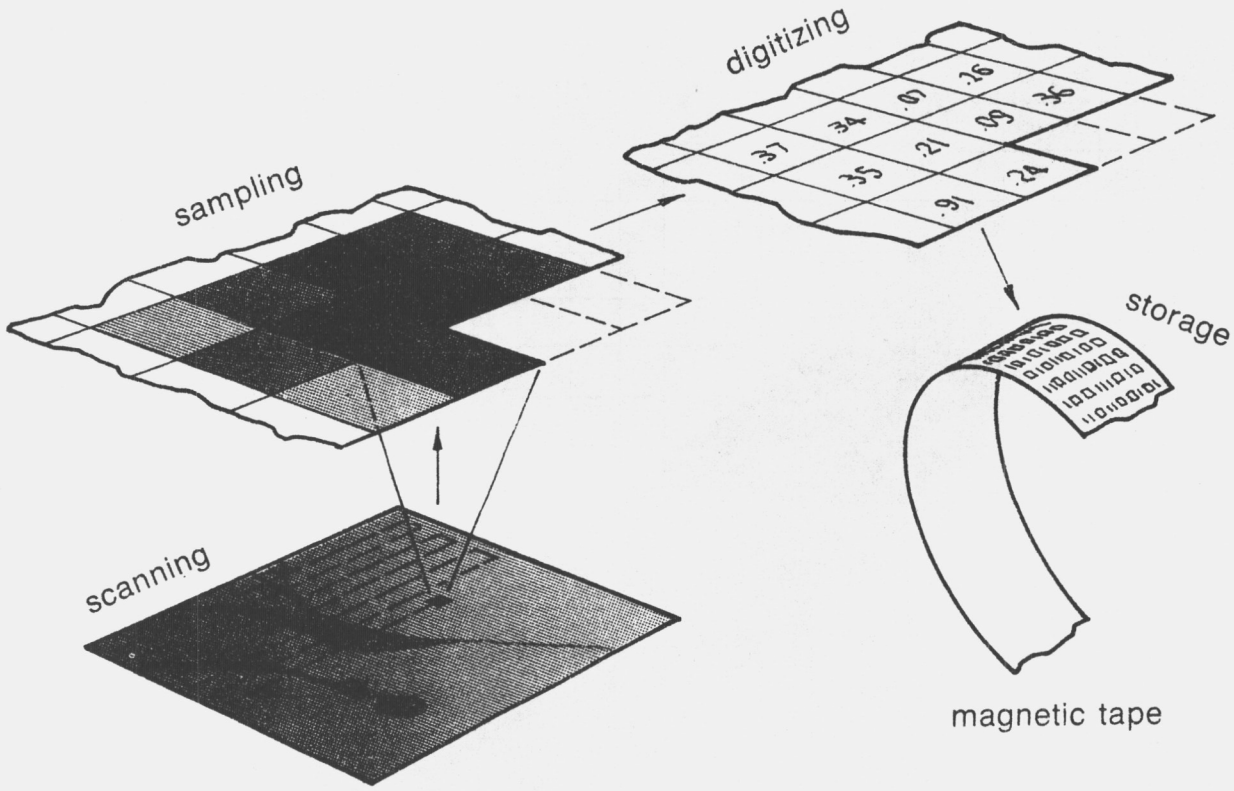

1 Photo Digitizer - an analog photo is transformed into a "numerical image" and stored.

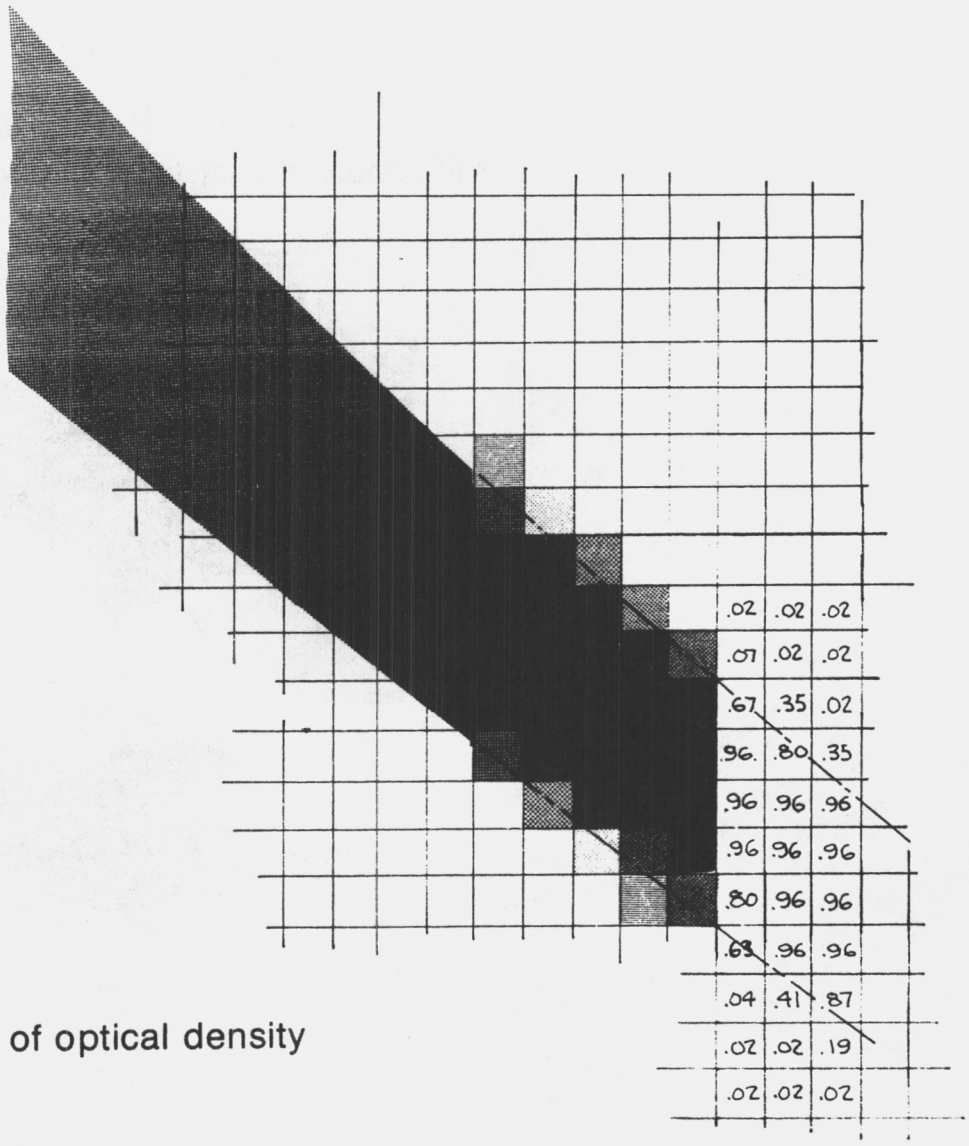

2 Analog-to-digital conversion of optical density modulations.

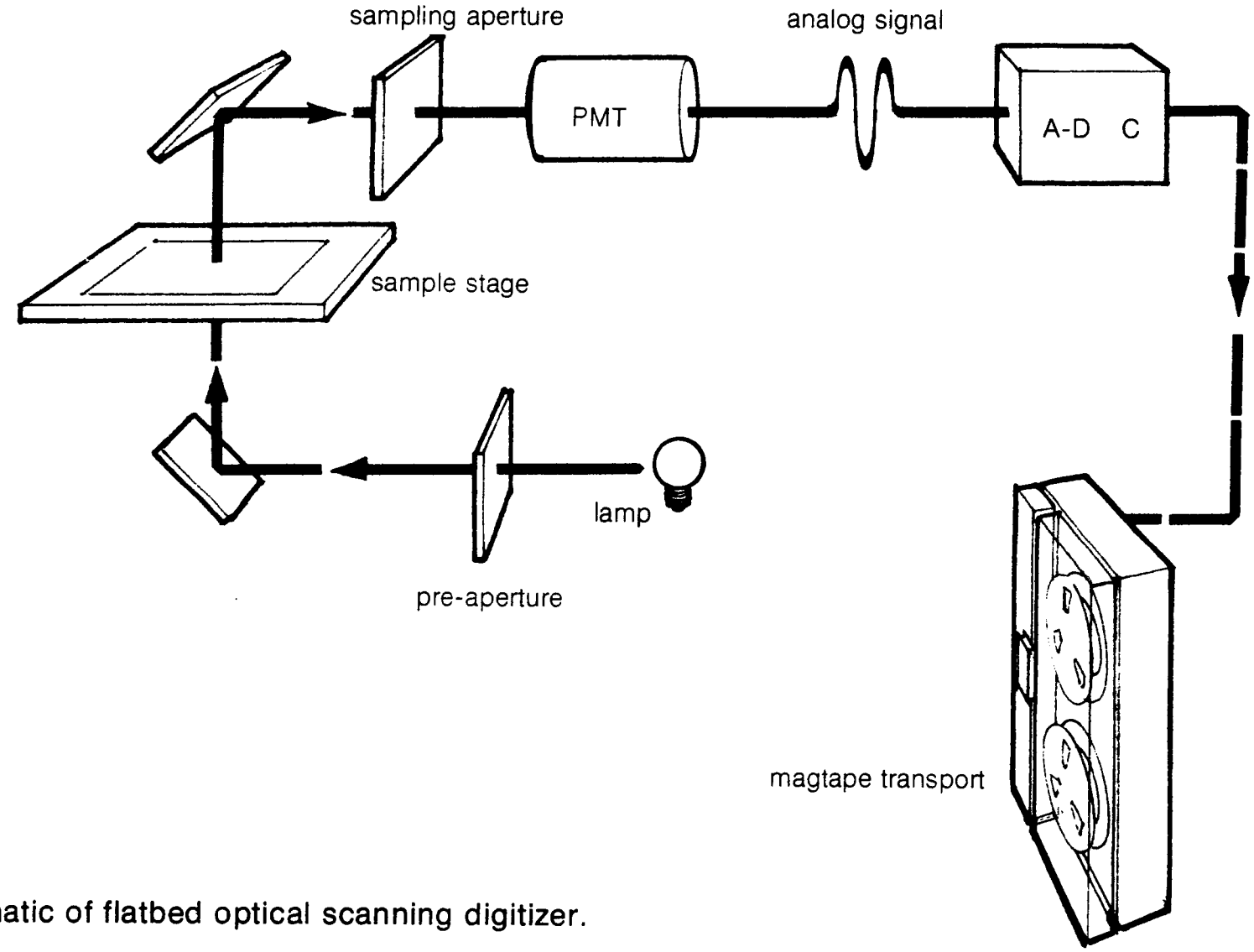

3 Schematic of flatbed optical scanning digitizer.

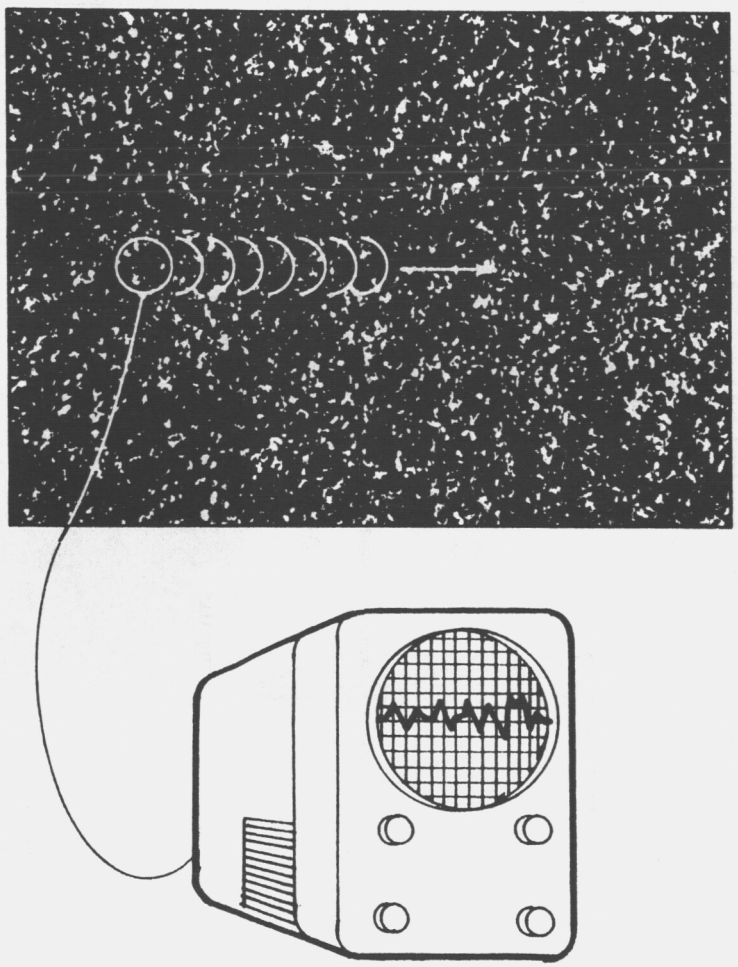

4 Microdensitometer trace of uniform density area of film showing effects of granularity.

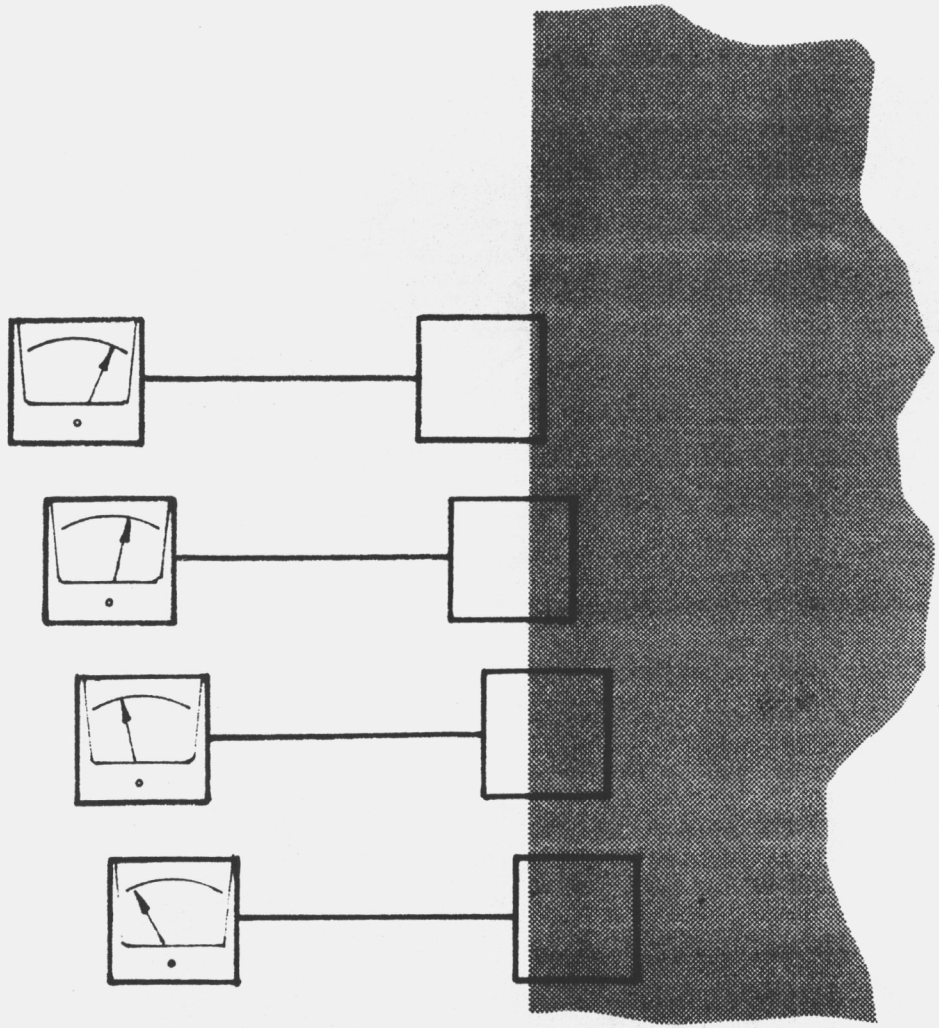

5 Effect of changes in pixel location.

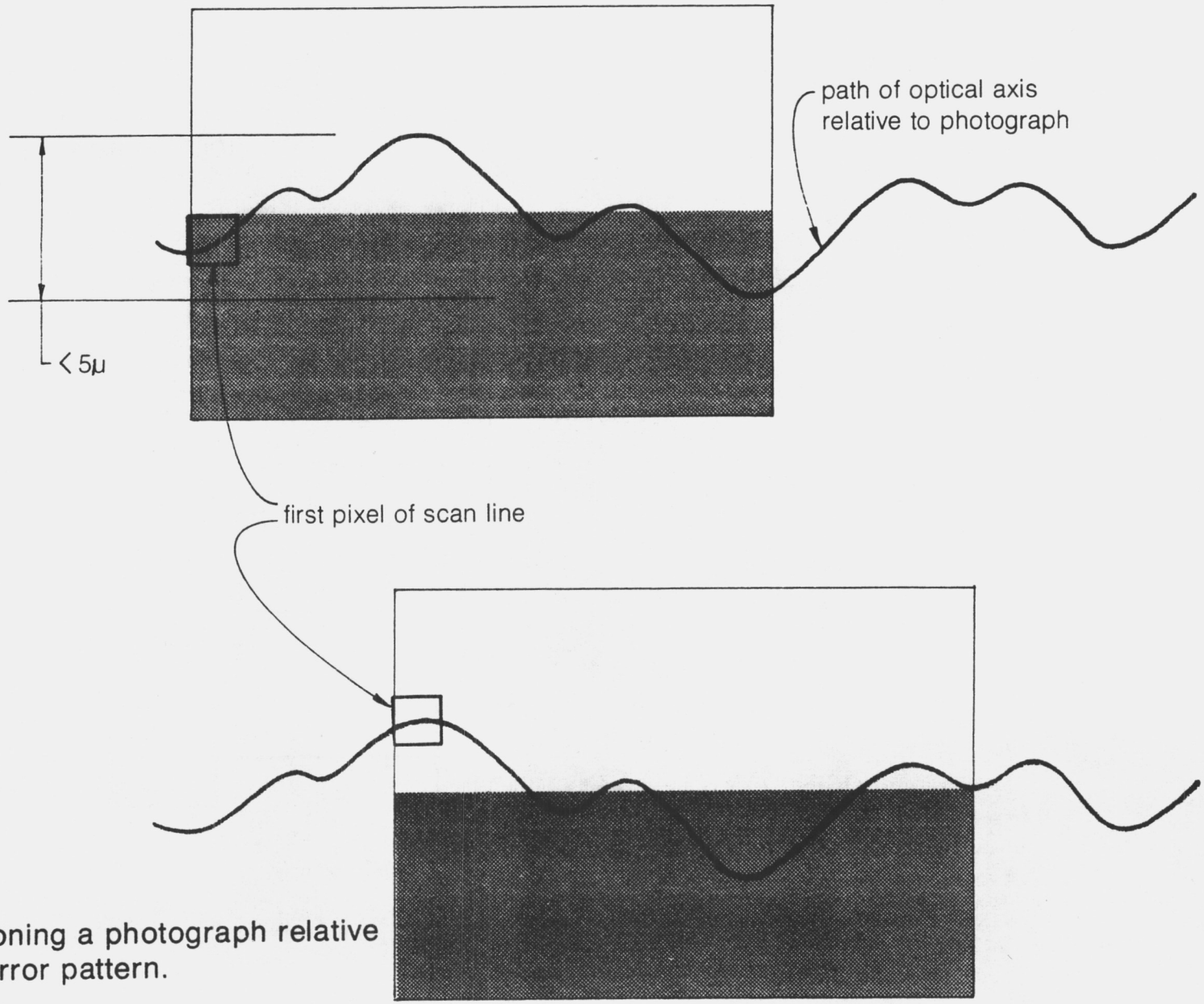

6 Effect of repositioning a photograph relative to the scanner error pattern.

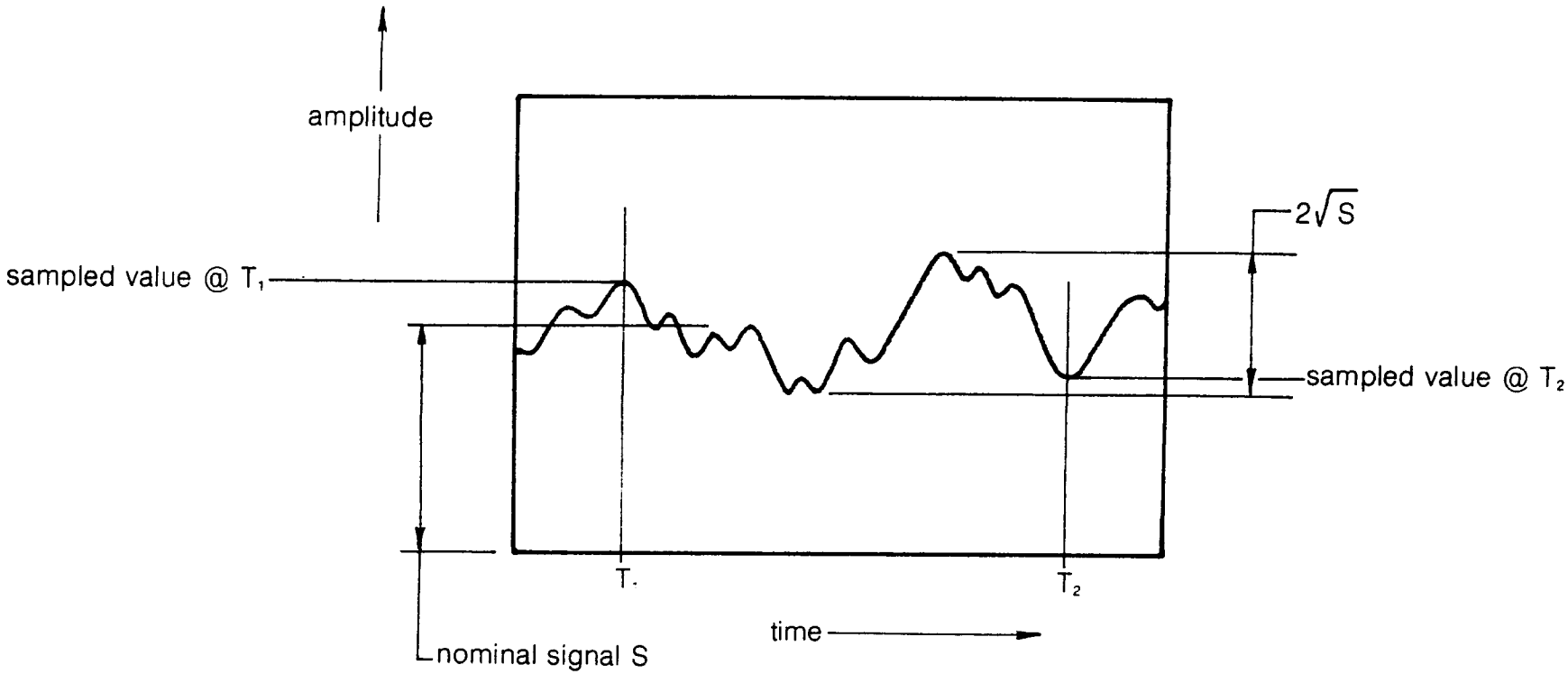

7 Noise-in-signal.

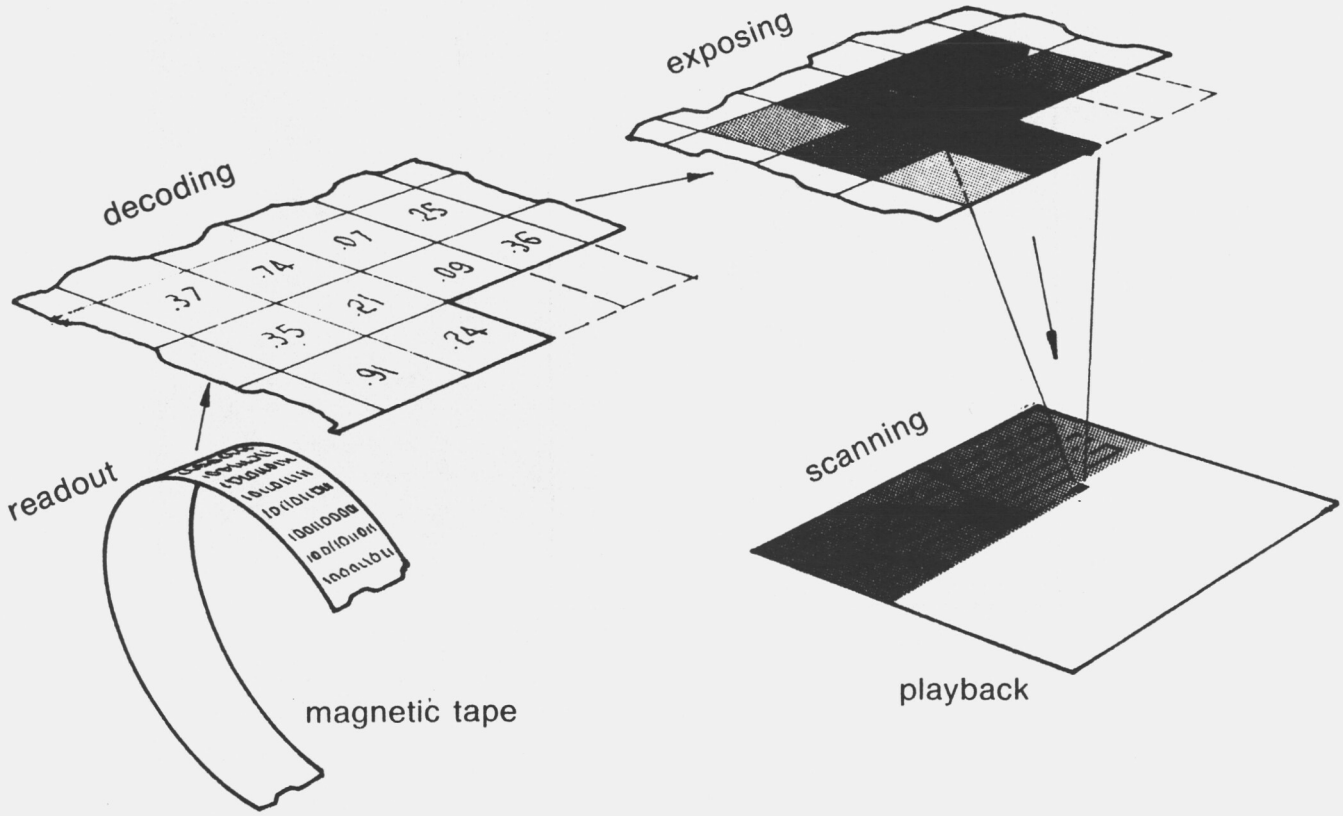

8 Photographic Playback - a "numerical image" is converted into a visual representation.

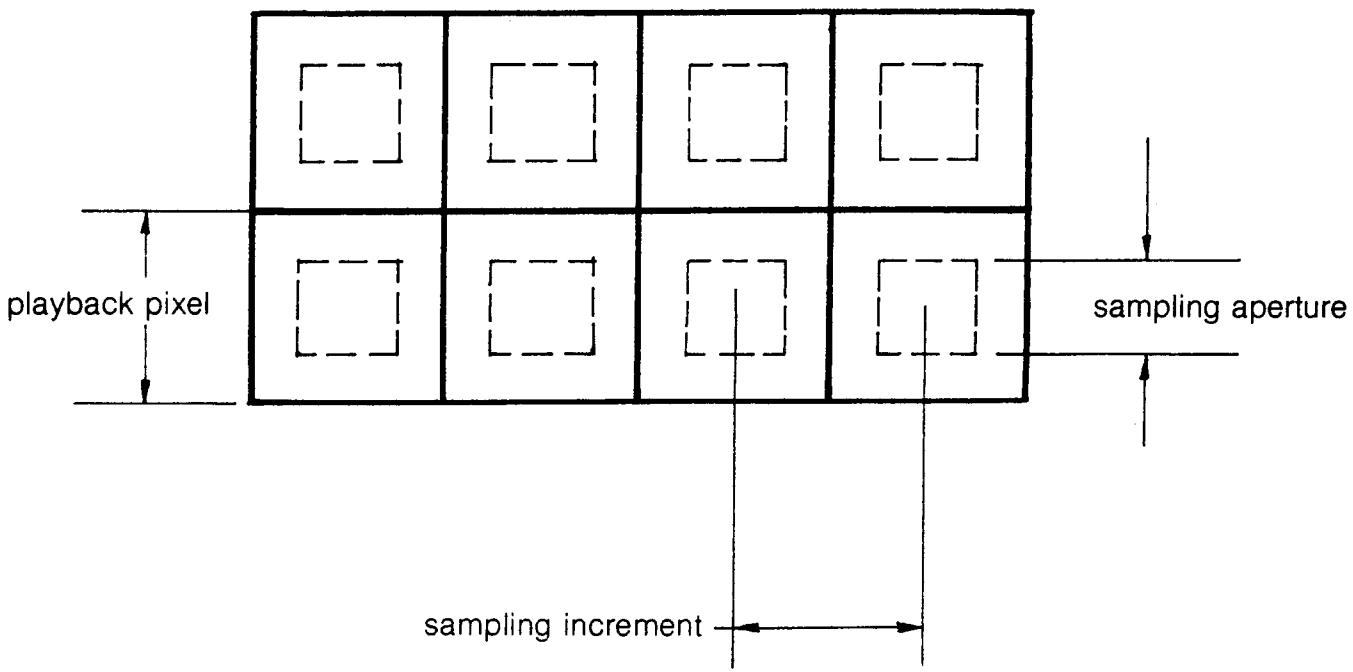

9 Scheme to make stored data insensitive to sampling aperture positioning errors.

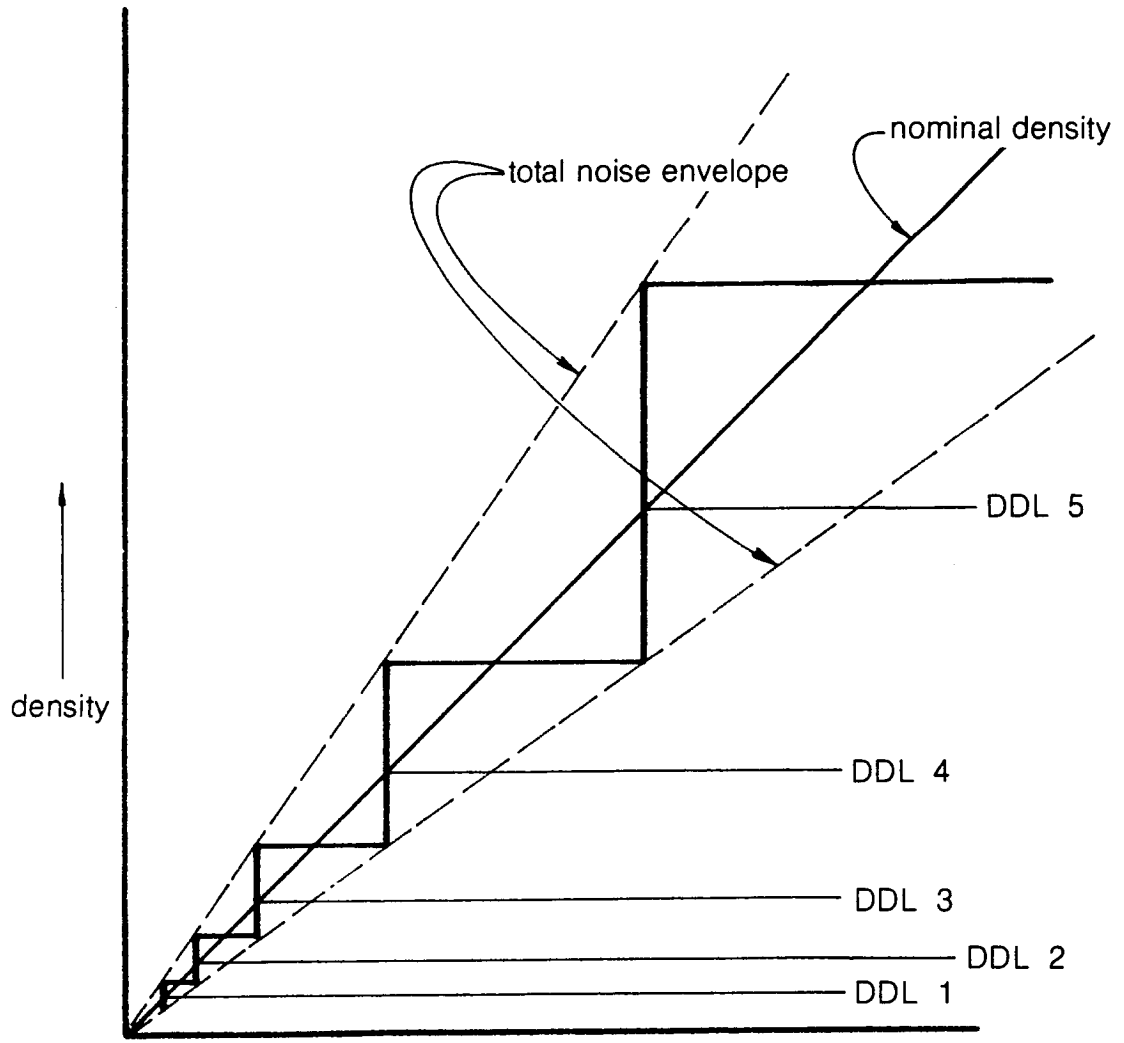

10 Distinguishable density levels.

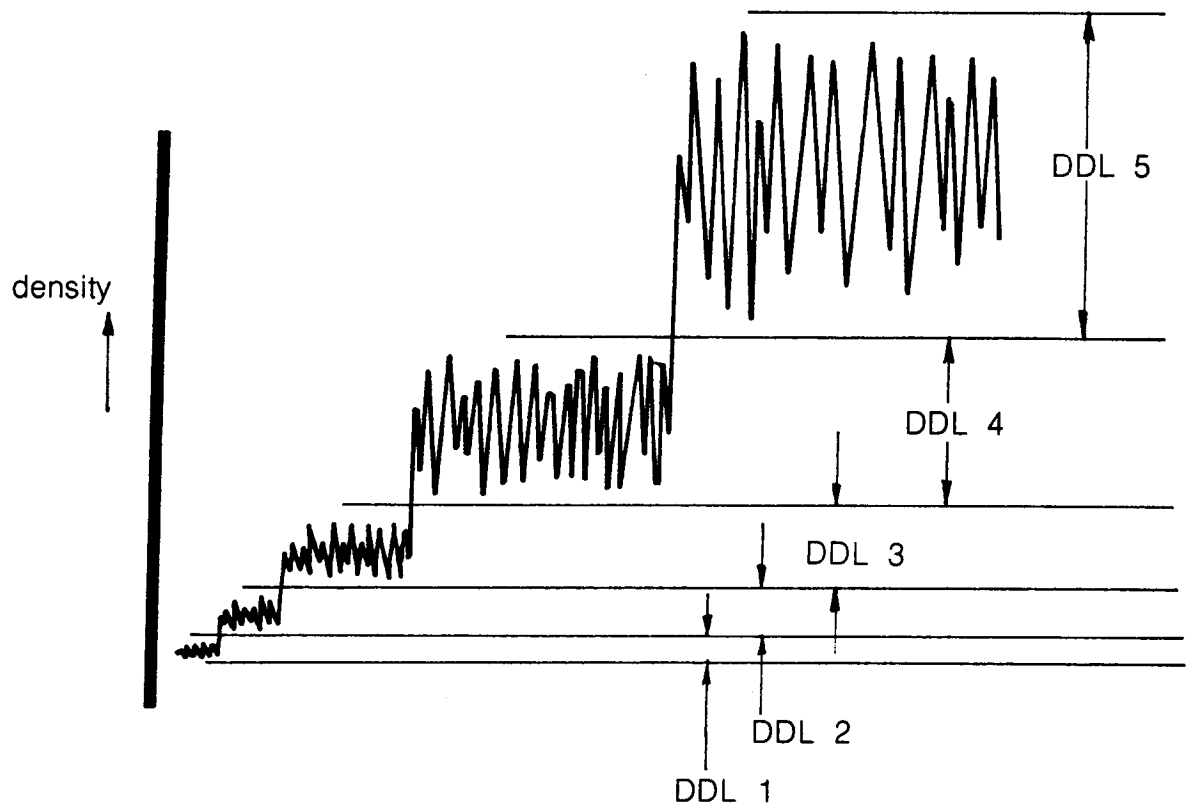

11 All values within a distinguishable density level are identified as the nominal DDL value.

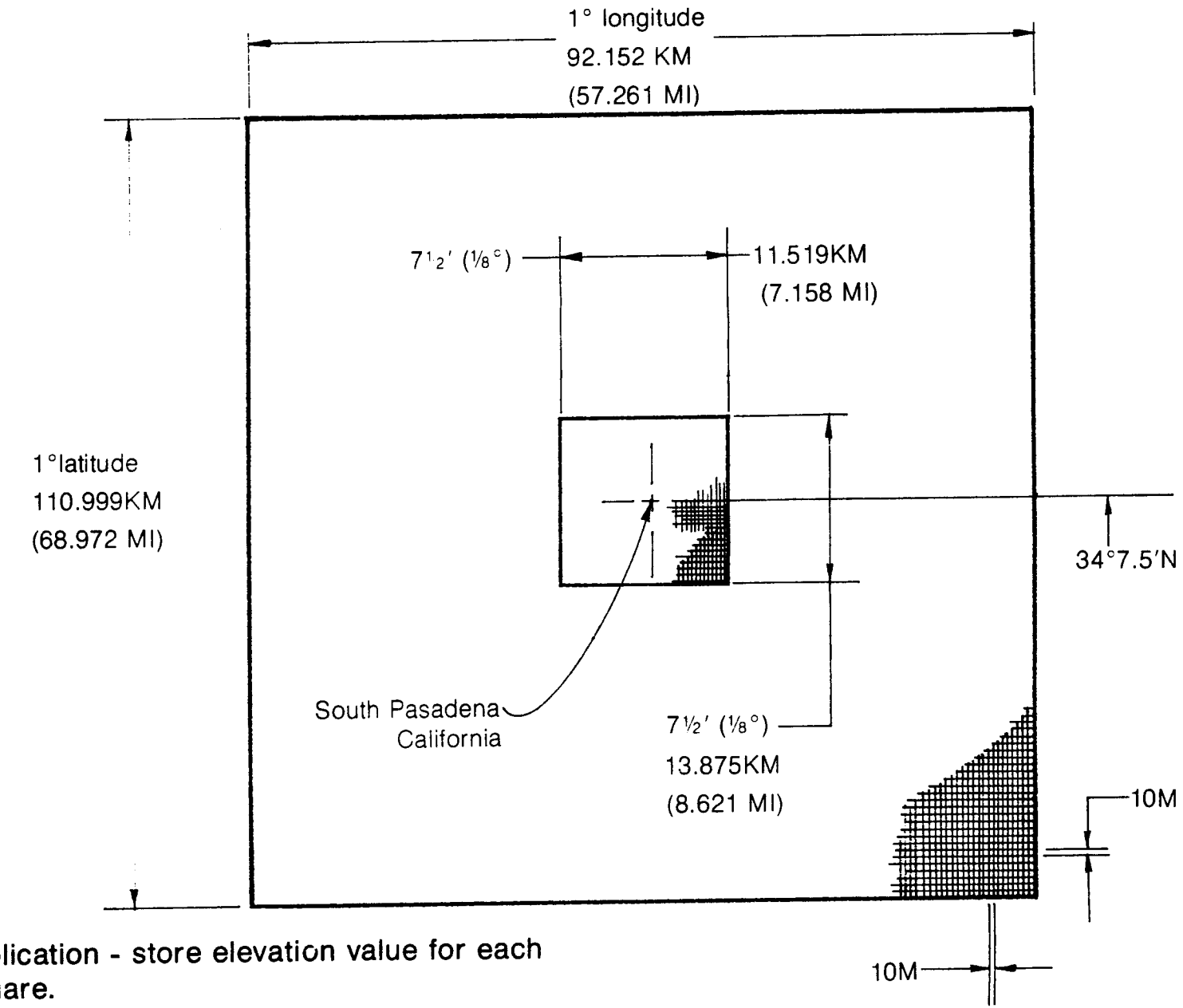

12 Mapping application - store elevation value for each 10-meter square.

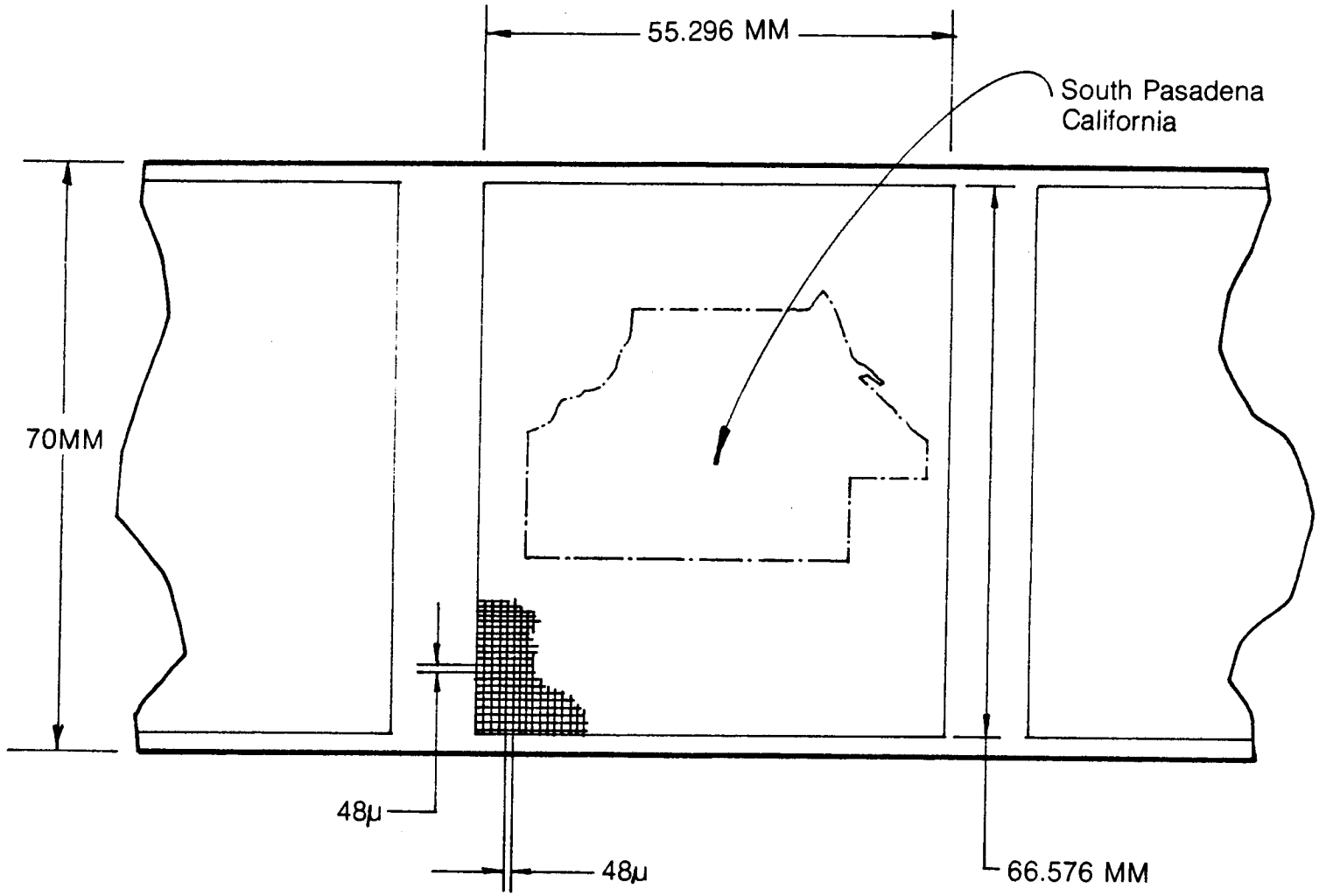

13 7½′ quad stored on 70MM film.

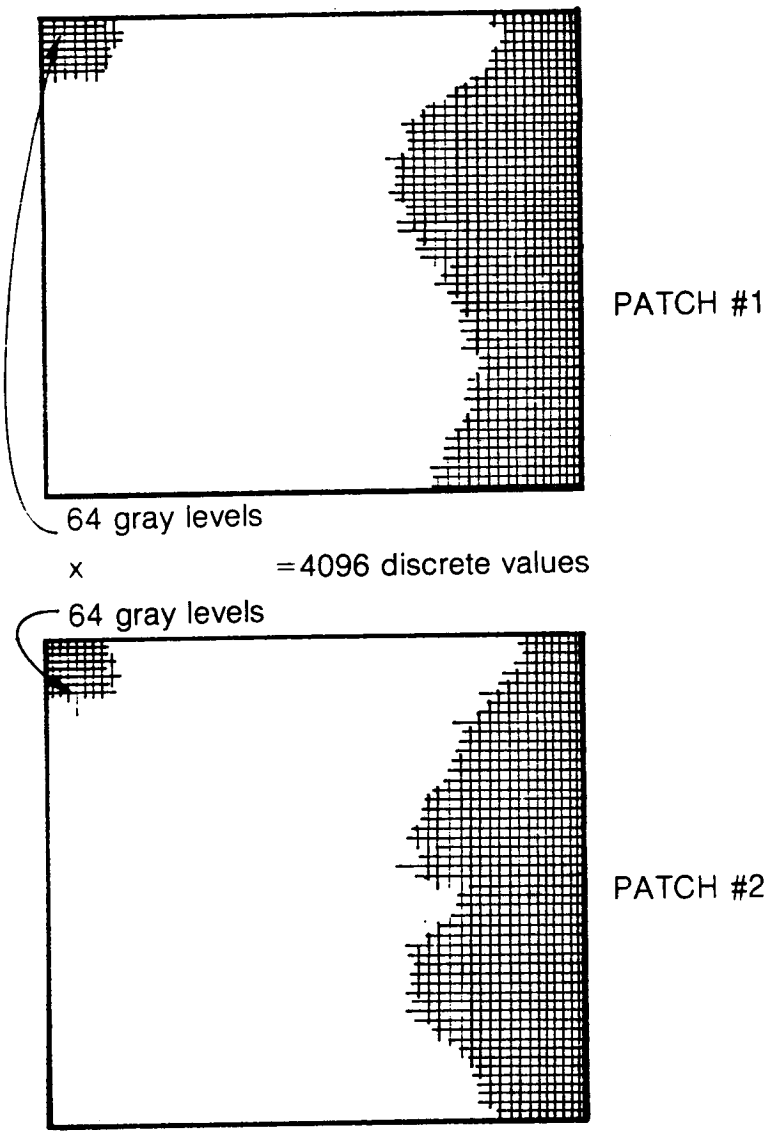

14 Multiplexing of high- and low-order pixels.

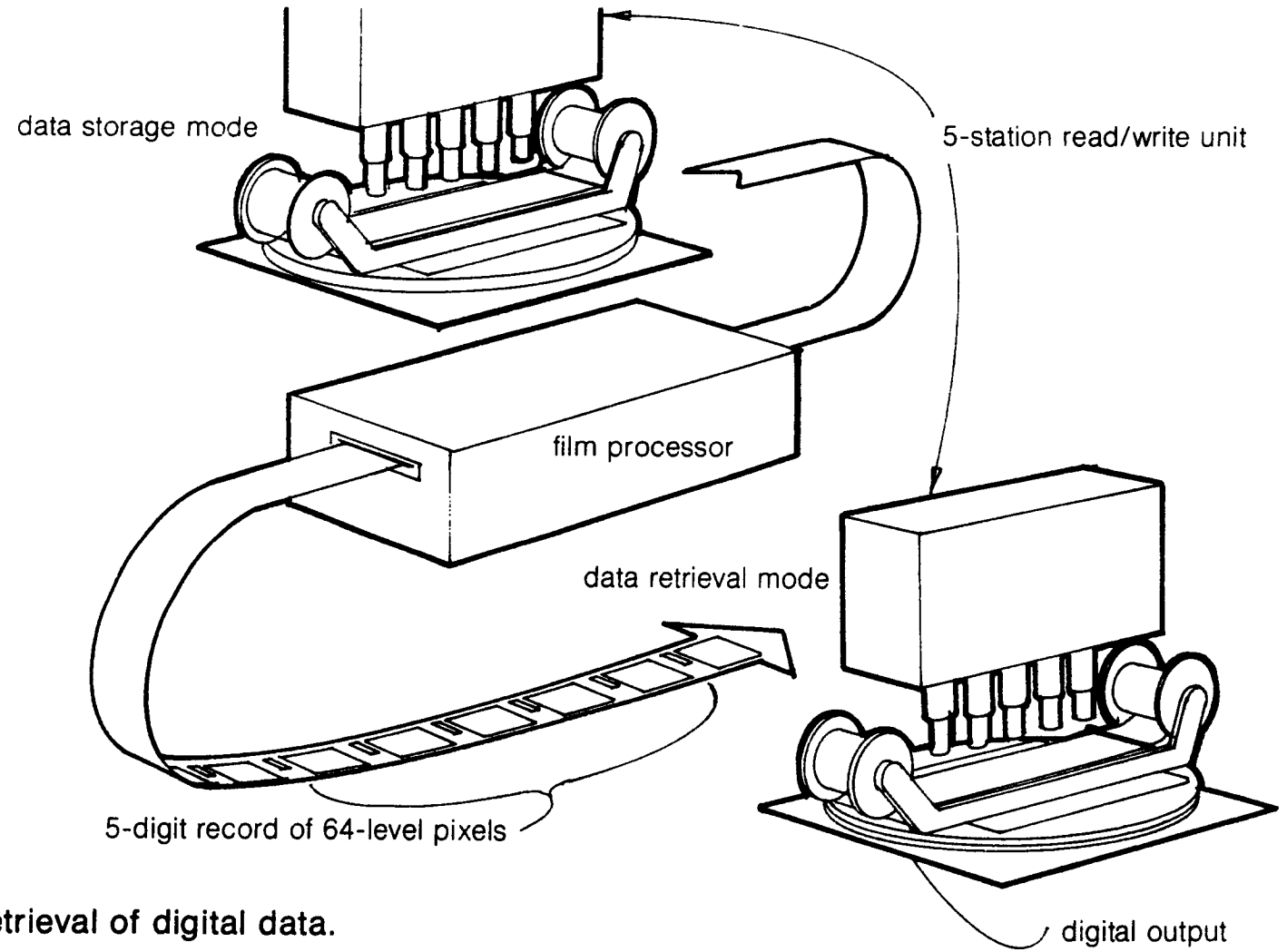

15 The storage and retrieval of digital data.

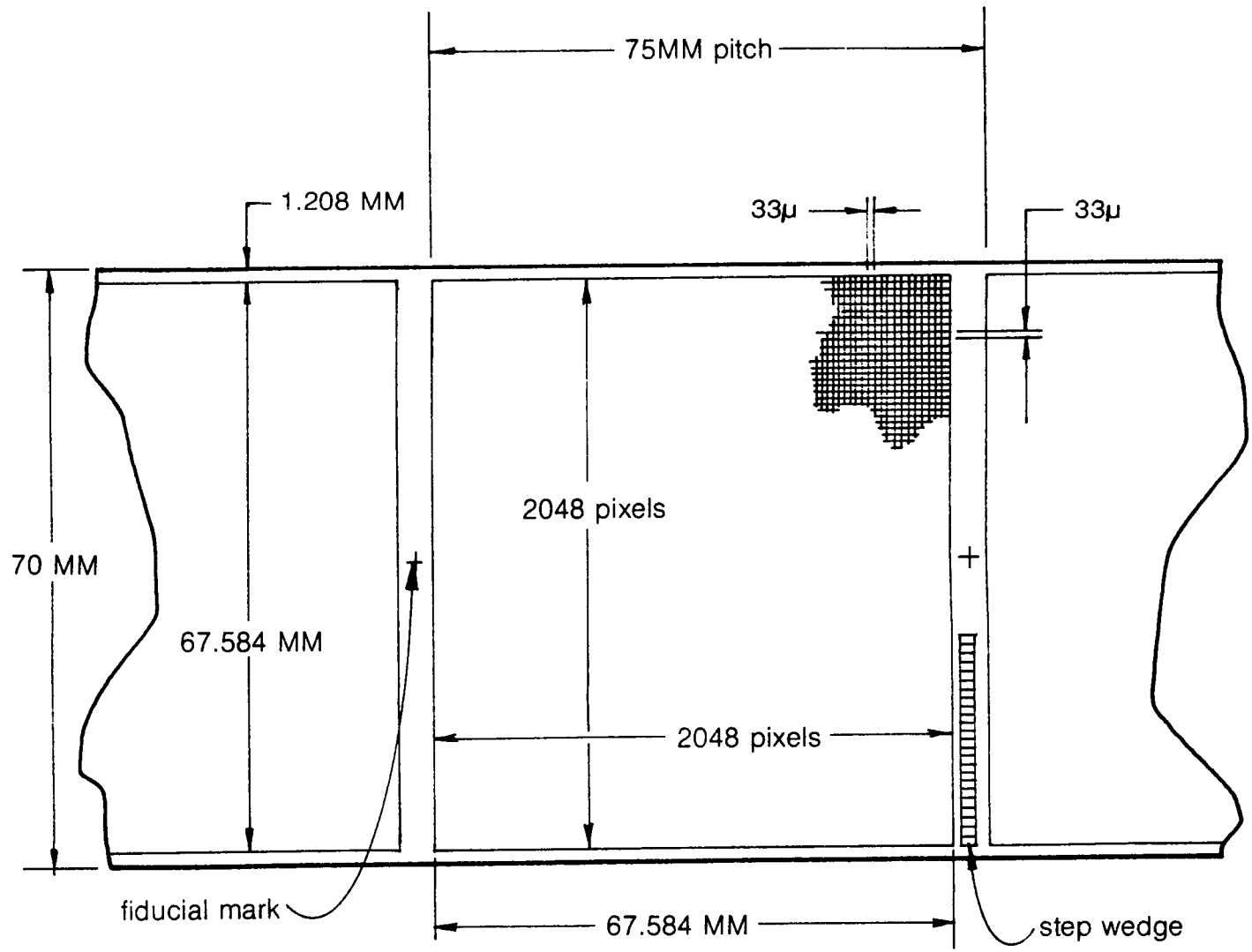

16 Maximum data format.

Poland: I have a comment Jim. I essentially did this. We have a Renticon detector in a telescope in Hawaii that takes images of solar Corona from the earth and does some special electronic processing for you, too. So we have electronic images on tape. We fill a tape every 20 minutes and they send these tapes back to Boulder and we make photographs of them on the Dicomed just so we can see what the Corona looked like and on each of these I put a step wedge on each line just like you talk about—so each line has a step wedge on each side and the digital date....we didn't need the high accuracy a lot of people talk about. Four or five bits was enough for long-term storage anyway. So essentially, we had numerical data we could process immediately. We made pictures that we could look at and then when we wanted to retrieve them a few years later, we could then put them on PDS, digitize the photograph, retrieve the data and look at it. We were writing with 50 micron sizes and reading back with 25.

Horton: Did you do any density stretching

Poland: Right.....yeah we had a internal calibration machine. The Dicomed writer was a limiting factor. It wasn't linear and it didn't write the same all over the film. So we had to calibrate all that.

Horton: Well, that same thing can be done with a PDS microdensitometer which is the point of this. Since you do have 64 different levels available from a reasonable film you could encode the information so that you can get a data compression by just using five or six bits out of 64.

Wells: Did you actually build this. Because it looks like a proposal for something DOD would fund. (laughter)

Horton: It was a pre-proposal.

POSTER SESSION

The abstracts presented here are from posters that were presented at an evening reception on Wednesday, May 11, 1983 held at the Goddard Space Flight Center Visitor's Center.

THE ROLE OF THE AUTOMATED PLATE MEASURING (APM) MACHINE IN DEVELOPING A PROGRAM TO DISCOVER QSOs AUTOMATICALLY

D. Turnshek, F. Briggs and C. Hazard, Department of Physics and Astronomy, University of Pittsburgh, and R. McMahon, R. Terlevich, E. Kibblewhite and M. Irwin, Institute of Astronomy, Cambridge University.

During the past several years Hazard, Terlevich and collaborators have visually assessed a wide variety of photographic 1.2-m UK Schmidt data (primarily IIIaJ objective prism plates) in an effort to discover QSOs. Their selection criteria were carefully appraised and revised by considering the results of large telescope spectroscopy and radio surveys in the regions under study. In view of the considerable work in various selected regions, we are now beginning to develop automatic discovery procedures. We discuss the general role of the APM type machine (developed by Kibblewhite at Cambridge University) in a program to discover QSOs automatically. Due to our current interests, we are only emphasizing the application of APM data to QSO discovery programs. In general, however, the methods we employ can be used to study stars and galaxies as well. We describe three aspects of our work. (1) The scanning of a direct plate with the APM machine. This results in the automated selection and description of images. (2) The selection of QSO candidates based on color-color diagrams constructed from the APM image data. (3) The analysis of APM raster data for QSOs selected visually from objective prism plates.

(1) Scanning A Direct Plate. The APM machine is programmed to operate in basically one of two modes. The discovery mode is used for extracting and preprocessing relevant data for all object images present on a photographic plate. A 15 parameter description of each image (with background subtracted) is deduced. The 15 parameters give the position, shape, size and density distribution for an image. By describing each image with only 15 parameters (there are typically of order 100,000 images on a 4 by 4 degrees region of a UK Schmidt field out of the galactic plane), only the less than 2 million important pieces of information on a plate need be saved on disk or tape for analysis. This should be compared to the approximately 1 billion pieces of information originally assessed. This aproach, although inadequate for some applications of analyzing photographic plates, emphasizes the use of the photographic plate as the most efficient medium for raw data storage. The approach is feasible since the APM machine can scan a plate quickly. For our purposes in this work, the image descriptions are used to classify the images into either stellar, non-stellar or flaws based on an empirical assessment of what a stellar image profile is. This was done for several deep IIIaJ UK Schmidt plates at 08h 57m +17deg. The IIIaJ plates typically have a limiting magnitude of 22 to 23. For the purposes of studying QSOs, we have eliminated all non-stellar images from the catalog of objects in the region. We have also included color information in the catalog by incorporating into our data set scans of the standard copies of the original PSS O and E plates and a scan of a UVR 3 color Palomar Schmidt plate. The resulting data set is the positions and intensities of colors for approximately 57,000 stellar images in the 4 by 4 degrees area of the sky. Although all objects generally have J, O and E images, the 3 color plate has a limiting magnitude less than 20 and, therefore, there is not UVR information for the faintest objects. Our future work utilizes separate direct U, B, V, R and I plates. Thus, the findings presented here are only preliminary.

(2) QSOs In Color-Color Diagrams. Although a photometric calibration has not been applied to the J, O, E, U, V and R data, the uncalibrated color-color diagrams illustrate how effectively QSOs can be identified solely on the basis of color. The QSOs in the diagrams were tediously selected on the basis of visually inspecting UK Schmidt IIIaJ objective prism plates. The QSOs were also confirmed using large telescope spectroscopy. Our long term goals are to develope liberal broad band color criteria for selecting QSO candidates automatically in photometrically calibrated

U, B, V, R and I fields. The unbiased selection of QSO candidates can then be used to study (i) selection effects, (ii) QSO emission/absorption line morphology and (iii) the space density, luminosity function and possible clustering of QSOs. However, in order to achieve these two goals efficiently, we intend to use APM scans of objective prism plates and narrow band filter plates to extract information on the certainty of a candidte's ID and, if possible, obtain a redshift. By doing so we will, for many candidates, eliminate the needless use of large telescope time for confirmation of IDs and obtaining redshifts. It will be possible to use Schmidt telescope data as an investigative tool in its own right. This kind of approach is made possible by the speed and data handeling capabilities of an APM type facility.

(3) Raster Scans Of QSOs On Objective Prism Plates. We have assessed how reliably objective prism data can be used to identify a QSO and determine a redshift. We compare large telescope spectra to raster scans of the visually selected QSO candidates on two different objective prism plates. Making an APM raster scan of a region (where density is recorded on tape for each pixel) is the second mode of operation for the APM machine. This mode is generally used for making a more detailed study of images for which software needs change or are somewhat special purpose. For example, we will eventually analyze the objective prism raster scans of all QSO candidates automatically selected on the basis of color. Although emission lines are often visible on the objective prism plate raster scans, it is not always possible to unambiguously deduce a QSO's redshift. However, sometimes the color characteristics of an objective prism spectrum indicate that an object is a QSO. In the future, the large wavelength range covered by the many narrow band filter plates we have had made will be used to constrain redshift determinations.

In summary, the APM facitlity provides an efficient mean of assessing a large amount of photographic plate material. In general, it allows astronomers to design programs in which 20 or more photographic plates from one region of the sky must be evaluated. Statistical studies of the color or variability properties of large samples of objects become possible.

RIMSTAR: Rapid Image Scanning Technology and Archiving

Eric R. Craine

and

John S. Scott

Steward Observatory
University of Arizona
Tucson, Arizona

I. INTRODUCTION

In recent years, techniques of obtaining astronomical imagery have been experiencing a conversion from traditional photographic emulsions to electronic arrays as the detection devices of choice. In spite of the great promise of linear scanners and area arrays, using CCDs or photodiodes as detectors, this transition has been evolutionary rather than revolutionary. Indeed, for many large volume applications, such as sky surveys, the photographic emulsion has remained highly desirable not only as the detector but as the archiving and display medium as well.

Further, in spite of apparently declining use of photographic emulsions for smaller scale astronomical projects, the proliferation of very large astronomical photographic data bases seems well established. Examples include photographic sky surveys recently completed, or in progress, at Steward Observatory, Hale Observatories, and the European Southern Observatory. These large projects, conducted with wide field telescopes, yield immense quantities of data, much of it never analyzed due to the difficulties of reducing photographic data.

A clear compromise to this dichotomy has emerged in the increasing use of data generated through digitization of photographic material. This is in many respects the best of both worlds, but suffers some severe limitations, largely in terms of the time required to digitize the data. Current astronomical digitization projects generally involve very small numbers of photographs (usually well under 100) and are frequently conducted using very slow scanning rate techniques (i.e. typically PDS microdensitometry).

For such small projects, this technique is acceptable. We suspect, however, that the digitization techniques currently in vogue in the astronomical community contribute to the very restricted nature of the projects attempted.

Further, there are numerous military and scientific problems which require digitization, either of direct or analog imagery, at high speed and in immense volumes. A potential solution of considerable interest in regard to these problems is the development of direct digital cameras. The principal drivers for these applications are speed, and the related aspect of the overall size of digital camera formats. Both the problems of speed of data acquisition and the overall image size (and hence achievable resolution) may be attacked by schemes of optical multiplexing of many individual digital detectors.

We are presently exploring designs for linking one- or two-dimensional detector arrays in large mosaics without gaps between elements of the detectors. These techniques essentially allow construction of arbitrarily large detector mosaics, for which high speed is preserved because individual array components can be read out in parallel.

As an example, one design envisions a 1000 x 1000 element array with a frame rate of one per millisecond, 300 times faster than for comparable conventional monolithic detectors.

Clear applications for this technology are recognized in the following areas:

* large scale, real time digital imagery, e.g. surveillance, guidance, etc.

* rapid digitization and archiving of documents, e.g. maps, recon photgraphs, text, etc.

II. NIPSS: A Representative Astronomical Problem

The Near Infrared Photographic Sky Survey (NIPSS) is a unique, visual and near infrared, electro-optically intensified, photographic survey of the northern sky, which was conducted in part as a support tool for the identification of optical counterparts to infrared sources detected by the Infrared Astronomy Satellite (IRAS). The survey consists of nearly 4,000 photographs, each subtending 4.5 degrees on the sky at a scale of about 115 arcsec/mm. The limiting magnitudes are approximately 19 mag and 16.5 mag in V and I respectively (Craine 1978).

It has been demonstrated (c.f. Horner and Craine 1980) that this survey can be very useful for identification of optical counterparts to infrared sources, but any manual extraction of these data from the photographs is tedious and slow and not feasible for more than a small number of survey fields (c.f. Craine et al. 1979).

For the NIPSS data to support IRAS to the greatest extent possible, it is essential to generate a list of potential infrared source candidates which can be read and manipulated by computer. Because of the diversity of infrared sources, as well as the broad range of application of the NIPSS data, it is clear that the most useful list is a complete catalog of the contents of the survey photographs rather than some arbitrary subset thereof.

The digitization of the NIPSS data base is just one example of large digitization projects (> 1,000 images) for which there is a need at present. Other areas generating large digitizing requirements include aerial reconnaissance in civil and military programs, including both remote sensing and airborne geophysical surveys. Clear needs for high volume, large format image digitization are also demonstrable in many disciplines of the medical profession. Numerous industrial applications are likewise evolving, as, for example, in areas of computer aided design and image enhanced quality control of high cost items such as helicopter rotor blades. A primary driver for implementation of many of these applications is the speed at which digitization may be achieved. In particular, all of these applications require, or would substantially benefit from, routine scan rates of one or two orders of magnitude faster than commonly available.

We have explored several possible techniques for accomplishing these tasks, concluding that conventional schemes for digitizing large volumes of photographic data are far too costly and time consuming to encourage the undertaking of the more ambitious of these projects using traditional technology. There is a distinct need for fast digitizing systems such as could be derived from development of large format, optically multiplexed CCD systems designed to address these problems.

III. Mosaic Description

One method of producing a high speed digitizer, capable of addressing some of the problems outlined above, involves the optical multiplexing of linear CCD arrays as arbitrarily long arrays with no gaps between individual elements. This may be achieved by securing 1 x n element CCDs on alternating segments

of the orthogonal faces of a long beamsplitter, thus obtaining a single array of length n times the number of chips used. The chips are placed such that, in the composite image plane, the sensitive elements of the adjacent arrays just abut, thus eliminating gaps between adjacent chips caused by the chips' surrounding packaging.

Digitizers of this type have been successfully constructed and have demonstrated particular potential value in computer aided design (CAD) applications. Very large arrays are now in the planning stage (1 x 40,000 pixels), but several problems remain under study (see below).

One interesting aspect of applying this approach to astronomical imagery is that an option exists to use the mosaicked detectors in either image or collimation space, the latter case being of lower cost and allowing use of additional schemes for reducing the effects of scattered light in the emulsion.

In spite of the attractiveness of optically multiplexed, linear CCD arrays, it is the extension of this technique to the two-dimensional array mosaic that offers real versatility and depth of application. The two-dimensional array opens possibilities of high resolution, large format real time digitization, as well as digital color imaging capabilities.

The optical multiplexing of two-dimensional CCD arrays is achieved by stacking multiple beamsplitters. A full two-dimensional array requires four image planes, and hence three stacked beamsplitters.

Figure 1 shows a typical multiplexing configuration, in this case the optical juxtaposition of 25 two-dimensional CCD chips. The resulting composite image plane view, as seen by the component chips in the system, is shown in Figure 2.

The stepped configuration of Figure 1 is a consequence of ensuring equal path lengths to each chip in the array, as is required to maintain compatible scale in image space.

If a collimated beam is providing illumination it is, of course, possible (perhaps desirable) to use a single column configuration. In either event, it should be noted that a first approximation to equal levels of illumination at each beamsplitter face can be achieved by careful matching of the reflectances and transmittances of the beamsplitters, or by use of filters in the system.

CCD chips are used as detectors in these designs to take advantage of their following properties:

* digital recording
* high dynamic range
* low geometric distortion
* high sensitivity
* available off-shelf

IV. Data Handling

Individual CCD chips may be read out at speeds of from 2 to 10 MHz. This high speed data stream is preprocessed on-line through one or more of a variety of techniques (e.g. bit compression, thresholding, filtering, run-link encoding, etc.), using one or more very high speed, bit slice processors. The bit slice processors have a true instruction clock rate of 10 MHz, and are used in a pipeline processor to sustain the rate of data flow at the clock rate.

The data are then transported to the main onboard computer, via appropriate FIFO buffers utilized to handle data bursts of 60 MHz, for further processing, and intermediate or long-term storage and display.

As an example, a 1 x 40,000 linear, mechanically scanned array can digitize a large chart (60 x 90cm military standard) at 25 microns resolution in about 1.5 min. With a 100:1 compression factor, the storage requirements of the compressed image would be 4.3 Mbytes.

V. Light Scattering

The application of optically multiplexed CCDs to the digitization of analog transparencies is handicapped in some instances. If the precise preservation of photometric data is of critical importance, the scattering of light in the photographic emulsion is of concern, though it should be recalled that in many instances the goals of a digitizing project can be readily met without resort to remedies to this problem. Indeed, we are aware of some digitizing projects which are making great efforts at photometric precision; this while digitizing high gamma photographic reproductions!

The one-dimensional CCD multiplexed linear scanner has an advantage over the two-dimensional machine in that it allows for reduced light scattering by use of polaroids in the optical path. A pair of polaroids and a slit can be used with the

linear system to mitigate the effects of scattered light. The polaroids should be oriented to minimize the scattering angle along the length of the slit; while the slit itself limits the problem in the orthogonal direction.

A second remedy for scattered light is feasible for systems operating in collimation space. Since cost effective, all reflective optics are now possible, a low frequency light source may be used to illuminate the film, thus substantially reducing scattering in the emulsion. A Class II, near infrared laser, with a beam expander, has ample energy density to serve as the source in most instances.

VI. Other Applications

The low levels of financial support which regrettably characterize astronomical research often preclude the routine development, and widespread availability, of techniques which might dramatically extend our ability to process astronomical data in an efficient and timely manner. One great advantage of developing digital cameras to more sophisticated levels is the wide demand for such devices in areas other than astronomy.

As an example, distinct military applications for these systems, which could provide substantive support for their development, include, but are by no means limited to, the following:

* ground/air launched cruise missile (GLCM/ALCM) mapping systems
* Pershing II mapping systems
* surveillance systems (satellite/RPVs)
* Army Helicopter Improvement Programs (AHIPS)
* map storage (Defense Mapping Agency)
* high speed ballistic studies

The civilian community also has considerable incentive to exploit this technology, largely driven by well defined needs in the analysis and storage of medical imagery and documents. This wide base of interest represents an unusual opportunity for astronomers to seek out diverse sources of support, as well as to develop a new generation of devices for image digitization.

This work is proceeding as a joint effort by Io, Inc. and E/ERG, Inc. of Tucson, Arizona. The collaboration of F. Pingal and T. Sargent is gratefully acknowledged.

references:

Craine, E.R. A.J., 83, 1598 (1978).

Craine, E.R., Duerr, R., Horner, V.M., Routsis, D., Swihart, D., and Turnshek, D. NIPSS Cont. No. 3, Steward Observatory, Tuson (1979).

Horner, V.M. and Craine, E.R. P.A.S.P., 92, 209 (1980).

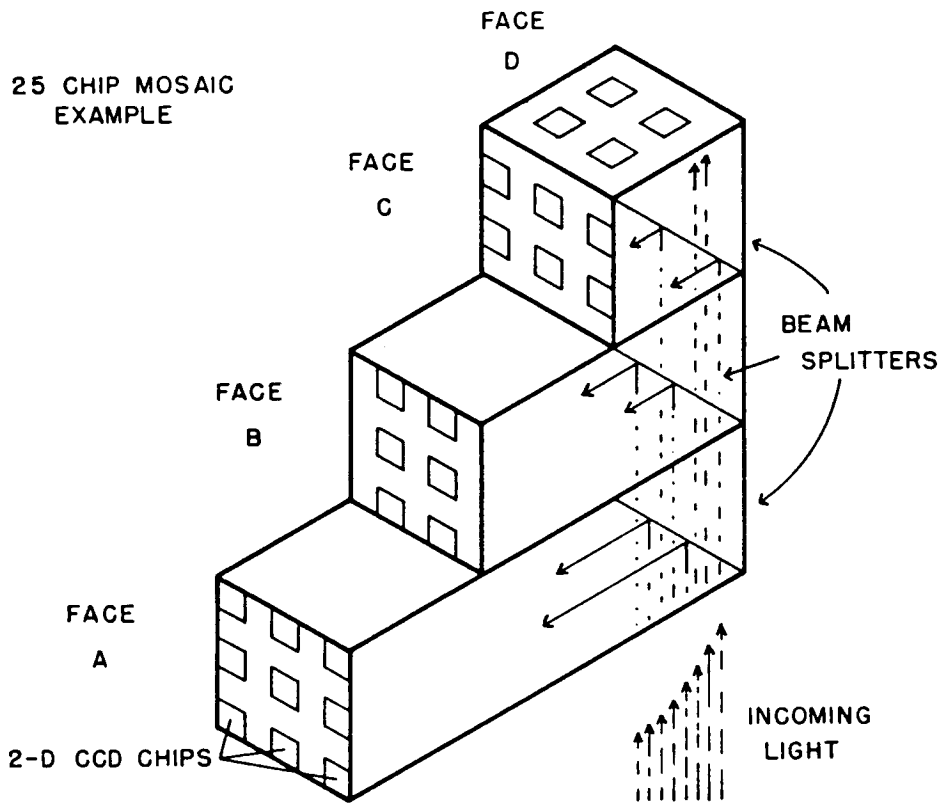

Figure 1. Two-dimensional optical multiplexing system.

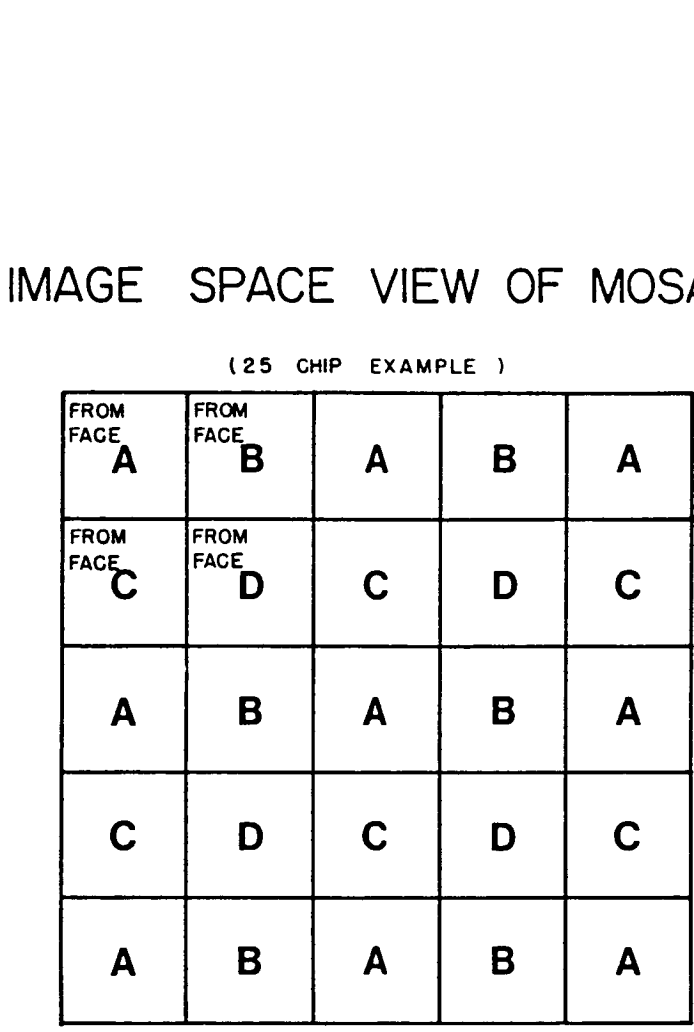

Figure 2. Image plane view of mosaicked array.

Computer Simulation of the Effects of Transmission-Averaging in Microdensitometry

Harry M. Heckathorn

E. O. Hulburt Center for Space Research
U. S. Naval Research Laboratory
Code 4143, Washington, D. C. 20375

One of the principal advantages of electrography when compared to photography is the nearly linear relationship between source intensity versus resulting image density. This property allows for simplified and more accurate photometric calibration and permits a certain degree of extrapolation of the calibration to beyond the limits of the faintest "photoelectric standard" on an exposure. The desires to extract quantitative photometric information from electrographic (or photographic) negatives and to convert this information into a digital format for computer analysis or enhancement have lead to the widespread use of scanning microdensitometers to perform this "A-to-D" conversion. Therefore it is of vital importance to understand and, if practical, to avoid any non-linearities which may be introduced during microdensitometry of electrographic emulsions.

A microdensitometer, or perhaps it should more properly be called a microphotometer, measures the relative optical transmission (T) through a spot projected on the emulsion, not the optical density (D) which is desired. Transmission and density are related by $D = -\log_{10} T$, but the equation is valid only if the opacity of the emulsion is uniform within the area of the spot. The quantity actually measured by the microdensitometer is the average transmission and, in the presence of image gradients, this is not equivalent to measuring the average density. This leads to an underestimate of the true density and can be a principal source of non-linearity in the digitization process. Since in electrographic recording density is directly proportional to intensity over a large range (not to its logarithm as on the "linear" portion of the photographic characteristic curve), density gradients are typically steeper than for photography. This is true even for high contrast astronomical emulsions such as IIIa-J where $4 < \gamma < 5$. Hence, the deleterious effects of transmission-averaging are potentially more severe in the case of electrography and have been investigated by means of a computer simulation.**

**NOTE: This investigation closely parallels that of Zinn and Newell (AAS Photo-Bulletin, No. 2, p. 6, 1972) with the exceptions that Gaussian fitting functions are not used in the computation of "measured" image density and a more complete range of parameter space has been investigated. It should be remembered that the findings do not relate directly to digitization of photographic emulsions since, unlike electrography, true density profiles of recorded objects which differ only in intensity have different shapes. The warning of the photometric consequences of transmission-averaging still pertains, however.

The steepest image gradients encountered in practice are those produced either from a point source or from a spectral emission or absorption line where the image profile is essentially the point spread function (PSF) of the instrument. The intrinsic intensity profiles of such images closely resemble a Gaussian. Therefore, the smooth density (∽intensity) distributions of stellar images were represented as digital arrays generated from rotationally-symmetric, noise-free Gaussians. The amplitude (∽intensity) of simulated images varied over the range from 1 to 256 (arbitrary units covering 6 stellar magnitudes) -- typical of the maximum measurable dynamic range on an electrographic exposure. The characteristic image size, as represented by the standard deviation (σ) of the Gaussian, was assumed constant (i.e., the PSF was assumed independent of intensity).

The digital density arrays $D_{true}(x,y)$ covered square areas $\pm 8\sigma$ from the image centers and were comprised of 4096 x 4096 pixels. To simulate sampling of these arrays by a transmission-averaging microdensitometer, square apertures of size (R) ranging from $\sigma/256$ to 2σ were passed over the central $\pm 6\sigma$ (areas containing essentially all of the image density) in a raster pattern with a stepping increment of $\sigma/256$. The average transmission through the aperture <T> was computed at each point and converted to a "measured" density value $D_{meas}(x,y) = -\log_{10} \langle T \rangle$. The "measured" intensity of each image was the sum $I' = \Sigma D_{meas}(x,y)$. This could be compared to the true integrated intensity $I = \Sigma D_{true}(x,y)$ computed from the original digital arrays.

As an example, the first figure shows normalized cross sections which pass through the peaks of two simulated star images differing in intensity by a factor of 32. The distorted image profiles show the result obtained with the simulated transmission-averaging densitometer using a square aperture of $R = \sigma/2$ (21.3% of the FWHM of the true image density profile). For the weaker image the net result is a 0.8% underestimate of the intensity. But for the brighter image the error is an intolerable 14.1%. This difference increases with larger scanning apertures and/or with larger intensity differences -- representing a potential source of systematic error. The second figure illustrates this trend while the table presents numerical values for the correction factor by which the "measured" intensity could be adjusted to compensate for the effect.

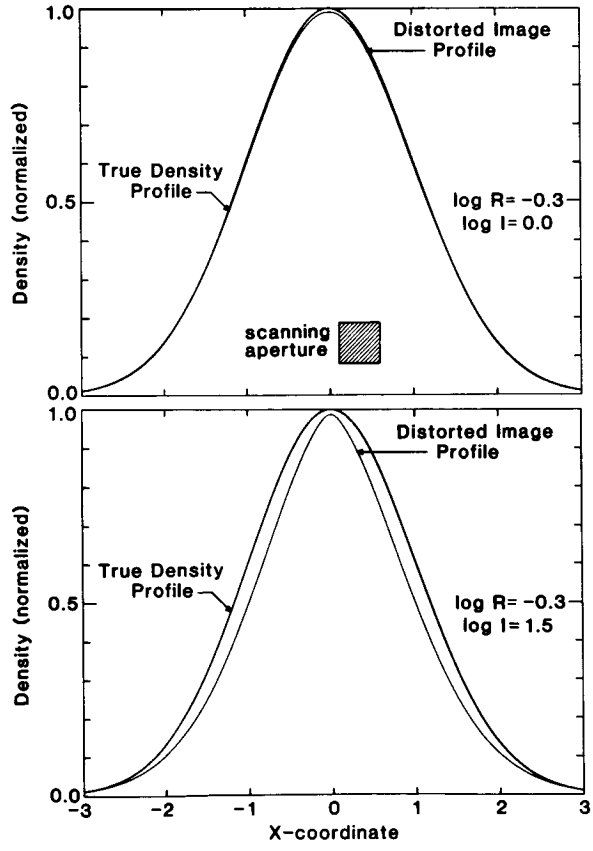

The error is fundamental, but its effect can be minimized or practically eliminated by using a scanning aperture as small as possible (and yet consistent with the noise characteristics and stability of the microdensitometer) or by the application of correction factors which may be determined from a sequence of star field images of varying exposure times (assuming photometric conditions and accurate timing) or from an image of a field containing photometric standards of sufficient range in magnitude.

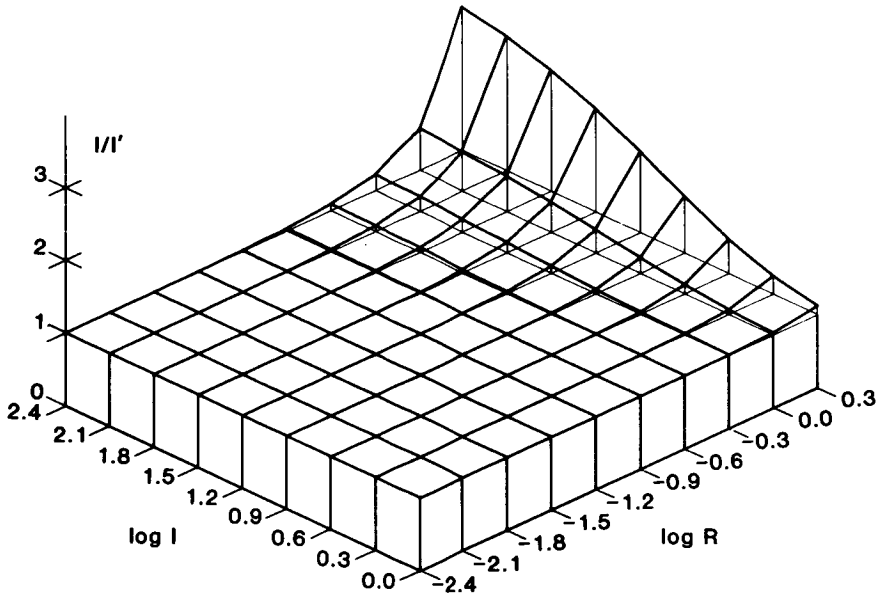

R

log I \ R	1/256	1/128	1/64	1/32	1/16	1/8	1/4	1/2	1	2	I
2.4	1.000	1.000	1.002	1.006	1.016	1.039	1.092	1.218	1.569	2.962	256
2.1	1.000	1.000	1.001	1.004	1.012	1.032	1.081	1.201	1.535	2.841	128
1.8	1.000	1.000	1.000	1.002	1.007	1.024	1.066	1.176	1.484	2.660	64
1.5	1.000	1.000	1.000	1.001	1.004	1.015	1.048	1.141	1.412	2.412	32
1.2	1.000	1.000	1.000	1.001	1.002	1.008	1.030	1.101	1.319	2.107	16
0.9	1.000	1.000	1.000	1.000	1.001	1.004	1.016	1.062	1.217	1.775	8
0.6	1.000	1.000	1.000	1.000	1.001	1.002	1.008	1.033	1.127	1.470	4
0.3	1.000	1.000	1.000	1.000	1.000	1.001	1.004	1.017	1.066	1.248	2
0.0	1.000	1.000	1.000	1.000	1.000	1.001	1.002	1.008	1.033	1.121	1
	-2.4	-2.1	-1.8	-1.5	-1.2	-0.9	-0.6	-0.3	0.0	0.3	

log R

Figure caption: Correction factor (I/I') which could be applied to the measured "density volume" of a stellar image based on the computer simulation of a transmission-averaging microdensitometer for various image intensities and scanning apertures relative to the width of the image. The values of I/I' for particular intensities (I) and relative aperture sizes (R) are indicative only but may be useful in selecting aperture sizes sufficiently small to avoid the undesirable photometric consequences of transmission-averaging. Identical information appears in the table.

1. Report No. NASA CP-2317	2. Government Accession No.	3. Recipient's Catalog No.
4. Title and Subtitle ASTRONOMICAL MICRODENSITOMETRY CONFERENCE		5. Report Date July 1984 6. Performing Organization Code 685.0
7. Author(s) Daniel A. Klinglesmith, Editor		8. Performing Organization Report No. 84F5182
9. Performing Organization Name and Address NASA Goddard Space Flight Center Greenbelt, Maryland 20771		10. Work Unit No. 11. Contract or Grant No. 13. Type of Report and Period Covered Conference Publication
12. Sponsoring Agency Name and Address National Aeronautics and Space Administration Washington, D.C. 20546		14. Sponsoring Agency Code

15. Supplementary Notes

16. Abstract

These proceedings contain the papers presented at the Astronomical Microdensitometry Conference held at Goddard Space Flight Center May 11 through 13, 1983. The program was designed to bring together astronomers from all over the world to discuss the status of the current microdensitometers used for digitizing astronomical imagery. The conference proceedings describe the many tests and improvements that have and can be made to the PDS microdensitometer, the standard workhorse of microdensitometry for astronomy. A session was devoted to the various types of microdensitometers that currently exist in the world. The attendees also presented papers on the future needs and the data processing problems associated with digitizing large images.

17. Key Words (Selected by Author(s))	18. Distribution Statement
Microdensitometry PDS Photometry Astrometry Microdensitometer	Unclassified - Unlimited Subject Category 35

19. Security Classif. (of this report)	20. Security Classif. (of this page)	21. No. of Pages	22. Price
Unclassified	Unclassified	431	A19

For sale by the National Technical Information Service, Springfield, Virginia 22161.

NASA-Langley, 1984